Springer Protocols

Methods in Molecular Biology 590

Molecular Endocrinology

Methods and Protocols

Edited by
Ok-Kyong Park-Sarge
Thomas E. Curry, Jr.

Humana Press

METHODS IN MOLECULAR BIOLOGY™

Series Editor
John M. Walker
School of Life Sciences
University of Hertfordshire
Hatfield, Hertfordshire, AL10 9AB, UK

For other titles published in this series, go to
www.springer.com/series/7651

Molecular Endocrinology

Methods and Protocols

Edited by

Ok-Kyong Park-Sarge and Thomas E. Curry, Jr.

University of Kentucky, Lexington, KY, USA

Humana Press

Editors
Ok-Kyong Park-Sarge
Department of Physiology
University of Kentucky
College of Medicine
800 Rose Street
MS-508 Albert B. Chandler
Medical Center
Lexington KY 40536-0298
USA
okps@uky.edu

Thomas E. Curry, Jr.
Department of Obstetrics & Gynecology
Division of Reproductive Endocrinology
University of Kentucky
800 Rose Street
C-355 Albert B. Chandler Medical Center
Lexington KY 40536-0293
USA
tecurry@uky.edu

ISSN 1064-3745 e-ISSN 1940-6029
ISBN 978-1-60327-377-0 e-ISBN 978-1-60327-378-7
DOI 10.1007/978-1-60327-378-7

Library of Congress Control Number: 2009935058

Cover illustration: Chapter 4 Figure 1C

Printed on acid-free paper

springer.com

Preface

Endocrinology is classically defined as the study of the biosynthesis, storage, chemistry, and physiological function of hormones. The origins of this discipline can be traced as far back as 200 BC when the Chinese isolated sex and pituitary hormones from human urine and used them for medicinal purposes (Temple, Robert, *The Genius of China*). There were many early descriptions of substances (i.e., hormones) emanating from animal and human organs (Rolleston, 1937 Br Med J1(3984):1033–1036) however, the term "endocrine" and "endocrinology" did not appear in common usage until the mid- to late 1800 s. In 1902, Bayliss and Starling first defined a hormone as a chemical that must be produced by an organ, released into the blood, and transported by the blood to a distant organ to exert its specific function. Since this early description of a hormone, our understanding of hormone action and the field of endocrinology has blossomed due to technological breakthroughs. Early work identified hormones such as insulin which led to the Noble Prize in Medicine for Drs. Banting, Best, and Macleod in 1923. In 1947, the mechanisms of hormonal feedback in regulating carbohydrate metabolism by extracts of the anterior pituitary led to the Nobel Prize for Dr. Bernardo Houssay. This work laid the foundation for the study of hormonal feedback control which is central to all aspects of modern endocrinology. In 1950, the Nobel Prize was shared by Drs. Hench, Kendall, and Reichstein for their work on the discovery of hormones from the adrenal cortex such as cortisone, their structure, and biological effects. Our understanding of hormone actions was further expanded by the work of Dr. Roger Guillemin and Dr. Andrew Schally for their elucidation of releasing factors such as thyroid releasing factor and gonadotropin releasing factor. These releasing factors were demonstrated to have neuroendocrine actions for which the scientists received the Nobel Prize in 1977. This same year they shared the Prize in Medicine with Dr. Rosalyn Yalow who, along with Dr. Soloman Berson, developed the radio-immunoassay to measure insulin.

Although all of these "pioneers" in our field have laid a path to advance our understanding of hormone structure, hormone action, and their biological effects, there has been a continuous advancement of our understanding on a day to day, week by week, year to year basis using new and novel techniques. In this volume, *Molecular Endocrinology: Methods and Protocols*, we have invited leaders in the field to share a diverse array of cutting-edge techniques that are becoming routinely employed in our quest to further understand hormone action. We have attempted to include a step-by-step protocol that allows investigators at all stages of their scientific career to successfully perform these techniques. We are indebted to the numerous investigators who have provided their time and expertise to make the techniques in their labs come to life in this volume. For all of us involved in this guide, it has been a learning experience, and hopefully this will translate into a simple, easy to follow step-by-step guide for the reader. We are grateful for the advice and guidance of Dr. John Walker throughout the process of compiling this book. We are also appreciative of

Humana Press for the opportunity to publish this volume. Finally, we are extremely indebted to Kathy Rosewell for all of her work in shepherding the editors throughout this entire process, which is analogous to herding cats! We hope you enjoy this volume of *Methods in Molecular Biology*.

Contents

Contributors

Ashok Agarwal • *Center for Reproductive Medicine, Glickman Urological and Kidney Institute and Obstetrics and Gynecology and Women's Health Institute, Cleveland Clinic, Cleveland, OH, USA*

Krassimira Angelova • *Department of Biochemistry and Molecular Biology, University of Georgia, Athens, GA, USA*

John D. Brannian • *Department of Obstetrics and Gynecology, Sanford School of Medicine of The University of South Dakota, Sioux Falls, SD, USA*

Illya Bronshteyn • *Transgenic and Gene-Targeting Institutional Facility, University of Kansas Medical Center, Kansas City, KS, USA*

Carole Bryant • *Department of Obstetrics and Gynecology, University of Kentucky College of Medicine, Lexington, KY, USA*

Michel Canis • *CHU Clermont-Ferrand, Polyclinique-Hôtel-Dieu, Gynécologie Obstétrique et Médecine de la Reproduction, Clermont-Ferrand Cédex, France*

Evangelia Charmandari • *Division of Endocrinology and Metabolism, Section on Pediatric Endocrinology, Biomedical Research Foundation of the Academy of Athens, Athens, Greece*

Wei-Min Chen • *Department of Public Health Sciences, Center for Public Health Genomics, University of Virginia, Charlottesville, VA, USA*

George P. Chrousos • *Department of Pediatrics, Athens University Medical School, Athens, Greece*

Thomas E. Curry, Jr • *Department of Obstetrics and Gynecology, University of Kentucky College of Medicine, Lexington, KY, USA*

Tamika Tyson Duplessis • *Department of Structural & Cellular Biology and Tulane University School of Medicine and Louisiana Cancer Research Consortium, New Orleans, LA, USA*

Kathleen M. Eyster • *Division of Basic Biomedical Sciences, Sanford School of Medicine, University of South Dakota, Vermillion, SD, USA*

Jeff Falk • *Aviva Systems Biology, San Diego, CA, USA*

Michael A. Frohman • *Department of Pharmacological Sciences, Centers for Molecular Medicine, Stony Brook University, Stony Brook, NY, USA*

Linda C. Giudice • *Department of Obstetrics, Gynecology and Reproductive Sciences, University of California, San Francisco, CA, USA*

Anelia Horvath • *Section on Endocrinology & Genetics (SEGEN), Program on Developmental Endocrinology & Genetics (PDEGEN), National Institute of Child Health and Human Development (NICHD), National Institutes of Health, Bethesda, MD, USA*

Huiyan Huang • *Center for Developmental Genetics, Graduate Program in Genetics, Stony Brook University, Stony Brook, NY, USA*

Tim H-M. Huang • *Human Cancer Genetics Program, The Ohio State University Comprehensive Cancer Center, Columbus, OH, USA*

Tomoshige Kino • *Program in Reproductive and Adult Endocrinology, Eunice Kennedy Shriver, National Institute of Child Health and Human Development, National Institutes of Health, Bethesda, MD, USA*
Jingjing L. Kipp • *Department of Biochemistry, Molecular Biology and Cell Biology, Center for Reproductive Science, Northwestern University, Evanston, IL, USA*
Kristen L. Koterba • *Department of Biochemistry, and Cancer Biology, University of Toledo College of Medicine, Toledo, OH, USA*
T. Rajendra Kumar • *Departments of Molecular & Integrative Physiology, Pathology and Laboratory Medicine, and Institute of Maternal and Fetal Biology, Center for Reproductive Sciences, University of Kansas Medical Center, Kansas City, KS, USA*
Melissa Larson • *Department of Molecular and Integrative Physiology, University of Kansas Medical Center, Kansas City, KS, USA*
Varsha S. Likhite • *Department of Biochemistry, University of Illinois, Urbana, IL, USA*
Gerard Mage • *CHU Clermont-Ferrand, Polyclinique-Hôtel-Dieu, Gynécologie Obstétrique et Médecine de la Reproduction, Clermont-Ferrand Cédex, France*
Adriana Maggi • *Department of Pharmacological Sciences, Center of Excellence on Neurodegenerative Diseases, University of Milan, Milan, Italy*
Carolyn G. Marsden • *Department of Structural & Cellular Biology, Center for Gene Therapy, Tulane University School of Medicine and Louisiana Cancer Research Consortium, New Orleans, LA, USA*
Sachiko Matsuzaki • *CHU Clermont-Ferrand, Polyclinique-Hôtel-Dieu, Gynécologie Obstétrique et Médecine de la Reproduction, Clermont-Ferrand Cédex, France*
Kelly E. Mayo • *Departments of Neurobiology & Physiology and Biochemistry, Molecular Biology and Cell Biology, Center for Reproductive Science, Northwestern University, Evanston, IL, USA*
Jeff McDermott • *Transgenic and Gene-Targeting Institutional Facility, University of Kansas Medical Center, Kansas City, KS, USA*
John Moore • *Department of Obstetrics and Gynecology, University of Kentucky College of Medicine, Lexington, KY, USA*
Latha Muniappan • *Molecular & Cellular Biochemistry, University of Kentucky College of Medicine, Lexington, KY, USA*
Josyf C. Mychaleckyj • *Department of Public Health Sciences, Center for Public Health Genomics, University of Virginia, Charlottesville, VA, USA*
Ann M. Nardulli • *Department of Molecular and Integrative Physiology, University of Illinois, Urbana, IL, USA*
Mary Osisami • *Center for Developmental Genetics, Graduate Program in Genetics, Stony Brook University, Stony Brook, NY, USA*
Sabire Özcan • *Department of Molecular & Cellular Biochemistry, University of Kentucky College of Medicine, Lexington, KY, USA*
Ok-Kyong Park-Sarge • *Department of Physiology, University of Kentucky College of Medicine, Lexington, KY, USA*
Radhika Pochampally • *Department of Pharmacology, Center for Gene Therapy, Tulane University School of Medicine and Louisiana Cancer Research Consortium, New Orleans, LA, USA*

David Puett • *Department of Biochemistry and Molecular Biology, University of Georgia, Athens, GA, USA*
Sudhanshu P. Raikwar • *Department of Internal Medicine, Division of Allergy and Immunology, Roy J. and Lucille A. Carver College of Medicine, University of Iowa and Veterans Affairs Medical Center, Iowa City, IA, USA*
Gianpaolo Rando • *Department of Pharmacological Sciences, Center of Excellence on Neurodegenerative Diseases, University of Milan, Milan, Italy*
Katherine L. Rosewell • *Department of Obstetrics and Gynecology, University of Kentucky College of Medicine, Lexington, KY, USA*
Brian G. Rowan • *Department of Structural & Cellular Biology and Tulane University School of Medicine and Louisiana Cancer Research Consortium, New Orleans, LA, USA*
Michèle M. Sale • *Departments of Medicine and Public Health Sciences, Center for Public Health Genomics, University of Virginia, Charlottesville, VA, USA*
Kevin D. Sarge • *Department of Molecular and Cellular Biochemistry, University of Kentucky College of Medicine, Lexington, KY, USA*
Ricardo Francalacci Savaris • *Departamento de Ginecologia e Obstetrícia Faculdade de Medicina,Universidade Federal do Rio Grande do Sul, Porto Alegre, RS, Brazil*
Jennifer R. Schultz-Norton • *Department of Molecular and Integrative Physiology, University of Illinois, Urbana, IL, USA*
Elizabeth Scotto-Lavino • *Department of Pharmacology, Program in Molecular and Cellular Pharmacology and the Medical Scientist Training Program, Stony Brook University, Stony Brook, NY, USA*
Rakesh K. Sharma • *Center for Reproductive Medicine, Glickman Urological and Kidney Institute and Obstetrics and Gynecology and Women's Health Institute, Cleveland Clinic, Cleveland, OH, USA*
Lirim Shemshedini • *Department of Biological Sciences, University of Toledo, Toledo, OH, USA*
Constantine Stratakis • *Section on Endocrinology & Genetics (SEGEN), Program on Developmental Endocrinology & Genetics (PDEGEN), National Institute of Child Health and Human Development (NICHD), National Institutes of Health, Bethesda, MD, USA*
Yunguang Tong • *Department of Medicine, Cedars-Sinai Research Institute, David Geffen School of Medicine at UCLA, Los Angeles, CA, USA*
Alex C. Varghese • *Center for Reproductive Medicine, Glickman Urological and Kidney Institute and Obstetrics and Gynecology and Women's Health Institute, Cleveland Clinic, Cleveland, OH, USA*
Huizhen Wang • *Department of Molecular and Integrative Physiology, Center for Reproductive Sciences, University of Kansas Medical Center, Kansas City, KS, USA*
Yu-I Weng • *Human Cancer Genetics Program, The Ohio State University Comprehensive Cancer Center, Columbus, OH, USA*
Mary Jo Wright • *Department of Surgery, Section of Breast Surgery, Louisiana Cancer Research Consortium, New Orleans, LA, USA*
Hongyan Xing • *Department of Molecular and Cellular Biochemistry, University of Kentucky College of Medicine, Lexington, KY, USA*

Pearlly S. Yan • *Human Cancer Genetics Program, The Ohio State University Comprehensive Cancer Center, Columbus, OH, USA*

Oladapo Yeku • *Department of Pharmacology, Center for Developmental Genetics, Stony Brook University, Stony Brook, NY, USA*

Nicholas Zavazava • *Department of Internal Medicine and Immunology Graduate Program, Division of Allergy and Immunology, Roy J. and Lucille A. Carver College of Medicine, University of Iowa and Veterans Affairs Medical Center, Iowa City, IA, USA*

Yvonne S. Ziegler • *Department of Molecular and Integrative Physiology, University of Illinois, Urbana, IL, USA*

Chapter 1

Determining the Affinity of Hormone–Receptor Interaction

David Puett and Krassimira Angelova

Abstract

Characterization of the binding of a hormone to its cognate receptor is a cornerstone of many studies in molecular and cellular endocrinology since this event represents the beginning of a specific cellular response, generally from a highly regulated extracellular messenger. The premise of hormone–receptor interaction follows from the law of mass action describing a reversible second-order reaction, hormone plus receptor, to give a non-covalently associated hormone-receptor complex. From this basic principle, a host of useful experimental parameters are available to the interested investigator. This chapter is focused on development of the experimental and mathematical underpinning of hormone–receptor interaction, with emphasis on a gonadotropin, chorionic gonadotropin (or luteinizing hormone), binding to the luteinizing hormone receptor, a member of the G protein-coupled receptor family. The general concepts and approaches developed herein are, however, valid to most interacting systems.

Key words: Hormones, gonadotropin, receptors, G protein-coupled receptors, hormone–receptor binding, kinetics of association and dissociation, saturation binding, competitive binding, thermodynamics of binding.

1. Introduction

The concept of receptors as an important and essential mediator of hormone action at the cellular level formed a major breakthrough in the development of endocrinology. The history of the field, beginning with the work of Claude Bernard and Paul Erhlich in the 19th and early 20th centuries, has been well documented and described by Limbird (1) in her seminal book on cell surface receptors. Although neither Bernard nor Erhlich used the term "receptor," they nonetheless provided critical thinking that stimulated others to pursue the field and unequivocally demonstrate that all classes of hormones act via specific cell surface or intracellular receptors. The basic concept,

O.-K. Park-Sarge, T.E. Curry, Jr. (eds.), *Molecular Endocrinology,* Methods in Molecular Biology 590,
DOI 10.1007/978-1-60327-378-7_1,

deceptively simple and straight-forward, is based on the principle of mass action: $H + R \leftrightarrow HR$ (1, 2). Here, *H* denotes the hormone (peptide, polypeptide, glycoprotein, steroid, thyroid, etc.), *R* refers to the unbound receptor, and *HR* the reversible complex that mediates the biological response(s) associated with the hormone.

Once this fundamental concept was firmly established, rapid advances in mathematical formulations and methodologies for quantitatively measuring HR were forthcoming. The low concentration of circulating hormones and the high affinity between hormone and receptor necessitated the development of radiolabeled hormones and sensitive techniques for measuring complexes. Most studies with peptide or protein-based hormones utilize [^{125}I] labeling because of its high specific radioactivity and reasonably long half-life (~60 days).

This chapter focuses on the binding of the heterodimeric human chorionic gonadotropin (hCG) [or luteinizing hormone (LH)] to the LH receptor (LHR) expressed in transfected human embryonic kidney (HEK) 293 cells. LHR is a G protein-coupled receptor expressed in gonadal cells (3–5). Thus, for quantitative binding studies, one can use appropridate ovarian or testicular cells, transiently or stably transfected mammalian cells (6–9), or membrane fractions from cells or tissues. The application of LH/hCG-LHR binding techniques has proven extremely useful in clinical endocrinology as many reports have appeared showing that naturally occurring mutations of the LHR receptor gene can lead to loss-of-function or gain-of-function, generally with pronounced phenotype, e.g. hypergonadotropic hypogonadism in females and males, and precocious puberty in males (cf. reviews in **refs.** 3–5). Characterization of mutant receptor functionality in transfected cells has permitted a better understanding of normal receptor function and the consequences of reduced hormone binding, normal binding but deficient signaling, hormone-independent receptor activation, reduced membrane trafficking, etc. Lastly, a few cases of gonadotropin β-subunit gene mutations have been characterized that show reduced receptor binding, consistent with the clinical presentation (4, 5). In the emerging area of molecular clinical endocrinology, the ability to combine and correlate genetic mutations with cellular and whole body phenotype will assume even more importance, elevating the need for better and more sensitive hormone-receptor binding assays.

The experimental scheme presented herein is applicable to other plasma membrane-associated receptors, albeit with important experimental differences associated with each system. The mathematical formulation provided applies to all reversibly interacting systems, including steroid and thyroid hormones binding to their respective intracellular receptors. Consistent with the theme of this chapter, the focus is on determination of the IC_{50} (the inhibitory concentration of unlabeled hormone that displaces 50% of a trace amount of specifically bound

radioactively labeled hormone) and the K_d (the equilibrium dissociation constant of the hormone–receptor complex) from binding measurements. We will also show how B_{max} (the maximum number of receptors per cell or per mg membrane protein) can be determined. Signaling measurements should also be performed to correlate binding and responsiveness, at least to ensure that the receptors binding hormone are functional.

2. Materials

2.1. Preparation of Hormone Stock Solutions

1. hCG, recombinant or natural (purified from pregnancy urine) can be purchased from various suppliers (Dr. Albert Parlow, NIDDK, NIH, Torrance, CA; Sigma Chemical Co., St. Louis, MO), or provided by several pharmaceutical firms, with stock solutions made in phosphate buffered saline (PBS) (Sigma-Aldrich Corp., St. Louis, MO) (*see* **Note 1**).
2. Radioiodinated hCG (50 μCi, specific activity >50 mCi/mg) can be purchased from a commercial vendor such as Perkin Elmer Life Science (Boston, MA). Alternatively, the investigator may prefer to iodinate hCG in their own laboratory (*see* **Note 2**).
3. Weymouth's medium with 20 mM HEPES (Life Science Technologies).
4. 0.1% Bovine serum albumin (BSA) (Sigma Chemical Co., St. Louis, MO).
5. Low ionic strength Binding Buffer: 278 mM sucrose, 0.1% glucose, 5 mM HEPES, 5 mM KCl, 1.2 mM $MgSO_4$, 1 mM $NaHCO_3$, 1 mM $CaCl_2.2H_2O$, and 1.2 mM KH_2PO_4 (6–9).

2.2. Transfection of HEK 293 Cells with the LHR cDNA

1. HEK 293 cells are obtained from the American Type Culture Collection (ATCC) (*see* **Note 3**).
2. Growth medium: Dulbecco's Modified Eagle's Medium (DMEM, Cellgro Mediatech, Inc.) supplemented with 10% (v/v) newborn calf serum (Life Science technologies), 10 mM HEPES, pH 7.4, 50 U/mL penicillin, 50 μg/mL streptomycin, and 0.125 μg/mL amphotericin B (all antibiotics from Invitrogen).
3. 83 cm^2 Filter Cap Flasks (Fisher Scientific, Pittsburgh, PA).
4. Lipofectamine (Invitrogen Corp.).
5. The human and rat LHR cDNAs, as well as cDNAs from other species, are available gratis from a number of investigators throughout the world. These are normally received in a transfection vector, e.g. pcDNA3 or pSVL.

2.3. hCG Binding to LHR-Expressing HEK 293 Cells

1. HEK 293 cells, transfected with LH receptor.
2. [^{125}I]hCG.
3. 1 N NaOH.
4. 1470 Wizard gamma counter (Wallac, Oy, Finland).
5. Prism software (GraphPad Software, San Diego, CA).

3. Methods

3.1. Preparation of Hormone Stock Solutions

1. Stock solutions of hCG are prepared by accurately weighing a small amount of lyophilized, salt-free hormone and dissolving it in PBS to give a concentration of 1 mg/mL.
2. The stock solution of hCG should then be aliquoted (100 μL) into plastic Eppendorf tubes and stored at −20°C. Although hCG is quite stable, it is recommended that the frozen solutions be thawed and refrozen no more than a few times.
3. A working solution of commercial [^{125}I]hCG is prepared by diluting the stock solution in Weymouths medium or Binding Buffer (*see* **Section 2.1**) to the desired concentration (*see* **Note 4**).

3.2. Transfection of HEK 293 Cells with the LHR cDNA

1. Frozen HEK 293 cells or cells in passage are plated into straight neck 83 cm^2 Filter Cap Flasks containing 15 mL growth medium at 37°C in humidified air with 5% CO_2.
2. Change media as necessary depending on the growth rate of the cells.
3. Cells are transfected with 15 or 30 μL lipofectamine using 5 or 10 μg LH-R cDNA, to achieve a ratio of lipofectamine: cDNA of 1:3, depending on the receptor density desired.

3.3. hCG Binding to LHR-Expressing HEK 293 Cells

1. Equilibrium and kinetic binding studies are performed in growth medium supplemented with 0.1% bovine serum.
2. The transfected HEK 293 cells are replated into 12-well or 24-well plates, e.g. 1×10^5 cells per well of 12-well plates.
3. Cells are allowed to attach overnight. If different buffers are considered, then optimized conditions need to be employed (*see* **Note 4**). If one wishes to use membrane fractions instead of intact cells, *see* **Note 5**.
4. Add appropriate amount of [^{125}I]hCG to the cells.
    1. For a saturation binding assay, add [^{125}I]hCG to the cells, in the range of 0–10 nM, which provides ample experimental points below and above the K_d (*see* **Note 6**).

2. For a competition binding assay, all plates receive a constant amount of [^{125}I]hCG that should be less than the K_d, but of a sufficient amount that accuracy is maintained as the specific binding decreases upon addition of unlabeled hCG (50–100 pM is recommended).
3. For a competition binding assay, a dose–response curve with increasing concentrations of hCG should be performed in which (unlabeled) hCG is added to an amount that gives complete or nearly complete competition with the radiolabeled hormone. A reasonable range is 0–10 nM. As stated above, an excess of hCG should be included in alternate wells to permit later correction for non-specific binding.
5. To minimize internalization of the hormone–receptor complex an incubation temperature of 4°C is recommended, along with an incubation time of 18–24 h (*see* **Note 7**). For measurements of kinetic constants for the rate of association (k_1) and the rate of dissociation (k_{-1}), and assuming a bimolecular reaction where $K_d = k_{-1}/k_1$, a series of hormone concentrations needs to be utilized with the amount of binding being determined at a number of time intervals for measurement of k_1 (*see* **Note 8**).
6. At the conclusion of the binding experiment, the medium is removed by aspiration.
7. The cells are quickly washed twice with 0.5 mL PBS.
8. The PBS is removed and NaOH is added to the flask, swirled and transferred to a glass tube. This step is repeated.
9. 1 mL of the NaOH solution is counted in a gamma counter (*see* **Note 9**).
10. It is recommended that particular care be given to units in obtaining and reporting binding data (*see* **Note 10**).
11. After the radioactivity has been measured for each sample and corrected for non-specific binding, the data can be analyzed using non-linear regression with Prism software from GraphPad Software, San Diego, CA. This software package also provides programs for preparing and analyzing Scatchard, Hill, and competitive binding plots (discussed below), and for statistical analysis and evaluation of replicate binding studies.

3.4. Data Analysis

3.4.1. Saturation Equilibrium Hormone–Receptor Binding

For a simple bimolecular and reversible reaction such as hormone binding to receptor (Eq. 1), the equilibrium association and kinetic rate constants are described in Eq. 2.

$$H + R \underset{k_{-1}}{\overset{k_1}{\leftrightarrow}} \mathrm{HR} \qquad (1)$$

$$K_a = (\mathrm{HR})/[(H)(R)] = k_1/k_{-1} = 1/K_d \quad (2)$$

Importantly, K_a is the equilibrium association constant; (H) and (R) refer, respectively, to the concentrations of free (unbound) hormone, and free (unoccupied) receptor, with (HR) being the concentration of bound or occupied receptor (*see* **Note 11**). From the conservation of mass, one can write the following relationships.

$$(H_t) = (H) + (H_b) \quad (3)$$

$$(R_t) = (R) + (R_b) \quad (4)$$

In Eqs. 3 and 4, (H_t) and (R_t) denote the total concentrations of hormone and receptor, respectively, while (H_b) and (R_b) refer to the respective concentrations of bound hormone and bound or occupied receptor. In all cases parentheses are used to denote concentrations, although more rigorously they should refer to activities. In biological systems, however, the activity coefficient is assumed to be 1.0 and thus the activity is approximated by the concentration. From the general assumption that the stoichiometry of binding is one molecule of hormone bound per molecule of receptor, Eqs. 3 and 4 can be rewritten as follows.

$$(H_t) = (H) + (HR), \text{ or } (\mathrm{H}) = (\mathrm{H_t}) - (\mathrm{HR}) \quad (5)$$

$$(R_t) = (R) + (\mathrm{HR}), \text{ or } (\mathrm{R}) = (\mathrm{R_t}) - (\mathrm{HR}) \quad (6)$$

Equation 2 can be expressed as shown in Eq. 7 taking advantage of the substitution for (HR) given in Eq. 6, and since $K_d = 1/K_a$, Eq. 7 can rewritten (Eq. 8).

$$K_a = (\mathrm{HR})/\{(H)[(R_t) - (\mathrm{HR})]\} \quad (7)$$

$$(\mathrm{HR})\, K_d = (H)[(R_t) - (\mathrm{HR})] \quad (8)$$

Denoting (HR) as (B), i.e. the concentration of bound hormone (or occupied receptor), and (R_t) as B_{max}, i.e. the concentration of total receptor, one can solve for (B) in Eq. 8 and obtain Eq. 9, which is often represented as a fractional occupancy of receptor, α $(= (B)/B_{max})$ and ranges from 0 with no receptors occupied to 1.0 with all receptors occupied (Eq. 10).

$$(B) = [(B_{max})(H)]/[K_d + (H)] \quad (9)$$

$$\alpha = (H)/[K_d + (H)] \quad (10)$$

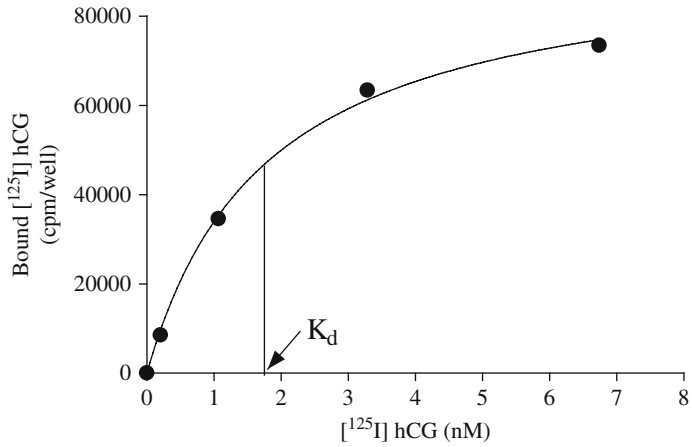

Fig. 1.1. A plot of specific binding of bound [^{125}I]hCG (in units of counts per minute, cpm/well) vs. [^{125}I]hCG concentration (in units of nM) in transiently transfected HEK 293 cells expressing the human LHR. The resulting saturation binding curve is a rectangular hyperbola representing a simple single site bimolecular reaction (see Eq. 9). The two important experimental variables, determined by Prism, are the K_d (2.0 nM), and B_{max} (9.45 $\times$ 10^4 cpm/well), both of which are indicted on the figure. Knowing the specific radioactivity of the radiolabeled hormone (932 cpm/fmol in this experiment) and the number of cells per well (ca. 10^5 for this experiment), or the total protein concentration, the bound radioactivity can be converted to moles (or fmol) bound, and this can be expressed as fmol bound per cell (using stably transfected cells), as fmol bound per cell corrected for cell number and transfection efficiency (transiently transfected cells), or as fmol bound per mg protein in cells, membranes, or tissue (or as per unit volume). The results shown are from a typical saturation binding isotherm and, for graphical clarity, only mean values are given and no SEMs. In practice, one would show the SEMs for each data point and perform replicate experiments to obtain meaningful K_d and B_{max} values. Statistical packages are available to provide rigorous analyses of the results.

Thus, a plot of (B) or α vs. (H) yields a rectangular hyperbola. A typical plot is shown in **Fig. 1.1** where the specific binding of [^{125}I]hCG] to the LHR expressed on transiently transfected HEK293 cells is plotted at various concentrations of [^{125}I]hCG (under the conditions used, the total and unbound concentrations of the radiolabeled hormone are nearly the same). It is noteworthy that the two experimental parameters of equilibrium binding, K_d and B_{max}, are readily obtainable from a binding isotherm (**Fig. 1.1**), as easily demonstrated from Eq. 9. For example, as (H) becomes very large, $K_d + (H) \rightarrow (H)$, which cancels (H) in the numerator, and $B \rightarrow B_{max}$. When $(B) = (1/2)B_{max}$, it follows that the concentration of (H) satisfying this condition corresponds to K_d. From **Fig. 1.1**, the K_d and B_{max} are 1.8 nM and 9.45 $\times$ 10^4 cpm/well (101 fmol/well), respectively, as determined by the Prism software package. Knowing the number of cells in the well, the specific radioactivity of the hormone, the transfection efficiency, or the amount of protein in the well, one can express B_{max} as the number of receptors per cell or per mg protein.

Table 1.1
Experimental Binding (Specific) Data for Figure 1.1

[^{125}I] hCG Total (nM)	[^{125}I] hCG Total (10^{-4} cpm)	[^{125}I] hCG Bound (10^{-4} cpm)	[^{125}I] hCG Free (10^{-4} cpm)
0.2	15.97	0.85	15.12
1.3	112.82	3.46	109.36
2.7	233.80	6.34	227.46
6.1	524.43	7.34	517.08

The actual experimental values shown in **Fig. 1.1** are given in **Table** 1.1, where the numbers testify to the relatively small amount of [^{125}I]hCG added to cells binds specifically. The data points in **Fig. 1.1** show mean values only for a representative binding experiment. Typically one would collect more data points and show the mean ± standard error of the mean (SEM); only a few points are shown and SEMs are omitted in this and subsequent figures for graphical clarity.

In practice it is rather difficult to experimentally measure B_{max} because of the relatively high concentration of radiolabeled hormone required to reach within even 10–20% of the saturation plateau. Since the K_d is defined as the concentration of unlabeled hormone leading to 50% of receptor occupancy, the lack of an accurate determination of B_{max} compromises the accuracy of obtaining K_d. To overcome these experimental limitations, graphical techniques are used to extrapolate from degrees of binding at non-saturable concentrations of hormone to that expected at an infinite concentration of hormone; moreover, statistical methods are available to provide accurate assessments of these values. These graphical methods that yield linear relationships instead of the rectangular hyperbole (**Fig. 1.1**) can be drawn with Prism or done using linear regression to obtain slopes and intercepts.

Most early binding studies utilized the Scatchard plot to recast the rectangular hyperbola into a linear relationship. The Scatchard equation readily follows from Eq. 9 which can be rearranged to give Eq. 11. Then, a simple rearrangement gives Eq. 12.

$$(B)[K_d + (H)] = B_{max}(H) \tag{11}$$

$$(B)/(H) = [B_{max}/K_d] - (B)/K_d \tag{12}$$

From Eq. 12, it is seen that a plot of $(B)/(H)$ vs. (B) results in a line of slope $-1/K_d$ (or $-K_a$). The extrapolated intercept at $(B)/(H) = 0$, i.e. on the x-axis, gives B_{max}. **Figure 1.2** shows a Scatchard plot of the data shown in **Fig. 1.1**. Here, the ratio of bound to free [^{125}I]hCG is plotted at various concentrations of

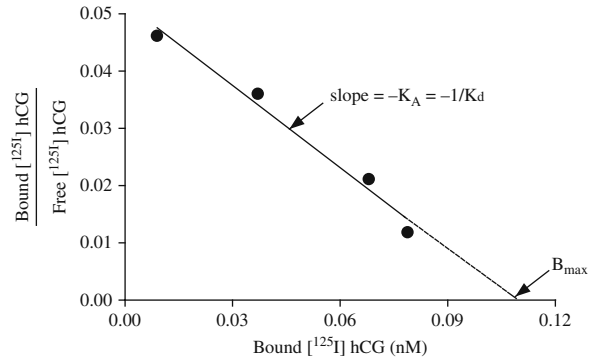

Fig. 1.2. A Scatchard plot of the data in **Fig. 1.1** shown as bound/free [^{125}I]hCG, equivalent to $(B)/(H)$, vs. bound [^{125}]hCG, i.e. (B). This plot represents a linear transformation of the rectangular hyperbola (**Fig. 1.1**) now recast as indicated in Eq. 12. The slope of the line is $-1/K_d$ or $-K_a$, and the extrapolated intercept at $(B)/(H) = 0$, i.e. on the *x*-axis, yields B_{max}. These parameters (obtained by Prism) are indicated on the figure. From these data, the values of K_d and B_{max} are 2.1 nM and, after conversion to the units in **Fig. 1.1**, 10.0×10^4 cpm/well (108 fmol/well), respectively. Any deviation from linearity implies the presence of multiple binding sites or cooperativity in hormone-receptor binding. As in **Fig. 1.1**, only mean values from a representative experiment are presented.

bound hormone, yielding a linear relationship from which the K_d and B_{max} can be obtained. Often the ratio, $(B)/(H)$, is given as B/F, where the parentheses are omitted but both B and F denote concentrations of B (bound) and F (free or unbound hormone). The K_d is 2.1 nM and the B_{max} value shown corresponds to 10.0×10^4 cpm/well (108 fmol/well), both parameters being very similar to those obtained from the saturation binding curve (**Fig. 1.1**). **Table 1.2** lists the B/F ratios plotted in **Fig. 1.2**. Increasing the number of data points will obviously improve the reliability of the results, as will replicate studies and rigorous statistical analyses.

Table 1.2
Experimental Binding (Specific) Data for Figures 1.2 (2 left columns) and 1.3 (2 right columns)

Bound/free	[^{125}I] hCG Bound (nM)	α	$\log_{10}[\alpha/(1-\alpha)]$
0.0462	0.0090	0.0904	−1.003
0.0360	0.0371	0.3659	−0.239
0.0211	0.0680	0.6709	0.309
0.0118	0.0788	0.7772	0.543

The Hill plot was originally introduced to explain oxygen binding to hemoglobin, which was known to exhibit positive cooperativity. This formulation was based on the assumption that a certain number of O_2 molecules, n, bind simultaneously to the hemoglobin tetrameter as outlined in Eq. 13. For the type of equilibrium depicted, the association constant can be written as shown in Eq. 14, where, consistent with our treatment of hormone–receptor interactions and the terms introduced earlier, H for O_2 and R for Hb, are used.

$$\mathrm{nO_2 + Hb \leftrightarrow Hb(O_2)_n} \tag{13}$$

$$K_a = (\mathrm{RH^n})/[(H)^n(R)] \tag{14}$$

If we now substitute $K_d = 1/K_a$ and $\alpha = B/B_{max}$, Eq. 14 can be expressed in a form shown in Eq. 15, which is readily rearranged to give Eq. 16. Taking the logarithm (base 10) of each side of Eq. 16 gives Eq. 17, showing that a plot of $\log_{10}[\alpha/(1-\alpha]$ vs. $\log_{10}(H)$ results in a linear relationship of slope n. The K_d can also be obtained as $(H)^n$ when $\log_{10}[\alpha/(1-\alpha)] = 0$. **Figure 1.3** shows a Hill plot of the data presented in **Fig. 1.1**. In this case, binding is non-cooperative, and thus the slope is 1.0. The K_d from this plot is 1.8 nM, in excellent agreement with the values obtained from non-linear regression and the Scatchard plot. Values for α and $\log_{10}[\alpha/(1-\alpha)]$ are given in **Table 1.2**. One can obtain B_{max} from Eq. 17: when $\log_{10}(H) = 0$, $[\alpha/(1-\alpha)] = -K_d$, or $B_{max} = [1-(1/K_d)]B$. This approach, however, is rarely used.

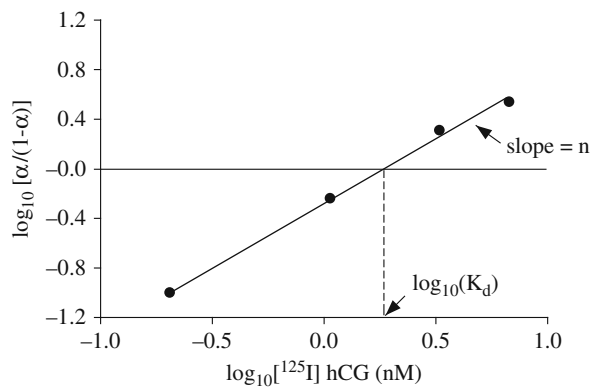

Fig. 1.3. A Hill plot of the data given in **Fig. 1.1.** showing $\log_{10}[\alpha/(1-\alpha)]$ vs. $\log_{10}$(free cpm), or (H), which represents a linear transformation of the rectangular hyperbola shown in **Fig. 1.1.** (see Eq. 17). In this case the binding is non-cooperative, and thus the slope (n) = 1.0 and K_d = 1.8 nM (analyzed by Prism). If the binding were positively or negatively cooperative, the slope would be greater or smaller than 1.0, respectively. For clarity, only mean values are shown.

$$\alpha = (H)^n/[K_d + (H)^n] \quad (15)$$

$$\alpha/(1-\alpha) = (H)^n/K_d \quad (16)$$

$$\log_{10}[\alpha/(1-\alpha)] = n\log_{10}(H) - \log_{10}K_d \quad (17)$$

While based on non-realistic assumptions, Eq. 17 is useful in distinguishing non-cooperative binding from cooperative binding. For example, if $n = 1.0$, the hormone–receptor binding is non-cooperative (as defined in Eqs. **1**–**12**) Values of n greater than or less than 1.0 indicate positive or negative cooperativity, respectively. A more realistic approach can be taken to treat each molecule of O_2 binding to hemoglobin separately, but since cooperativity is not a major issue with hCG binding to the LHR, these formulations will not be introduced.

3.4.2. Competitive Equilibrium Hormone–Receptor Binding

The above sections were based on the implicit premise that the hormone was radiolabeled with high specific radioactivity, e.g. [^{125}I]hCG; in this section such a labeled hormone will be denoted as $^*H$ to distinguish it from unlabeled hormone, H. In widely used competition studies, one adds a small amount of $^*H$ and various concentrations of unlabeled hormone, H, for competitive binding to the receptor. This approach does not provide a true thermodynamic dissociation constant since the affinity parameter measured, the IC_{50} or inhibitory concentration for 50% displacement of $^*H$, depends on many experimental conditions. Nonetheless, under achievable conditions, the IC_{50} is approximately equivalent to the K_d; also, this approach utilizes much less radiolabeled hormone than does saturation binding and is particularly useful in screening combinatorial libraries or mutants of either the hormone or the receptor.

The mathematical formulation underlying competitive binding is a bit more involved than that describing saturation binding since two forms of the hormone are used, e.g. H and $^*H$, and thus there is the possibility that the respective K_d's for receptor binding differ one from the other. Fortunately this can be experimentally determined (1), and any differences between hCG and [^{125}I]hCG binding to the LHR have been found to be negligible. To greatly simplify the mass action equation, it is assumed that H and $^*H$ bind to the LHR with the same affinity. Thus, for the equilibrium presented in Eq. 18 and the conservation of masses shown in Eqs. 19 and 20, one can obtain the expression given in Eq. 21 (1, 2). This rather simple equation is, however, derived from a much more complex relationship (1) and holds only under certain experimental conditions.

$$H + {}^*H + R \leftrightarrow HR + {}^*HR \quad (18)$$

$$(H) + ({}^{*}H) + (HR) + ({}^{*}HR) = (H_{\mathrm{t}}) \tag{19}$$

$$(R) + (HR) + ({}^{*}HR) = (R_{\mathrm{t}}) \tag{20}$$

$$\mathrm{IC}_{50} = K_d + ({}^{*}H) \tag{21}$$

If one wishes to compete the binding of the natural radiolabeled ligand with a derivative or small molecule screen, then the above equation must be modified somewhat (1, 2, 10, 11).

A plot of (**B*), or (**HR*), vs. $\log_{10}(H)$ gives a displacement curve such as that presented in **Fig. 1.4**. The figure is given in a form consistent with most experimental studies where the radioactivity associated with binding **H*, with no competing *H* present, is normalized to 100% and the concentration of the competing unlabeled hormone is graphed on a base_{10} logarithmic scale. The latter is done because in a complete competitive curve several orders of concentrations of the unlabeled hormone are used. At increasingly higher concentrations of hCG, the amount of [^{125}I]hCG bound to receptor is diminished due to competition with hCG. An important binding parameter obtained from competition curves is the IC_{50}, the concentration that reduces the amount of bound radiolabeled hormone by 50% **(Fig. 1.4)**. In

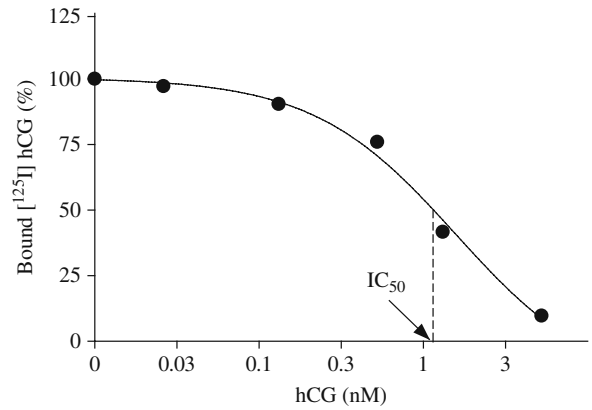

Fig. 1.4. A competitive binding plot of bound [^{125}I]hCG, or (**B*), vs. a logarithmic plot of (hCG), where the ordinate indicates the trace amount of radiolabeled hormone bound to human LHR (cpm/well), and the abscissa gives the concentration in units of nM. Each well contains transiently transfected HEK 293cells with 0.1 nM [^{125}I]hCG. In this plot, as is commonly done, the maximum binding of the trace radiolabeled hormone is normalized to 100% in the absence of any added unlabeled hormone; as increasing concentrations of unlabeled hormone (*H*) compete with (**H*), the curve goes to zero. The major experimental parameter directly available from this plot is the IC_{50} (1.6 nM from Prism). An estimate of B_{max} (20.1×10^4 cpm/well or 69 fmol/well, with [^{125}I]hCG having a specific radioactivity of 2,290 cpm/fmol) can be made from the following relationship: $[(B_{\mathrm{o}}) \times (\mathrm{IC}_{50})/({}^{*}H)]$, where B_{o} is the concentration of bound **H* with no added unlabeled hormone and (**H*) is the concentration of radiolabeled hormone added. While mean values only are given in the figure, one would always have replicates and use statistical packages for a complete analysis of the results.

this particular experiment, the IC_{50} is 1.6 nM; when corrected for the concentration of radiolabeled ligand (Eq. 21), 0.1 nM, a K_d and B_{max} of 1.5 nM and 20.1 $\times$ 10^4 cpm/well (69 fmol/well) are obtained. The experimental values for specific binding in the presence of hCG and [^{125}I]hCG are listed in **Table 1.3**. This experiment refers to a different transfection and thus the difference in B_{max} values.] These results emphasize that differences in values of K_d and B_{max} are dependent to some extent on the type of binding experiment performed or even the type of analysis used on the same data set, thus emphasizing the need of replicate studies and rigorous statistical evaluation of the results. B_{max} values do of course vary more than K_d, particularly in different transfections. One method to alleviate this problem is to use stable transformants (12).

Table 1.3
Experimental binding (specific) data for Figures 1.4 (2 left columns) and 1.5 (2 right columns)

hCG (nM) added	[^{125}I] hCG Bound (10^{-4} cpm)	$(HR_t)/(HR_{eq})$	Time (h)
0.000	2.600	0.370	1
0.026	2.528	0.586	2
0.132	2.350	0.863	4
0.526	1.976	0.965	8
1.316	1.084		
5.263	0.252		

3.4.3. Hormone–Receptor Binding Kinetics

It is often desirable and useful to measure the kinetics of hormone binding to the receptor and the kinetics of dissociation of bound hormone from the receptor. It has been found with many hormone–receptor interactions that the rate constant of association is nearly a diffusion-limited event. Rather than presenting a detailed derivation of binding kinetics for bimolecular reactions, this section will provide an overview with the salient formulae required to obtain the two important rate constants, k_1 and k_{-1}, from experimental measurements. Numerous sources offer a rigorous derivation of the equations if desired (1, 2).The basic differential equation giving the rate of formation of the (HR) complex as a function of time, Eq. 22, follows from Eq. 1. It is useful at this time to introduce a term referred to as the observed rate constant, k_{ob}, as defined in Eq. 23.

$$d(HR)/dt = k_1(H)(R) - k_{-1}(HR) \qquad (22)$$

$$k_{ob} = k_1(H) + k_{-1} = k_1[(H) + K_d] \tag{23}$$

Experimentally, one adds various concentrations of radiolabeled hormone to LHR-expressing cells and measures the change in specific binding as a function of time, $(HR)_t$, permitting the reaction to go to equilibrium to give $(HR)_{eq}$ for that particular concentration of added hormone. This is repeated at different concentrations, and a plot of $\ln\{(HR)_{eq}/[(HR)_{eq} - (HR)_t]\}$ vs. time (t) gives a linear relationship of slope k_{ob} as shown in Eq. 24. **Figure** 1.5 shows such a plot of [^{125}I]hCG binding to LHR at various times, and the corresponding values of $[(HR_t)/(HR_{eq})]$ are given in **Table 1.3**.

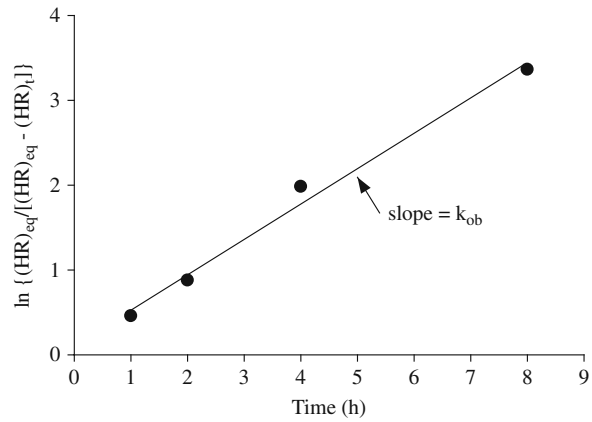

Fig. 1.5 The kinetics of binding 50 pM [^{125}I] hCG to the rat LHR expressed in transiently transfected COS7 cells. A linear transformation of kinetic binding data was made (only mean values shown), $\ln\{(*HR)_{eq}/[(*HR)_{eq} - (*HR)_t]\}$ vs. time, where the slope (from Prism) is K_{ob} which equals 7.2×10^{-3} min^{-1} (see Eq. 24). $(*HR)_{eq}$ and $(*HR)_t$ represent the equilibrium binding and the binding at any time t, respectively.

$$\ln\{(HR)_{eq}/[(HR)_{eq} - (HR)_t]\} = k_{ob}t \tag{24}$$

With values of k_{ob} at different concentrations of hormone, one can plot k_{ob} vs. (H) (see Eq. 23) to obtain a linear relationship of slope k_1 and intercept on the y-axis, when $(H) = 0$, of k_{-1}. Alternatively, knowing the K_d one can obtain the kinetic rate constants using Eqs. 2 and 23. From the equilibrium binding data for hCG-LHR, the values for K_d (average of 1.8_5 nM) and k_{ob} (7.2×10^{-3} min^{-1}) yield a k_1 of 3.8×10^6 min^{-1}M^{-1}and a k_{-1} of 7.0×10^{-3} min^{-1}. As shown elsewhere (13), the association rate constant for hCG binding to the LHR is dependent on the buffer composition and is particularly influenced by ionic strength. Lastly, k_{-1} can be measured directly by utilizing conditions where a preformed HR complex is allowed to dissociate and the amount of free hormone is

sufficiently low that negligible binding or rebinding occurs to the receptor (*see* **Note 9**). Under these conditions, replacing H by $^*H$ in Eq. 22, gives Eq. 25, integration of which yields Eq. 26 where $(^*HR)_t$ and $(^*HR)_o$ represent, respectively, the amount of complex, monitored by cpm, at time t and at zero time, i.e. when the binding solution is diluted or excess H added.

$$d(^*HR)/dt = -k_{-1}(^*HR) \tag{25}$$

$$\ln[(^*HR)_t/(^*HR)_o] = -k_{-1}t \tag{26}$$

Equation 26 shows that a plot of $\ln[(^*HR)_t/(^*HR)_o]$ vs. t gives a linear relationship with a slope of $-k_{-1}$. Knowing the value of (H) in Eq. 23, it is possible to calculate k_1 from the values of k_{ob} and k_{-1}. The determination of k_{-1} by the methods outlined should give reasonably consistent agreement. Also, independent measurements of K_d, k_1, and k_{-1} should satisfy, within reasonable limits, the relationship embodied in Eq. 2.

Any significant deviation from linearity in the plots suggested by Eqs. 23, 24, and 26 indicates that simple bimolecular binding is not occurring or that different binding states of the receptor (or hormone) may exist. Kinetic data are often more sensitive to the above differences than are apparent equilibrium binding results. The absolute values of the kinetic rate constants are useful when attempting to understand the molecular mechanisms involved. For example, a rate constant of association that is expected for a diffusion-controlled reaction implies that the receptor contact site is available for occupancy and the time-limiting factor is a properly oriented collision with hormone. In contrast, if k_1 is much less than that expected from a diffusion-limited reaction, this suggests that the receptor binding pocket is "closed" much of the time, as might be expected if the receptor oscillates between two conformational states, one in which the receptor binding site is blocked (the receptor state most of the time) and one in which binding can readily occur. For hCG binding to the LHR, the data suggest that the low values of K_d, i.e. high affinity, arise from both a relatively high k_1 (on the order of $10^6 - 10^7$ $M^{-1}min^{-1}$) and a relatively low k_{-1} (on the order of 10^{-3} min^{-1}). The association and dissociation rate constants reflect near diffusion-limited binding and slow dissociation of the hormone–receptor complexes, respectively, leading ultimately to the high affinity between hormone and cognate receptor.

3.4.4. Thermodynamic Parameters of Hormone–Receptor Binding

A complete elucidation of the nature of hormone binding to receptor includes determination of several thermodynamic parameters relating differences in the Gibbs standard free energy (ΔG), enthalpy (ΔH), and entropy (ΔS) between the reactants and products of the binding reaction, $H + R \leftrightarrow HR$. The standard free

energy of binding is given by Eq. 27 where R is the gas constant (1.99 cal/[mol·deg]), T is the absolute temperature (Kelvin = $^{o}C + 273$), and K_a the association constant. Since the reaction leading to the formation of the hormone–receptor complex is energetically favorable at physiologically relevant temperatures, ΔG will have a negative value. For hCG binding to the LHR, ΔG is between −13 and −14 kcal/mol. By measuring K_a at several temperatures, one can make a van't Hoff plot of ln (K_a) vs. $1/T$ and obtain ΔH from the slope which equals $-\Delta H/R$. Knowing ΔG and ΔH, ΔS is readily obtained (= $\Delta H - \Delta G)/T$).

$$\triangle G = -RT\ln K_a = RT\ln K_d = \triangle H - T\triangle S \qquad (27)$$

Few studies in molecular endocrinology evolve to the point of determining the thermodynamic parameters of binding. This is unfortunate since valuable information can be forthcoming from the signs and magnitudes, particularly of ΔH and ΔS. For example, a favorable reaction for a hormone–receptor complex to form must be accompanied by a negative free energy change, i.e. the energy of the complex is less than that of the free or unbound states of the hormone and receptor. Such a reaction is favored by a negative ΔH and a positive ΔS. Enthalpic changes generally reflect rather specific interactions between hormone and receptor, e.g. hydrogen bonds, ionic interactions, and dipole interactions, while entropic changes generally reflect changes in disorder, e.g. changes in the aqueous environment of interacting sites and the nature of hydrophobic interactions. Equation 27 clearly and simply demonstrates that favorable binding between hormone and receptor is always a balance between ΔH and ΔS. It is interesting that the low K_ds characteristic of hormone–receptor binding translate into some of the most favorable interaction free energies associated with biological systems. Yet, the corresponding free energies of binding, generally between −12 and −14 kcal/mol, reflect a net gain of several hydrogen bonds, hydrophobic bonds, ionic interactions, and dipole interactions, each contributing some −1 to −3 kcal/mol to the overall free energy. The situation is, however, much more complex as ΔG is dictated by both ΔH and ΔS, neither of which can be computationally obtained with any degree of confidence. As an example, from the crystal structure of the FSH-FSH receptor ectodomain complex (14), with the contact sites between hormone and receptor clearly delineated, it is not possible to use this information to predict the K_d (or ΔG) of binding. Much additional research is required before one can use structural information to rationalize and quantify the ensuing binding affinity and thermodynamic parameters.

4. Notes

1. Some investigators may prefer to express and purify the hormone from mammalian or insect cells. The former provides glycan structures more like that of natural hCG, although bioactive hCG can be expressed in insect cells. Purified hCG should have a stated potency in the range of 12,000–15,000 international units (IUs)/mg. For non-specific binding corrections, a much less expensive crude preparation (ca. 3,000 IU mg, Sigma-Aldrich Corp.) can be substituted for purified hCG.
2. One may prefer to iodinate hCG in the laboratory using either an enzymatic or chemical oxidizing reagent. ^{125}I is preferred over ^{131}I because of its 60-day half-life and its relatively high specific radioactivity and low energy γ emission. Pierce Biotechnology, Inc. (Rockford, IL) provides a number of reagents to facilitate iodination, and the Iodo-Gen reagent (or Iodo-Beads) works very well with hCG. [Na^{125}I] can be obtained from a standard vendor such as Perkin-Elmer Life Science (5 mCi, 629 GBq/mg). To iodinate hCG in the laboratory, a Pierce Iodo-Gen or Iodo-Bead regeant can be used to give bioactive [^{125}I]hCG following the instructions recommended by the vendor. Separation of free [^{125}I] and [^{125}I]hCG is accomplished by gel filtration chromatography (1 $\times$ 20 cm column of Sephadex G-100) in which the column is prewashed first with 1% (w/v) BSA and then with 50 mL PBS. The reaction mixture is added to the column which is developed with PBS. Collection of approximately 20-drop fractions in glass tubes ensures a good separation of [^{125}I]protein and [^{125}I]. The peak protein tubes (5–6 tubes) are pooled and counted; then 4% (w/v) BSA is added to the pooled material to a final concentration of 0.25% (w/v). and the stock solution of [^{125}I]hCG is aliquoted and stored at -20^{o}C. Radiolabeling should not drastically alter the binding properties of the hormone, and this can be documented by comparing parameters obtained from saturation and competition binding.
3. Target cells can be obtained from the ovaries and testes of a variety of species, either as primary cells or immortalized cells (the latter from ATCC or individual scientists). For investigators interested in studying binding of LH and hCG to human LHR and perhaps early downstream signaling, e.g. cAMP, most studies are done with one of several transfected cell lines, HEK 293, COS7, or CHO cells.
4. Before embarking on a concerted investigation of hormone binding to its cognate receptor, it is important to screen a number of buffers since many cases have been reported where

a single ion, for example Na^+, K^+, or Ca^{++}, may significantly affect binding. Also, conditions must be chosen such that non-specific binding is low compared to total binding. If large corrections are required to obtain specific binding, then the experimental accuracy is considerably compromised.

5. If membrane fractions are used, the concepts and steps are similar to those given for intact cells; however, incubation should be done in tubes that are gently agitated throughout the experiment. Following centrifugation to pellet the membrane-associated receptors, the membrane fractions are collected for counting.
6. For each concentration chosen, it is important to repeat the exact conditions in the presence of 1 μg of unlabeled hCG/mL to enable the non-specific binding to be subtracted from the total binding to give specific binding. For example, the specific counts bound = total counts − non-specific counts. From a knowledge of the specific radioactivity of the iodinated hormone, the counter efficiency, and experimental conditions, the concentration in nM or pM can be determined.
7. The kinetics of hormone–receptor internalization should be determined to ensure that the observed specific binding is attributable to cell surface receptor binding and has little or no contribution from internalized complexes (*see* **ref.** 15 for methodologies). Shorter incubation times can be used at the more physiologically relevant temperature of 37°C, but some of the apparent binding of hormone will be attributable to internalization. A compromise set of conditions is to incubate hCG and the LHR at 25°C for 16–18 h.
8. It is important that the incubation time be sufficient to permit equilibrium to be reached under the conditions used at each concentration of hormone. As above, the specific binding must be calculated in each case. While k_{-1} can be calculated as a simple product, $k_{-1} = k_1 K_d$, it is always advisable to make direct experimental measurements of k_{-1}. Two approaches can be used to determine k_{-1} experimentally. In both, sufficient radioiodinated hormone is added and equilibrated such that accurate measurements can be made of the amount bound as the degree of binding is reduced. It is important that conditions be met that minimize reassociation of radiolabeled hormone, originally bound but that has dissociated with time, from rebinding to the receptor. This is accomplished by either performing: (i) an "infinite dilution", i.e. removing the media containing radiolabeled hormone from the cells and adding excess

media devoid of radiolabeled hormone back to the cells, or by (ii) adding an excess of unlabeled hormone to minimize any rebinding of radioiodinated hormone to the receptor.

9. There are other methodologies for separating bound and free hormone (1, 16), including equilibrium dialysis, vacuum filtration, and chromatographic methods. Some of these techniques, however, require either a solubilized LHR (or at least the ectodomain responsible for high affinity and specific LH binding) or dispersed membrane preparations. Surface plasmon resonance, which requires no radiolabeling, can also be used for binding studies, but solubilized LHR or the LHR ectodomain is generally required.
10. Hormone concentrations can be reported as unit weight/ unit volume, e.g. ng/mL, but it is preferable to use molarity whenever possible, e.g. nM. Although many reports appear giving hormone concentrations in units (U)/mL, international units (IU)/mL, or mIU/mL, authors and editors should strive to have these units translated into molarity or weight/unit volume whenever possible; K_a is in units of M^{-1} (or nM^{-1}); $K_d$and IC_{50} are in units of M (or nM); the rate constant of association, k_1, is in units of $min^{-1}M^{-1}$ (or $s^{-1}M^{-1}$); and the rate constant of dissociation, k_{-1}, and k_{ob} are in units of min^{-1} (or s^{-1}). ΔG, ΔH, and ΔS are, respectively, in units of cal/mol (or kcal/mol), cal (or kcal), and cal/deg (or kcal/deg), the former referred to as an entropy unit.
11. One must be cognizant that (H) denotes free hormone concentration, but often $(H)_t$ is approximately equal to (H).

Acknowledgments

This chapter is dedicated to the memory of Yongsheng Li who contributed significantly to research on gonadotropins and their receptors. It is a pleasure to thank Geneva DeMars for helpful comments and assistance. Supported by NIH research grants DK33973 and DK69711.

References

1. Limbird, L. E. (1996) *Cell Surface Receptors: A Short Course on Theory and Methods*, 2nd edition, Kluwer Academic Publishers, Boston, MA.
2. Hulme, E. C. (1999) Analysis of binding data, in *Methods in Molecular Biology, Vol. 106: Receptor Binding Techniques* (Keen, M., ed.), Humana Press, Totowa, NJ, pp. 139–185.
3. Themmen, A. P. (2005) An update of the pathophysiology of human gonadotropin and receptor gene mutations and polymorphisms. *Reproduction* **130**, 263–274.
4. Piersma, D., Verhoef-Post, M., Berns, E. M. J. J., and Themmen, A. P. N. (2007) LH receptor gene mutations and polymorphisms: An overview. *Mol. Cell. Endocrinol.* **260–262**, 282–286.

5. Ascoli, M. and Puett, D. (2009) The gonadotropin hormones and their receptors, in *Yen and Jaffe's Reproductive Endocrinology*, Sixth Edition (Strauss, III, J. F. and Barbieri, R., eds.), Elsevier, Inc., Philadelphia, PA, pp. 35–55.
6. Angelova, K. and Puett, D. (2002) Differential responses of an invariant region in the ectodomain of three glycoprotein hormone receptors to mutagenesis and assay conditions. *Endocrine* **19**, 147–154.
7. Angelova, K. Fanelli, F., and Puett, D. (2002) A model for constitutive lutropin receptor activation based on molecular simulation and engineered mutations in transmembrane helices 6 and 7. *J. Biol. Chem.* **277**, 32202–32213.
8. Angelova, K., Narayan, P., and Puett, D. (2003) The luteinizing hormone receptor: Influence of buffer composition on ligand binding and signaling of wild type and mutant receptors. *Mol. Cell. Endocrinol.* **204**, 1–9.
9. Angelova, K., Fanelli, F., and Puett, D. (2008) Contributions of intracellular loops 2 and 3 of the lutropin receptor in Gs coupling. *Mol. Endocrinol.* **22**, 126–138.
10. Cheng, Y. and Prusoff, W. H. (1973) Relationship between the inhibition constant (K_I) and the concentration of an inhibitor that causes a 50% inhibition (I_{50}) of an enzymatic reaction. *Biochem. Pharmacol.* **22**, 3099–3108.
11. Chou, T.-C. (1974) Relationships between inhibition constants and fractional inhibition in enzyme-catalyzed reactions with different numbers of reactants, different reaction mechanisms, and different types and mechanisms of inhibition. *Mol. Pharmacol.* **10**, 235–247.
12. Warrenfeltz, S.W., Lott, S.A., Palmer, T.M., Gray, J., and Puett, D. (2008) Luteinizing hormone-induced up-regulation of ErbB-2 is insufficient stimulant of growth and invasion in ovarian cancer cells. *Mol. Cancer Res.* **6**, 1775–1785.
13. Galet, C. and Ascoli, M. (2005) The differential binding affinities of the luteinizing hormone (LH)/choriogonadotropin receptor for LH and choriogonadotropin are dictated by different extracellular domain residues. *Mol. Endocrinol.* **19**, 1263–1276.
14. Fan, Q. R. and Hendrickson, W. A. (2005) Structure of human follicle-stimulating hormone in complex with its receptor. *Nature* **433**, 269–277.
15. Kishi, M. and Ascoli, M. (2000) The C-terminal tail of the rat lutropin/choriogonadotropin (CG) receptor independently modulates human (h) CG-induced internalization of the cell surface receptor and the lysosomal targeting of the internalized hCG-receptor complex. *Mol. Endocrinol.* **14**, 926–936.
16. Qume, M. (1999) Overview of ligand-receptor binding techniques, in *Methods in Molecular Biology, Vol. 106: Receptor Binding Techniques* (Keen, M., ed.), Humana Press, Totowa, NJ, pp. 3–23.

Chapter 2

Determination of Serum Estradiol Levels by Radiometric and Chemiluminescent Techniques

Carole Bryant, John Moore, and Thomas E. Curry, Jr.

Abstract

The ability to precisely measure circulating levels of hormones is a foundation of modern endocrinology. For assisted reproductive technologies such as in vitro fertilization (IVF), accurate determination of circulating levels of estradiol are crucial for patient management, retrieval of fertilizable oocytes, and successful pregnancy outcome. For many years, circulating levels of estradiol were determined by radioimmunoassay. More recently, nonradioactive techniques such as ELISAs or chemiluminescent approaches have replaced traditional radioimmunoassays. In the current chapter, we outline the procedures for analysis of circulating levels of estradiol by both radioimmunoassay and chemiluminescent techniques.

Key words: Radioimmunoassay, chemiluminescence, estradiol, Immulite, hormone detection.

1. Introduction

A major breakthrough in the field of endocrinology was the development of sensitive, specific, quantitative assays to determine the concentrations of hormones. In 1977, Dr. Rosalyn Yalow received the Nobel Prize in Medicine for the development of a radioimmunoassay (RIA) for insulin. The RIA developed by Drs. Yalow and Berson replaced bioassays and was the first technique that allowed for the precise measurement of previously undetectable levels of hormones (1). RIA is based upon a competitive binding reaction where a known amount of radiolabeled hormone "competes" with an unknown quantity of the hormone found in serum (or other biological fluid or tissue) for an antibody against the hormone. As the concentration of the hormone in the sample increases, more of the hormone binds to

O.-K. Park-Sarge, T.E. Curry, Jr. (eds.), *Molecular Endocrinology,* Methods in Molecular Biology 590,
DOI 10.1007/978-1-60327-378-7_2,

the antibody and displaces the radiolabeled hormone. Thus as the hormone concentration increases, the ratio of the antibody-bound radiolabeled hormone to free radiolabeled hormone decreases. The antibody bound hormones are separated from the unbound hormones and the radioactivity measured. The amount of hormone present in the serum can be determined by plotting the outcomes on a binding curve.

Since the early discovery of RIA, kits have become commercially available to measure a vast array of hormones. In our laboratory, we use the Siemens Coat-A-Count kits (Siemens Medical Solutions Diagnostics, Los Angeles, CA) to measure estradiol. The estradiol Coat-A-Count kits are a solid phase RIA based on a specific antibody to estradiol immobilized to the wall of a polypropylene tube. ^{125}I-labeled estradiol competes for a fixed time with estradiol in the patient sample for antibody binding sites on the wall of the tube. After incubation, separation of bound estradiol from free hormone is achieved by decanting. The tube is then counted in a gamma counter, the counts per minute (CPM) being inversely related to the amount of estradiol present in the patient sample. In other words, the higher the concentration of estradiol in the serum, the more radiolabeled estradiol is displaced from the antibody binding sites resulting in lower counts per minute. The quantity of estradiol in the sample is determined either through a computer program or by comparing the counts to a calibration curve.

Although the RIA technique is extremely sensitive and specific, nonradioactive techniques have gained increasing popularity in recent years primarily due to the problems associated with storage and disposal of radioisotopes. Our laboratory has replaced the radiometric estradiol assay with a chemiluminescent procedure. The Siemens IMMULITE 1000 Estradiol procedure is based upon the same principles as the RIA but instead uses a solid-phase, competitive binding chemiluminescent enzyme immunoassay. Instead of radiolabeled hormone, alkaline phosphate conjugated estradiol is employed. The detection of alkaline phosphate conjugated estradiol is accomplished by the ability of alkaline phosphate to hydrolyze a phosphate ester of a chemiluminescent substrate (adamantyl dioxetane). The cleavage of the chemiluminescent substrate is detected spectrophotometrically by a luminometer (2). The photon counts can be used in the same manner as the radiometric counts to determine the concentration of estradiol in the sample. In this chapter, we detail the methodology to determine the serum concentrations of estradiol by both RIA and chemiluminescence. This procedure is the cornerstone to assess a woman's responsiveness to exogenous gondadotropin stimulation during assisted reproductive technology procedures.

2. Materials

2.1. Specimen (Serum) Collection and Storage

1. Evacuated Serum Collection Tubes (BD Vacutainer Systems, Preanalytical Solutions, Franklin Lakes, NJ).
2. Holder/Adapter—use with the evacuated collection system. (BD Vacutainer Systems).
3. Tourniquet.
4. Alcohol Wipes—70% isopropyl alcohol.
5. Gauze sponges—for application on the site from which the needle is withdrawn.
6. Adhesive bandages/tape—protects the venipuncture site after collection.
7. Sharps disposal unit—BD Vacutainer Systems (*see* **Note 1**).
8. Gloves.

2.2. Radioimmunoassay

1. Reagents for radiometric measurement of estradiol are obtained in kit form from Siemens Medical Solutions Diagnostics, Los Angeles, CA. All reagents should be stored at 2–8°C and are stable for at least 30 days after opening. A single 100 tube kit (TKE21) (*see* **Note 2**) contains the following:
   a. Estradiol Antibody Coated Tubes: 100 polypropylene tubes coated with rabbit antibodies to estradiol and packaged in zip-lock bags.
   b. (125I) Estradiol: Iodinated synthetic estradiol in liquid form, ready to use. Each vial contains 105 ml.
   c. Zero standard (A Calibrator), 1 vial, 5 ml.
   d. Estradiol Calibrators B through G: 6 vials, 2 mls each. The calibrators contain respectively 20, 50, 150, 500, 1800, and 3600 picograms of estradiol per milliliter (pg/ml); equivalently: 0.07, 0.18, 0.55, 1.84, 6.61, and 13.2 nanomoles per liter (nmol/L).
2. Quality control specimens: CON6 Multivalent Control Module (Siemens, Catalog Number CON6) is an assayed, human serum based, tri-level control. Each set of CON6 controls consists of lyophilized material which is reconstituted by adding exactly 6.0 ml of distilled or deionized water. Let it stand for 30 minutes, then mix by inversion until completely dissolved. The controls are stable for 7 days at 2–8°C or for 2 months frozen at –20°C. Aliquot if necessary in tightly capped plastic containers to avoid repeated freeze-thaw cycles and evaporation.
3. Disposable polypropylene tubes, 12 × 75 mm.

4. Pipettor for 100–1000 µl.
5. Disposable 100 and 1000 µl tips.
6. Vortex mixer.
7. Centrifuge.
8. Distilled or deionized water.

2.3. Radioimmunoassay Analysis and Quantification of Estradiol

1. Gamma counter (Beckman, Inc).

2.4. Chemiluminescence

1. Reagents are obtained in kit form (Catalog Number LKE21) from Siemens Medical Solutions Diagnostics.
2. All reagents, test units, and wedges should be stored at 2–8°C and are stable until the expiration dates stated on the packaging.
3. There are three components in each kit (the test units, reagent wedge, and adjustors) which represent a matched set. Bar-codes encode information about the test, including expiration dates, component lot numbers, adjustment and master curve parameters.
4. Estradiol Test Units: 25 test units per re-sealable pack. Each bar-coded-labeled test unit contains one bead coated with polyclonal anti-estradiol antibody. The test unit packs are packaged in re-sealable bags with desiccant and are stable until the expiration date on the label when stored refrigerated at 2–8°C.
5. Estradiol Reagent Wedge: One barcode reagent wedge, containing 7.5 ml bovine calf intestine alkaline phosphatase conjugated to estradiol in human protein based matrix. Store refrigerated at 2–8°C to maintain stability until the expiration date on the wedge label (*see* **Note 3**).
6. Estradiol Adjustors: one set of two vials. 2 ml each, designated low and high concentrations of estradiol in processed human serum. Store refrigerated at 2–8°C for 30 days after opening. Stable at −20°C for 6 months after reconstitution.
7. Quality control specimens: CON6 Multivalent Control Module (Siemens, Catalog Number CON6) is an assayed, human serum based, tri-level control. Each set of CON6 controls consists of lyophilized material which is reconstituted by adding exactly 6.0 ml of distilled or deionized water. Let it stand for 30 minutes, then mix by inversion until completely dissolved. The controls are stable for 7 days at 2–8°C or for

2 months frozen at −20°C. Aliquot if necessary in tightly capped plastic containers to avoid repeated freeze-thaw cycles and evaporation.

8. Chemiluminescent Substrate (Catalog Number LSUBX): Each box of Chemiluminescent Substrate includes two bottles of Chemiluminescent Substrate. Prior to use, the Chemiluminescent Substrate is stored refrigerated at 2–8°C. The substrate can remain on the instrument for up to 30 days.
9. Probe Wash: Each box of Probe Wash (Siemens Catalog Number LPWS2) contains two bottles of Probe Wash Concentrate that should be stored at room temperature. Before using, each 100 ml bottle must be diluted with 900 ml of distilled water (1:10 dilution).
10. Immulite 1000 sample cups (Catalog Number LSCP).
11. Immulite cups holder set (Catalog Number LCH).
12. Transfer pipets (Sarstedt, Newton, NC).
13. Centrifuge.
14. Distilled or deionized water.

3. Methods

3.1. Specimen (Serum) Collection and Storage

1. Label vacutainer collection tube with patient identification information.
2. Don gloves and prepare the collection site (*see* **Note 4**) by swabbing the area with alcohol wipes.
3. Place a tourniquet above the collection area tight enough to make the vein bulge. Insert the needle into the vein at a 15 degree angle.
4. Push the vacutainer (blood specimen collection tube) into the holder, keeping the needle steady. The vacutainer will automatically begin filling. Draw the correct volume of blood allowing the vacuum in the tube to be exhausted (*see* **Note 5**).
5. When the collection is finished, remove the needle from the collection site by pulling it out at the same angle at which it was inserted.
6. Remove the tourniquet.
7. Apply a dry gauze to the site and apply pressure. Immediately dispose of the collection needle by placing it in a sharps container. Do NOT recap the needle.
8. Gently invert the tube 5 times.

9. After 2 or 3 minutes, remove the gauze and cover the collection site with an adhesive bandage.
10. Allow the specimen to coagulate by sitting at room temperature (22–26°C) 20–30 minutes.
11. Centrifuge at 1300–1800 *g* for 10 minutes to separate the serum from the cells.
12. The samples may be stored at 2–8°C for 7 days, or up to 2 months frozen at −20°C (*see* **Note 6**).

3.2. Radioimmunoassay

1. Allow all reagents, specimens and CON6 controls to come to room temperature (22–26°C) before using (*see* **Note 7**).
2. Label two plain (uncoated) 12 × 75 mm polypropylene tubes as T (total counts) and two plain (uncoated) 12 × 75 mm polypropylene tubes as NSB (nonspecific binding) (*see* **Note 8**).
3. Label Estradiol Ab-Coated Tubes as A (0 pg/ml, maximum binding) and B through G (20, 50, 150, 500, 1800, and 3600 pg/ml) in duplicate (total of 14 tubes). Label additional antibody-coated tubes, also in duplicate for controls and patient samples controls.
4. Pipet 100 µl of the zero calibrator A into the NSB and A tubes (0 pg/ml) and 100 µl of each of the calibrators B through G into correspondingly labeled tubes. Pipet 100 µl of each control and patient sample into the tubes prepared (*see* **Notes 9–11**).
5. Add 1.0 ml of (125I) estradiol to every tube and vortex all tubes.
6. Cap the total count tubes to avoid accidental decantation at the end of incubation.
7. Cover and incubate at room temperature for 3 hours.
8. Decant thoroughly all tubes except the total count tubes (*see* **Note 12**).

3.3. Radioimmunoassay Analysis and Quantification of Estradiol

1. Count each tube for 1 minute in a gamma counter. Results will be expressed as counts per minute (CPM).
2. For each pair of tubes calculate the average NSB corrected counts per minute. This is accomplished by subtracting the NSB from each tube as follows: Average NSB corrected CPM (or Net Counts) = CPM − Average NSB CPM. Determine the binding of each pair of tubes as a percentage of maximum binding (MB), with the NSB-corrected counts of the A tubes (0 pg/ml) taken as 100%: Percent Bound = (Net Counts/Net MB Counts) × 100. Note: The calculation can be simplified by omitting the correction for nonspecific binding; samples within range of the calibrators yield virtually the same results when Percent Bound is calculated from the Average CPM.

3. Most gamma counters will have a program to determine binding kinetics. However if necessary use logit-log graph paper, plot Percent Bound on the vertical (probability or ordinate) axis against Concentration on the horizontal (logarithmic or abscissa) axis for each of the nonzero calibrators, and draw a line approximating the path of these points (**Fig. 2.1**). Results for the unknowns may then be calculated from the line by interpolation (3) (*see* **Note 13**).

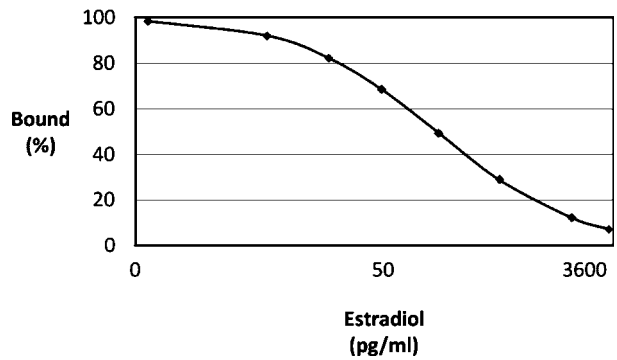

Fig. 2.1. Logit-Log standard curve for calculating estradiol concentration. The cpm for the estradiol standards are converted to percent bound which is plotted on the standard curve to generate the binding curve. The amount of estradiol in the patient sample is calculated from the binding curve.

3.4. Chemiluminescence

The Siemens IMMULITE 1000 Estradiol procedure is a solid-phase, competitive binding chemiluminescent enzyme immunoassay. The solid phase test unit contains a polystyrene bead coated with polyclonal rabbit anti-estradiol. The patient sample along with a known amount of estradiol conjugated to alkaline phosphate are simultaneously introduced into the reaction tube containing the bead and incubated for 60 minutes at 37°C with intermittent agitation. During the incubation, estradiol in the sample competes with the alkaline phosphate estradiol conjugate for a limited number of antibody binding sites on the bead. Unbound enzyme labeled conjugate and unbound sample are then removed by a centrifugal wash, after which substrate is added and the reaction tube is incubated for 5 minutes. The chemiluminescent substrate undergoes hydrolysis in the presence of alkaline phosphate yielding the sustained emission of light. After the 5 minute incubation at 37°C, the light signal reaches a maximum and the photon counts are measured by the photomultiplier tube (PTM). Counts per second (cps) are converted to analyte concentrations (doses) using stored master curves. The IMMULITE 1000 calculates test results for controls and patient samples from the observed signal (counts per second), using a stored master curve (2) (*see* **Note 14**). The bound complex and thus also the photon counts, as measured by the luminometer, is inversely proportional to the concentration of estradiol in the sample (4).

1. Place the bags of estradiol test units UNOPENED at room temperature on the bench for 30 minutes. Do not open immediately after removing from the refrigerator as condensation will form on the beads.
2. Place the three CON6 controls on the bench and allow them to thaw while doing other set-up.
3. Place the Estradiol Reagent Wedge on the Reagent Carousel. Load the wedge into the Reagent Carousel by inserting the tab at the bottom of the wedge into the slot on the outer rim of the Reagent Tray. Press down firmly until it snaps into place.
4. Open the cap of the reagent wedge and remove bubbles in the reagent wedge. Do this by poking the liquid in the wedge with a pipette tip. Bubbles may cause false level sensing and a short sample or reagent draw.
5. Place the Reagent Carousel into the Reagent Chamber by positioning the Reagent Carousel so the line on the tray handle is aligned with the line on the carousel spindle. (The Reagent Carousel can only be seated on the carousel spindle if the two lines are properly aligned.) Close the lid covering the Reagent Carousel (**Fig. 2.2**).
6. Check the volume of water and probe wash on the LED level indicator on the left side instrument. Add water (labeled on the lid with a blue dot) if needed, (*see* **Note 15**). Add probe wash (yellow dot on lid) if needed.
7. Check the volume in the chemiluminescent substrate bottle (brown bottle on top of the Immulite). If it is empty, replace it with a new bottle. To replace, remove the old bottle by pulling it straight up off the spike. Remove the red cap that reads "flip off" from the new bottle and push the inverted bottle onto the spike. Push the gray prime button (just below the Chemiluminescent substrate bottle but above the fill level line) module 2 times (*see* **Note 16**).
8. Turn the Immulite monitor on and double click the Immulite 1000 icon. Press the "Run Immulite" button.
9. Enter your name or initials in the User ID box and press enter. The instrument will download programs. (This takes a few minutes.) The action takes you to the "Home" screen.
10. Clicking "Worklist" on the top tool bar will advance to the Worklist Entry Screen. At this screen, turn on "Auto Increment" by clicking it in the "Entry Options" panel on the left near the top of the screen. In the center of the screen, type the number "1" in the Sample Cup Box and press "Enter."
11. Click "Control" on the left panel. Tab to "Control Name." Click the down arrow to open the pull down box and select CON6. Press enter.

12. At the "Control Lot#" box, select the lot number on the bottom of the list and press enter. At the "Control Level" box, select "4." Then press "Accept."
13. Because the Auto Increment was turned on in step 10, the sample cup number will now read "2." Repeat steps 11–12 to enter the Controls 5 and 6 respectively.
14. Sample cup holders 1, 2, and 3 should remain in the sample cup holder rack. Place sample cups in the sample cup holders.
15. Vortex, then pipette CON6 controls 4, 5, and 6 into sample cup holders 1, 2, and 3 respectively using sample transfer pipets.
16. Sample Cup # now reads "4." In the panel on the left, click "Patient" then tab to "Accession Number." This is a required field on the Immulite 1000. You may either enter the patient accession number (i.e. hospital identifier number) or create your own identifier for your samples. Click the "Accept" at the bottom of the screen. This will advance the next screen.
17. Transfer a patient sample into a plastic sample cup and place the cup into Sample Cup Holder #4. The minimum volume required for estradiol is 125 µl. 100 µl is necessary as "dead volume" while 25 µl is the actual amount pipetted by the Immulite during operation (*see* **Note 17**). Ensure there are no bubbles on the surface of the sample or reagents. Bubbles may cause false level-sensing and a short sample or reagent draw.
18. Repeat steps 16–17 for each sample being assayed.
19. Press the green "GO" button on the Immulite screen. This message will appear: *DPC IMMULITE INITIALIZING.* Please wait. Next, the following prompt appears: *Remove all tubes from the load chain. Press GO when completed.* Do this.
20. Lift the cover on the Immulite. Remove any Test Units or sample cups between the first green arrow on the Load Platform and the Main Carousel.
21. After a brief initialization, the prompt will read: *Load water and substrate containers. Empty waste container and press GO.* Ignore this as you have already done this. Simply press GO.
22. The message will read: *IMMULITE is priming the syringes. Please wait.* The Immulite will prime the syringes once. As the Immulite primes the Hamilton Syringe Pump, watch for air bubbles in the lines and large air spaces in the syringes (**Fig. 2.2**). These should go away as the instrument primes the syringes. If there are large air spaces or bubbles when priming is finished, manually prime the pump again. Do this by pushing the "Prime" button on the pump. Repeat this until major bubbles and spaces are gone.

23. This message will now appear: *Prime the syringes, substrate and water. Press GO when done.* To do this, unscrew the long silver thumbscrew which is located below and to the left of the substrate bottle on the Substrate Heater. Gently lift the Substrate Heater and check for white precipitate at the end of the Substrate Heater Nozzle. If necessary, wipe the nozzle with a moist lint-free tissue with distilled water. Prime the Substrate Pump by pushing the black button on the substrate pump (**Fig. 2.2**). (Catch the waste substrate in a suitable container and discard it.) Push the prime button AT LEAST four times.
24. Lift the thin tubing next to the Substrate Heater pump. Push the black button on the Water Pump AT LEAST four times (**Fig. 2.2**). (Catch the waste water in a suitable container and discard it.)
25. Put the gray plastic connector for the thin tubing back into hole. Place the Substrate Heater pump back into place and tighten the thumbscrew. Press GO.
26. The Immulite will display the following prompt: *IMMULITE is priming the syringes. Please wait.* The large syringe will prime and the following message will appear: *Load reagents, samples and test units. Press GO to read reagents.*
27. The reagents in the reagent carousel, water, chemiluminescent substrate and probe wash were placed on board in earlier steps so it will not be necessary to load the reagents at this point. Only samples and test units must be loaded on the load platform (**Fig. 2.2**).
28. To print a copy of the worklist, click the "Worklist" box in the bottom left corner of the screen. To print, click the "Print Worklist" box at the bottom. To exit this screen, click "Close."

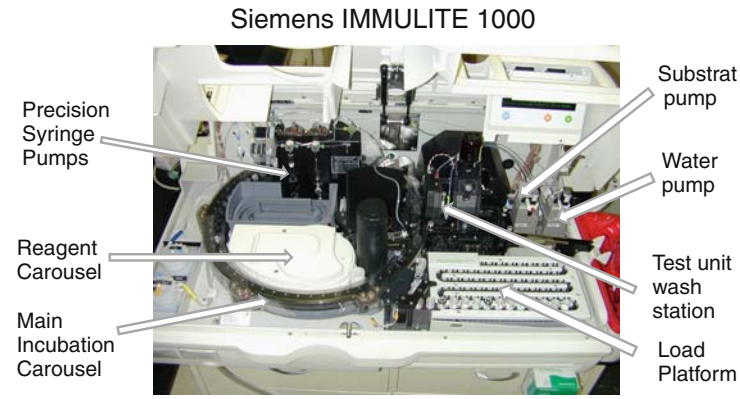

Fig. 2.2. Photograph illustrating the key components of the Siemens IMMULITE 1000 used for chemiluminescent detection of estradiol.

4. Notes

1. Needles should be placed in a proper disposal unit IMMEDIATELY after their use.
2. Estradiol kits are available in different sizes as follows: 100 tubes (catalog number TKE21), 200 tubes (TKE22), 500 tubes (TKE 25), and 1000 tubes (TKE2X).
3. When starting a new wedge, remove the foil seal and any gummy residue. Then check the surface of the liquid for bubbles. Break any bubbles with a disposable pipette tip.
4. The most common location for collecting blood is the median cubital vein which runs down the inner part of the forearm. This is an optimum collection site because the vein is close to the skin surface and there are not many nerves surrounding it.
5. If using a syringe and needle system manually pull back on the syringe plunger to fill the syringe with blood.
6. Aliquot, if necessary, to avoid repeated thawing and freezing of serum.
7. Before assay, allow the samples to come to room temperature and mix by gently swirling or inversion.
8. Because nonspecific binding in the Coat-A-Count procedure is characteristically low, the NSB tubes may be safely omitted without compromising accuracy or quality control.
9. Pipet directly into the bottom of the tubes.
10. Use a disposable tip micropipette and change the tip between samples to avoid carryover contamination.
11. Patient samples expected to contain concentrations of estradiol greater than the highest calibrator (3600 pg/ml) should be diluted in the zero calibrator before assay.
12. To greatly enhance precision it is important to remove all visible moisture from each tube.
13. Analysis may also be performed by implementation of the 4 parameter logistic.
14. Each new kit must be adjusted with the adjustors supplied in the kit before being used to process patient samples in order to ensure the applicability or the lot-specific stored master curve. Thereafter, while the same lot remains in use, the adjustment procedure for the IMMULITE 1000 estradiol assay should be repeated every 2 weeks. Criteria for calibration curve acceptance (slope and intercept) after adjustment have been established are lot specific. Each curve is electronically evaluated by the IMMULITE 1000 microprocessor.

Unacceptable adjustments are flagged. After adjustment, all controls must be within 2 SD range of the monthly calculated mean for acceptability of calibration curve adjustments. Siemens CON6 Multivalent Control Module is used as quality control material. Two of the three controls must be within the 2 SD range of the monthly calculated mean for acceptability of patient results. The upper limit of linearity for the estradiol assay is 2000 pg/dL. The linearity of the assay varies from 91 to 113% (see package insert for dilutions).

15. Distilled water of consistent quality is required. Water should meet NCCLS Type 1 reagent water standards at the time of preparation.
16. An alarm will sound when the bottle of chemiluminescent substrate is low. There will be enough chemiluminescent substrate in the Immulite to run 20–25 test units once the alarm sounds. The Immulite WILL run with the chemiluminescent substrate bottle removed.
17. While the minimum sample volume required for estradiol assay by the Immulite 1000 is 125 µl, we recommended using at least 150 µl. If the Immulite 1000 system senses insufficient volume, an error message appears and the Test Unit is shown as a white circle on the Home screen.

Acknowledgements

This work was supported by NIH grant RP20 RR15592 and HDO57446 (to TEC).

References

1. Yalow RS, Berson SA.1960 Immunoassay of endogenous plasma insulin in man. J Clin Invest 39: 1157–75.
2. Immulite Operators Manual 2003 Document Number 600467 revision C, version 5.xx November 2003. Copyright 2002–2003.
3. Dudley RA, et al.1985 Guidelines for immunoassay data reduction. Clin Chem 31:1264–71.
4. Babson AL, Olson DR, Palmieri T, Ross AF, Becker DM, Mulqueen PJ. 1991. The IMMULITE assay tube; a new approach to heterogeneous ligand. Clin Chem 37: 1521–1522.

Chapter 3

Identification of Natural Human Glucocorticoid Receptor (hGR) Mutations or Polymorphisms and Their Functional Consequences at the Hormone–Receptor Interaction Level

Evangelia Charmandari, George P. Chrousos, and Tomoshige Kino

Abstract

Glucocorticoids regulate a broad spectrum of physiologic functions essential for life and play an important role in the maintenance of basal and stress-related homeostasis. At the cellular level, the actions of glucocorticoids are mediated by the human glucocorticoid receptor α (hGRα), a ligand-dependent transcription factor ubiquitously expressed in almost all tissues and cells. The molecular mechanisms of hGRα action involve (a) binding to glucocorticoids, (b) cytoplasmic to nuclear translocation, (c) binding/association to DNA/chromatin, and (d) transcriptional activation or repression by interacting with cofactors and other transcription factors. Mutations or polymorphisms in the hGR gene may impair these molecular mechanisms of hGRα action, thereby altering tissue sensitivity to glucocorticoids. The latter may take the form of glucocorticoid resistance or glucocorticoid hypersensitivity and may be associated with significant morbidity. The identification of natural pathologic mutations in patients' hGR gene and the subsequent examination of the functional defects of the natural mutant hGRα receptors would enhance our understanding of the molecular mechanisms of hGRα action and highlight the importance of integrated cellular and molecular signaling mechanisms for maintaining homeostasis and preserving normal physiology.

Key words: Cytoplasmic to nuclear translocation, dexamethasone binding assay, gene sequencing, fluorescent recovery after photobleaching, glucocorticoid receptor, glucocorticoid resistance, glucocorticoid hypersensitivity, green fluorescent protein, glutathione-S transferase pull-down assay, reporter assay, thymidine incorporation assay, transfection.

1. Introduction

Glucocorticoids are steroid hormones synthesized and secreted by the adrenal cortices under the influence of the hypothalamic-pituitary-adrenal (HPA) axis. Glucocorticoids regulate a

O.-K. Park-Sarge, T.E. Curry, Jr. (eds.), *Molecular Endocrinology,* Methods in Molecular Biology 590,
DOI 10.1007/978-1-60327-378-7_3,

broad spectrum of physiologic functions essential for life and play an important role in the maintenance of basal and stress-related homeostasis (1–3). At the cellular level, the actions of glucocorticoids are mediated by the human glucocorticoid receptor α (hGRα), a ligand-dependent transcription factor ubiquitously expressed in almost all tissues and cells (4, 5). The gene encoding hGRα (hGR gene) is located in the long arm of chromosome 5 (q31.3), and consists of 9 exons, spanning over 150 kb (**Fig. 3.1A**). Expressed hGRα is a panel of 8 amino terminal translational isoforms of varying lengths, each of which consists of three subdomains, the N-terminal (NTD), the DNA-binding (DBD) and the ligand-binding (LBD) domains. In our expression and functional studies referred to here, we have employed as representative the longest GRα isoform consisting of 777 amino acids. The GR gene also produces an equal number of hGRβ isoforms by the use of an alternative 3' exon 9β, which cannot bind glucocorticoids and function as dominant negative isoforms for hGRα (1).

In the absence of ligand, hGRα resides mostly in the cytoplasm of cells as part of a hetero-oligomeric complex, which contains chaperone heat shock proteins (HSPs) 90, 70, 23, and FKBP51, as well as other proteins (6) (**Fig. 3.1B**). Upon ligand-induced activation, the receptor dissociates from this multiprotein complex and translocates into the nucleus through the nuclear pore by an energy-dependent mechanism that includes importin α and β. Inside the nucleus, hGRα binds as a homodimer to glucocorticoid response elements (GREs) in the promoter regions of target genes and regulates their expression positively or negatively (6–9). The ligand-activated hGRα can also modulate gene expression without binding to DNA by interacting with other transcription factors, such as activator protein-1 (AP-1), nuclear factor-κB (NF-κB), p53 and signal transducers and activators of transcription (STATs) (10–13).

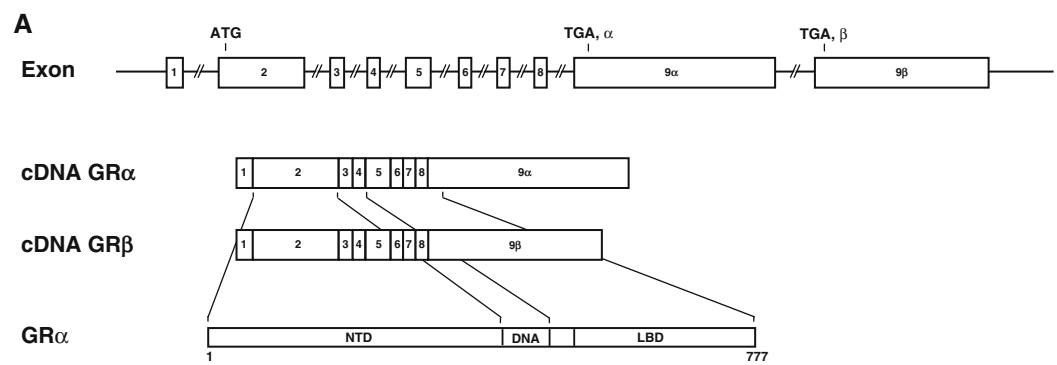

Fig. 3.1. Structures of the hGR gene and the hGRα protein, and hGRα-mediated transduction of the glucocorticoid signal. **(A)** Genomic, complementary cDNA and protein structures of the hGRα. DBD: DNA-binding domain, GR: glucocorticoid receptor; LBD: ligand-binding domain, NTD: N-terminal domain.

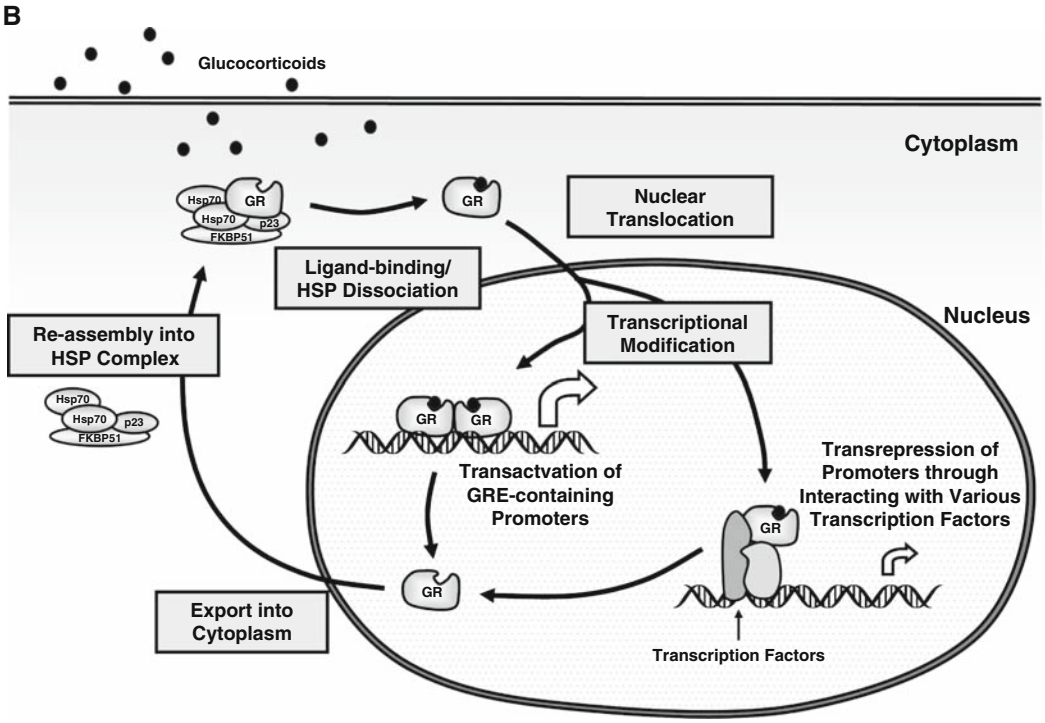

Fig. 3.1. **(B)** Circulation of hGRα between the cytoplasm and the nucleus. Upon binding to ligand, hGRα dissociates from HSPs and translocates into the nucleus, where it binds to GREs in the promoter region of target genes or communicates with other transcription factors to modulate the transcription. After changing the transcriptional rates of glucocorticoid-responsive genes, hGRα is exported to the cytoplasm and is re-assembled into the complex with HSPs.GR: glucocorticoid receptor; HSP: heat shock protein.

To initiate transcription, hGRα uses its transcriptional activation domains, activation function (AF)-1 and AF-2, located in NTD and LBD, respectively to interact with nuclear receptor coactivators and chromatin-remodeling complexes (14–18). The p160 coactivators, including the steroid receptor coactivator 1 and the glucocorticoid receptor-interacting protein 1 (GRIP1), play an important role in the hGRα-mediated transactivation of glucocorticoid-responsive genes. These coactivators interact directly with both the AF-1 of hGRα through their carboxyl-terminal domain and the AF-2 through multiple amphipathic LXXLL signature motifs located in their nuclear receptor-binding (NRB) domain (19). They also have histone acetyltransferase activity through which they acetylate multiple lysine residues located in the N-terminal tail of chromatin-associated histones. This acetylation facilitates access of other transcription factors, cofactors and the transcription initiation complex composing the RNA-polymerase II and its ancillary components to initiate and promote transcription (14–17) (**Fig. 3.1C**).

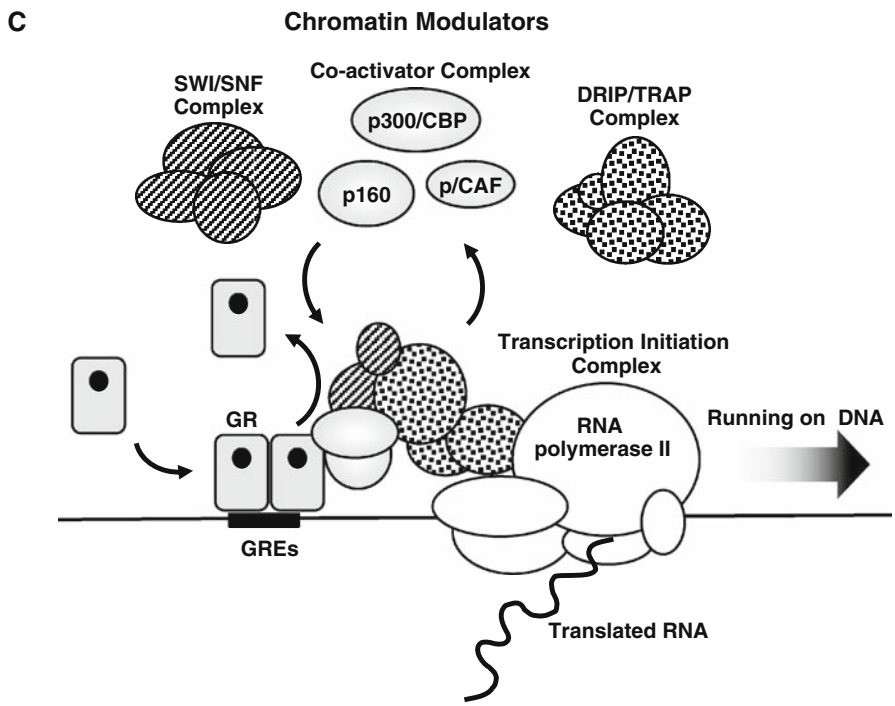

Fig. 3.1. **(C)** Schematic representation of the interaction of hGRα with coactivators on a GRE-driven promoter. DRIP/TRAP: vitamin D receptor-interacting protein/thyroid hormone receptor-associated protein; GR: glucocorticoid receptor; GREs: glucocorticoid response elements; p/CAF: p300/CBP-associating factor; SWI/SNF: switching/sucrose non-fermenting.

Mutations or polymorphisms in the hGR gene impair one or more of the molecular mechanisms of hGRα action and alter tissue sensitivity to glucocorticoids (**Fig. 3.2A, B**). Alterations in tissue sensitivity to glucocorticoids may take the form of glucocorticoid resistance or glucocorticoid hypersensitivity and may be associated with significant morbidity (20–22). In previous studies, we have identified most of the known pathologic mutations in the hGR gene by sequencing the patients' genomic DNA, and have systematically investigated the molecular mechanisms through which various natural hGRα mutant receptors affect glucocorticoid signal transduction (**Fig. 3.2A**). In this chapter, we will describe the methods and techniques for detecting mutations and polymorphisms in the hGR gene and for examining their functional defects. The flow chart that illustrates the functional characterization that we usually perform in all cases of the hGRα mutations/polymorphisms is shown in **Fig. 3.3**. In patients with suspected glucocorticoid resistance/hypersensitivity on clinical and/or biochemical grounds, blood samples are taken for gene analysis and functional examination of their hGRs in thymidine incorporation and whole cell dexamethasone-binding assays. The thymidine incorporation assay examines the sensitivity of patients' lymphocytes

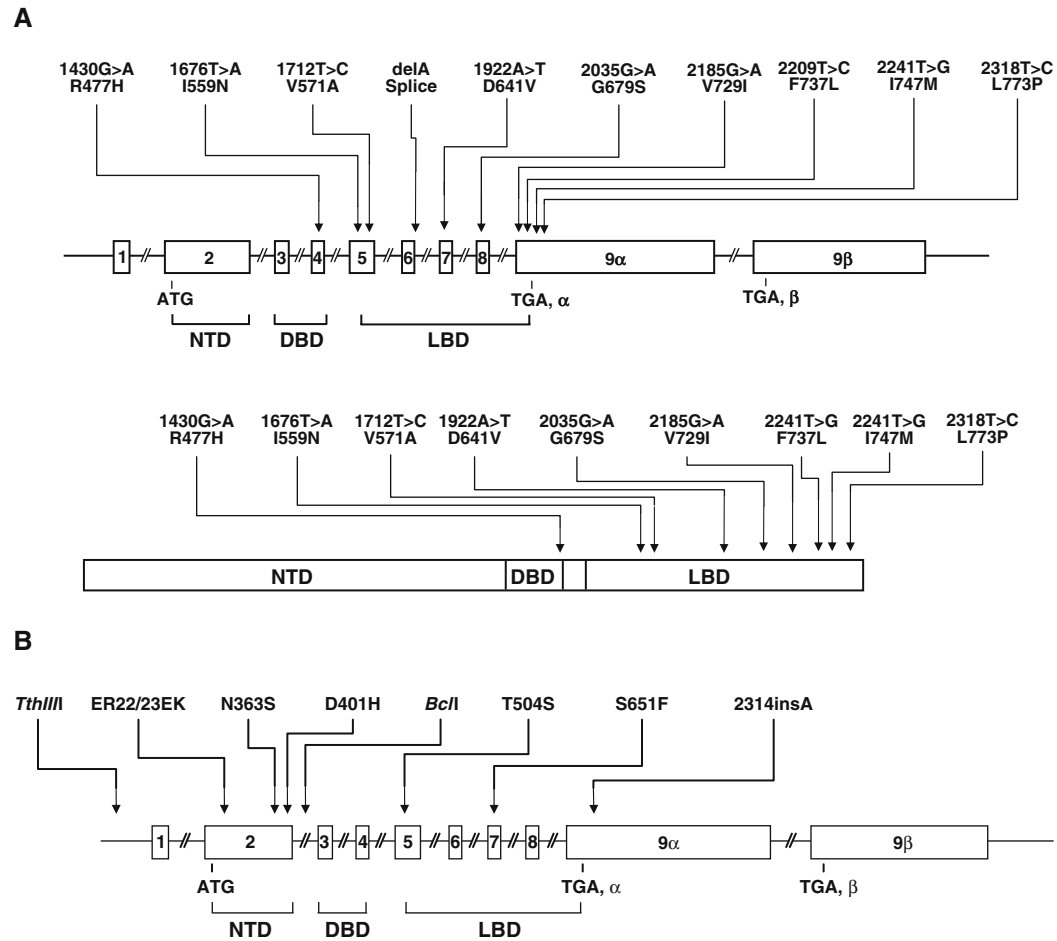

Fig. 3.2. Location of the known mutations (**A**) and polymorphisms (**B**) of the hGR gene. DBD: DNA-binding domain; GR: glucocorticoid receptor; GREs: glucocorticoid response elements; NTD: N-terminal domain; LBD: ligand-binding domain.

to glucocorticoid dexamethasone by evaluating the suppressive effect of this steroid on the incorporation of thymidine into the cell DNA. The latter whole cell dexamethasone-binding assay examines the affinity of the hGRαs to dexamethasone and the number of the hGRα molecules (or binding sites for dexamethasone). Once mutations/polymorphisms are identified in patients' hGR gene, the functions of the mutated hGRα are further examined using several techniques, which employ exogenous expression of mutant hGRαs. These include (a) subcellular localization and nuclear translocation of the mutant hGRαs, (b) evaluation of the ability of the mutant hGRαs to stimulate transcription, and (c) determination of the size and/or expression levels of the mutant hGRα by Western blots. In this chapter, we discuss the methods used for the identification of endogenous hGRα in the circulating mononuclear cells of patients and for the evaluation of the functional defects of mutant hGRαs.

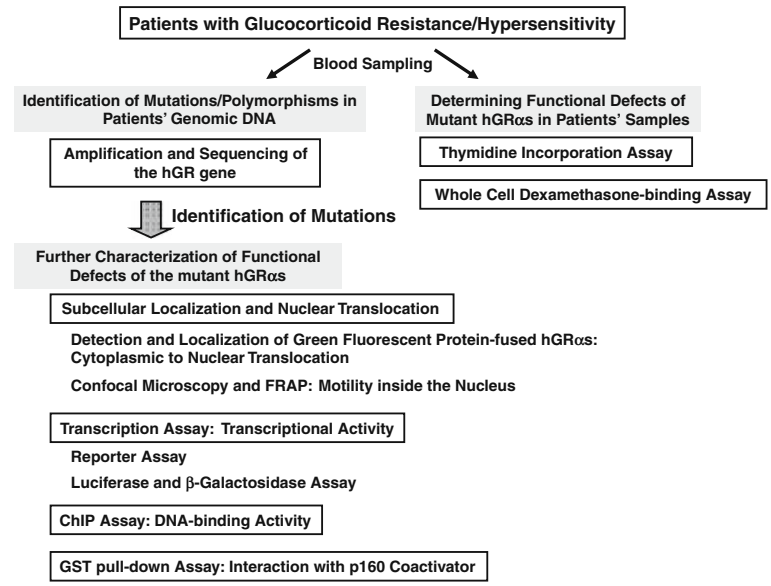

Fig. 3.3. Flow chart for the analyses of the hGR gene mutations/polymorphisms.

2. Materials

2.1. Identification of Endogenous hGRα in the Circulating Mononuclear Cells of the Patients

2.1.1. Purification of Circulating Mononuclear Leukocytes from Patients' Blood by Ficoll-Paque PLUS Gradient Method

1. RPMI1640 medium (Invitrogen) supplemented with or without 10% fetal bovine serum (FBS, HyClone, Ogden, UT) and antibiotics (Invitrogen).
2. Ficoll-Paque PLUS (GE Healthcare, Piscataway, NJ).
3. Culture medium from B95 cells, which contains the infective Epstein-Bar virus (EBV).

2.1.2. Thymidine Incorporation Assays

1. Thymidine, [Methyl-3H], 40–60 Ci/mmol; 1.48–2.22 TBq/mmol (MP Biologicals, Solon, OH).
2. Phytohaemagglutinin (PHA) (Sigma Chemical Co.).
3. β-Counter (Beckman LS6000IC counter, Beckman Coulter Inc., Fullerton, CA).

2.1.3. Whole Cell Dexamethasone-Binding Assays

1. [1,2,4,6,7-^{3}H]-Dexamethasone, 70-110 Ci/mmol, 2.6–4.1 TBq/mmol (GE Healthcare).
2. Non-radioactive dexamethasone (Sigma Chemical Co., St Louis, MO).

3. β-Counter (Beckman LS6000IC counter, Beckman Coulter Inc.).

2.1.4. Amplification and Sequencing of the hGR Gene

1. AmpliTaq DNA Polymerase (Invitrogen, Carlsbad, CA).
2. BigDye Terminator v3.1 Cycle Sequencing Kit (Applied Biosystems, Foster City, CA).
3. Wizard Genomic DNA Purification Kit (Promega Corp. Madison, WI).
4. GeneAmp PCR System 9700 (Applied Biosystems).
5. ABI Prism 310 Genetic Analyzer (Applied Biosystems).

2.2. Evaluation of the Functional Defects of the Mutant hGRα: Subcellular Localization and Nuclear Translocation of the Mutant hGRα

2.2.1. Cell Culture and Transient Transfection Assays

1. CV-1 and COS-7 embryonic African green monkey kidney cells and HeLa human cervical uterine carcinoma cells, purchased from American Type Culture Collection (Manassas, VA).
2. Phenol red-containing or -free Dulbecco's Modified Eagle medium (DMEM) (Invitrogen) supplemented with 10% FBS and antibiotics.
3. McCoy's 5A medium (Invitrogen) supplemented with 10% FBS, neomycin (G418) and antibiotics.
4. Trypsin EDTA 0.25% (Invitrogen).
5. Lipofectin (Invitrogen).
6. FuGENE 6 (Roche Applied Science, Indianapolis, IN).
7. Opti-MEM (Invitrogen)

2.2.2. Subcellular Localization and Nuclear Translocation of the Mutant Green Fluorescence Protein (GFP)-hGRα

1. The pF25GFP vector (a gift from Dr. G.N. Pavlakis, National Institutes of Health, Frederick, MD), pEGFP-C1 vector (Clontech).
2. The green fluorescent protein (GFP)-fused plasmid expressing hGRα, which is constructed by subcloning the hGRα cDNA into the pF25GFP vector/pEGFP-C1, as previously described (23). pF25GFP-hGRα and pEGFP-C1-hGRα contain the hGRα cDNA 5' terminally fused respectively to the GFP or the EGFP cDNA in an in-frame fashion, and the Cytomegalovirus promoter drives the expression of the fusion genes. pEGFP-C1 has the neomycin-resistant (for mammalian cells) and the kanamycin resistant (for bacteria) cassettes, while pF-25GFP contains the ampicillin resistant cassette (for bacteria) only.
3. The GFP-fused plasmids expressing mutant hGRα are constructed by introducing the corresponding mutations into the pF25GFP-hGRα using PCR-assisted site-directed mutagenesis using the QuickChange® II XL Site-Directed Mutagenesis Kit (Stratagene, La Jolla CA).
4. 10% charcoal/dextran-treated FBS (Hyclone).

5. Inverted fluorescence microscope (Leica DM IRB, Wetzlar, Germany) with fluorescent source, or a confocal microscope (Zeiss LSM510 Inverted Meta/Zeiss Axiovert 200 M microscope, Carl Zeiss, Thornwood, NY).
6. Digital charge-coupled device (CCD) camera (Hamamatsu Photonics K.K., Hamamatsu, Japan).
7. Openlab software (Improvision, Boston, MA).

2.2.3. Confocal Microscopy and Fluorescent Recovery After Photobleaching (FRAP) to Evaluate Motility of the Mutant hGRαs Inside the Nucleus in Living Cells

1. Plasmids expressing GFP-fused wild type and mutant hGRα receptors.
2. African monkey kidney COS-7 cells.
3. Delta-T culture dishes (Bioptechs, Butler, PA).
4. Zeiss LSM510 upright 2-photon meta/Zeiss Axioskop 2 microscope (Carl Zeiss).
5. Water immersion Zeiss Achroplan × 63, 0.9 NA, IR (working distance 2.2 mm) objective lens (Carl Zeiss).

2.3. Evaluation of the Functional Defects of the Mutant hGRαs: Transcription Assays Using GRE-Driven Reporter Genes

1. The pRShGRα plasmid, which expresses high levels of hGRα under the control of the Rous sarcoma virus (RSV) promoter in mammalian cells. This plasmid was originally constructed by Dr. R.M. Evans (Salk Institute, La Jolla, CA), and is now commercially available in the American Type Culture Collection (Manassas, VA).
2. The plasmids expressing various natural hGRα mutant receptors are constructed by introducing the corresponding mutations into the pRShGRα plasmid using PCR-assisted site-directed mutagenesis (Stratagene, La Jolla, CA). The plasmids expressing known hGRα mutant receptors are described in the references (24–32).
3. The pMMTV-luc plasmid, which expresses luciferase under the control of the glucocorticoid-responsive mouse mammary tumor virus (MMTV) promoter (a gift from Dr. G.L. Hager, National Institutes of Health, Bethesda, MD).
4. The pSV40-β-gal plasmid, which encodes the β-galactosidase gene under the control of the simian virus (SV) 40 promoter (Promega Corp.).
5. Opti-MEM (Invitrogen).
6. Dexamethasone (Sigma Chemical Co.).

2.3.1. Transfection

2.3.2. Luciferase and β-Galactosidase Assays

1. 5x Reporter lysis buffer (Promega Corp.). 1x Buffer solution used for lysing cells can be made by diluting the original 5x solution with 4 volumes of water.

2. Reporter assay buffer: 25 mM Gly-Gly (Sigma Chemical Co.), pH 8.0, 10 mM ATP, 25 mM $MgSO_4$, 1% Triton-X 100.
3. Monolight 3010 Luminometer (BD PharMingen, San Diego, CA).
4. D-Luciferin sodium salt solution (BD PharMingen).
5. β-Galactosidase enzyme assay system (Galacto-Light Plus, Tropix, Bedford, MA).

2.4. Evaluation of the Functional Defects of the Mutant hGRαs for Their Ability to Interact with GRE: Chromatin Immunoprecipitation (ChIP) Assays

1. HCT-116 human colon carcinoma cells (purchased from American Type Culture Collection) stably transfected with pMAM-neo-luc (Clontech, Palo Alto, CA), which contains the full-length mouse mammary tumor virus promoter and a neomycin (G418)-resistant cassette.
2. 1% formaldehyde.
3. Protease inhibitors (Complete™, Roche Applied Science).
4. ChIP lysis buffer: 10 mM Tris-HCl, pH 7.5, 3 mM $CaCl_2$, 2 mM $MgCl_2$.
5. Nonidet P-40 (NP-40) lysis buffer: 10 mM Tris-HCl, pH 7.5, 10 mM NaCl, 3 mM $MgCl_2$, 0.5% NP-40.
6. Nuclear buffer: 50 mM Tris-HCl, pH 8.0, 25% glycerol, 5 mM $Mg(CH_3COO)_2$, 0.1 mM EDTA.
7. ChIP dilution buffer: 16.7 mM Tris-HCl, pH 8.1, 167 mM NaCl, 0.01% SDS, 1.1% Triton X-100, 1.2 mM EDTA, protease inhibitors (1 tablet/50 ml of lysate) (Complete™, Roche Applied Science).
8. Misonix sonicator 3000 (Misonix Inc., Farmingdale, NY).
9. Anti-hGRα antibody (Affinity Bioreagents, Golden, CO).
10. Low salt wash buffer: 20 mM Tris-HCl, pH 8.1, 150 mM NaCl, 0.1% SDS, 1% Triton X-100, 2 mM EDTA.
11. High salt wash buffer: 20 mM Tris-HCl, pH 8.1, 500 mM NaCl, 0.1% SDS, 1% Triton 10 X-100, 2 mM EDTA.
12. LiCl wash buffer: 10 mM Tris-HCl, pH 8.1, 0.25 M LiCl, 1% NP40, 1% deoxycholate, 1 mM EDTA.
13. TE buffer: 10 mM Tris-HCl, pH 8.0, 1 mM EDTA.
14. ChIP elution buffer: 100 mM $NaHCO_3$, 1% SDS.
15. Primer set: forward primer: 5'-AACCTTGCGGTTCCCAG-3'; reverse primer: 5'-GCATTTACATAAGATTTGG-3'. This primer pair amplifies the promoter region −219 to −47 of the MMTV long terminal repeat (fragment size: 173), which contains two functional GREs.
16. Agarose (Invitrogen) for DNA gels.
17. Ethidium bromide (Sigma Chemical Co.).

2.5. Evaluation of the Functional Defects of the Mutant hGRαs for Their Ability to Interact with the p160 Coactivator: Glutathione-S Transferase (GST) Pull-Down Assays

1. The pGEX-4T3 vector (GE Healthcare).
2. The plasmids pGEX-4T3-GRIP1(1-1462), pGEX-4T3-GRIP1(596-774) and pGEX-4T3-GRIP1(740-1217), which express GST-fused full-length-GRIP1, nuclear receptor-binding fragment of GRIP1 and carboxyl-terminal fragment of GRIP1, respectively, are constructed by subcloning the corresponding GRIP1 fragments of cDNA into the pGEX-4T3 vector.
3. E. coli, BL21 strain (Stratagene).
4. Isopropyl β-D-1-thiogalactopyranoside (IPTG) (GE Healthcare).
5. Glutathione Sepharose 4B Fast Flow beads (GE Healthcare).
6. GST binding buffer: 50 mM Tris-HCl, pH 8.0, 50 mM NaCl, 0.1% NP-40, 1 mM EDTA, 10% glycerol, 1 mg/ml of bovine serum albumin fraction V (Sigma Chemical Co.).
7. Coupled in vitro transcription/translation reactions (TNT Quick Coupled Transcription/Translation System, Promega Corp.).
8. [^{35}S] L-methionine, >400 Ci/mmol; >14.8 TBq/mmol Solution, in vitro translation grade (MP Biologicals).
9. The pBK-CMV vector (Stratagene).
10. The pBK/CMV-wild type and mutant hGRα-expressing plasmids are constructed by subcloning the corresponding cDNA into the pBK-CMV vector (22).
11. Tris-Glycine SDS Sample Buffer (2x) (Invitrogen).
12. 8% SDS-PAGE gel.
13. Enlightning buffer (NEN Life Science Products, Inc., Boston, MA).
14. Luria-Bertani (LB) broth.
15. X-ray films.

2.6. Determining the Size and/or Expression Levels of the Mutant hGRαs: Western Blots

1. Western blot lysis buffer: 100 mM Tris-HCl, pH 8.5, 250 mM NaCl, 1% Nonidet P-40, protease inhibitors (Complete™ 1 tablet/50 ml of lysate) (Complete™, Roche Applied Science).
2. Tris-Glycine SDS Sample Buffer (2x) (Invitrogen).
3. Molecular weight prestained markers (SeeBlue Plus 2 Prestained Protein Standard, Invitrogen).
4. 8% Tris-Glycine Gel (Invitrogen).
5. Hybond C nitrocellulose membranes (GE Healthcare).
6. TBS-T buffer: 50 mM of 1 M Tris-HCl, pH 8.5, 10 mM 5 M NaCl, 0.5% Tween 20.
7. Blocking solution: 5% dry milk powder/TBS-T buffer.

8. Purified specific rabbit polyclonal anti-hGRα antibody (Affinity BioReagents).
9. Horseradish peroxidase-conjugated goat anti-rabbit IgG (Affinity BioReagents).
10. ECL Plus Western Blotting Detection System (GE Healthcare).
11. High performance chemiluminescence film (Hyperfilm ECL, GE Healthcare).

3. Methods

3.1. Identification of Endogenous hGRα in the Circulating Mononuclear Cells of Patients

3.1.1. Purification of Circulating Mononuclear Leukocytes from Patients' Blood by the Ficoll-Paque Gradient Method

1. The patients' blood is drawn using heparinized tubes and circulating mononuclear leukocytes are purified with the Ficoll-Paque PLUS following the company's protocol. Briefly, blood samples diluted with equal volume of balanced salt solution are overlaid on the Ficoll-Paque PLUS in appropriate tubes, and are centrifuged at $\times 400\ g$ for 20–40 min at 18–20°C. The leukocyte layer is harvested after taking out the upper layer, centrifuged at $\times 60$–$100\ g$ for 10 min at 18–20°C, and leukocytes are resuspended in RPMI medium. They are washed with RPMI medium once (*see* **Note 1**).
2. Mononuclear leukocytes can be transformed with EBV, as the transformed cells grow continuously and are used as source of patients' genomic DNA. Briefly, mononuclear leukocytes are cultured in medium consisting of an equal volume of fresh RPMI medium containing 10% FBS and antibiotics, and the culture medium obtained from B95 cells subsequently passed through the filter with 0.45 μM pore size. The medium can be replaced with regular culture RPMI1640 medium with the supplements once the cells start replicating (usually takes several days).

3.1.2. Determining Functionality of Endogenous GR by Thymidine Incorporation Assay

1. Mononuclear leukocytes isolated from patients and control subjects are seeded in 24-well plates (10^5cells/well) with 0.5 ml of RPMI1640 supplemented with 10% FBS and antibiotics, and are incubated at 37°C for 2 h.
2. They are then stimulated with PHA (5 μg/well) and exposed to seven different concentrations (0 nM, 2.5 nM, 10 nM, 25 nM, 100 nM, 250 nM, and 1000 nM) of dexamethasone.

3. Following incubation at 37°C for 72 h, [^{3}H]-thymidine is added to each well (0.1 μCi/well) and incubation is continued for a further 4 h.
4. Subsequently, cells are transferred to eppendorf tubes, centrifuged for 1–2 min at 3000 rpm, and 0.5 ml of 10% trichloracetic acid is added to each tube after removing the supernatant (*see* **Note 2** and **3**).
5. Cell lysates are transferred to scintillation vials and the radioactivity is measured using a β-counter. Representative results of the thymidine incorporation assay are shown in **Fig. 3.4**.

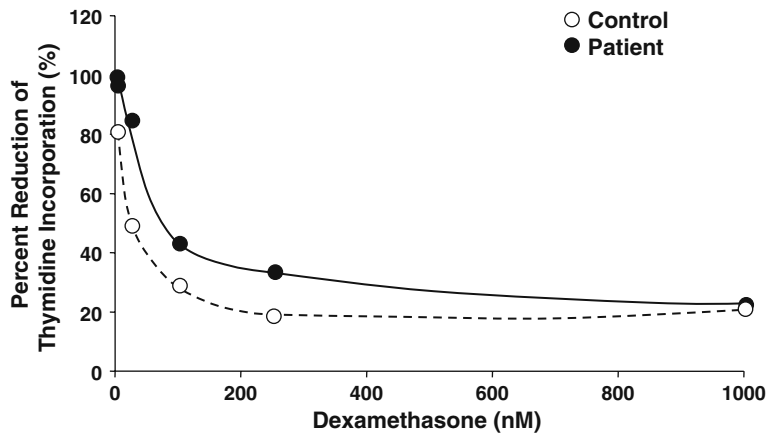

Fig. 3.4. Thymidine incorporation assays performed on circulating mononuclear leukocytes harboring the heterozygotic hGR L773P mutation. There was increased resistance to dexamethasone-induced suppression of phytohemagglutinin-stimulated thymidine incorporation in the patient compared to the control subject. [FROM (27)]

3.1.3. Evaluation of Affinity of the Endogenous GR to Glucocorticoids by Whole Cell Dexamethasone-Binding Assays

1. Mononuclear leukocytes isolated from patients and control subjects were seeded in 96-well plates (1–3 × 10^6cells/well).
2. Cells are incubated in plain RPMI with six different concentrations (1.56 nM, 3.125 nM, 6.25 nM, 12.5 nM, 25 nM, and 50 nM) of [1,2,4,6,7-^{3}H]-Dexamethasone at 37°C in the presence or absence of a 500-fold molar excess of non-radioactive dexamethasone for 1 h (See **Note 4**).
3. After incubation, cells are transferred to tubes and are washed with PBS three times to remove free steroid.
4. Cells are transferred to scintillation vials, and the radioactivity is measured using a β-counter.
5. Specific binding is calculated by subtracting nonspecific from total binding, and these data are analyzed using the Scatchard method. Binding capacity is expressed as

fentomoles per 10^6cells, and the apparent dissociation constant (Kd) is expressed in nanomolar concentrations (nM) (*see* **Notes 3 and 5**). Representative results of the whole cell dexamethasone-binding assay are shown in **Fig. 3.5**.

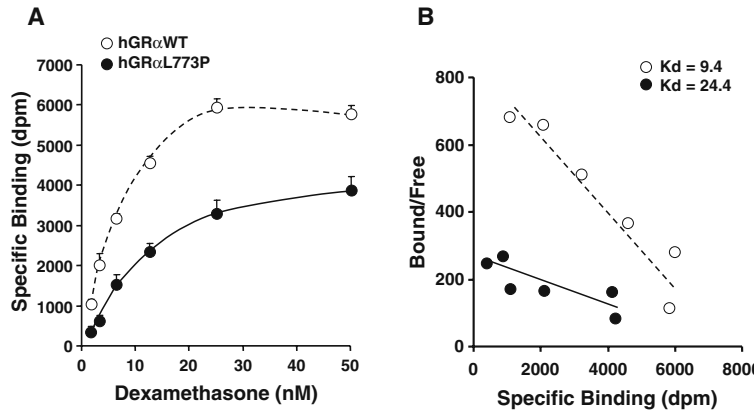

Fig. 3.5. Whole cell dexamethasone-binding assays for hGRαL773P. The mutant receptor hGRαL773P demonstrated decreased affinity for the ligand compared to the wild type receptor. Binding curves of radioactive (hot) dexamethasone to the wild type hGRα and hGRαL773P are shown in panel **A**, while results of their scatchard analysis are demonstrated in panel **B**. Binding curves indicate that the apparent dissociation constant (Kd) of hGRαL773P was higher than that of the wild type receptor. COS7 cells, transfected with the wild type hGRα- or hGRαL773P-expressing plasmid, were used in the assays. [FROM (27)]

3.1.4. Amplification and Sequencing of Patients' hGR Gene

1. Genomic DNA is extracted from circulating mononuclear leukocytes using the Wizard Genomic DNA Purification Kit, according to the instructions of the manufacturer (Promega Corp.).
2. Eight exonic sequences of the GR gene, which contain the coding region of the hGRα, are amplified by the polymerase chain reaction (PCR) using the AmpliTaq DNA polymerase in the GeneAmp PCR System 9700. The primers used for PCR amplification of genomic DNA are designed using the exon/intron junction sequences (**Table 3.1**). Initiation is performed at 94°C for 7 min, followed by 30 cycles of denaturation at 94°C for 45 s, annealing at 55°C (exons 3-7, 9) or 60°C (exons 2, 8) for 30 s and extension at 72°C for 1 min, and a final period of extension at 72°C for 7 min (*see* **Note 6**).
3. Amplified DNAs are further sequenced using the BigDye Terminator v3.1 Cycle Sequencing Kit and one of the primers is used for the amplification or appropriate internal primers, according to the instructions of the manufacturer (Applied Biosystems). We use an automatic sequencer (ABI Prism 310 Genetic Analyzer) to read sequences (*see* **Note 6**). A representative sequence result of the mutated hGR gene is shown in **Fig. 3.6**.

Table 3.1
Primer pairs for amplification of exonic sequences of the hGR gene

Exons amplified		Primer sequence
Exon 2	Forward	5'-GATTCGGAGTTAACTAAAAG-3'
	Reverse	5'-GTCCATTCTTAAGAAACAG-3'
Exon 3	Forward	5'-AGTTCACTGTGAGCATTCTG-3'
	Reverse	5'-CGTGAGAAATAAAACCAAGT-3'
Exon 4	Forward	5'-GACAGAAGGCTGTCCTTATA-3'
	Reverse	5'-CATTATGCGTATCAAGCATA-3'
Exon 5	Forward	5'-GAATAAACTGTGTAGCGCAG-3'
	Reverse	5'-TAGTCCCCAGAACTAAGAGA-3'
Exon 6	Forward	5'-GATCTTCTGAAGAGTGTTGC-3'
	Reverse	5'-GGGAAAATGACACACATACA-3'
Exon 7	Forward	5'-GAAAGTTCTCCAAAATTCTG-3'
	Reverse	5'-TTGGTGTCACTTACTGTGCC-3'
Exon 8	Forward	5'-GACACAGTGAGACCCTATCT-3'
	Reverse	5'-CACCAACATCCACAAACTGG-3'
Exon 9	Forward	5'-GGAATTCCAGTGAGATTGGT-3'
	Reverse	5'-TATAAACCACATGTAGTGCG-3'

Exon 1 does not contain coding sequence of the hGRα.
[FROM (27)]

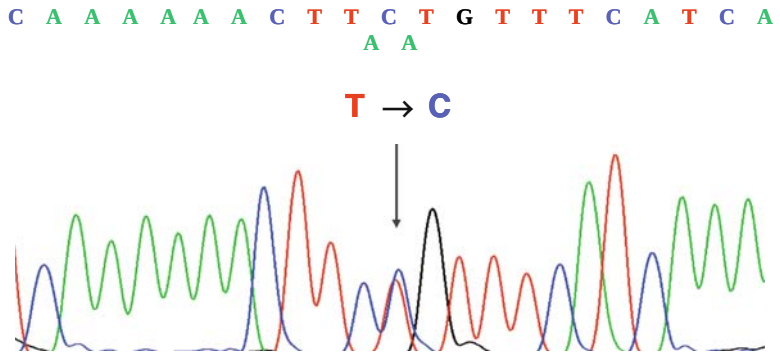

Fig. 3.6. sequence analyses identifying the hGRαL773P mutation in the hGR gene. sequencing of the coding region of the hGR gene revealed a single heterozygous thymine to cytosine (T→C) substitution at nucleotide position 2318 (EXON 9), resulting in leucine to proline substitution (C T G→C C G) at amino acid 773 in the LBD of the receptor. [FROM (27)]

3.2. Evaluation of Functional Defects of Mutant hGRαs: Subcellular Localization and Nuclear Translocation of the Mutant hGRα

3.2.1. Cell Culture and Transient Transfection Assay

1. CV-1 and COS-7 embryonic African green monkey kidney cells, and HeLa human cervical uterine carcinoma cells are grown in DMEM supplemented with 10% FBS and antibiotics. Cells are incubated in a humidified atmosphere of 5% CO_2 at 37°C and passaged every 3 to 4 days (*see* **Note 1**).
2. Twenty-four hours before transfection, subconfluent cells are removed from their flasks by trypsinization, resuspended in supplemented medium, and plated in six-well plates (CV-1, COS-7), 75 cm^2 flasks (CV-1, COS-7), 35-mm-diameter dishes (HeLa), or 150-mm-diameter dishes (HCT-116) at a concentration of 1.5×10^5 cells/well, 1×10^6 cells/flask, 1.5×10^5 cells/35-mm dish, and 2.5×10^6 cells/150-mm dish, respectively.
3. CV-1, COS-7, and HCT-116 cells are transfected using the lipofectin method, as previously described (33).
4. HeLa cells are transfected using FuGENE 6 reagent according to the instructions of the manufacturer (Roche Applied Science). The FuGENE 6 to transfected DNA ratio is 2:1.

3.2.2. Subcellular Localization and Nuclear Translocation of the Mutant Green Fluorescence Protein (GFP)-hGRα

1. HeLa cells are plated on coated 35-mm-diameter dishes (1.5×10^5 cells/well) in supplemented DMEM. Twenty-fours hours later, cells are transfected with GFP-fused wild type or mutant hGRα-expressing plasmids (2 μg/dish) using FuGENE 6. In further experiments, and in order to determine the effect of the mutant receptors upon the nuclear translocation of the wild type receptor, HeLa cells are transfected with equal amounts of GFP-fused wild type and mutant hGRα (1 μg/dish).
2. Forty-eight hours after transfection, the medium is replaced by phenol red-free DMEM supplemented with 10% charcoal/dextran-treated FBS and antibiotics.
3. Sixteen hours later, cells are exposed to dexamethasone (10^{-6} M) and fluorescence is detected sequentially by an inverted fluorescence microscope or a confocal microscope, as previously described (*see* **Note 7**) (34). Twelve-bit black-and-white images are captured using a digital CCD camera. Image analysis and presentation are performed using the Openlab software. Representative images of the nuclear translocation of GFP-hGRα and EGFP-hGRα mutants are shown in **Fig. 3.7**.

3.2.3. Confocal Microscopy and Fluorescent Recovery After Photobleaching (FRAP) to Evaluate Motility of the Mutant hGRαs Inside the Nucleus in Living Cells

1. COS-7 cells, cultured in Delta-T culture dishes and transfected with pF25-hGRαs are treated for 4 h with 10^{-6}M dexamethasone 24 h after transfection.
2. Before photobleaching, the media are replaced with Hanks balanced salt solution (HBSS) containing 10% FBS, and the cells are examined under a microscope.

3. Emitted signals are recorded at 37 ± 0.5°C with the Zeiss LSM510 upright 2-photon meta/Zeiss Axioskop 2 microscope (26, 35). A water immersion Zeiss Achroplan × 63, 0.9 NA, IR (working distance 2.2 mm) objective lens is used for image acquisition. Confocal images are built point by point by collecting the intensities from the photo-multiplier tube using Zeiss LSM 5 software version 3.2 (Carl Zeiss) (*see* **Note** 7).
4. For FRAP, GFP is excited with an argon laser at 488 nm, and emission is collected using the Meta detector with custom emission range from 495 to 590 nm. Images are taken every 63 ms at zoom factor 3 and resolution 128 × 128 pixels (pixel size, 0.38 × 0.38 μm; pixel time, 3.84 s). After the first 2 images, a selected rectangular region of fixed size (11.02 × 2.28 μm^2) in the nucleus is bleached at a set laser power of 15 mW for 50 iterations. Fluorescence in the bleached region is measured as a function of time using the

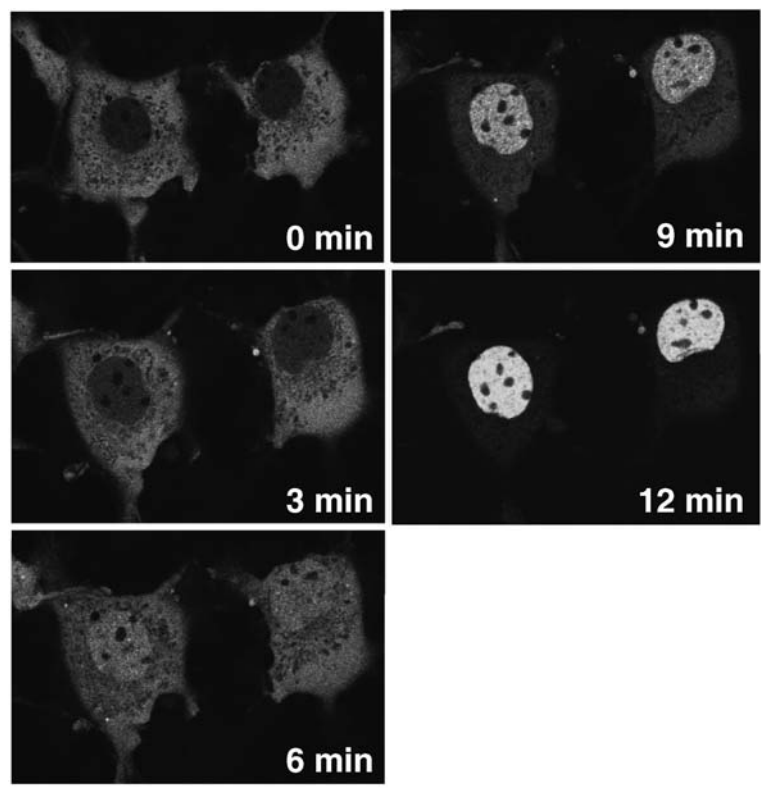

Fig. 3.7. Subcellular localization of the mutated hGRα and their translocation into the nucleus. (**A**) Nuclear translocation of GFP-fused wild type hGRα. HeLa cells were transfected with pF25-hGRα and images were recorded under a confocal microscope every 3 min after addition of 10^{-6}M of dexamethasone.

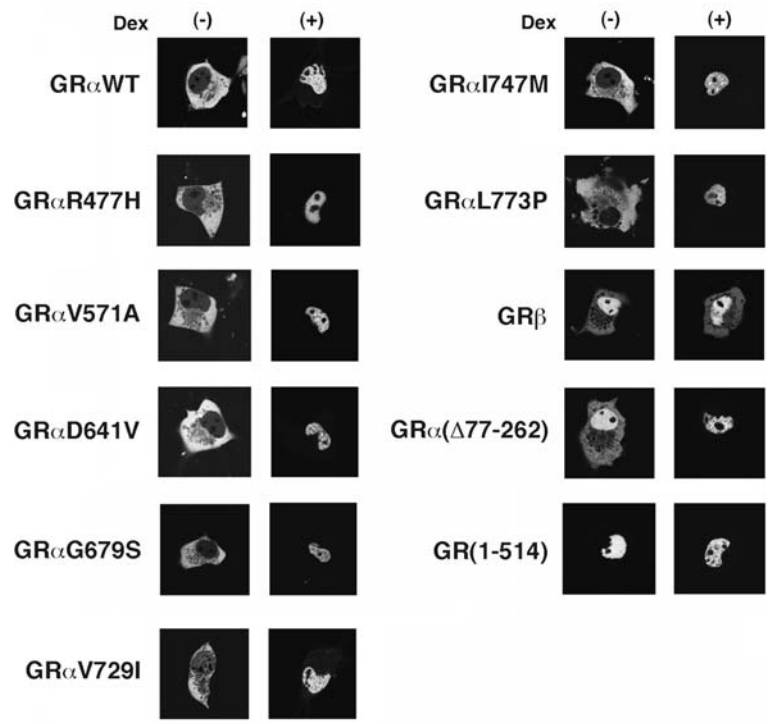

Fig. 3.7. (**B**) Subcellular localization of the mutatant hGRαs in the absence and presence of dexamethasone. HeLa cells were transfected with pF25-hGRα wild type and mutants and images were recorded under a confocal microscope in the absence or presence of 10^{-6} M of dexamethasone.

LSM software. To account for bleaching to laser scanning, the intensity of an identical area in a distant nuclear area is also measured with time (26).

5. To correct for differences in the expression level between individual cells, fluorescence data for the bleached and control areas in the nucleus are normalized as fractional recovery: $R = (F-F_0)/(F_{\text{infinite}}-F_0)$. In addition, results obtained from the bleached area are normalized to those obtained from the control area to account for attenuation of fluorescence due to laser scanning, as previously described (36).
6. Using the obtained FRAP curve, the $t_{1/2}$ of maximal recovery is determined, which is defined as the time point after bleaching at which the normalized fluorescence has increased to half the amount of the maximal recovery. A representative FRAP curve is shown with analysis (**Fig. 3.8A**) and photobleaching images (**Fig. 3.8B**) (26). Recovery $t_{1/2}$ values obtained from a population of cells for each procedure are statistically analyzed. Representative results of $t_{1/2}$ values of the mutant hGRαs are shown in **Table 3.2**.

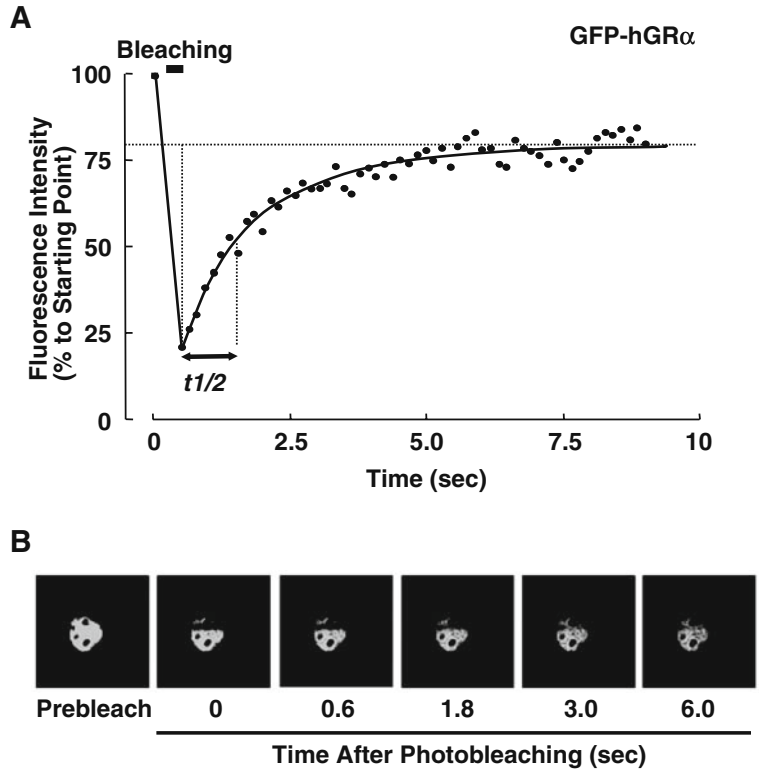

Fig. 3.8. Fluorescent recovery after photobleaching (FRAP) of GFP-hGRα. **(A)** Recovery of GFP-hGRα fluorescence intensity in the nucleus after photobleaching and calculation of $t_{1/2}$. COS-7 cells were transfected with pF25-hGRα, treated with 10^{-6} M dexamethasone and photo-bleached in the nucleus. Fluorescence intensity was traced time-sequentially, and the recovery $t_{1/2}$ was estimated from the recovery curve produced. (**B**) Representative photobleaching [adapted from (31)]. [From (26)]

Table 3.2
Half recovery time ($t_{1/2}$) of GR mutants in FRAP

hGRs	$t_{1/2}$ Mean ± SD (s)
hGRαWT	1.116 ± 0.207
hGRαR477H	0.641 ± 0.172 **
hGRαV571A	0.729 ± 0.143 **
hGRαD641V	0.930 ± 0.094 **
hGRαG679S	0.900 ± 0.124 **
hGRαV729I	0.825 ± 0.097 *

(continued)

Table 3.2 (continued)

hGRs	$t_{1/2}$ Mean ± SD (s)
hGRαI747M	0.835 ± 0.125 *
hGRαL773P	0.843 ± 0.145 *
hGRβ	0.656 ± 0.205 **
hGRα (Δ77-262)	0.645 ± 0.101 **
hGR(1-514)	0.415 ± 0.121 **

**: $p < 0.01$; *: $p < 0.05$, compared to GRα WT
[From (26)]

3.3. Evaluation of the Ability of the Mutant hGRα to Stimulate the Transcription: Transcription Assays Using GRE-Driven Reporter Genes

3.3.1. Transfection

1. CV-1 cells are seeded in six-well plates at a concentration of 1.5×10^5 cells/well. Twenty-four hours later, cells are cotransfected with wild-type hGRα, mutant hGRα or a control plasmid (pRSV-erbA^{-1}) (0.05 μg/well), pMMTV-luc (0.5 μg/well), and pSV40-β-gal (0.1 μg/well).
2. For experiments designed to determine whether the mutant receptor exerts a dominant negative or positive effect upon the wild-type receptor, CV-1 cells are cotransfected with pMMTV-luc (0.5 μg/well), pSV40-β-gal (0.1 μg/well), a constant amount of wild-type hGRα (0.05 μg/well) and five, progressively increasing concentrations of the mutant receptor, so that the ratio between the wild-type and mutant receptor would range from 1:0 to 1:10 (1:0, 1:1, 1:3, 1:6, 1:10). pRSV-erbA^{-1} is added in appropriate quantities to maintain a constant amount of DNA in each well.
3. Twenty-four hours later, the transfection medium is replaced with supplemented DMEM. Forty-eight hours after transfection, dexamethasone or vehicle (100% ethanol) is added to the medium at a concentration of 10^{-6} M.

3.3.2. Luciferase and β-Galactosidase Assays

1. Seventy-two hours after transfection, cells are washed with PBS twice, and lysed at room temperature with 150 μl of reporter lysis buffer. Cell lysates are collected and stored at −20°C.
2. 350 μl of reporter assay buffer are added to 50 μl of cell lysates.
3. Luciferase activity in the cell lysates is determined in a Monolight 3010 Luminometer using as substrate 100 μl of 1 mM D-Luciferin sodium salt solution, as previously described (37).

4. β-Galactosidase activity is determined in the same samples using a β-galactosidase enzyme assay system according to the instructions of the manufacturer (Tropix).
5. Luciferase activity is divided by β-galactosidase activity to account for transfection efficiency. Representative results of a transcription assay using glucocorticoid-responsive MMTV promoter is shown in **Fig. 3.9**.

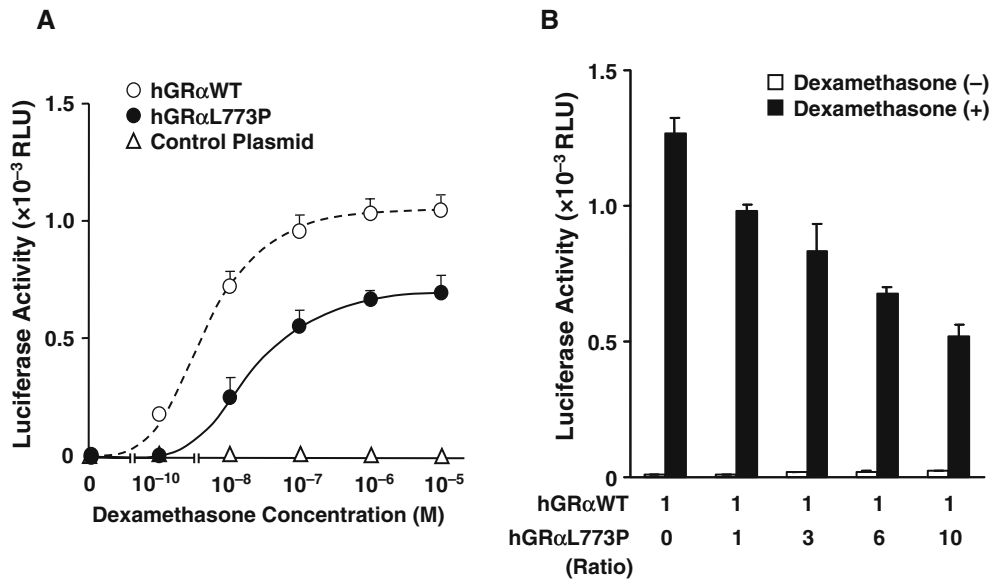

Fig. 3.9. Transcription assays for hGRαL773P. (**A**) Transcriptional activity of the wild type hGRα, the mutant receptor hGRαL773P and a control plasmid. Compared to the wild type receptor, the mutant receptor demonstrated a 2-fold reduction in the ability to transactivate the MMTV promoter in response to dexamethasone (10^{-12} to 10^{-5} M). Bars represent mean ± SEM of at least three independent experiments. (**B**) Dominant negative effect of hGRα L773P upon the wild type hGRα. Cotransfection with a constant amount of hGRα and five, progressively increasing concentrations of hGRαL773P, revealed a dose-dependent inhibition of hGRα-mediated transactivation of the MMTV promoter. Bars represent mean ± SEM of at least three independent experiments. [From (27)]

3.4. Evaluation of the Functional Defects of the Mutant hGRα for Their Ability to Interact with GRE: Chromatin Immunoprecipitation (ChIP) Assays

1. HCT-116 human colon carcinoma cells stably transfected with pMAM-neo-luc are seeded in 150-mm-diameter dishes (2.5×10^6 cells/dish) and grown in supplemented McCoy's 5A medium. Subconfluent cells are transiently transfected with wild-type or mutant pRShGRα (15 μg/dish) using lipofectin (33). Three hours later, the transfection medium is replaced with supplemented McCoy's 5A medium.
2. Sixteen hours after transfection, cells are treated with dexamethasone (10^{-6} M) or vehicle (100% ethanol) for 3–6 h. Cells are cross-linked using 1% formaldehyde at 37°C for 10 min.Cross-linked cells are collected by

using cell-scrapers, and harvested by centrifuging at 3,000 *g* for 5 min, and washed 3 times with PBS, each time collecting cells by centrifuging at 3,000 *g* for 5 min.

3. Cells are resuspended with equal volumes (5 ml each) of ChIP lysis buffer and NP-40 lysis buffer, homogenized in a Dounce homogenizer, and centrifuged at 21,000 *g* at 4°C for 5 min. Nuclear pellets are stored in a nuclear buffer at −80°C (27).

4. Equal amounts of nuclei (100 μg) are used for each immunoprecipitation experiment. Nuclei are diluted in 500 μl of ChIP dilution buffer, sonicated 8 times for 10 s (at 10 s intervals) and centrifuged at 21,000 *g* for 5 min.

5. Supernatants are precleared and the amount of DNA-protein complexes present in each sample is measured at 260 nm. Equal amounts of chromatosomes are immunoprecipitated with anti-hGRα antibody at 4°C for 14 h. Immunocomplexes are captured on protein A-agarose, washed sequentially with low salt wash buffer, high salt wash buffer, LiCl wash buffer and twice with TE buffer (*see* **Note 8**).

6. Samples are eluted with freshly prepared ChIP elution buffer at room temperature for 15 min twice, and after adding 20 μl of 5 M NaCl, cross-linking is reverted at 65°C for 4 h.

7. After addition of 10 μl of 0.5 M EDTA (to stop reversion of cross-linking) and subsequent incubation with 20 μl of proteinase K (10 mg/ml in 1 M Tris-HCl, pH 6.5) at 45°C for 1 h, genomic DNA fragments are extracted with phenol/chloroform and precipitated with ethanol.

8. The primer set is designed to amplify the MMTV promoter region, which contains two GREs. Equal volumes of DNA are used for PCR amplification of the MMTV promoter region. Initiation is performed at 94°C for 7 min, followed by 30 cycles of denaturation at 94°C for 1 min, annealing at 50°C for 1 min and extension at 72°C for 1 min, and a final period of extension at 72°C for 7 min.

9. PCR-amplified products (173 bp) are electrophoresed on 2% agarose gel and visualized by ethidium bromide staining. Representative results of the ChIP assay are shown in **Fig. 3.10**.

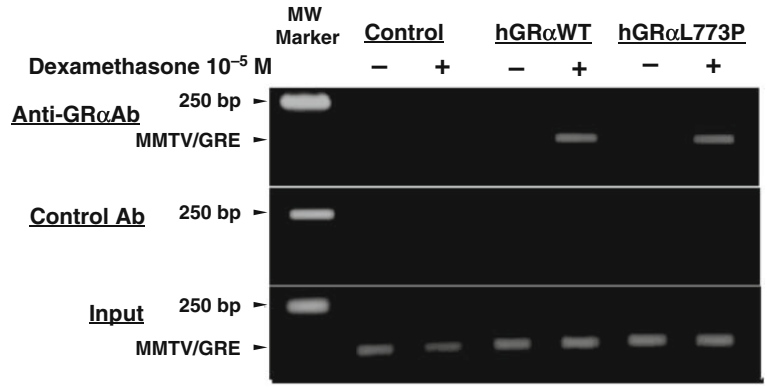

Fig. 3.10. ChIP assays for evaluating the DNA binding activity of hGRαL773P in vivo. ChIP assays were performed on HCT-116 cells stably transfected with MMTV. The cells were transiently transfected with control, wild type hGRα-or hGRαL773P-expressing plasmid. Both the wild type hGRα and hGRαL773P coprecipitated with MMTV GREs in a ligand-dependent fashion, indicating that the mutant receptor preserves its ability to bind to DNA. MW: Molecular weight. [FROM (27)]

3.5. Evaluation of the Functional Defects of the Mutant hGRα for Their Ability to Interact with the p160 Coactivator: Glutathione-S Transferase (GST) Pull-Down Assays

1. E. coli (B21 strain) are transformed with GST-fusion protein expression vectors [GST-fused GRIP1 (1-1462), GRIP1(559-774) and GRIP1(740-1217)], and are grown in LB broth overnight.
2. On the day of purifying GST-fused proteins, transformed bacteria are cultured at 37°C for 2–3 h by adding 1/10 volume of its confluent solution into LB broth.
3. When OD600nm of the culture reaches to 0.6–0.8, IPTG (0.5 mM) is added to express GST fusion proteins, and cells are further cultured for 2 h (*see* **Note 9**).
4. Cells are then collected by centrifugation at 5,000*g* for 10 min, resuspended in 900 µl of PBS, and cell-extracts are generated by pulse sonication (Misonix Sonicator 3000) on ice (10 s) (*see* **Note 9**).
5. Cell debris is then pelleted at 21,000*g* at 4°C for 10 min.
6. A 50% slurry of Glutathione Sepharose 4B Fast Flow beads (*see* **Note 10**) (60 µl) is added to the cell extracts and allowed to bind by gentle agitation at 4°C for 5 min.The beads with the bound GST fusion protein are then pelleted by centrifugation at 400*g* for 1 min.
7. The beads with the bound GST fusion protein are washed with 1 ml of GST binding buffer for 3 times by centrifuging them at 400*g* for 1 min, and analyzed by SDS-PAGE for the amount of protein bound to the GST-beads (38).

8. Coupled in vitro transcription/translation reactions are used to produce ^{35}S-labelled wild type (WT) and mutant hGRα in rabbit reticulocyte lysate by using pBK/CMV-hGRαWT and pBK/CMV-hGRα mutant, respectively, as templates.
9. ^{35}S-labelled wild type and mutant hGRαs (4–20 µl of crude translated protein) are incubated with GST fusion proteins bound to Glutathione Sepharose 4B beads, washed, eluted with Tris-Glycine SDS Sample Buffer (2x) (Invitrogen).
10. Samples are loaded and electrophoresed on an 8% SDS-PAGE gel. The percent of starting material loaded in input lanes is 3 or 5%. The gel is fixed, treated with Enlightning buffer and dried. Radioactivity is detected by exposing a film on the gel (*see* **Note 11**). Representative results of the GST pull-down assay using the GST-fused GRIP1 fragment proteins are shown in **Fig. 3.11**.

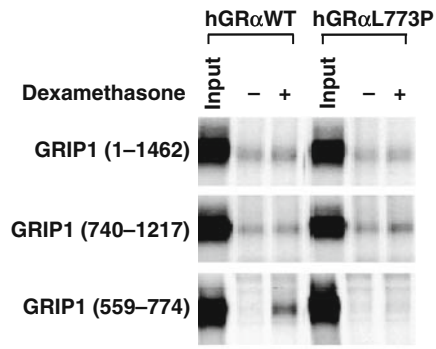

Fig. 3.11. GST pull-down assays examining the association of hGRαL773P and GST-fused GRIP1 fragments. In vitro translated and ^{35}S-labeled hGRαWT and hGRαL773P were incubated with bacterially produced GST-fused GRIP1(1-1462), GRIP1(597-774) and GRIP1(740-1217) in the absence or presence of dexamethasone (10^{-5}M). There was no interaction between the mutant receptor and the NRB fragment of GRIP1 in vitro, indicating that the AF-2 domain of hGRαL773P is ineffective. [From (27)]

3.6. Determining the Size and/or expression Levels of the Mutant hGRα by Western Blots

1. CV-1 and COS-7 cells are seeded in 75 cm^2 flasks at a concentration of 1×10^6 cells/flask and grown in supplemented DMEM. Subconfluent cells are transfected with wild-type or mutant hGRα (15 µg/flask) using the lipofectin method (33). Twenty-four hours (CV-1) or six hours (COS-7) after transfection, the transfection medium is replaced with supplemented DMEM.
2. Twenty-four hours later, cells are washed with ice-cold PBS three times, gently scraped from their flasks, centrifuged briefly at 200 *g* for 5 min and lysed using a Western blot lysis buffer (1–2 ml).

3. The cell lysates are centrifuged (500 *g* at 4°C) for 5 min to obtain whole cell extracts.
4. Whole cell extracts are mixed with an equal amount of Tris-Glycine SDS Sample Buffer (2x), heated to 95°C for 3 min, and electrophoresed alongside molecular weight prestained markers through 8% Tris-Glycine Gel.
5. Following electroblotting (25 V/0.8 mA/cm^2) onto Hybond C nitrocellulose membranes, proteins are incubated with blocking solution for 4 h.
6. Immunoblotting is performed at 4°C overnight, using purified specific rabbit polyclonal anti-hGRα antibody at 10 μg/ml. After washing with TBS-T three times, membranes are incubated with horseradish peroxidase-conjugated goat anti-rabbit IgG at 1:1000 dilution at room temperature for 1 h.
7. Membranes are washed with TBS-T three times.
8. The wild-type and mutant hGRα receptors are visualized using the ECL Plus Western Blotting Detection System and exposed to high-performance chemiluminescence film (*see* **Note 6**).

4. Notes

1. For all methods using live cells, the cell viability is very important to obtain reproducible results. Keep cells in a good condition by replating them every 3–4 days, depending on their growth rates.
2. Some of the cells are tightly attached on the bottom of the plates after 3 days of culture. Trypsinization may be required for harvesting them.
3. Thymidine incorporation assays and whole cell dexamethasone-binding assays can also be performed in COS7 cells transfected with hGRα-expressing plasmids, or in EBV-transformed mononuclear leukocytes.
4. Dexamethasone and other steroids are usually dissolved easily in 100% ethanol. Add them directly into culture media or reactions at a final dilution of 1:1000. These concentrated solutions can be kept at −20 and −80°C over 6 months.
5. Radioactivity of the culture media should be counted to estimate the concentrations of free radioactive dexamethasone for the Scatchard method. Total incubation volume should be 200 μl/well. Add nonradioactive (cold) and

radioactive (hot) dexamethasone into the incubation at a 1:10 fold dilution. If the signal from hot dexamethasone is low, increase amounts of mononuclear leukocytes up to 1×10^7cells/well.

6. Concentrations of $MgCl_2$ should be adjusted in the PCR for appropriate amplification of the hGRα exons from the patients' genomic DNA. If several non-specific bands are amplified with the target DNA, gel-purification of the band may be required for obtaining clear sequence results. Ready Reaction Mixture of the BigDye Terminator v3.1 Cycle Sequencing Kit can be used with ½ or ¼ volumes of the original reaction by adding the 5x Sequence buffer supplied with the kit. After PCR reactions using the sequencing kit, samples should be further purified with ethanol precipitation or appropriate columns to remove free fluorescent dyes.
7. GFP-fused hGRα easily leaks from the cytoplasm into the nucleus in cells with over-loaded expression. Such cells sometimes show delayed nuclear translocation of the GFP-hGRα. Thus, cells with appropriate expression should be selected for the analyses. At least 5–10 different cells should be tested to evaluate the time required for cytoplasmic to nuclear translocation of GFP-hGRα. Exposure to the laser beam can damage cells and easily bleach GFP. Thus, exposure of the cells with laser should be kept as short as possible.
8. Since PCR can detect trace amounts of the MMTV GREs, contamination of GR-unbound DNA could cause false-positive results. Thus, the washing steps are crucial for successful reactions in ChIP assays. Quantitative real-time PCRs using the TaqMAN or the SYBR Green-based system represent an alternative to the regular PCR and subsequent gel analyses. ChIP assays can be also performed in patients' mononuclear lymphocytes using the primer pairs detecting the endogenous glucocorticoid-responsive genes, such as the glucocorticoid-induced leucine zipper protein (GILZ), the interferon regulatory factor 8 (IRF8), and the insulin-like growth factor (IGF)-binding protein 1 (IGFBP1) (39).
9. If bacteria express low levels of GST-fused proteins, culture at 30°C with extended incubation may improve their production. Large-scale purification using the Glutathione Sepharose 4B Pre-packed Columns (bed volume: 1 or 5 ml) and the automated injection pump/fraction collector system (GE Healthcare) may be convenient for making stock of the GST-fused proteins. Cell lysis with sonication is complete when the cloudy cell suspension becomes translucent. The frequency and intensity of sonication should be adjusted, so that complete lysis will occur in 10 s, without frothing

(frothing may denature proteins). Before treating with Enlightning buffer, gels should be fixed by incubating them with a fixing buffer containing 10% methanol and 10% glacial acetic acid for 20 min, followed by washing with distilled water for an additional 20 min.

10. GST beads purchased from GE Healthcare come as an 80% slurry containing 20% ethanol. The beads should be washed with 1000 μl of PBS two times and once with the same volume of GST binding buffer, by centrifuging them at 400 *g* for 1 min. GST beads are then resuspended in GST binding buffer to make them 50% slurry.
11. Multiple protein bands usually appear with anti-GR antibody due to the presence of N-terminal translational isoforms of the hGRα (12, 40).

Acknowledgements

This book chapter was created based on the work supported in part by the Intramural Research Program of the *Eunice Kennedy Shriver* National Institute of Child Health and Human Development, National Institutes of Health, Bethesda, MD.

References

1. Kino, T., and Chrousos, G. P. (2004) Glucocorticoid effect on gene expression. In *Handbook on Stress and the Brain Part 1* (Steckler, T., Kalin, N. H., and Reul, J. M. H. M., eds) pp. 295–312, Elsevier BV, Amsterdam.
2. Chrousos, G. P., Charmandari, E., and Kino, T. (2004) Glucocorticoid action networks–an introduction to systems biology. *J Clin Endocrinol Metab* 89, 563–564.
3. Chrousos, G. P. (2004) The glucocorticoid receptor gene, longevity, and the complex disorders of Western societies. *Am J Med* 117, 204–207.
4. Zhou, J., and Cidlowski, J. A. (2005) The human glucocorticoid receptor: one gene, multiple proteins and diverse responses. *Steroids* 70, 407–417.
5. Duma, D., Jewell, C. M., and Cidlowski, J. A. (2006) Multiple glucocorticoid receptor isoforms and mechanisms of post-translational modification. *J Steroid Biochem Mol Biol* 102, 11–21.
6. Pratt, W. B. (1993) The role of heat shock proteins in regulating the function, folding, and trafficking of the glucocorticoid receptor. *J Biol Chem* 268, 21455–21458.
7. Terry, L. J., Shows, E. B., and Wente, S. R. (2007) Crossing the nuclear envelope: hierarchical regulation of nucleocytoplasmic transport. *Science* 318, 1412–1416.
8. Bamberger, C. M., Schulte, H. M., and Chrousos, G. P. (1996) Molecular determinants of glucocorticoid receptor function and tissue sensitivity to glucocorticoids. *Endocr Rev* 17, 245–261.
9. Schaaf, M. J., and Cidlowski, J. A. (2002) Molecular mechanisms of glucocorticoid action and resistance. *J Steroid Biochem Mol Biol* 83, 37–48.
10. Jonat, C., Rahmsdorf, H. J., Park, K. K., Cato, A. C., Gebel, S., Ponta, H., and Herrlich, P. (1990) Antitumor promotion and antiinflammation: down-modulation of AP–1 (Fos/Jun) activity by glucocorticoid hormone. *Cell* 62, 1189–1204.

11. Scheinman, R. I., Gualberto, A., Jewell, C. M., Cidlowski, J. A., and Baldwin, A. S., Jr. (1995) Characterization of mechanisms involved in transrepression of NF-κB by activated glucocorticoid receptors. *Mol Cell Biol* 15, 943–953.
12. Chrousos, G. P., and Kino, T. (2005) Intracellular glucocorticoid signaling: a formerly simple system turns stochastic. *Sci STKE*, pe48.
13. Kino, T., and Chrousos, G. P. (2002) Tissue-specific glucocorticoid resistance-hypersensitivity syndromes: multifactorial states of clinical importance. *J Allergy Clin Immunol* 109, 609–613.
14. McKenna, N. J., Xu, J., Nawaz, Z., Tsai, S. Y., Tsai, M. J., and O'Malley, B. W. (1999) Nuclear receptor coactivators: multiple enzymes, multiple complexes, multiple functions. *J Steroid Biochem Mol Biol* 69, 3–12.
15. McKenna, N. J., Lanz, R. B., and O'Malley, B. W. (1999) Nuclear receptor coregulators: cellular and molecular biology. *Endocr Rev* 20, 321–344.
16. McKenna, N. J., and O'Malley, B. W. (2002) Combinatorial control of gene expression by nuclear receptors and coregulators. *Cell* 108,465–474.
17. Auboeuf, D., Honig, A., Berget, S. M., and O'Malley, B. W. (2002) Coordinate regulation of transcription and splicing by steroid receptor coregulators. *Science* 298, 416–419.
18. Hittelman, A. B., Burakov, D., Iniguez-Lluhi, J. A., Freedman, L. P., and Garabedian, M. J. (1999) Differential regulation of glucocorticoid receptor transcriptional activation via AF-1-associated proteins. *EMBO J* 18, 5380–5388.
19. Heery, D. M., Kalkhoven, E., Hoare, S., and Parker, M. G. (1997) A signature motif in transcriptional co-activators mediates binding to nuclear receptors. *Nature* 387, 733–736.
20. Kino, T., De Martino, M. U., Charmandari, E., Mirani, M., and Chrousos, G. P. (2003) Tissue glucocorticoid resistance/hypersensitivity syndromes. *J Steroid Biochem Mol Biol* 85, 457–467.
21. Chrousos, G. P., and Kino, T. (2007) Glucocorticoid action networks and complex psychiatric and/or somatic disorders. *Stress* 10, 213–219.
22. Charmandari, E., Kino, T., Ichijo, T., and Chrousos, G. P. (2008) Generalized glucocorticoid resistance: clinical aspects, molecular mechanisms, and implications of a rare genetic disorder. *J Clin Endocrinol Metab* 93, 1563–1572.
23. Kino, T., Stauber, R. H., Resau, J. H., Pavlakis, G. N., and Chrousos, G. P. (2001) Pathologic human GR mutant has a transdominant negative effect on the wild-type GR by inhibiting its translocation into the nucleus: importance of the ligand-binding domain for intracellular GR trafficking. *J Clin Endocrinol Metab* 86, 5600–5608.
24. Charmandari, E., Kino, T., Ichijo, T., Jubiz, W., Mejia, L., Zachman, K., and Chrousos, G. P. (2007) A novel point mutation in helix 11 of the ligand-binding domain of the human glucocorticoid receptor gene causing generalized glucocorticoid resistance. *J Clin Endocrinol Metab* 92, 3986–3990.
25. Charmandari, E., Kino, T., Ichijo, T., Zachman, K., Alatsatianos, A., and Chrousos, G. P. (2006) Functional characterization of the natural human glucocorticoid receptor (hGR) mutants hGRαR477H and hGRαG679S associated with generalized glucocorticoid resistance. *J Clin Endocrinol Metab* 91, 1535–1543.
26. Kino, T., Liou, S. H., Charmandari, E., and Chrousos, G. P. (2004) Glucocorticoid receptor mutants demonstrate increased motility inside the nucleus of living cells: time of fluorescence recovery after photobleaching (FRAP) is an integrated measure of receptor function. *Mol Med* 10, 80–88.
27. Charmandari, E., Raji, A., Kino, T., Ichijo, T., Tiulpakov, A., Zachman, K., and Chrousos, G. P. (2005) A novel point mutation in the ligand-binding domain (LBD) of the human glucocorticoid receptor (hGR) causing generalized glucocorticoid resistance: the importance of the C terminus of hGR LBD in conferring transactivational activity. *J Clin Endocrinol Metab* 90, 3696–3705.
28. Charmandari, E., Kino, T., Souvatzoglou, E., Vottero, A., Bhattacharyya, N., and Chrousos, G. P. (2004) Natural glucocorticoid receptor mutants causing generalized glucocorticoid resistance: molecular genotype, genetic transmission, and clinical phenotype. *J Clin Endocrinol Metab* 89, 1939–1949.
29. Vottero, A., Kino, T., Combe, H., Lecomte, P., and Chrousos, G. P. (2002) A novel, C-terminal dominant negative mutation of the GR causes familial glucocorticoid resistance through abnormal interactions with p160 steroid receptor coactivators. *J Clin Endocrinol Metab* 87, 2658–2667.
30. Karl, M., Lamberts, S. W., Koper, J. W., Katz, D. A., Huizenga, N. E., Kino, T.,

Haddad, B. R., Hughes, M. R., and Chrousos, G. P. (1996) Cushing's disease preceded by generalized glucocorticoid resistance: clinical consequences of a novel, dominant-negative glucocorticoid receptor mutation. *Proc Assoc Am Physicians* 108, 296–307.

31. Karl, M., Lamberts, S. W., Detera-Wadleigh, S. D., Encio, I. J., Stratakis, C. A., Hurley, D. M., Accili, D., and Chrousos, G. P. (1993) Familial glucocorticoid resistance caused by a splice site deletion in the human glucocorticoid receptor gene. *J Clin Endocrinol Metab* 76, 683–689.
32. Hurley, D. M., Accili, D., Stratakis, C. A., Karl, M., Vamvakopoulos, N., Rorer, E., Constantine, K., Taylor, S. I., and Chrousos, G. P. (1991) Point mutation causing a single amino acid substitution in the hormone binding domain of the glucocorticoid receptor in familial glucocorticoid resistance. *J Clin Invest* 87, 680–686.
33. Felgner, P. L., Gadek, T. R., Holm, M., Roman, R., Chan, H. W., Wenz, M., Northrop, J. P., Ringold, G. M., and Danielsen, M. (1987) Lipofection: a highly efficient, lipid-mediated DNA-transfection procedure. *Proc Natl Acad Sci USA* 84, 7413–7417.
34. Stauber, R. H., Horie, K., Carney, P., Hudson, E. A., Tarasova, N. I., Gaitanaris, G. A., and Pavlakis, G. N. (1998) Development and applications of enhanced green fluorescent protein mutants. *Biotechniques* 24, 462–466, 468–471.
35. Kino, T., Tiulpakov, A., Ichijo, T., Chheng, L., Kozasa, T., and Chrousos, G. P. (2005) G protein β interacts with the glucocorticoid receptor and suppresses its transcriptional activity in the nucleus. *J Cell Biol* 169, 885–896.
36. Schaaf, M. J., and Cidlowski, J. A. (2003) Molecular determinants of glucocorticoid receptor mobility in living cells: the importance of ligand affinity. *Mol Cell Biol* 23, 1922–1934.
37. Brasier, A. R., Tate, J. E., and Habener, J. F. (1989) Optimized use of the firefly luciferase assay as a reporter gene in mammalian cell lines. *Biotechniques* 7, 1116–1122.
38. Bhattacharyya, N., Dey, A., Minucci, S., Zimmer, A., John, S., Hager, G., and Ozato, K. (1997) Retinoid-induced chromatin structure alterations in the retinoic acid receptor β2 promoter. *Mol Cell Biol* 17, 6481–6490.
39. Chen, W., Rogatsky, I., and Garabedian, M. J. (2006) MED14 and MED1 differentially regulate target-specific gene activation by the glucocorticoid receptor. *Mol Endocrinol* 20, 560–572.
40. Lu, N. Z., and Cidlowski, J. A. (2005) Translational regulatory mechanisms generate N-terminal glucocorticoid receptor isoforms with unique transcriptional target genes. *Mol Cell* 18, 331–342.

Chapter 4

Monitoring Insulin-Stimulated Production of Signaling Lipids at the Plasma Membrane

Mary Osisami, Huiyan Huang, and Michael A. Frohman

Abstract

Lipid second messengers play important roles in many cell signaling cascades. Lipid signaling molecules allow for high specificity, rapid transduction, and rapid reversibility of localized stimulation events. Fluorescent sensors capable of detecting individual signaling lipids enable their production and degradation to be followed, revealing the nature and dynamics of signaling pathways. The following sections outline a method for using lipid sensors to monitor the production of signaling lipids on the plasma membrane of C2C12 myotubes in response to insulin signaling.

Key words: Lipid second messengers, lipid sensors, green fluorescent protein.

1. Introduction

Agonist-stimulated cell-signaling cascades invariably result in the generation of lipid second messengers such as diacylglycerol (DAG), phosphatidylinositol 3-phosphate (PI3P), phosphatidylinositol 5-phosphate (PI5P), phosphatidylinositol 4,5-bisphosphate ($PI4,5P_2$), phosphatidylinositol 3,4,5-triphosphate (PIP_3), and phosphatidic acid (PA). These lipid second messengers are highly specific, aid in rapid transduction of the initial signal/stimulus, and can cause changes in the biophysical properties of the subcellular membranes on which they are generated (***reviewed in*** 1–3). The signaling lipids are produced by enzymes localized to specific membrane sites or compartments, and their diffusion is limited by the actin cytoskeleton; this assists in restricting the signaling to specific subcellular regions (4). Once produced, lipid signaling molecules

O.-K. Park-Sarge, T.E. Curry, Jr. (eds.), *Molecular Endocrinology,* Methods in Molecular Biology 590,
DOI 10.1007/978-1-60327-378-7_4,

recruit effector proteins that carry out localized actions or propagate the signaling cascade (***reviewed in*** 1–3). The effector proteins have very specific regions that mediate the binding to signaling lipids, and when fused to reporter proteins such as Enhanced Green Fluorescent Protein (EGFP), many retain their ability to bind to the signaling lipids with great specificity (5–7). Fusing the lipid binding domains to EGFP thus permits the visualization of signaling lipids during dynamic cellular responses to agonist stimulation.

Described in the following sections is a method for detecting the signaling lipid PA, which can be generated by the action of members of the Phospholipase D, DAG Kinase, and LysoPA acetyltransferase families of signaling enzymes. In the sample protocol provided, we will describe a method for visualizing PA production in C2C12 myotubes in response to insulin. This signaling pathway, which results in translocation of vesicles containing the Glut-4 glucose transporter to the plasma membrane, has been shown in fat cells to require the production of PA by Phospholipase D1 at the plasma membrane (8). This protocol utilizes a PA-sensor described previously (9, 10), which was generated by our group by fusion of EGFP with a 40-amino acid PA-binding domain (PABD) from the yeast SNARE protein Spo20p (11). Alternate PA sensors have been described, based on the PA-binding domains of RAF-1 kinase (5, 12) and the Son-of Sevenless (SOS) Ras exchange factor (13). The protocol can also be used with sensors for other signaling lipids, including DAG, PI3P, PI4,5P_2, PI3,4P_2, and PIP_3 (6, 7, 14–16).

In this chapter, we described protocols for monitoring the generation of signaling lipids using C2C12 myotubes with sensors for PA. Acquisition of signal is one step of the process; however, it is often important to normalize the amount of signal detected to the amount of membrane locally present, since changes in cell morphology can lead to changes in membrane thickness in a confocal optical section. Approaches to take this factor into account are discussed.

2. Materials

2.1. Cell Culture

1. C2C12 muscle cells (available from ATCC), ideally ones stably transfected with exofacial myc-glut-4 (17) and the PA sensors described below (*see* **Section 3.1.1**). Note, however, that long-term and/or high-level overexpression of lipid sensors can interfere with biological processes; hence it may be necessary to select cell lines that have only moderate or low levels of expression of the sensors, or to express them using transient transfection.

2. C2C12 proliferation media: Dulbecco's Modified Eagle's Medium (DMEM) supplemented with 10% fetal bovine serum (FBS).
3. C2C12 differentiation media: DMEM supplemented with 2% horse serum.
4. Phosphate Buffered Saline (PBS).
5. 1x TrypLE^{TM} Express trypsin-like solution (Invitrogen).
6. Wild-type (wt) PA sensor (GFP-Spo20-PABD, *see* **Note 1**) and a mutant (mt) PA sensor (GFP-Spo20-PABD-L67R) that does not bind PA (*see* **Note 2**).
7. 0.2% gelatin solution.
8. 18 × 18 mm glass coverslips (Fisher).
9. 25% glutaraldehyde (Sigma) diluted in PBS to 0.001%.

2.2. Insulin Stimulation and Immunofluorescence

1. Insulin, 167 μM, 1000x stock solution (Sigma). This can be purchased as a liquid solution or as a powder and diluted in water. The working concentration is 167 nM.
2. 4% paraformaldehyde made fresh in PBS before use.
3. Blocking buffer: 5% bovine serum albumin, 0.1% glycine, 5% normal goat serum in PBS.
4. 9E10 anti-myc primary antibody (mouse monoclonal, Sigma).
5. Secondary antibody: Alexa647-labeled goat anti-mouse IgG (Invitrogen).
6. Chamber slides (Nunc).
7. Krebs-Ringer phosphate HEPES (KRPH) buffer: 5 mM Na_2HPO_4, 20 mM HEPES, pH 7.4, 1 mM $MgSO_4$, 1 mM $CaCl_2$, 136 mM NaCl, 4.7 mM KCl.
8. VectaShield® mounting medium (Vector laboratories Inc.).
9. Clear nail polish.
10. Confocal microscope with a capacity of live cell imaging and a heating chamber to maintain cells at 37°C.

3. Methods

3.1. C2C12 Culture and Differentiation

1. Maintenance culture: C2C12 cells stably expressing exofacial myc-glut-4 and either wild-type PABD-EGFP (EGFP-Spo20-PABD) or mutant PABD-EGFP (EGFP-Spo20-PABD-L67R) should be maintained by passaging as they approach confluency, using TrypLE^{TM} Express to release the cells (typically, 5' incubation at 37°C). A 1:20 split every

2 days is recommended to ensure that the cells retain the ability to differentiate efficiently (*see* **Note 3**). The following steps include two separate cultures of C2C12 cells expressing either wild type PABD-EGFP or mutant PABD-EGFP.

2. Coating coverslips with gelatin: Place coverslips into the tissue culture plates that will be used for culture and add enough gelatin solution to cover them. Incubate for 15 min, then remove the gelatin and add glutaraldehyde solution for 10 min to fix the slides. Remove the glutaraldehyde and wash the coverslips 4 times with PBS and once with proliferation media.
3. Differentiation: Plate harvested cells onto gelatin-coated coverslips in 35 mm tissue culture plates at 15,000 cells/cm^2 (*see* **Note 4**). The appearance of multinucleated muscle fibers should begin on day 2 of differentiation and continue on through day 8 (see **Fig. 4.1**).
4. The next day, wash the plates once with warm PBS, and culture for 6 days in C2C12 differentiation media, changing the media every 2 days. When washing the plates, make sure that the PBS is pipetted on to the sides of the plates to avoid dislodging the cells from the coverslips. The cells will adhere quite tightly at the beginning of the differentiation process but become less adherent as they mature into large myotubes.

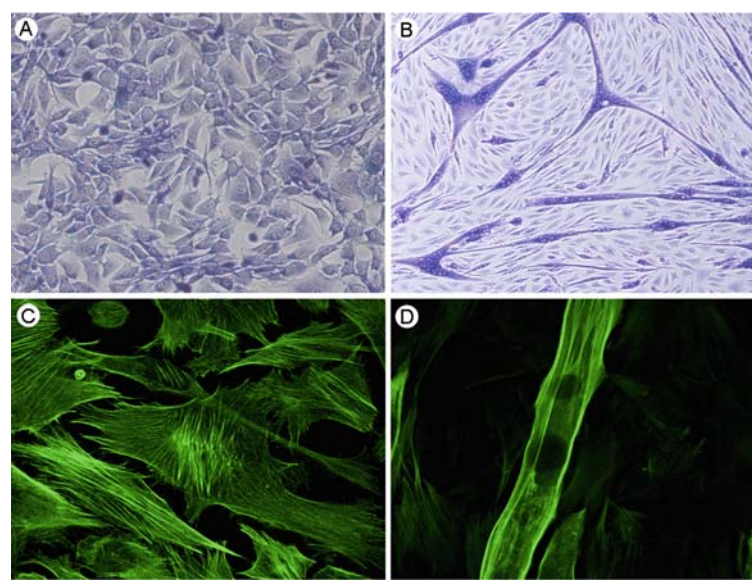

Fig. 4.1. Morphological changes during C2C12 muscle differentiation. C2C12 cells stained with Giemsa to show cell shape (**A**, **B**) or Alexa Fluor 488 phalloidin to image F-actin (**C**, **D**). (**A**, **C**) Proliferating myoblasts before induction of differentiation. (**B**, **D**) C2C12 myotubes 6 days-post induction of differentiation.

3.2. Insulin Stimulation and Immunofluorescence

1. After allowing the cells to differentiate for 6 days, remove the differentiation media by aspiration, wash the cells twice with warm PBS, and culture in serum-free DMEM for 4 hours to bring the cells to rest and to basal levels of the signaling lipid PA (*see* **Section 3.4**).
2. Wash the cells twice with warm KRPH buffer followed by a 30 min incubation at 37°C in KRPH buffer with or without 167 nM insulin, using the non-stimulated plate as a control.
3. Aspirate the media and wash the plates three times with cold PBS and fix in paraformaldehyde for 10 min.
4. Remove the paraformaldehyde solution and wash the cells 3 times for 5 min each in PBS.
5. Incubate the cells with blocking buffer for at least one hour at room temperature.
6. Remove the blocking buffer and replace with anti-myc primary antibody diluted 1:500 in blocking buffer for one hour at room temperature (*see* **Note 5**).
7. Remove the primary antibody solution and wash the cells 3 times for 5 min each in PBS at room temperature.
8. Incubate with Alexa Fluor 647 goat anti-mouse IgG diluted 1:500 in blocking buffer at room temperature in the dark for one hour (*see* **Note 6**).
9. Remove the secondary antibody solution and wash 3 times for 5 min each in PBS at room temperature in the dark.
10. After the final wash, remove the PBS and place the coverslips face-down on microscope slides dotted with 10 μl of Vecta-Shield and allow them to dry in the dark.
11. Seal the edges of the coverslips onto the microscope slides using clear nail polish.
12. The slide should be viewed under phase contrast to locate the cells and under confocal microscopy to image them. Alternatively, cells can be located using DAPI stain (0.001 mg/ml) under UV light with an excitation/emission of 358/461. Wavelengths of 495/519 nm and 650/668 nm are used to visualize GFP and Alexa Fluor 647 respectively. Software such as Photoshop can be used to overlay images. An example of what can be anticipated when imaging translocation of the PA sensor to the plasma membrane is shown in **Fig. 4.2**.

3.3. Live Cell Confocal Microscopy

1. Plate cells onto gelatin-coated chamber slides at 15,000 cells/cm^2. To coat the chamber slides with gelatin, see **Section 3.1.2**.
2. Differentiate and serum-starve the cells as described above (as in step 3.2.1). During the last 20 min of serum starvation, begin to warm up the heating chamber of the confocal microscope.

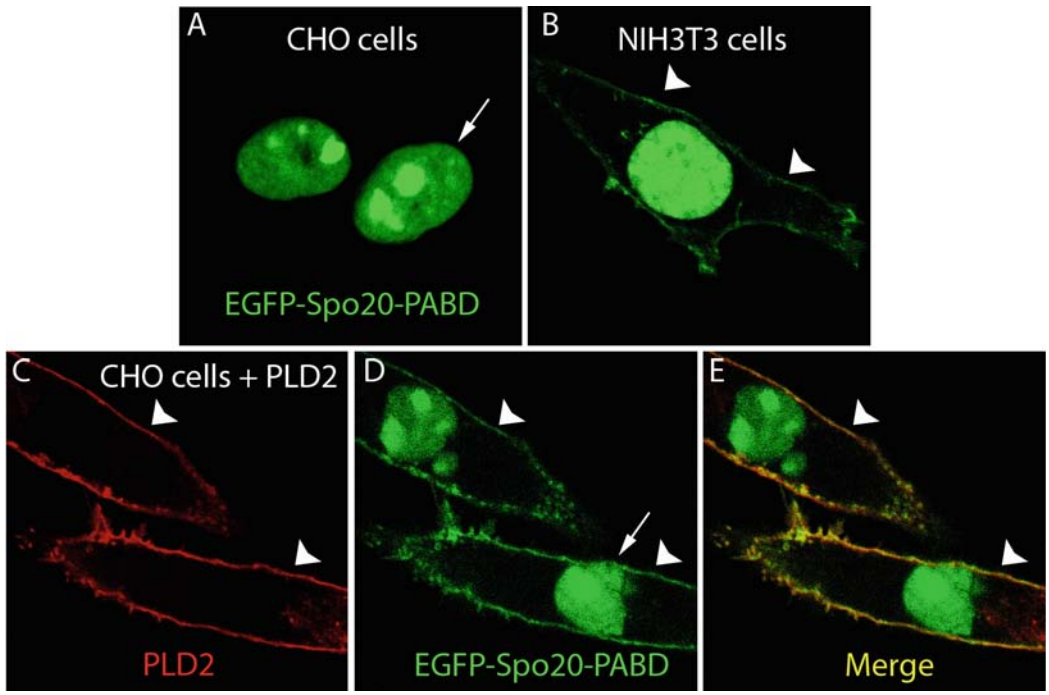

Fig. 4.2. Translocation of the PA sensor, EGFP-Spo20-PABD, to the plasma membrane upon PA generation. (**A**) In serum-starved CHO cells, all of the PA sensor is found in the nuclei (*arrow*). (**B**) In NIH3T3 cells cultured in 10% serum, most of the sensor is in the nucleus, but a small amount is detected on the plasma membrane (*arrowheads*). (**C**) In PLD2-overexpressing cells (which are also being stimulated with PMA, an activator of PLD), PLD2 localizes to the plasma membrane (*arrowheads*). (**D**) Although some of the PA sensor remains in the nucleus, a greater fraction is now seen at the plasma membrane, (**E**) as shown in the merged image.

3. Wash the cells 3 times with warm KRPH buffer. Replace the final wash with fresh KRPH buffer and quickly move the slides to the heating chamber of the confocal microscope.
4. In the heating chamber and on the microscope stage, stimulate the cells by adding insulin to the medium (final concentration of insulin: 167 nM).
5. Visualize the cells as described above (as in step 3.2.12); however, set the confocal software for constant imaging by taking an image of the slide every 2 min.
6. Use image enhancement and normalization as needed to optimize the series of images (*see* **Note 7**).

3.4. Anticipated Results

Prior to insulin stimulation, both the wt and mutant sensors should be distributed evenly throughout the cytoplasm in many cell types, because the sensors exhibit unrestrained movement in the absence of sufficient target lipid to recruit them to a membrane surface. In some cells, sensor accumulation may be noted in the nucleus, due to a tendency for EGFP to localize there

(an example of this type of finding is shown in **Fig. 4.2**). Upon insulin or other agonist stimulation, readily visible movement of the sensor to the plasma membrane should be apparent for the wild-type but not the mutant sensor. Examples of this type of translocation can be seen in several publications (9, 10, 13). The optimal time point to examine membrane translocation of the sensor will vary according to the signal being followed. PIP_3, for example, typically rises and falls quite fast, and may peak within seconds to minutes of the addition of agonist. PA generally takes longer to begin to rise (seconds to minutes), peaking at 15–30 min after stimulation.

4. Notes

1. There are sensors that can image many other types of lipids, such as DAG, PI3P, PI4,5P_2, PI3,4P_2, and PIP_3 (6, 7, 14–16). These sensors can be used in similar protocols for a multitude of cell lines and signaling pathways. The EGFP on the sensors can be changed to other fluorophores such as mCherry, mPlum, and Venus (yellow fluorescent protein) as needed to enable multi-color detection (18, 19). It should be noted that several of the available lipid sensors will detect lipid changes only on specific membranes (e.g. Golgi or endocytic vesicles, **reviewed in** 1).
2. The mutant PABD is used as a negative control, since it does not bind to PA.
3. Never allow myoblasts to become confluent. If the cells become confluent, there will be a reduction in fusion competency. If the cells are not ready to be passaged on the second day post passaging, then replace the old media with fresh media.
4. Some investigators have reported that glut-4 overexpression C2C12 cell lines do not differentiate well (20). If this happens, mix wild-type C2C12 cells with the glut-4 overexpression cells in a 1:1 ratio; this should result in near wild-type differentiation efficiency while maintaining detectable levels of exofacial myc glut-4 and the lipid sensor.
5. Exofacial myc-Glu-4 is a construct that contains a myc-tag on the first exofacial loop of glut-4 (17). The myc tag becomes detectable on the cell surface (for non-permeabilized cells) only once glut-4-containing vesicles have fused into the plasma membrane. In contrast, the EGFP tag can be imaged in real-time using living cells. Permeabilization is omitted

when it is desired to detect only the cell-surface myc-epitope tag, but if a different system and pathway is used, permeabilization with 0.1% triton X-100 for 10 min after fixation or with 0.05% saponin during blocking may be needed for the primary and secondary antibody immunostaining.

6. In this protocol, translocated glut-4 is used as a plasma membrane marker. Alternate approaches include using antibodies that illuminate the plasma membrane, such as Snap25 or NCX1, as well as performing direct staining of the plasma membrane using commercially available dyes such as Alexa Fluor 594 WGA or CellMask^{TM} Orange plasma membrane stain (Invitrogen, Carlsbad, CA). When changing the protocol to use sensors to image a different subcellular membrane compartment, a membrane marker for the region of interest should be employed to enable normalization and image signal enhancement (see below).
7. There are several methods available to normalize the readout from lipid sensors. One method includes the use of FRET-based sensors (21, 22). This method allows for monitoring the level of sensor "activation" as well as normalization to the total amount of membrane of the organelle/membrane of interest.

   Another method, which is useful for the protocol described here, is based on simultaneous expression of both the wt and mt sensors tagged with different fluorophores simultaneously in the same cell. To pursue this approach, one would use two myoblast stable cell lines, one expressing the exofacial myc-Glut-4 and the wt PA EGFP sensor, and the other expressing the mt sensor tagged to mCherry. Upon differentiation, the red and green myoblasts will fuse to generate doubly expressing myotubes (*see* **Note 4**). To prepare for imaging, the differentiation step should be performed by mixing both cell lines in the same plate in a 1:1 ratio. For imaging, monitor and calculate the ratio of green to red output at the plasma membrane as detected using the translocated Glut-4, which can be imaged using a third color, such as far-red-labeled secondary antibody. Alternately, the PM membrane stains and markers described above can be used for normalization, such as Alexa Fluor 594 WGA or CellMask^{TM} Orange plasma membrane stain.
8. If the signal from either the Glut-4 or the lipid sensors are weak, then the signals can be digitally enhanced by using a program such as Photoshop and performing a "masking" operation. This masking operation is a coincidence detection method that will only show pixels that are in common, i.e. where there is co-localization.

Acknowledgments

This work was supported by NIH award GM071520 to MAF and an NIH NIDDK NRSA award and the Turner Foundation to MO.

References

1. Balla, T., Bondeva, T., and Varnai, P. (2000) How accurately can we image inositol lipids in living cells? *Trends Pharmacol Sci* **21**, 238–241
2. Hurley, J. H., and Meyer, T. (2001) Subcellular targeting by membrane lipids. *Curr Opin Cell Biol* **13**, 146–152
3. Spiegel, S., Foster, D., and Kolesnick, R. (1996) Signal transduction through lipid second messengers. *Curr Opin Cell Biol* **8**, 159–167
4. Morone, N., Fujiwara, T., Murase, K., Kasai, R. S., Ike, H., Yuasa, S., Usukura, J., and Kusumi, A. (2006) Three-dimensional reconstruction of the membrane skeleton at the plasma membrane interface by electron tomography. *J Cell Biol* **174**, 851–862
5. Ghosh, S., Strum, J. C., Sciorra, V. A., Daniel, L., and Bell, R. M. (1996) Raf-1 kinase possesses distinct binding domains for phosphatidylserine and phosphatidic acid. Phosphatidic acid regulates the translocation of Raf-1 in 12-O-tetradecanoylphorbol-13-acetate-stimulated Madin-Darby canine kidney cells. *J Biol Chem* **271**, 8472–8480
6. Oancea, E., Teruel, M. N., Quest, A. F., and Meyer, T. (1998) Green fluorescent protein (GFP)-tagged cysteine-rich domains from protein kinase C as fluorescent indicators for diacylglycerol signaling in living cells. *J Cell Biol* **140**, 485–498
7. Holz, R. W., Hlubek, M. D., Sorensen, S. D., Fisher, S. K., Balla, T., Ozaki, S., Prestwich, G. D., Stuenkel, E. L., and Bittner, M. A. (2000) A pleckstrin homology domain specific for phosphatidylinositol 4, 5-bisphosphate (PtdIns-4,5-P2) and fused to green fluorescent protein identifies plasma membrane PtdIns-4,5-P2 as being important in exocytosis. *J Biol Chem* **275**, 17878–17885
8. Huang, P., Altshuller, Y. M., Hou, J. C., Pessin, J. E., and Frohman, M. A. (2005) Insulin-stimulated plasma membrane fusion of Glut4 glucose transporter-containing vesicles is regulated by phospholipase D1. *Mol Biol Cell* **16**, 2614–2623
9. Zeniou-Meyer, M., Zabari, N., Ashery, U., Chasserot-Golaz, S., Haeberle, A. M., Demais, V., Bailly, Y., Gottfried, I., Nakanishi, H., Neiman, A. M., Du, G., Frohman, M. A., Bader, M. F., and Vitale, N. (2007) Phospholipase D1 production of phosphatidic acid at the plasma membrane promotes exocytosis of large dense-core granules at a late stage. *J Biol Chem* **282**, 21746–21757
10. Su, W., Yeku, O., Olepu, S., Genna, A., Park, J. S., Ren, H., Du, G., Gelb, M., Morris, A., and Frohman, M. A. (2009) FIPI: A Phospholipase D pharmacological inhibitor that alters cell spreading and inhibits chemotaxis. *Mol. Pharm.* **75**, 437–466
11. Nakanishi, H., de los Santos, P., and Neiman, A. M. (2004) Positive and negative regulation of a SNARE protein by control of intracellular localization. *Mol Biol Cell* **15**, 1802–1815
12. Corrotte, M., Chasserot-Golaz, S., Huang, P., Du, G., Ktistakis, N. T., Frohman, M. A., Vitale, N., Bader, M. F., and Grant, N. J. (2006) Dynamics and function of phospholipase D and phosphatidic acid during phagocytosis. *Traffic (Copenhagen, Denmark)* **7**, 365–377
13. Zhao, C., Du, G., Skowronek, K., Frohman, M. A., and Bar-Sagi, D. (2007) Phospholipase D2-generated phosphatidic acid couples EGFR stimulation to Ras activation by Sos. *Nat Cell Biol* **9**, 707–712
14. Gray, A., Van Der Kaay, J., and Downes, C. P. (1999) The pleckstrin homology domains of protein kinase B and GRP1 (general receptor for phosphoinositides-1) are sensitive and selective probes for the cellular detection of phosphatidylinositol 3,4-bisphosphate and/or phosphatidylinositol 3,4,5-trisphosphate in vivo. *Biochem J* **344 Pt 3**, 929–936
15. Lindsay, Y., McCoull, D., Davidson, L., Leslie, N. R., Fairservice, A., Gray, A., Lucocq, J., and Downes, C. P. (2006)

Localization of agonist-sensitive PtdIns (3,4,5) P3 reveals a nuclear pool that is insensitive to PTEN expression. *J Cell Sci* **119**, 5160–5168

16. Blatner, N. R., Stahelin, R. V., Diraviyam, K., Hawkins, P. T., Hong, W., Murray, D., and Cho, W. (2004) The molecular basis of the differential subcellular localization of FYVE domains. *J Biol Chem* **279**, 53818–53827
17. Bogan, J. S., McKee, A. E., and Lodish, H. F. (2001) Insulin-responsive compartments containing glut4 in 3t3-l1 and cho cells: regulation by amino acid concentrations. *Mol Cell Biol* **21**, 4785–4806
18. Shaner, N. C., Campbell, R. E., Steinbach, P. A., Giepmans, B. N., Palmer, A. E., and Tsien, R. Y. (2004) Improved monomeric red, orange and yellow fluorescent proteins derived from Discosoma sp. red fluorescent protein. *Nat Biotechnol* **22**, 1567–1572
19. Shaner, N. C., Steinbach, P. A., and Tsien, R. Y. (2005) A guide to choosing fluorescent proteins. *Nature Methods* **2**, 905–909
20. Nedachi, T., and Kanzaki, M. (2006) Regulation of glucose transporters by insulin and extracellular glucose in C2C12 myotubes. *Am J Physiol Endocrinol Metab* **291**, E817–828
21. Gallegos, L. L., Kunkel, M. T., and Newton, A. C. (2006) Targeting protein kinase C activity reporter to discrete intracellular regions reveals spatiotemporal differences in agonist-dependent signaling. *J Biol Chem* **281**, 30947–30956
22. Sato, M., Ueda, Y., and Umezawa, Y. (2006) Imaging diacylglycerol dynamics at organelle membranes. *Nature Methods* **3**, 797–799

Chapter 5

Gene Expression Profiling in the Aging Ovary

Kathleen M. Eyster and John D. Brannian

Abstract

DNA microarray is an important discovery technology that allows the analysis of the expression of thousands of genes at a time. Data from DNA microarrays elucidate fundamental biological processes through discovery of differential expression of genes not previously known or predicted to be involved in a particular process. In the ovary and other hormone-responsive tissues, the technology can be used to examine the effects of gene mutations, pharmaceutical agents, disease, hormones, developmental changes, or changes in gene expression related to aging.

Key words: Microarray, ovary, aging, obesity, gene expression, CodeLink Whole Mouse Genome microarrays, Agilent RNA 6000 Nano LabChip.

1. Introduction

Obesity is associated with progressive health disorders, e.g. metabolic syndrome, and has a negative impact on fertility. A major reproductive disorder related to obesity is polycystic ovary syndrome (PCOS), which is the most prevalent endocrinopathy of reproductive age women. Moreover, women with PCOS are at greater risk for developing type II diabetes and cardiovascular disease as they age (1).

Mice heterozygous for the Lethal Yellow (LY) mutation at the agouti gene locus exhibit distinct characteristics including yellow coat color, adult-onset obesity, insulin resistance (2), hyperleptinemia (3), and accelerated reproductive senescence (3, 4). Declining ovarian function in aging LY mice is directly related to progressive obesity and hyperleptinemia (3). Because of the adult-onset, progressive obesity characteristic of LY mice, these

O.-K. Park-Sarge, T.E. Curry, Jr. (eds.), *Molecular Endocrinology,* Methods in Molecular Biology 590,
DOI 10.1007/978-1-60327-378-7_5,

mice more closely mimic typical human obesity than many other mouse models of obesity, e.g. *ob/ob* or *db/db* mice. Therefore, we have used the obese LY mouse and their lean black littermates to study the effects of aging and progressive obesity on gene expression in the ovary (3, 5).

DNA microarray is a powerful technology that allows the analysis of the expression of thousands of genes at a time. As such, it is an important discovery technology. DNA microarrays are often used to elucidate fundamental biological processes through discovery of differential expression of genes not previously known or predicted to be involved in a particular process. In the ovary, the technology can be used to examine the effects of pharmaceutical agents (5), disease, hormones, developmental changes, or changes in gene expression related to aging. Differential gene expression can be measured in whole synchronized ovaries, in isolated granulosa cells, or in isolated corpora lutea. The present chapter outlines the methodology behind microarray analysis to examine changes in ovarian gene expression during the aging process in genetically obese LY mice.

2. Materials

2.1. Preparation of Synchronized Mouse Ovaries for RNA Extraction

1. Lethal Yellow mice (C57BL/6J A^y/a) and their lean black littermates (C57BL/6J a/a) were obtained from the Augustana College Biology Department (Sioux Falls, SD) breeding colony. The breeding colony was founded by breeder mice obtained from Jackson Laboratory (Bar Harbor, ME, current strain number KK Cg-A^y/J). Mice were housed and fed as described (5).
2. GnRH antagonist, Antide© (Bachem, Torrance, CA).
3. Equine chorionic gonadotropin (eCG, Sigma) has primarily follicle stimulating hormone activity in the mouse. Human chorionic gonadotropin (hCG, Sigma) has luteinizing hormone activity.
4. 1.8 ml cryovial (Nunc).
5. PBS + 0.1% BSA.
6. RNAlater (Ambion, Austin, TX) is an RNA-preserving reagent.

2.2. RNA Hygiene

1. RNase ZAP (Ambion).
2. Diethylpyrocarbonate (DEPC, Sigma).

2.3. RNA Extraction

1. TRI reagent (Molecular Research Center, Cincinnati, OH)
2. Bromochloropropane (Molecular Research Center, Cincinnati, OH).

3. 3 M sodium acetate (Sigma).
4. Silica gel membrane and buffers (RW1 and RPE) for purification of RNA (RNeasy, Qiagen, Valencia, CA).
5. β-mercaptoethanol (Sigma). Add 10 µl β-mercaptoethanol per 1000 µl to guanidine isothiocyanate-containing lysis/binding buffer such as RNeasy Lysis Buffer (RLT buffer, Qiagen), before use.
6. 100% molecular grade ethanol (Sigma).
7. RNase-free DNase (Qiagen): Mix 10 µl DNase stock solution with 70 µl of DNase dilution buffer (RDD) and add the diluted DNase directly to the gel membrane of the column.

2.4. Analysis and Quantitation of RNA

1. Agilent Bioanalyzer 2100.
2. RNA 6000 Nano Chip (Agilent, Santa Clara, CA). The RNA 6000 Nano Chip kit contains the gel matrix, spin filter columns, dye concentrate, marker mixture diluent, the RNA ladder (molecular weight markers), and the RNA chip. The priming station for pressurizing the chip is purchased separately.

2.5. Synthesis of First and Second Strand cDNA and cRNA

1. The MessageAmp II-Biotin Enhanced kit (Ambion #AM1791, Austin, TX). This kit contains all reagents for the synthesis of first and second strand cDNA and for the in vitro transcription synthesis of cRNA. This includes T7 Oligo (dT) primer, 10x first strand buffer, dNTP mix, RNase inhibitor, reverse transcriptase, 10x second strand buffer, DNA polymerase, RNase H, biotin-NTP mix, T7 10x reaction buffer, T7 enzyme mix, and filter cartridges and buffers for purification of cDNA and cRNA.
2. Non-DEPC-treated nuclease-free water (Ambion).
3. Bacterial RNA spikes were obtained from Applied Microarrays (Tempe, AZ).
4. MessageAmp II aRNA Amplification Kit (Ambion) if two rounds of cRNA synthesis are needed.
5. In vitro transcription (IVT) master mix: 12 µl biotin-NTP mix, 4 µl T7 10x reaction buffer, and 4 µl T7 enzyme mix per sample plus 5% volume overage.

2.6. Hybridization

1. CodeLink Whole Mouse Genome microarrays (Applied Microarrays, Tempe, AZ).
2. 5x Fragmentation buffer: 200 mM Tris acetate, pH 8.2, 500 mM potassium acetate, 150 mM magnesium acetate.
3. Hybridization buffer components A and B (Applied Microarrays, Tempe, AZ).

4. 0.75x TNT wash buffer: 75 ml of 1 M Tris-HCl, pH 7.6, 22.5 ml of 5 M NaCl, 0.375 ml of Tween 20, 902 ml of DEPC-treated water. Filter through a 0.2 μm filter.
5. 1x TNT buffer: 100 ml of 1 M Tris-HCl, pH 7.6, 30 ml of 5 M NaCl, 0.5 ml of Tween 20, 870 ml of DEPC-treated water. Filter through 0.2 μm filter.
6. 0.1x SSC/0.05%Tween 20 wash buffer: 5 ml of 20x SSC buffer (Sigma), 0.5 ml of Tween 20 (Sigma), 994.5 ml of DEPC-treated water. Filter through a 0.2 μm filter.
7. TNB buffer: Dissolve 1 g NEN blocking reagent (Perkin-Elmer, Waltham, MA) in 200 ml 1x TNT. Heat to 60°C then stir overnight, reheat to 60°C then filter through 0.88 μm filter. Freeze at −20°C in 50 ml aliquots.
8. Streptavidin-Alexa 647 (Molecular Probes): Stock solution: Add 1 ml of 1x PBS to 1 mg lyophilized Streptavidin-Alexa 647. Freeze at −70°C in 100 μl aliquots. Working dilution of Streptavidin-Alexa 647: Mix 6.8 μl Streptavidin-Alexa 647 stock solution with 3.39 ml TNB buffer for each microarray plus 10% volume overage.

3. Methods

3.1. Preparation of Synchronized Mouse Ovaries for RNA Extraction

1. Maintain adult (90-, 120-, 150-, or 180-day old) female mice on a 14:10 light/dark cycle with lights on at 0600.
2. To exclude gonadotropin-mediated effects, suppress late estrus/metestrus mice with a GnRH antagonist (Antide©, Bachem, Torrance, CA). Antide treatment may be initiated at any time during metestrus or diestrus. Inject mice (i.p.) with 10 μg/g body weight (BW) Antide on the morning of Day 1 of treatment and again on the morning of Day 4.
3. On the evening of Day 5 (∼36 h after the last Antide injection), inject mice with 1 IU eCG (Sigma) per 5 gram BW (i.e. 5 IU for a ∼25 g mouse) to stimulate coordinated follicle development. Euthanize the mice by cervical dislocation 36 h after eCG injection (*see* **Note 1**).
4. Quickly dissect the ovaries free from surrounding tissue and immediately place them in a sterile glass petri dish in ice-cold PBS + 0.1 % BSA (RNAlater can be substituted for PBS/BSA in this dissection). Rapidly trim all surrounding fat and connective tissue from the ovaries under a dissecting microscope. One ovary is placed in a 1.8 ml cryovial containing 1.0 ml RNAlater and placed on ice for 5−10 min. After 5−10 min,

cryovials are placed in a −70°C freezer or in liquid nitrogen until RNA extraction. The contralateral ovary may be placed in cell lysis buffer (Sigma), homogenized, centrifuged, and extracts stored at −70°C for later protein analysis by immunoblot, or it may be fixed and embedded for immunohistochemistry.

3.2. RNA Hygiene

1. Ribonucleases (RNases) are very sturdy enzymes and are ubiquitous in the environment. The surface of the skin is an especially rich source of RNases. In order to preserve the integrity of RNA during the extraction and processing of samples it is important to practice careful RNA hygiene.
2. Purified water (resistivity of 18.2 MΩ) should be treated with diethylpyrocarbonate (*see* **Note 2**) to destroy RNases. For enzyme reactions, use commercial nuclease-free water rather than DEPC-treated water as DEPC may interfere with some enzymes. DEPC will also interfere with UV spectrophotometry so use commercial nuclease-free water to dilute nucleic acids for spectrophotometry.
3. Treat instruments with an RNase reducing agent such as RNase ZAP and rinse with DEPC-treated water. Autoclaving alone does not destroy RNases. Pipet tips, centrifuge tubes, and other disposables should be certified nuclease-free. Gloves should be worn at all times when working with RNA.

3.3. RNA Extraction

1. To extract RNA, blot the RNAlater from the ovaries, weigh the tissues, and mince the ovaries into 600 µl TRI reagent. A single mouse ovary weighs 2.4–4.0 mg. If ovaries are being pooled, 30–50 mg of tissue can be processed in the volumes specified.
2. Homogenize the tissues with a Polytron homogenizer using a 7 mm probe. (The 7 mm probe fits well in a 12 × 75 mm test tube or a 1.5 ml Eppendorf centrifuge tube.) The probe must be thoroughly cleaned before use (*see* **Note 3**). Place the tube containing the sample in a beaker of ice. Homogenize the sample for two pulses of 10 s each, separated by 30 s rest on ice to prevent overheating of the sample. Run the Polytron probe in 400 µl fresh TRI reagent to rinse any residual tissue fragments from the probe.
3. Combine the two aliquots of TRI reagent into one (*see* **Note 4**). Add 200 µl bromochloropropane and 60 µl 3 M sodium acetate to the homogenate in TRI reagent, mix well, then incubate on ice for 15 min.
4. Transfer the sample to a 1.5 ml centrifuge tube and centrifuge for 5 min at 8,000 *g*. The clear aqueous (top) layer contains the total RNA.

5. Remove the aqueous layer, carefully avoiding the interface between layers (*see* **Note 5**). Add 1 ml RLT buffer to the aqueous phase (approximately 450 µl) and mix. Add 1.2 ml of 100% ethanol and mix.
6. For each sample, place a silica gel membrane spin column (RNeasy column) in a collection tube. Add 700 µl of the sample mixture to the membrane and centrifuge for 30 s at 10,000 *g*.
7. Discard the flow through and repeat the addition of sample mixture in 700 µl aliquots until all of the sample has been centrifuged through the membrane.
8. Wash the membrane with 350 µl of wash buffer RW1 and discard the flow through.
9. Add 80 µl of diluted DNase directly to the silica gel column and incubate at room temperature for 15 min. This step is necessary to ensure removal of residual DNA. DNA does not bind well to this silica gel membrane, but since the RNA will be used for microarray it is imperative that all traces of genomic DNA be removed from the sample.
10. After the incubation, add 350 µl of wash buffer RW1 to the membrane and centrifuge for 30 s at 10,000 *g* and discard the flow through.
11. Wash the membrane twice with 500 µl RPE wash buffer, passing each wash through the membrane by centrifugation for 30 s at 10,000 *g* and discarding the flow through.
12. Centrifuge the membrane without adding buffer for 2 min at 14,000 *g* to dry the membrane. Move the membrane to a new, well-labeled 1.5 ml collection tube.
13. To elute the RNA, add 50 µl nuclease-free water to the center of the membrane. Incubate for 10 min at room temperature.
14. Centrifuge the membrane for 1 min at 10,000 *g*. Repeat the elution step with another 50 µl of nuclease-free water, incubate at room temperature for 10 min, and centrifuge into the same collection tube.
15. Discard the membrane. The purified RNA is now located in 100 µl of nuclease-free water (*see* **Note 6**). Store the purified RNA at −70°C.

3.4. Analysis and Quantitation of RNA

1. Assess the quality and quantity of the purified total RNA using the Agilent RNA 6000 Nano LabChip in an Agilent Bioanalyzer. This microfluidics chip replaces both quantitation by UV spectrophotometry and analysis of quality by agarose gel electrophoresis and uses only 1 µl of RNA sample.
2. Place 550 µl of the gel matrix on a spin filter cartridge included with the reagent kit and centrifuge for 10 min at 1500 *g*. Store at 4°C in 65 µl aliquots.

3. Before use, bring reagents to room temperature including one 65 µl aliquot of gel matrix, the dye concentrate, and the marker mixture diluent. Vortex the dye concentrate and centrifuge 5–10 s at 10,000 *g*.
4. Add 1 µl of dye concentrate to the aliquot of gel matrix. Vortex well to mix and centrifuge at 13,000 *g* for 10 min in a 1.5 ml centrifuge tube.
5. Pipet 9 µl of the gel matrix into the 3 specified wells on the chip and pressurize one specified well with the accompanying priming station.
6. Pipet 5 µl marker mixture diluent into the 12 sample wells as well as the RNA ladder well. Denature the RNA samples and ladder at 70°C for 2 min and chill on ice. Add 1 µl of ladder to the appropriate well and 1 µl of sample to each sample well.
7. Vortex the chip for 1 min at 2400 rpm using the vortex adaptor.
8. Place the chip in the Agilent Bioanalyzer for analysis. The readout from the Agilent Bioanalyzer is illustrated in **Fig. 5.1**.

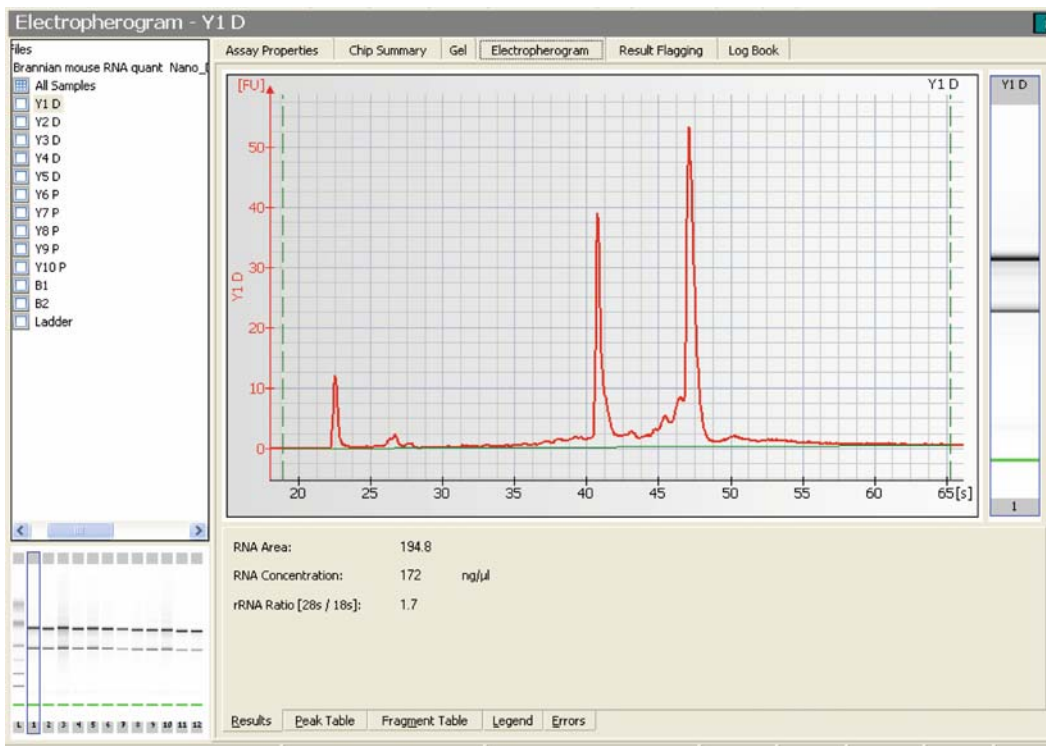

Fig. 5.1. Readout from Agilent Bioanalyzer RNA 6000 Nano LabChip. The bioanalyzer scans each RNA sample and produces an electropherogram for each sample. The electropherograms are interpreted into an gel view that mimics the appearance of the traditional agarose gel (bottom left corner) showing the RNA molecular weight marker ladder and the 18s and 28s ribosomal RNA bands of the 12 samples. In the figure, sample 1 is highlighted. The individual electropherogram for sample 1 is shown in the center of the figure with the gel view for that sample to its right. The RNA concentration is shown below in ng/µl.

3.5. Synthesis of First and Second Strand cDNA and cRNA

1. This protocol is designed to synthesize enough labeled cRNA for one microarray using 0.2–2.0 μg total RNA as the starting material (*see* **Note 7**). The volume of total RNA must be 10 μl or less. If the volume is greater than 10 μl, use vacuum concentration (i.e., SpeedVac) to reduce the volume. If the volume is less than 10 μl, add nuclease-free water.
2. Mix the 10 μl of total RNA with 1 μl of diluted bacterial control spike RNA and 1 μl of T7 Oligo (dT) primer. Incubate the mixture for 10 min at 70°C then chill the sample on ice. The bacterial control RNA is carried through the entire reaction series and serves as a control for the reaction series and also for the hybridization as bacterial samples are spotted on the microarrays as well as genes of the species of interest. The T7 Oligo (dT) primer is composed of a tract of oligo (dT) sequence and the sequence of the T7 promoter. The oligo (dT) section of the primer hybridizes with the poly-A tail of messenger RNAs in the sample. During the reverse transcription reaction in the next step, the sequence of the T7 promoter is added to each mRNA that is reverse transcribed.
3. Prepare a reverse transcription (RT) master mix during the priming reaction. The RT master mix contains 2 μl of 10x first strand buffer, 4 μl dNTP mix, 1 μl RNase inhibitor, and 1 μl ArrayScript reverse transcriptase for each sample of the reaction plus an additional 5% volume overage.
4. Pipet 8 μl of RT master mix into each RNA sample, mix by pipetting, and centrifuge briefly to collect all volume at the bottom of the tube. Incubate at 42°C for 2 h then chill on ice.
5. Prepare second strand master mix during the first strand synthesis incubation. For each sample, include 63 μl nuclease-free water, 10 μl second strand buffer, 4 μl dNTP mix, 2 μl DNA polymerase, and 1 μl RNase H plus 5% volume overage.
6. Add 80 μl second strand master mix to each sample, mix by pipetting, and centrifuge briefly. Incubate for 2 h at 16°C. This reaction is especially sensitive to temperature, to the extent that if using a thermal cycler with a heated lid the heat should be turned off or the lid should be left open because the heated lid will prevent the reaction from occurring at the appropriate temperature.
7. During the second strand synthesis reaction nuclease-free water should be heated to 50–55°C for the cDNA purification step.
8. When the second strand cDNA incubation is completed, add 250 μl of cDNA binding buffer to each sample and mix by pipetting up and down.

9. Transfer the mixture to a cDNA filter cartridge that is seated in a 1.5 ml collection tube for removal of salts and enzymes. Centrifuge the filter cartridge for 1 min at 10,000 *g* and discard the flow through.
10. Wash the filter cartridge once with 500 µl wash buffer, centrifuge for 1 min at 10,000 *g*, and discard the flow through. Centrifuge the filter cartridge for 1 min at 10,000 *g* without the addition of buffer to dry the cartridge, then move the filter cartridge to a new, well-labeled 1.5 ml collection tube.
11. Pipet 12 µl of preheated (50–55°C) nuclease free water onto the center of each cartridge. Incubate at room temperature for 2 min then centrifuge for 1.5 min at 10,000 *g* to elute the cDNA.
12. Add a second 12 µl aliquot of preheated nuclease-free water to each cartridge, incubate for 2 min at room temperature, and centrifuge at 10,000 *g* for 1.5 min to elute into the same collection tube.
13. The purified double-stranded cDNA is now located in the approximately 20 µl volume that was eluted in two steps from the filter cartridge. Discard the cartridge. Store the purified cDNA at −20°C or proceed with the in vitro transcription (IVT) reaction for the synthesis of biotinylated cRNA.
14. The IVT master mix can be prepared during the second strand cDNA incubation and held on ice during the cDNA purification step.
15. Add 20 µl of IVT master mix to each sample of purified double-stranded cDNA (20 µl) and mix by pipetting.
16. The IVT reaction is incubated at 37°C for 14 h. The T7 enzyme is an RNA polymerase that will transcribe any sequence containing the double-stranded T7 promoter at its 5' end. Because the T7 oligo (dT) primer used in the reverse transcription reaction (step 3.5.2 above) contained the sequence of the T7 promoter, each double-stranded cDNA transcript synthesized in step 3.5.6 will contain a double-stranded promoter for the T7 RNA polymerase enzyme at its 5' end and will thus serve as a template for the T7 RNA polymerase. The biotin-NTP mix contains ATP, GTP, CTP, and biotin-11-UTP, consequently the cRNA synthesized in the IVT reaction is labeled with biotin.
17. Add room temperature nuclease-free water (60 µl) and RNA binding buffer (350 µl) to the IVT reaction product.
18. Add 100% ethanol (250 µl) to each sample, pipet 3 times to mix, and transfer immediately to an RNA filter cartridge seated in a collection tube (*see* **Note 8**). This step is performed to remove enzymes, salts, and excess nucleotides from the cRNA.

19. Centrifuge the filter cartridges for 1 min at 10,000 *g* and discard the flow through.
20. Wash each cartridge with 650 µl wash buffer and centrifuge for 1 min at 10,000 *g*. Centrifuge the filter cartridge for 1 min at 10,000 *g* without the addition of buffer to dry the cartridge, then move the filter cartridge to a new, well-labeled tube.
21. Pipet 100 µl of preheated (50–60°C) nuclease-free water onto the filter cartridge and incubate at room temperature for 2 min. Nuclease-free water must be heated to 50–60°C before beginning cRNA purification.
22. Centrifuge the cartridge for 1.5 min at 10,000 *g* to elute the cRNA from the cartridge. Discard the cartridge.
23. Quantitate cRNA: Dilute 2 µl of cRNA in 78 µl nuclease-free water (dilution factor of 40) and read the UV absorbance at 260 nm and 280 nm using an 80 µl quartz cuvette.
24. Calculate the concentration of cRNA by the equation:

$$\text{Absorbance}_{260} \times \text{dilution factor} \times 40\ \mu\text{g/ml} \times 0.001\ \text{ml}/\mu\text{l} = \text{concentration in } \mu\text{g}/\mu\text{l}.$$

25. If the absorbance of cRNA at 260 nm is 0.54 then the concentration of cRNA is 0.864 µg/µl (0.54 × 40 × 40 × 0.001). Store the purified cRNA at −70°C or proceed to the next step.

3.6. Hybridization

1. cRNA must be fragmented prior to hybridization. 10 µg of purified biotinylated cRNA is needed for each microarray in a volume of 20 µl or less. If the volume containing 10 µg is greater than 20 µl, the sample should be concentrated using a vacuum centrifuge (i.e., SpeedVac).
2. Using the sample in the example in step 3.5.25 above, 11.57 µl of sample will contain 10 µg cRNA (10 µg/0.864 µg/µl = 11.57 µl). Add 8.43 µl of nuclease-free water to 10 µg cRNA to bring the volume to 20 µl.
3. If the synthesis reaction did not yield 10 µg of cRNA (this typically occurs if the starting material is less than 0.2 µg of total RNA), two rounds of cRNA synthesis may be employed in order to provide enough cRNA for the microarray. In this case, the first round of cRNA synthesis is the same as a single round synthesis protocol except that none of the NTP's in the IVT reaction are modified; biotinylated cRNA cannot be used as the source material for cDNA synthesis.
   a. The purified, unmodified single-stranded cRNA (up to 2 µg in a maximum of 10 µl) from the first strand reaction is primed for the second round of cDNA synthesis using 2 µl of random primers. Incubate at 70°C for 10 min then chill on ice.

b. Mix 2 µl 10x first strand buffer, 4 µl dNTP mix, 1 µl RNase inhibitor, and 1 µl reverse transcriptase plus 5% volume overage for each sample to prepare a first strand master mix.

c. Add 8 µl of this master mix to each sample, mix, and incubate at 42°C for 2 h.

d. Add 1 µl RNase H to each sample and incubate for 30 min at 37°C. The RNase removes the cRNA template so that only the newly synthesized first strand cDNA remains to serve as the template for second strand cDNA synthesis.

e. Add 5 µl T7 Oligo (dT) primer to each sample and incubate at 70°C for 10 min then chill on ice. This is the same primer used for the reverse transcription reaction in the first round of amplification. It will prime the second strand synthesis of cDNA and ensure that each transcript bears the T7 promoter sequence required for the IVT reaction.

f. Prepare the second strand master mix while the priming reaction incubates. Include 58 µl nuclease-free water, 10 µl 10x second strand buffer, 4 µl dNTP mix, and 2 µl DNA polymerase per sample plus 5% volume overage.

g. Add 74 µl second strand master mix to each sample and incubate at 16°C for 2 h. Complete the purification of double-stranded cDNA.Synthesize, purify, and quantitate biotinylated cRNA as described above.

4. Add 5 µl of Fragmentation buffer to 10 µg cRNA and incubate the sample at 94°C for 20 min, then chill on ice for a minimum of 5 min (*see* **Note 9**).

5. Prepare a hybridization solution master mix containing 78 µl hybridization buffer component A, 130 µl component B, and 27 µl nuclease-free water for each sample plus 5% volume overage.

6. Add 235 µl of the hybridization solution master mix to each fragmented sample of cRNA. Mix the samples by vortexing and denature the cRNA by incubating at 90°C for 5 min. Chill samples on ice for 5 min before loading the microarrays.

7. Use CodeLink (6–8) Whole Mouse Genome microarrays. These microarrays contain approximately 30,000 single-stranded 30-mer oligonucleotide probes for mouse genes/transcribed sequences. CodeLink microarrays are treated glass microscope slides designed with a removable flexible coverslip with a tab. The coverslip is glued around the edges with a port at each of the four corners.

8. Using a wide-bore 1 ml pipet tip, 250 µl of hybridization solution containing fragmented biotinylated cRNA is slowly injected through one of the ports.

9. The ports are sealed with sealing strips and the microarrays are incubated at 37°C for 18 h in a shaking incubator set at 300 rpm.
10. In preparation for post-hybridization wash steps, 240 ml of 0.75x TNT buffer should be brought to 46°C in a waterbath overnight.

3.7. Post-hybridization Processing

1. Remove the microarrays from the hybridization incubator and carefully peel off the flexible coverslips by lifting the tab. Place the microarrays in room temperature 0.75x TNT until all coverslips have been removed.
2. Place a rack holding all of the microarrays into 0.75x TNT buffer at 46°C, and incubate the arrays for exactly 1 h to remove non-hybridized and non-specifically hybridized cRNA.
3. Move the rack of microarrays into a tray containing Streptavidin-Alexa 647 (*see* **Note 10**) and incubate covered at room temperature for 30 min.
4. Fill four 250 ml reservoirs with 1x TNT buffer at room temperature. Move the rack of microarrays from the Streptavidin-Alexa fluor 647 into the first reservoir and incubate for 5 min.
5. Wash 3 more times in fresh 1x TNT, 5 min each wash. Wash the slides a final time in 0.1x SSC/0.05% Tween 20 for 30 s with continuous movement up and down of the slides in the buffer.
6. Dry the slides by centrifugation using a 96-well plate rotor to carry the rack holding the microarrays. Place the slides in an opaque slide box until they can be scanned.
7. Scan the microarrays with a GenePix Pro 4000B scanner (Molecular Devices, Sunnyvale, CA). The scanner should be turned on and the GenePix Pro software opened 15 min before use. Scan the slides, saving each with a unique name that includes the serial number of the microarray.
8. If regions of high background are identified in the scans, the final washing step in 0.1x SSC/0.05% Tween 20 for 30 s should be repeated and the slide scanned again.

3.8. Analysis of Microarray Data

1. Scanned microarray images are imported into CodeLink 5.0 software (**Fig. 5.2A**). This software associates the image of each spot on the array with an expression value that reflects the pixel intensity of the fluorescence of the hybridized sample (**Fig. 5.2B**). The software also associates the expression value of each spot with gene identifiers (i.e., gene name, GenBank accession number, Locus Link identifier). CodeLink software also provides several tools to analyze the quality of the microarrays. For example, the number of spots with background contamination can be visualized as well as the coefficient of variation of the microarray slide set.

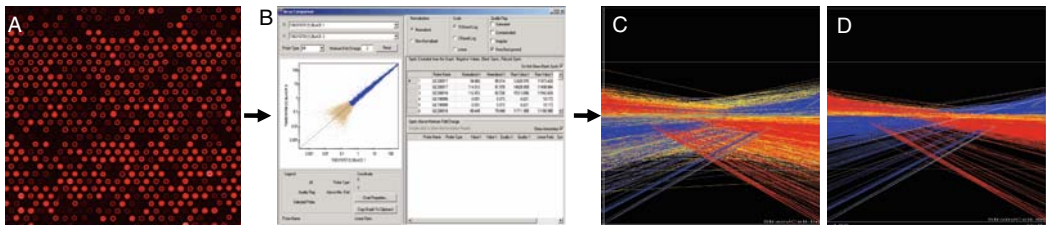

Fig. 5.2. Images of DNA microarray analysis. **Panel A** shows the appearance of raw data from the microarray scanner; the varying intensities of each spot on the array can be seen. **Panel B** illustrates data from CodeLink 5.0 software which assigns a numeric value to the pixel intensity of each spot on the array associates that information with the gene name. Data from GeneSpring 7.0 software comparison of gene expression in the ovaries of 90 versus 180-day-old lethal yellow mice are shown in **Panels C** and **D**. Each line in these graphs represents one gene. All genes on the microarray are shown in the graph in **Panel C**, whereas **Panel D** shows only the genes that were found to be significantly different between 90- and 180-day-old mouse ovaries.

2. A useful tool allows all of the spots on one microarray to be graphed against all of the spots on a second microarray. When two arrays measuring gene expression from the same tissue are graphed against each other, there is a strong correlation between the two data sets because the majority of genes are expressed identically (**Fig. 5.3A**). The broadening of the line into an arrow shape reflects genes whose expression is near background. In contrast, when there is a problem with a sample, the graph yields a "cloud effect" (**Fig. 5.3B**).

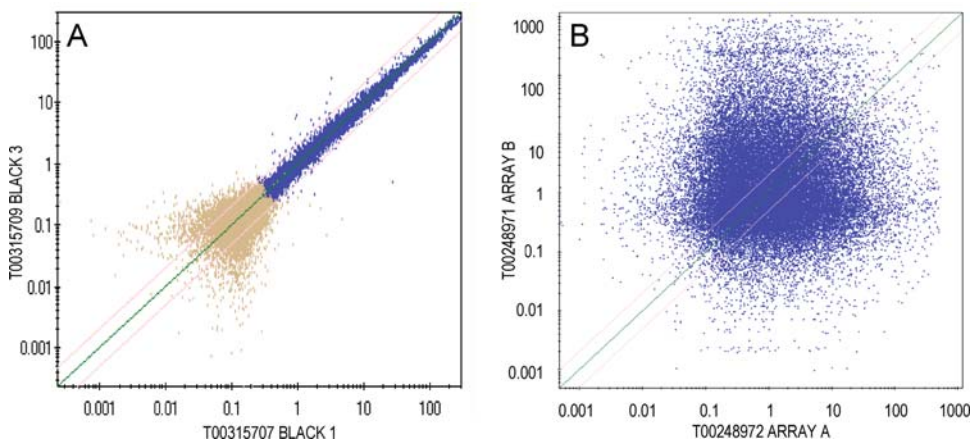

Fig. 5.3. Log base 10 data from two microarrays are graphed against each other. **Panel A**: The majority of genes in a given tissue are expressed equally; therefore, graphing the log base 10 data from two microarrays shows a strong correlation with less than 2-fold difference in expression. (The faint lines on each side of the regression line illustrate 2-fold difference in expression.) The broadening of the data into an arrow shape, shown in lighter gray, reflects genes whose expression is near background. **Panel B** illustrates the "cloud effect" observed when a failed microarray is graphed against a valid microarray. The data from the microarray in **Panel B** was discarded.

3. If the cloud effect is observed when two biological replicates are graphed, then the array that is the source of the problem must be discarded and the microarray for that sample run again.
4. Data can be exported from CodeLink software in a variety of formats that support software programs for further analysis of microarray data. We routinely export data in Excel format and in a tab-delimited format specified for upload to GeneSpring software (*see* **Note 11**).
   a) Data from the Excel output are uploaded to Acuity software (Axon). This program is the first point at which we can observe gene names associated with expression values.
   b) Data from the tab-delimited format are uploaded to GeneSpring 7.0 (Agilent) (**Fig. 5.2C**). GeneSpring is used to normalize the data.
   c) The expression of each gene is normalized to the median gene expression, and each microarray is normalized to the 50th percentile of gene expression. Gene Spring also transforms the data to log base 10. Statistical analysis is performed using the normalized and log-transformed data.
   d) GeneSpring 7.0 performs t-tests for comparisons of two groups or analysis of variance for comparisons of multiple groups. The p value can be varied and should be set at 0.05 or lower.
   e) Since thousands of comparisons are performed across the microarray, a multiple testing correction such as the Benjamini and Hochberg False Discovery Rate should be applied. With this test, approximately 5% of the genes pass the test by chance. GeneSpring also provides tools for cluster analysis and for gene ontologies (*see* **Note 12**).
   f) Many genes, sometimes several thousand, are often identified as exhibiting significantly different expression (**Fig. 5.2D**). The significance lists include genes whose expression is near the limits of detection (near background) as well as genes for which the difference between the comparison groups is minimal. To make the lists of genes more manageable, we eliminate genes for which the means of all comparison groups are near background (<0.02) as well as genes for which the group means are not greater than 2-fold different from each other ($\pm 10\%$) (*see* **Note 13**).
   g) CodeLink microarrays contain many expressed sequence tags (ESTs) and gene sequences that are not named and whose functions are unknown. These genes are typically set aside but not discarded. With time, these genes will be associated with a name and function and it will be possible to fit them into known gene ontologies (**Table 5.1**).

Table 5.1
Gene expression data from DNA microarray analysis

GenBank ACCN#	Expressed Sequence Tag Description	90 d	180 d	P value	Fold Exp
AK087684	2 days pregnant adult ovary cDNA, RIKEN clone:E330004G06	0.22	1.70	0.048	7.7
AK054275*	2 days pregnant adult ovary cDNA, RIKEN clone:E330009D23	0.63	1.99	0.030	3.2
AK054483	2 days pregnant adult ovary cDNA, RIKEN clone:E330031A18	0.61	1.41	0.026	2.3
AK054536	2 days pregnant adult ovary cDNA, RIKEN clone:E330038L21	1.82	4.95	0.017	2.7
AW553537	Mouse Newborn Ovary cDNA Library cDNA clone L0228E02 3′	1.34	0.52	0.018	0.4
AW555412	Mouse Newborn Ovary cDNA Library cDNA clone L0255E08 3′	0.21	0.44	0.038	2.2
BB556413	RIKEN 2 days pregnant adult ovary cDNA clone E330023M09 3′	0.63	1.33	0.013	2.1
BB559749	RIKEN 2 days pregnant adult ovary cDNA clone E330040F24 3′	1.53	4.67	0.013	3.1
AV093810	C57BL/6 J ES cell cDNA clone 2400004K12	19.62	141.63	0.01	7.2

Genes expressed in the ovaries of 90-day-old (90 d) versus 180-day-old (180 d) lethal yellow mice were compared. Shown here are the expression values at 90 and 180 days for 9 expressed sequence tags that represent unnamed genes cloned from ovary tissue or embryonic stem cells. In addition to the gene name or description of the expressed sequence tag and expression data, other types of data that can be obtained from DNA microarray analysis include the p value that denotes significant differences in gene expression and fold expression values (Fold Exp) (expression at 180 days divided by expression at 90 days). In addition, the GenBank accession number allows searching of NCBI databases for a variety of types of gene and protein information.Expressed sequence tags eventually are identified and associated with a cellular function. For example, an NCBI search found that AK054275, denoted with an asterisk in the table, has been identified as Lcor, a ligand-dependent nuclear receptor corepressor, also known as transcription factor Mlr2 (13).

h) Other software packages are available that are designed specifically to identify relationships among differentially expressed genes in a given experimental paradigm, such as Ingenuity Pathways Analysis (Redwood City, CA) and Ariadne Pathway Studio (Rockville, MD). These programs can be useful for data analysis. However, there is no substitute for analyzing your own data. The pathway analysis software programs recognize relationships that fit specific algorithms. If relationships in your data do not fit those algorithms, the relationships will be missed by the software.

i) It is important to carry out confirmatory studies with selected genes using complementary technologies. Real time RT-PCR (5, 6) confirms differential gene expression. Similarly, immunoblot (6), enzyme linked immunosorbent assay, and immunohistochemistry (5) confirm differential expression of the protein products of selected genes.

j) Microarray data should be deposited in a public database such as the Gene Expression Omnibus (GEO) database that is maintained by the National Center for Biotechnology Information (www.ncbi.nlm.nih.gov/geo) as recommended by Minimum Information About a Microarray (MIAME) standards (9). Many journals require public deposition of microarray data before publication.

k) The study of the effect of aging and obesity on gene expression in the mouse ovary (10) is a good example of the types of data and results that can be gained from DNA microarray experiments. Gene expression data were compared between young (90 day) versus old (180 day) mice with the lethal yellow gene mutation and 90 versus 180-day-old lean black littermates. In addition, comparisons were made between black versus lethal yellow at 90 days of age and between black versus lethal yellow at 180 days of age. A number of genes related to sterol synthesis and metabolism were shown to be differentially expressed in the ovaries of aging (180 day old) lethal yellow mice compared to black mice but those genes were not differentially expressed at 90 days of age. The data suggest that differential expression of these genes is directly related to acquired obesity and not to the mutation that causes the lethal yellow phenotype.

4. NOTES

1. The synchronization with Antide should yield ovaries comparable to a natural cycle on the morning of proestrus. The timing may be adjusted to obtain earlier or later stage ovaries. To obtain luteinized ovaries, hCG (1 IU/5 g BW) may be given 48 h after eCG with euthanasia 12–24 h later.
2. Add 1 ml of DEPC to 999 ml water and stir on a stir plate overnight. Autoclave the water to destroy the DEPC.
3. To clean the 7 mm Polytron probe, fill a 50 ml graduated cylinder with DEPC-treated water and laboratory detergent. Run the Polytron probe in the soapy water. Run the

Polytron probe in clean DEPC-treated water several times to rinse. Spray the outside and inside of the probe with RNase ZAP and rinse thoroughly with DEPC-treated water. When homogenizing multiple tissues, run the probe in a graduated cylinder of DEPC-treated water between each sample to prevent cross contamination of samples. It is also important to clean the homogenizer probe immediately after use. TRI reagent is corrosive and will ruin the probe if it is not removed. Clean with laboratory detergent in DEPC-treated water as at the beginning of the homogenizations.

4. When working with small quantities of tissue this technique rescues the residual sample that is retained in the Polytron probe and would otherwise be lost. An alternate method when working with very small samples is to use a reagent kit such as the Ambion RNAqueous micro kit.
5. After centrifugation, the aqueous (clear, top) layer contains the RNA, the organic (pink, bottom) layer contains proteins, and the DNA is at the interface. It is important to avoid the interface when withdrawing the RNA layer in order to reduce DNA contamination of the RNA sample. Proteins can be extracted from the organic layer as described elsewhere (11).
6. The RNA can be eluted into a smaller volume, but our experience is that recovery is better if we use two elution steps with 50 μl volume each. If the sample is too dilute for downstream purposes the RNA can be concentrated with a SpeedVac concentrator (Thermo Fisher Scientific, Waltham, MA). In our hands, the silica gel membranes yield a more consistent RNA sample than the previous method using phenol/chloroform/isoamyl alcohol (11). The spin column purification technologies for RNA continue to evolve and a variety of these matrices are now available. The RNeasy silica gel membranes exclude RNA species smaller than 200 nucleotides so this method cannot be used if microRNAs are desired; however, the RNAqueous micro kit (Ambion) uses a similar spin column technology and will recover microRNAs.
7. If less than 0.2 μg total RNA is available, two successive rounds of cRNA synthesis can be employed—see Section 3.6.3. Be aware of the time demands of this protocol. From initiation of the synthesis of first strand cDNA to the final scanning of microarray slides requires 3 days. There are several points (noted in the methods) at which the samples can be frozen and the experiment resumed at a later time.

8. Add the water and RNA binding buffer to all of the samples. Add ethanol to one sample and transfer that sample to its filter cartridge before adding ethanol to the next sample. The cRNA is in a semi-precipitated state after addition of the ethanol so it is important to transfer it to the cartridge rapidly.
9. The cRNA is fragmented by metal-induced hydrolysis. The purpose of fragmentation of the cRNA is to reduce secondary and tertiary RNA structure that interferes with RNA hybridization to oligonucleotide spotted on the microarray slide, thereby improving hybridization kinetics (12).
10. The Alexa 647 fluorescent signal does not photobleach as rapidly as some other fluorescent probes.
11. More recent versions of GeneSpring appear to have changed their algorithms for statistical analysis as well as the user interface and are less user friendly than the 7.0 version.
12. CodeLink microarrays use a single sample on each array, and therefore a single dye for each array. Data analysis therefore deals with fluorescent intensity rather than intensity ratios.
13. The 2-fold cut-off is an arbitrary point widely used in gene expression studies. It is based on the assumption that if the means of two groups differ by less than 2-fold, the differences are not likely to be biologically significant even if they are mathematically significant. It is certain that some biologically important genes will be missed by using the 2-fold cut-off, but it is expected that the majority of genes will be identified in most tissues.

Acknowledgments

This work was supported in part by NSF IBN-0315717, NIH R15 HD044438 and by NIH INBRE 2P20 RR16479. The authors would like to thank Sandy Bradley for assistance with preparation of the manuscript.

References

1. Pasquali, R., Gambineri, A. (2006) Polycystic ovary syndrome. A multifaceted disease from adolescence to adult age. *Ann. N.Y. Acad. Sci.* **1092,** 158–174.
2. Klebig, M., Wilkinson, J., Geisler, J., and Woychik, R. (1995) Ectopic expression of the agouti gene in transgenic mice causes obesity, features of type II diabetes, and yellow fur. *Proc. Natl. Acad. Sci. USA* **92**, 4728–4732.
3. Brannian, J.D., Furman, G.M., Diggins, M. (2005) Declining fertility in the Lethal Yellow mouse is related to progressive hyperleptinemia and leptin resistance. *Reprod. Nutr. Dev.* **45**, 143–150.
4. Granholm, N. and Dickens, G. (1986) Effects of reciprocal ovary transplantation on reproductive performance of lethal yellow mice. *J. Reprod. Fertil.* **78**, 749–753.

5. Brannian, J.D., Eyster, K.M., Weber, M., and Diggins, M. (2008a) Pioglitazone administration alters ovarian gene expression in aging obese lethal yellow mice. *Reprod. Biol. Endocr.* **6**,10 doi:10.1186/1477-7827-6-10.
6. Eyster, K.M., Klinkova, O., Kennedy, V., Hansen, K.A. (2007) Whole genome deoxyribonucleic acid microarray analysis of gene expression in ectopic vs. eutopic endometrium. *Fertil. Steril.*, **88**, 1505–1533.
7. Shippy, R., Sendera, T.J., Lockner, R., Palaniappan, C., Kaysser-Kranich, T., Watts, G., Alsobrook, J. (2004) Performance evaluation of commercial short-oligonucleotide microarrays and the impact of noise in making cross-platform correlations. *BMC Genomics* **5**, 61.
8. Yauk, C.L., Berndt, M.L., Williams, A., Douglas, G.R. (2004) Comprehensive comparison of six microarray technologies. *Nucleic Acids Res.* **32**, e124.
9. Brazma, A., Hingamp, P., Quackenbush, J., Sherlock, G., Spellman, P., Stoecker, C., et al. (2001) Minimum information about a microarray experiment (MIAME)—toward standards for microarray data. *Nat. Genet.* **29**, 365–371.
10. Brannian, J., Eyster, K., Greenway, M., TeSlaa, K., Diggins, M. (2008b) Obesity-related modification of ovarian gene expression and glucocorticoid metabolism in aging lethal yellow mice. *Biol. Reprod. Suppl.* 1 **78**, 243.
11. Rodrigo, M.C., Martin, D.S., Redetzke, R.A., Eyster, K.M. (2002) A method for the extraction of high quality RNA and protein from single small samples of arteries and veins preserved in RNAlater. *J. Pharmacol.-Toxicol. Meth.* **47**, 87–92.
12. Mehlmann, M., Townsend, M.B., Stears, R.L., Kuchta, R.D., Rowlen, K.L. (2005) Optimization of fragmentation conditions for microarray analysis of viral RNA. *Anal. Biochem.* **347**, 316–323.
13. Kunieda, T., Park, J.-M., Takeuchi, H., Kubo, T. (2003) Identification and characterization of *Mlr1,2*: two mouse homologues of *Mblk-1*, a transcription factor from the honeybee brain. *FEBS Lett* **535,** 61–65.

Chapter 6

Genomics Analysis: Endometrium

Ricardo Francalacci Savaris and Linda C. Giudice

Abstract

Microarray technology has been used widely in gynecology. Numerous studies have used this method to address biological questions related to human endometrium. The cyclic changes of endometrium confer special characteristics that should be considered before genomic analysis. The present study reviews these considerations and the principles of transcriptomic analysis through an example of a comparison of three different phases of the menstrual cycle.

Key words: Endometrium, genomic analysis, transcriptome, microarray, human.

1. Introduction

In the last few years, several investigators using microarray technology have pursued analysis of endometrial gene expression. This approach provides a snapshot of the current events, at the transcript level, in a distinctive tissue under certain conditions. With this technique, it is possible to compare the biological events between a pathological condition versus control. Contrary to traditional methods, such as real-time PCR, or immunohistochemistry, where the expression of one or a few genes is analyzed across 2 or more groups, in gene expression microarrays thousands of genes can be analyzed at the same time. The first paper reporting on the transcriptome of human endometrial cells in culture was published in 2000 (1). Since then, a remarkable number of studies have used this technology, as summarized in Horcajadas et al. (2).

Endometrium is a dynamic tissue that regenerates all of its cellular constituents on a cyclic basis, in response to steroid hormones. The 28-day human menstrual cycle is divided into

O.-K. Park-Sarge, T.E. Curry, Jr. (eds.), *Molecular Endocrinology,* Methods in Molecular Biology 590,
DOI 10.1007/978-1-60327-378-7_6,

Table 6.1
Phases of the menstrual cycle

Phase	Days of the cycle	
Menses	1–4	
	Proliferative	Secretory
Early	5–7	15–22
Middle	8–10	23–25
Late	11–14	26–28

phases: proliferative (early, mid, late), secretory or luteal (early, mid, late), and menstrual (3) (**Table 6.1**). These phases are distinct from each other with regard to cellular proliferation, differentiation, and function (4). Moreover, the endometrium is a complex mucosa composed of two major compartments: the basalis layer, which remains intact from cycle to cycle, and the functionalis layer, which is shed during menses (3). The functionalis layer has luminal and glandular epithelia; whereas, the basalis has only glandular epithelium. Both have stromal compartments comprised of fibroblasts, immune cells, vascular endothelium, smooth muscle cells, and pericytes. Thus, intrinsic variability needs to be considered in designing and analyzing studies on the endometrium. Furthermore, this tissue also has abnormal states, such as dysfunctional bleeding, infection, hyperplasia, cancer and adverse effects on its anatomy and physiology, such as leiomyomata and polyps, which can alter some of the endometrial gene profile (5).

In order to conduct a microarray study, it is necessary to plan 9 steps:

1. Study design.
2. Collection of the samples.
3. RNA extraction.
4. In vitro transcription.
5. Labeling.
6. Chip hybridization.
7. Scanning the fluorescence generated from the chip.
8. Data analysis and data mining.
9. Validation of the results.

Steps from 4 through 7 can be conducted in core facilities. This review will focus on steps 1, 2, and 8, with the endometrium as the tissue of consideration.

1.1. Study Design

Normal endometrium has at least 7 intrinsic collection points from the different cycle phases (as shown in **Table 6.1**) that can be used for comparison with pathologic states of the tissue. For example, if an investigator wants to identify genes associated with abnormal uterine bleeding in women who use contraceptive steroids, subjects should be those with and without abnormal uterine bleeding, using the same type of contraceptive, for a comparable time of use, but without the other confounding factors, such as presence of cancer or infections. A challenging issue in studies on endometrium is that of "normal" controls. Also, the use of medication should be noted, because these may have an effect on the endometrial transcriptome (6). The same principle may be applied to the presence of submucosal leiomyomata (5), hydrosalpinges (7), polycystic ovaries, and other conditions that may impact endometrial gene expression. The present study compares the transcriptome of three different phases of the menstrual cycle (proliferative, and mid and late secretory phases). With this example, different biological processes and gene expression in the tissue over time (menstrual cycle) can be identified.

1.2. Sample Size

The sample size and power of a study are normally used for clinical trials, but only recently have microarray studies addressed this important issue. There are many methods and reviews for calculating sample size (8–12). Calculation of sample size is a demonstration of the power of the study. It takes into account the variance of individual measurements, the acceptable false-positive rate (alpha error), and the desired discriminatory power of the microarray. The alpha (α) and beta (β) errors are also known as false positive error (type I error), and false negative error (type II error), respectively. An $\alpha = 0.05$ means that the researcher is willing to accept 5% of false positive cases. Likewise, a $\beta = 0.2$ means that the researcher is willing to accept 20% falsely negative cases. Because of the large number of genes involved (over 40,000), a general guideline is to choose $\alpha = 0.001$ and $\beta = 0.05$ (13). Other parameters that should be taken into consideration include the fold change between two conditions. In this situation, the researcher will try to identify the genes that have a 2-fold change or higher between two conditions. The higher the fold-change, the lower the sample size. Another parameter is the standard deviation (σ) of the logarithmic expression level among samples. The logarithmic expression relates to data transformation, usually done by a data analysis software, such as GeneSpring. The log transformation will give the data a Gaussian distribution, an imperative condition to use a parametric test, with the Student's *t*-test being the most commonly used. Our lab has verified that endometrial samples have a standard deviation of 0.2 in Affymetrix HG-U133 Plus 2 gene chip array (data not published). Liu et al. proposed a quick calculation for sample size between 2 groups, considering a False Discovery

Rate of 5%, and the proportion of non-differentially expressed genes (π_0) at 0.50, 0.90, and 0.95 (10). In this scenario, it is necessary to have a minimum of 4 samples in each group to obtain at least 80% power, and a $\pi_0 = 0.9$. For 3 or more groups, using the same scenario, it is necessary to have 7 samples in each group (10). For a power of 0.95, 8 samples in each group would be required. A simple estimate of the number of biological replicates in a microarray experiment is based on degrees of freedom (*df*). A reasonable guide is to have $df = 5$ or greater. This can be determined by counting the number of independent biological replicates (e.g., independent subjects, independent animals, independent cell lines, or independent pools of microdissected tissues) and subtracting the number of distinct treatments from the number of independent biological replicates (13). For a single-factor experiment with *N* patients divided into *p* treatment groups, the residual *df* are N – p (14). For instance, if we want to compare 2 groups, in order to have a $df = 5$, it would be necessary to have, at least, 7 samples (i.e., 4 cases and 3 controls). Lee et al. (13) have presented a modified formula based on sample size calculation for comparing two means:

$$n = \frac{4(z_\alpha + z_\beta)^2}{\left(\frac{\delta}{\sigma}\right)^2}, \text{where}$$

α error (two tails) = 0.001 = 3.29 (value obtained from a *z*-distribution table)
β error = 0.05 = 1.645 (95% power)
δ = fold change in log scale (× 2; i.e. $\log_2 = 1$)
σ = standard deviation of gene array (microarray chip), 0.2 in our samples

2. Materials

An endometrial biopsy was performed in 12 healthy, fertile subjects according to the three phases of the menstrual cycle [early proliferative ($n = 4$), mid ($n = 4$) and late secretory ($n = 4$)], based on the date of last menstrual period and luteal hormone (LH) surge (day 13 of the menstrual cycle). Sample size was calculated based on degrees of freedom ($df = 9$). Samples were stored in cryotubes, snap frozen in liquid nitrogen, and kept at –80°C until further analysis.

2.1. RNA Extraction

The TRIzol® method has been used in our laboratory for RNA extraction. The procedure is done under sterile conditions, using high grade materials.

2.1.1. Hardware

1. Fume hood.
2. 14 mL sterile plastic tube.
3. Rack for 14 mL tubes.
4. Pipette 1000 μL and 200 μL.
5. Sterile tips for 1000 μL and 200 μL pipette.
6. Rotor-stator homogenizer (Pro Scientific Inc. Oxford, CT, USA).
7. Microcentrifuge with temperature control (Eppendorf centrifuge 5415R, Eppendorf, Westbury, NY).
8. Centrifuge without temperature control (Eppendorf 5417C, Eppendorf).

2.1.2. Reagents

1. TRIzol ® (Invitrogen, Carlsbad, CA, USA).
2. H_2O RNAse free.
3. Ethanol 70% and 100%.
4. 14.3 M β-mercaptoethanol.
5. Chloroform.
6. Isopropyl alcohol.
7. Tris/HCl 1 M (USB, Cleveland, OH)—make a 10 mM solution.

2.2. RNA Purification

RNA purification is done with RNeasy Plus Mini Kit (QIAGEN, Valencia, CA).

2.3. Probe Preparation and GeneChip® Hybridization

Purified RNA with known concentration and analysis of the purification.

1. Core facility for in vitro transcription, labeling, GeneChip® hybridization, washing, staining, and scanning.
2. GeneChip Array: Human Genome—U133 Plus 2 (Affymetrix Inc., Santa Clara, CA) with 54,646 gene probes (one for each sample).

2.4. Analysis of the Genes

1. CEL files sent by the core facility.
2. Software for analysis: GeneSpring GX 7.3.1 (Agilent Technologies , Inc. Santa Clara, CA).

2.5. Interpretation of the Gene List

1. Ingenuity Pathways Analysis (IPA) 5.5.1 (Ingenuity, Redwood City, CA). Our lab has been using this software for gene interpretation.
2. Gene list from ANOVA generated from GeneSpring in an Excel spreadsheet.

3. Methods

3.1. RNA Extraction

To prevent cross-contamination among the samples, prepare 3 tubes (#1: 4 mL H_2O RNAse free; #2: 4 mL ethanol 100%; #3: H_2O RNAse free) to rinse the rotor.

1. Put 1 mL of TRIzol into a 14 mL Falcon® tube, add the endometrial sample, and homogenize it completely until a homogeneous solution is obtained and tissue pieces are not observed.
2. Transfer the homogenate into a labeled 1.5 mL tube, add 200 μL of chloroform, and vortex for 15 s.
3. Centrifuge at 16,100 *g* at 4°C for 15 min. It will yield 3 layers, an aqueous upper phase (containing the RNA), a white, and a pink phase.
4. Take the supernatant with a 200 μL pipette and put into a new 1.5 mL labeled tube. Avoid the white layer interface. Discard the white and the pink phase into hazardous waste.
5. Add an equal amount of isopropyl alcohol into the tube, i.e., if 210 μL of supernatant are removed, add 210 μL of isopropyl alcohol.
6. Vortex for 15 s, and let the sample sit for 10 min.
7. Centrifuge at 16,100 *g* at 4°C for 10 min. Remove supernatant into the hazardous waste and keep the pellet.
8. Dry the opening part of the tube with a paper towel. Decant the liquid by placing the tube upside down.
9. Add 1 mL of ethanol 70%. You will be able to see the pellet at this point.
10. Centrifuge at 16,100 *g* at 4°C for 5 min.
11. Remove and discard the supernatant. Dry the opening part of the tube with a paper towel and allow the pellet to dry. Flick the tube occasionally to verify if the pellet moves or not. If it moves, it means it is not dry enough.
12. Add 100 μL of RNAse free H_2O and leave in the thermal plate at 4°C.

Determine the amount of RNA in the spectrophotometer according to one's laboratory protocol. The ratio of 260/280 should be between 1.9 and 2.1 to verify RNA purity. If the ratio is below 1.9, there is protein contamination; if it is higher, it could be RNA degradation or other sort of contamination. If the ratio is below 1.9, do not proceed with the microarray.

3.2. RNA Purification

It is important to know how much total RNA there is in the sample. If <50 μg use everything for purification; otherwise, save for later. One will need 50 μg of total RNA for column purification. Adjust the volume to 100 μL. For instance, if the original sample has 250 μg of total RNA suspended in 98 μL, to obtain 50 μg, the calculation is $(50 \times 98)/250 = 19.6$ μL; thus take 19.6 μL of the original sample (total RNA sample) and add 80.4 μL of RNAse free H_2O for a final volume of 100 μL.

1. Take the RLT Plus from the QIAGEN RNeasy Plus Mini kit and the β-Mercaptoethanol (β-ME 14.3 M) under the fume hood. Make a 1:100 dilution of β-ME as follows: 1 mL of RLT + 10 μL of β-ME = RLT + β-ME.
2. Take the RNA sample (100 μL with ≤50 μg of RNA) and mix with 350 μL of RLT + β-ME, put into the gDNA Eliminator Mini Spin Column, and spin at 16,100 *g* for 30 s. There should be 450 μL (100 μL of RNA sample + 350 μL of RLT buffer solution). Discard the column and save the flow-through.
3. Add 1 volume of 70% ethanol (±450 μL, i.e., the same amount of the flow-through) to the flow-through, and mix well by pipetting. Do not centrifuge. It should yield 900 μL.
4. Transfer 700 μL of the sample, including any precipitate that may have formed, to an RNeasy spin column in a 2 mL collection tube (the pink tube). Close the lid gently, and spin at 16,100 *g* for 15 s. Discard the flow-through in the hazardous waste. If the amount of RNA from step 3 is higher than 700 μL, repeat the same step in the same RNeasy spin column. One can put 2 × 450 μL, because you have 900 μL from step 3.
5. Add 700 μL of Buffer RW1 to the RNeasy pink tube. Close the lid and spin at 16,100 *g* for 15 s to wash the spin column. Discard the flow-through.
6. Add 500 μL of Buffer RPE to the RNeasy pink tube. Spin at 16,100 *g* for 2 min to wash the spin column.
7. (Optional to further dry the RNA) Place the RNeasy spin column in a new 2 mL collection tube (round bottom). Spin at 16,100 *g* for 1 min to dry the RNA and remove the buffer.
8. Place the RNeasy spin column in a new 1.5 mL collection tube supplied by QIAGEN. Add 30 μL of RNAse free water directly to the spin column membrane. Close the lid and centrifuge at 16,100 *g* for 1 min.

This should yield purified RNA whose concentration can be determined by spectrometry. Label the tube as pRNA with the sample # and the concentration on the side of the tube—for instance 0.182 μg/μL.

3.3. Probe Preparation and GeneChip® Hybridization

Purified RNA is then sent to the microarray core facility for in vitro transcription, labeling, GeneChip® hybridization, washing, staining, and scanning. Our lab has been using the Human Genome U133 Plus 2.0 array from Affymetrix because it has the complete human genome with 54,646 gene probes. The fluorescent readings are sent by the facility core in electronic files (.CEL files). These .CEL files are specific from Affymetrix. Each sample hybridized with a single GeneChip® will generate a corresponding .CEL file.

3.4. Analysis of the Genes

Once the .CEL files from each sample are sent from the core facility, the normal workflow in microarray data analysis follows these steps:

1. Import data and set up the experiment (see **Section 3.5**).
2. Verify the quality of microarray data.
3. Filter for differential expression.
4. Statistical analysis.
5. Reference to known biology.
6. Export results.

3.4.1. Steps for Data Analysis

1. Data mining starts from .CEL files, which represents the data derived from the scanned GeneChip. Every .CEL file should be named accordingly (*see* **Note 1**). Import the .CEL files into the GeneSpring GX program.
2. Choose the correct chip, in this case Affymetrix HG-U133_Plus_2 (*see* **Note 2**).
3. Pre-normalize the .CEL files using Robust Multi-array Analysis (RMA) (13) (*see* **Note 3**).
4. After pre-normalization, name the experiment and its parameters.
5. Normalize the samples "per gene: Normalize to median" (*see* **Note 4**).
6. Give parameters for the samples, in order to identify replicates. We use the phase of the cycle as the replicate parameters (Prol, MSE, LSE).
7. Interpretation of the sample data should be determined next. Keep a parameter, in this case "phase," as a categorical variable for sample analysis and to identify replicates (*see* **Note 5**).
    1. Check quality of the experiment at the sample level (*see* **Note 6**).
    2. Perform ANOVA analysis using all genes (54,646) as the reference.
8. Compare the sample replicates (Prolif. vs. MSE vs. LSE) using "phase" as the parameter.

9. Assume that the test is parametric with equal variances (because of the normalizations).
10. Choose a false discovery rate of 5% or lower.
11. Choose the Multiple Test correction as Benjamini and Hochberg False Discovery Rate (*see* **Note 7**).
12. Choose the post-hoc test as Tukey (this post-hoc test compares all groups to each other).
13. Run the analysis.
14. Identify the gene list of the post-tests (a 3 × 3 table).
15. Choose the post-test that shows significant genes.
16. Make a list of these genes in a separate folder and save it in Excel.
17. Apply a filter from the list of genes identified in the post-hoc test, using a threshold of interest. We normally use ≥2 or ≤2-fold change, comparing one condition (i.e. Prol.) vs. another condition (i.e. MSE). By so doing, the significant genes between the 2 groups are further filtered by fold change for up or down regulation.
18. If the experiment has only 2 groups, *see* **Note 8**.
19. After having the gene list from ANOVA, cluster the samples using Hierarchical analysis based on a condition tree. Use the individual samples for clustering. The Pearson correlation should be the measurement of similarity, and the average linkage should be the clustering algorithm (*see* **Note 9**).
20. For a non-supervised analysis, use Principal Component Analysis (PCA). From the menu "Tools" choose "Principal Component Analysis." Use the "all genes" as a reference gene list. Identify the behavior of all of the samples based on condition by using PCA. We normally use the mean centering and scaling for the analysis (*see* **Note 10**). After having the gene list of interest (**Table 6.2**), one needs to interpret the identified genes. In our lab, we have used Ingenuity Pathways Analysis for interpretation of genes.

3.5. Interpretation of the Gene List (see Note 11)

1. Select the gene list from ANOVA generated in GeneSpring GX and save in Excel.
2. Change values below 1 to the negative value (*see* **Note 12**).
3. Create a new Excel file for IPA (*see* **Note 13**).
4. Prepare the gene list to upload to Ingenuity Pathways Analysis. We generally up-load the whole gene list derived from ANOVA .
5. Get the fluorescence intensity values in each condition and the *P*-values of the comparison derived from ANOVA and add them to the Excel spreadsheet (*see* **Note 12**).

Table 6.2
An example of gene list generated from GeneSpring GX. Gene Id: gene identification; Prol: proliferative endometrium, MSE: midsecretor endometrium; LSE: late secretory endometrium. The Normalized values represent the mean fluorescent values from the samples; the *P*-value is based from ANOVA. Fold change can be obtained by the geometric mean of the values from two conditions

		Normalized values				
Gene Id	**Gene Symbol**	**Prol**	**MSE**	**LSE**	***P*-value**	**Description**
212531_at	LCN2	0.747	1.416	6.685	0.00124	lipocalin 2 (oncogene 24p3)
201925_s_at	DAF	0.673	0.873	4.175	7.36E-06	decay accelerating factor for complement (CD55, Cromer blood group system)
226926_at	ZD52F10	0.76	0.846	4.566	7.52E-08	Dermokine
217022_s_at	IGHA1; IGHA2; MGC27165	0.578	1.068	3.395	0.000395	immunoglobulin heavy constant alpha 1; immunoglobulin heavy constant alpha 2 (A2m marker); hypothetical protein MGC27165
225242_s_at	URB	0.567	0.917	3.211	2.24E-06	steroid sensitive gene 1
217388_s_at	KYNU	0.643	0.981	3.633	0.000838	kynureninase (L-kynurenine hydrolase)
238625_at	C1orf168	0.565	0.922	3.17	3.16E-05	chromosome 1 open reading frame 168
227297_at	ITGA9	0.613	0.673	3.184	1.57E-05	Integrin, alpha 9
213800_at	CFH	0.815	0.99	4.058	4.58E-06	complement factor H
209116_x_at	HBB	0.383	0.48	1.88	0.0347	hemoglobin, beta;
211699_x_at	HBA1; HBA2	0.5	0.574	2.435	0.021	hemoglobin, alpha 1; hemoglobin, alpha 2;
227070_at	GLT8D2	0.641	0.741	3.109	4.63E-05	glycosyltransferase 8 domain containing 2
205403_at	IL1R2	0.641	1.079	3.098	0.000175	interleukin 1 receptor, type II
228302_x_at	CAMK2N1	0.826	1.095	3.963	3.72E-07	calcium/calmodulin-dependent protein kinase II inhibitor 1

214247_s_at	DKK3	0.583	0.645	2.721	3.15E-05	dickkopf homolog 3 (Xenopus laevis)
218824_at	FLJ10781	0.555	0.653	2.481	4.45E-05	hypothetical protein FLJ10781
225081_s_at	CDCA7L	0.646	0.946	2.866	1.30E-07	cell division cycle associated 7-like
219148_at	PBK	0.758	0.922	3.342	0.00011	PDZ binding kinase
226930_at	FNDC1	0.778	0.982	3.353	0.0013	fibronectin type III domain containing 1
202709_at	FMOD	0.685	0.954	2.95	9.66E-08	fibromodulin
209458_x_at	HBA1; HBA2	0.478	0.529	2.052	0.0281	hemoglobin, alpha 1; hemoglobin, alpha 2;
211745_x_at	HBA1; HBA2	0.484	0.538	2.069	0.0277	hemoglobin, alpha 1; hemoglobin, alpha 2;

6. Upload the saved file into Ingenuity server (Ctrl-U). A new dialog box will open.
7. Select the File Format as "flexible format" from the drop-down menu.
8. Check that the column header is present.
9. Choose Affymetrix as the identifier from the dropdown menu.
10. Choose array platform HG-U133 Plus 2.
11. Use log ratio as observation, and edit the observation names to a short name (Prol, MSE, LSE).
12. Save the dataset in a New Project in the project manager box in IPA.
13. Highlight the dataset to be analyzed.
14. Perform a new core analysis from "NEW."
15. Choose the parameters for cut-off. Log ratio as 2.0 both up and down regulated identifiers.
16. Choose the *P*-value as 0.05.
17. Click on Recalculate. It will show how many molecules are eligible for generating networks (*see* **Note 14**).
18. Run the analysis and save it.
19. Identify the analysis and right click on it. Choose "New Core, Tox Or Metabolomics Analysis."
20. In our example, we have select Prol, MSE, and LSE groups for comparison and run the comparison.
21. After the comparison is done, select the file and identify the main networks, functions, and canonical pathways.
22. Core and Metabolomics Analyses allow you to interpret datasets in the context of biological processes, pathways, and molecular networks. With multiple datasets that represent multiple time points or dosage treatments, use "Comparison Analysis" to understand which biological processes and/or diseases are relevant to each time point or dose.
23. Identify the main canonical pathways involving the significant genes (*see* **Note 15**).
24. Identify the main significant canonical pathways and overlay the gene expression with the *P*-values (**Fig. 6.1**) (*see* **Note 15**).
26. If no canonical pathway of interest is identified, go to functional analysis to identify the main functions across the conditions and the genes related to each function (**Fig. 6.2**).

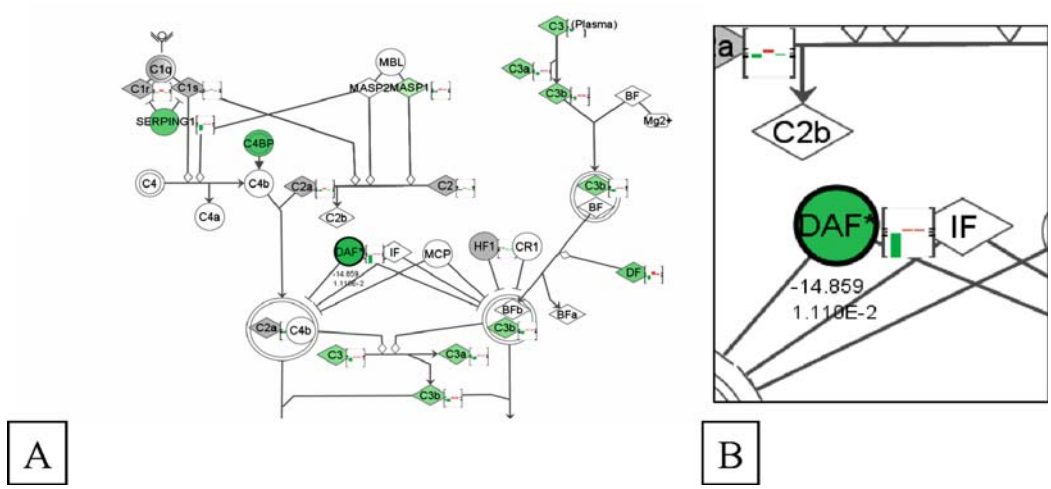

Fig. 6.1. The complement cascade is partially shown is this example below (**A**). In **Table 6.2**, DAF appears as a significant gene down-regulated in proliferative endometrium. IPA identifies that this gene has a significant probability to belong to the Complement cascade. Here, we identify that DAF is down-regulated (which would appear as the green color) after another statistical analysis performed by IPA, described in step 17, from Section 3.4. The little bar chart seen in the magnification (**B**) on the side of the gene represents its fluorescence expression over the three different conditions (Proliferative, MSE, and LSE). The current value of DAF represents the expression of this gene in the Proliferative condition (i.e., comparing to the other conditions, DAF is –14.859-fold negative, and this down-regulation is significant $P = 0.011$). The bottom *arrows* go to the formation of the membrane attack complex (not shown).

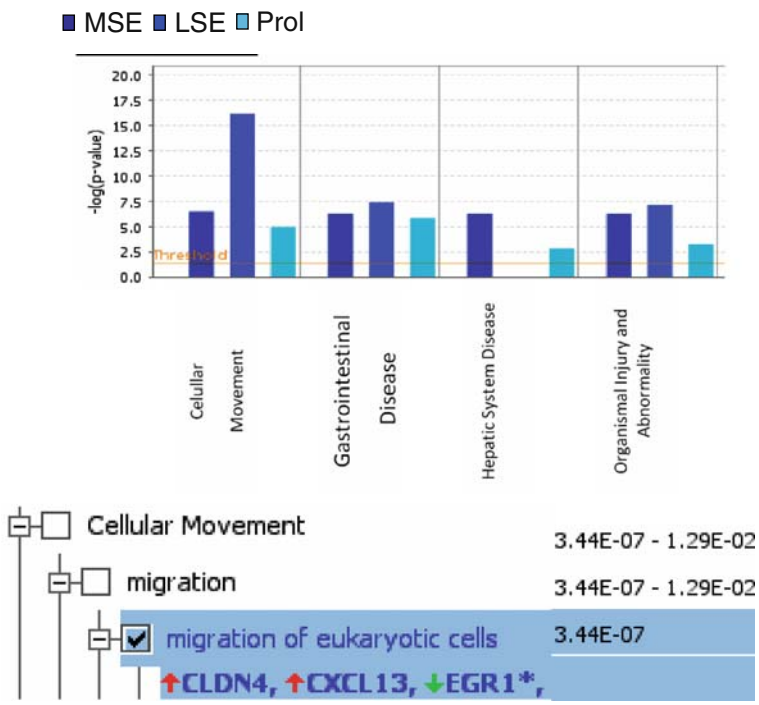

Fig. 6.2. Example of biological functions across the conditions. Cellular movement is expressed mainly in the LSE, followed by MSE and Prol. In MSE, the genes related to cellular movement, more specifically to migration are depicted. CLDN4 and CXCL13 have positive fluorescence intensity values in MSE, while in EGR1, it is decreased. The values on the right side are *P*-values ranges, when it includes more than one process. When one process is shown alone, the individual *P*-value is shown.

27. After this, one will have the genes and their functions in the context of a pathway and one can study in more detail each gene and relevant processes. This is a very time consuming step of the study, mainly if one is not familiar with the canonical pathway or with the biological process. In our lab we use all available resources to understand these canonical pathways and biological process. For example, in a recent paper, we found that matrix metallopeptidase 7 (MMP7) was up-regulated in the endometrium of women with ectopic pregnancy, compared to non-pregnant MSE (15). Of note, this peptidase has active and non-active forms, and a validation method with immunohistochemistry, using an antibody against the active form was imperative. Other examples of discovering new functions and genes can be seen in other publications (16, 17).

4. Notes

1. If many projects are running at the same time, it is advised to make 2 folders for the .CEL files. One will be used as the main folder for .CEL files, and the other for a specific experiment. The .CEL file naming should be consistent and as informative as possible. For example: Gladstone-MSE-M153-normal-HGU133Plus2.CEL. This name will give information from where the hybridization was performed (Gladstone core facility), phase of the menstrual cycle (mid-secretory phase), sample code# (M153), if it has any disease (in this case: normal), what chip was hybridized (HG-U133 Plus 2). It is not necessary to use a date, because the file normally displays the date, which gives us reference about the hybridization method. This file should not be removed or renamed from the main folder. For a specific project, this .CEL file is copied and pasted into another folder for the experiment. The file should be renamed for the sake of clarity in the array. For instance, named as MSE1 and put into one's notes that this sample is MSE1 = M153. The reason for doing that is for better visualization in the hierarchical clustering and for the experiment, when graphs are generated.
2. Always keep the annotation up to date. In GeneSpring GX, go to Annotations from menu bar → update annotations from Agilent. As in any software, new versions are constantly launched. In January 2008, a new version of GeneSpring GX (version 9.0.0) was released. Five newer intermediate updated versions were available. The reader should access

the website for up-to-date information about the software. For further details, see http://www.chem.agilent.com/Scripts/Generic.ASP?lPage=64589&PF=Y (accessed on July 15, 2008).

3. The Robust Multi-array Analysis normalization corrects the background of the chip. By using only the perfect match (PM) probe set, normalize the expression across chips and make a summarization of the expression measured. This is done using log-transformed PM values, after carrying out a global background adjustment and across-array normalization (13).
4. Because of the RMA normalization steps, special data transformation, such as setting the measurements less than 0.01 to 0.01 and per chip, should be precluded. However, normalization can be performed at the gene level, using the option "per gene: Normalize to median." This normalization improves visualization of expression pattern, and normalizes each gene across conditions, i.e., all the samples, to a median of 1. An example is given in **Table 6.3**. In one-color arrays, it is possible to normalize the samples to specific samples, but we do not generally perform this option.
5. In this step, the parameters of the samples are defined. The parameters are important because they will identify the replicates for each condition for later analysis. For

Table 6.3
Example of "per Gene: Normalize to median." This table is an example of how gene normalization is performed. For instance, gene ID 2134_at represents a specific gene out of the whole genome. The values 0.182, 0.471 and 0.181 are the fluorescent intensity obtained from the scanning of the GeneChip®, after RMA prenormalization. The gene normalization by median is a way to give the gene expression values a Gaussian distribution across all the samples. In this example, sample#1 is the median value. All other samples will be divided by this median value, in this case 0.182. In order to simplify, only 3 out of 12 samples are shown here.

Gene ID	After RMA prenormalization			Calculation		After per gene normalization		
	Sample #1	Sample #2	Sample #3	Median of gene among samples	Equation Sample #/ median	Sample 1	Sample 2	Sample 3
2134_at	0.182	0.471	0.181	0.182		1	2.588	0.998

Table 6.4
Expression of gene 1007_s_at across different conditions and replicates samples. This table is central for understanding the microarray analysis. The 3 groups are seen (MSE, LSE, and Prol), with their respective replicates (MSE = 8; LSE = 6; Prol = 9). In this example, more than 4 samples are used to show the importance of sample variation, a fact that would not be possible with 4 samples. Each value in the column express the fluorescent expression of the gene in each sample, after normalization. GeneSpring will use ANOVA with these values and groups for statistical analysis. The process is repeated with all 54,646 gene probes

Replicate	MSE	LSE	Prol
1	10.43	7.908	8.743
2	8.587	6.009	7.455
3	2.932	1	6.375
4	2.652	0.687	5.127
5	0.997	0.683	1.685
6	0.738	0.194	0.731
7	0.407		0.663
8	0.375		0.611
9			0.091
Mean	3.38	2.74	3.49
SD	3.92	3.32	3.41

example, we have 23 samples (**Table 6.4**) and we are analyzing the transcriptome of the endometrium across 3 phases: proliferative, mid (MSE), and late (LSE) secretory. The endometrial phases will identify the groups, and individual samples will be categorized according to the phases ($n = 8$ in MSE; $n = 6$ in LSE; $n = 9$ in Prol), identifying the replicates. After identifying one's samples, some software can enable displaying the parameters as parametric (i.e., hours, time), or non-parametric data (i.e., with disease/without disease). Another important step is to present the data as the log of the ratio within the replicates, so the data will have a Gaussian distribution. The mean of normalized values will be displayed and used for analysis. **Figure 6.3** shows the distribution of the samples among the 3 groups. The expression levels were normalized (by RMA and appear in the

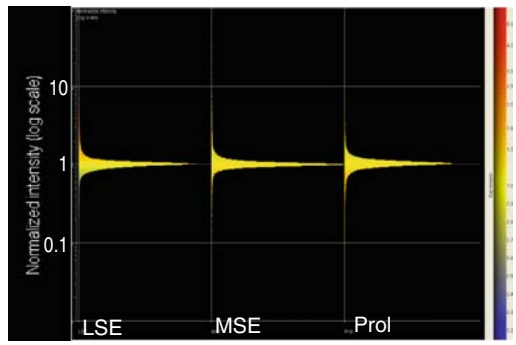

Fig. 6.3. Distribution of the intensity of fluorescence of the genes across the conditions (LSE, MSE, Prol). Note the bell shape distribution of the intensity of gene expression around 1. This normal distribution confers the possibility to use parametrical tests for statistical analysis.

log of ratio). If the data have a normal distribution, the statistical methods for normally distributed samples (Student *t*-test, ANOVA) can be used; otherwise, their equivalent non-parametric test should be used (Wilcoxon-Mann-Whitney test, Kruskal-Wallis, respectively).

6. Quality control at the sample level can be verified by using a box plot or scatter plot on samples, having the whole human genome as default. It is important to remove poor quality samples before analysis, because it is expected that samples within the same condition should have similar expression at a global level. However, this also can represent the biological variability of the samples, and the researcher should be alert to this. **Figures 6.4** and **6.5** show the dispersion of each sample as a box plot and scatter plot, respectively. For instance, **Table 6.4** shows a gene expression in 23 samples. Samples #1, #2, #3, #4 from MSE are quite different from the rest, and eventually the researcher discovered that these samples had an associated condition, such as endometriosis. The box plot and the scatter plot can show this difference in a global gene level. The box plot would be different, or the dot from a group would not cluster with its group. Thus, if the researcher removes samples 1,2, and 3 the new analysis of the gene would be significant ($P = 0.03$ – ANOVA). It is important to stress that these differences could represent biological variance, and the removal of a sample may mislead the results. In addition, another filter can be used at the gene level. Instead of removing a sample, a gene is removed. The quality control at the gene level can be performed through different filters. The two commons filters used in our lab are filter on error and confidence, but these steps can be skipped if one uses another filter such as ANOVA. The statistical test will show that these genes are not significantly different.

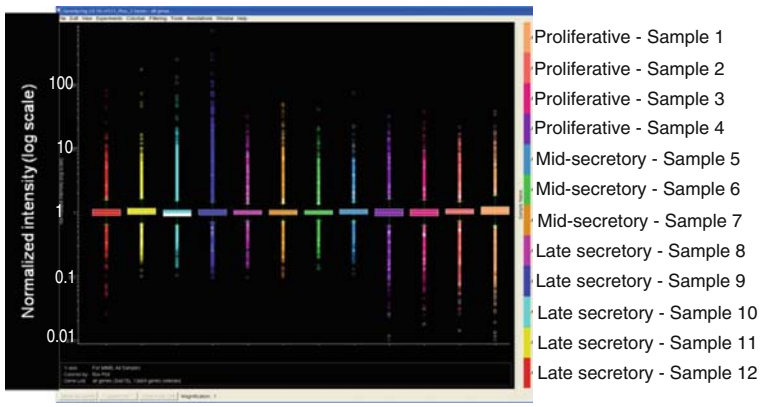

Fig. 6.4. Box plot of the samples. Each box plot represents a sample with the intensity of the genes. Here 12 box-plot are seen, and they correspond to the 12 samples. These box plots show the normalized fluorescence intensity of the genes in the individual sample. If one of the box plots (i.e., one of the samples) is very different from its group, it signifies that the sample is an "outlier." An outlier sample would reduce the chances of finding a significant difference when groups are compared, thus the researcher might want to remove the sample from the analysis, if an additional variable was found, e.g. that case had endometriosis.

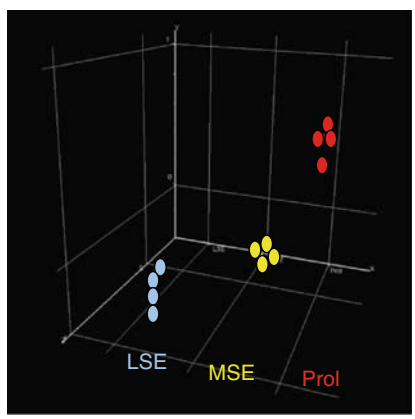

Fig. 6.5. Scatter plot of the samples. Note that replicates tend to cluster. The different shaded dots represent proliferative, mid, and late secretory samples respectively. If one of the dots (an individual sample) was located away, it would signify that the sample was an "outlier." An outlier would reduce the chances of finding a significant difference.

Filtering on error: The gene must appear at least in one of the conditions and should have no more than 3 standard deviations of the mean, which is 1. This filter removes genes that are outliers across conditions, even after the normalization, which can limit statistically significant findings. However, by doing this, one may eliminate an important gene. Poor-quality samples or genes can affect the statistical significance of clustering analysis findings. For instance, consider the following gene expression after normalization in the three conditions

(MSE, LSE, Prol) and their replicates for the gene 1007_s_at, as shown in **Table 6.4**. The filter was done using the parameter "filter outlier genes that have 3 or more standard deviations from the mean of the condition." It means that no sample was excluded. If one performs a statistical analysis with these data, they will not be significant, and this gene will be out of the significant gene list. If one uses ANOVA, this statistical test will perform this exclusion, so it is unnecessary to use this filter.

Filtering on confidence: Filter genes with *P*-values ≥ 0.05 within at least one condition. Filtering on Confidence using *t*-test compares the mean of the replicates of a gene within the same condition to the hypothetical mean of 1. This identifies genes with unreliable measurements and removes it from the experiment. Carrying poor-quality samples or genes with a wide spread of expression can affect the statistical significance of the cluster analysis. Once again, this is not necessary, because further statistical analyses will subsequently be performed.

7. Multiple test correction: In a typical microarray experiment, thousands of genes are simultaneously measured across different conditions. When a Student *t*-test is performed on a gene, the *P*-value of 5% is normally chosen. This means that there is a 5% chance that the mean expression of the gene in one condition is different from the other by chance alone, although it is shown as significant, so this is a case of a false positive by chance. If 50,000 genes are tested between 2 conditions, and a *P*-value of 5% is used, 2,500 genes can be false positives. In order to overcome this problem, multiple testing corrections are used to reduce the false positive rate. There are a few types of multiple testing corrections: the Bonferroni method, which is the most stringent, and the Benjamini and Hochberg False Discovery Rate, the less stringent. There is a trade-off in the use of stringency. The higher the stringency, the higher the number of false negatives; whereas, the lower the stringency, the greater the number of false positives. Our group normally uses the latter. This correction tolerates more false positives, and it works by ranking the *P*-values from the largest to the smallest. The first in the rank has no correction, the second *P*-value in the rank is multiplied by $(n/n - 1)$ where n is the total number of genes. The third *P*-value is multiplied by $(n/n - 2)$, the fourth by $(n/n - 3)$, and so on. If the corrected *P*-value is <0.05, the gene is considered significant.

8. In situations where one has only 2 groups, one can use the Volcano Plot. The Volcano Plot takes in consideration the Student *t*-test and the fold change at the same time (14). To use the Volcano Plot, take the gene list with all genes or after quality control filtering as the list of genes to be analyzed. Compare two samples of replicates (e.g., Prol vs. MSE).
   a. Choose a cut-off as 5% and false discovery rate of 5% or lower.
   b. Choose a filter of 2-fold, or as desired: the higher the fold-change chosen, the higher the stringency.
   c. Run the program, and the resulting gene list contains the genes of interest with a 2-fold change (up and down regulated, with a *P*-value <0.05).
   d. Save the gene list in a separate folder.
9. The aim of clustering is to group samples according to their genomic content. A typical example would be to carry out clustering analysis on multiple samples. Typical clustering analysis can be carried out within GeneSpring GX. We have generally used the Pearson correlation for measuring similarity and the average linkage for clustering algorithm. The use of a significant gene list (such as ANOVA) will yield a different clustering among the samples, compared to use of the whole gene list. It is preferred to use the gene list derived from a statistical test).
10. PCA is not a clustering technique. It is a tool to characterize the most abundant themes or building blocks that reoccur in many genes in an experiment. With the results, PCA shows a sample that is an outlier; which may or may not be removed from the analysis. PCA on conditions calculates the standard correlation between each condition vector and each principal component vector [eigenvector, (from German eigen, own) + vector]. Calculating scores this way has the advantage of scaling them to be between –1 and 1. PCA facilitates reducing the complexity of the data by discovering a number of principal components that define most of the data variability.
11. The following steps were used in IPA 5.5.1 (October 2007). Please note that the workflows within IPA have been updated to reflect new features. For information on the most current workflows within IPA, please contact support@ingenuity.com or visit http://www.ingenuity.com
12. Note that some software's, such as GeneSpring GX 7.3, give a list of significant genes with a *P*-value <0.05 and a fold change $\geq$ or ≤ 2. However, the negative fold change is normally expressed as values below 1. For instance, if the fold change is 0.2, it means –5-fold. In order to transform a

long list of fractional values for posterior analysis Excel is quite useful. Copy the gene list generated in GeneSpring GX to a spreadsheet, having the Gene identification and fold change in different columns, and use the "IF" formula, a feature commonly used in Excel, to change the fractional values into their negative inverse. For instance, consider cell A1 and A2 from the spreadsheet. Cell A1 has the Gene Id, and cell A2 has the fold change. On cell A3 write the formula "= IF(A2<1;-1/A2;A2)." It means that, if the number is <1, it should be divided by −1, otherwise keep the number as it is).

Currently in IPA 7.0, it is not necessary to calculate the negative inverse of fractional values. Fractional values that indicate down-regulated values can be indicated in the data upload process using the ratio expression value type.

13. IPA v. 5 uses a file format called "Flexible Format," which is any Excel 1997/2003 file. The identifiers should be in one column and can be mixed identifiers. Flexible Format allows you to upload up to 20 observations (groups) simultaneously with up to three expression value types per observation. In this study, we used Format B Template, which preceded the Flexible format and is no longer available for download from Ingenuity.

    Alternatively, GeneSpring GX 7.3 and later, and Ingenuity Pathways Analysis (version 5 and later) are connected through a script, which allows the integration between GeneSpring GX, with the Ingenuity Pathways Analysis tool. The integration consists of three scripts for GeneSpring GX that will allow sending gene lists with experimental data for analysis in IPA and create networks of interacting genes and proteins. Install a ZIP file in GeneSpring GX. Be sure to install the correct version. Download from the GeneSpring GX site and save this version on the hard drive. Drag the ZIP file onto the GeneSpring GX window. Follow the instructions on the screen. Upon restarting GeneSpring GX, three new scripts will appear within the Scripts folder of the GeneSpring GX navigator window. Each script will send data directly to IPA, perform a specified analysis in IPA, and send data from IPA directly back to GeneSpring GX. In addition, GeneSpring is now in version 10. Please refer to GeneSpring's website (http://www.chem.agilent.com/en-US/products/software/lifesciencesinformatics/genespringgx/pages/gp41630.aspx−−accessed on December 12, 2008) for the most current directions on how to install the connector, as the instructions may have changed with this new version.

14. Use the Recalculate button after setting your analysis parameters to see the number of Eligible Genes you have for your analysis. For networks, IPA suggests that for the best results, you should have <800. This ensures that IPA is not analyzing noise in the dataset. If you have >800 genes eligible for network generation, try increasing the stringency of your cutoff values, either by a higher fold change, or setting a $P < 0.01$.
15. Ingenuity updates the main canonical pathway periodically. It will show a graph with the expression of genes in each canonical pathway and a *P*-value. This *P*-value represents the probability that a certain gene belongs to that particular canonical pathway. The status of the pathway, i.e., if it is active or inhibited, must be study case by case. Even if a Canonical Pathway does not meet statistical significance or have a high ratio, it is still useful for the user to open Canonical Pathways that are biologically interesting to them or that have something to do with their hypothesis/scientific question. The reason is because a Canonical Pathway might have only one gene or molecule affected, but if it is a rate-limiting enzyme or critical molecule within that pathway, it could have a significant biological effect (even though it is not statistically significant). IPA 7 has a new feature that describes each Canonical Pathway. This function helps you to understand this particular pathway. To access the descriptions, find the corresponding Canonical Pathway in the Canonical Pathways library, then right click on it, and choose "Show Description." Canonical Pathways now are also divided up into categories to help with interpretation of the data. It can be worthwhile to spend an extra time looking at Canonical Pathways. The use of auxiliary literature to understand the pathways, its mechanisms of inhibition or activation, is essential to look at individual genes that may have different functions depending on certain conditions, i.e., tissue, phase of the cycle, presence or not of diseases.

Acknowledgements

This research was supported by NICHD/NIH through cooperative agreement 1U54HD055764-01 as part of the Specialized Cooperative Centers Program in Reproduction and Infertility Research (Dr. Giudice) and Coordenacao de Aperfeicoamento de Pessoal de Nivel Superior (CAPES) Grant BEX3656-06-3 (Dr. Savaris).

References

1. Popovici RM, Kao LC, Giudice LC. (2000) Discovery of new inducible genes in in vitro decidualized human endometrial stromal cells using microarray technology. Endocrinology; 141:3510–3513.
2. Horcajadas JA, Diaz-Gimeno P, Pellicer A, Simon C. (2007) Uterine receptivity and the ramifications of ovarian stimulation on endometrial function. Semin Reprod Med; 25:454–460.
3. Dockery P. The fine structure of the mature human endometrium. In: Glasser SR, Aplin JD, Giudice LC, Tabibzadeh S, eds. The Endometrium. New York: Taylor & Francis; 2002:21–38.
4. Talbi S, Hamilton AE, Vo KC, Tulac S, Overgaard MT, Dosiou C, Le Shay N, Nezhat CN, Kempson R, Lessey BA, Nayak NR, Giudice LC. (2006) Molecular phenotyping of human endometrium distinguishes menstrual cycle phases and underlying biological processes in normo-ovulatory women. Endocrinology; 147: 1097–1121.
5. Horcajadas JA, Goyri E, Higon MA, Martinez-Conejero JA, Gambadauro P, Garcia G, Meseguer M, Simon C, Pellicer A. (2008) Endometrial receptivity and implantation are not affected by the presence of uterine intramural leiomyomas: a clinical and functional genomics analysis. J Clin Endocrinol Metab Sep; 93(9):3490–3498. Epub Jun 17, 2008.
6. Martinez-Conejero JA, Simon C, Pellicer A, Horcajadas JA. (2007) Is ovarian stimulation detrimental to the endometrium? Reprod Biomed Online; 15:45–50.
7. Savaris RF, Giudice LC. (2007) The influence of hydrosalpinx on markers of endometrial receptivity. Semin Reprod Med; 25:476–482.
8. Black MA, Doerge RW. (2002) Calculation of the minimum number of replicate spots required for detection of significant gene expression fold change in microarray experiments. Bioinformatics; 18:1609–1616.
9. Qiu W, Lee ML. (2006) SPCalc: A web-based calculator for sample size and power calculations in micro-array studies. Bioinformation; 1:251–252.
10. Liu P, Hwang JT. (2007) Quick calculation for sample size while controlling false discovery rate with application to microarray analysis. Bioinformatics; 23:739–746.
11. Ferreira JA, Zwinderman A. (2006) Approximate sample size calculations with microarray data: an illustration. Stat Appl Genet Mol Biol; 5:Article25. Epub Oct 9, 2006.
12. Jung SH. (2005) Sample size for FDR-control in microarray data analysis. Bioinformatics; 21:3097–3104.
13. Lee NH, Saeed AI. (2007) Microarrays: an overview. Methods Mol Biol; 353:265–300.
14. Churchill GA. (2002) Fundamentals of experimental design for cDNA microarrays. Nat Genet; 32 Suppl:490–495.
15. Savaris RF, Hamilton AE, Lessey BA, Giudice LC. (2008) Endometrial Gene Expression in Early Pregnancy: Lessons From Human Ectopic Pregnancy. Reprod Sci: Oct; 15(8):797–816. Epub Jun 30, 2008.
16. Macklon NS, van der Gaast MH, Hamilton A, Fauser BC, Giudice LC. (2008) The impact of ovarian stimulation with recombinant FSH in combination with GnRH antagonist on the endometrial transcriptome in the window of implantation. Reprod Sci; 15:357–365.
17. Burney RO, Talbi S, Hamilton AE, Vo KC, Nyegaard M, Nezhat CR, Lessey BA, Giudice LC. (2007) Gene expression analysis of endometrium reveals progesterone resistance and candidate susceptibility genes in women with endometriosis. Endocrinology; 148:3814–3826.

Chapter 7

Detection of Ovarian Matrix Metalloproteinase mRNAs by In Situ Hybridization

Katherine L. Rosewell and Thomas E. Curry, Jr.

Abstract

In situ hybridization represents a powerful technique to localize DNA or RNA of interest at the chromosomal or cellular level. In endocrine tissues composed of diverse and varied cell types, in situ hybridization has allowed the identification of specific cells responsible for the expression of genes controlling the function of the tissue. Our laboratory has routinely used this approach to understand the cellular expression of genes associated with the growth of the ovarian follicle, rupture of the follicle, and transformation of the ruptured follicle into the corpus luteum. The current study outlines the procedural details of in situ detection of mRNA in tissues and illustrates the utility of this approach in identifying the ovarian cells expressing the matrix metalloproteinases and their endogenous inhibitors, the TIMPs, in the human ovary.

Key words: Ovary, in situ hybridization, matrix metalloproteinase, TIMP, human.

1. Introduction

The development of in situ hybridization (ISH) has allowed investigators to identify specific DNA or RNA sequences within tissues, cells, or chromosomes of interest. The technique was originally described for the detection of ribosomal gene sequences in cells using labeled ribosomal RNA (1, 2). ISH has evolved to utilize complementary DNA, RNA, or oligonucleotides which are labeled (i.e., probe) to allow cellular detection, localization, and identification of nucleic acid sequences. Some laboratories subsequently quantitate the in situ reaction product as (1) the number of labeled cells or (2) the relative amount of reaction product per unit area.

O.-K. Park-Sarge, T.E. Curry, Jr. (eds.), *Molecular Endocrinology,* Methods in Molecular Biology 590,
DOI 10.1007/978-1-60327-378-7_7,

The label for detection of the DNA, RNA, or oligonucleotide of interest can either be fluorescent, radioactive, or colorimetric. Fluorescent labeled probes have been widely used with fluorescent DNA ISH or FISH to routinely diagnose chromosome structure and assess chromosomal integrity (3). For radiolabeled probes, the most common isotope employed is ^{35}S, although ^{3}H, ^{32}P, ^{33}P have also revealed nucleic acid sequences of interest (4). Colorimetric probes have utilized various methods of detection including biotin, alkaline phosphatase, and digoxigenin. Colorimetric approaches have the advantage of a rapid development and turnaround time without the problems associated with the use and disposal of radionucleotides. Although colorimetric ISH was initially reported to have less sensitivity than the radiometric ISH, there has been considerable debate as to the comparative sensitivities between the two methodologies with different laboratories favoring one or another of the approaches. For example, Warford reported that comparison of ^{35}S and ^{3}H probes with biotin labeled probes has shown that optimized nonradioactive methods can give results equivalent or superior to radiolabeled probes but that for certain probe/target combinations, radioactive methods were preferable (3). Likewise, Emson noted that the sensitivity of detection depends on the reporter used and that the most sensitive radiolabeled ribonucleotide probes may exceed the sensitivity of the best non-radioactive probes (5). However, the use of multiple digoxigenin- or alkaline phosphatase labeled probes exhibit sensitivities that are at least equivalent to isotopic in situ hybridization (5). Wilcox compared various colorimetric and radiometric techniques and concluded that ^{35}S labeled riboprobes represent the most sensitive method for the detection of mRNA in tissue sections (4). Our laboratory routinely uses radiolabeled probes and in this chapter we detail the procedure for labeling and detection of ^{35}S cRNA probes for detection of mRNA sequences of interest in the ovary.

A major advantage of ISH is the detection of nucleic acid sequences at the level of the individual cell. This advantage is readily apparent in tissues with a diverse array of cell types as typically found in endocrine tissues. In the ovary, there are multiple cell types in the ovarian follicle, the corpus luteum, and in the stroma. In our studies examining the expression of the ovarian matrix metalloproteinases (MMPs) and their associated inhibitors, the tissue inhibitors of metalloproteinases or TIMPs, we have employed in situ hybridization to identify the cells responsible for producing this family of proteinases and their inhibitors. We have observed that when RNA levels are examined by Northern blot or PCR methodologies in whole or intact ovarian tissue collected as ovulation approaches, there are often negligible changes in mRNA expression patterns. However, when these same time points are examined by ISH, striking changes in

the localization patterns are observed. For example, *Timp3* mRNA levels are relatively unchanged in whole rat or mouse ovaries collected after the administration of human chorionic gonadotropin to induce follicular rupture and oocyte release (6–8). Yet the pattern of *Timp3* mRNA is rapidly and highly induced in granulosa cells of preovulatory follicles (9–11). In this chapter we describe the ISH procedure and apply this technique to identify members of the MMP family in the human ovary.

2. Materials

2.1. Tissue Preparation

1. Tissue-Tek® O.C.T. Compound (VWR).
2. Fisherbrand® ProbeOn™ Plus microscope slides (charged and precleaned).
3. Microscope slide boxes for ultra-low freezer storage (−80°C).
4. Human ovarian tissue obtained from specimens in surgical pathology. All procedures for these experiments utilizing human tissue were approved by the University of Kentucky Institutional Review Board.

2.2. Synthesis of cRNA Probe

1. Template DNA (1 μg).
2. 10X Transcription Buffer (Ambion).
3. NTP mix (combine in 1:1:1 ratio from 10 mM each: ATP, CTP, GTP, store at −20°C; Ambion).
4. UTP (10 μM; diluted in RNase free water (RFW), *see* **Note 1**, from 10 mM stock, store at −20°C; Ambion).
5. Uridine-5′-Triphosphate, [α - ^{35}S] (Specific. Activity. 1200 Ci/mmol; 44.4 TBq/mmol 5 mM Tris, pH 7.4 with 10 mM DTT 10 mCi/ml; 370 MBq/ml) store at −80°C (MP Biomedicals).
6. RNA Polymerase specific for vector, store at -20°C (*see* **Note 2**).
7. DNase I, store at −20°C (Ambion).
8. Ethylenediaminetetraacetic acid disodium salt dehydrate (EDTA, 0.25 M; Sigma-Aldrich).
9. Mini Quick Spin RNA columns, store at 4°C, (Roche Applied Science).
10. Urea Gel: For 5% add 8 ml of Sequagel-4.75 (National Diagnostics), 2 ml of Sequagel complete buffer (National Diagnostics) and 80 μl Ammonium persulfate (APS, 10% w/v; Bio-Rad). APS is prepared as a 10% solution in RFW, aliquot 80 μl per microfuge tube and store at −20°C.

11. Snap-A-Gels™ mini cassette, 1.5 mm (Jule, Inc.)
12. Gel Loading Buffer II (Ambion)
13. Kodak Biomax XAR film (Thermo Fisher).

2.3. Preparation of Slides Before Hybridization

1. Phosphate buffer saline (PBS): Prepare a 10X stock with 1.37 M NaCl, 27 mM KCl, 101 mM Na_2HPO_4. Adjust pH to 7.4–7.6, autoclave and store at room temperature (RT). Dilute to 1x concentration with RFW for working solution.
2. Paraformaldehyde (Sigma-Aldrich): Prepare a fresh 4% (w/v) solution in PBS for the total number of slide dishes used. The solution is carefully heated to 55°C (not more than 62°C at any time) to dissolve and when cooled, pH to 7.4–7.6 with 1 M sodium hydroxide (NaOH) added dropwise. Filter before use.
3. Triethanolamine (TEA; Sigma-Aldrich): Prepare a 1.5% (v/v) solution in RFW (adjust pH to 8.0 if necessary).
4. Acetic anhydride (Sigma-Aldrich).
5. Sodium Chloride/Sodium Citrate buffer (SSC): Prepare a 20X stock with 3 M NaCl and 300 mM $C_6H_5Na_{23}O_7{\cdot}2H_2O$ in RFW and pH to 7.0. Used in preparation of tissue sections at 2X and 1X concentrations and in post-hybridization washes at 2X and 0.2X concentrations.
6. Ethanol (EtOH): 70% and 80% diluted in RFW. 95% and 100% EtOH (ThermoFisher).
7. Chloroform (Sigma-Aldrich).

2.4. Hybridization

1. RNA mix: For every ml of RFW add 2.5 mg salmon sperm DNA (Sigma-Aldrich), 6.25 mg yeast total RNA (store at −20°C; Invitrogen) and 6.25 mg yeast tRNA (store at −20°C; Invitrogen). Boil salmon sperm DNA once for 10 minutes before adding. Store remaining portion at −20°C.
2. Hybridization Cocktail containing 45% Formamide (Amresco).
3. Sodium dodecyl sulfate (SDS; ThermoFisher): Prepare a 10% (w/v) solution in RFW, store at room temperature.
4. Sodium thiosulfate (Sigma-Aldrich): Prepare a 10% (w/v) solution in RFW, store at room temperature.
5. Sodium acetate (Sigma-Aldrich): Prepare a 0.1 M solution in RFW and pH to 5.2.
6. UltraPure™ Dithiothreitol (Clelands Reagent, DTT; Invitrogen): Prepare a 5 M solution in 0.1 M sodium acetate pH 5.2 (store at -20°C).
7. Coverslips (*see* **Note 3**).
8. Hybridization chamber (*see* **Note 4**).
9. Formamide (Sigma-Aldrich): Prepare a 50% solution (v/v) in RFW and store at room temperature.

2.5. Post-hybridization Washes

1. SSC solution: *see* **Section 2.3.5**
2. DTT: *see* **Section 2.4.6**
3. RNAse buffer: Prepare a fresh 1X stock solution of 1 M Trizma base (Sigma-Aldrich), 397 mM NaCl, and 0.5 M EDTA. Check to make sure pH is 8.0 (*see* **Note 5**).
4. RNAse A (Amresco).
5. Ethanol (EtOH): 70% and 90% diluted in RFW.
6. Kodak Biomax XAR film (Thermo Fisher).

2.6. Dipping Slides in Photographic Emulsion

1. Kodak NBT 2 Emulsion, diluted 1:1 in RFW (VWR; *see* **Note 6**).
2. Waterbath set to 45°C.
3. Plain glass slides.
4. Some type of rack to keep slides upright while they dry.
5. Slide boxes for storage.
6. Electrical tape.
7. Scissors.
8. Aluminum foil.

2.7. Developing Slides

1. Kodak Professional D-19 Developer (Sigma-Aldrich).
2. Kodak Professional Fixer (Sigma-Aldrich).
3. Slide staining racks and containers.

2.8. Counterstaining Slides

1. Hematoxylin Stain Gill's Formulation #2 (ThermoFisher).
2. Scott's Tap Water Substitute (ThermoFisher).
3. CitriSolv Clearing Agent (ThermoFisher).
4. Ethanol (EtOH): 70% and 80%, diluted in RFW. 95% and 100% EtOH (ThermoFisher).
5. Permount (ThermoFisher).
6. Coverslips.

3. Methods

3.1. Tissue Preparation

Tissues are collected, embedded in OCT, immediately frozen on dry ice, and stored at −80°C. When ready to use, cut 10 μm sections on a cryostat, place on Fisherbrand® ProbeOn™ Plus microscope slides and store in microscope slide boxes for ultra-low freezer storage (*see* **Note 7**). For human ovaries, we place 1 section per slide. For rodent ovaries, we place 4 sections per slide but each section is 50 μm apart. Thus for the rodent we have a group of

5 slides ready; the first section goes on slide 1, the second section goes on slide 2, the third section goes on slide 3. . .the sixth section goes on slide 1, the seventh section goes on slide 2, etc.

3.2. Synthesis of cRNA Probe

1. Add the following in order: 1 μg of your template DNA (not more than 7 μl per reaction), 2 μl of 10X Transcription Buffer, 3 μl NTP mix, 2.4 μl UTP (10 μM), 5.6 μl ^{35}S-UTP and 2 μl of the appropriate RNA Polymerase.
2. Place at 37°C in water bath for 45 minutes.
3. Add another 1 μl of RNA Polymerase, incubate for an additional 30 minutes. This is known as "spiking" and is useful to boost the probe yield.
4. Add 1 μl DNase I and incubate for an additional 15 minutes.
5. Stop the reaction by the addition of 2 μl 0.25 M EDTA.
6. While incubating with DNase, prepare the Mini Quick Spin RNA columns.
   a. Let the columns come to RT.
   b. Remove the top cap first and then bottom, place in a 1.5 ml eppendorf microcentrifuge tube and spin at 1,000*g* (RCF) for 1 minute at RT.
   c. Place column in a newly labeled 1.5 ml microcentrifuge tube.
7. Add labeled probe after EDTA addition (*see* **Section 3.2.5**) and spin at 1,000*g* (RCF) for 4 minutes at RT.
8. Count 1 μl of eluted probe. We aim for 1×10^6 cpm/μl (*see* **Note 8**).
9. Prepare a 5% Urea Gel while the probe is synthesizing, make sure gel is set before diluting probe to load.
10. Dilute probe to 1×10^6 cpm/μl, add 1 μl of the diluted probe to 8 μl Gel Loading Buffer II.
11. Heat denature probe for 5 minutes at 95°C.
12. Load on the gel and run at 240 V for approximately 20 minutes.
13. Oppose to Kodak Biomax XAR film for at least 1 hour or overnight in the dark. Develop film.

3.3. Preparation of Slides Before Hybridization

1. Remove slides from the -80°C freezer and place them in metal slide racks that are setting on aluminum foil on dry ice. Once you have chosen the slides you need to use, wrap them in the foil and allow them to thaw on the bench top approximately 10 minutes before putting them in step #2.
2. All the subsequent incubations use 400 ml of solutions and are preformed at RT unless otherwise stated. Place in 4% paraformaldehyde solution for 15 minutes.

3. Wash in 1X PBS twice for 5 minutes each, use fresh PBS each time.
4. Wash in TEA buffer that is in a fume hood stirring with a stir bar. Immediately before placing the slide rack in the dish add 1 ml acetic anhydride, break up any micelles that form by moving the dish around the stir plate. Allow to incubate for 10 minutes.
5. Wash in 2X SSC for 5 minutes.
6. Wash in 1X SSC for 5 minutes.
7. Wash in fresh 1X SSC for 1 minute.
8. Dehydrate samples according to the following schedule: 70% EtOH for 1 minute; 80% EtOH for 1 minute; 95% EtOH for 2 minutes; 100% EtOH for 2 minutes.
9. Transfer to a slide dish in a fume hood containing Chloroform for 5 minutes.
10. Place slides back in 100% EtOH for 1 minute, followed by 95% EtOH for 1 minute. Allow slides to dry thoroughly before proceeding to the hybridization step.

3.4. Hybridization

1. Calculate how many slides you will be using because the probe mix and hybridization mix are calculated on a per slide basis. You will be adding 1×10^6 cpm of your radioactive probe to each slide. See example below (*see* **Note 9**).
2. Prepare hybridization mix:
   a. Prepare the probe mix (6 µl/slide is the volume needed) by adding:
      i. Calculated amount of RFW.
      ii. 2 µl of RNA mix per slide.
      iii. 1×10^6 cpm of radioactive probe per slide.

      For example, if you have 10 slides and your probe is 1.5×10^6 cpm/µl; you would need a total of 60 µl of probe mix:

$$2\ \mu l\ of\ RNA\ mix \times 10\ slides = 20\ \mu l\ RNA\ mix$$

$$Need\ 1 \times 10^6 cpm \times 10\ slides = 1 \times 10^7 cpm;\ you\ have\ 1.5 \times 10^6 cpm/\mu l\ so\ you\ would\ need$$

$$1 \times 10^7 cpm / 1.5 \times 10^6 cpm/\mu l = 6.66\ \mu l\ of\ radioactive\ probe$$

$$60\ \mu l\ total - (20\ \mu l\ RNA\ mix + 6.66\ \mu l\ of\ radioactive\ probe) = 33.34\ \mu l\ of\ RFW\ needed$$

   b. Heat the probe mix to 95°C for 5 minutes, then place on ice for 5 minutes.

c. Mix together in appropriate size tube (44 µl/slide is the volume needed):
   i. 42 µl of hybridization cocktail per slide.
   ii. 0.5 µl of 10% SDS per slide.
   iii. 0.5 µl of sodium thiosulfate per slide.
   iv. 1 µl of 5 M DTT per slide

3. Carefully add the probe mix into the tube with the hybridization mix and finger flick to mix. Avoid vortexing because it induces bubbles.
4. Apply 50 µl of the hybridization mix/slide to center of slide, coverslip, and place in a hybridization chamber that has been soaked in a 50% formamide solution.
5. Place in hybridization oven set to the appropriate temperature for your cDNA hybridization for 16 hours. We typically hybridize at 55°C. Place a pan of water in the oven to maintain humidity. Do not allow the slides to dry out!

3.5. Post-hybridization Washes

1. You can dilute the 20X SSC to the 2X and 0.2X solutions with water the night before and leave on the bench at room temperature.
2. Turn on water baths in the morning and let them achieve the appropriate temperature while you are preparing the wash solutions.
3. Allow the 5 M DTT to melt in a 37°C water bath. *Caution:* The DTT is added to the solution in the dish right before the transfer of the slides. That way we are certain that it has been added. The in situ will not work if you forget to add DTT to any of the washes where it is listed.
4. Briefly rinse individual slides in 2X SSC to carefully remove the coverslips and place the slides into a metal slide rack submersed in 2X SSC + 4 mM DTT (320 µl/400 ml) for 30 minutes at room temperature. Place the waste solutions into an appropriate container for your radioactive waste department to collect. The subsequent washes can be poured down the drain if your institution allows.
5. Wash in 2X SSC + 4 mM DTT (320 µl/400 ml) for 30 minutes at 37°C.
6. Wash in RNAse buffer with RNase A (10 mg/400 ml) + 2 mM DTT (160 µl/400 ml) for 30 minutes at 37°C.
7. Wash in RNAse buffer + 2 mM DTT (160 µl/400 ml) for 30 minutes at 37°C.
8. Wash in 0.2X SSC + 2 mM DTT (160 µl/400 ml) twice for 15 minutes each at room temperature.

9. Wash in 0.2X SSC + 2 mM DTT (160 µl/400 ml) for 60 minutes at 60°C.
10. Briefly rinse in 0.2X SSC + 2 mM DTT (160 µl/400 ml) at room temperature.
11. Brief 10 second rinses in RFW, 70% EtOH and 90% EtOH.
12. Allow slides to air dry with aluminum foil over them so no dust gets on the uncovered tissue.
13. Place representative slides for each treatment and time point against Kodak Biomax XAR film X-ray film in the dark overnight to check labeling.

3.6. Dipping Slides in Photographic Emulsion

1. Working with emulsion needs to be done in the dark with a safe light. The safe light in the dark room can be used but needs time to warm. Fill water bath with warm tap water and set to 45°C.
2. Arrange work area in the darkroom before turning out the room lights. Place the foil wrapped emulsion in the waterbath to liquefy, along with a small container to use to dip the slides in (*see* **Note 10**). Have bench paper down in the area you will use to blot the slides and the drying area. You will need some plain glass slides to check if the emulsion is ready to use as well as paper towels to blot the slides on. You will also need some type of rack to keep the dipped slides upright during the drying period.
3. Turn off room light and wait ~30 minutes for the emulsion to liquefy. Emulsion is a solid at 4°C.
4. Bring the in situ slides to the darkroom. LEAVE OVERHEAD LIGHT OFF.
5. Unwrap tube of emulsion carefully, do not shake. *Carefully* pour emulsion into your dipping container being very careful not to introduce any bubbles into the emulsion. Let emulsion sit in water bath ~10 minutes so that any bubbles can settle out of the solution.
6. Use a plain glass slide to dip in the emulsion for 3 seconds, blot and look for bubbles. If there are no (or very few) bubbles it is ready to use. It is important to have an even coating on the slides; bubbles will cause areas of no signal. Check emulsion in this way anytime you need to add more emulsion to the dipping container.
7. Carefully dip each slide(s) in the warm emulsion (*see* **Note 11**), again being careful not to introduce any bubbles into the emulsion. Dip each slide straight into and out of the emulsion so that there is an even coating of emulsion on each slide and that the area of the tissue is covered. As you are dipping, check frequently to make sure that tissue is covered, refill emulsion container as needed.

8. Blot the bottom onto paper towels to remove excess emulsion.
9. Place slides upright into rack. When rack is filled set it aside in the drying area.
10. Allow slides to dry for 4 hours. You can turn off the safelight to conserve the bulb life but remember it will take time to warm up again when you are packing the slides away.
11. After 4 hours, return to the darkroom bringing slide boxes, electrical tape, scissors, and aluminum foil. Turn on safelight and allow it to warm up.
12. Place slides into black slide boxes, tape around lids with black electrical tape, and wrap each box in aluminum foil. Only at this time can the overhead lights be turned on. Label with date dipped, probe, your name, etc.
13. Store boxes at 4°C, *nowhere near any radioactivity*. Exposure time will differ depending on probe used but we typically allow the slides to develop 2–4 weeks.

3.7. Developing Slides

1. Allow boxed, foil-wrapped slides to come to room temperature. Turn on safelight in the darkroom to warm up.
2. Pour Kodak Professional Fixer in staining container so that the slides will be totally immersed. Place in an ice/water mix to rapidly cool down to 13–15°C.
3. While the Fixer is cooling, dilute the Developer 1:1 with water that has been refrigerated at 4°C. For the tap water wash, mix half tap water with half cold water. This should result in the solutions being 13–15°C. For optimal development the three solutions should not vary in temperature more than 1°C.
4. Proceed quickly to the darkroom for the development of the slides.
5. In dark room, select the slides to develop and load into rack, remaining as far away from safe light source as possible.
6. Develop in Kodak Professional D-19 developer for 4 minutes.
7. Stop development in tap water for 1 minute.
8. Fix in Kodak Professional Fixer for 4 minutes. At this point, the slides can be exposed to light.
9. Keep slides in tap water until counterstained.

3.8. Counterstaining Slides

1. Place slide rack with developed slides into Hematoxylin Stain Gill's Formulation #2 (*see* **Note 12**) for 2 minutes.
2. Rinse slides briefly in a 4 liter beaker of tap water, then move to another 4 liter beaker of tap water for 2 minutes.
3. Place slide rack into Scott's Tap Water Substitute for 1 minute.

4. Rinse in tap water for 30 seconds.
5. Brief 10 second rinses in 70%, 80%, 95%, and then 100% EtOH.
6. Place slide rack into CitriSolv Clearing Agent until ready to coverslip.
7. Coverslip slides using Permount and allow to air dry.
8. Slides can now be observed using a microscope equipped with either brightfield or darkfield illumination.
9. With darkfield illumination, the silver grains from the in situ reaction product appear white against a black background. Representative darkfield in situ hybridization results in human ovarian tissue are illustrated in **Fig. 7.1** and **Fig. 7.2**.

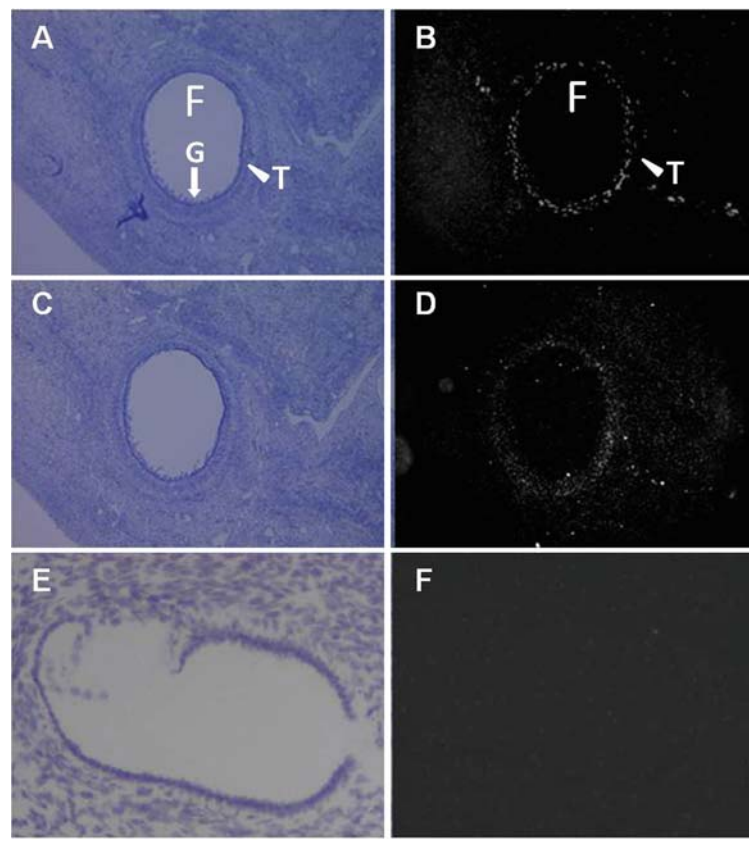

Fig. 7.1. In situ hybridization of members of the MMP family in ovarian follicles. ^{35}S-labeled complimentary RNA probes were hybridized with sections of human ovaries overnight and processed as described. Panels **A**, **C, and E** are stained with hematoxylin. In situ hybridization reactions were visualized by autoradiographic detection of silver grains (*white* areas in panels **B** and **D**). Adjacent sections of an antral follicle exhibit expression for collagenase mRNA (MMP1, Fig. 7.1A,B) and stromelysin 3 (MMP11, Fig. 7.1C,D) in the theca cell layer. Collagenase is also observed associated with blood vessels in the ovarian stoma. Panel **F** is hybridized to the stomelysin 3 sense probe as a negative control. F, follicle; G, granulosa cell layer, T, theca cell layer.

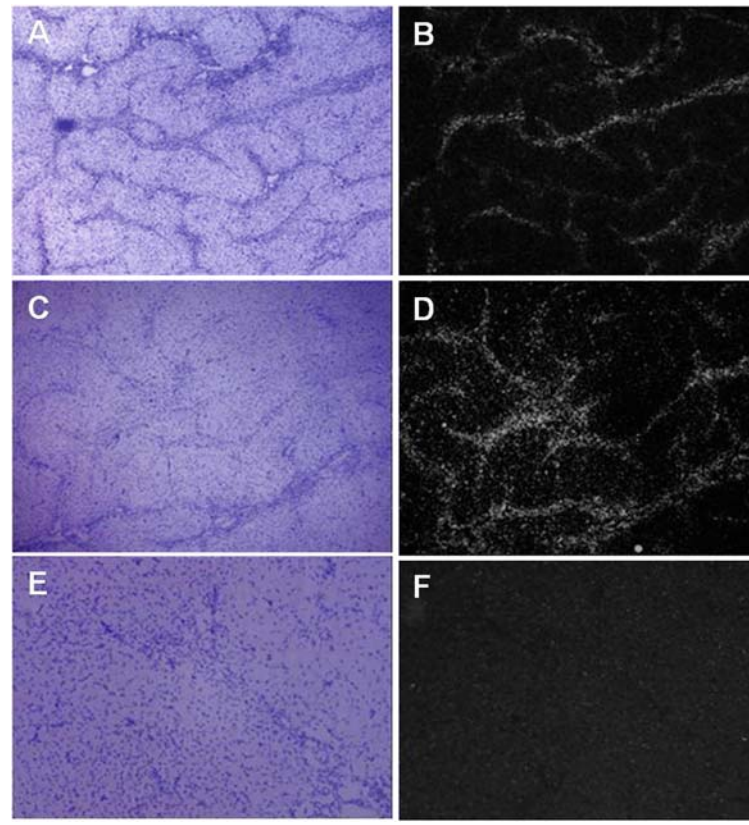

Fig. 7.2. In situ hybridization of members of the MMP family in corpus luteum. ^{35}S-labeled complimentary RNA probes were hybridized with sections of human ovaries containing a corpus luteum (CL) overnight and processed as described. Panels **A**, **C**, and **E** are stained with hematoxylin. In situ hybridization reactions were visualized by autoradiographic detection of silver grains (*white* areas in panels **B** and **D**). Adjacent sections of a corpus luteum demonstrate membrane type 1 matrix metalloproteinase mRNA (MMP14, Fig. 7.1A,B) and the tissue inhibitor of metalloproteinase 2 (TIMP2, Fig. 7.1C,D) in the stroma of the CL. Panel **F** is hybridized to the sense probe as a negative control.

4. Notes

1. All solutions should be made in RNase free water (RFW) that has a resistivity of 18.2 MΩ-cm. Water may be treated with diethyl pyrocarbonate (DEPC; Sigma-Aldrich), 1 ml per liter, overnight and then autoclaved to deactivate DEPC. Currently we use a Milli-Q® Synthesis water purification system (Millipore) which provides RFW without further treatment. All glassware should be covered with foil to keep out dust and heated to 180°C for 6 hours or 250°C for 4 hours and

allowed to cool in the oven overnight before opening the door to remove glassware for storage. Materials that cannot be heated in this manner can be treated with RNaseZap (Ambion). Chemicals for solutions are handled using gloves and spatulas that have been made RNase free.

2. We use TOPO® cloning kits (Invitrogen) for insertion of our PCR products of interest. Generally they contain promoter sites for Sp6, T3, and T7 depending on the particular kit.
3. We use 24 × 40 mm No. 1 glass coverslips which completely cover the useable area of the Fisherbrand® ProbeOn™ Plus microscope slides. The hybridization mix volume is calculated based on this size coverslip. Alternatively you can make coverslips from Parafilm M®, these have the advantage of easier removal after hybridization and before the washes. Remember to handle coverslips and Parafilm M® with gloved hands to keep them RNase free.
4. We use a Nunc Bio-Assay dish (243 × 243 × 18 mm) as a hybridization chamber. Whatman Gel Blot paper (200 × 250 mm) is placed in the dish and 8 wood craft sticks (i.e. popsicle sticks) are used to support the slides in the chamber. The chamber will hold 16 slides; 4 slides on 2 wood craft sticks. Use ~75 ml of 50% formamide solution to wet the paper.
5. RNase A is difficult to remove from glassware. We have glassware set aside specifically dedicated for preparation and use of RNase buffer.
6. Dilute the Kodak NBT 2 Emulsion (VWR) in a dark room under safe light conditions as follows. Emulsion comes in a 4 oz container in a small cardboard box. The box may be opened in the light, but not the container. In the darkroom, place the container with the lid still on in the 45°C waterbath for an hour in order to liquefy the emulsion. Place an equal volume (118 ml) of RFW in a 500 ml flask in the waterbath. At the end of the hour, *carefully* pour the emulsion into the beaker containing RFW. Rinse the emulsion container with a little of the diluted solution, emulsion is expensive. Gently swirl the mixture then put it back in the waterbath for a few minutes for even mixing. Aliquot ~40 ml each into 50 ml conical tubes. Wrap individual tubes in foil and store at 4°C, nowhere near any radioactivity! Diluted emulsion is good for ~ 6 months.
7. We pre-label our slides using a pencil; do not label with lab markers because the writing will come off in the EtOH washes.
8. We use 1×10^6 cpm/μl as index of the efficiency of the probe labeling. The integrity of the probe is confirmed by gel electrophoresis (Section 3.2.9). If the efficiency of the probe

labeling is low or the integrity of the probe is not a single band of the expected size, do not proceed. Repeat the probe labeling in Section 3.2

9. Our laboratory has routinely used 1×10^6 cpm/slide for hybridization. However, amount of probe added to the slides may vary with your probe sequence, length of your probe, type of tissue and whether you are going to quantitate the in situ reaction product. The specific activity can be calculated if necessary.
10. Since the emulsion is expensive we use a small oblong glass vial that holds ~ 10 ml of emulsion. We dip 2 slides back to back in the vial for 3 seconds, draining emulsion back into the vial by scraping the edge of the slides along the edge of the vial. Make sure that there is an even coating of emulsion on the slides, there will be areas of no signal without emulsion. Blot the slides on paper towels and then separate the slides to dry. Add emulsion to the vial when the volume falls below the tissue sections on the slide. Generally we can dip a rack of 30 slides in 10 ml. We have also used coplin jars as a dipping vessel but the volume of emulsion needed is greater. Do not reuse the emulsion that has had slides dipped in it. Emulsion that has been heated but not used may be stored and used in the future.
11. In designing the experiment we add a few additional slides that can be used to determine the time needed for development of a significant signal. These "test" slides are dipped in emulsion along with the rest but placed in a separate box. That way we can develop a slide or two without disturbing the "experimental" slides.
12. Hematoxylin Stain Gill's Formulation #2 should be filtered before use to remove particulates.

Acknowledgements

We are indebted to Ms. Sarah Wheeler-Price and Ms. Lauren Thomas for their assistance with the in situ hybridization. This work was supported by grants to TEC (NIH HDO57446 and NCRR P20 RR15592).

References

1. John HA, Birnstiel ML, Jones KW 1969 RNA–DNA hybrids at the cytological level. Nature 223 582–587
2. Gall JG, Pardue ML 1969 Formation and detection of RNA-DNA hybrid molecules in cytological preparations. Proc Natl Acad Sci U S A 63:378–383
3. Warford A, Lauder I 1991 In situ hybridisation in perspective. J Clin Pathol 44:177–181

4. Wilcox JN 1993 Fundamental principles of in situ hybridization. J Histochem Cytochem 41: 1725–1733
5. Emson PC 1993 In-situ hybridization as a methodological tool for the neuroscientist. Trends Neurosci 16:9–16
6. Curry TE, Jr., Nothnick WB 1996 Changes in ovarian tissue inhibitor of metalloproteinase (TIMP) expression during follicular growth, ovulation, and the luteal period in the rat. Proceedings of Inhibitors of Metalloproteinases in Development and Disease. Banff: 119–126
7. Hagglund AC, Ny A, Leonardsson G, Ny T 1999 Regulation and localization of matrix metalloproteinases and tissue inhibitors of metalloproteinases in the mouse ovary during gonadotropin-induced ovulation. Endocrinology 140:4351–4358
8. Nothnick WB, Soloway P, Curry TE, Jr. 1997 Assessment of the role of tissue inhibitor of metalloproteinase-1 (TIMP-1) during the periovulatory period in female mice lacking a functional TIMP-1 gene. Biol Reprod 56:1181–1188
9. Simpson KS, Byers MJ, Curry TE, Jr. 2000 Spatiotemporal mRNA expression of the tissue inhibitors of metalloproteinases (TIMPs) in the ovary throughout the rat estrous cycle. Endocrinology 142:2058–2069
10. Liu K, Olofsson JI, Wahlberg P, Ny T 1999 Distinct expression of gelatinase A [matrix metalloproteinase (MMP)-2], collagenase-3 (MMP-13), membrane type MMP 1 (MMP-14), and tissue inhibitor of MMPs Type 1 mediated by physiological signals during formation and regression of the rat corpus luteum. Endocrinology 140:5330–5338
11. Curry TE, Jr., Song L, Wheeler SE 2001 Cellular localization of gelatinases and tissue inhibitors of metalloproteinases during follicular growth, ovulation and early luteal formation in the rat. Biol Reprod 65:855–865

Chapter 8

Adenoviral Gene Transfer into Isolated Pancreatic Islets

Latha Muniappan and Sabire Özcan

Abstract

The beta cells within the pancreatic islets are responsible for production of insulin, a peptide hormone required for maintaining normoglycemia. The establishment of efficient gene transfer into pancreatic islets is very important for studies of insulin and glucagon production and secretion, as well as for gene therapy purposes for the treatment of diabetes. We describe here in detail a protocol for adenoviral gene transfer into isolated mouse islets of the pancreas. Effective gene transfer into pancreatic islets using recombinant adenoviruses can be achieved with a multiplicity of infection (MOI) of 10. However, if the islets are not dispersed, adenoviral gene transfer is limited only to the cells on the periphery of the islets, which represent the glucagon-producing alpha cells in rodents. Dispersion of pancreatic islets with EGTA increases the efficiency of gene transfer into the cells within the core of the islets, which consist of insulin-producing beta cells.

Key words: Recombinant adenovirus, pancreatic islets, diabetes, gene therapy, insulin, gene transfer, GFP.

1. Introduction

The insulin-producing beta cells within the islets of the pancreas are essential for maintaining glucose homeostasis. Lack of or decreased insulin production and secretion results in type 1 and type 2 diabetes. Therefore the pancreatic beta cells are a major target for gene therapy in the treatment of diabetes (1, 2). The islets of the pancreas consist of four different cell types, of which about 70% are insulin producing beta cells, surrounded by glucagon-producing alpha cells in rodents. Targeting the pancreatic islets could potentially intervene or even reverse the course of diabetes by modulating the immune response, preventing beta cell death and promoting neogenesis of the islets.

O.-K. Park-Sarge, T.E. Curry, Jr. (eds.), *Molecular Endocrinology,* Methods in Molecular Biology 590,
DOI 10.1007/978-1-60327-378-7_8,

Current research is mainly directed to develop highly efficient and non-toxic vectors for gene transfer in primary insulin producing cells. There are a number of non-viral and viral gene transfer strategies available for transfection of cells. Non-viral methods that are routinely utilized for gene transfer into many cell types include calcium phosphate precipitation, cationic liposome, and the biolistic method (3). Viral gene transfer methods are more efficient in pancreatic islets (4) and utilize many different recombinant viruses, including retroviruses (4), lentiviruses (4), adeno-associated viruses (AAV) (5), and adenoviruses (4, 6–8). Retroviral gene transfer requires the transfection of dividing cells and is not suitable for islet cells, which are nondividing cells. Lentiviruses, which belong to the HIV family of viruses, are effective in transfer of genes to both dividing and nondividing cells, but the safety of the recombinant lentiviruses for gene transfection purposes in a clinical setting has not been confirmed. AAV can transduce nondividing cells and integrates into the host genome, but is considered inadequate for gene transfection into islet cells due to the need of high dose of recombinant viruses (6, 8). Adenoviral gene transfer offers the advantage of a high gene transfer efficiency into pancreatic islets and does not interfere with islet function (4, 9). Together with lentivirus and AAV, adenovirus is the most commonly used recombinant virus in current beta-cell research (8). However, one important limitation of the adenoviral mediated gene transfer is that adenoviruses cannot reach and transfect the cells within the core of pancreatic islets, which contain the insulin-producing beta cells.

To achieve a more beta-cell specific gene expression, new adenoviral vectors have been developed, which contain beta-cell specific promoters including the insulin promoter (10). This insures the expression of the desired gene only in insulin-producing beta-cells. Also a number of inducible adenoviral vectors are available, where the gene of interest is under the control of a tetracycline-regulated (11) or hormone-inducible promoter (12).

The adenoviral gene transfer method described in this chapter is optimized and standardized using the pAdEasy adenoviral system (13). The efficiency of viral gene transfer depends on many factors including the stability and toxicity of the expressed protein in islets. Infection of islets with various titers of recombinant adenoviruses resulted in 70% efficiency with an adenoviral titer of 2.3×10^7 plaque-forming unit (pfu)/mL. This corresponds to a multiplicity of infection (MOI) 10. Using an MOI of 50, the infection efficiency could be increased to 85–90%; however, high concentrations of virus are toxic and cause cell death. Low virus titers such as an MOI of 10 resulted in 70% efficiency with no increase in islet cell death (**Fig. 8.1**). Since the pAdEasy system contains green fluorescent protein (GFP), transfection efficiency could be easily followed and GFP positive cells were observed 16 h

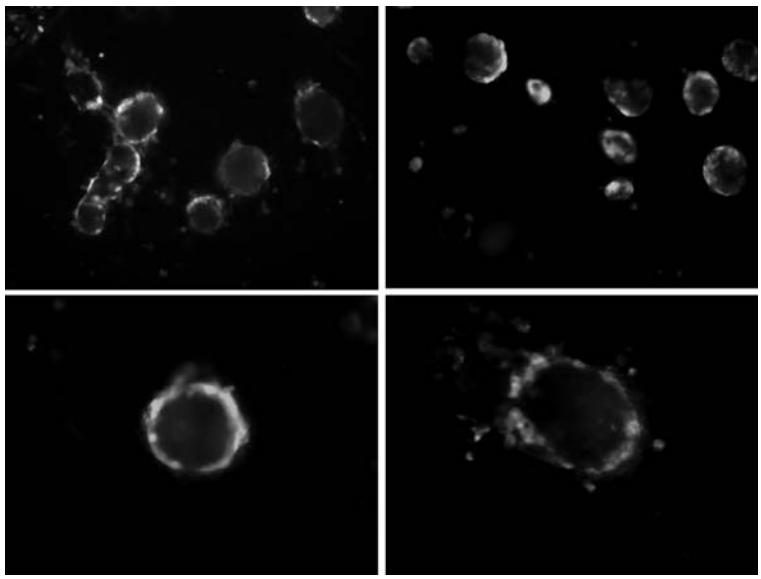

Fig. 8.1. Adenoviral mediated gene transfer into mouse islets. Islets were first incubated with the GFP adenovirus for 10 min at 37°C with gentle agitation and then placed in a 37°C humidified incubator for 24 h. Islets were visualized using fluorescence microscopy.

after infection using fluorescence microscopy. Analysis of the transfected islets using confocal microscopy indicated that GFP expression was restricted to the outermost layer (first to two layers) of cells, while the core of the islet was GFP-negative (**Fig. 8.2A**). Since the insulin-producing beta cells are more abundant in the center of the islet, only a few beta cells are transfected after adenoviral infection of intact islets (**Fig. 8.3**). Large islets were more difficult to infect compared to smaller ones (14, 15). This is likely due to necrosis of cells in the core of the islet, since they lack nutrients due to limited nutrition diffusion.

In order to reach the core of the islet and also to improve adenoviral transfection efficiency, the cell-to-cell contact of the intact islets was disrupted transiently by utilizing 2 mM of ethylene glycol tetraacetic acid (EGTA), which increases cell permeability (16). This led to an increase in gene transfer efficiency. Analysis of the EGTA treated islets using confocal microscopy indicated an increased distribution of GFP positive cells throughout the islet rather than being confined to the periphery (**Fig. 8.2B**). However, most of the cells located within the core of the islet were still GFP-negative.

Considering the compact structure of the pancreatic islet, a more efficient vector for gene transfer would have to be able to not only transfect the periphery of the islet, but also penetrate to the core of the islet. This is highly important, as the insulin producing beta cells are mainly situated in the core of the islet surrounded by a mantle of non-beta cells at the periphery.

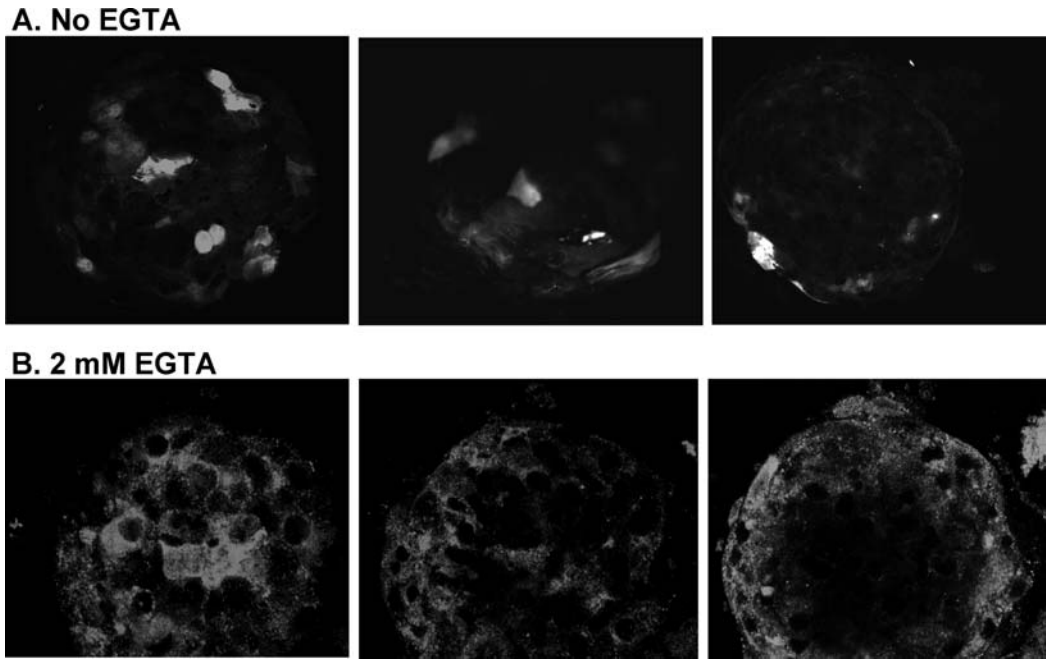

Fig. 8.2. Analysis of GFP expression in mouse islets following adenoviral-mediated gene transfection with a GFP adenovirus by confocal microscopy. Islets were pretreated without (**A**) or with (**B**) 2 mM EGTA for 15 min at 37°C with gentle agitation, then infected with adenovirus of MOI 10 and placed in a 37°C humidified incubator for 24 h. The transfection efficiency was determined by detection of GFP fluorescence using a confocal microscope.

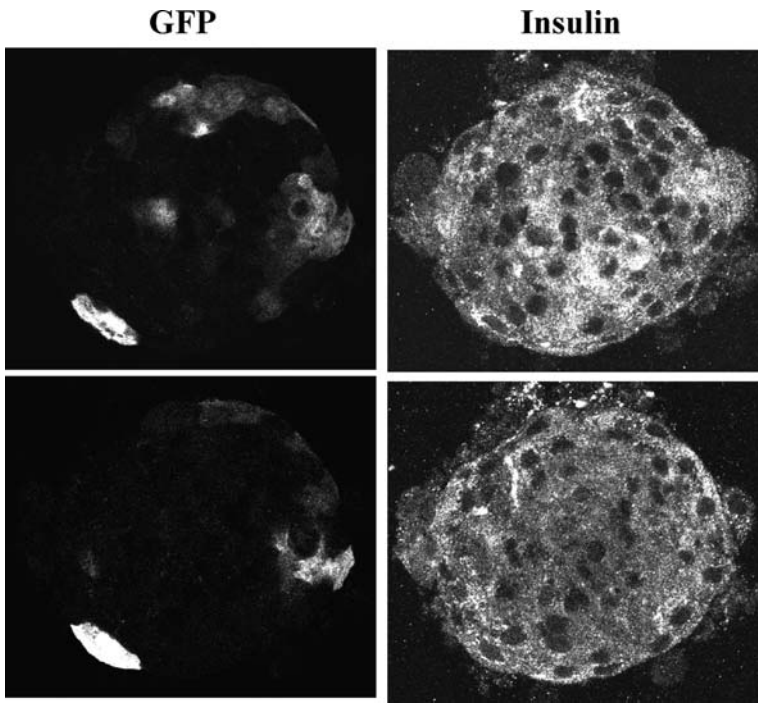

Fig. 8.3. Analysis of adenoviral gene transfer into pancreatic beta cells. Twenty-four hours after adenoviral gene transfection with the GFP adenovirus, islets were fixed, permeabilized and stained for insulin. GFP and insulin staining was visualized using immunofluorescence microscopy.

2. Materials

All media were sterilized by filtration through a 0.22 μm filter.

2.1. Isolation of Mouse Pancreatic Islets

1. Dulbecco's Modified Eagle's Medium (DMEM): DMEM supplemented with 4.5 g/L glucose, 2 mM glutamine, 50 μM penicillin and streptomycin (Gibco/BRL).
2. Ca^{++}- and Mg^{++}-free Hanks' Balanced Salt Solution (HBSS): 400 mg/L KCl, 60 mg/L KH_2PO_4, 350 mg/L $NaHCO_3$, 8 g/L NaCl, 48 mg/L Na_2HPO_4, 1 g/L D-Glucose, 10 mg/L Phenol Red (Gibco/BRL).
3. 1x Phosphate-buffered saline (PBS), pH, 7.4: 150 mM NaCl, 2.7 mM KCl, 4.3 mM Na_2HPO_4, 1.4 mM KH_2PO_4.
4. Dissociation medium: RPMI-1640 supplemented with 1 mg/mL collagenase type V (Sigma), 2 mg/mL STI (Sigma) and 2% BSA fraction V (Sigma).
5. RPMI-1640: RPMI-1640 supplemented with 2 mM glutamine, 50 μM penicillin and streptomycin (Gibco/BRL).
6. RPMI-1640 + 10% FBS: RPMI-1640 supplemented with 10% volume/volume fetal bovine serum (Sigma), 2 mM glutamine, 50 μM penicillin and streptomycin (Gibco/BRL).
7. Matrigel (BD Biosciences): To treat the tissue culture dishes with matrigel, dilute matrigel with RPMI-1640 medium to a final concentration of 6.3 mg/mL in a 50 mL tube. Centrifuge at 2,800 *g* for 20 min at 4°C to remove debris. Transfer supernatant to a sterile falcon tube. For a 60-mm dish add 300 μL matrigel with a sterile pipette and use a sterile cell scraper to evenly spread the matrigel. Incubate at 37°C for 30 min until matrigel polymerizes. Add 2 mL of medium to each dish coated with matrigel.
8. Wrist-action shaker.
9. Dissecting microscope.
10. Dissecting tools: Scissors, Tweezers, Scalpels.
11. Cell dissociation sieve—60 mesh(Sigma-Aldrich S1020-5EA).

2.2. Dispersion of Isolated Islets

1. Ca^{++}- and Mg^{++}-free HBSS supplemented with 2 mM ethylene glycol tetra-acetic acid (EGTA) (Sigma).

2.3. Adenoviral Transfection of Isolated Mouse Islets

1. Recombinant adenoviruses—Recombinant adenoviruses expressing GFP were constructed using the pAdEAsy system (13, 17) and amplified as described previously.
2. RPMI-1640.

3. RPMI-1640 + 10% FBS solution.
4. 1x PBS.
5. Inverted Fluorescence Microscope (Olympus).

2.4. Immunofluoresence

1. Microscope cover slips (22 × 40 × 0.15 mm) (Fisher).
2. 1x PBS.
3. Paraformaldehyde (Fisher): Prepare a 4% (w/v) solution in 1x PBS fresh for each experiment. The solution may need to be carefully heated (use a stirring hot-plate in a fume hood) to dissolve and then cool to room temperature for use.
4. Quench solution: 100 mM glycine in 1x PBS.
5. Permeabilization solution: 0.5% (v/v) Triton X-100 in 1x PBS.
6. Blocking buffer: 3% (w/v) BSA in 1x PBS.
7. Vectashield mounting medium with DAPI (4, 6-diamino-2-phenylindole; Vector Laboratories). Store at 4°C in the dark.

2.5. Insulin Staining

1. Insulin antibody: Monoclonal anti-insulin serum (Cat. No. I2018, Sigma).
2. Secondary antibody: TRITC (tetramethylrhodamine β isothiocyanate)-conjugated secondary antibody against mouse (Molecular Probes).
3. Leica SP2 laser scanning confocal microscope or equivalent.

3. Methods

3.1. Isolation of Mouse Pancreatic Islets

The procedure described below is for five 6–8 weeks old C57BL6 mice. Surgery and islet isolation should be performed as quickly as possible to minimize tissue degradation. The method used to isolate pancreatic islets is based on the protocol developed by Gotoh et al. (18) and Shewade et al. (19) with some modifications.

1. After the animal is deeply anesthetized by intraperitoneal injection of Nebutal (40–60 mg/kg body weight), clean the midline incision site with 70% ethanol. Make a midline incision through the skin and separate the skin from the muscle using scissors and forceps.
2. Make a U-shaped incision through the abdominal muscle and pull the tissue flap upward. Remove the intestine and stomach out of the body cavity to expose the spleen attached with pancreas.
3. Separate the pancreas and immediately place it into a 50 mL falcon tube containing 10–20 mL ice-cold DMEM and keep on ice.

4. Wash the pancreata 3 times with 3 mL of 1x PBS by centrifuging at 180 *g* for 5 min at 4°C to remove the fatty tissue and blood clots by aspirating media (*see* **Note 1**).
5. Place the pancreata in a petri dish with 3 mL PBS, and using scalpel and scissors, chop the tissue into small sized pieces, leaving no heavy chunks of tissue.
6. Wash the chopped pancreatic tissue 2 times with 3 mL of 1x PBS.
7. Wash the chopped tissue 2 times with 3 mL of DMEM by centrifugation at 180 *g* for 5 min and remove the floating fatty tissue by aspirating the supernatant.
8. Add 15 mL of dissociation medium to the chopped tissue from five mouse pancreata.
9. Place the tubes into a wrist-action shaker water bath at 37°C and incubate for at least 15–20 min (optimize for each lot of collagenase and animal strain) (*see* **Note 2**).
10. After the incubation time, shake the tubes vigorously. If the digestion is complete, the tissue should fall apart and have a "creamy" texture (*see* **Note 3**).
11. When the digestion is complete, stop the collagenase reaction by adding 10 mL of ice-cold RPMI-1640 + 10% FBS to the tubes.
12. Centrifuge the mixture at 180 *g* for 5 min at 4°C
13. Discard the supernatant and repeat the wash for 2 more times with ice cold RPMI-1640 + 10% FBS. Be very cautious not to aspirate the pellet.
14. Seed the pellet in a 60-mm cell culture dish containing RPMI-1640 + 10% FBS. The islets can now be cultured at 37°C with 5% CO_2 for 48 h.
15. After 48 h, the floating islets should be picked manually using a Pasteur pipette under a dissection microscope and used for experiments. Smaller islets are preferred for adenoviral gene transfer (*see* **Notes 4–6**).

3.2. Dispersion of Isolated Islets

1. Plate the desired number of islets (*see* **Note 7**) in a 60-mm dish for adenoviral gene transfection.
2. Rinse the islets with 3 mL of RPMI-1640 + 10% FBS and allow the islets to adhere to culture dishes coated with matrigel as prepared in Section 2.1.
3. Incubate the cells with RPMI-1640 + 10% FBS.
4. After 24 h, disperse the islets by treating with 2 mM EGTA as in steps 5–6. To increase the adenoviral transfection efficiency, islets are pretreated with 2 mM EGTA to disrupt the cell-to-cell contact (*see* **Note 8**).
5. For dispersion: Aspirate the RPMI-1640 media and wash the cells 2 times with 2 mL of 1x PBS.

6. Incubate the isolated islets in a 2 mL of Ca^{2+}- and Mg^{2+}-free HBSS containing 2 mM EGTA to disrupt the cells. After 15 min of incubation at 37°C with gentle agitation, disrupt the remaining intact islets mechanically by pipetting.
7. Once the cells are dispersed, they can be used for transfection with recombinant adenoviruses.

3.3. Adenoviral Transfection of Isolated Mouse Islets

1. Thaw the frozen recombinant adenovirus expressing GFP stock on ice. For preparation of recombinant adenovirus, see the previously published methods (13, 17).
2. Aspirate the media from the islets in a tissue culture hood, and wash the islets twice with 2 mL of 1x PBS.
3. Add 500–1000 μL of recombinant adenovirus resuspended in RPMI-1640 medium without FBS with MOI of 5, 10, or 50 (*see* **Notes 10–11**).
4. Islets need to be completely covered with media.
5. To ensure the even distribution of the virus, incubate the islets with virus for 10 min at 37°C with mild agitation in a tissue culture hood.
6. Add 1 mL of RPMI-1640 + 10% FBS and maintain the islets for 24 h at 37°C in a humidified incubator with 5% CO_2 and 95% air.
7. To determine the efficiency of viral transfection, analyze the number of GFP expressing cells under the fluorescence microscope after 16 h of transfection.
8. Change the media every 24 h if the cells need to be kept for a longer period of time (for more than 2–3 days).
9. After the desired transfection efficiency is observed, the transfected islets can be used for immunofluorescence, immunoblotting, or PCR reactions etc.

3.4. Immunofluorescence

1. Quickly rinse the islets twice with ice-cold 1x PBS.
2. Incubate the islets with 4% paraformaldehyde (PFA) solution for 10 min at room temperature to fix the cells.
3. Discard the PFA (into a hazardous waste container) and wash the samples twice for 5 min each with 1x PBS.
4. Quench the residual formaldehyde by incubating with 100 mM glycine for 10 min at room temperature, followed by two washes with 1x PBS.
5. Permeabilize the cells by incubation in PBS/0.5% Triton X-100 for 5 min at room temperature and then rinse the cells twice with 1x PBS.

6. Incubate the cells with 15 μL of Vectashield mounting medium with DAPI (1.5 μg/mL) for 10 min at room temperature to stain the DNA in the nucleus.
7. As the sample is on a cover slip, carefully invert the cover slip into a drop of mounting medium on a microscope slide. Seal the sample using Nail varnish. The sample can be viewed immediately after the varnish is dry or be stored in the dark at 4°C for up to a month.

3.5. Insulin Staining

Following 3.3.1–3.3.5,

1. Block the samples with 3% (w/v) BSA in 1x PBS at room temperature for 30 min.
2. Remove the blocking solution and incubate with primary anti insulin antibody (dilution 1:100 in 3% BSA) at 4°C overnight in a humidified chamber.
3. Wash the samples 3 times for 5 min each with 1x PBS.
4. Incubate the cells with TRITC (tetra-methylrhodamine β−isocyanate)-conjugated secondary antibody against mouse (dilution 1:250 in 1x PBS) for 1 h at 37°C in a humidified chamber protected from light.
5. Process the cover slips as in steps 6–7 of Section 3.4.
6. View the slides under phase contrast microscope (to locate the cells and identify focal plane) and capture the images on a Leica SP2 laser scanning confocal microscope using a $\times 63$ oil immersion objective. Emitted light is detected at >515 nm for GFP (green) or >560 nm for insulin (red).

4. Notes

1. Pancreata should be washed thoroughly to ensure that they are not contaminated with any fatty tissue. Contamination with fatty tissue will decrease islet yield. The fatty tissue and blood clots should be removed by aspirating the media after washing the cells.
2. The batch of collagenase used for islet isolation is very important since the collagenase activity varies with lot number from the same supplier and source. We use Type V collagenase (Sigma), which is optimal for pancreas digestion. The quantity of collagenase required to digest the pancreas varies with the strain and age of animal used. The duration of collagenase digestion also depends on collagenase activity. To test a new

batch of collagenase start with a 5 min digestion period. If the time required to digest the pancreatic tissue exceeds 15 min, increase the amount of collagenase.

3. The endpoint for collagenase digestion is determined visually. Completely digested pancreata will have no tissue chunks and appear smooth with a "creamy" texture.
4. We used smaller islets for adenoviral gene transfer, because larger islets with diameters > 150 microns are more prone to core cell death (14). On average a rodent pancreas has 3 times more small islets than large ones and the small islets have been shown to have about 20% higher viability (14). Incubation of islets at low temperatures (26°C) appears to be effective in prevention of core cell damage (15).
5. Islets can also be purified by using a Ficoll (type 400DL, Sigma) gradient as described previously (20). The islets form a ring at the interphase of the medium and Ficoll and are recovered using a micropipette.
6. Islets can also be identified by staining with dithiozone (21) and appear red under the microscope. To stain islets with dithiozone, use a very small aliquot of the islet preparation, since dithiozone is toxic to cells.
7. The number of islets required depends on the type of the experiment. For immunostaining 20–30 islets are sufficient, while for Western blotting, RNA extraction, and siRNA transfection 200–400 islets are required.
8. In a recently described method, a transfection efficiency of 100% was achieved with an MOI of 5 using a two-step digestion protocol (22). In this method, the islets are first dispersed by digestion with collagenase and EGTA/dispase. After adenovirus-mediated gene transfer, the cells are reorganized to islet like structures.
9. The pAdEasy adenoviral expression system used in this protocol is described in reference 13. Although we used the GFP adenovirus for adenoviral gene transfer into pancreatic islets, the same procedure or protocol also applies for any other type of recombinant adenovirus.
10. The amount of islets, the MOI and the length of incubation with adenovirus depends on the type of the gene to be expressed and the type of experiment.
11. Low adenovirus titers result in decreased gene transfer efficiency (**Fig. 8.1**) Although, transfections with high adenoviral titers result in increased transfection efficiency, they also lead to increased cell death.

Acknowledgements

This work was supported by grants from NIH/NIDDK R01DK067581 and American Diabetes Association 1-05-CD-15 to S.Ö. L. M. is a recipient of the American Heart Association Great Rivers Affiliate Postdoctoral Fellowship.

References

1. Wajchenberg, B. L. (2007) Beta-cell failure in diabetes and preservation by clinical treatment. *Endocr. Rev.* **28,** 187–218.
2. Zaia, J. A. (2007) The status of gene vectors for the treatment of diabetes. *Cell Biochem. Biophys.***48,**183190.
3. Gainer, A. L., Korbutt, G. S., Rajotte, R. V., Warnock, G. L., and Elliott, J. F. (1996) Successful biolistic transformation of mouse pancreatic islets while preserving cellular function. *Transplantation.* **61,** 1567–1571.
4. Leibowitz, G., Beattie, G. M., Kafri, T., Cirulli, V., Lopez, A. D., Hayek, A. et al. (1999) Gene transfer to human pancreatic endocrine cells using viral vectors. *Diabetes.* **48,** 745–753.
5. Prasad, K. M., Yang, Z., Bleich, D., and Nadler, J. L. (2000) Adeno-associated virus vector mediated gene transfer to pancreatic beta cells. *Gene Ther.* **7,** 1553–1561.
6. Sigalla, J., David, A., Anegon, I., Fiche, M., Huvelin, J. M., Boeffard, F. et al. (1997) Adenovirus-mediated gene transfer into isolated mouse adult pancreatic islets: normal beta-cell function despite induction of an anti-adenovirus immune response. *Hum. Gene Ther.* **8,** 1625–1634.
7. Barbu, A. R., Akusjarvi, G., and Welsh, N. (2002) Adenoviral-induced islet cell cytotoxicity is not counteracted by Bcl-2 overexpression. *Mol. Med.* **8,** 733–741.
8. Mukai, E., Fujimoto, S., Sakurai, F., Kawabata, K., Yamashita, M., Inagaki, N. et al. (2007) Efficient gene transfer into murine pancreatic islets using adenovirus vectors. *J. Control Release.* **119,** 136–141.
9. Csete, M. E., Afra, R., Mullen, Y., Drazan, K. E., Benhamou, P. Y., and Shaked, A. (1994) Adenoviral-mediated gene transfer to pancreatic islets does not alter islet function. *Transplant. Proc.* **26,** 756–757.
10. Wang, X., Olmsted-Davis, E., Davis, A., Liu, S., Li, Z., Yang, J. et al. (2006) Specific targeting of pancreatic islet cells in vivo by insulin-promoter-driven adenoviral conjugated reporter genes. *World J. Surg.* **30,** 1543–1552.
11. Takahashi, R., Ishihara, H., Takahashi, K., Tamura, A., Yamaguchi, S., Yamada, T. et al. (2007) Efficient and controlled gene expression in mouse pancreatic islets by arterial delivery of tetracycline-inducible adenoviral vectors. *J. Mol. Endocrinol.* **38,** 127–136.
12. Xu, Z. L., Mizuguchi, H., Mayumi, T., and Hayakawa, T. (2003) Regulated gene expression from adenovirus vectors: a systematic comparison of various inducible systems. *Gene.* **309,** 145–151.
13. He, T. C., Zhou, S., da Costa, L. T., Yu, J., Kinzler, K. W., and Vogelstein, B. (1998) A simplified system for generating recombinant adenoviruses. *Proc. Natl. Acad. Sci. USA* **95,** 2509–2514.
14. MacGregor, R. R., Williams, S. J., Tong, P. Y., Kover, K., Moore, W. V., and Stehno-Bittel, L. (2006) Small rat islets are superior to large islets in in vitro function and in transplantation outcomes. *Am. J. Physiol. Endocrinol. Metab.* **290,** E771–E779.
15. Cui, Y. F., Ma, M., Wang, G. Y., Han, D. E., Vollmar, B., and Menger, M. D. (2005) Prevention of core cell damage in isolated islets of Langerhans by low temperature preconditioning. *World J. Gastroenterol.***11,**545–550.
16. Barbu, A. R., Bodin, B., Welsh, M., Jansson, L., and Welsh, N. (2006) A perfusion protocol for highly efficient transduction of intact pancreatic islets of Langerhans. *Diabetologia.* **49,** 2388–2391.
17. Mosley, A. L. and Ozcan, S. (2003) Adenoviral gene transfer into beta-cell lines. *Methods Mol. Med.***83,**73–79.
18. Gotoh, M., Maki, T., Kiyoizumi, T., Satomi, S., and Monaco, A. P. (1985) An improved method for isolation of mouse pancreatic islets. *Transplantation.* **40,** 437–438.
19. Shewade, Y. M., Umrani, M., and Bhonde, R. R. (1999) Large-scale isolation of islets by tissue culture of adult mouse pancreas. *Transplant. Proc.* **31,** 1721–1723.
20. Kelly, C. B., Blair, L. A., Corbett, J. A., and Scarim, A. L. (2003) Isolation of islets of

Langerhans from rodent pancreas. *Meth. Mol. Med.* **83,** 3–14.

21. Clark, S. A., Borland, K. M., Sherman, S. D., Rusack, T. C., and Chick, W. L. (1994) Staining and in vitro toxicity of dithizone with canine, porcine, and bovine islets. *Cell Transplant.* **3,** 299–306.
22. Tsukiyama, S., Matsushita, M., Matsumoto, S., Morita, T., Tsuruga, Y., Takahashi, T. et al. (2008) Noble gene transduction into pancreatic beta-cells by singularizing islet cells with low doses of recombinant adenoviral vector. *Artif. Organs.* **32,** 188–194.

Chapter 9

Basic Molecular Techniques for the Detection of Single Nucleotide Polymorphisms: Genome-Wide Applications in Search for Endocrine Tumor Related Genes

Anelia Horvath and Constantine Stratakis

Abstract

The necessity of genotyping high number of variations in extended sample sets has become apparent in the era of large genomic studies of common complex disorders, in cancer and in pharmacogenomics. The single nucleotide polymorphisms' (SNPs) apparent advantages over other genetic markers such as high frequency, relative stability, and statistically random distribution across the genome have made them a method of choice for most of these genome-wide oriented applications. The requirement for simultaneous genotyping of high number of SNPs, keeping at the same time reasonable price and reliable accuracy, triggered the rise of the genotyping throughput, and led to the development of the array-based technologies. The present chapter briefly reviews the methodological and historical aspect of the basic SNP detecting techniques that lie in the basis of the modern high-throughput technologies, providing at the same time detailed guide on the application of one of the most advanced SNP microarray platform on the market: the genome-wide SNP Array 6.0 recently developed by Affymetrix, which we have used to study families with Catney complex and Micronodular adrenocortical hyperplasia. In addition, we discuss practical clues and tips aiming at extending applications and improving performance.

Key words: SNP, variation, microarray, endocrinology, genome.

1. Introduction

1.1. Background

The completion of the Human Genome Project opened a whole new era in genetic studies (1, 2). Subsequently, the International HapMap Project provided further insight into the extent of human genetic diversity and delivered new tools for the study of genetics (3, 4). Genome variations result from the concurrent action of mutational events and evolutionary selection. These two factors

O.-K. Park-Sarge, T.E. Curry, Jr. (eds.), *Molecular Endocrinology,* Methods in Molecular Biology 590,
DOI 10.1007/978-1-60327-378-7_9,

have favored the accumulation of base substitutions, making the single nucleotide polymorphisms (SNPs) the most common variation of the human genome. More than 11 million SNPs are reported so far in the databases, with an overall appearance of 1 per every 100–300 bp (5, 6). SNP is defined as a point variation located at a specific position in the genome, with minor allele frequency (MAF) above 1% in at least one non-selected population. However, not all SNPs strictly match this definition—nowadays many variants, including small insertions, deletions, and variations with less than 1% MAF are also referred to us as SNPs. Most frequently SNPs occur in non-coding regions of the genome; when located in the regulatory sequences of a gene, such as promoters, enhancers, silencers, and transcription-binding sites, they can affect the levels of expression of the particular protein, and are referred to us as regulatory SNPs (rSNPs) (**reviewed in** 6). Although less frequently, SNPs are also found in the coding sequences, where they may alter protein structure and function, and, apart as genetic markers, can serve as functional variants.

The most important revelation of the HapMap project was that the human genome is organized into discrete linkage disequilibrium (LD) blocks with relative evolutionary stability and boundaries defined by the break-points of a recombination event (4). The association between neighboring SNPs significantly reduces the genome variation complexity and enables the use of limited number of representative SNPs (tag-SNPs) for the prediction of all the major haplotypes, thus greatly improving genotyping accuracy and reducing its cost; it is estimated that approximately 500,000 tag SNPs are sufficient for the full genotyping of an individual of European descent (7–9).

The necessity of genotyping high number of variations in extended sample sets has become apparent in the studies of common complex disorders, cancer, and pharmacogenomics. In contrast to the rare Mendelian diseases, in which variation in a single gene is sufficient to cause the disease phenotype, common disorders are thought to be due to the combined effect of a number of susceptibility DNA variations acting in concert with the environment. Genome-wide association (GWA) approaches require large number of SNPs (10^6–10^7) that are spread all over the human genome, to be genotyped in large cohorts of individuals. Because of its comprehensiveness, reliability, and reproducibility, GWA studies are rapidly replacing the more traditional candidate-gene and linkage mapping strategies that have dominated genetics in the past. In our laboratory, genotyping more than 10,000 SNPs and looking for both association and loss of heterozygosity (LOH), we were able to identify variations in the genes coding for phosphodiesterases (*PDE11A* and *PDE8B*) to contribute to the phenotype of micronodular adrenocortical hyperplasia (MAD) (10, 11). More recently, a number of GWA studies shed light on

the genetics of common endocrine disorders such as type 2 diabetes (T2D) (12–17), obesity (18, 19), and height (20, 21). The identification of the Wnt-signaling pathway member *TCF7L2* [transcription factor 7-like 2 (T-cell specific, HMG-box)] as one of the major contributing factors to T2D is considered one of the most essential findings in the arena of complex disease to date), and has been indeed repeated in European, Asian, and African populations (12–17). Further, variations in *INSIG2* (insulin-induced gene 2) and *FTO* (fat mass and obesity associated) were shown to associate with both adult and childhood obesity from GWA studies performed for obesity separately as well as a component of T2D (18, 19). Height was reported to associate with common variation in the *HMGA2* oncogene (high-mobility group AT-hook 2), again, as a result of GWA study (20); subsequent analysis of related GWA datasets revealed a second locus—*GDF5-UQCC* (growth differentiation factor 5 and ubiquinol-cytochrome c reductase complex chaperone)—yeast homolog CBP3 to also contribute to height variations (21).

When applied on cancer studies, highly parallel SNP genotyping have shown incomparable potential to identify different types of genetic changes simultaneously, thus deciphering the initiation and progression of the tumorigenic processes **(reviewed in** 22, 23**)**. For example, GWA scans revealed two closely related loci on 8q24 to associate with prostate cancer in both European and African-American population (24–27). Finally, in pharmacogenomics, a whole field relies on the ability to accurately genotype multiple genetic variations in an individual drug response genes in order to provide optimized therapeutic outcome **(reviewed in** 6**)**. All these possible applications make high-throughput SNP genotyping a tool of unparalleled usefulness for studying the genetic and/or genomic basis of human diseases and to design new molecular therapies.

1.2. Genotyping Technologies

The SNPs' apparent advantages over other genetic markers such as high frequency, relative stability, and statistically random distribution across the genome have made them a method of choice for most of the genome-wide oriented applications. The requirement for simultaneous genotyping of high number of SNPs, at a reasonable price and with high reliability and accuracy, triggered the rise of the genotyping throughput, and led to the development of the array-based technologies. In addition to the high-throughput genotyping, SNP-arrays provide platforms for analyzing several more types of genetic alterations simultaneously: methylation patterns, all types of dosage changes, including allelic gains and losses, LOH and copy number variations, as well as expression profiles.

Although three- and tetra-allelic SNPs have been described, the vast majority of the SNPs are bi-allelic, thus triggering the technological challenge toward discrimination between two

alternative genetic variants. Two principal approaches for distinguishing of the alternative alleles lie in the bases of the majority of the modern high-throughput technologies: primer extension and hybridization. Some other approaches, such as enzymatic cleavage, ligation and single strand conformation polymorphism (SSCP) analysis have been successfully applied for studying many individual genetic variants, but have limited application in the high-throughput arena. Finally, the emerging new generation sequencing technologies are a promising tool for ultimate genome analysis in the very near future. A brief overview of the physico-chemical basis of the listed approaches is provided below.

Primer extension techniques are based on allele-specific incorporation of nucleotides complementary to the DNA template of interest (28). They may employ a common primer, which 3' end anneals with the base adjacent to the SNP, or two allele specific primers, which are identical except for their 3' nucleotide that is complementary to the corresponding alternative SNP allele; both approaches utilize the fidelity of the polymerase in extending accurately the nucleotide chain. To identify the extended nucleotide, either mass spectroscopy or fluorescent detection is applied, in the later case the different nucleotides are labeled with different fluorescent dyes.

Hybridization technologies employ the difference in the thermal stability of the DNA duplexes between perfectly complementary strands and mismatches. Accordingly, a crucial requirement is to optimize conditions favoring stringent hybridization between the complementary species; the major factors to determine the potential to accurately discriminate the alleles are the length and the sequence of the hybridizing molecules and the position of the mismatch. Significant advantage of the hybridization based approaches is that they do not require enzymatic discrimination of the alternative alleles. Therefore, these approaches are feasible for high-throughput applications, yet keeping the challenge of physico-chemical conditioning.

Ligation approaches are based on the ability of the ligase to discriminate between perfectly complementary adjacent nucleotides and mismatches; a bond is generated only when two adjacent 3' and 5' nucleotides are complementary to the template (29). Hence, the ligation-based technologies typically employ three nucleotides—two allele-specific and a common one —with 3'end immediately next to the variable position. The potential for multiplicity of the ligation based approaches have been explored in several assays—combinatorial fluorescence energy transfer (CFET) (30), Padlock technology (31, 32)—with the highest throughput achieved by its modification employing molecular inversion probe (MIP) which was able to detect accurately up to 12,000 per reaction (33).

Enzymatic cleavage is based on the ability of the certain classes' endonucleases to recognize and cleave DNA at specific sequences. Although one of the earliest techniques to detect DNA variations, and, also, implemented in classic technologies as Southern blot and Restriction Fragment Length Polymorphism (RFLP), the enzymatic cleavage is naturally restricted to the SNPs that change recognizable by the restriction endonucleases sequences (34). In an attempt to extend the RFLP application, a mismatch PCR-RFLP method has been designed, in which a restriction site is incorporated next to the SNP by a mismatched primer (35).

Single-strand confirmation polymorphism (SSCP) analysis employs the difference in the gel mobility of molecules with different conformation; it is applied on single stranded DNA fragments under non-denaturating conditions triggering the formation of different secondary conformation (36). The advantage of the SSCP is that it can be applied for screening for unknown SNPs in the particular PCR-amplified DNA fragment. Similarly to the hybridization, SSCP does not employ enzymatic features and is based only on the physico-chemical characteristics of the alternative molecules. Hence, it requires stringent optimization and may miss some variants which do not cause detectable difference in the physical features of the molecule under the applied conditions. A high-throughput application of SSCP has been recently explored with capillary array electrophoresis (37).

Sequencing: Nowadays, the whole-genome re-sequencing is acknowledged as an ultimate research tool to provide essential impact on the understanding of genome. Until recently, whole genome re-sequencing has been limited by the cost, time, and labor—effectiveness of the current technologies. Today, the growing recognition of its necessity is driving an exponential progress in the novel sequencing technologies development (38, 39). Although currently the re-sequencing of individual genomes requires resources that are beyond those of a single laboratory, realistic and affordable cost and time lines for their availability are seen in the very near future. Until then, DNA microarrays present an alternative practical way to study hundreds and thousands of individual genomes. Advances in microarray-based approaches have enabled to study not only the SNPs, but also all the main forms of genomic variation (amplifications, deletions, insertions and complex rearrangements). Below is provided a brief overview of the main steps in the development of the microarray technologies and their most advanced applications.

1.3. SNP Microarray Technology Development

The first SNP array-based assay was reported in 1998. It achieved reasonable accuracy in the simultaneous discrimination of 558 SNPs on a single array using hybridization-based approach (40). The major challenge in terms of labor-effectiveness was to

optimize the multiplex PCR toward minimal number of reactions per sample. This study opened the way for the development of array based high-throughput technologies.

Two years later, scientists from Affymetrix attained significant improvement in the reliability of the array-based genotyping: they included additional redundant probes for each SNP locus. These probes searched not only the polymorphic base but also four additional bases for each allele, thus increasing the competitiveness of the hybridization (41). In addition, this group explored a novel essential application of array-based SNP genotyping, allelic imbalance. Analyzing SNP strings in paired tumor and germ-line DNA samples in two major types of human tumors—neurofibromatosis type 2 and esophageal adenocarcinoma—the researchers demonstrated the capacity of the approach not only to detect LOH, but also to distinguish LOH in a mixed population of normal and neoplastic cells, which is the case in most tumor samples. At the same year, another group explored independently the SNP genotyping for tumor studies (42). Their analysis on human small-cell lung carcinoma validated accurate detection of LOH, but failed to prove that SNP arrays are reliable for studying of genomic amplifications. Nevertheless, these two steps in the novel SNP array application opened the way for the exploration of the SNP arrays to simultaneously characterize two major genome features—sequence and allelic imbalance.

Further progress in SNP genotyping throughput was technologically directed toward the improvement of two major factors: number of the analyzed in parallel assays and multiplexing of the sample preparation. The effort to optimize the multiplex PCR continued in the following years, leading to the development of several successful approaches for highly parallel genotyping. From them, the *Golden Gate assay* is one of the most successful and has been adopted by the company Illumina for their commercial SNP genotyping platform (43, 44). Human genome complexity emerged as a major challenge for next generation genotyping technologies. The first whole genome SNP array was developed 3 years later by Affymetrix researchers (45). The technique combined genome amplification and reduction of genome complexity by the following principal steps: restriction digestion, adaptor-based amplification, fragmentation, and labeling, followed by hybridization to the oligonucleotide array. The non locus-specific approach for amplification significantly increased the number of the SNPs analyzed, and in 2004 the first commercial array designed to genotype 10,000 SNPs simultaneously was released (46). The development of whole genome amplification approaches enhanced the applicability of the SNP microarrays to cancer tissues, and their ability to analyze copy number changes was explored in several studies, including endocrine malignancies (47, 48). In the following years, the coverage of the Affymetrix chips continuously improved

to 100 K, 500 K, and, lately, to approximately 1 million with an additional 946,000 probes for detection of copy number variation (CNV), arrayed on the most advanced Affymetrix released chip version—Genome-Wide Human SNP Array 6.0.

At the same time another major technological achievement emerged on the bio-market: the BeadChip microarray technology developed by Illumina. The protocol employs single tube whole genome amplification followed by fragmentation to approximately 300 to 600 bp, and subsequent hybridization onto locus specific capture probes on beads; the allele discrimination is achieved by enzyme mediated single base extension (47, 48). The most recent product of this technology—Human1M-Duo BeadChip—analyzes more than 1.1 million loci per sample, with a median spacing between markers of 1.5 kb and additional throughput acquired by the ability to genotype two DNA samples simultaneously.

Thus, the two leading products in the SNP array development are made by the Affymetrix and Illumina companies, respectively. Their results are similar in labor- and cost-effectiveness and quality (49). Both vendors provide user-friendly software for the analysis of the generated datasets: Birdseed from Affymetrix and BeadStudio from Illumina. The current chapter intends to combine ours and others experience in an attempt to provide practical tips to the use of one of the two leading technologies—Affymetrix SNP array, in its most advanced versions. We will emphasize on the laboratory preparation and handling of the samples that ensure successful data generation; a comprehensively guide on the machine operations is provided on the Affymetrix website (http://www.affymetrix. com/products_services/arrays/specific/genome_wide_snp6/genome_wide_ snp_6.affx).

2. Materials

2.1. DNA Extraction and Preparation

1. QIAamp Blood Mini Kit (Qiagen).
2. Microcon or Centricon (Milipore).
3. DNA extraction Masterpure Protocol (Epicentre).
4. Nucleon DNA extraction kit (BACC2, Amersham Biosciences).
5. Xylene.
6. 100% ethanol.
7. 80% ethanol.
8. 70% ethanol.
9. Phosphate Buffered Saline (PBS) without Calcium or Magnesium, pH 7.4 (Gibco).

10. Reduced EDTA TE buffer (TEKnova): 10 mM Tris-HCl, 0.1 mM EDTA, pH8.0.
11. 7.5 M NH_4OAc.
12. Glycogen (5 mg/mL) (Sigma-Aldrich).

2.2. Restriction Digestion

1. *Nsp* I, 10,000 U/ml, 125 μl vial (New England Biolabs).
2. *Sty* I, 10,000 U/ml, 300 μl vial (New England Biolabs).
3. AccuGENE water (recommended from Affymetrix as the water used for the optimization of the suggested protocol).

2.3. Ligation

1. T4 DNA ligase, 250 ml vial (New England Biolabs).
2. Adaptor *Sty*I or *Nsp* I (50 μM) (Affymetrix, included in the Genome-Wide Human SNP Assay Kit 5.0/6.0).
3. AccuGENE water.

2.4. PCR

1. TITANIUM DNA Amplification kit (Clontech): includes AccuGENE water, TITANIUM Taq PCR Buffer (10x), GC-Melt (5 M), dNTP (2.5 mM each), TITANIUM Taq DNA polymerase (50x).
2. PCR Primer 002 (100 μM): (Affymetrix, included in the Genome-Wide Human SNP Assay Kit 5.0/6.0).

2.5. Pooling, Purification, and Quantization of the PCR Product

1. Magnetic beads (Agencourt).
2. Filter plate (E & K Scientific).
3. Elute plate (Bio-Rad).
4. Millipore Vacuum manifold.
5. MicroAmp clear adhesive film (Applied Biosystems).
6. Buffer EB (Qiagen).
7. Jitterbug Microplate Incubator Shaker.
8. UV Spectrophotometer plate reader (Spectramax).

2.6. Fragmentation of the PCR Amplicons

1. 10x Fragmentation Buffer (Affymetrix, included in the Human SNP 6.0 Assay Kit for Automated Target Preparation).
2. Fragmentation agent (*DNAse* I) (Affymetrix, included in the Human SNP 6.0 Assay Kit for Automated Target Preparation).

2.7. Labeling of the Fragmented Products

1. 5x TdT buffer (Affymetrix, included in the Human SNP 6.0 Assay Kit for Automated Target Preparation).
2. DNA labeling reagent (30 mM).
3. TdT enzyme (30 U/μl).

2.8. Target Hybridization, Washing, Staining, and Scanning Arrays

1. Genome-Wide Human SNP Nsp/Sty Assay Kit 5.0/6.0 (Affymetrix).
2. GeneChip Hybridization Oven 645 (Affymetrix).
3. GeneChip Fluidic Station 450: (Affymetrix).
4. GeneChip Scanner 3000 7G (Affymetrix).
5. Pipettes (single- and multi-channel).

2.9. Data Analysis

1. Birdseed (v2) (Affymetrix).

3. Methods

An useful example of time- and work-flow for the entire experiment, with recommended points to stop, is provided in **Table 9.1**. Please note that this workflow is recommended for one operator and could be efficiently modified to save time if two or more operators are performing the steps simultaneously (*see* **Note 1**).

3.1. DNA Extraction and Preparation

The general recommendation for relatively intact, high-quality DNA, isolated from fresh lymphocytes or tissue material is advisable also for the SNP-array genotyping. However, since often no fresh materials are available, tips for genotyping-sufficient extracting DNA from frozen samples or paraffin embedded material are also provided. The recommended minimal amount input DNA is 500 ng (250 ng for each restriction enzyme—*Nsp* I and *Sty*I) at concentration 50 μg/μl stored in reduced EDTA TE buffer (*see* **Note 2**). This DNA must be free of contaminants that may interfere with the enzymatic activity. The integrity of the purified genomic DNA may be checked on a 1% agarose gel (*see* **Note 3**).

3.1.1. DNA from Peripheral Blood Lymphocytes

For isolation of sufficient quality DNA from peripheral blood lymphocytes for genotyping on SNP 6.0 Array, QIAamp Blood Mini Kit (Qiagen), following the manufacturer recommendation, is validated and recommended by Affymetrix.

3.1.2. DNA from Cell Cultures

Several methods have proven to be suitable for high-quality DNA isolation from cell cultures: standard protocols for SDS/Proteinase K digestion, phenol/chlorophorm extraction, or Microcon or Centricon (Milipore) ultrapurification and concentration, according to the manufacturer instructions.

3.1.3. DNA from Buccal Swab

Successful SNP array 6.0 genotyping on DNA from buccal swabs has been achieved using DNA extraction Masterpure Protocol (Epicentre), according to the manufacturer recommendations (50).

Table 9.1.
Time- and work-flow for SNP 6.0 genotyping

Day	Procedures	Time	Recommended stop
Day 1	DNA preparation	varies	Yes
Day 2	Restriction Digest (*Sty*I); 1 *Sty*I plate	2 h 45 min	
	Ligation (*Sty*I); 1 *Sty*I plate	3 h 45 min	
	PCR (*Sty*I); 3 *Sty*I plates	1 h for the hands-on; the PCR reaction can run overnight	Yes
Day 3	Restriction Digest (*Nsp*I);1 *Nsp*I plate	2 h 45 min	
	Ligation (*Sty*I); 1 *Nsp*I plate	3 h 45 min	
	PCR (*Nsp*I); 4 *Nsp*I plates	1 h for the hands-on; the PCR reaction can run overnight	Yes
Day 4	*Sty*I and *Nsp*I PCR products pooled	20 min	
	PCR product purification	3 h	
	PCR product quantitation	1 h 30 min	Yes
Day 5	Fragmentation	2 h	
	Labeling	5 h 20 min	
	Hybridization onto Arrays	1 h for the hands-on; the hybridization reaction run overnight to a total of 16–18 h	Yes
Day 6	Washing, staining and scanning the arrays	automated	NA

3.1.4. DNA from Frozen Tissue

To isolate high-quality DNA from frozen tissue, Nucleon DNA extraction kit (BACC2, Amersham Biosciences) has been validated on SNP array 6.0 genotyping.

3.1.5. DNA from Paraffin Embedded

DNA from formalin-fixed paraffin-embedded tissues is often degraded, at least to a certain degree, and requires some additional caution in order to achieve the genotyping results that are normally produced using high-quality DNA. We provide here an approach that has been used for successful SNP array 6.0 genotyping of formalin-fixed paraffin embedded-tissues and have been proven to lead

to high-quality data with several modification of the original genotyping protocol (provided in the appropriate further sections) (51). DNA extraction is performed according to the following protocol:

1. Select paraffin blocks that have at least 70% of the required cell types. Use at least 20 slices of 10 mM-thick sections.
2. Add 1 ml xylene to the microtube containing tissue sections for 30 min, repeat twice.
3. Add 100% ethanol and incubate 30 min, repeat the step twice.
4. Add 75% ethanol and incubate 15 min, repeat the step twice.
5. Add 1 ml PBS for 15 min, repeat the step twice.
6. Dry the pellet; re-suspend the dried pellet in 180 µl buffer ATL (QIAamp DNA Mini Tissue Kit, Qiagen) and follow the manufacturer instructions.
7. Elute in 50 µl reduced EDTA TE buffer.

3.1.6. Additional DNA Purification Through Ethanol Precipitation

This step is only required in case the extracted DNA is suspected to contain inhibitors. Purify genomic DNA as follows:

1. Add 0.5 volumes 7.5 M NH_4OAc, 2.5 volumes cold 100% ethanol, and 0.5 µl of glycogen.
2. Vortex, incubate at –20°C for 1 h, and centrifuge at 12,000 *g* at room temperature for 20 min.
3. Remove supernatant, wash pellet with 80% ethanol and centrifuge at 12,000 *g* at room temperature for 5 min; repeat step
4. Resuspend the pellet in reduced EDTA TE buffer; the volume must be sufficient to ensure DNA concentration 50 ng/µl).

3.2. Restriction Digestion

At this step, separate restriction reactions with *Sty* I and *Nsp* I are performed according to the manufacturer instructions (NEB). Briefly, the following steps are included:

1. Aliquot 5 µl genomic DNA (equivalent to 250 ng) into a 96-well plate (*see* **Note 4**). Two replicates of each sample are required for this step—one for *Sty* I and one for *Nsp* I.
2. Prepare *Sty* I and *Nsp* I digestion Master Mix for the number of the samples plus 15% extra as follows (the sample is for the recommended 48 reactions) (*see* **Note 5**):

	1 rxn	**48 rxns + 15%**
AccuGENE water	11.55 µl	637.6
NEB buffer 3 for *Sty* I or 2 for *Nsp* I (10x)	2 µl	110.4 µl
BSA (100x, 10 mg/ml)	0.2 µl	11.04 µl
Sty I or *Nsp* I (10U/µl, NEB)	1 µl	55.2 µl
Total	14.75 µl	814.24 µl

3. Aliquot 14.75 μl of the Master mix to each DNA sample (the total volume of the restriction reaction is 19.75 μl); the plate must be on the cooling chamber and seal the plate.
4. Vortex and spin the plate, ensure that the mixture is on the bottom of the wells.
5. Incubate on the thermal cycler for 2 h on 37°C followed by 20 min on 65°C and hold on 4°C until the next step.

3.3. Ligation

In this step each digested DNA sample from the step 5 in the **Section 3.2** is ligated to adaptors that recognize the cohesive 4 bp overhangs (steps 1–4) and subsequently diluted to a total volume of 100 μl (step 5).

1. Prepare *Sty* I and *Nsp* I ligation Master Mix for the number of the samples plus 25% extra as follows (the sample is for the recommended 48 reactions):

	1 rxn	**48 rxns + 25%**
T4 ligation buffer (10x)	2.5 μl	150 μl
Adaptor *Sty* I or *Nsp* I (50 μM)	0.75 μl	45 μl
T4 DNA ligase (400 U/μl)	2 μl	120 μl
Total	5.25 μl	315 μl

2. Add 5.25 μl of the *Sty* I and *Nsp* I ligation Master Mix to the corresponding restriction reaction (19.75 μl). Now the reaction total is 25 μl.
3. Seal, vortex, and spin the plate, ensure that the mixture is on the bottom of the wells.
4. Incubate on the thermal cycler for 3 h on 16°C followed by 20 min on 70°C and hold on 4°C until the next step.
5. Dilute each reaction by adding of 75 μl AccuGENE water.

3.4. PCR (see Note 6)

1. Transfer 10 μl of each diluted ligation sample into a clean fresh PCR plate. Three PCR plates are required for *Sty* I, and four are required for *Nsp* I (because the *Nsp* I sites harbor high number of CNV, and robust amplification is required to ensure appropriate representation of fragments). Accordingly, 30 μl of the *Sty* I ligation reaction and 40 μl of the *Nsp* I ligation reaction need to be transferred in 7 new PCR tubes (10 μl per well (**Fig. 9.1**).

2. Prepare PCR master mixes (48 × 3 = 144 reactions for *Sty*I and 48 × 4 = 172 reactions for *Nsp*I plus 15% extra as follows:

***Sty* I PCR mix**	**1 rxn**	**144 rxns + 15%**
AccuGENE water	39.5 µl	6541.2 µl
TITANIUM Taq PCR Buffer (10x)	10 µl	1656 µl
GC-Melt (5 M)	20 µl	3312 µl
dNTP (2.5 mM each)	14 µl	2318.4 µl
PCR Primer 002 (100 µM)	4.5 µl	745.2 µl
TITANIUM Taq DNA polymerase (50x)	2 µl	331.2 µl
Total	90 µl	14904 µl

***Nsp* I PCR mix**	**1 rxn**	**172 rxns + 15%**
AccuGENE water	39.5 µl	7813.1 µl
TITANIUM Taq PCR Buffer (10x)	10 µl	1978 µl
GC-Melt (5 M)	20 µl	3956 µl
dNTP (2.5 mM each)	14 µl	2769.2 µl
PCR Primer 002 (100 µM)	4.5 µl	890.1 µl
TITANIUM Taq DNA polymerase (50x)	2 µl	395.6 µl
Total	90 µl	17802 µl

3. Add 90 µl PCR Master Mix to each of the aliqouted diluted ligation reactions (10 µl); the total volume is 100 µl.
4. Seal, vortex, and spin the plate, ensure that the mixture is on the bottom of the wells.
5. Run the PCR on the thermal cycler using the following conditions: denaturation at 94°C for 3 min, 30 cycles of denaturation at 94°C for 30 s, annealing at 60°C for 30 s and elongation at 68°C for 15 s, followed by final elongation at 68°C for 7 min.
6. Verify the PCR by loading and running 3 µl of the reaction on 2% TBE gel. The fragments should appear as a dominant smear in the range 200–1100 bp.

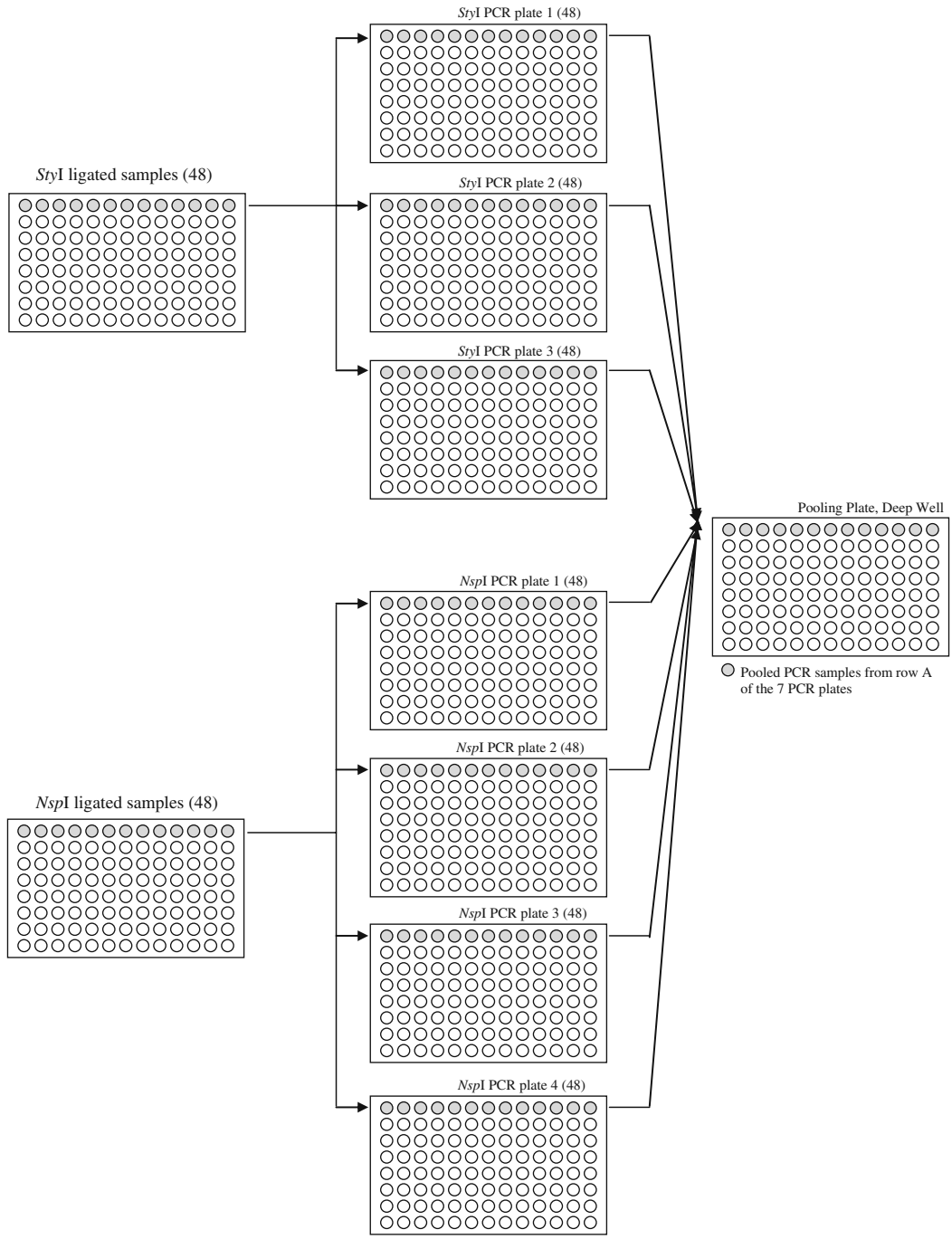

Fig. 9.1. StyI and NsiI ligation, PCR reactions, and pooling into a deep well plate.

3.5. 5. Pooling, Purification, and Quantization of the PCR Product

At this stage you have a total of 7 PCR reactions per sample (3 for *Sty* I and 4 for *Nsp* I digested DNA); pool them together (to a total of 700 µl), and purify the pooled PCR product through binding to magnetic beads.

1. Vortex and spin the plate; ensure that the mixture is on the bottom of the wells.
2. Using 12-channel pipette set to 110 µl transfer the 7 PCR reactions to a deep well pooling plate (*see* **Fig. 9.1**).
3. Prepare the magnetic beads by mixing them through vigorous shaking until homogenously dispersed; pour them into a mixing boat.
4. Using 12-channel pipette transfer 1 ml magnetic beads into each well in the deep-well collection plate, already containing 700 µl pooled PCR reaction, mix well by pipetting.
5. Transfer each reaction from the pooling plate to the corresponding row of the filter plate that is placed on the Millipore Vacuum manifold; the mixture is sticky and viscous (*see* **Fig. 9.1**). To ensure appropriate vacuum pressure, seal the unused wells with a MicroAmp clear adhesive film.
6. Using vacuum (20–24 in Hg) dry the samples for 60–90 min or until they appear completely dry. Carefully inspect the wells with flashlight to ensure they are completely dry; if they are not, continue the vacuum dry.
7. Add 1.8 ml 75% ethanol to each reaction and wash under the vacuum (20–24 in Hg) for 10–20 min, inspect the wells carefully to ensure they are dry, remove the plate and tap it on paper towel to blot off any residual liquid, return the plate to the vacuum manifold and vacuum for an additional 10 min, tap off on paper towels again.
8. Attach the elution plate to the bottom of the filter plate, fixating it with lab tape. Add 55 µl of Buffer EB to each well, ensure that the EB buffer is on the bottom of the wells, place the plate on Jitterbug Microplate Incubator Shaker for 10 min; ensure that the beads are homogeneously re-suspended. Elute using the vacuum manifold at 20–24 in Hg in deep well collar for 15–30 min or until all the wells are completely dry (inspect with a flashlight). Seal the plate with adhesive film and centrifuge at 1400*g* for 5 min.
9. Transfer 45 µl of each eluate to a fresh PCR plate for quantitation and fragmentation.

10. For quantitation, prepare 100x diluted aliquots in an optical plate by mixing 2 µl of the purified samples with 198 µl Accugene water; make sure to set a raw with water only for the blank.
11. Using spectrophotometer plate reader, measure the OD at 260, 280, and 320 nm, and calculate the concentration of the diluted, and subsequently, undiluted sample.

3.6. Fragmentation of the PCR Amplicons

1. Using 12-channel pipette transfer 5 µl of Fragmentation Buffer (10x) to each sample in the 96-well reaction plate (the total volume of each well is now 50 µl).
2. Dilute the fragmentation agent (*DNAse* I) to 0.1 U/µl with Accugene water and add 5 µl diluted fragmentation reagent to each sample (the total volume of each well is now 55 µl). This procedure should be performed quickly and on ice, because the fragmentation reagent is extremely temperature sensitive (*see* **Note 8**).
3. Seal tightly, vortex, and spin the plate, then incubate it on the thermal cycler for 35 min on 37°C followed by 15 min on 95°C and hold on 4°C until the next step (*see* **Note 5**).
4. Check the fragmentation products by loading and running 1.5 µl of the reaction on 4% TBE gel. Average fragments size is below 160 bp.

3.7. Labeling of the Fragmented Products

1. Prepare the labeling master mix for the number of the samples plus 15% extra as follows (the sample is for the recommended 48 reactions):

	1 rxn	**48 rxns + 15%**
TdT buffer (5x)	14 µl	772.8 µl
DNA labeling reagent (30 mM)	2 µl	110.4 µl
TdT enzyme (30 U/µl)	3.5 µl	193.2 µl
Total	19.5 µl	1076.4 µl

2. Add 19.5 µl of the labeling master mix to the fragmented DNA (53.5 µl); the total volume of the mixture is 73 µl.
3. Seal tightly, vortex, and spin the plate, then incubate it on the thermal cycler for 4 h on 37°C followed by 15 min on 95°C and hold on 4°C until the next step.

3.8. Target hybridization, Washing, Staining, and Scanning Arrays

1. Load each reaction onto the SNP Array 6.0.
2. Follow manufacture's protocol for gene amplification. The protocol recommends 2 approaches dependent on PCR systems that are suitable for this step: GeneAmp PCR system 9700, Applied Biosystems 2720 Thermal Cycler and MJ Tetrad PTC-225 Thermal Cycler (http://www.affymetrix.com/index.affx).
3. Washing, Staining, and Scanning Arrays using Fluidic Station 450 and GeneChip Scanner 3000 7G according to the recommended protocols and software handbook. (http://www.affymetrix.com/index.affx).

3.9. Data Analysis

Once the datasets are generated, they can be analyzed by the provided user-friendly software in the desired downstream application. (http://www.affymetrix.com/index.affx). As every method, SNP arrays have limitations: like other array-based methods, SNP arrays cannot detect balanced genomic, chromosomal and gene rearrangements. In addition, since DNA is extracted from multiple cells in a tissue or from various cell populations in a sample, SNP arrays cannot achieve the single cell experiments resolution that allows assessment of intra-sample variability. More complete results may soon be generated by the combination of SNP arrays with methods such as Fluorescent in situ hybridization (FISH). However, the tremendous amount of information derived from SNP microarray studies along with improvements in software and other analytical tools has accelerated dramatically the rate with which new genetic associations are found. Certain unique features of the most advanced SNP arrays that allow simultaneous analysis of both DNA dosage alterations and copy number variations provide unparalleled power. This is whole new era in genetics and genomics, and SNPs made that possible.

4. Notes

1. Before starting, plan carefully when and where you will need to interrupt the process. Be sure to use the recommended and validated reagents, consumables, and conditions. The experiment is sensitive to minimal changes in the protocol.
2. Proper DNA extraction approach is a necessary pre-requisite for successful downstream protocol accomplishment. DNA extraction protocols that involve boiling or strong denaturants must be avoided because of their high potential to isolate single stranded DNA. Efforts should be made to ensure that

DNA is clean of any inhibitors that may interfere with the enzymatic reaction. Common inhibitors are high EDTA concentrations, salts, and heme from blood. Therefore, salt- and heme-free input DNA in reduced EDTA TE buffer must be used. If a genomic DNA is expected to be contaminated with inhibitors, an additional purification through ethanol precipitation is necessary.

3. Since the success of the assay requires the amplification of DNA fragments between 200 and 1100 bp, the minimal size of the input DNA should exceed 2000 bp. High quality genomic DNA is expected to run as a major band in the range of 10 and 20 kb. The DNA quality and quantity is easily assessable on 1% agarose gel. Insufficient DNA samples can be amplified with Repli-G whole genome amplification kit provided by Qiagen. The input DNA is 30 μl; the amplified DNA can be directly used in the subsequent steps of the protocol as recommended.
4. Uniform quantity of 250 ng genomic DNA for *Nsp* I and *Sty* I digestion steps is necessary. Excess amounts of genomic DNA are reported to result in a decrease of the average overall call rate (Nishida Tajima 431 bmc genomics 2008).
5. Work with master mixes for each reaction is essential for uniform sample processing. Positive and negative controls must be included with every set of sample run. Multichannel pipette is a must and proficiency using it is required. For the majority of the reactions, a 12-channel pipette is recommended to disperse the master mix that is previously aliquoted in 12 strips or poured into a clean solution basin immediately before the beginning of the reaction. At each step when you are using the multichannel pipette (digestion, ligation, pooling, etc.) be very careful not to cross contaminate the neighboring wells with small droplets. It is helpful to cut the seal between each row on the 96-well plates so it can be removed one raw at a time and processed accordingly.
6. Since the adaptor-based amplification is not locus-specific, any contamination may severely affect the genotyping accuracy; therefore, stringent requirements for clean lab, equipment, and samples handling are necessary prerequisite for the accurate SNP genotyping (see Affymetrics instructions for separating the protocol steps at different lab space (http://www.affymetrix.com/index.affx).
7. When using DNA extracted from formalin-fixed paraffin-embedded tissues, better PCR yield is reported by splitting the ligation product into 9 plates and performing 9 independent PCR reactions. The 9 PCR independent

reactions are then pooled and processed further according to the recommended protocol (51). Pool and processes the 9 independent PCR reactions according to the recommended protocol (51). For DNA extracted from formalin fixed paraffin embedded tissues, better fragmentation results are reported when performing three consecutive fragmentation reactions, 10 min each, instead of the recommended 1 reaction for 35 min (51).

References

1. Lander ES, Linton LM, Birren B, Nusbaum C, Zody MC, Baldwin J, et al. (2001) International Human Genome Sequencing Consortium. Initial sequencing and analysis of the human genome. *Nature*. **409**, 860–921.
2. International Human Genome Sequencing Consortium (2004) Finishing the euchromatic sequence of the human genome. *Nature*. **431**, 931–45.
3. The International HapMap Consortium (2003) The International HapMap Project. *Nature*. **426**, 789–96.
4. International HapMap Consortium (2005) A haplotype map of the human genome. *Nature*. **437**, 1299–320.
5. Botstein D, Risch N. (2003) Discovering genotypes underlying human phenotypes: past successes for mendelian disease, future approaches for complex disease. *Nat Genet*. **33** Suppl, 228–37.
6. Chorley BN, Wang X, Campbell MR, Pittman GS, Noureddine MA, Bell DA. (2008) Discovery and verification of functional single nucleotide polymorphisms in regulatory genomic regions: current and developing technologies. *Mutat Res*. **659**, 147–57.
7. Gabriel SB, Schaffner SF, Nguyen H, Moore JM, Roy J, Blumenstiel B, et al. (2002) The structure of haplotype blocks in the human genome. *Science*. **296**, 2225–9.
8. Nicolas P, Sun F, Li LM. (2006) A model-based approach to selection of tag SNPs. *BMC Bioinformatics*. **15**, 7:303.
9. Steemers FJ, Chang W, Lee G, Barker DL, Shen R, Gunderson KL. (2006) Whole-genome genotyping with the single-base extension assay. *Nat Methods*. **3**, 31–3.
10. Horvath A, Boikos S, Giatzakis C, Robinson-White A, Groussin L, Griffin KJ, et al. (2006) A genome-wide scan identifies mutations in the gene encoding phosphodiesterase 11A4 (*PDE11A4*) in individuals with adrenocortical hyperplasia. *Nat Genet*. **38**, 794–800.
11. Horvath A, Mericq V, Stratakis CA. (2008) Mutation in *PDE8B*, a cyclic AMP-specific phosphodiesterase in adrenal hyperplasia. *N Engl J Med*. **358**, 750–2.
12. Sladek R, Rocheleau G, Rung J, Dina C, Shen L, Serre D, et al. (2007) A genome-wide association study identifies novel risk loci for type 2 diabetes. *Nature*. **445**, 881–5.
13. Wellcome Trust Case Control Consortium (2007). Genome-wide association study of 14,000 cases of seven common diseases and 3,000 shared controls. *Nature*. **447**, 661–78.
14. Saxena R, Voight BF, Lyssenko V, Burtt NP, de Bakker PI, Chen H, et al. (*2007) Genome-wide association analysis identifies loci for type 2 diabetes and triglyceride levels. Science*. **316**, 1331–6.
15. Zeggini E, Weedon MN, Lindgren CM, Frayling TM, Elliott KS, Lango H, et al. (2007) Replication of genome-wide association signals in UK samples reveals risk loci for type 2 diabetes. *Science*. **316**, 1336–41.
16. Scott LJ, Mohlke KL, Bonnycastle LL, Willer CJ, Li Y, Duren WL, et al. (2007) A genome-wide association study of type 2 diabetes in Finns detects multiple susceptibility variants. *Science*. **316**, 1341–5.
17. Grant SF, Thorleifsson G, Reynisdottir I, Benediktsson R, Manolescu A, Sainz J, et al. (2006) Variant of transcription factor 7-like 2 (TCF7L2) gene confers risk of type 2 diabetes. *Nat Genet*. **38**, 320–3.
18. Herbert A, Gerry NP, McQueen MB, Heid IM, Pfeufer A, Illig T, et al. (2006) A common genetic variant is associated with adult and childhood obesity. *Science*. **312**, 279–83.
19. Frayling TM, Timpson NJ, Weedon MN, Zeggini E, Freathy RM, Lindgren CM, et al. (2007) A common variant in the FTO gene is associated with body mass

index and predisposes to childhood and adult obesity. *Science.* **316**, 889–94.

20. Weedon MN, Lettre G, Freathy RM, Lindgren CM, Voight BF, Perry JR, et al. (2007) A common variant of HMGA2 is associated with adult and childhood height in the general population. *Nat Genet.* **39**, 1245–50.
21. Sanna S, Jackson AU, Nagaraja R, Willer CJ, Chen WM, Bonnycastle LL, et al. (2008) Common variants in the GDF5-UQCC region are associated with variation in human height. *Nat Genet.* **40**, 198–203.
22. Dutt A, Beroukhim R. (2007) Single nucleotide polymorphism array analysis of cancer. *Curr Opin Oncol.* **19**, 43–9.
23. Mao X, Young BD, Lu YJ. (2007) The application of single nucleotide polymorphism microarrays in cancer research. *Curr Genomics.* **8**, 219–28.
24. Amundadottir LT, Sulem P, Gudmundsson J, Helgason A, Baker A, Agnarsson BA, et al. (2006) A common variant associated with prostate cancer in European and African populations. *Nat Genet.* **38**, 652–8.
25. Gudmundsson J, Sulem P, Manolescu A, Amundadottir LT, Gudbjartsson D, Helgason A, et al. (2007) Genome-wide association study identifies a second prostate cancer susceptibility variant at 8q24. *Nat Genet.* **39**, 631–7.
26. Yeager M, Orr N, Hayes RB, Jacobs KB, Kraft P, Wacholder S, et al. (2007) Genome-wide association study of prostate cancer identifies a second risk locus at 8q24. *Nat Genet.* **39**, 645–9.
27. Haiman CA, Patterson N, Freedman ML, Myers SR, Pike MC, Waliszewska A, et al. (2007) Multiple regions within 8q24 independently affect risk for prostate cancer. Nat Genet. **39**, 638–44.
28. Sokolov BP. (1990) Primer extension technique for the detection of single nucleotide in genomic DNA. *Nucleic Acids Res.* **18**, 3671.
29. Landegren U, Kaiser R, Sanders J, Hood L. (1988) A ligase-mediated gene detection technique. *Science.* **241**, 1077–80.
30. Tong AK, Li Z, Jones GS, Russo JJ, Ju J. (2001) Combinatorial fluorescence energy transfer tags for multiplex biological assays. *Nat Biotechnol.* **19**, 756–9.
31. Nilsson M, Malmgren H, Samiotaki M, Kwiatkowski M, Chowdhary BP, Landegren U. (1994) Padlock probes: circularizing oligonucleotides for localized DNA detection. *Science.* **265**, 2085–8.
32. Lizardi PM, Huang X, Zhu Z, Bray-Ward P, Thomas DC, Ward DC. (1998) Mutation detection and single-molecule counting using isothermal rolling-circle amplification. *Nat Genet.* **19**, 225–32.
33. Hardenbol P, Yu F, Belmont J, Mackenzie J, Bruckner C, Brundage et al. (2005) Highly multiplexed molecular inversion probe genotyping: over 10,000 targeted SNPs genotyped in a single tube assay. *Genome Res.* **15**, 269–75.
34. Botstein D, White RL, Skolnick M, Davis RW. (1980) Construction of a genetic linkage map in man using restriction fragment length polymorphisms. *Am J Hum Genet.* **32**, 314–31.
35. Love-Gregory LD, Dyer JA, Grasela J, Hillman RE, Phillips CL. (2001) Carrier detection and rapid newborn diagnostic test for the common Y393N maple syrup urine disease allele by PCR-RFLP: culturally permissible testing in the Mennonite community. *J Inherit Metab Dis.* **24**, 393–403.
36. Orita M, Suzuki Y, Sekiya T, Hayashi K. (1989) Rapid and sensitive detection of point mutations and DNA polymorphisms using the polymerase chain reaction. *Genomics.* **5**, 874–9.
37. Kukita Y, Higasa K, Baba S, Nakamura M, Manago S, Suzuki A, et al. (2002) A single-strand conformation polymorphism method for the large-scale analysis of mutations/polymorphisms using capillary array electrophoresis. *Electrophoresis.* **23**, 2259–66.
38. Bennett ST, Barnes C, Cox A, Davies L, Brown C. (2005) Toward the 1,000 dollars human genome. *Pharmacogenomics.* **6**, 373–82.
39. Strausberg RL, Levy S, Rogers YH. (2008) Emerging DNA sequencing technologies for human genomic medicine. *Drug Discov Today.* **13**, 569–77.
40. Wang DG, Fan JB, Siao CJ, Berno A, Young P, Sapolsky R, et al. (1998) Large-scale identification, mapping, and genotyping of single-nucleotide polymorphisms in the human genome. *Science.* **280**, 1077–82.
41. Mei R, Galipeau PC, Prass C, Berno A, Ghandour G, Patil N, et al. (2000) Genome-wide detection of allelic imbalance using human SNPs and high-density DNA arrays. *Genome Res.* **10**, 1126–37.
42. Lindblad-Toh K, Tanenbaum DM, Daly MJ, Winchester E, Lui WO, Villapakkam A, et al. (2000) Loss-of-heterozygosity analysis of small-cell lung carcinomas using single-nucleotide polymorphism arrays. *Nat Biotechnol.* 18, 1001–5.

43. Fan JB, Chee MS, Gunderson KL. (2006) Highly parallel genomic assays. *Nat Rev Genet.* **7**, 632–44.
44. Fan JB, Oliphant A, Shen R, Kermani BG, Garcia F, Gunderson KL, et al. (2003) Highly parallel SNP genotyping. *Cold Spring Harb Symp Quant Biol.* **68**, 69–78.
45. Kennedy GC, Matsuzaki H, Dong S, Liu WM, Huang J, Liu G, et al. (2003) Large-scale genotyping of complex DNA. *Nat Biotechnol.* **21**, 1233–7.
46. Matsuzaki H, Loi H, Dong S, Tsai YY, Fang J, Law J, et al. (2004) Parallel genotyping of over 10,000 SNPs using a one-primer assay on a high-density oligonucleotide array. *Genome Res.* 14, 414–25.
47. Gunderson KL, Steemers FJ, Lee G, Mendoza LG, Chee MS. (2005) A genome-wide scalable SNP genotyping assay using microarray technology. *Nat Genet.* **37**, 549–54.
48. Steemers FJ, Chang W, Lee G, Barker DL, Shen R, Gunderson KL. (2006) Whole-genome genotyping with the single-base extension assay. *Nat Methods.* **3**, 31–3.
49. Grant SF, Hakonarson H. (2008) Microarray technology and applications in the arena of genome-wide association. *Clin Chem.* **54**, 1116–24.
50. Mick E, Neale B, Middleton FA, McGough JJ, Faraone SV. (2008) Genome-wide association study of response to methylphenidate in 187 children with attention-deficit/hyperactivity disorder. *Am J Med Genet B Neuropsychiatr Genet.* 147B, 1412–8.
51. Tuefferd M, De Bondt A, Van Den Wyngaert I, Talloen W, Verbeke T, Carvalho B, et al. (2008) Genome-wide copy number alterations detection in fresh frozen and matched FFPE samples using SNP 6.0 arrays. *Genes Chromosomes Cancer.* **47**, 957–64.

Chapter 10

Methylated DNA Immunoprecipitation and Microarray-Based Analysis: Detection of DNA Methylation in Breast Cancer Cell Lines

Yu-I Weng, Tim H.-M. Huang, and Pearlly S. Yan

Abstract

The methylated DNA immunoprecipitation microarray (MeDIP-chip) is a genome-wide, high-resolution approach to detect DNA methylation in whole genome or CpG (cytosine base followed by a guanine base) islands. The method utilizes anti-methylcytosine antibody to immunoprecipitate DNA that contains highly methylated CpG sites. Enriched methylated DNA can be interrogated using DNA microarrays or by massive parallel sequencing techniques. This combined approach allows researchers to rapidly identify methylated regions in a genome-wide manner, and compare DNA methylation patterns between two samples with diversely different DNA methylation status. MeDIP-chip has been applied successfully for analyses of methylated DNA in the different targets including animal and plant tissues *(1, 2)*. Here we present a MeDIP-chip protocol that is routinely used in our laboratory, illustrated with specific examples from MeDIP-chip analysis of breast cancer cell lines. Potential technical pitfalls and solutions are also provided to serve as workflow guidelines.

Key words: DNA methylation, epigenetics, MeDIP-chip, microarray, cancer.

1. Introduction

Epigenetic modification involves DNA methylation, covalent modification of histones and small inhibitory RNA molecules known as microRNAs (miRNAs) (3). DNA methylation is a heritable, enzyme-induced modification without changing the nucleotide sequence of the DNA base pairs. DNA methylation involves transfer of a methyl-group to the 5-carbon on the cytosine in a CpG dinucleotide via DNA methyltransferases (DNMT1, DNMT3A, and DNMT3B) (4). Most of the CpG dinucleotides

O.-K. Park-Sarge, T.E. Curry, Jr. (eds.), *Molecular Endocrinology,* Methods in Molecular Biology 590,
DOI 10.1007/978-1-60327-378-7_10,

are unevenly distributed within the genome and regions high in these dinucleotides termed CpG islands. The haploid human genome consists of 29,848,753 CpGs and about 6% of all CpGs are located in the CpG islands (5). These islands are frequently located in the 5'-untranslated region and the first exon of approximately 60% of all genes. Methylation of CpG islands affects the transcriptional activation of genes. It is generally accepted that a high level of promoter CpG island methylation results in gene silencing (6). In the normal genome, DNA methylation is essential for proper development, chromosomal integrity, maintenance of gene expression states, and X chromosome inactivation (7, 8). In primary human tumors, methylation patterns are severely altered. This includes hypermethylation of CpG islands and genome-wide hypomethylation (9, 10). Because DNA methylation has significant effects on gene function and expression, detection of DNA methylation becomes an active area of research for the understanding of normal biological processes and tumorigenesis.

There are several methods available for the determination of methylation patterns and the quantitative assessment of methylation levels in sample tissues (11). These include methods for interrogating the combined methylation status of several CpG sites in a single gene (methylation-specific polymerase chain reaction or MSP and MethyLight; 12, 13), methods for interrogating methylation status of individual CpG sites present in a gene (combined bisulfite restriction analysis or COBRA and methylation-specific single-nucleotide primer extension or MS-SNuPE; 14, 15), methods for interrogating multiple CpG loci in many genes (methylation-specific oligonucleotide microarray or MSO microarray; 16), and methods for high-throughput, genome-wide epigenetic analysis (differential methylation hybridization or DMH; 17).

A large number of currently available techniques used for studying global methylation differences involve the use of methylation sensitive restriction enzyme(s) thereby limiting these approaches to profile genomic regions containing these restriction site motifs. In this regard, the methylated DNA immunoprecipitation (MeDIP)-chip approach is less biased and therefore more appealing (2, 18). The general strategy for the MeDIP-chip procedure is outlined in **Fig. 10.1**. Genomic DNA is sheared to low molecular weight fragments (average 400 bp) (*see* **Note 1**). Methylated DNAs are immunoprecipitated with the anti-methylcytosine antibody, and may be PCR-amplified if source material is limited (*see* **Note 2**). Input and methylated DNA can be subsequently labeled with fluorescent dyes Cy3 (green) and Cy5 (red), pooled, denatured, and hybridized to a microarray slide containing all the annotated human CpG islands (n = 27,800) or other whole genome or promoter microarray designs (*see* **Note 3**). The slide is scanned using a GenePix 4000B scanner and each image is analyzed with the GenePix Pro 6.0 image analysis software.

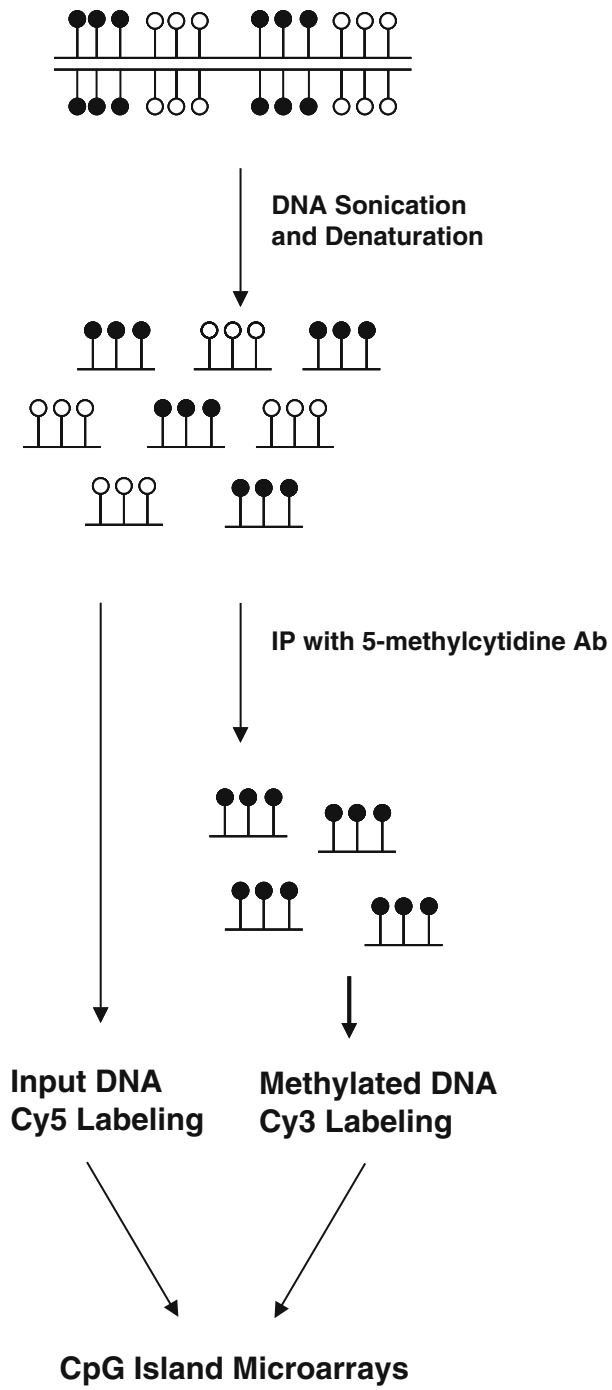

Fig. 10.1. Overview of the MeDIP protocol. The genomic DNA is sonicated into small fragments and then immunoprecipitated with an antibody directed against 5-methylcytidine. Input DNA and methylated DNA (*black circle*) can be differentially labeled with Cy5 (red) and Cy3 (green) and co-hybridized as a two-color experiment on microarrays, or used for data validation.

MeDIP-chip has proven to be an efficient and robust method for analyzing DNA methylation at a genome-wide scale. Recently, several different companies have provided array designs to fit customer needs including whole-genome survey sets and promoter sets so that you can obtain comprehensive data from your methylation samples.

2. Materials

2.1. Preparation of Genomic DNA

1. Qiagen QIAamp DNA Mini kit (Valencia, CA).

2.2. Sonication of Genomic DNA

1. Bioruptor model 200 (Diagenode, Sparta, NJ).
2. Microcentrifuge (Thermo Scientific, Waltham, MA).
3. Water bath at 37°C , 50°C and 95°C (Thermo Scientific).

2.3. Immunoprecipitation of methylated DNA (MeDIP)

1. Mouse monoclonal 5-methylcytidine antibody, MAb-5MECYT-500 (Diagenode, Sparta, NJ).
2. Dynabeads Protein G (Invitrogen, Carlsbad, CA).
3. Phase lock, heavy tubes (Eppendorf, Westbury, NY).
4. Magnetic rack for 1.5-ml tubes (Invitrogen).
5. Rotating/rocking platform (Fisher Scientific, Pittsburgh, PA).
6. Proteinase K solution (Invitrogen).
7. 10x IP buffer: 100 mM Na-Phosphate, pH 7.0, 1.4 M NaCl, 0.5% Triton X-100.
8. TE buffer: 10 mM Tris-HCl, pH 7.5, 1 mM EDTA.
9. Digestion buffer: 50 mM Tris, pH 8.0, 10 mM EDTA, 0.5% SDS.

2.4. Purification of Methylated DNA

1. Glycogen (Roche, Indianapolis, IN).
2. Phenol:chloroform:isoamyl alcohol (Fluka, St. Louis, MO).
3. 5 M NaCl.
4. TE buffer: 10 mM Tris-HCl, pH 7.5, 1 mM EDTA.
5. NanoDrop ND-3300 Fluorospectrometer (Thermo Scientific).
6. Thermocycler (Applied Biosystems, Foster City, CA).

2.5. Analysis by CpG Island Microarrays

1. Cy3/Cy5 labeling kit (GE Healthcare, Piscataway, NJ).
2. Agilent Technologies Human CpG island microarray G4492A (Santa Clara, CA).

2.6. Data Validation (Components for a Combined Bisulfite Restriction Analysis or COBRA)

1. Universal Methylated DNA Standard (Zymo Research, Orange, CA) or prepare methylated positive control using *Sss*I methylase (New England Biolabs, Ipswich, MA).
2. EZ DNA Methylation-Gold Kit (Zymo Research).
3. PCR primers reflecting the bisulfite-converted genome sequence of region of interest (Illumina, San Diego, CA).
4. AmpliTaq Gold DNA Polymerase (Applied Biosystems, Foster City, CA).
5. Methylation sensitive restriction enzyme such as *Bst*UI (New England Biolabs).
6. Agarose (Fisher Scientific).

3. Methods

3.1. Preparation of Genomic DNA

1. Extract genomic DNA using Qiagen QIAamp DNA Mini kit, following the manufacturer's protocol (*see* **Note 4**).
2. The quantity and quality of genomic DNA (preferably eluted in water) needs to be carefully determined (*see* **Note 5**).

3.2. Sonication of Genomic DNA

1. Sonicate purified genomic DNA using Diagenode Bioruptor 200, as follows:

   Dilute 20 μg genomic DNA in 300−450 μl IP buffer (use 10x IP buffer to adjust the buffer concentration to 1x strength) in a 1.5 ml eppendorf tube. As we have observed inconsistencies in DNA fragmentation patterns between runs, we resort to careful control of the sonication conditions. If that is not your experience, you can skip the following section.
2. Prior to the beginning of the sonication process, remove all the ice particles using a strainer and add a predetermined amount of fresh ice. Bring the water level to a preset mark.
3. Turn sonicator on 30 s then off 30 s for 20 times. We replenish ice after the first two cycles and replace both fresh ice and ice-cold water after 4th cycle.
4. Load 4 μl on a 2% agarose gel to verify fragment size of DNA (mean size should be 200–800 bp; average 400 bp) (*see* **Note 6** and **Fig. 10.2**).
5. Aliquot 100–150 μl sonicated DNA to three eppendorf tubes; each tube contains 6–7 μg DNA.

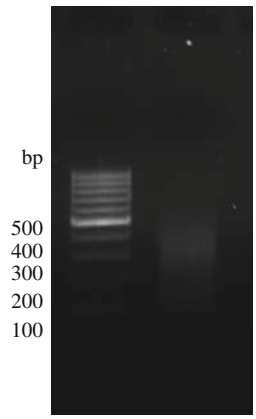

Fig. 10.2. The gel represents sonicated genomic DNA isolated from MCF-7 run on a 2% agarose gel. Most of the sheared fragments have a size between 200 and 800 bp.

3.3. Immunoprecipitation of Methylated DNA (MeDIP)

1. Heat-denature the samples (DNA) for 10 min in boiling water, and immediately cool on ice for 10 min.
2. Save one tube of the heat-denatured DNA, and store at -20°C for use as an input control.
3. Add 10 µg of antibody (monoclonal mouse anti-5-methyl cytidine) (*see* **Notes 7–8**).
4. Incubate the mixture overnight on a rotating platform at 4°C.
5. Add 50 µl of Dynabeads Protein G to the DNA-antibody mixture.
6. Incubate 2 h on a rotating platform at 4°C.
7. The washing steps are simplified by the use of an Invitrogen magnetic rack. Once the magnetized Dynabeads are tightly held by the magnet in the rack, remove unbound DNA-antibody mixture. Remove tubes from the rack. Add 1 ml of 1x IP buffer and flick gently to wash. Replace the tubes to the rack and repeat this washing step three times.
8. Resuspend the beads in 250 µl digestion buffer.
9. Add 5 µl Proteinase K (20 mg/ml stock).
10. Incubate overnight on a rotating platform at 50°C.

3.4. Purification of Methylated DNA

1. For 200 µl volume, add 400 µl phenol:chloroform:isoamyl alcohol, vortex for 30 s. For a clean separation of the two phases, employ a 2 ml heavy Eppendorf phaselock tube whereby the organic phase is located above the gel and can be cleanly removed (follow instructions provided by Eppendorf).
2. Transfer the aqueous supernatant to a new tube.

3. Add 1.5 μl glycogen (20 mg/ml stock) and mix well.
4. Add 16 μl 5 M NaCl and then 800 μl 100% ethanol.
5. Precipitate in -80°C freezer for 30 min or overnight.
6. Centrifuge at 20,000*g* for 10 min at 4°C. Carefully remove the supernatant. Wash pellets by adding 500 μl of 80% EtOH. Vortexing to resuspend pellet and spin again at 20,000*g* for 5 min at 4°C.
7. Resuspend the DNA pellet in 70 μl TE buffer.
8. Measure DNA concentration (*see* **Note 9**).
9. Save 5 μl of immunoprecipitated DNA to check for enrichment in the immunoprecipitation samples using gene-specific qPCR (*see* **Note 10**).

3.5. Analysis by CpG Island Microarrays

1. Cy3/Cy5 labeling of MeDIP-enriched and input DNA, array hybridization, and array washing were performed using a previously published protocol *(*19*)*.
2. An example of a commercially available microarray suitable for MeDIP-chip experiment is described here. Agilent Technologies Human CpG island microarray (G4492A) contains 45–60 mers oligonucleotide probes tiling all the CpG islands as defined by the University of California-Santa Cruz Genome Browser. This slide format has 195,000 probes covering a total of 27,800 human CpG islands. The average spacing between probes is 116 bp. Probes are selected for uniqueness within the genome (repeat sequence masked) and predicted hybridization properties according to standard Agilent probe design criteria was used in the design with the exception of theoretical Tm window restriction. This restriction cannot be used due to high GC content in CpG islands. As such, the standard Tm restriction is lifted to achieve the appropriate spacing.
3. Other appropriate microarrays for MeDIP analysis include NimbleGen HD2 Whole Genome Tiling Array Sets and the University Health Network HCG12K Human CpG Island Microarray (for additional designs, *see* **Note 3**).
4. As the Agilent CpG island microarray is our platform of choice, we use the Agilent DNA Analytics program (version 4.0.76) to identify regions that are enriched by the 5-methylcytidine antibody. For researchers who do not have quick access to biostatisticians to assist in data analysis, this is the most reasonable approach.

3.6. Data Validation

1. The combined bisulfite restriction analysis (COBRA) is a preferred way to validate MeDIP-chip data. This protocol is as much a gold standard in DNA methylation analysis as bisulfite sequencing (14). The steps that follow represent useful insight for smooth adaptation of this protocol.

2. Positive methylation control can be purchased but can also be prepared by following the protocol that comes with *Sss*I methylase. Because the methyl-donor SAM is quite labile, we spike the reaction mixture with another dose of SAM half way through the recommended reaction time.
3. Blood DNA and sperm DNA are good choices for negative control used in COBRA as these DNA are known to lack DNA methylation. Blood DNA, though not as devoid of methylation as sperm DNA, is far easier to work with in the subsequent bisulfite conversion step and the PCR step.
4. Bisulfite conversion of MeDIP DNA, positive and negative DNA is achieved by using the Easy DNA Methylation kit. For most validation targets, bisulfite converted DNA derived from this straight forward approach is sufficient to yield methylation status. There are, however, regions in the genome that are less accessible to the chemicals used in the bisulfite modification reaction. This will require the more tedious protocol described elsewhere (14).
5. Bisulfite PCR products from the region of interest are divided into two equal portions. One portion is restricted by methylation-sensitive enzyme and the other is mock-restricted. Both portions are then purified and run out on agarose gel (PAGE gel is used if better separation is desired). This scheme provides an uncut PCR fragment with intensity approximate that of a sample devoid of DNA methylation. When a sample has methylation sites close to one end of the PCR product or just having low level of methylation, the disappearance of the unrestricted band in comparison to the mock-restricted sample will add confidence to the methylation call.
6. A representation of validation is depicted in **Fig. 10.3**. Herein we validate promoter methylation found in tamoxifen-resistant MCF-7 cells (OHT) but not in regular MCF-

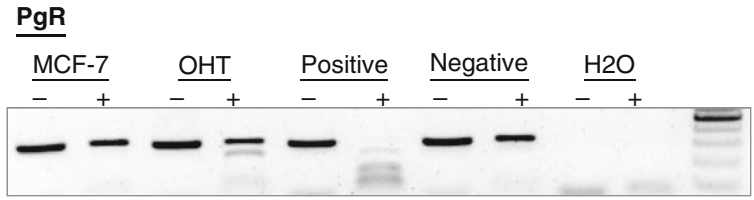

Fig. 10.3. COBRA validation of *PgR* promoter methylation in OHT (tamoxifen-resistant MCF-7 cells) but not in untreated MCF-7 cells. Positive control (genomic DNA methylated with *Sss*I) showed 100% in the interrogated region. Negative control (blood DNA) should little to no restricted bands by *Bst*UI (not methylated in this region). The parental MCF-7 cells harbored no methylation in this region whereas tamoxifen-resistant OHT cells showed signs of methylation in the *PgR* promoter, potentially signifying the onset of gene silencing.

7 cells. In this figure, positive control was derived from genomic DNA methylated by *Sss*I enzyme prior to bisulfite conversion to retain this methylation information. The negative control was bisulfite converted blood DNA known to lack DNA methylation. Control and sample DNA were interrogated by *Bst*UI to reveal methylated CpG dinucleotides within the region bracketed by the PgR promoter primers. The presence of restricted fragments with a concomitant decrease in the top unrestricted band signified the presence of methylation in the *PgR* promoter.

7. Other assays suitable for data validations include quantitative methylation-specific PCR (qMSP, 12) and the time- and resources-expensive bisulfite sequencing.

4. Notes

1. Different researchers have suggested widely varying values from 200 to 1000 bp. For example, a study reported a fragment size of 600 bp (20) whereas another reported a lower fragment size of 300–600 bp (21) in their MeDIP protocol. In the protocol listed by a commercial company (NimbleGen System, Inc) a much wider fragment size range (200–1000 bp) is cited. The protocols of chromatin immunoprecipitation (ChIP) are very similar to MeDIP. The average fragment size after sonication is around 200–600 bp (21, 22).
2. The amount of immunoprecipitated DNA is typically very small. One solution is to perform multiple pull down experiments. If source material is limited, one can amplify the pull down DNA prior to labeling and microarray analysis. There are several approaches described in the literature for this step, they include whole genome amplification using the Sigma WGA2 kit, ligation-mediated PCR (LM-PCR; http://www.chiponchip.org/protocol_itm3.html) or T7 amplication (23). After amplifying MeDIP and input samples, the resultant amplicons should be evaluated on an agarose gel to validate that their fragment size range matches the pull down DNA and input DNA. It is also pertinent that there should not be distinct banding pattern present in the amplified products.

3.

Company	Array designs	Total probes	Probe length
NimbleGen	Whole-Genome	2.1 million	50– mer
	CpG island-Plus-Promoter	385,000	50–75 mer
Agilent Technologies	Human CpG island	237,220	95 bp
	Mouse CpG island	97,652	95 bp
Phalanx Biotech	Human One Array	32050	60 mer
	Mouse One Array	31802	71 Mer

4. There are several genomic DNA isolation kits commercial available now, you can choose one of them. Purity is determined by calculating the ratio of absorbance at 260 nm to absorbance at 280 nm. Pure DNA has an A260/A280 ratio of 1.8–2.0 indicating the absence of protein and an A260/230 ratio of >2.0, indicating the absence of other organic compounds such as ethanol. Impure DNA will lead to nonspecific binding and affect MeDIP pull down.
5. After isolation of genomic DNA from your samples, run a 1.5% agarose gel to check the quality of the DNA and make sure there is no contamination with RNA, since the antibody also can recognize 5-methylcytidine in RNA. If there is a contamination with RNA, you may see smear RNA located in the front of the gel.
6. Wide range of genomic DNA can be successfully fragmented by sonication (from breast progenitor cells to breast cancer cell lines). However, the efficiency of sonication varies with DNA concentration, and machine itself (probe-type sonicator produces different outcomes in comparison to Bioruptor). Therefore, it is very important to systematically check the size of the fragmented DNA. Some of the factors that will alter the fragment size such as water temperature, ice/water ratio in the sonication vessel, DNA dissolved in the water or IP buffer, duration of reset between each energy pulse, DNA concentration and volume of DNA per tube, and batch of the eppendorf tubes, etc.
7. MeDIP-chip is only limited to identify CpG islands that are highly methylated in genomes. This is because the antibody used in the assay can only bind to >4 nearby methylated CpG sites. Therefore, low-density methylation of CpG islands is likely not detectable by MeDIP-chip. To improve the methylation coverage by MeDIP-chip, methyl-CpG immunoprecipitation (MCIp, 24) assay is one of the alternative methods.

8. There are several different 5-methylcytidine antibodies available now.

Clone	Host Species	Type	Company	Quantity
33D3	Mouse	Monoclonal Ab	GenWay	1 mg/ml
33D3	Mouse	Monoclonal Ab	Eurogentec	1 mg/ml
33D3	Mouse	Monoclonal Ab	ProSci	0.05 mg
33D3	Mouse	Monoclonal Ab	Calbiochem	
33D3	Mouse	Monoclonal Ab	Epigentek	1 mg/ml
33D3	Mouse	Monoclonal Ab	Affinity BioReagents	100 μg
33D3	Mouse	Monoclonal Ab	Santa Cruze	50 μg/0.5 ml
33D3	Mouse	Monoclonal Ab	AbCam	50 μg
33D3	Mouse	Monoclonal Ab	AbD SeroTec	0.1 mg

9. NanoDrop ND-3300 Fluorospectrometer uses PicoGreen dye to stain nucleic acid for quantitating double-stranded DNA (dsDNA). The PicoGreen assay provides a highly sensitive means of dsDNA quantiation with minimal consumption of sample. The ND-3300 fluorospectrometer has demonstrated a detection range for dsDNA bound with PicoGreen reagent of 1 –1000 pg/μl. Compared to the NanoDrop ND-1000, ND-3300 provides more accurate readout especially for the immunoprecipitation DNA samples.
10. In order to evaluate the enrichment of methylated DNA after MeDIP, we use quantitative PCR to measure the change of Ct between immunoprecipitation DNA and input DNA. We usually can have 40–200-fold increase after MeDIP based on different target genes.

References

1. Zilberman, D., Gehring, M., Tran, R.K., Ballinger, T., Henikoff, S. (2007) Genome-wide analysis of *Arabidopsis thaliana* DNA methylation uncovers an interdependence between methylation and transcription. *Nat. Genet.* ***39***, 61–69.
2. Rauch, T., Wang, Z., Zhang, X., Zhong, X., Wu, X., Lau, S. K., Kernstine, K. H., Riggs, A. D., Pfeifer, G. P., (2007) Homeobox gene methylation in lung cancer studied by genome-wide analysis with a microarray-based methylated CpG island recovery assay. *Proc. Natl. Acad. Sci.****104***, 5527–5532.
3. Esteller, M. (2008) Epigenetics in Cancer. *N. Engl. J. Med.* ***358***, 1148–1159.
4. Liu, K., Wang, Y. F., Cantemir, C., Muller, M. T. (2003) Endogenous assays of DNA methyltransferases: Evidence for differential activities of DNMT1, DNMT2, and DNMT3 in mammalian cells in vivo. *Mol. Cell Biol.* ***23***, 2709–19.
5. Rollings, R.A., Haghighi, F., Edwards, J.R., Das, R., Zhang, M.Q., Ju, J., Bestor, T.H. (2006) Large-scale structure of genomic methylation patterns. *Genome Res.* ***16***, 157–163.

6. Laird, P.W. (2005) Cancer epigenetics. *Hum. Mol. Genet.* ***14***, R65–76.
7. Bird, A. (2002) DNA methylation patterns and epigenetic memory. *Genes Dev.* ***16***, 6–21.
8. Jaenisch, R., Bird, A. (2003) Epigenetic regulation of gene expression: how the genome integrates intrinsic and environmental signals. *Nat. Genet.* ***33***, 245–254.
9. Das, P. M., Signal, R. (2004) DNA methylation and cancer. *J. Clin. Oncol.****22***, 4632–4642.
10. Feinberg, A. P., Tycko, B. (2004) The history of cancer epigenetics. *Nat. Rev. Cancer* ***4***, 143–153.
11. Suzuki, M. M., Bird, A. (2008) DNA methylation landscapes: provocative insights from epigenomics. *Nat. Rev. Genet.* ***9***, 465–476.
12. Herman, J. G., Graff, J. R., Myohanen, S. et al. (1996) Methylation-specific PCR: a novel PCR assay for methylation status of CpG islands. *Proc. Natl. Acad. Sci. USA* 93, 9821–9826.
13. Eads, C. A., Danenberg, K. D., Kawakami, K., et al. (1999) CpG island hypermethylation in human colorectal tumors is not associated with DNA methyltransferase overexpression. *Cancer Res.* ***59***, 2302–2306.
14. Xion, Z., Laird, P. W. (1997) COBRA: a sensitive and quantitative DNA methylation assay. *Nucleic Acids Res.* ***25***, 2532–2534.
15. Gonzalgo, M. L., Jones, P. A. (1997) Rapid quantitation of methylation differences at specific sites using methylation-sensitive single nucleotide primer extension (Ms-SNuPE). ***25***, 2529–2531.
16. Gitan, R. S., Shi, H., Chen, C. M., Yan, P. S., Huang, T. H. (2002) Methylation-specific oligonucleotides microarray: a new potential for high-throughout methylation analysis. *Genome Res.* ***12***, 158–164.
17. Yan, P. S., Chen, C. M., Shi, H., Rahmatpanah F., Wei, S. H., Huang, T. H. (2002) Applications of CpG island microarrays for high-throughout analysis of DNA methylation. *J. Nutr.* ***132***, 2430S–2434S.
18. Weber, M., Davies, J. J., Wittig, D., Oakeley, E. L., Haase, M., Lam, W. L., Schübeler, D. (2005) Chromosome-wide and promoter-specific analyses identify sites of differential DNA methylation in normal and transformed human cells. *Nat. Genet.* ***37***, 853–862.
19. Lee, T.I., Johnstone, S.E., Young, R.A., (2006) Chromatin immunoprecipitation and microarray-based analysis of protein location. *Nature Protocols* ***1***, 729–748.
20. Down, T.A., Rakyan, V.K., Turner, D.J., Flicek, P., Li, H., Kulesha, E., Graf, S., Johnson, N., Herrero, J., Tomazou, E.M., Thorne, N.P., Backdahl, L., Herberth, M., Howe, K.L., Jackson, D.K., Miretti, M.M., Marioni, J.C., Birney, E., Hubbard, T.J.P., Durbin, R., Tavare, S., Beck, S., (2008) A Bayesian deconvolution strategy for immunoprecipitation-based DNA methylome analysis. *Nat. Biotech.* ***26***, 779–785.
21. Jacinto, F.V., Ballestar, E., Esteller, M., (2008) Methyl-DNA immunoprecipitation (MeDIP): hunting down the DNA methylation. *Biotechniques* ***44***, 35–43.
22. Kininis, M., Chen, B.S., Diehl, A.G., Isaacs, G.D., Zhang, T., Siepel, A.C., Clark, A.G., Kraus, W.L., (2007) Genomic analyses of transcription factor binding, histone acetylation, and gene expression reveal mechanistically distinct classes of estrogen-regulated promoters. *Mol. Cell. Biol.* ***27***, 5090–5104.
23. Liu, C.L., Schreiber, S.L., Bernstein, B.E. (2003) Development and validation of a T7 based linear amplification for genomic DNA. *BMC Genomics* ***4***, 19.
24. Schilling, E., Rehli, M. (2007) Global, comparative analysis of tissue-specific promoter CpG methylation. *Genomics.* ***90***, 314–323.

Chapter 11

Use of Reporter Genes to Study the Activity of Promoters in Ovarian Granulosa Cells

Jingjing L. Kipp and Kelly E. Mayo

Abstract

Use of reporter genes provides a convenient way to study the activity and regulation of promoters and examine the rate and control of gene transcription. Many reporter genes and transfection methods can be efficiently used for this purpose. To investigate gene regulation and signaling pathway interactions during ovarian follicle development, we have examined promoter activities of several key follicle-regulating genes in the mouse ovary. In this chapter, we describe use of luciferase and β-galactosidase genes as reporters and a cationic liposome mediated cell transfection method for studying regulation of activin subunit- and estrogen receptor α (ERα)-promoter activities. We have demonstrated that estrogen suppresses activin subunit gene promoter activity while activin increases ERα promoter activity and increases functional ER activity, suggesting a reciprocal regulation between activin and estrogen signaling in the ovary. We also discuss more broadly some key considerations in the use of reporter genes and cell-based transfection assays in endocrine research.

Key words: Reporter genes, luciferase, β-galactosidase, promoter activity, estrogen, estrogen receptor, activin.

1. Introduction

There are many approaches to investigate gene expression in eukaryotic cells. Ultimately, one is often interested in the levels, modification, localization, or activity of the protein encoded by the gene of interest, as such measurements are perhaps most closely correlated with the biological response. However, in many cases, it is useful to measure levels of the RNA transcript, for example between cell or tissue types, in response to a stimulus, or over time. Thus, many assays for RNA measurement have been developed, including S1 nuclease protection, primer extension, Northern blot hybridization,

O.-K. Park-Sarge, T.E. Curry, Jr. (eds.), *Molecular Endocrinology,* Methods in Molecular Biology 590,
DOI 10.1007/978-1-60327-378-7_11,

and RT-PCR. However, these assays all measure mRNA transcript levels which are, of course, affected by both the rate of transcription and the rate of mRNA degradation (and potentially by other steps including RNA processing and transport). To investigate directly the rate of gene transcription, an important assay is nuclear run-on transcription, which allows transcription to continue in isolated nuclei and then hybridizes labeled transcripts to known DNA for identification (1, 2). This assay provides a direct way to assess which genes are active in a given cell and examine the effects of environmental conditions on gene transcription (3, 4). Using this assay, gene transcription occurs largely in its native structural and cellular context. However, some paused RNA polymerases may be artificially activated thus leading to incorrect interpretation of the results (5). Isolation of purified nuclei can also be technically difficult for some cells (6). A complementary assay is the measurement using RT-PCR of unspliced nuclear pre-mRNA precursors using primers that span introns (7). While both are very valuable assays and give fairly direct measurements of gene transcription, they are complex assays most often utilized in specialized circumstances.

An alternative way to indirectly measure gene transcription is to study gene promoter activities using reporter genes, where a reporter is placed next to and controlled by the promoter region of a gene of interest and the accumulation of the reporter gene mRNA or protein product is measured as an indicator of the promoter activity. Mutations can also be introduced into the promoter region to identify important regulatory elements, and ultimately, transcription factors controlling its activity.

A reporter gene encodes a product that can be easily and quantitatively measured. Examples of common reporter genes include the gene that encodes jellyfish green fluorescent protein (GFP) which emits green fluorescent light when excited by appropriate wavelengths (8, 9), the luciferase genes that encode firefly or Renella luciferases which catalyze a reaction in which the substrate luciferin is acted upon to produce light (10, 11), the *LacZ* gene that encodes the enzyme β-galactosidase which catalyzes a reaction in which the substrate analog X-gal gives a blue colored product (12) or 1,2-dioxetane substrates produce light (13–16), the bacterial gene that encodes the enzyme chloramphenicol acetyl transferase (CAT) whose enzymetic activity can be measured with thin layer chromatography or immunological assays, and the human growth hormone gene that encodes growth hormone which can be secreted into the culture medium and measured by radioimmunoassay (17). There are many others that can be used in the appropriate context. A reporter gene normally is not endogenously expressed or only expressed at a very low level. Although endogenous β-glactosidase activity can be detected in most mammalian cell lines, through manipulating assay conditions, the endogenous β-glactosidase activity can be minimized.

The luciferase gene and the *LacZ* gene have been widely used as reporter genes to study promoter activities due to the fact that they can be quickly translated into proteins, these proteins are enzymes which allow for amplification of the signal, the enzymatic activity can be measured with simple, highly sensitive, and quantitative assays, and no radioactive materials are involved. In addition, luciferase has a fast turn-over rate, which reduces accumulation in an inducible system and provides a more dynamic view of gene transcription (18). In this chapter, we describe use of these two reporter genes to study promoter activities in endocrine systems.

A promoter-reporter DNA construct is most often produced and propagated using bacterial plasmids. The plasmid DNA can be introduced into mammalian cells through transient or stable transfection (19). The former is widely used as an initial testing step and is described in this chapter. If a promoter does not show strong activity in transiently transfected cells, stable transfection may be considered. There are numerous ways of transfecting cells with DNA, including calcium phosphate precipitation, lipid vesicle encapsulated DNA transfer, and electroporation (20). We have been using a cationic liposome mediated transfection method to study promoter activities in ovarian granulosa cells. This process involves encapsulating DNA with lipid, transfecting cells with the DNA/lipid mix, collecting cell lysates, and performing luciferase or β-galactosidase assays to quantitatively measure promoter activity (**Fig. 11.1**).

Using reporter genes to study the activity of promoters is convenient, sensitive, and reliable. It is however important to understand that this assay is an indirect measurement, and it assumes that the amount of reporter gene product is a reasonable indicator of transcription rate and therefore promoter activity. This assumption is justified if reporter mRNA turnover or translational rate is not affected by the treatment conditions being employed. Using reporter genes to study the activity of promoters may also introduce bias due to the incorporation of foreign elements from the vector or elimination of intrinsic elements from the endogenous gene within the test genes (21). Therefore, a particular promoter-reporter system needs to be carefully evaluated and validated before use. Indeed, this approach is perhaps best applied once other methods like nuclear run-on have been used to verify that what is being studied is actually a transcriptional effect. Reporter gene assays then allow this transcriptional effect to be studied in greater detail. Finally, transfection efficiency, cell viability, and sample recovery play a critical role in interpreting results; therefore, internal controls need to be included in each assay. Although not described in detail here, for internal control purposes, dual-reporters are commonly employed, where one plasmid containing an experimental reporter gene is co-transfected with another plasmid containing a distinct control reporter gene whose activity can be measured using a different assay. The experimental reporter gene is normally driven by a promoter of interest and the control

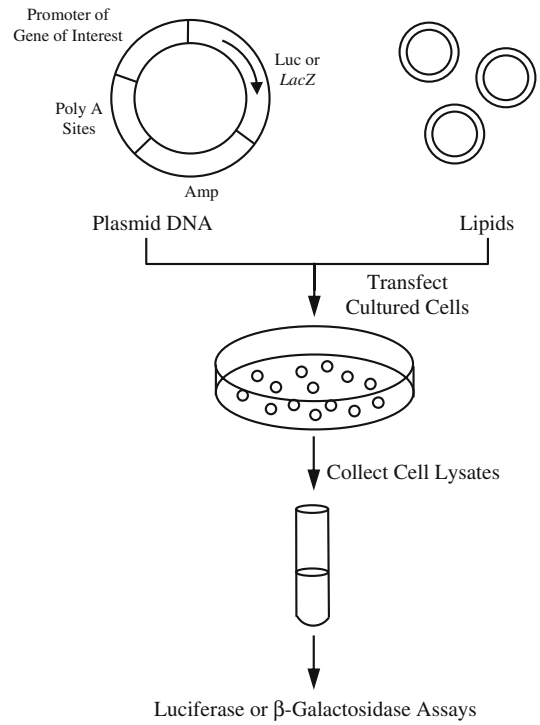

Fig. 11.1. Flow chart showing the use of reporter genes and cationic liposome-mediated cell transfection to study promoter activity. Plasmid DNA is mixed with a liposome suspension. Cells are transfected via incubating with the DNA/lipid mix. Cell lysates are then collected and luciferase or β-galactosidase assays are performed to measure promoter activity. Luc: luciferase reporter gene that encodes firefly luciferase. *LacZ*: *LacZ* reporter gene that encodes β-galactosidase. Amp: gene for ampicillin resistance in *E. coli*. *Arrow* within the Luc gene shown in the circular plasmid indicates the direction of transcription.

reporter is normally driven by a constitutive viral promoter whose activity is not affected by the experimental conditions (19, 22). Although the dual-reporters can be a combination of any two distinct reporter genes, the dual-luciferase reporter system, where firefly luciferase is used as an experimental reporter and Renilla luciferase is used as a control reporter, allows detection of both reporters using the same assay but with different substrates (22).

We are interested in investigating interactions between the signaling pathways involving the steroid hormone estrogen and the TGF-β superfamily member activin. We have demonstrated that estrogen suppresses activin subunit expression and decreases activin signaling in the early mouse ovary (23), while activin stimulates estrogen receptor α and estrogen receptor β (ERα and ERβ) expression (24). To further examine if this reciprocal regulation is at the level of gene transcription and to confirm an effect of activin on functional ER activity, we used reporter genes to study the promoter activities of the activin subunits and ERα as well as the activation of

estrogen response element (ERE). We have shown that estrogen suppresses activin subunit gene promoter activities while activin increases ERα promoter activity and increases functional ER activity (23, 24). Select examples from this work related to the use of reporter genes will be used for illustrative purposes in presenting the specific methods used in these cell-based transfection assays.

2. Materials

2.1. Cell Culture

1. CD-1 mice at 21–23 day of age for primary granulosa cell culture.
2. GRMO2 cells: from a mouse granulosa cell line provided by N.V. Innogenetics, Ghent, Belgium (25, 26).
3. Medium for primary cell culture (4F medium): phenol red-free D-MEM/F-12 medium (Invitrogen Corporation, Grand Island, NY) supplemented with 2 μg/ml insulin, 5 nM sodium selenite, 5 μg/ml transferrin, 0.04 μg/ml hydrocortisone, and 50 μg/ml sodium pyruvate. To obtain 4F medium containing serum, add 10% charcoal/dextran treated fetal bovine serum (Hyclone, Logan, UT) (see **Note 1**).
4. Pre-incubation medium: 0.5 M sucrose and 10 mM EGTA in 4F medium (without serum).
5. Medium for GRMO2 cell culture (HDTIS medium): phenol red-free D-MEM/F-12 medium (Invitrogen Corporation, Grand Island, NY) supplemented with 5 μg/ml insulin, 5 nM sodium selenite, 10 μg/ml transferrin, 50 μg/ml sodium pyruvate, and 2% charcoal/dextran-treated fetal bovine serum (Hyclone, Logan, UT) (*see* **Note 1**).
6. 12-well (# 92012, Techno Plastic Products Ltd., Zurich, Switzerland) or 24-well tissue culture plates (#662-160, Greiner Bio-One, Monroe, NC).
7. Cell strainer (#352340, 40 μm, BD Falcon, Bedford, MA).

2.2. Lipid and Transfection

1. Plasmid DNA: DNA construct that contains a promoter fragment of a gene of interest linked to a luciferase reporter gene or a β-galactosidase reporter gene.
2. Liposomes: Dissolve 100 mg of DDAB (Dimethyldioctadecylammonium bromide) (Sigma # D-2779. Powder stored at room temperature) in 1 ml chloroform. Add 100 μl of PtdEtn (L-a-phosphatidylethanolamine, dioleoyl[C18:1, cis9]) (Sigma #P-0510. Supplied in 10 mg/ml chloroform, stored at −20°C) and 4 μl of DDAB solution in a microcentrifuge tube. Dry in a speed vac and store at −20°C (*see* **Note 2**) (27).

3. Liposome suspension: Resuspend the liposome pellet in 101 µl of 100% ethanol. Take 1 ml of sterile distilled water in a 15 ml polystyrene tube. Pipette 50 µl of the 101 µl resuspended pellet into the water while vortexing the tube at medium speed (27). Store at 4°C and can be used for up to 4–5 months.
4. Polystyrene tubes (#2058 Falcon 5 ml tubes and #2057 Falcon 14 ml tubes) (*see* **Note 3**).
5. Phenol red-free Opti-MEM: #11058-021, Invitrogen Corporation, Grand Island, NY (*see* **Note 4** for preparation of regular phenol red containing Opti-MEM).

2.3. Transfection Efficiency Evaluation

1. Poly-L-Lysine: #P4832, SIGMA, St. Louis, MO. Store at 2–8°C.
2. Microscope cover slips (12 mm, circle): #12-545-80, Fisher Scientific, Pittsburgh, MA.
3. Fixative: prepare a 1% (w/v) paraformaldehyde solution in PBS fresh before use. To dissolve paraformaldehyde in PBS, heat at low to medium settings (avoid boiling) and then cool to room temperature.
4. Pmax green fluorescent protein (pmax GFP) control DNA is obtained from Amaxa (Cologne, Germany) (*see* **Note 5**).
5. DAPI mounting medium (Vector Laboratories, Inc.).
6. Fluorescent microscope (Leica DM 5000B).

2.4. Luciferase Assay and β-galactosidase Assay

1. Luciferase assay cell lysis buffer: 25 mM HEPES (pH 7.8), 15 mM $MgSO_4$, 4 mM EGTA, 1 mM dithiothreitol (DTT), and 0.1% Triton X-100 in ddH_2O.
2. Luciferase assay reaction buffer: 25 mM HEPES, pH 7.8; 15 mM $MgSO_4$, 4 mM EGTA, 2.5 mM ATP, 1 mM DTT and 1 µg/ml BSA in ddH_2O (*see* **Note 6**).
3. Luciferin: aliquot 10 mM luciferin stock solution (sodium salt) (Analytical Bioluminescence Lab, San Diego, CA) into 500 µl aliquots and store at −20°C.
4. β-galactosidase assay kit: Galacto-Light Plus Systems kit (Applied Biosystems, Bedford, MA).
5. Luminometer (Analytical Luminescence Laboratory Monolight 2010).
6. Luminometer cuvettes (#556862, 12 × 75 mm, BD Biosciences Pharmingen).
7. Bio-Rad protein assay reagent (Bio-Rad Laboratories, Inc., Richmond, CA).
8. Teflon cell scrapers (Fisher).

3. Methods

Use of reporter genes provides a convenient way to study the function and regulation of promoters. Herein we describe a cationic liposome mediated transfection method to study regulation of activin subunit- and ERα-promoter activities as well as activation of a synthetic ERE in primary cultured granulosa cells and in a mouse granulosa cell line, GRMO2 cells. Using this transfection method, DNA plasmids are encapsulated by cationic liposomes. The cationic liposomes can be attracted to negatively charged cell surface where they can fuse with plasma membranes and thus lead to uptake and expression of the DNA in transfected cells (20).

For most mammalian cells, transfection efficiency is generally poor. However, this can be optimized by varying DNA concentration, transfection reagent, and transfection time. The optimal procedure or reagent for transfection varies between cell lines or primary cell types. The protocol described in this chapter has been optimized for transfecting mouse granulosa cells and it has also been successfully used with many other cell types, including 293/293T cells, 3T3 cells, and JEG3 cells. To optimize the transfection method and to facilitate the interpretation of experimental results, a protocol for evaluating transfection efficiency is also detailed below. For experimental control purposes, each transfection assay should include a mock transfection negative control (no plasmid), an empty vector negative control (omit promoter), and a constitutively active viral promoter positive control.

To further analyze promoter function and identify important regulatory elements within a promoter and ultimately, the transcription factors that occupy these sites, 5' deletion mapping and site-directed mutagenesis can be utilized. The flow chart shown in **Fig. 11.2** outlines the basic steps to generate 5' deletion mutations of a promoter at different lengths and plasmids containing these promoter fragments. The plasmids can then be transfected into cells to study changes in promoter activity. To make site-directed mutations, we generally use a QuickChange site-directed mutagenesis kit (Stratagene). A detailed protocol can be found in the manufacturer's instruction manual, and this technique is therefore not included in this chapter.

Using luciferase or *LacZ*as reporter genes, we have studied the effect of estrogen on activin βA and βB promoter activities, the effect of activin on ERα promoter activity and the effect of activin on ERE activation, and shown a negative regulatory feedback system between these two important signaling pathways.

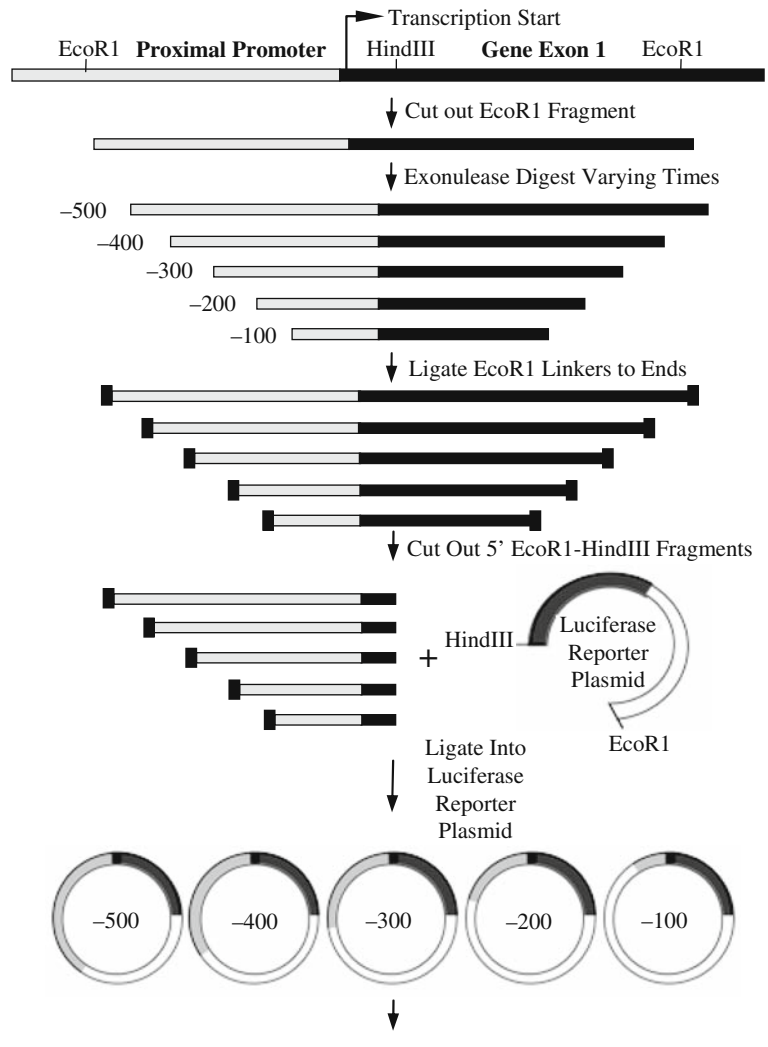

Fig. 11.2. Flow chart showing the basic steps to generate 5' deletion mutations. The plasmids containing the promoter fragments can then be transfected into cells to study the activity of the different promoter fragments. Although not shown here, rather than non-specific exonucleases, termini are often defined by unique restriction enzyme recognition sites.

3.1. Preparation of Primary Cultured Granulosa Cells and GRMO2 Cells for Transfection

Granulosa cells are collected through follicle puncture as reported previously by our laboratory in rats (28–32) and in mouse (24). Preparation of mouse cells is described below.

1. CD-1 mice are sacrificed on postnatal days 21–23. Ovaries from 5–10 animals are rapidly dissected out and collected into a 10 cm petridish containing cold 4F medium.
2. Dissect out fat and oviduct under a dissection microscope. Transfer ovaries to a clean 10 cm petridish and wash the ovaries twice with cold 4F medium.

3. Transfer the ovaries into a 15 ml Corning tube containing 10 ml pre-incubation medium and incubate at 37°C for 30 min, or until the ovaries sink (*see* **Note 7**). The purpose of this step is to disrupt gap junctions and improve cell integrity and yield (33).
4. After the ovaries have gravitated to the bottom of the tube, wash ovaries 2–3 times with cold fresh medium and transfer the ovaries along with 5 ml medium to a 10 cm petridish.
5. Use a 25 gauge needle to hold an ovary steady and use another needle to puncture follicles. Release of granulosa cells from follicles can be clearly observed under a dissection microscope. Continue puncturing until no more granulosa cells are extruded. Discard the punctured ovary and move on to a fresh one.
6. After all the ovaries are punctured and discarded, collect the extruded granulosa cells from the petridish into a 15 ml Corning tube under a cell culture hood. Centrifuge the cells at 150*g* for 5 min. Aspirate the medium and resuspend cells in 5 ml of 4F medium. Centrifuge again and aspirate the medium.
7. Repeat this wash once with 4F medium and once with 4F medium containing serum. Resuspend the final cell pellet in 1–2 ml of 4F medium containing serum. Filter out oocytes and small follicles with a 40 μm cell strainer.
8. Count viable cells using Trypan-blue exclusion and plate approximately 5×10^5 cells per well in 12-well plates or 2×10^5 cells per well in 24-well plates in 4F medium containing serum.
9. Cells are cultured in a humidified incubator at 37°C and 5% CO_2, and they normally attach to the bottom of the plates within 1 or 2 days.
10. If GRMO2 cells are to be used, cells are thawed and cultured in 12-well plates in a humidified incubator at 37°C and 5% CO_2 in HDTIS medium.
11. Start transfection when the cells are about 50–70% confluent.

3.2. Transfection

1. After 3- days of culture in the estrogen-deprived condition and when the cells reach the desired confluency, primary cultured granulosa cells or GRMO2 cells are transiently transfected with DNA constructs using cationic liposomes in a phenol red free Opti-MEM medium. The DNA constructs used here are either an activin βA subunit promoter-luciferase reporter construct (34), an activin βB subunit promoter-luciferase reporter construct (28), a 2x estrogen response element (ERE)—luciferase reporter construct (kindly provided by Dr. Larry Jameson from Northwestern University (35)), or a mouse ERα-promoter-β-galactosidase construct (kindly provided by Dr. Alessandro Weisz from Seconda Università degli Studi di Napoli, Italy (36)).

2. Transfection reagent is prepared as listed in **Table 11.1**. Typically, we use 0.25 μg DNA per well for 24-well plates and 0.5 μg DNA per well for 12-well plates. First, the DNA mix and lipid mix are prepared separately by combining appropriate amount of DNA or lipid with an equal amount of OptiMEM. Second, these two mixes are combined and incubated at room temperature for at least 20 min. Finally, the combined mixes are diluted with a larger volume of OptiMEM (see **Table 11.1**). This final mix is used to transfect cells.

Table 11.1
Preparation of transfection reagent

	DNA Mix		Lipid Mix			
Plate Size	DNA per well (ug)	OptiMEM (ul)	Lipid per well (ul)	OptiMEM (ul)	Diluent OptiMEM (ul)	Final Volume (ml)
24 well	0.25–1	25	5	25	200	~ 0.25
12 well	0.5–2	50	10	50	400	~ 0.5
6 well	2–5	100	15	100	800	~ 1
6 cm	5–10	200	25	200	1600	~ 2
10 cm	10–20	400	45	400	3200	~ 4

3. If co-transfection of a promoter-reporter gene construct together with a particular gene-expression construct is desired, add 0.025–0.05 μg of the gene-expression construct to the above DNA mix. Total DNA contents need to be normalized in all samples with appropriate vectors.
4. Aspirate medium from cells and wash once with PBS. Add the transfection mix to each well and incubate in a humidified CO_2 incubator for 6 h (*see* **Note 8**).
5. After 6 h transfection, the transfection mix is aspirated and cells are maintained in fresh culture medium for 14–16 h (overnight) to recover. Transfection efficiency evaluation or luciferase/β-galactosidase assays can then be performed. In our studies, after recovery, fresh medium containing various hormonal treatments (see result figures later) is given to the cells for an additional 24 h to examine effects of those treatments on the promoter activities.

3.3. Transfection Efficiency Evaluation

1. Lysine coat coverslips: heat coverslips in a loosely covered glass beaker in 1 M HCl at 50–60°C for 4–16 h; cool and wash coverslips extensively in dH_2O and then ddH_2O; rinse coverslips in 100% ethanol and leave to dry; coat coverslips in bulk in 10–15 ml 1 mg/ml poly-L-lysine with gentle shaking for 30 min in a 10 cm petridish; wash the coverslips in dH_2O and then ddH_2O at least 5 changes in each; rinse coverslips in 100% ethanol and let dry before use (*see* **Note 9**).
2. Plate cells in 24-well plates with a lysine-coated cover slip on the bottom of each well. Transfect cells with pmaxGFP control DNA (0.5 μg/μl, use 0.5 μl for each well) for 6 h following transfection protocol described above.
3. After overnight recovery, aspirate medium and rinse cells briefly with PBS. Add 0.5 ml of 1% paraformaldehyde to each well and fix cells at 4°C for 30 min. Aspirate the fixative and rinse cells with PBS once. Add several drops of PBS to each well so the cover slips are easy to pick up with a forceps.
4. Each slide can accommodate three 12 mm diameter circle coverslips. Add three drops of DAPI mounting medium on a slide and make sure that they are separated enough, then put one coverslip on each drop, cell side facing down. Use a Kimwipe to absorb excess DAPI mounting medium and seal with nail polish.
5. Let nail polish dry and take pictures from randomly selected 10–20 fields using a fluorescent microscope. Count the number of transfected cells (GFP, green) and the total number of cells (DAPI nuclear stained, blue) in each field, calculate transfection efficiency by dividing the number of transfected cells by the total number of cells, and then average the results from all fields. Examples in **Fig. 11.3** show that in a particular field, 6 out of 16 primary cultured granulosa cells were transfected and 9 out of 53 GRMO2 cells were transfected. The final transfection efficiency was 26% for primary cultured granulosa cells and 6% for GRMO2 cells after averaging results from 15 different fields.

3.4. Luciferase Assay and β-Galactosidase Assay

1. For luciferase assay, prepare cell lysis buffer as described in Materials.
2. Aspirate medium from wells and wash cells 1–2 times with cold PBS. Add 150 μl of lysis buffer to each well (12-well or 24-well culture plates). Incubate on ice for 20–30 min with gentle shaking.

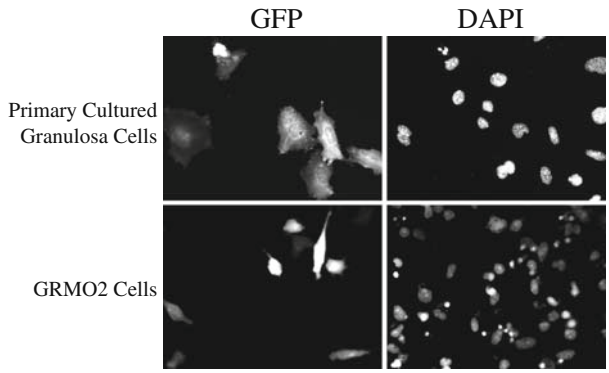

Fig. 11.3. Examples for transfection efficiency evaluation in primary cultured mouse granulosa cells and in GRMO2 cells. Using the cationic liposome-mediated cell transfection method described in this chapter, cells were transfected with 250 ng per well pmax GFP control DNA in 24-well plates. Cells were then fixed and pictures were taken under a fluorescent microscope. GFP: shows cells that were transfected and gave green fluorescent light. DAPI: shows the total number of cells that were nuclear stained with DAPI. In the particular fields shown here, 6 out of 16 primary cultured granulosa cells were transfected and 9 out of 53 GRMO2 cells were transfected. The final transfection efficiency was 26% for primary cultured granulosa cells and 6% for GRMO2 cells after averaging results from 15 different fields.

3. Tilt the plates, scrap the bottom of each well with cell scrapers, and collect lysates into chilled eppendorf tubes. Store the collected lysates on ice until ready to use or store at −80°C for later use (*see* **Note 10**).
4. Dilute 10 mM luciferin to 1 mM in ddH_2O and prepare luciferase assay reaction buffer as described in Materials. Aliquot 400 µl of reaction buffer into luminometer cuvettes.
5. Set the luminometer so that it injects 100 µl of substrate (luciferin) and collects data for 10 s (see **Note 11**).
6. Centrifuge cell lysates at maximal speed using a table top centrifuge before use to remove cell debris. Add 100 µl of cell lysates to 400 µl of reaction buffer, immediately inject 100 µl of 1 mM luciferin using the automatic injector, and measure emitted luminescence using the luminometer for 10 s.
7. For β-galactosidase assay, a Galacto-Light Plus Systems kit is used following the manufacturer's instructions.
8. Use the remaining cell lysates to measure protein concentration in each sample with the Bio-Rad protein assay reagent: add 5–10 µl of cell lysate to 100 µl diluted Bio-Rad assay reagent in a 96-well plate and read absorbance at 595 nm wave length with a 96-well plate reader.

9. Normalize relative light units obtained from luciferase assay or β-galactosidase assay with the protein content in each sample (*see* **Note 12**). The normalization allows one to control possible variations in the number of cells, cell growth rate and recovery of samples. Example results using a luciferase reporter gene to study effect of estrogen on activin βA and βB subunit promoter activities are shown in **Fig. 11.4**. Example results using *LacZ* reporter gene to study effect of activin on ERα promoter activity are shown in **Fig. 11.5**. Example results using luciferase reporter gene to study effect of activin on ERE activation are shown in **Fig. 11.6**.

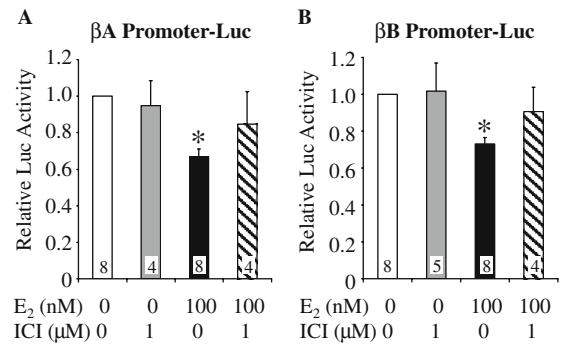

Fig. 11.4. Effects of E_2 and ICI 182, 780 on activinβA- and βB-promoter activities in transfected GRMO2 granulosa cells. All the treatments were given for 24 h. The numbers at the bottom of each bar indicate replicate experiments. Each measurement was done in triplicate. *P $<$ 0.05 (Reproduced from **ref.*22*** with permission from *The Endocrine Society*).

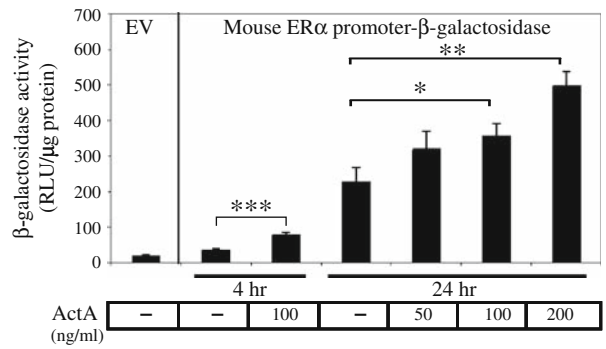

Fig. 11.5. Activin A increases ERα promoter activity. GRMO2 cells were deprived of estrogen for 3 days before being transfected with a mouse ERα promoter-β-galactosidase construct or empty vector (EV) overnight and then treated with activin A (ActA) at indicated doses for 4 or 24 h. Results are the average of three independent experiments each performed in triplicate. *P $<$ 0.05, **P $<$ 0.01, ***P $<$ 0.001 (Reproduced from **ref.*23*** with permission from the *Journal of Biological Chemistry*).

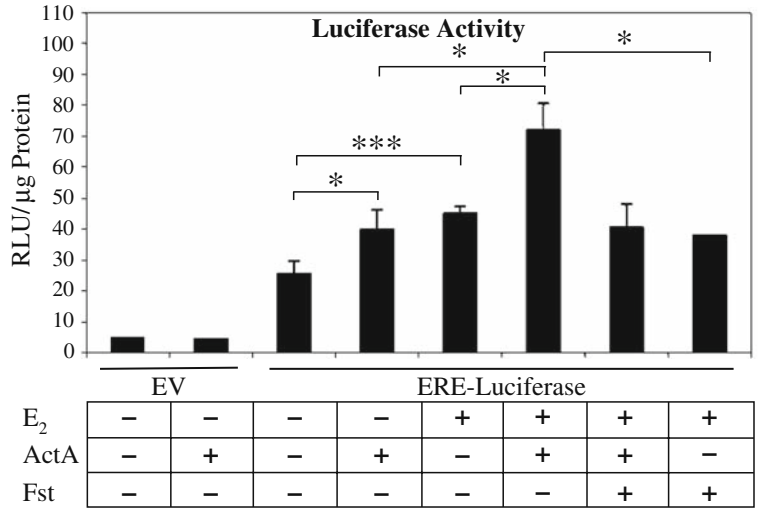

Fig. 11.6. Activin A increases ERE response to E_2. Primary granulosa cells were deprived of estrogen for 3 days before being transfected with an ERE-Luciferase construct or empty vector (EV) overnight. Transfected cells were then treated with activin A (ActA, 100 ng/ml), follistatin (Fst, 400 ng/ml), or a combination of these two compounds for 4–8 h followed by addition of E_2 (100 nM) or ethanol for another 24 hrs $n = 5$. *$P < 0.05$, ***$P < 0.001$ (Reproduced from **ref.*23*** with permission from the *Journal of Biological Chemistry*).

4. Notes

1. Estrogen-free culture conditions are used to minimize any interference from this steroid as this study measures estrogen effects as well as ER levels. If the estrogenic properties of phenol red containing culture medium or of serum are not a concern, use regular D-MEM/F-12 medium and regular fetal bovine serum.
2. Alternatively, a commercially available product such as Lipofectamine (Invitrogen) can be used and transfection can be performed following its manufacturer's instructions, although the homemade liposome preparation described in this protocol is very cost efficient.
3. Polystyrene tubes are the clear ones, not the opaque ones. The opaque ones are polypropylene tubes and lipids tend to adhere to the walls of this kind of tube.
4. Prepare regular Opti-MEM if the estrogenic effects of phenol red are not a concern: dissolve 13.6 g of Opti-MEM I powder (# 22600-050, Invitrogen Corporation, Grand Island, NY) in 1L of ddH_2O, add 2.4 g $NaHCO_3$, pH to 7.3, filter, and store at 4°C.

5. Although we use the pmax GFP control DNA from Amaxa, any other GFP-encoding plasmid will work.
6. Leave the ATP aliquot on ice and add it to the reaction solution just before use to minimize degradation at room temperature.
7. Incubation for 30 min is normally enough. Prolonged incubation (>45 min) can cause significant loss of cells due to cell death.
8. Transfection time may vary between 6 and 16 h depending on use of cell types and transfection reagents. Prolonged transfection times may cause cell toxiticity.
9. Treatment with HCl helps cells and polyaminoacids stick to glass. After acid treatment, coverslips can be stored for 1 year without polyaminoacid coating. After polyaminoacid coating, coverslips can also be stored for 1 year and rinsed with 100% ethanol before use. Polyaminoacid can be saved at −20°C and reused for 3–4 times.
10. We have observed that freezing the lysates at −80°C for at least 1 hr before use gives more consistent results between experiments.
11. The amount of reaction buffer and substrate used can be scaled down if desired or if using a different type of luminometer or luminometer cuvettes.
12. Relative light units can also be normalized with an internal luciferase control if using a dual-luciferase reporter assay system, or with another reporter gene expressed from a control constitutive promoter.

References

1. Derman, E., Krauter, K., Walling, L., Weinberger, C., Ray, M., Darnell, J.E. Jr. (1981) Transcriptional control in the production of liver-specific mRNAs. *Cell* **23**:731–739.
2. Greenberg, M.E., Ziff, E.B. (1984) Stimulation of 3T3 cells induces transcription of the c-fos proto-oncogene. *Nature* **311**:433–438.
3. Weaver, R.F. (1999) Molecular Biology. 1st ed: McGraw-Hill Companies, Inc.
4. Hu, Z.W., Hoffman, B.B. (2000) Nuclear run-on assays for measurement of adrenergic receptor transcription rate. *Methods in Molecular Biology* **126**:169–180.
5. Eick, D., Kohlhuber, F., Wolf, D.A., Strobl, L.J. (1994) Activation of pausing RNA polymerases by nuclear run-on experiments. *Analytical Biochemistry* **218**:347–351.
6. Sandoval, J., Rodriguez, J.L., Tur, G., et al. (2004) RNAPol-ChIP: a novel application of chromatin immunoprecipitation to the analysis of real-time gene transcription. *Nucleic Acids Research* **32**:e88.
7. Lipson, K.E., Baserga, R. (1989) Transcriptional activity of the human thymidine kinase gene determined by a method using the polymerase chain reaction and an intron-specific probe. *Proceedings of the National Academy of Sciences of the United States of America* **86**:9774–9777.
8. Prendergast, F.G., Mann, K.G. (1978) Chemical and physical properties of aequorin and the green fluorescent protein isolated from Aequorea forskalea. *Biochemistry* **17**: 3448–3453.

9. Tsien, R.Y. (1998) The green fluorescent protein. *Annual Review of Biochemistry* **67**: 509–544.
10. Ow, D.W., JR DEW, Helinski, D.R., Howell, S.H., Wood, K.V., Deluca, M. (1986) Transient and stable expression of the firefly luciferase gene in plant cells and transgenic plants. *Science* **234**:856–859.
11. de Wet JR, Wood, K.V., DeLuca, M., Helinski, D.R., Subramani, S. (1987) Firefly luciferase gene: structure and expression in mammalian cells. *Molecular and Cellular Biology* 7:725–737.
12. Joung, J.K., Ramm, E.I., Pabo, C.O. (2000) A bacterial two-hybrid selection system for studying protein-DNA and protein-protein interactions. *Proceedings of the National Academy of Sciences of the United States of America* **97**:7382–7387.
13. Jain, V.K., Magrath, I.T. (1991) A chemiluminescent assay for quantitation of beta-galactosidase in the femtogram range: application to quantitation of beta-dgalactosidase in lacZ-transfected cells. *Analytical Biochemistry* **199**:119–124.
14. Bronstein, I., Fortin, J., Stanley, P.E., Stewart, G.S., Kricka, L.J. (1994) Chemiluminescent and bioluminescent reporter gene assays. *Analytical Biochemistry* **219**:169–181.
15. Bronstein, I., Fortin, J.J., Voyta, J.C., et al. (1994) Chemiluminescent reporter gene assays: sensitive detection of the GUS and SEAP gene products. *BioTechniques* **17**: 172–174, 6–7.
16. Bronstein, I., Martin, C.S., Fortin, J.J., Olesen, C.E., Voyta, J.C. (1996) Chemiluminescence: sensitive detection technology for reporter gene assays. *Clinical Chemistry* **42**: 1542–1546.
17. Kingston, R.E., Sheen, J., Moore, D. (2001) Isotopic assays for reporter gene activity. Current protocols in molecular biology, edited by Frederick M Ausubel et al. Chapter 9:Unit9 7A.
18. Thompson, J.F., Hayes, L.S., Lloyd, D.B. (1991) Modulation of firefly luciferase stability and impact on studies of gene regulation. *Gene* **103**:171–177.
19. Carey, M., Smale, S.T. (1999) Functional Assays for Promoter Analysis. In: Transcriptional Regulation in Eukaryotes: Concepts, Strategies, and Techniques: Cold Spring Harbor Laboratory Press, pp. 137–92.
20. Felgner, P.L., Gadek, T.R., Holm, M., et al. (1987) Lipofection: a highly efficient, lipid-mediated DNA-transfection procedure. *Proceedings of the National Academy of Sciences of the United States of America* **84**: 7413–7417.
21. Zhang, K., Kurachi, S., Kurachi, K. (2003) Limitation in use of heterologous reporter genes for gene promoter analysis. Silencer activity associated with the cloramphenicol acetyltransferase reporter gene. *Journal of Biological Chemistry* **278**:4826–4830.
22. Sherf, B.A. NSL, Hannah, R.R. and Wood, K.V. Dual-Luciferase, T.M. (1996) Reporter Assay: An Advanced Co-Reporter Technology Integrating Firefly and Renilla Luciferase Assays. *Promega Notes Magazine* **57**: 02.
23. Kipp, J.L., Kilen, S.M., Bristol-Gould, S., Woodruff, T.K., Mayo, K.E. (2007) Neonatal exposure to estrogens suppresses activin expression and signaling in the mouse ovary. *Endocrinology* **148**: 1968–1976.
24. Kipp, J.L., Kilen, S.M., Woodruff, T.K., Mayo, K.E. (2007) Activin regulates estrogen receptor gene expression in the mouse ovary. *Journal of Biological Chemistry* **282**:36755–36765.
25. Briers, T.W., van de Voorde, A., Vanderstichele, H. (1993) Characterization of immortalized mouse granulosa cell lines. *In vitro Cellular & Developmental Biology* **29A**:847–854.
26. Vanderstichele, H., Delaey, B., de Winter, J., et al. (1994) Secretion of steroids, growth factors, and cytokines by immortalized mouse granulosa cell lines. *Biology of Reproduction* **50**:1190–1202.
27. Campbell, M.J. (1995) Lipofection reagents prepared by a simple ethanol injection technique. *BioTechniques* **18**:1027–1032.
28. Dykema, J.C., Mayo, K.E. (1994) Two messenger ribonucleic acids encoding the common beta B-chain of inhibin and activin have distinct 5′-initiation sites and are differentially regulated in rat granulosa cells. *Endocrinology* **135**:702–711.
29. Mukherjee, A., Park-Sarge, O.K., Mayo, K.E. (1996) Gonadotropins induce rapid phosphorylation of the 3′,5′-cyclic adenosine monophosphate response element binding protein in ovarian granulosa cells. *Endocrinology* **137**:3234–3245.
30. Park-Sarge, O.K., Mayo, K.E. (1994) Regulation of the progesterone receptor gene by gonadotropins and cyclic adenosine 3′,5′-monophosphate in rat granulosa cells. *Endocrinology* **134**:709–718.
31. Pei, L., Dodson, R., Schoderbek, W.E., Maurer, R.A., Mayo, K.E. (1991) Regulation of the alpha inhibin gene by cyclic adenosine 3′,5′-monophosphate after transfection into

rat granulosa cells. *Molecular Endocrinology* **5**:521–534.

32. Burkart, A.D., Mukherjee, A., Mayo, K.E. (2006) Mechanism of repression of the inhibin alpha-subunit gene by inducible 3′,5′-cyclic adenosine monophosphate early repressor. *Molecular Endocrinology* **20**: 584–597.
33. Campbell, K.L. (1979) Ovarian granulosa cells isolated with EGTA and hypertonic sucrose: cellular integrity and function. *Biology of Reproduction* **21**:773–786.
34. Ardekani, A.M., Romanelli, J.C., Mayo, K.E. (1998) Structure of the rat inhibin and activin betaA-subunit gene and regulation in an ovarian granulosa cell line. *Endocrinology* **139**:3271–3279.
35. Gehm, B.D., McAndrews, J.M., Chien, P.Y., Jameson, J.L. (1997) Resveratrol, a polyphenolic compound found in grapes and wine, is an agonist for the estrogen receptor. *Proceedings of the National Academy of Sciences of the United States of America* **94**:14138–14143.
36. Cicatiello, L., Cobellis, G., Addeo, R., et al. (1995) In vivo functional analysis of the mouse estrogen receptor gene promoter: a transgenic mouse model to study tissue-specific and developmental regulation of estrogen receptor gene transcription. *Molecular Endocrinology* **9**: 1077–1090.

Chapter 12

Use of Reporter Genes to Study Promoters of the Androgen Receptor

Lirim Shemshedini

Abstract

As a transcriptional regulator, the androgen receptor (AR) regulates the expression of many genes that are essential for male sexual differentiation, including the development of both normal prostate and prostate cancer. The AR acts by binding to regulatory DNA sequences found on the promoters of regulated genes. The study of AR activity on such responsive promoters is greatly facilitated by the use of the reporter gene assay, which provides a quantitative and reproducible method for studying the activity of such promoters. Among the several reporter genes that can be used, the genes encoding luciferase (Luc) and chloramphenicol acetyltransferase (CAT) have been used most widely and successfully by researchers interested in AR-regulated promoters. Such studies have led to the identification and characterization of DNA regulatory elements mediating AR activity on responsive promoters and to an improved understanding of how AR regulates the transcription process. Described in this chapter is a method by which to generate and utilize Luc and CAT reporter gene plasmids driven by the promoter of a novel androgen-regulated gene, ETV1.

Key words: Prostate cancer, androgen receptor, androgen, luciferase, β-galactosidase, chloramphenicol acetyltransferase.

1. Introduction

Transcriptional activation depends on the interaction of transcriptional activators with promoters of regulated genes. The androgen receptor (AR) is one such protein that, in response to binding androgens, regulates the expression of multiple genes necessary for and controlling proper male sexual differentiation (1). Among the multitude of AR target tissues, the best studied and perhaps the most medically interesting because of its diseased form is the prostate. This small bean-shaped gland is found only in males and

O.-K. Park-Sarge, T.E. Curry, Jr. (eds.), *Molecular Endocrinology,* Methods in Molecular Biology 590,
DOI 10.1007/978-1-60327-378-7_12,

its proper development is under the direct control of androgens and AR (2). Surprisingly, androgens and AR also mediate the transformation of normal prostate cells to prostate cancer cells (3), a process that results from changes in AR-regulated gene expression (4).

AR functions by binding to specific DNA sequences called androgen-responsive elements (AREs), which are found in the promoters of AR-regulated genes (5). To study AR activity on such promoters, reporter gene assays are employed. A reporter gene assay depends on the construction of a reporter plasmid, which harbors a reporter gene under the control of an AR-regulated promoter. The two most commonly used reporter genes in the AR research field are luciferase *(Luc)* and chloramphenicol acetyltransferase (*CAT*), which encode enzymes whose activity can be used as a direct measure of promoter activity (6). The source of the promoter can be another plasmid that contains an already cloned promoter or genomic DNA for a novel promoter, which can be used as a template for the polymerase chain reaction (PCR) with subsequent sub-cloning of the PCR product into an empty reporter gene plasmid. This chapter describes the latter method that was used to generate Luc and CAT reporter gene plasmids under the control of the ETV1 promoter, a novel AR-regulated promoter (7). The reporter gene plasmid is usually transfected into the prostate cancer cell lines LNCaP (8) and PC-3 (9). Because LNCaP and PC-3 cells represent two highly divergent states of prostate cancer (10), most researchers employing reporter gene assays to study AR utilize these two cell lines.

2. Materials

2.1. Constructing a Reporter Gene Plasmid Containing an AR-Inducible Promoter

1. pGL3-Basic containing the luciferase reporter gene (Promega, Madison, WI).
2. pCAT3-Basic containing the chloramphenicol acetyltransferase (*CAT*) reporter gene (Promega).
3. NheI and BglII restriction enzymes (Promega).
4. ETV1 synthetic PCR primers (Integrated DNA Technologies, Coralville, IA):
   Upstream: 5′-GATCGCTAGCGATCTAATTTTAGTTGAG-3′
   Downstream: 5′-GATCAGATCTGCTGGAGATTTCCTCAGG-3′
5. QIAquick gel extraction columns (Qiagen, Valencia, CA).
6. Agarose (Promega).

7. Trizol Reagent (Invitrogen, Carlsbad, CA).
8. 0.1 M sodium citrate ($Na_3C_6H_5O_7$) (Sigma-Aldrich, St. Louis, MO).

2.2. Transfecting Reporter Plasmids into Prostate Cancer Cells

1. RPMI-1640 (without phenol red) medium (Sigma-Aldrich).
2. F12K medium (Sigma-Aldrich).
3. OPTI-MEM medium (Invitrogen).
4. Penicillin-streptomycin solution (Sigma-Aldrich) stored as 20 ml aliquots at −20°C and added to 4 liters of medium. The final concentrations are 50 units/ml (penicillin) and 0.05 mg/ml (streptomycin).
5. Fetal bovine serum (FBS) or FBS extracted with dextran-coated charcoal (DCC) (Hyclone, Ogden, UT).
6. Corning Mammalian cell culture tubes (100 mm dishes and 12-well plates) (Fisher Scientific, Pittsburgh, PA).
7. R1881 (Sigma-Aldrich), an AR agonist, is dissolved in ethanol (EtOH) at a 1000x stock concentration of 1 μM and stored at −20°C. It is added as a 1/1000 volume to cell medium to dilute to the working concentration of 1 nM (*see* **Note 1**).
8. Casodex (Sigma-Aldrich), an AR antagonist, is dissolved in dimethyl sulfoxide (DMSO) at a 1000x stock concentration of 10 μM and stored at −20°C. It is added as a 1/1000 volume to cell medium to dilute to the working concentration of 10 nM.
9. Lipofectamine 2000 (Invitrogen) (*see* **Note 2**).
10. AR-inducible reporter plasmids and pCH110 ("public domain" that is widely available) as an internal control reporter plasmid (*see* **Note 3**).

2.3. Measuring Luciferase Reporter Gene Activity

1. Dulbecco's Phosphate-Buffered Saline (D-PBS) (Sigma-Aldrich): Prepared as 1x with filtered ddH_2O and stored at 4°C.
2. M-Per Mammalian Protein Extraction Reagent (Pierce Biotechnology, Rockford, IL).
3. Luciferase Buffer: 25 mM Gly-Gly (Sigma-Aldrich), 4 mM EGTA, 15 mM $MgSO_4$, 15 mM K_2HPO_4. Store at 4°C.
4. Luciferin: 1 mM D-Luciferin (Pierce Biotechnology), 10 mM DTT, 25 mM Gly-Gly. Store in 1-ml aliquots in gray (opaque) 1.5-ml microtubes at −80°C.
5. 1 M DTT (dithiothreitol). Store at −20°C.
6. 100 mM ATP (adenosine triphosphate). Store at −20°C.
7. 250 mM Gly-Gly (Sigma-Aldrich). Store at 4°C.

8. β-Gal Buffer: 60 mM Na_2HPO_4, 40 mM NaH_2PO_4, 10 mM KCl, 1 mM $MgSO_4$. Just before using, mix for each reaction 200 µl β-Gal Buffer with 40 µl ONPG (o-nitrophenyl-β-D-galactopyranoside) and 0.64 µl 2-mercaptoethanol. Because 0.64 µl is difficult to measure accurately, this reagent is made as a pool for multiple reactions. The ONPG stock solution is 4 mg/ml prepared in ddH_2O and stored in 1-ml aliquots at −20°C.
9. Lmax Luminometer (from Molecular Devices, Sunnyvale, CA).
10. Vmax Spectrophotometer (from Molecular Devices).

2.4. Measuring CAT Reporter Gene Activity

1. β-Gal Lysis Buffer: 250 mM Tris-HCl, pH 7.5, 5 mM DTT, 15% glycerol. Store at 4°C.
2. [^{14}C]chloramphenicol: [dichloroacetyl-1,2-^{14}C]chloramphenicol at 50 mCi/mmol and 50 mCi/ml (PerkinElmer Life and Analytical Sciences, Inc., Waltham, MA). Store at −20°C.
3. 5 mg/ml n-butyryl coenzyme A (CoA) (Sigma-Aldrich). Store at −20°C.
4. 250 mM Tris-HCl, pH 8.
5. Mixed xylenes: 3-[(Z)-(3-butyl-4-Oxo-2-thioxo-1,3-thiazolidin-5-ylidene) methyl]-2-[4-(2-hydroxyethyl)-1-piperazinyl]-4H-pyrido[1,2-A]pyrimidin-4-one Sigma-Aldrich).
5. Rubber policeman (cell scraper) for harvesting cells (Fisher).
6. Ready-Safe Scintillation Cocktail (Beckman Coulter Inc., Fullerton, CA).

3. Methods

The reporter gene assay has been very important in studying the role of AR in transcription. This assay enables researchers to identify AREs in AR-regulated promoters (5), to study the effects of mutations of such promoters on AR activity (11), and to detect any changes in AR activity that exist in different prostate cancer cell lines (12). The reporter gene assay consists of (a) transient transfection of cultured mammalian cells, (b) preparation of cytoplasmic extracts, (c) and measuring the activities of an AR-inducible reporter gene and a constitutively expressed internal control gene. The reporter gene most commonly used today is the firefly luciferase gene, which encodes an enzyme whose activity can be easily measured (6). Another reporter gene commonly used is the bacterial *CAT*, whose enzyme product can also be easily quantified (6). As for the internal control, the *lacZ*-encoded β-Galactosidase

(β-Gal) provides a consistent measure of transfection efficiency (13). The AR-inducible reporter plasmid harbors an AR-regulated promoter driving the expression of the reporter gene. The promoter can be a known DNA sequence or may come from a novel gene, requiring the cloning of this new promoter using genomic DNA and PCR, a method that is described below.

LNCaP and PC-3 cells represent the two most widely studied prostate cancer cell lines used for reporter gene assays studying AR-responsive promoters. LNCaP cells have endogenous AR and thus exhibit androgen-dependent gene expression and cell proliferation (8). In contrast, PC-3 cells have lost expression of endogenous AR and of many AR-regulated genes and thus do not respond to androgen signaling (9). As such, LNCaP and PC-3 cells represent two highly divergent states of prostate cancer, AR-positive and AR-negative (10).

3.1. Constructing a Reporter Gene Plasmid Containing an AR-Inducible Promoter

1. The source of the promoter DNA sequence can be either a restriction fragment from another plasmid that contains this sequence, or more likely, a PCR product using genomic DNA. The latter is particularly important for studying newly identified AR-regulated promoters. What follows is a method by which to generate a PCR product of the promoter of a newly identified AR-induced gene, ETV1 (7), in LNCaP cells.
2. Grow LNCaP cells in 60-mm dishes containing RPMI-1640 medium with 10% FBS until they reach confluency.
3. To harvest the cells, add 1 ml Trizol to the cells and scrape them off the dish with a rubber policeman. Place the homogenized cells in a 1.5 ml microtube. Incubate the homogenate for 10 min at room temperature to completely dissociate the nucleoprotein complexes.
4. Add 0.2 ml chloroform, vortex for 15 s, and incubate at room temperature for 3 min. Spin in a microcentrifuge at 14,000*g* for 15 min at 4°C, after which the mixture will separate into an upper aqueous phase and a lower organic phase with an interphase between them. The genomic DNA is found in the interphase and lower organic phase.
5. Remove carefully the aqueous phase without disturbing the interphase (*see* **Note 4**). Precipitate the DNA found in the interphase and organic phase by adding 0.3 ml 100% EtOH and mixing by inversion. Incubate for 3 min at room temperature and pellet the precipitated DNA by centrifuging at 2,000 *g* for 5 min at 4°C.
6. Discard the supernatant and wash the DNA pellet by adding 1 ml 0.1 M sodium citrate ($Na_3C_6H_5O_7$) in 10% EtOH, incubating for 30 min at room temperature, and then centrifuging at 2,000*g* for 5 min at 4°C. Repeat this step.

7. After the second wash, resuspend the DNA pellet in 1.5 ml 75% EtOH and incubate for 20 min at room temperature. Centrifuge at 2,000*g* for 5 min at 4°C and discard the supernatant.
8. Air dry the DNA pellet for 15 min at room temperature (*see* **Note 5**). Dissolve the DNA in about 100 µl 8 mM NaOH and store overnight at 4°C. Quantify the DNA by measuring the A_{260} (*see* **Note 6**). For long-term storage, adjust the pH from about 9 to 8 by adding 10 µl 0.1 M HEPES per 100 µl of DNA sample. Store the DNA at −20°C.
9. Use 100 ng of the genomic DNA as a template for a PCR reaction with two synthetic oligonucleotides that amplify the ETV1 promoter region that extends from about +40 to −1000 and includes the putative ARE (*see* **Notes 7, 8**). The PCR conditions are as follows: 1 cycle, 95° C, 4 min; 35 cycles, Denature (95°C, 2 min), Anneal (52°C, 3 min), Extend (72°C, 1 min); 1 cycle, 72°C, 7 min.
10. Run the PCR product on a 1% electrophoretic agarose gel, extract the PCR fragment followed by purification using a QIAquick gel extraction column.
11. Clone the PCR product into either the pGL3-Basic or pCAT3-Basic vector using the restriction enzymes NheI (upstream) and BglII (downstream) and standard ligation and transformation protocols (*see* **Note 9**). Maps of these two plasmids are shown in **Fig. 12.1**.

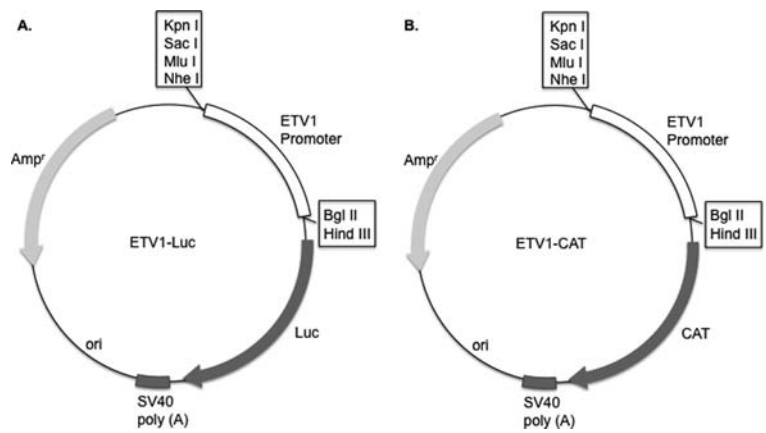

Fig. 12.1. Maps of two reporter gene plasmids containing the ETV1 promoter. The ETV1 promoter from +40 to −1000 was PCR amplified using genomic DNA from LNCaP cells and was sub-cloned into the NheI and BglII sites of either (**A**) pGL3-Basic or (**B**) pCAT3-Basic to make ETV1-Luc or ETV1-CAT, respectively. The promoter nucleotide sequence information of ETV1 was obtained from the human genome database (NIH) and analyzed by using an online program (bimas.dcrt.gov/molbio/matrixs/), which revealed the presence of a consensus TATA box sequence and a near consensus androgen-responsive element (ARE) (75%) within the first 1 kb. upstream of the identified exon 1.

12. Measure AR activity on this newly cloned promoter using transient transfection experiments in LNCaP or PC-3 cells as described above in Sections 3.2–3.4. Be certain to use in this experiment both a positive control, e.g. PSA-Luc or MMTV-CAT reporter plasmid, and a negative control, e.g. empty pGL3-Basic or pCAT3-Basic vector (*see* **Note 10**).

3.2. Transfecting Reporter Plasmids into Prostate Cancer Cells

1. Two widely used prostate cancer cell lines are LNCaP and PC-3 (*see* **Note 11**). LNCaP cells are grown in RPMI-1640 medium (without phenol red) (*see* **Note 12**) supplemented with 10% FBS. PC-3 cells are grown in F12K medium supplemented with 10% FBS. Both the RPMI-1640 and F12K media contain the antibiotics penicillin (50 units/ml) and streptomycin (0.05 mg/ml). The two cell lines are grown in Corning 100-mm tissue culture dishes and at confluency are split 1:2 into new 100-mm dishes for maintenance. After another 3–4 days (for LNCaP cells) or 2–3 days (for PC-3 cells), the cells will reach confluency and can be split into new 100-mm dishes or multiwell plates for transfection.
2. For transfection experiments, cells from each confluent 100-mm dish are split into two Corning 12-well plates (*see* **Note 13**) and grown in 500 µl per well of the same media as above (step 1) for 2–3 days (for LNCaP cells) or overnight (PC-3 cells), after which the cells should have reached about 70% confluency. The old medium is replaced with serum- and phenol red-free RPMI-1640 (LNCaP cells) or F12K medium (PC-3 cells), neither of which has antibiotics (*see* **Note 14**). One hour later, the cells are transfected with the appropriate plasmids.
3. Lipofectamine 2000 is a highly efficient transfection reagent for both LNCaP and PC-3 cells. Other transfection reagents can also be used (*see* **Note 2**). For a transfection with Lipofectamine 2000, 1 µg of total plasmid DNA (*see* **Note 15**) is mixed with 75 µl of OPTI-MEM medium in one microtube and another 75 µl aliquot of OPTI-MEM is mixed with 3 µl of Lipofectamine 2000 in a second microtube, giving a ratio of 1 µg DNA to 3 µl Lipofectamine 2000 (*see* **Note 16**). Mix by tapping the tubes and incubate the two tubes for 5 min at room temperature.
4. Pool the two OPTI-MEM aliquots and mix them together with a micropipettor and incubate for 20 min at room temperature.
5. Add dropwise the mixture of plasmid DNA and Lipofectamine 2000 to the cells on 12-well plates and move the plates slowly in a figure "8" shape to distribute the DNA evenly.
6. Place the cells in an incubator for 5–8 h, and then gently add 500 µl of new medium (RPMI-1640 or F12K) supplemented with 20% DCC-extracted FBS. Since this new medium is

going into wells already containing approximately 500 µl of serum-free medium, the new FBS concentration found in each will be about 10%.

7. After an overnight incubation, aspirate away the old medium and gently add new medium (RPMI-1640 or F12K) supplemented with 10% DCC-extracted FBS and then add 1 nM R1881, an androgen agonist. This is added as 1 µl of a 1 µM R1881 stock concentration in EtOH, and 1 µl EtOH is added as a vehicle control. Also, to demonstrate that androgen activation of the promoter is dependent on AR, have some wells receiving both androgen and the anti-androgen Casodex (also known as Bicalutamide). The Casodex is added as 1 µl of a 10 µM stock concentration in DMSO. 1 µl DMSO is used as a vehicle control.
8. After an overnight incubation, cells are harvested for measuring reporter gene activity.

3.3. Measuring Luciferase Reporter Gene Activity

1. Before extraction, the cells in the 12-well plate are washed using cold PBS. This is done by aspirating away the medium and gently adding 1 ml PBS, moving in a figure "8," and aspirating. Repeat this step twice.
2. Add 100 µl of M-Per Protein Extraction Reagent to each well and place on a shaker at room temperature for 10 min.
3. Transfer the cell extract to a microtube and spin in microcentrifuge for 5 min at 14,000*g* at room temperature.
4. Remove 90 µl of supernatant and place in a new microtube. Be careful not to remove any of the pellet found at the bottom of the tube. Half the extract should be used for the luciferase assay and the other half for the β-Gal assay (*see* **Note 17**).
5. To carry out the luciferase assay, transfer 45 µl of cell extract into each well of a 96-well nontransparent plate and place the plate into an Lmax Luminometer (from Molecular Devices, Sunnyvale, CA) or the equivalent instrument. Prepare in two 12 × 75 mm polypropylene tubes the following solutions:

ATP Solution	Luciferase Buffer	5 ml
	1 M DTT	5 µl
	100 mM ATP	100 µl
Luciferin Solution	Luciferin (thaw on ice)	1 ml
	250 mM Gly-Gly	0.5 ml
	1 M DTT	5 µl
	ddH_2O	3.5 ml

The 5-ml volume of each solution is enough for 100 luciferase reactions. Place the tubes in the two slots on the luminometer and perform the following injection protocol: inject 50 µl ATP Solution, wait 1.6 s, inject 50 µl Luciferin Solution, wait 1.6 s, and then read light emission.

6. To carry out the β-Gal assay, transfer 40 µl of cell extract into each well of a 96-well transparent plate and mix with 240 µl β-Gal Buffer containing freshly added ONPG and 2-mercaptoethanol. Allow the reaction to take place at 37°C for 6 h (LNCaP cells) or 30 min (PC-3 cells) (*see* **Note 18**). Read absorbance at 420 nm using a Vmax spectrophotometer (from Molecular Devices) or equivalent instrument.
7. To normalize luciferase activity for transfection efficiency, divide the readings from the luciferase assay by the readings from the β-Gal assay. This will control for any differences in transfection efficiency (*see* **Note 19**). An example result is shown in **Fig. 12.2**.

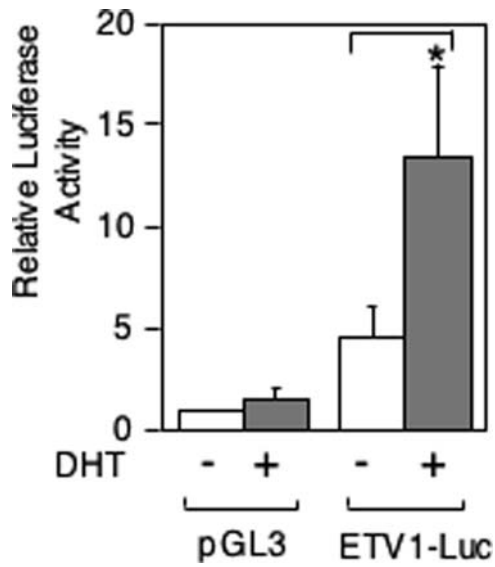

Fig. 12.2. Androgen-inducible transactivation of the ETV1 promoter fused to the *luciferase* reporter gene in LNCaP cells. LNCaP cells were transfected with ETV1-Luc or the empty pGL3 plasmid, using Lipofectamine 2000, and then treated with or without 100 nM DHT, as indicated. All Luciferase activities shown are relative to β-Gal activity, which was used to standardize for differences in transfection efficiency. Note that the Luciferase activity is represented relative to the activity of pGL3, and this activity was set to 1. *Asterisks* indicate statistical significance ($p < 0.05$), as indicated. (Reproduced from **ref. 7** with permission from the Endocrine Society.)

3.4. Measuring CAT Reporter Gene Activity

1. Harvest the transfected cells with a rubber policeman (scraper) and place the cells in a 1.5-ml microcentrifuge tube. Pellet the cells by centrifuging for 3 min at 2,000*g*, followed by washing 2x with 1 ml PBS each time and centrifugation. Be careful not to dislodge the cells during the washing.

2. Resuspend the cells in 100 µl β-Gal Lysis Buffer and lyse the cells using 4 cycles of freezing (in liquid nitrogen) and thawing (in a 37°C water bath).
3. Spin at 14,000*g* for 15 min at 4° C and transfer 90 µl of supernatant to a fresh tube sitting in ice. Be careful not to remove any of the pellet. Use 50 µl for the CAT assay and 40 µl for β-Gal assay. Perform the β-Gal assay as described above in step 6 of Section 3.2.
4. To carry out the CAT assay, prepare the following mixture in a 1.5-ml microcentrifuge tube for each reaction:

Cell Extract	45 µl
[^{14}C]Chloramphenicol (at 0.05 mCi/ml)	3 µl
5 mg/ml n-Butyryl CoA	5 µl
250 mM Tris-HCl	72 µl

Also prepare a negative control reaction in which 50 µl β-Gal Lysis Buffer, not Cell Extract, is added to the tube.

5. Incubate the reactions for 1–2 h at 37°C.
6. Add 300 µl ice-cold Mixed Xylenes to stop the reaction and extract the product. The n-butyryl chloramphenicol partitions mainly in the Xylene phase.
7. Vortex for 30 s and spin at 14,000*g* for 5 min.
8. Remove 250 µl of upper (Xylene) layer and put it a fresh tube. Add 100 µl 250 mM Tris-HCl, pH 8, to this tube and repeat step 7.
9. Remove 200 µl of upper layer and transfer to a scintillation vial. Add 5 ml Ready-Safe scintillation cocktail (or equivalent) and count cpm in a scintillation counter.
10. Calculate CAT activity as cpm/β-Gal unit.

4. Notes

1. Dihydroxytestosterone (DHT) can also be used. Because DHT is less chemically stable than R1881, it is best to use 10–100 nM of DHT in the assay. Like R1881, a 1000x stock of DHT can be prepared in EtOH and stored at −20°C.
2. Fugene 6 (Roche Diagnostics Corp., Indianapolis, IN) is more efficient for transfection of PC-3 cells than LNCaP cells and X-treme Reagent (Roche Diagnostics Corp.) is

best for siRNA transfection of prostate cancer cells with subsequent monitoring of cell growth or apoptosis. For both reagents, the transfection conditions are the same as for Lipofectamine 2000, with the ratio of DNA to transfection reagent being different. Follow the specific manufacturer's recommended ratios for these two reagents.

3. The plasmid pcDNA3.1/myc-His/LacZ, which is commercially available from Invitrogen, can be used in place of pCH110.
4. Since the aqueous phase contains RNA, it is critical that this aqueous phase is carefully removed to produce quality of genomic DNA that can successfully be used as a template for PCR.
5. Drying the DNA in a speed vac will make it more difficult to solubilize the DNA.
6. The 100 μl should yield a DNA concentration of about 0.2 mg/ml. Quantify the amount of DNA by A_{260} spectrophotometry and adjust the volume accordingly to reach that concentration.
7. For amplifying promoter fragments 1000 bp long or less, Taq polymerase (Invitrogen) can be used. If the fragment is longer than 1000 bp, use Vent Polymerase (New England Biolabs, Ipswich, MA), which has proofreading ability. Use online promoter analysis programs, such http://linux1.softberry.com/berry.phtml to analyze genomic DNA sequence for the presence of putative AREs.
8. It is important that the promoter region cloned into the vector extends at least 30 bp downstream of the transcriptional start site for that promoter, which will ensure correct transcriptional initiation from this reporter plasmid. The promoter fragment must also contain at least one ARE (androgen-regulated element), through which the AR will activate the promoter.
9. Because the pGL3-Basic and pCAT3-Basic contain multiple cloning restriction enzyme sites, other restriction enzymes can be used.
10. As positive controls, there are many reporter plasmids with well-characterized AR-regulated promoters. In addition to the PSA promoter, there are hKLK2-Luc, MMTV-Luc, and several others. However, these reporter plasmids are not commercially available and thus can be obtained from several research labs studying AR activity.
11. While LNCaP and PC-3 cells are recommended, other cell lines can be used. This would include other prostate cancer cell lines, such as DU145, VCaP, CWR22-Rv1, Mda-P109

cells, and non-prostate cancer cell lines, including HeLa and Cos cells. It is important to mention that some of these cells (DU145, HeLa, and Cos) do not express endogenous AR and thus must be transfected with an AR expression plasmid in order to study AR-induced promoters.

12. Because phenol red has androgenic activity in LNCaP cells, medium without phenol red is used with these cells.
13. Transfections can also be done in 60 mm dishes or 6- or 24-well plates, depending on transfection efficiency and magnitude of promoter activity. The amounts of transfection reagent and plasmid DNA have to be adjusted according to the number of cells.
14. Antibiotics can interfere with transfection efficiency.
15. The total amount of plasmid DNA for each well of a 12-well plate is 1 μg. The 1 μg consists of 0.25 μg of AR-inducible reporter plasmid, 0.25 μg of internal control reporter plasmid (pCH110), and the remainder can be promoter-less control plasmid (for LNCaP cells) or AR expression plasmid (for PC-3 cells, which do not express endogenous AR protein). The pCH110 contains the Lac Z gene under the control of the constitutive SV40 promoter and thus encodes β-Gal, which can be monitored by β-Gal assay.
16. A ratio of 1 μg DNA to 3 μl of Lipofectamine 2000 reagent is optimal for LNCaP cells. For PC-3 cells, the ratio can be from 1:2 to 1:3, depending on the sensitivity of your particular batch of PC-3 cells.
17. The measure of β-Gal activity will allow you to monitor transfection efficiency and thus standardize the transfection experiment. While protein concentration can be used for this standardization, β-Gal activity is a preferred method of standardization since it can reveal transfection efficiency differences between cells receiving different plasmids.
18. The OD_{420} readings must be at least 0.1 to be useful. If the reading falls below 0.1, the assay must be repeated either using more cell extract or incubating for a longer period of time. In the worst case, the transfection experiment will have to repeated if the β-Gal activity is too low (OD_{420} is below 0.1). On the other hand, if the OD_{420} is greater than 1.0, repeat the β-Gal assay either using less cell extract or incubating for a shorter period of time.
19. It is also possible to use luciferase activity as a control for transfection efficiency, as is found in the Dual Luciferase Reporter Assay system offered by Promega. In this case, cells are co-transfected with an AR-inducible luciferase reporter plasmid and pRL-TK-Luc (Promega), instead of pCH110

(*see* **Note 15**). The inducible reporter expresses the firefly luciferase and the pRL plasmid the *Renilla* Luciferase, which are measured sequentially using the Promega system. However, we have found the β-gal activity more consistent than the *Renilla* Luciferase activity for measuring transfection efficiency of LNCaP and PC-3 cells.

Acknowledgments

The author would like to thank Chen-Lin Hsieh for critical reading of the manuscript. This work was supported by R15 DK067059.

References

1. Wilson, J.D., Griffin, J.E., George, F.W., and Leshin, M. (1981) The role of gonadal steroids in sexual differentiation. *Rec. Prog. Horm. Res.* **37,**1–39.
2. Lee, C. (1996) Role of androgen in prostate growth and regression: stromal-epithelial interaction. *Prostate Suppl.* **6,** 52–56.
3. Taplin, M.E. (2007) Drug insight: role of the androgen receptor in the development and progression of prostate cancer. *Nat. Clin. Pract. Oncol.* **4,** 236–244.
4. Gregory, C.W., Hamil, K.G., Kim, D., Hall. S.H., Pretlow, T.G., Mohler, J.L., et al. (1998) Androgen receptor expression in androgen-independent prostate cancer is associated with increased expression of androgen-regulated genes. *Cancer Res.* **58,** 5718–5724.
5. Kato, S., Matsumoto, T., Kawano, H., Sato, T, and Takeyama, K. (2004) Function of androgen receptor in gene regulations. *J. Steroid Biochem. Mol. Biol.* **89–90,** 627–633.
6. Arnone, M.I., Dmochowski, I.J., and Gache, C. (2004) Using reporter genes to study cis-regulatory elements. *Methods Cell Biol.* **74,** 621–652.
7. Cai, C., Hsieh, C.L., Omwancha, J., Zheng, Z., Chen, S.Y., Baert, J.L., et al. (2007) ETV1 is a novel androgen receptor-regulated gene that mediates prostate cancer cell invasion. *Mol. Endocrinol.* **21,** 1835–1846.
8. Horoszewicz, J.S., Leong, S.S., Kawinski, E., Karr, J.P., Rosenthal, H., Chu, et al. (1983) LNCaP model of human prostatic carcinoma. *Cancer Res.* **43,** 1809–1818.
9. Heisler, L.E., Evangelou, A., Lew, A.M., Trachtenberg, J., Elsholtz, H.P., and Brown, T.J. (1997) Androgen-dependent cell cycle arrest and apoptotic death in PC-3 prostatic cell cultures expressing a full-length human androgen receptor. *Mol. Cell. Endocrinol.* **126,** 59–73.
10. Jenster, G. (1999) The role of the androgen receptor in the development and progression of prostate cancer. *Semin Oncol.* **26**407–421.
11. Jain, A., Lam, A., Vivanco, I., Carey, M.F., and Reiter, R.E. (2002) Identification of an androgen-dependent enhancer within the prostate stem cell antigen gene. *Mol. Endocrinol.* **16,** 2323–2337.
12. Marques, R.B., van Weerden, W.M., Erkens-Schulze, S, de Ridder, C.M., Bangma, C.H., Trapman, J., et al. (2006) The human PC346 xenograft and cell line panel: a model system for prostate cancer progression. *Eur. Urol.* **49,** 245–257.
13. Shemshedini, L., Knauthe, R., Sassone-Corsi, P., Pornon, A., and Gronemeyer, H. (1991) Cell-specific inhibitory and stimulatory effects of Fos and Jun on transcription activation by nuclear receptors. *EMBO J.* **10**, 3839–3849.

Chapter 13

Isolation of Proteins Associated with the DNA-Bound Estrogen Receptor α

Jennifer R. Schultz-Norton, Yvonne S. Ziegler, Varsha S. Likhite, and Ann M. Nardulli

Abstract

Regulating gene expression is a complex process requiring the interaction of multiple transcription factors with their cognate recognition sequences. While these DNA-bound transcription factors are the primary drivers of gene expression, the capacity of a transcription factor to alter gene expression is tempered by its association with a host of coregulatory proteins that are recruited to the DNA-bound transcription factor. We have developed a novel approach to isolate large complexes of proteins associated with the DNA-bound estrogen receptor α (ERα) using an agarose-based electrophoretic mobility shift assay (EMSA). This method should be readily adapted to a variety of cultured cell lines, DNA sequences, and transcription factors and has the potential to provide valuable information about a wide variety of regulatory proteins involved in influencing gene expression.

Key words: Transcription factor, estrogen receptor, complex isolation, agarose-based electrophoretic mobility shift assay, protein–DNA complex.

1. Introduction

Estrogen receptor α (ERα also referred to as ESR1) is a member of a large superfamily of nuclear receptors that function as ligand-inducible transcription factors (1). Upon binding hormone, ERα undergoes a conformational change, binds to estrogen response elements (EREs) residing in estrogen-responsive genes, and initiates changes in gene expression. We and others have demonstrated that, in addition to conformational change induced by hormone binding, individual ERE sequences function as allosteric modulators of ERα conformation (2–7). Thus, both hormone and DNA influence ERα structure.

The ERE-bound ERα recruits a multitude of coregulatory proteins to estrogen-responsive genes and requires the participation of these proteins to effectively modulate transcription (reviewed in

O.-K. Park-Sarge, T.E. Curry, Jr. (eds.), *Molecular Endocrinology,* Methods in Molecular Biology 590,
DOI 10.1007/978-1-60327-378-7_13,

8, 9). The identification of coregulatory proteins has been extremely useful in helping to define mechanisms involved in regulating transcription. Initially, the majority of coregulatory proteins identified were isolated through their interaction with a discrete functional domain of the receptor, most commonly the ligand binding domain.

To better understand how ERα regulates transcription of estrogen-responsive genes, we have developed a method of isolating novel proteins associated with the estrogen- and DNA-bound ERα. This agarose-based electrophoretic mobility shift assay (EMSA) utilizes full-length purified ERα and endogenously expressed nuclear proteins and takes into consideration ligand- and DNA-induced changes in receptor conformation, which we feel more faithfully represents the transcriptionally active DNA-bound receptor than the free receptor or individual receptor domains. Using this method, we have isolated and identified more than 100 proteins associated with the ERE-bound ERα and shown that more than a dozen of these proteins interact with ERα and influence estrogen-responsive gene expression (*see* **Table13.1**, **refs**. 10–18 and unpublished work). Thus, our agarose-

Table 13.1
ERα-interacting proteins isolated from agarose gel complexes. Proteins associated with the DNA-bound ERα were identified by mass spectrometry analysis. The effects of some of these ERα-associated proteins on the ERα-ERE interaction and ERα-mediated transcription are indicated. ↑/↓ represents gene-specific effects

Protein	ERα-ERE interaction	ERα-mediatedTranscription	References
APE1	↑	↑/↓	*(22)*
FEN1	↑	↑/↓	*(15)*
MPG	↑	↓	*(11)*
NM23-H1	↑	↓	*(17)*
PCNA	↑	↑ basal	*(13)*
PDI	↑	↑/↓	*(14)*
pp32	↑	↓	*(12)*
RbAp46	not done	↑/↓	*(21)*
RbAp48	not done	↓	*(21)*
Rho-GDI	↑	↑/↓	*(16)*
SOD1	↑	↑	*(18)*
TAF-1β	↑	↓	*(10)*
Trx	–	↑/↓	*(23)*
TrxR	↑	↑/↓	*(23)*

based EMSA has been very effective in isolating novel regulatory proteins that associate with the ERE-bound ERα and influence receptor activity. This method could be applicable in isolating proteins that influence the activity of other DNA-bound transcription factors.

2. Materials

2.1. HeLa Cell Culture, Lysis, and Nuclear Extract Purification

1. Dulbecco's Modified Eagle Medium:Nutrient Mix F-12, pH 7.4 containing 15 mM HEPES and L-glutamine (Invitrogen, Carlsbad, CA) (*see* **Note 1**).
2. 10% fetal bovine serum (FBS, Atlanta Biologicals, Norcross, GA).
3. 100 U/ml penicillin, 100 μg/ml streptomycin, 25 μg/ml gentamycin
4. Hank's Balanced Salt Solution (HBSS): 10 mM HEPES pH 7.6, 0.075% sodium bicarbonate.
5. HBSS-EDTA (HE): 10 mM HEPES pH 7.6, 0.075% sodium bicarbonate, 1.2 mM EDTA pH 7.4.
6. TEG: 50 mM Tris pH 7.4, 0.1 mM EDTA, 10% glycerol.
7. TEG-500: 50 mM Tris pH 7.4, 0.1 mM EDTA, 10% glycerol, 0.5 M KCl.
8. Protease Inhibitor Cocktail (PIC, P8340, Sigma, St. Louis, MO) containing 4-(2-aminoethyl)-benzenesulfonyl fluoride (AEBSF), pepstatin A, E-64, bestatin, leupeptin, and aprotinin. Dilute the 100x stock 1:100 into the sample as needed.
9. Trypan blue.
10. Tissue grinder with B pestle (Kontes, Vineland, NJ).

2.2. Protein Assay

1. BioRad Protein Assay Kit II, containing 5x Protein Assay Solution and Bovine Serum Albumin (BioRad, Hercules, CA). 5x Protein Assay Solution is diluted 1:5 in deionized H_2O (dH_2O) and filtered through a Whatman filter (#1001-150, Fisher Scientific).
2. Disposable glass culture tubes (Fisher Scientific).

2.3. Preparation of ^{32}P-Labeled Oligos

1. Oligos containing the *Xenopus laevis* vitellogenin A2 estrogen response element: 5′-CTA GAT TAC AGG TCA CAG TGA CCT TAC TCA-3′ and 5′-GAT CTG AGT AAG GTC ACT GTG ACC TGT AAT CTA G-3′ (IDT, Coralville, IA).
2. Oligos containing a nonspecific DNA sequence: 5′-CTA GAT TAC TTC TCA TGT TAG ACA TAC TCA-3′ and 5′-GAT CTG AGT ATG TCT AAC ATG AGA AGT AAT CTA G-3′.

3. 10x Annealing Buffer: 10 mM Tris pH 7.8, 10 mM $MgCl_2$, 50 mM KCl, 1 mM EDTA, 1 mM EGTA.
4. $^{32}\gamma$P-ATP with a specific activity of 7000 Ci/mmol (MP Biomedicals, Solon, OH).
5. T4 Kinase (10U/μl, Invitrogen).

2.4. DNA Binding Reactions

1. 10x Reaction Buffer: 150 mM Tris pH 7.9, 2 mM EDTA, 800 mM KCl, 500 μM $ZnCl_2$, 50 mM MgOAc, 40 mM DTT, 0.5 μM 17β-estradiol. Make fresh from stock solutions. 1 M DTT stock solution, which is stored at −20°C, should not be refrozen. 17β-estradiol should be prepared in ethanol.
2. Salmon sperm DNA: 10 mg/ml stock diluted to 1 mg/ml in dH_2O (Invitrogen).
3. BSA: 50 mg/ml stock diluted to 1 mg/ml in dH_2O (Invitrogen) or ovalbumin, 20 mg/ml stock diluted to 1 mg/ml in dH_2O (Roche Diagnostics Corp., Indianapolis, IN).
4. Poly-deoxyinosine/deoxycytidine: resuspended to 1 mg/ml in dH_2O (Amersham Biosciences, Piscataway, NJ).
5. 50% glycerol.
6. HeLa nuclear extracts prepared as described in **Section 3.1**.
7. Purified ERα can be prepared as described (2, 19) or purchased from a commercial supplier.
8. ERα-specific antibody (sc-8002, Santa Cruz Biotechnology, Santa Cruz, CA).
9. Nonspecific antibody (YY1-specific, sc-7341, Santa Cruz Biotechnology).

2.5. Agarose Gel Electrophoresis for Initial Protein/DNA Complex Characterization

1. 10x Running Buffer: 5.4 g Tris base, 27.4 g boric acid, 11.2 g $MgOAc \cdot 4H_2O$, 20 ml 0.5 M EDTA. Bring to 1L with dH_2O.
2. Molecular biology grade agarose (BioRad) (*see* **Note 2**).
3. DE81 ion exchange cellulose acetate (Whatman, Florham Park, NJ).
4. Biomax XAR autoradiography film (Carestream Health, Inc, Rochester, NY).

2.6. Agarose Gel Electrophoresis for Complex Isolation and Protein Extraction

1. 10x Running Buffer as described in **Section 2.5.1**.
2. Molecular biology grade agarose (BioRad).
3. Biomax XAR autoradiography film (Carestream Health, Inc).
4. Montage gel extraction kit (Millipore, Billerica, MA).
5. Microcon YM-10 size exclusion columns (Millipore).

3. Methods

Small agarose gels should be used initially to determine the conditions required for protein–DNA complex formation. ^{32}P-labeled ERE-containing oligos, HeLa nuclear extracts, which contain full-length endogenously expressed coregulatory proteins, and purified ERα are used for these small-scale experiments. To ensure that a protein-DNA complex formed is specific, a number of steps should be taken. First, ^{32}P-labeled oligos containing a nonspecific DNA sequence should be run in parallel with the ^{32}P-labeled ERE-containing oligos. A specific protein–DNA complex will be formed with the ERE-containing oligos, but not with oligos containing a nonspecific DNA sequence (data not shown). Second, the receptor and HeLa nuclear extract can be added alone and in combination to demonstrate that protein–DNA complex formation requires the addition of both the receptor and the nuclear proteins (**Fig. 13.1**, Lane 4) and that neither the receptor (Lane 2) nor the nuclear proteins (Lane 3) alone are sufficient for complex formation. Third, competition assays should be carried out with an excess (50–100x) of unlabeled ERE-containing oligos and unlabeled oligos lacking an ERE to demonstrate that ERE-containing oligos decrease protein–DNA complex formation (Lanes 5-6), but that the same molar excess of oligos containing a nonspecific DNA sequence does not affect complex formation (Lanes 7–8). Fourth, an ERα-specific antibody can be added to the binding reaction to demonstrate that the protein–DNA complex is supershifted and that ERα is present in the complex (**Fig. 13.2**, Lane 5). In contrast, a nonspecific antibody is unable to alter the migration of the protein–DNA complex (**Fig. 13.2**, Lane 6).

Once the gel conditions required for formation of a specific protein–DNA complex have been identified, the reactions can be scaled up and run on larger gels to isolate sufficient amounts of protein for further analysis. Mass spectrometry analysis can be used to identify novel proteins associated with the DNA-bound ERα and Western blots can be performed to confirm that a protein is present in the protein–DNA complex when the ERE-containing oligos are utilized, but not present when oligos containing a nonspecific DNA sequence are utilized. This method has been extremely useful in identifying proteins associated with the DNA-bound ERα using HeLa nuclear extracts and purified ERα as well as MCF-7 nuclear extracts, which contain endogenously expressed ERα (13–18, 21–23) and should be amenable for use with other cell types and systems.

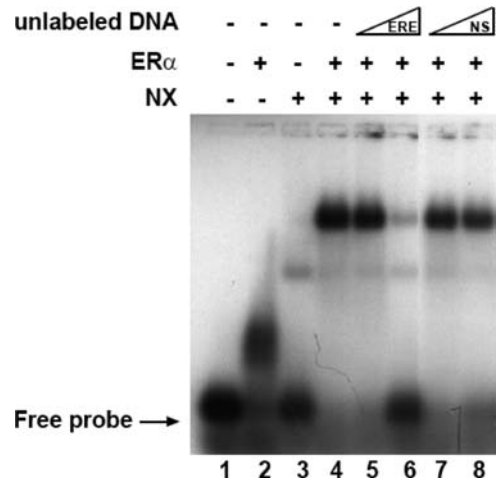

Fig. 13.1. Small-scale agarose-based gel mobility shift assay with unlabeled competitor DNA. ^{32}P-labeled, ERE-containing oligos were incubated without (lanes 1–2) or with HeLa nuclear extracts (NX, lanes 3–8). Purified ERα (lanes 2, 4–8) was included as indicated. Increasing amounts of unlabeled oligos containing ERE (lanes 5–6) or nonspecific DNA sequence (lanes 7–8) were included in the binding reaction as indicated. Complexes were resolved on an agarose gel and visualized by autoradiography.

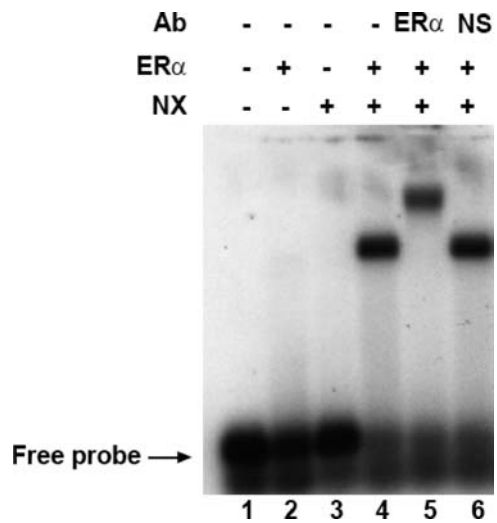

Fig. 13.2. Small-scale agarose-based gel mobility shift assay with antibody supershift. ^{32}P-labeled, ERE-containing oligos were incubated without (lanes 1–2) or with HeLa nuclear extracts (lanes 3–6). Purified ERα (lanes 2, 4–6) was included as indicated. ERα-specific (lane 5) or nonspecific (lane 6) antibody was included as indicated. Complexes were resolved on an agarose gel and visualized by autoradiography.

3.1. HeLa Cell Culture, Lysis, and Nuclear Extract Purification

1. HeLa cells are grown in T175 flasks at 37°C until 80–90% confluent. Approximately 20 flasks are used for a typical preparation. The media should be changed the day before harvest (*see* **Note 3**).
2. Wash each flask with 10 ml HBSS.

3. Harvest the cells by adding 2 ml HE to each flask and incubate at 37°C for 2 min. Tap the flasks to release the cells. Add 25 ml HBSS to the first flask. Collect the cells and transfer to the next flask. Repeat this procedure for 8–10 flasks and transfer the cells to a 250 ml centrifuge bottle on ice. Add 10 ml HBSS to a flask to remove any cells still adhering to the flask and transfer the remaining cells sequentially to 4 flasks. Repeat this process until all of the flasks have been rinsed. Transfer the remaining cells to the centrifuge bottle.
4. Centrifuge the cells for 5 min at 4°C at 150*g*.
5. Aspirate the media. From this point forward, keep the cells on ice and work quickly to limit protein degradation.
6. Resuspend the cell pellet in 200 µl of TEG with 1x PIC at 4°C for each T175 flask harvested. Loosen the cell pellet by tapping the centrifuge bottle. Transfer the resuspended cells to a chilled tissue grinder and homogenize on ice with 25 shallow strokes of a B pestle. Check at this point to ensure that the cells have been lysed and that the nuclei are intact. Combine 10 µl cell lysate with 1 µl Trypan blue and examine under a microscope. The nuclei, but not the intact cells, will appear blue. If all cells are not lysed, homogenize the cells with an additional 10 shallow strokes of a B pestle.
7. Transfer the homogenate to a chilled 11 ml polyallomer high speed centrifuge tube on ice. Rinse the homogenizer with 200 µl of TEG containing 1x PIC and add to the polyallomer tube.
8. Pellet the homogenate for 10 s at 4°C at 10,200*g*
9. Quickly place the pelleted nuclei on ice and remove the supernatant.
10. Resuspend the nuclei in 75 µl of TEG-500 with 1x PIC at 4°C for each T175 flask harvested by pipetting the nuclei through a 1-ml pipette tip 5–7 times. For example, 1.5 ml of TEG-500 will be needed for 20 flasks of cells. Incubate on ice for 20 min and vortex every 5 min.
11. Centrifuge the nuclear extract for 30 min at 4°C at 142,000*g*.
12. Transfer the supernatant to a clean microcentrifuge tube and aliquot. Freeze aliquots quickly on dry ice and store at −80°C.

3.2. Protein Assay

1. Dissolve 12.5 µg BSA per ml dH_2O (12.5 µg/ml) and store at 4°C. Prepare standards to generate a standard curve by diluting the BSA to 10 µg/ml, 7.5 µg/ml, 5 µg/ml, and 2.5 µg/ml in dH_2O.
2. Aliquot 1 ml of 1x Protein Assay Solution into each of 12 disposable glass culture tubes. Reserve 2 tubes for blanks. Add

10 µl of each diluted BSA standard in duplicate to the remaining 10 tubes. The final concentrations of BSA in the tubes will be 0, 25, 50, 75, 100, and 125 ng/ml. Vortex.

3. Incubate at room temperature for 5 min.
4. Determine the absorbance of each standard at 595 nm using a spectrophotometer. Plot the standards on a curve with the concentration on the *x*-axis and absorbance on the *y*-axis.
5. Determine the concentration of the nuclear extract prepared in Section 3.1 by diluting 1–2 µl of the extract in 10 µl dH_2O and add to 1 ml of 1x Protein Assay Solution in a disposable test tube. Prepare duplicates for each sample. Vortex. The same 1x Protein Assay Solution should be used for samples and standards, but samples should be prepared after the standard curve is determined to ensure that the amount of sample used falls on the standard curve.
6. Incubate at room temperature for 5 min.
7. Measure the absorbance at 595 nm and use the standard curve to determine the concentration of protein in the sample.

3.3. Preparation of ^{32}P-Labeled Oligos

1. Anneal 2 nmol of complimentary oligos in 1x Annealing Buffer in a thermalcycler. The annealing mixture should be brought to 85°C for 2 min and the temperature reduced 1°C per minute for 60 min followed by incubation on ice. Alternatively, the mixture could be boiled in a hot block and allowed to cool in the hot block at room temperature for 1 h. The annealed mixture should be kept on ice until ready to end-label.
2. End label 40 pmol of the annealed oligos with 1 µl γ ^{32}P ATP using 2 µl of T4 Kinase (10 U/µl, Invitrogen) according to manufacturer's directions.

3.4. DNA Binding Reactions

1. For initial optimization and characterization of protein–DNA complexes, prepare Small-scale Reaction Mixes. On ice, combine 20,000–40,000 cpm ^{32}P-labeled oligos, 400 fmol purified ERα, 1 µl of salmon sperm DNA (1 mg/ml), 1 µl of BSA (1 mg/ml) or ovalbumin (1 mg/ml), 1 µl of polydeoxyinosine/deoxycytidine (1 mg/ml), 1.2 µl of 10x Reaction Buffer, and 2.4 µl of glycerol (50%). Bring the reaction to 12 µl of final volume with dH_2O. Incubate for 10 min at room temperature once all reagents are added.
2. For isolation of protein–DNA complexes, prepare Large-scale Reaction Mixes. On ice, combine 50 pmol unlabeled ERE-containing oligos, 18 pmol ERα, 262 µg HeLa nuclear extract, 16 µl of salmon sperm DNA (1 mg/ml), 16 µl of BSA (1 mg/ml) or ovalbumin (1 mg/ml), 16 µl of polydeoxyinosine/deoxycytidine (1 mg/ml), 20 µl of 10x

Reaction Buffer, and 40 µl of glycerol (50%). Bring the reaction to 200 µl with dH_2O. ERα-specific antibody can be added to help stabilize the protein–DNA complex.

3.5. Agarose Gel Electrophoresis for Initial Protein/DNA Complex Characterization

1. Prepare a 6.5 × 10 cm 1–1.25% agarose gel in 25 ml of 1x Running Buffer. Allow the gel to solidify at room temperature. Chill the gel at 4°C for 15 min prior to removing the comb (*see* **Note 4**).
2. Set up the 4°C gel with 1x Running Buffer at 4°C in a cold room and chill thoroughly (*see* **Note 5**).
3. While the gel is chilling, prepare the Small-scale Reaction Mix (~10 µl) described in Section 3.4.1 on ice. Unlabeled oligos containing an ERE or nonspecific DNA sequence (50–100-fold excess) and ERα-specific and nonspecific antibodies can also be added at this point. Incubate for 10 min at room temperature.
4. Add 10 µg HeLa nuclear extract to the Reaction Mix for a final volume of 12.5 µl and incubate for 20 min at room temperature (*see* **Note 6**).
5. Load the samples onto a horizontal gel and electrophorese at 100 V for 1–2 h at 4°C (*see* **Note 7**).
6. Place the gel on a piece of DE81 cellulose acetate with two pieces of Whatman blotting paper underneath. Dry the gel at 65°C for 30 min on a vacuum gel dryer. Expose the dried gel to autoradiography film overnight to determine the position of the protein–DNA complexes and the free oligos.

3.6. Agarose Gel Electrophoresis for Complex Isolation and Protein Extraction

1. For isolation of proteins, prepare a 15 × 10 cm 1–1.25% agarose gel in 50 ml of 1x Running Buffer using a prep-style comb. Alternatively, the teeth of a comb can be taped with electrical tape to increase the well size, as shown in **Fig. 13.3A**. Chill the gel at 4°C for 15 min prior to removing the comb.
2. While the gel is chilling, prepare the Large-scale Reaction Mix described in Section 3.4.2 on ice. ERα-specific antibody can be added to help stabilize the protein–DNA complex. Prepare Small-scale Reaction Mixes described in Section 3.4.1 with ^{32}P-labeled ERE-containing oligos, which are run adjacent to the large-scale reactions with the unlabeled ERE-containing oligos to identify the location of each protein–DNA complex (*see* **Note 8**).
3. Load the samples onto the horizontal gel and separate the complexes at 100 V at 4°C for the time required to separate the protein–DNA complex from the free DNA.
4. After fractionation, the wet gel is wrapped in plastic and exposed to autoradiography film overnight at 4°C. The position of each protein–DNA complex will be defined by the

radiolabeled protein-DNA complexes, which are run in parallel (*see* **Fig. 13.3B**). Draw 2 lines across the autoradiogram to define the position of the unlabeled protein–DNA complexes (arrowheads). Using a single-edge razor, cut a 3-sided flap in the autoradiogram where each unlabeled protein–DNA complex has migrated (dashed lines). Place the autoradiogram directly over the agarose gel. Pull back the 3-sided flap, fold it back along the solid line shown in **Fig. 13.3B**, and excise the gel region containing the protein–DNA complex. Recover the proteins from the gel with a Montage gel extraction kit according to manufacturer's directions (*see* **Note 9**).

5. The extracted proteins can be concentrated with Microcon size-exclusion columns according to manufacturer's directions. An appropriate molecular weight cutoff should be used to ensure that low molecular weight proteins of interest are not lost (*see* **Note 10**). The identity of the proteins present in the complexes can be determined by mass spectrometry analysis and the presence of a particular protein can be verified by Western blot analysis.

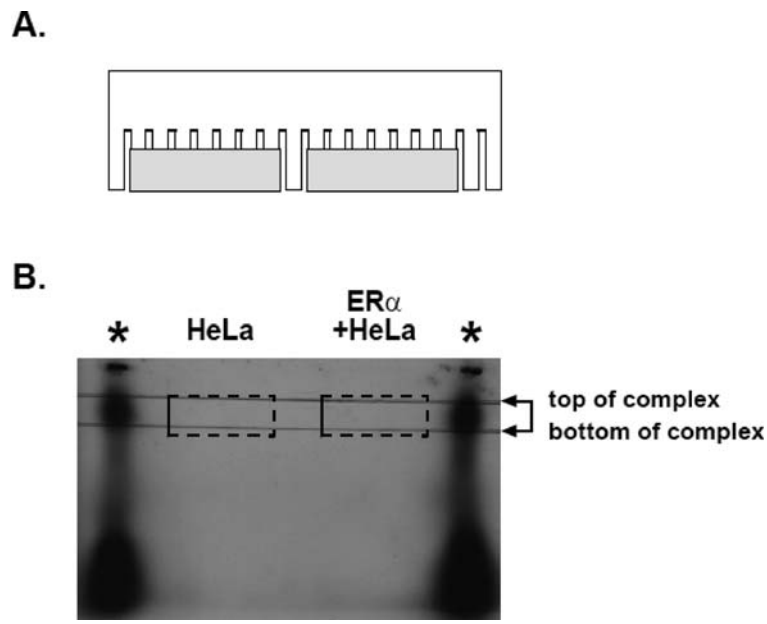

Fig. 13.3. Large-scale agarose-based gel mobility shift assay. (**A**) Schematic drawing of a comb with taped teeth utilized for large-scale isolation of ERα-containing protein–DNA complexes. (**B**) Unlabeled ERE-containing oligos were incubated with HeLa nuclear extracts in the absence or in the presence of purified ERα. Small-scale reactions containing HeLa nuclear extract, ERα and ^{32}P-labeled, ERE-containing oligos were run on the outside lanes (*) to indicate where the protein–DNA complexes were located. The underlying gel was excised from the regions beneath the boxed areas. Proteins were extracted from the gel regions from control (HeLa) or protein–DNA complex (ERα+HeLa) lanes and were identified by mass spectrometry analysis.

4. Notes

1. All cell culture reagents are from Invitrogen, Carlsbad, CA, unless otherwise stated.
2. We have successfully used low-melt, megabase, and SeaKem agarose to isolate protein–DNA complexes.
3. HeLa cells can be grown in spinner flasks, which is useful if larger numbers of cells are needed. For spinner flask cultures, maintain the cells at a density of 2×10^6 cells/ml. Pour cells into 250-ml centrifuge bottles and skip to step 3.1.4 of the protocol.
4. If more wells are needed, use 1–1.25% agarose in 50 ml of Running Buffer for an 18-well gel using the BioRad Wide Mini Sub Cell gel system. If a nebulizer will be used for extracting complexes, do not exceed 1.25% agarose as it will clog the filter.
5. Some protein complexes may be more stable at lower temperatures. In this case the gel box can be placed in an ice bath to maintain it at a lower temperature throughout the run.
6. This protocol can be adapted to use extracts from multiple cell lines. We have successfully formed specific protein–DNA complexes using nuclear extracts from HeLa and MDA-MB-231 cell nuclear extracts in combination with purified ERα and with MCF-7 cell nuclear extracts, which contain endogenously expressed ERα.
7. The duration of electrophoresis will depend on the size of the protein–DNA complex and the length of the oligos and should be determined empirically. No loading buffer is needed since the glycerol in the reaction mix will allow the sample to sink to the bottom of the well. Dyes should generally not be used since they may interfere with protein–DNA complex formation.
8. Unlabeled oligos are utilized for large-scale reaction mixes to prevent contamination of mass spectrometry equipment with the ^{32}P-labeled probe. Large-scale reaction mixes should be kept in as small a volume as possible.
9. We have found that the Montage gel extraction kit is far more efficient in isolating ERα and its associated proteins than acetone or trichloroacetic acid precipitation.
10. We typically use a filter with a 10 kDa molecular weight cut-off. A small amount of Triton X-100 (0.2 mM) can be added during the concentration step to minimize the amount of

protein that sticks to the plastic or filter (20). Micro-liquid chromatography electrospray ionization tandem mass spectrometry combined with database searches can be used to identify proteins by correlating experimental spectra to protein sequences in the human sequence database. Mass spectrometry analysis can be performed at a number of commercial and academic facilities on a fee for service basis. The presence of a protein in the protein–DNA complex can be confirmed by Western analysis of the eluted proteins.

Acknowledgements

We are indebted to J. Yates and coworkers for their mass spectrometry analysis of the proteins isolated. This work was supported by NIH grant R01 DK 53884 (to AMN). JRS-N was supported by an NIH Reproductive Biology Program Training Grant (T32 HD07028).

References

1. Beato, M., Herrlich, P., and Schutz, G. (1995) Steroid hormone receptors: Many actors in search of a plot. *Cell.* **83,** 851–57.
2. Wood, J. R., Greene, G. L., and Nardulli, A. M. (1998) Estrogen response elements function as allosteric modulators of estrogen receptor conformation. *Mol Cell Biol.* **18,** 1927–34.
3. Wood, J. R., Likhite, V. S., Loven, M. A., and Nardulli, A. M. (2001) Allosteric modulation of estrogen receptor conformation by different estrogen response elements. *Mol Endocrinol.* **15,** 1114–26.
4. Loven, M. A., Likhite, V. S., Choi, I., and Nardulli, A. M. (2001) Estrogen response elements alter coactivator recruitment through allosteric modulation of estrogen receptor beta conformation. *J Biol Chem.* **276,** 45282–88.
5. Loven, M. A., Wood, J. A., and Nardulli, A. M. (2001) Interaction of estrogen receptors alpha and beta with estrogen response elements. *Mol Cell Endocrinol.* **181,** 151–63.
6. Klinge, C. M. (2001) Estrogen receptor interaction with estrogen response elements. *Nucleic Acids Res.* **29,** 2905–19.
7. Hall, J. M., McDonnell, D. P., and Korach, K. S. (2002) Allosteric regulation of estrogen receptor structure, function, and coactivator recruitment by different estrogen response elements. *Mol Endocrinol.* **16,** 469–86.
8. Robyr, D., Wolffe, A. P., and Wahli, W. (2000) Nuclear hormone receptor coregulators in action: Diversity for shared tasks. *Mol Endocrinol.* **14,** 329–47.
9. Torchia, J., Glass, C., and Rosenfeld, M. G. (1998) Co-activators and co-repressors in the integration of transcriptional responses. *Curr Opin Cell Biol.* **10,** 373–83.
10. Loven, M. A., Muster, N., Yates, J. R., and Nardulli, A. M. (2003) A novel estrogen receptor alpha associated protein, template activating factor I beta, inhibits acetylation and transactivation. *Mol Endocrinol.* **17,** 67–78.
11. Likhite, V. S., Cass, E. I., Anderson, S. D., Yates, J. R., and Nardulli, A. M. (2004) Interaction of estrogen receptor alpha with 3-methyladenine DNA glycosylase modulates transcription and DNA repair. *J Biol Chem.* **279,** 16875–82.
12. Loven, M. A., Davis, R. E., Curtis, C. D., Muster, N., Yates, J. R., and Nardulli, A. M. (2004) A novel estrogen receptor alpha-associated protein alters receptor-deoxyribonucleic acid interactions and represses receptor-mediated transcription. *Mol Endocrinol.* **18,** 2649–59.

13. Schultz-Norton, J. R., Gabisi, V. A., Ziegler, Y. S., McLeod, I. X., Yates, J. R., and Nardulli, A. M. (2007) Interaction of estrogen receptor alpha with proliferating cell nuclear antigen. *Nucleic Acids Res.* **35,** 5028–38.
14. Schultz-Norton, J. R., McDonald, W. H., Yates, J. R., and Nardulli, A. M. (2006) Protein disulfide isomerase serves as a molecular chaperone to maintain estrogen receptor {alpha} structure and function. *Mol Endocrinol.* **20,** 1982–95.
15. Schultz-Norton, J. R., Walt, K. A., Ziegler, Y. S., McLeod, I. X., Yates, J. R., Raetzman, L. T., and Nardulli, A. M. (2007) The deoxyribonucleic acid repair protein flap endonuclease-1 modulates estrogen-responsive gene expression. *Mol Endocrinol.* **21,** 1569–80.
16. El Marzouk, S., Schultz-Norton, J. R., Likhite, V. S., McLeod, I. X., Yates, J. R., and Nardulli, A. M. (2007) Rho GDP dissociation inhibitor alpha interacts with estrogen receptor alpha and influences estrogen responsiveness. *J Mol Endocrinol.* **39,** 249–59.
17. Curtis, C. D., Likhite, V. S., McLeod, I. X., Yates, J. R., and Nardulli, A. M. (2007) Interaction of the tumor metastasis suppressor nonmetastatic protein 23 homologue H1 and estrogen receptor alpha alters estrogen-responsive gene expression. *Cancer Res.* **67,** 10600–7.
18. Rao, A. K., Ziegler, Y. S., McLeod, I. X., Yates, J. R., and Nardulli, A. M. (2008) Effects of Cu/Zn superoxide dismutase on estrogen responsiveness and oxidative stress in human breast cancer cells. *Molecular Endocrinololgy.* **22,** 1113–24.
19. Kraus, W. L., and Kadonaga, J. T. (1998) p300 and estrogen receptor cooperatively activate transcription via differential enhancement of initiation and reinitiation. *Genes Dev.* **12,** 331–42.
20. Suelter, C. H., and DeLuca, M. (1983) How to prevent losses of protein by adsorption to glass and plastic. *Anal Biochem.* **135,** 112–9.
21. Creekmore, A. L., Walt, K. J., Schultz-Norton, J. R., Ziegler, Y.S., McLeod, I. X., Yates, J. R., and Nardulli, A. M. The role of retinoblastoma associated proteins 46 and 48 in estrogen receptor α mediated gene expression. *Mol. Cell Endocrinol.* **291**, 79–86.
22. Curtis, C.D., Thorngren, D.L., Ziegler, Y.S., Sarkeshik A., Yates, J.R., Nardulli, A.M. (2009) Apurinic/apyrimidinic endonuclease 1 alters estrogen receptor activity and estrogen responsive gene expression. *Mol Endocrinol.* **23**, 1346–59.
23. Rao, A., Ziegler, Y.S., McLeod, I.X., Yates, J.R., Nardulli, A.M. (2009) Thioredoxin and thioredoxin reductase influence estrogen receptor α mediated gene expression in human breast cancer cells. *J Mol Endocrinol.* In Press.

Chapter 14

Chromosome-Wide Analysis of Protein Binding and Modifications

Kevin D. Sarge, Hongyan Xing, and Ok-Kyong Park-Sarge

Abstract

In order to fully understand the functions of a DNA-binding protein it is necessary to identify all of its binding sites in chromosomes and assess the role of each site in the overall biological function of the factor. An approach ChIP-on-Chip which combines the chromatin immunoprecipitation technique with chromosomal DNA microarray analysis, has proven to be a powerful means for the chromosome-wide identification of protein binding sites. This approach can also be used to characterize chromosome-wide variations in patterns of post-translational protein modifications, for example histone modifications. This chapter presents methodologies for the ChIP-on-Chip analysis, using as an example the identification of chromosome-wide binding sites for the TATA-binding protein in mitotic cells.

Key words: Chromatin immunoprecipitation, ChIP-on-Chip, chromosome-wide, TBP, epigenetics, method.

1. Introduction

One method for identifying new binding sites of factors for which a consensus recognition sequence has been determined is to perform database searches to identify matches to this sequence in the genome. The chromatin immunoprecipitation technique could then be used to test whether these identified sites are actually bound by the factor. However, this approach is not only inefficient, in that it would likely involve analyzing many sites that turn out not to be actual binding sites for the protein, but would also likely miss many actual binding sites whose sequences are similar to but don't exactly match the test sequence(s) used to perform the database searching. In the ChIP-on-Chip approach, DNA fragments isolated by

O.-K. Park-Sarge, T.E. Curry, Jr. (eds.), *Molecular Endocrinology,* Methods in Molecular Biology 590,
DOI 10.1007/978-1-60327-378-7_14,

chromatin immunoprecipitation using an antibody against the protein of interest are used to probe a DNA Chip containing an array of genomic DNA sequences. Thus, this experimental methodology has the advantages of being able (a) to identify binding sites of a protein in a way that is not biased with respect to the DNA sequence bound, and (b) to simultaneously identify binding sites over very large regions of genomic DNA. This technique can provide important new insights not only into the genomic DNA binding sites of DNA-binding proteins, but also into the variations in patterns of post-translational modifications of proteins such as histones throughout chromosomes (1–8). In this chapter we describe the key experimental details involved in performing ChIP-on-Chip experiments. To illustrate the types of data that can be obtained using these methodologies we present figures showing the results of chromatin immunoprecipitation and ChIP-on-Chip identification of chromosome-wide binding sites of the general transcription factor TATA-binding protein (TBP) in mitotic cells (9).

2. Materials

2.1. Chromatin Immunoprecipitation Analysis

1. Cells expressing the protein of interest.
2. Tissue culture media and associated reagents appropriate for the cells being used.
3. Formaldehyde (37% stock solution).
4. 1 M Glycine.
5. 0.5 M PMSF (phenylmethylsulfonyl fluoride) in absolute100% ethanol.
6. NP40 lysis buffer: 50 mM Tris-HCl, pH 8.0, 85 mM KCl, 0.5% NP40, 1 mM PMSF (PMSF added fresh).
7. Phosphate-Buffered Saline (PBS): 137 mM NaCl, 2.7 mM KCl, 4.3 mM Na_2HPO_4, and 1.5 mM KH_2PO_4.
8. SDS lysis buffer: 50 mM Tris-HCl, pH 8.0, 1% SDS, 10 mM EDTA, 1 mM PMSF (PMSF added fresh).
9. ChIP assay kit (Upstate Biotechnology, Lake Placid, NY).
10. Sonicator.
11. ChIP Dilution buffer: 20 mM Tris-HCl, pH 8.0, 0.01% SDS, 1% Triton X-100, 1.2 mM EDTA, 167 mM NaCl.
12. Protein G-sepharose or protein A-sepharose (Upstate).
13. Salmon sperm DNA saturated-protein A agarose beads (Upstate).
14. Primary antibody capable of immunoprecipitating protein of interest and species-matched non-specific IgG.

15. Low salt wash buffer: 20 mM Tris-HCl, pH 8.0, 0.1% SDS, 1% Triton X-100, 2 mM EDTA, 150 mM NaCl.
16. High salt wash buffer: 20 mM Tris-HCl, pH 8.0, 0.1% SDS, 1% Triton X-100, 2 mM EDTA, 500 mM NaCl.
17. LiCl wash buffer: 10 mM Tris-HCl, pH 8.0, 250 mM LiCl, 1% NP40, 1% deoxycholic acid, 1 mM EDTA.
18. ChIP Wash buffer: 100 mM Tris-HCl, pH 8.0, 500 mM LiCl, 1% NP40, 1% deoxycholic acid.
19. 1 x TE: 10 mM Tris-HCl, pH 8.0, 1 mM EDTA.
20. ChIP elution buffer: 1% SDS, 100 mM $NaHCO_3$.
21. DNA purification column designed for DNA fragments (e.g. Qiagen PCR kit).
22. Quantitative PCR machine, or regular PCR machine and native gel electrophoresis equipment and solutions.

2.2. Probing Genomic DNA Chips with Fluorescent-Labeled DNAs from ChIP Assay

1. Random primers for linear PCR amplification.
2. DNA biotin labeling kit (Affymetrix, Santa Clara, CA)
3. Human Cot1 DNA.
4. Access to Microarray hybridization incubators and detection instruments (e.g. Affymetrix) or a Microarray Facility.
5. Software to analyze the resulting data, for example, GeneChip Operating Software (GCOS) and TAS software (Affymetrix).

3. Methods

3.1. Chromatin Immunoprecipitation Analysis

In this first part of the ChIP-on-Chip experiment, cells are subjected to the chromatin immunoprecipitation assay using an antibody against the protein of interest in order to obtain protein-bound DNA fragments. These will later be labeled and used to probe the Chip arrays containing genomic DNA sequences in order to identify new binding sites for the protein. One can verify the specificity of the ChIP part of the procedure by performing PCR analysis of the resulting DNA fragments in two ways: (a) using primers that amplify a known binding site for the protein as well as a site which is known not to bind the factor and (b) using the antibodies against the protein vs. non-specific control antibodies. This verification may save time and effort that would result from using sub-optimal DNA fragment sets to probe the DNA Chip arrays in the second part of the ChIP-on-Chip experiment. **Figure 14.1** shows an example of such PCR analysis, in this case quantitative PCR analysis, to show the specific binding of TBP to the histone H4 promoter, a known binding site for this protein, in mitotic cells.

1. Grow tissue culture cells in media appropriate for that cell line. Cells capable of growing in suspension, such as human Jurkat cells, are often chosen for the reasons described in **Note 1**, but adherent cells have also been used successfully.
2. Cross-link exponentially growing cells (at least 10×10^6 cells per sample) by adding formaldehyde directly to the tissue culture medium to a final concentration of 1%.
3. After incubation for 10 minutes at 25°C with gentle rotation, quench (stop) crosslinking by adding glycine to a final concentration of 125 mM.
4. Pellet cross-linked cells by centrifuging at 3,000*g* for 5 minutes.
5. Wash cross-linked cells 3 times with PBS, each time collecting cells by centrifuging at 3,000*g* for 5 minutes.
6. Incubate washed cross-linked cells in NP40 lysis buffer (0.2 ml/1×10^6 cells) for 10 minutes on ice.
7. Pellet insoluble material containing cross-linked protein-DNA by centrifugation at 3,000*g* for 10 minutes at 4°C. Aspirate off the supernatant.
8. Incubate pellets in SDS lysis buffer (0.2 ml/1×10^6 cells) for 10 minutes on ice and solubilize by sonication to an average DNA length of 500–1000 bp (*see* **Note 2**).
9. Dilute sonicated chromatin 1:10 using ChIP Dilution buffer.
10. Pre-clear the soluble chromatin by adding 80 µl of a 50% slurry of salmon sperm DNA saturated-protein A agarose beads and 10 µl non-specific (control) rabbit IgG and incubating for 1 h at 4°C with rotation.
11. Centrifuge at 3,000*g* for 1 minute.
12. Take approximately 30 µl of the supernatant (pre-cleared chromatin) to be used later as the "Input" DNA sample.
13. To half of the rest of the supernatant (precleared chromatin) add the primary antibody against the protein of interest, and to the other half add species-matched non-specific control IgG, and incubate with rotation at 4°C for 16 hours. For ChIP assays we use primary antibodies at 1:200 dilutions (v:v).
14. To these tubes add 60 µl salmon sperm DNA saturated-protein A agarose beads and incubate for 1 hour at 4°C.
15. Centrifuge at 3,000*g* for 1 minute to collect beads, and discard the supernatant.
16. Wash beads once for 5 minutes at RT with low salt wash buffer and repeat step 15.
17. Wash beads once for 5 minutes at RT with high salt wash buffer and repeat step 15.

18. Wash beads once for 5 minutes at RT with LiCl wash buffer and repeat step 15.
19. Wash beads three times for 5 minutes at RT with ChIP Wash buffer and repeat step 15.
20. Wash beads twice for 5 minutes at RT with TE, each time repeating step 15.
21. Elute immune complexes by two successive incubations of the beads with 75 µl ChIP elution buffer and then pool elutions. In addition, the Input DNA sample collected in step 12 above should be made 1% in SDS and 100 mM in $NaHCO_3$ using stock solutions of each.
22. Reverse cross-links by adding NaCl to a concentration of 200 mM, and then heating at 67°C for at least 5 hours.
23. Concentrate and purify immunopurified and Input DNAs using a column designed for DNA fragments (such as Qiagen PCR purification kit). DNA is eluted in 30 µl 10 mM Tris-HCl, pH 8.5.
24. To test the specificity of the DNA fragments obtained from the chromatin IP, subject aliquots of 1 µl of the immunoprecipitated DNAs as well as input samples obtained prior to immunoprecipitation by PCR, using primers that amplify a known binding region and primers that amplify a region where the factor is known not to bind. Quantitative PCR analysis is preferred, but if not available then PCR products can be separated by agarose gel electrophoresis and visualized by ethidium bromide staining.

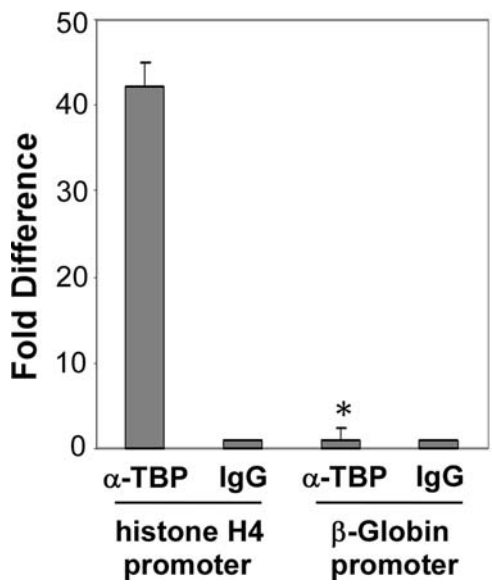

Fig. 14.1. Analysis of specificity of ChIP TBP promoter binding in mitotic cells. Chromatin immunoprecipitation (ChIP) assay was performed on mitotic (nocodazole-blocked) Jurkat cells using TBP antibodies or control IgG antibodies, followed by quantitative PCR assay using primer pairs specific to the H4 and β-globin gene promoters. Data are means ± s.d. ($n = 3$, $^*P < 0.0002$). This figure is from Xing et al. (9).

3.2. Probing Genomic DNA Chips with Fluorescent-Labeled DNAs from ChIP Assay

If the results of the analysis described at the end of **Section 3.1** above shows the specificity of the ChIP DNAs, these DNA fragments can then be used to probe the DNA Chip arrays containing the genomic sequences. In the first part of the ChIP-on-Chip, the DNA fragments isolated by immunoprecipitation using antibodies against the protein of interest, and the control Input DNA sample, is amplified by PCR and then labeled with biotin. In the second part of the ChIP-on-Chip, these labeled DNAs are then incubated with the Chips containing the genomic DNA arrays and the DNA spots that hybridize with the probes identified using specialized instruments designed for these purpose (e.g., Affymetrix equipment). The binding sites for the factor of interest are then determined by analyzing the data using computer software. **Figures 14.2, 14.13 and 14.4** illustrate the types of data output that can result from ChIP-on-Chip studies, in this case from our studies that characterized the binding sites of the TBP protein within chromosomal DNA of mitotic cells (9).

1. Subject 15–30 μl of the immunoprecipitated DNA and Input DNA samples to the first round of random primer PCR to amplify the DNA fragments (*see* **Note 3**).
2. Subject the DNA from the first round of amplification to a second round of amplification using a different primer (*see* **Note 4**).
3. Label the amplified DNAs with biotin following the manufacturer's protocol (e.g., Affymetrix).
4. Hybridize 10 μg of the labeled DNAs to the genomic DNA Chip arrays probes chosen for analysis (*see* **Note 5**) in the presence 15 μg human Cot1 DNA, using a specialized incubator and following the manufacturer's instructions (*see* **Note 6**). This step is typically done by a Microarray Facility, as is the following step.
5. Chips are washed, stained with fluorescent streptavidin-phycoerythrin, and scanned using specialized instruments (e.g., Affymetrix) are typically done in a dedicated Microarray Facility that has the required specialized machines.
6. Identify binding sites for the factor of interest by analyzing the resulting data using software from the manufacturer (*see* **Note 7**). For examples of data output, see **Figs 14.2, 14.3 and 14.4**.

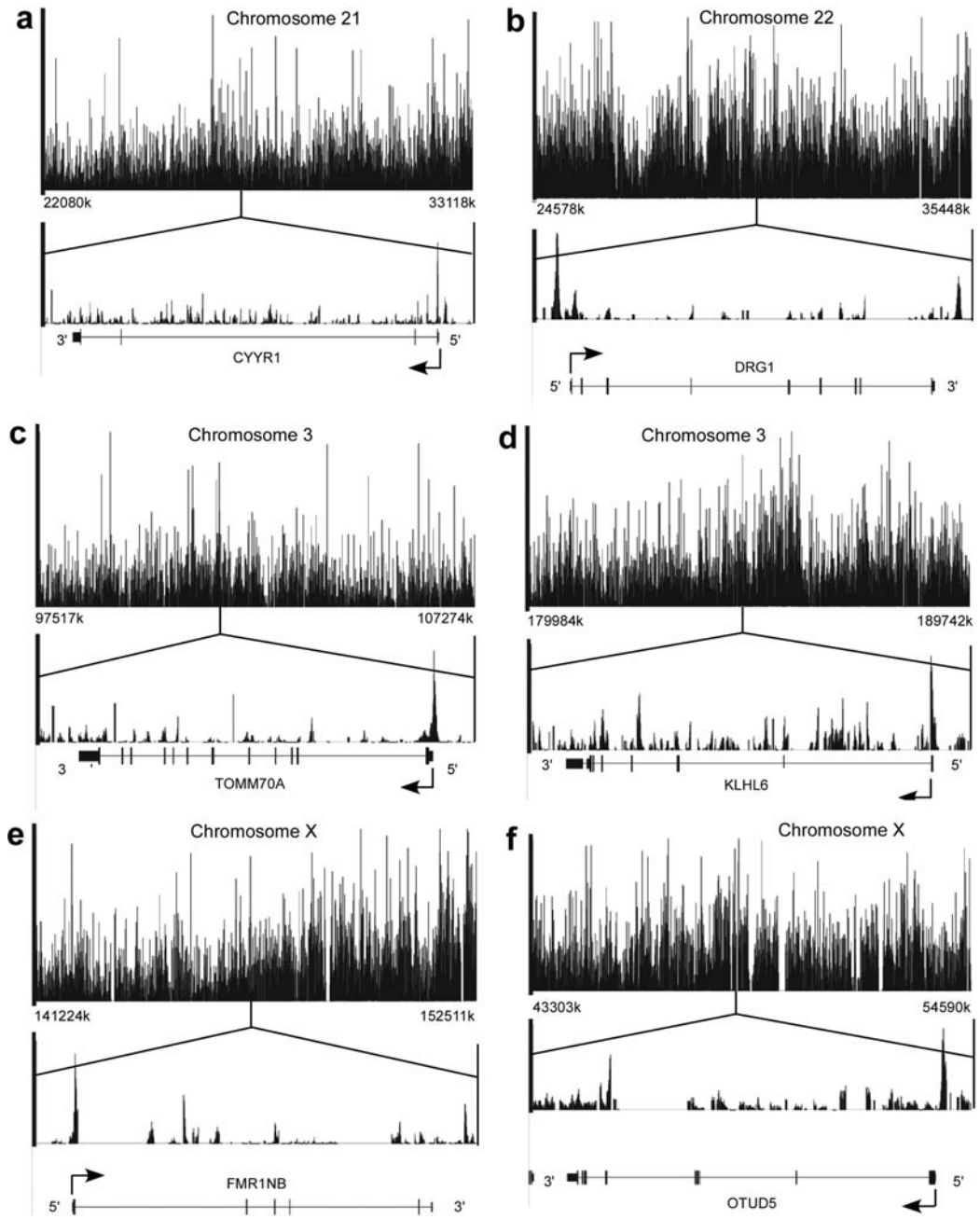

Fig. 14.2. TBP is bound to many chromosomal loci during mitosis. DNA fragments immunoprecipitated by TBP antibodies by ChIP assay using mitotic cells, with input genomic DNA as control, were hybridized to the Affymetrix Genechip human tiling array 2.0c, which includes genomic DNA arrays spanning human chromosomes 3, 21, 22, and X. Shown at the top of each panel are the locations of TBP binding in regions representing 10 million base-pair segments of the indicated chromosome. In the lower part of each panel are close-up views of TBP binding to a gene within that region, indicating the association of TBP with the promoter regions of each gene. The genes are CYRR1 (panel **a**), DRG1 (panel **b**), TOMM70A (panel **c**), KLHL6 (panel **d**), FMR1NB (panel **e**), and UTUD5 (panel **f**). This figure is from Xing et al. (9).

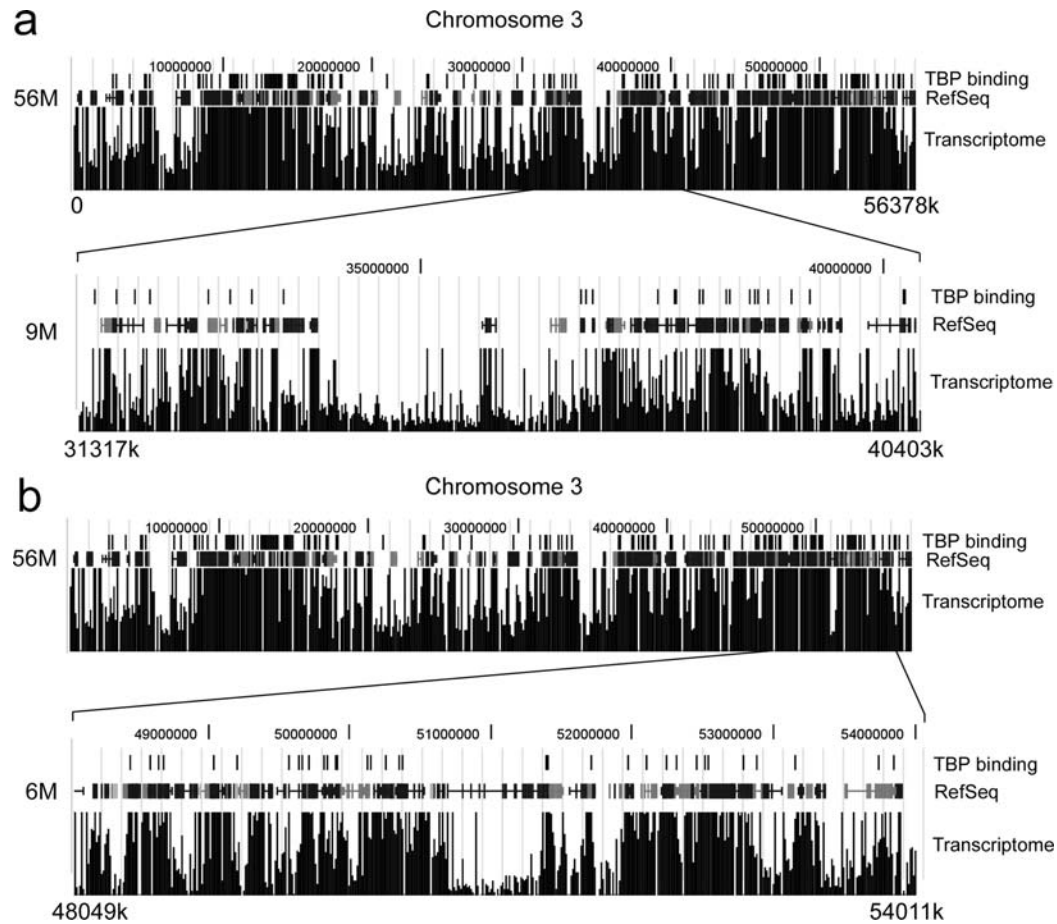

Fig. 14.3. Correlation between TBP binding and Transcriptome. The top parts of panels (**a)** and (**b)** show the data for TBP binding to a 56 million bp region of chromosome 3 (vertical lines represent locations of TBP binding), along with a depiction of the RefSeq genes and Transcriptome data (10) for this region. In the bottom parts of panels (a) and (b) are shown the same information for two different sub-portions of this 56 million bp region, one that is approximately 9 million bp long and the other 6 million bp in length. This figure is from the Supplementary data of Xing et al. (9).

Fig. 14.4. Lack of strong mitotic TBP binding in a chromosomal region containing pseudogenes, genes expressed in a tissue-restricted manner, and large regions lacking annotated genes. Panel (**a**) shows the data for TBP binding to the

4. Notes

1. Non-adherent cells are often chosen because (a) it is easier to grow the large numbers of cells required for these types of experiments, for example using spinner flasks, compared to adherent cells, and (b) it is likely that cross-linking is more efficient in such cells because more of their surface is exposed to the medium.
2. The sonication conditions used, such as the energy and duration, are dependent on the sonicator employed and must be empirically tested to find the conditions that yield fragments in this size range as observed on polyacrylamide gels stained with ethidium bromide.
3. In the Affymetrix protocol we followed, the initial round of linear amplification was carried out using random primer A [5′-GTTTCCCAGTCACGGTC$(N)_9$-3′], and utilized 4 cycles of 95°C, 4 minutes, 10°C, 5 minutes, ramp from 10°C to 37°C over 9 minutes, followed by 8 minutes at 37°C, using sequenase.
4. In the second round of amplification, in the Affymetrix protocol the DNA from the first round of amplification is then amplified using primer B (5'-GTTTCCCAGTCACGGTC-3') by Taq polymerase PCR using 32 cycles of 95°C, 30 s, 45°C, 30 s, 55°C, 30 s, 72°C, 1 minute.
5. For our experiments we used the Affymetrix Genechip Human tiling array 2.0 c, which contains genomic DNA spanning human chromosomes 3, 21, 22, X, and Y, including intergenic regions, promoters, untranslated regions, exons, introns, etc. However, DNA Chips are also available in which only known promoter regions are included, which may be desirable if you are studying a transcription factor and your goal is just to determine which promoters are bound by the factor of interest. The benefit of such a selective genomic DNA Chip is that one Chip can contain all the sequences one is interested in examining, whereas you would have to buy and hybridize many different Chips if you want to examine all of the genomic sequence. Of course, the disadvantage

Fig. 14.4 (continued) KLHL6 gene from Figure 14.2, but compressed so that its size is displayed relative to the region shown in panel (**b**). The *asterisk* indicates the TBP peak associated with this gene's promoter region, and the *dotted line* relates the height of this TBP signal to the TBP signals in panel (b). In panel (b) is shown a region of chromosome 21 that contains a number of pseudogenes, genes whose expression is tissue-restricted (C21orf99: testis and muscle; ANKRD21: testis; LOC441956: mammary gland), as well as regions that are devoid of any annotated genes. The position of each pseudogene is indicated by the vertical bar next to its identifier. The sizes of the two regions in panels (a) and (b) are displayed on the same relative scale, as are the magnitudes of the TBP binding signals. This figure is from the Supplementary data of Xing et al. (9).

of using a selective genomic DNA sequence Chip is that it would miss any binding sites for your factor that are not in the promoter sequences selected for inclusion on the Chip (e.g., not-yet-identified promoters, control DNA sequences that are within introns, or far upstream of proximal promoter regions, etc.). To have confidence in the results of the probing, it is suggested that three of each Chip be probed in each experiment (i.e., probing done in triplicate).

6. The steps of the procedure involving Chip hybridization, staining with fluorescent streptavidin-phycoerythrin, and scanning are typically done in a dedicated Microarray Facility that has the required specialized machines. For example, in our study the University of Kentucky Microarray Facility performed these steps using equipment including an Affymetrix GeneChip hybridization incubator 640, Fluidics Station 450, and GeneChip Scanner 3000 7G.
7. In our study, data were collected and analyzed using GeneChip Operating Software (GCOS) and TAS software (Affymetrix). The results (from three TBP IP DNA-probed chips and three genomic input DNA-probed chips) were quantile-normalized within treatment/control replicate groups. A Wilcox Rank Sum test was applied to the transformation log2 for data, testing the null hypothesis of the equality of the two population distribution functions against the alternative of a positive difference on location between the probability distribution of the treatment and that of the control. The Wilcoxon test was applied in a sliding window across the chromosomes. The chromosomal positions bound by TBP were identified based on a *P* value cut off of 0.005. Results were visualized using IGB software (Affymetrix) and the UCSC GenomeViewer, and compared to the RefSeq database (NCBI).

Acknowledgments

We are very grateful to David Rodgers for allowing us to use computers in his lab to analyze the data from our ChIP-on-Chip experiments.

References

1. Dietz, S. C., and Carroll, J. S. (2008) Interrogating the genome to understand oestrogen-receptor-mediated transcription. *Expert Rev. Mol. Med.* **10**, e10.
2. Trelle, M. B., and Jensen, O. N. (2007) Functional proteomics in histone research and epigenetics. *Expert Rev. Proteomics* **4**, 491–503.

3. Wade, J. T., Struhl, K., Busby, S. J., and Grainger, D. C. (2007) Genomic analysis of protein–DNA interactions in bacteria: insights into transcription and chromosome organization. *Mol. Microbiol.* **65**, 21–26.
4. Sandelin, A., Carninci, P., Lenhard, B., Ponjavic, J., Hayashizaki, Y., and Hume, D. A. (2007) Mammalian RNA polymerase II core promoters: insights from genome-wide studies. *Nat. Rev. Genet.* **8**, 424–436.
5. Elnitski, L., Jin, V. X., Farnham, P. J., and Jones, S. J. (2006) Locating mammalian transcription factor binding sites: a survey of computational and experimental techniques. *Genome Res.* **16**, 1455–1464.
6. Wu, J., Smith, L. T., Plass, C., and Huang, T. H. (2006) ChIP-chip comes of age for genome-wide functional analysis. *Cancer Res.* **66**, 6899–6902.
7. DeAngelis, J. T., Farrington, W. J., and Tollefsbol, T. O. (2008) An overview of epigenetic assays. *Mol. Biotechnol.* **38**, 179–183.
8. Callinan, P. A., and Feinberg, A. P. (2006) The emerging science of epigenomics. *Hum. Mol. Genet.* **15 Spec No 1**, R95–101.
9. Xing, H., Vanderford, N. L., and Sarge, K. D. (2008) The TBP-PP2A mitotic complex bookmarks genes by preventing condensin action. *Nat. Cell Biol.* **10**, 1318–1323.
10. Kapranov, P., Cheng, J., Dike, S., Nix, D. A., Duttagupta, R., Willingham, A. T., Stadler, P. F., Hertel, J., Hackermuller, J., Hofacker, I. L., Bell, I., Cheung, E., Drenkow, J., Dumais, E., Patel, S., Helt, G., Ganesh, M., Ghosh, S., Piccolboni, A., Sementchenko, V., Tammana, H., and Gingeras, T. R. (2007) RNA maps reveal new RNA classes and a possible function for pervasive transcription. *Science* **316**, 1484–1488.

Chapter 15

Genome-Wide Analysis for Protein–DNA Interaction: ChIP-Chip

Yunguang Tong and Jeff Falk

Abstract

Chromatin immunoprecipitation (ChIP) is a well-established procedure for protein–DNA interaction research. ChIP-chip, combining chromatin immunoprecipitation (ChIP) and microarray technology (Chip), enables scientists to survey genome-wide DNA binding sites for a given protein. The ChIP-chip technique has been used to identify transcription factor binding sites, explore epigenomic information and investigate factors in DNA replicate/repairs. Here we describe a protocol for ChIP-chip to study Pituitary Tumor Transforming Gene (PTTG1) in mammalian cells.

Key words: Chromatin immunoprecipitation, ChIP-chip, microarray, ChIP-GLAS, transcription factor, protein–DNA interaction; PTTG1.

1. Introduction

Chromatin immunoprecipitation (ChIP) is a powerful experimental approach for identifying the association of proteins with specific regions of the genome. The method involves crosslinking proteins with their genomic binding loci in live cells, shearing the chromatin into fragments, immunoprecipitating the protein bound DNA complex, and eluting the purified DNA (1). The traditional ChIP method is often coupled with Southern blot (2) or quantitative PCR, which are only applicable to analysis of small segments of known, pre-defined genomic loci and not helpful for the discovery of novel protein binding sites. ChIP-chip amplifies the ChIP purified DNA and analyzes the DNA using microarray elements covering all genomic binding sites, generating complete DNA binding information for a given protein (3, 4). Generally, the purified DNA is amplified, fluorescently

O.-K. Park-Sarge, T.E. Curry, Jr. (eds.), *Molecular Endocrinology,* Methods in Molecular Biology 590,
DOI 10.1007/978-1-60327-378-7_15,

labeled, and hybridized to DNA microarrays containing genomic DNA sequences along with a control DNA sample. The fluorescent signal from the significantly stronger ChIP DNA channel and input control are subsequently identified and mapped back to the genome (5). ChIP-chip has been used for a diverse and rapidly expanding set of applications. It has been used in investigating transcription factors and transcriptional machinery (6), the chromatin-modifying mechanism and architecture, histones and histone modifications (7), factors in DNA replication/repair (8), DNA methylation sites (9) and the linkage between transcription factor and nuclear-exporting machinery (10).

Several distinct ChIP-chip platforms have been developed with distinct differences in their DNA amplification, microarray, and visualization technologies. The two primary techniques used for DNA amplification include whole genome amplification (WGA) (11) and GLAS (Guided Ligation And Selection) based amplification (12). There are also three primary types of DNA microarray technologies: mechanically spotted cDNA or PCR-product arrays, mechanically spotted oligonucleotide arrays, and arrays with oligonucleotide synthesized in situ. Moreover, two types of dye systems exist including single color or two colors. Each of the different platforms require specific protocols for DNA amplification, labeling, hybridization, scanning, data analysis, and results interpretation (5, 13).

Here we describe a ChIP-chip protocol using a ChIP-GLAS technique to identify PTTG1 targeted genes. The advantage of this technology is that it has significantly enhanced sensitivity and decreased starting material requirements in comparison to other traditional ChIP-chip technologies. This is achieved by using a protocol that incorporates a number of important variations in the chromatin immunoprecipitation, DNA amplification, microarray hybridization steps, and centers around the use of a single array containing 20,000 human promoters. The parameters and conditions suggested may require further optimization for each protein and cell type investigated. The results of each step should be carefully evaluated before proceeding to the next step to assure overall accuracy of the ChIP-chip results. This protocol has been successfully used in surveying transcription factors in human cells (12, 14).

2. Materials

2.1. Chromatin Immunoprecipitation

1. Antibody of interested protein (*see* **Note 1**).
2. Negative control IgG (Rabbit control IgG, Abcam).

3. 10x PBS (Sigma): 1.37 M NaCl, 100 mM Phosphate, 27 mM KCl.
4. 10x Glycine (2.5 M).
5. 1x Ripa Lysis Buffer (Sigma): 150 mM NaCl, 50 mM Tris, 1% NP-40, 0.5%, Sodium deoxycholate, 0.1%SDS.
6. Dounce homogenizer (Wheaton).
7. 100x Protease Inhibitor Cocktail (PIC): (AEBSF, E-64, bestatin, leupeptin, aprotinin and EDTA)
8. PMSF (100 mM).
9. Preblocked Salmon Sperm DNA/Protein G agarose (Active Motif).
10. 1% SDS.
11. 1 M $NaHCO_3$.
12. 5 M NaCl.
13. RNase A (10 µg/µl).
14. 0.5 M EDTA.
15. 1 M Tris-Cl pH 6.5.
16. Proteinase K (10 µg/µl).
17. 20 mg/ml glycogen (Roche Applied science).
18. Neg Primer* (*see* **Note 2**).
    For (5′-ATGGTTGCCACTGGGGATCT-3′)
    Rev (5′-TGCCAAAGCCTAGGGGAAGA-3′)
19. 37% Formaldehyde (highly toxic by inhalation and should be used only in a ventilated hood).
20. 3 M Sodium acetate pH 5.2.
21. 25:24:1(v/v/v) Phenol/chloroform/isoamyl alcohol.
22. 100% Ethanol.
23. 70% Ethanol.
24. Qiagen MinElute PCR purification kit (Qiagen).
25. Rocking platform for culture plates.
26. Apparatus to rotate tubes end-to-end at 4°C (e.g., a Labquake from Barnstadt/Thermolyne).
27. Spectrophotometer.
28. Sonicator.
29. Taq polymerase and 10x PCR Buffer.
30. dNTP mixture (5 mM each dNTP).
31. Triton X-100.
32. LiCl.
33. IGEPAL CA-630.

34. Sodium deoxycholate.
35. Fixation solution: Add 2 ml of 38% formaldehyde to 74 ml minimal cell culture medium and mix thoroughly (final concentration is 1% formaldehyde).
36. Glycine Stop-Fix solution: Combine 4 ml 10x Glycine Buffer, 4 ml 10x PBS and 32 ml dH_2O. Mix well and leave at room temperature.
37. Cell Scraping Solution: Add 600 µl 10x PBS to 5.4 ml dH_2O, mix and place on ice. Add 30 µl 100 mM PMSF just before use.
38. Ice cold PBS.
39. ChIP Wash Buffer 1: 0.1% SDS, 1% Triton X-100, 2 mM EDTA, 20 mM Tris-HCl, pH 8.0, 150 mM NaCl.
40. ChIP Wash Buffer 2: 0.1% SDS, 1% Triton X-100, 2 mM EDTA, 20 mM Tris-HCl, pH 8.0, 500 mM NaCl.
41. ChIP Wash Buffer 3: 0.25 M LiCl, 1% IGEPAL CA-630, 1% sodium deoxycholate, 1 mM EDTA, 10 mM Tris-HCl, pH 8.0.
42. ChIP Wash Buffer 4: 1% SDS, 0.1 M $NaHCO_3$.

2.2. DNA Amplification, Labeling and Hybridization

1. Biotinylation Kit (Aviva Systems Biology): PHOTOPROBE® Biotin, 1 M MgCl2, 10 M Ammonium, Acetate, 2-Butanol, 0.1 M Tris, pH 9.5, Glycogen, λ DNA (100 ng/µl), TE Buffer.
2. Annealing and Ligation Kit (Aviva Systems Biology): 100% Ethanol, H_2OK-Oligo-Mix *(varies with different genome)*, Streptavidin-Coated Magnetic Beads, 2x Binding Buffer, GLAS Wash Buffer.
3. ChIP-GLAS amplification and labeling kit (Aviva Systems Biology): dNTP Mix, T7 Primer, T3 Primer, Atto 550-Labeled T7 Primer, Atto 647-Labeled T7 Primer.
4. Hybridization kits (Aviva Systems Biology): 100X PreWash Solution 1, 500x PreWash Solution 2, 40x PreWash Solution 3, 10x Blocking Buffer, 10% SDS, 20x SSC, Hybridization Solution.
5. Blocking Buffer (60 ml): 6 ml of 10x Blocking Buffer, 0.6 ml of 10% SDS, 53.4 ml of H_2O.
6. PreWash Solution 1 (300 ml): 3 ml of 100x PreWash Solution 1, 297 ml of H_2O.
7. PreWash Solution 2 (600 ml): 1.2 ml of 500x PreWash Solution 2, 598.8 ml of H_2O.
8. PreWash solution 3 (300 ml): 7.5 ml of 40x PreWash Solution 3, 292.5 ml of H_2O.

9. AmpliTaq Gold DNA Polymerase and Buffer (Applied Biosystems Cat. No. N8080241)
10. Taq DNA polymerase and Buffer (NEB).
11. 96-well Magnetic Holder (Dynal Inc.).
12. Microarray Slide (Aviva Systems Biology).
13. Hybridization Chamber (Aviva Systems Biology).
14. 24 × 60 mm or 22 × 60 mm Coverslips.
15. Wash Solution (300 ml warmed up to 50°C): 30 ml of 20x SSC, 3 ml of 10% SDS, 267 ml of H_2O.
16. 0.2x SSC 1 (600 ml): 6 ml of 20x SSC, 594 ml of H_2O.
17. 0.1x SSC (600 ml): 3 ml of 20x SSC, 597 ml of H_2O.
18. Jewelers Microforceps.

2.3. Scan and Analyze

1. Microarray scanner which can read a 25 mm by 75 mm glass slide (e.g., GenePix 4000B).
2. Scanning software (e.g., GenePix).

3. Methods

3.1. Chromatin Immunoprecipitation

This section describes preparation of chromatin from adherent cells in three 15 cm plates (~500–700 cm^2, ~5 × 10^7 cells) (*see* **Note 3** for processing frozen tissue).

1. Grow Human choriocarcinoma JEG-3 cells to ~80% confluence on three 15 cm plates.
2. Aspirate medium and add 20 ml of freshly made Fixation Solution to each plate. Incubate for 10 min at room temperature with gentle shaking (*see* **Note 4**).
3. Aspirate Fixation Solution off and wash by adding 20 ml ice-cold PBS to each plate, rock the plate for 5 s and then aspirate off the PBS.
4. Add 10 ml Glycine Stop-Fix solution to each of the plates, swirl to cover, and then rock at room temperature for 5 min.
5. Aspirate the Glycine Stop-Fix solution and add 20 ml ice-cold PBS, rock the plate for 5 s, and then remove the PBS.
6. Add 2 ml ice cold Cell Scraping Solution to each of the plates and scrape cells with a rubber policeman. Transfer the cells to a 15 ml conical tube on ice.
7. Pellet the pooled cells by centrifugation for 10 min 720*g* at 4°C.
8. Remove the supernatant. The pellet can be frozen for later use.

9. Resuspend the cell pellet in 1.5 ml ice-cold 1x Ripa Buffer supplemented with 15 µl 10x PIC and 15 µl 10x PMSF, by pipetting up and down. Incubate on ice for 30 min.
10. Transfer the cells to an ice-cold dounce homogenizer. Gently dounce on ice with 10 strokes to aid in nuclei release.
11. Transfer cells to a 15 ml conical tube and centrifuge at 2,400*g* for 10 min at 4°C to pellet the nuclei. Carefully remove the supernatant. Resuspend the nuclei pellet in 0.3 ml 1x Ripa Buffer supplemented with 10 µl 10x PIC.
12. Shear the chromatin by sonication of the sample in a volume of 0.3–0.5 ml in a V shaped eppendorf tube, 8–10 times for 10 s with 1 min on ice between each round of Sonication, using a Branson digital sonifier (Fisher) set at amplitude of 65%. Sonication conditions should be optimized to ensure proper shearing has been achieved (*see* **Note 5**).
13. Remove 5 µl of sonicated DNA and determine the extent of DNA shearing by analyzing the range of DNA fragment sizes gel electrophoresis using a 1% agarose gel. Optimal shearing will result in DNA ranging from 0.3 to 2 kb in size with most of the fragments concentrated in the 0.5–0.8 kb size range.
14. Centrifuge the sheared DNA samples at 16,000*g* in a 4°C microcentrifuge for 15 min. Transfer the supernatants to a fresh tube. Add 0.2 ml 1x Ripa lysis buffer. Aliquot the sheared chromatin into 10 tubes at 50 µl ($\sim 5 \times 10^6$ cells/tube). The samples can be stored at −80°C for later use.
15. Dilute each 50 µl chromatin to 500 µl using 1x Ripa buffer (supplement with PIC). Add 50 µl fully resuspended Protein G beads.
16. Rotate the tube at 4°C for 1–2 h.
17. Pellet the beads at 16,000*g* for 2 min. Let the tube on ice for 2 min to let the beads settle.
18. Transfer the supernatant (chromatin) to a fresh tube without disturbing the beads. Repeat to ensure that all beads are removed from the chromatin.
19. Transfer 20 µl of the pre-cleared chromatin to a microcentrifuge tube and store at −20°C. This sample is the "Input DNA." It will be treated to remove cross-links at a later stage
20. Use 1 and 3 µg of Anti-PTTG1 antibody (Zymed, Carlsbad, CA) for each ChIP reaction. Incubate the tubes 4 h to overnight on a rotator at 4°C *(sensitivity may be improved by overnight incubation)*.

21. Aliquot 100 µl of the fully resuspended beads into each of the antibody/chromatin incubations and Incubate the tubes on a rotator for 1.5 h at 4°C.
22. Each ChIP reaction will be washed using 1 ml of each of the wash buffers listed following, rotate for 5 min, once with ChIP Wash Buffer 1 + PIC, four times with ChIP Wash Buffer 2 + PIC, once with ChIP Wash Buffer 3 + PIC, and twice with ChIP Wash Buffer 4.
23. Freshly prepare 420 µl ChIP Elution Buffer for each ChIP reaction by adding 20 µl of 1 M $NaHCO_3$ to 400 µl 1% SDS and mixing thoroughly.
24. Add 50 µl ChIP Elution Buffer to each of the washed Protein G bead pellets in the 0.65 ml tubes. Cap tubes, vortex briefly, and incubate for 2 min at room temperature with gentle rotation. Repeat the elution once and pool the supernatant (total volume is 100 µl). Discard the beads.
25. Add 80 µl Elution buffer to the saved input DNA (20 µl) bringing the total volume to 100 µl.
26. Add 4 µl 5 M NaCl and 1 µl RNase A to each ChIP elution and to the sample of Input DNA.
27. Vortex to mix completely and centrifuge the tubes briefly to remove liquid from the sides of the tubes. Reverse the protein–DNA cross linking process by incubating at 65°C 4 h to overnight. The samples can be stored at −20°C for later use. The SDS in the samples may precipitate. Warm the tubes to room temperature and vortex to resuspend the SDS.
28. Remove tubes from 65°C incubator and centrifuge at 16,000*g* for 1 min to collect liquid.
29. Add the following to each tube: 2 µl 0.5 M EDTA, 2 µl 1 M Tris-HCl pH 6.5 and 2 µl Proteinase K solutions.
30. Vortex, centrifuge at 16,000*g* briefly and incubate at 42°C for 1.5–2 h to digest the proteins. During this incubation, prepare the reagents that will be needed for DNA purification in the next section.
31. Purify the DNA from the protein digest sample using Qiagen MinElute PCR cleanup kit by adding 600 µl PB buffer (Quiagen kit) to the sample, and following the manuscript's protocol.
32. Elute DNA with 19 µl TE buffer instead of the EB buffer from the Qiagen kit.
33. Evaluate quality of the purified DNA on a 1% agarose gel. An example is shown in **Fig. 15.1** (*see* **Note 6**).

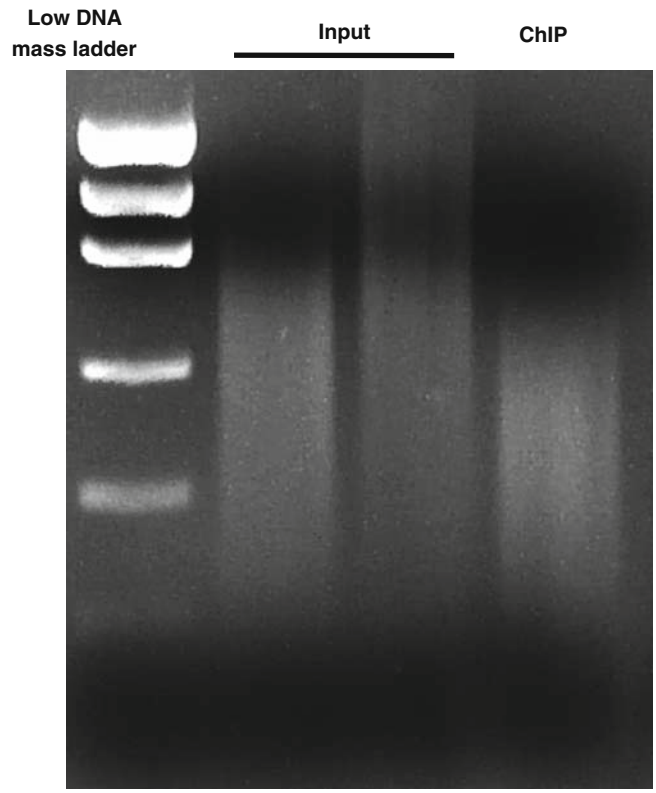

Fig. 15.1. Purified DNA (ChIP) as shown by agarose electrophoresis.

3.2. ChIP DNA Amplification, Labeling, and Hybridization to Microarray

This part of procedures varies a lot among different ChIP-chip techniques and platforms. The user may have to consult the microarray manufacturer before continuing. The ChIP-GLAS technology introduced here showed improved sensitivity which is useful when testing material is limited. However, unlike profiling studies conducted with tiling arrays, the binding interaction information derived from ChIP-DSL (Chromatin Immunoprecipitation DNA Selection and Ligation) studies is limited to the promoter regions.

1. Set up each biotinylation reaction in a PCR tube by adding 18 µl of DNA (ChIP or input), 1 µl of λDNA (100 ng/µl), and 1 µl of PHOTOPROBE® Biotin.
2. Mix, centrifuge, and cover the reaction with 20 µl mineral oil, incubate at 95°C for 10 min in a PCR machine.
3. Add 60 µl ddH_2O to the reaction, and pipette 80 µl from the bottom of the tube to a new 0.6 ml tube (*see* **Note 7**). Add 80 µl of 0.1 M Tris pH 9.5 and mix.
4. Add 160 µl of 2-butanol, vortex, and centrifuge at 14,000*g* for 3 min. Remove the upper butanol phase and repeat the extraction once (*see* **Note 8**).

5. Transfer the aqueous phase from the bottom of the tube into a new one.
6. Precipitate the DNA by adding 10 µl of 10 M Ammonium Acetate, 2 µl of 1 M $MgCl_2$, 1 µl of Glycogen, and 200 µl Cold 100% ethanol.
7. Mix and incubate at −20°C for 15 min. Centrifuge at 4°C, 14,000*g* for 15 min.
8. Carefully remove the supernatant without disturbing the pellet, as the pellet contains the biotinylated DNA, wash with 70% ethanol and centrifuge at 4°C, 14,000*g* for 5 min. Remove the supernatant and air dry the pellet.
9. Resuspend the pellet in 10 µl TE Buffer. Proceed to the annealing step. All the subsequent GLAS steps are done by placing reaction tubes in a PCR machine. Buffer changes at each of the following steps are carried out by placing tubes in a 96-well magnetic holder and using a pipette to remove the liquid.
10. Resuspend streptavidin-coated magnetic beads slurry and transfer 5 µl/reaction to each PCR tube. Add 150 µl of 2x Binding Buffer, mix, place the tube in a 96-well magnetic holder for 2 min and remove the supernatant. Repeat once and resuspend the beads in 2x Binding Buffer at a desired volume (5 µl/reaction).
11. Warm up GLAS Wash Buffer to 45°C and 1x Ligation Buffer to 45°C.
12. Set up annealing reactions in a PCR tube by adding 10 µl of Biotinylated DNA, 10 µl of H20K-Oligo-Mix, and 20 µl 2x Binding Buffer.
13. Incubate reaction tubes in a PCR machine at 95°C for 10 min, and then 45°C for 30 min.
14. Transfer 5 µl streptavidin-coated magnetic beads into each sample and mix. Incubate at 45°C for 1.5 h.
15. Wash beads with 180 µl of prewarmed GLAS Wash Buffer. Repeat this wash twice with GLAS Wash Buffer and once with 150 µl of prewarmed 1x Taq DNA Ligase Buffer.
16. Add 40 µl of 1x Taq DNA Ligation Buffer and 1 µl Taq DNA Ligase to each tube, incubate at 45°C for 1 hour.
17. Remove the supernatant and wash beads twice with 180 µl of prewarmed GLAS Wash Buffer. Remove residual solution after last wash. Proceed to the elution step.
18. Resuspend beads in 40 µl ddH_2O, incubate at 95°C for 5 min and then immediately chill on ice for 5 min. The supernatant containing the eluted DNA is transferred into a new tube.

19. Proceed to a diagnostic PCR amplification to check the quality of the GLAS reaction, or store the samples at −20°C for later use.
20. Assemble diagnostic PCR reactions (per reaction) by adding 2.5 µl of 10x PCR Buffer, 1.5 µl of 25 mM $MgCl_2$, 0.5 µl of 10 mM dNTPs, 0.5 µl of 30 pmol/ul T7 Primer, 0.5 µl of 30 pmol/µl T3 Primer, 2 µl of GLAS Sample, 0.4 µl of Taq DNA Polymerase, and 17.1 µl of ddH_2O.
21. PCR amplify the samples using the program of denaturation at 95°C for 5 min, 24 cycles of amplification at 95°C for 30 s, 54°C for 2 min, 72°C for 2 min, extension at 72°C for 5 min, and holding at 4°C until use.
22. Take 5 µl of reaction and analyze on a 2% agarose gel. If a weak band at ~120 bp is not detected, the experiment should be repeated from the beginning, paying close attention to the products from each step and preferably using increased amounts of starting material if this is feasible (*see* **Note 9**).
23. If a band is detected in the ChIP samples, proceed with labeling and amplifying the GLAS products by assembling the following PCR reaction:

	Input	ChIP	Mock
10x PCR Buffer	2.5 µl	2.5 µl	2.5 µl
25 mM $MgCl_2$	1.5 µl	1.5 µl	1.5 µl
10 mM dNTP Mix	0.5 µl	0.5 µl	0.5 µl
30 pmol/µl T3 Primer	0.5 µl	0.5 µl	0.5 µl
15 pmol/µl Atto	1 µl	–	–
15 pmol/µl Atto 647T7	–	1 µl	1 µl
GLAS sample	4 µl	4 µl	4 µl
Taq DNA Polymerase	0.4 µl	0.4 µl	0.4 µl
ddH_2O	14.6 µl	14.6 µl	14.6 µl

24. Place tubes in PCR machine and start PCR reaction using the program of denaturation at 95°C for 5 min, 29 cycles of amplification at 95°C for 30 s, 54°C for 2 min, 72°C for 2 min, extension at 72°C for 5 min, and holding at 4°C until use.
25. Take 5 µl of the PCR reaction and analyze on a 2% agarose gel. **Figure 15.2** shows an example of this analysis. This PCR should show a stronger band than the diagnostic PCR. The PCR reaction should be kept in dark until use in order to preserve the dyes intensity.

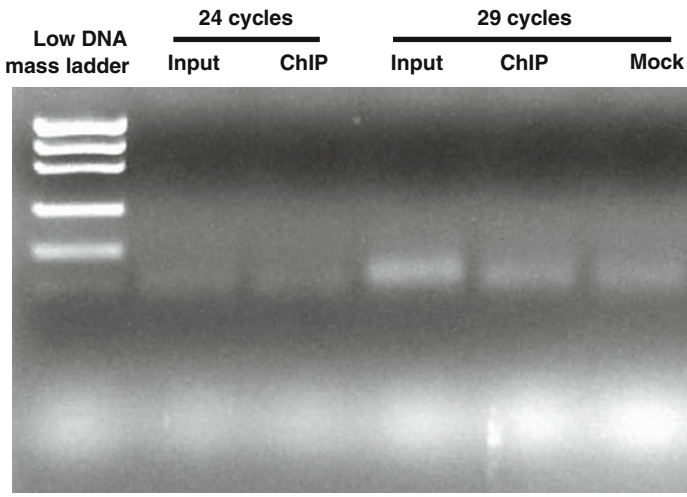

Fig 15.2. ChIP-DSL PCR results as shown by agarose electrophoresis. 29-cycle PCR products showed a stronger signal than 24-cycle's. ChIP sample showed a stronger signal than Mock sample.

26. Warm up 50 ml Blocking Buffer to 50°C in a Coplin Jar. Use 50 ml Blocking Buffer for every two slides.
27. Place microarray slides into a slide rack, submerged in 250 ml 1x PreWash Solution 1 in a Wheaton Glass Staining Dish (250 ml solution for five slides) with gentle shaking for 5 min, 50°C.
28. Wash the slides in 250 ml 1x PreWash Solution 2 with gentle shaking for 2 min, 50°C. Repeat once.
29. Wash the slides in 250 ml 1x PreWash Solution 3 with gentle shaking for 10 min, 50°C.
30. Wash the slides in 250 ml H_2O with gentle shaking for 1 min, 50°C.
31. Immediately transfer the slides to prewarmed Blocking Buffer. Incubate for 15 min at 50°C.
32. Wash the slides in 250 ml H_2O with gentle shaking for 1 min, 50°C.
33. Put the slides in slide container or 50 ml conical tubes, centrifuge at 1,000 *g* for 2 min to dry the slides.
34. Prepare hybridization mix in an amber tube (60 µl per reaction for H20K chip) by adding 30 µl of Hybridization Solution, 5 µl of Atto-550-labeled GLAS sample (Input), 10 µl of Atto-647-labeled GLAS sample (ChIP), and 15 µl of ddH_2O (*see* **Note 9**).
35. Incubate the mix at 95°C for 5 min and spin down briefly.
36. Place the blocked microarray slide with the label side facing up in a hybridization chamber.

37. Add 55 µl DNA hybridization mix onto the array. Carefully place coverslip (24 × 60 mm) on the top of the array *(see* **Note 10***)*. A #1 size coverslip is recommended since this will reduce the number of air bubbles trapped.
38. Add 50 µl H_2O to each side of the chamber and assemble the chamber.
39. Incubate the hybridization chambers without shaking at 50°C overnight.
40. Fill a Coplin jar with 50 ml prewarmed Wash Solution. Disassemble the hybridization cassettes and place slides into the jar (up to five slides).
41. After a brief gentle shaking for 1 min, remove each slide slowly from the Coplin jar with the cover glass left behind. It is important to not let the slides dry out during the washing process since this will significantly increase background levels.
42. Place the slides into a slide rack and wash them in the remaining 250 ml Wash Solution with gentle shaking for 10 min.
43. Wash slides in 250 ml 0.2x SSC with gentle shaking for 2 min. Repeat once.
44. Wash slides in 250 ml 0.1x SSC with gentle shaking. Repeat once.
45. Put the slides in slide containers or 50 ml conical tubes, centrifuge at 2000 rpm for 2 min to dry the slides and protect slides from light and dust until it is scanned.

3.3. Scan and Analyze

The microarray slides can be analyzed using any standard microarray scanner. The following protocol has been optimized for a Genepix 4000B scanner.

1. Turn on the scanner and place the slide in the machine with barcode facing downward.
2. Open the hardware setting dialog box, select double wavelength scan, and set PMT gain at 660 for both channels (635/562).
3. Perform a preview scan, and adjust PMT gain to avoid saturation.
4. Draw a scan area, perform image scan and save image.
5. Load the accompanied GAL (genepix array list) file, make sure each block and spot are properly aligned. Image processing involves identifying each microarray features, determining background and measuring fluorescent intensities of features. The GenePix Pro combines several different background subtraction methods to derive the final image and to remove stray fluorescent signals including local, global, negative control, and morphological background subtraction. Perform data analysis and save the row data results in a GPR file. Enrichment is represented as the ratio of the ChIP-derived DNA relative to the control input DNA.

6. Import the GPR files into a suitable microarray data analysis program. Various softwares are available on the market for microarray data analysis. We recommend the use of the single-array error model (14, 15) for data normalization and analysis, such as GenePix Acuity 4.0 from Molecular Device, R package (Internet download, www.r-project.org, free to public) for data analysis and normalization. A software package has also been developed by Dr. Ren, which is freely available at http://www.chiponchip.org/software.html. Another commonly used program is SAM, significance analysis of microarrays (Stanford, http://www-stat.stanford.edu/~tibs/SAM/, free for academic) for statistic analysis of replicates.
7. Once data is imported into Acuity 4.0, select the data sets to be normalized using the Query Wizard and normalize the data using lowess normalization. An example is shown in **Fig. 15.3**.

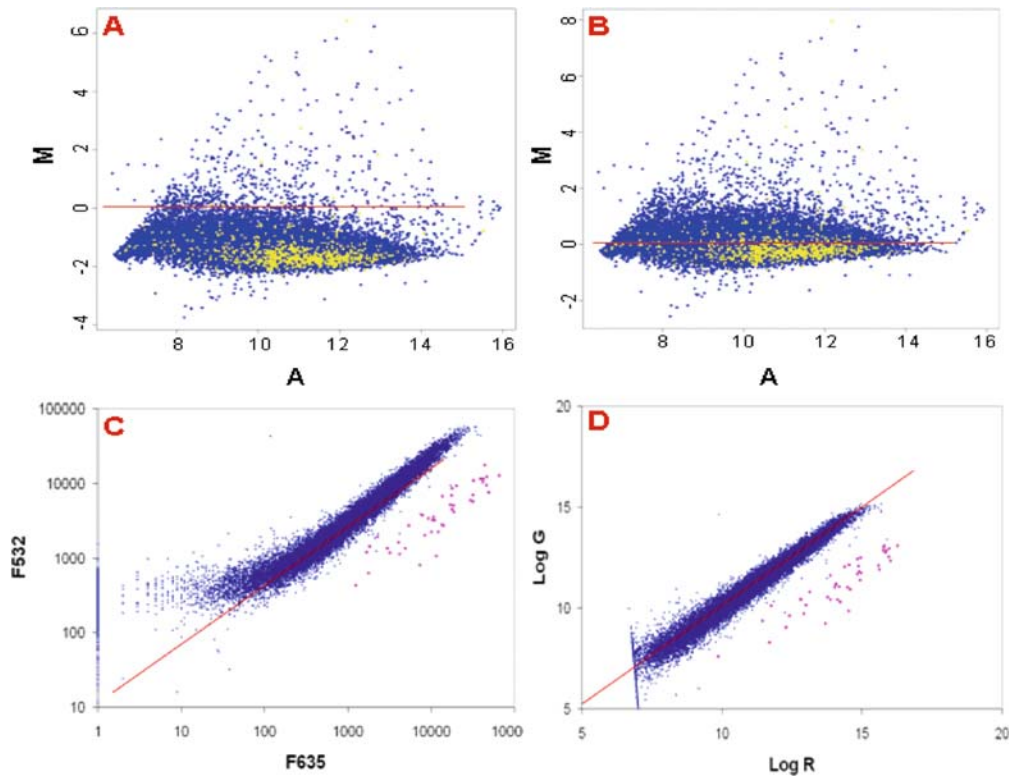

Fig. 15.3. ChIP-DSL data before and after normalization. Figures **A** and **B** are examples of M/A plots using linear normalization. Figures **C** and **D** are examples of standard Scatter plots of non-linear lowess normalization.

8. Plot the data for viewing using either a scatter plot or a M/A plot. Scatter plots will graph the log Atto 550 vs log Atto647, whereas M/A plots graph M, which represents the fold

enrichment expressed as the log2 ratio, versus A which represents the average of the intensity. M/A graphs are generally recommended since these plots increase the range of differential expression that can be easily viewed. An example is shown in **Fig. 15.4**.

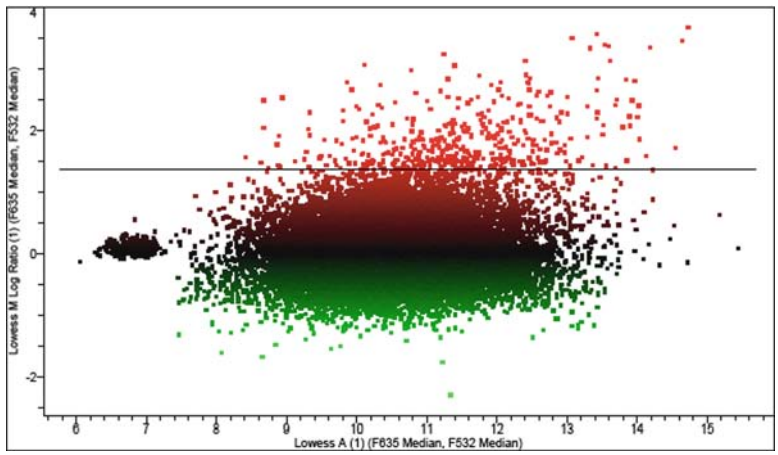

Fig. 15.4. Enriched binding of transcription factor. MA plot of ChIP-DSL genome-wide profiling data. ChIP-DSL Profile identified enriched promoters (above the cutoff line) (log2 M >1.4).

9. Data is generally ranked and compared between experiments based on the M value (log ratio) where log 2M of 1.4 = 2.5 fold enrichment. Changes in binding where M values are >1.4 are generally considered significant levels of enrichment.
10. As is true with any microarray experiment, the best way to quantify target binding in a dataset is to look at genes that have statistically significant binding among groups of arrays. This is best done by conducting multiple experimental repeats in order to generate statistical significant p values. This typically requires a minimum of three replicate trials in order to generate p values < 0.05.
11. The user may need to consult the array manufacturer (Aviva Systems Biology) and a bioinformatics specialist for proper data analysis and results interpretation.
12. If poor results are obtained from the ChIP-DSL assay a diagnostic assay can be performed using the Human Spike-In DNA Control Kit (Aviva Systems Biology) which can be used as positive control to assess specificity and sensitivity of DSL assay and provide insight as to whether the poor results are due to problems encountered in the ChIP or the DSL sections of the experiment. This assay contains 44 1 kb fragments spiked into a genomic DNA background in

proportions that mimic the enrichment of chromatin immunoprecipitation. This facilitates testing the DSL assay independently from the ChIP step to eliminate the factor of antibody efficiency for chromatin immunoprecipitation.

13. Targets identified by ChIP-DSL as having enriched factor-mediated binding should be validated using ChIP-qPCR studies where enrichment of each identified target is quantitated with respect to input DNA and negative control genes derived from naked genomic regions (15) (*see* **Note 11**).

4. Notes

1. The use of antibodies that are suitable for ChIP-based studies is the most critical step in any ChIP-Chip analysis. Many antibodies that perform well in other applications do not work in ChIP studies, with only 1 in 5 antibodies performing appropriately in ChIP-based applications (unpublished result, Aviva Systems Biology). ChIP performed with an unproven antibody must include appropriate controls to demonstrate that the antibody and the prepared chromatin are appropriate for ChIP-based studies. These studies generally entails conducting ChIP-qPCR validation studies with known positive control genes in order to demonstrate appropriate factor mediated binding (*see* **Note 5**). If there are no suitable antibodies for ChIP, the user may tag the given protein so that a ChIP-grade tag antibody can be used; however, this generally results in increased levels of background as compared to using a specific antibody.
2. Negative control primers. Because ChIP reactions are unavoidably contaminated with a small amount of non-specifically captured DNA. The negative control primers should be included in the PCR analysis to demonstrate the relative amount of contaminating DNA in different DNA samples.
3. Starting material. Generally successful ChIP-GLAS experiments require a minimum of 5×10^6 cells or 30 mg of frozen tissue per ChIP-GLAS assay. For frozen cells homogenize, or use a razor blade to cut small 1–3 mm pieces. In a 50 ml Corning tube combine tissue with 10 ml of PBS, add formaldehyde to 1% final concentration and proceed with the protocol as written.
4. Fixation conditions need to be optimized for different cell types. Excessive cross-linking may result in masking important epitopes on the protein resulting in reducing the immunoprecipitation efficiency, whereas too little cross-linking may lead to incomplete fixation. The 10 min, room temperature fixation

outlined in the procedure works well for most standard cell types; however, it is recommended that a fixation time course be performed with a small aliquot of cells in order to optimize fixation for the specific cell type being used.

5. It is recommended that sonication conditions be optimized prior to the actual ChIP-DSL experiment by performing a sonication time course and analyzing the products on a 1% agarose gel to identify the optimal conditions resulting in appropriate fragmentation sizes ranging from 0.3 to 2 kb. Shearing will be inefficient when the chromatin sample becomes emulsified. Lower shearing power and turn the power on gradually will effectively avoid this problem. The user can centrifuge the sample for 4 min at 8000 rpm in a microcentrifuge to remove trapped air in shearing.
6. PCR analysis of ChIP purified DNA. A successful ChIP results in enrichment, not complete purification of chromatin fragments that are bound by the protein of interest. Thus, DNA isolated by ChIP is inevitably contaminated with non-specifically captured DNA. If there are known targeted genes for the given protein, a diagnostic quantitative PCR should be performed to test the enrichment of ChIP purified DNA. The primers for the targeted gene should produce a stronger signal in ChIP antibody than Negative control IgG. The negative primers should produce similar signal in Negative control IgG and ChIP antibody. If using regular PCR, the PCR cycling should be stopped while the reaction is still in the linear stage of amplification since virtually all PCR primer pairs will produce a PCR product when use ChIP DNA as a template. Hot-start PCR methods are recommended to ensure consistent PCR amplification results. PCR analysis is extremely sensitive, precautions against contamination should be taken throughout the entire ChIP protocol. PCR primers should efficiently and specifically amplify the desired target.
7. The mineral oil contamination will be removed by the following butanol extraction.
8. The volume of the aqueous phase will be decreased to about 50–70 μl after the second extraction.
9. Stochastic PCR bias is the major source of non-specific background in ChIP-DSL experiments. This PCR bias occurs when there is a limiting number of starting templates. The low template concentrations during early cycles may lead to stochastic fluctuation in the interactions of primer annealing to the templates derived from ChIP DNA. To avoid this problem, the amount of DSL sample used as templates should be increased. In addition, splitting the sample into multiple PCR reaction tubes can also be useful in decreasing nonspecific background.

10. These volumes are good for using 24 × 60 mm cover glass. If using a larger size cover glass, volume should be increased accordingly
11. The user should practice a few times using an empty slide to avoid scratching and creating air bubbles.

Acknowledgments

This work was supported by NIH Grant CA 75979 (SM), T32 DK007770, and The Doris Factor Molecular Endocrinology Laboratory. We thank Dr. Shlomo Melmed for his critical discussion in preparing this protocol.

References

1. Strutt, H., and Paro, R. (1999) Mapping DNA target sites of chromatin proteins in vivo by formaldehyde crosslinking. Methods Mol. Biol. 119:455–467.
2. Southern, E.M. (1975) Detection of specific sequences among DNA fragments separated by gel electrophoresis. J. Mol. Biol. 98: 503–517.
3. Sandmann, T., Jakobsen, J.S., and Furlong, E.E. (2006) ChIP-on-chip protocol for genome-wide analysis of transcription factor binding in Drosophila melanogaster embryos. Nat. Protoc. 1: 2839–2855.
4. Lee, T.I., Johnstone, S.E., and Young, R.A. (2006) Chromatin immunoprecipitation and microarray-based analysis of protein location. Nat. Protoc. 1:729–748.
5. Buck, M.J., and Lieb, J.D. (2004) ChIP-chip: considerations for the design, analysis, and application of genome-wide chromatin immunoprecipitation experiments. Genomics 83:349–360.
6. Zhu, X., Gerstein, M., and Snyder, M. (2007) Getting connected: analysis and principles of biological networks. Genes Dev. 21: 1010–1024.
7. Hanlon, S.E., and Lieb, J.D. (2004) Progress and challenges in profiling the dynamics of chromatin and transcription factor binding with DNA microarrays. Curr. Opin. Genet. Dev. 14:697–705.
8. MacAlpine, D.M., and Bell, S.P. (2005) A genomic view of eukaryotic DNA replication. Chromosome. Res. 13:309–326.
9. van, S.B., and Henikoff, S. (2003) Epigenomic profiling using microarrays. Biotechniques 35:346–4, 356.
10. Ishii, K., Arib, G., Lin, C., Van, H.G., and Laemmli, U.K. (2002) Chromatin boundaries in budding yeast: the nuclear pore connection. Cell 109:551–562.
11. Barker, D.L., Hansen, M.S., Faruqi, A.F., Giannola, D., Irsula, O.R., Lasken, R.S., Latterich, M., Makarov, V., Oliphant, A., Pinter, J.H. et al (2004) Two methods of whole-genome amplification enable accurate genotyping across a 2320-SNP linkage panel. Genome Res. 14:901–907.
12. Tong, Y., Tan, Y., Zhou, C., and Melmed, S. (2007) Pituitary tumor transforming gene interacts with Sp1 to modulate G1/S cell phase transition. Oncogene 26:5596–5605.
13. Kim, T.H., Barrera,L.O., and Ren, B. (2007) ChIP-chip for genome-wid
14. Li, Z., Van, C.S., Qu, C., Cavenee, W.K., Zhang, M.Q., and Ren, B. (2003) A global transcriptional regulatory role for c-Myc in Burkitt's lymphoma cells. Proc. Natl. Acad. Sci. U. S. A 100:8164–8169.
15. Hughes, T.R., Marton, M.J., Jones, A.R., Roberts, C.J., Stoughton, R., Armour, C.D., Bennett, H.A., Coffey, E., Dai, H., He, Y.D. et al. (2000) Functional discovery via a compendium of expression profiles. Cell 102: 109–126.

Chapter 16

Detection of ERα-SRC-1 Interactions Using Bioluminescent Resonance Energy Transfer

Tamika T. Duplessis, Kristen L. Koterba, and Brian G. Rowan

Abstract

Bioluminescent Resonance Energy Transfer is a naturally occurring phenomenon that can be exploited to explore protein–protein interactions in real-time in intact cells and cellular extracts. It detects energy transferred between a bioluminescent donor enzyme (*Renilla* luciferase) fusion protein and a fluorescent (GFP^2, a mutant of Green Fluorescent Protein) acceptor fusion protein. Optimal detection of BRET^2 energy transfer relies on the distance and orientation generated by the fusion proteins. This chapter describes in detail the BRET^2 assay as it is used to examine the physical interaction between the nuclear receptor ERα and the transcriptional coactivator SRC-1. Description of methods include selection of donor and acceptor combinations, fusion construct generation and validation, cell culture and transfection, individual fluorescence and luminescence detection, BRET^2 detection, and data analysis.

Key words: Estrogen receptor, nuclear receptor, Steroid Receptor Coactivator-1 (SRC-1), protein–protein interaction, Bioluminescent Resonance Energy Transfer^2.

1. Introduction

Estrogen receptor alpha (ERα) is a member of the nuclear receptor superfamily of ligand-activated transcriptional regulators through which endogenous and environmental estrogens bind and elicit their effects. As a transcriptional regulator, the function of ERα is dependent on its ability to physically interact with other biomolecules such as DNA and other transcriptional regulatory proteins. In the absence of estrogen, ERα is complexed as part of a multiprotein inhibitory complex that includes heat shock proteins and immunophilins. Upon ligand binding, the receptor undergoes

O.-K. Park-Sarge, T.E. Curry, Jr. (eds.), *Molecular Endocrinology,* Methods in Molecular Biology 590,
DOI 10.1007/978-1-60327-378-7_16,

a conformational change that promotes homodimerization, recruitment of coregulators and results in binding to specific DNA binding sites in the promoter of target genes to regulate transcription (1, 2). At the promoters of ERα responsive genes, ligand-bound ERα recruits transcription coactivators such as members of the SRC-1 family that potentiate transcription through chromatin remodeling and interaction with general transcription factors. ERα may also regulate transcription through binding to transcription factors already bound to the promoter including SP-1 proteins (3–5), AP-1 proteins (6), NFkappaB (7), and GATA-1(8).

Given the importance of protein–protein interactions in nuclear receptor action, robust assays that measure these interactions in intact cells are an invaluable tool. Measurements of protein–proteins interactions in a live, cell-based system is possible using Bioluminescent Resonance Energy Transfer ($BRET^2$). Detection of protein–protein interaction using $BRET^2$ requires excited energy transfer between a bioluminescent donor molecule (*Renilla* luciferase) and a fluorescent acceptor molecule (a mutant of Green Fluorescent Protein-GFP^2). $BRET^2$ is one of several assays that detects protein–protein interactions using energy transfer between two molecules. Sensitivity and ease of optimization makes $BRET^2$ the assay of choice for evaluating specific physical interactions of nuclear receptors.

2. Materials

2.1. Cell Culture and Transfection

1. Cells suitable for transfection. Cell lines that yield high transfection efficiencies are especially useful (HEK-293, HeLa, and COS-1).
2. Basic growth medium such as Dulbecco's Modified Eagle's Medium (DMEM) supplemented with 0.3 mg/ml L-Glutamine, 1% Penicillin/Streptomycin, and 10% FBS or 5% charcoal dextran stripped FBS for HEK-293 cells.
3. 0.05 % Trypsin-EDTA.
4. 6-well cell culture dish.
5. Transfection reagent/system of choice. For example, Fugene 6 (Roche), Lipofectamine or Lipofectamine 2000 (Invitrogen).
6. cDNAs of proteins of interest to generate fusion proteins in $BRET^2$ expression vectors (**Fig. 16.1**).

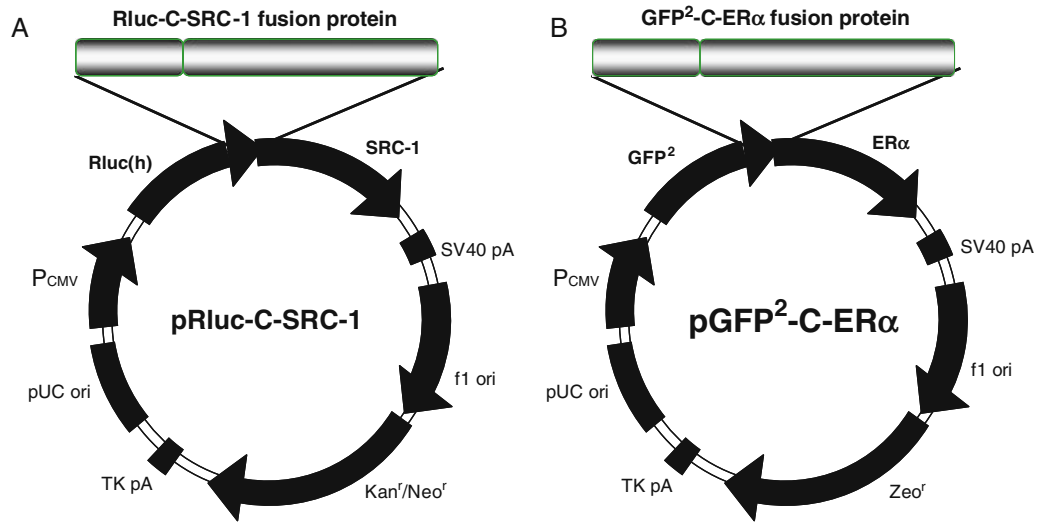

Fig. 16.1. Vector diagrams for the Rluc C SRC-1 and GFP^2C ERα used in the $BRET^2$ studies.

2.2. $BRET^2$ Preliminary and Standardization Experiments

1. $BRET^2$ Buffer: PBS supplemented with 0.1 g/l $CaCl_2$, 0.1 g/l $MgCl_2$, 1 g/l D-Glucose. Alternatively Dulbecco's Phosphate Buffered Saline (D-PBS) containing supplements is available from Gibco. Store at room temperature. Add 2 μg/ml Aprotinin (MP Biomedicals, Solon, OH) prior to use (*see* **Note 1**).
2. 96-well black Optiplate (PerkinElmer) (*see* **Note 2**).
3. Fluorescence microplate reader (FLUOstar Optima, BMG Labtech) (*see* **Note 3**).
4. 1 mM DeepBlueC stock (Coelenterazine 400 a): Reconstitute one vial (50 μg) with 125 μl (1 mM) absolute ethanol. Vortex. Store at −20°C protected from light (Biotium, Hayward, CA) (*see* **Note 4**).
5. 25 μM DeepBlueC working solution: Dilute from 1 mM stock to 25 μM working solution using $BRET^2$ Buffer with Aprotinin. Dilute solution just prior to use.
6. Luminescence microplate reader (FLUOstar Optima, BMG Labtech).
7. Aluminum foil.

2.3. $BRET^2$ Assay

1. $BRET^2$ Buffer.
2. 96-well white Optiplate (PerkinElmer).
3. 1 mM DeepBlueC stock (Coelenterazine 400 a).
4. 25 μM DeepBlueC working solution.
5. Dual Microplate reader with luminescence and fluorescence capabilities equipped with Rluc emission filter: 410 nm bandpass 80 nm and GFP^2 emission filter: 515 nm bandpass 30 nm (FLUOstar Optima, BMG Labtech) (9).

3. Methods

3.1. Cell Culture and Transfection

1. Select the Rluc (donor) and GFP^2 (acceptor) combination for BRET^2 determination to determine interaction of ERα and SRC-1.
2. Generate fusion constructs in BRET^2 expression vectors consisting of the cDNA for SRC-1 and ERA inserted in-frame with the cDNA for Rluc (donor) and GFP^2 (acceptor) proteins (**Fig. 16.1**) (*see* **Note 5**).
3. Plate HEK-293 cells in a 6-well cell culture dish in normal growth media so that cells will reach appropriate confluency levels according to transfection reagent/system protocol (*see* **Note 6**).
4. Usually 24 hours after plating, transfect cells with Rluc-C-SRC-1 and GFP^2-C-ERα to coexpress the Rluc-SRC-1(donor) and GFP^2-ERα (acceptor) fusion proteins of interest if these proteins are not already stably expressed (**Fig. 16.2**). Additionally, also express the Rluc fusion protein alone for analysis of the BRET^2 signal (*see* **Note 7**) and include appropriate positive- and negative-control proteins transfected in parallel (*see* **Note 8**). A 1:1 transfection ratio of Rluc and GFP^2 fusion proteins may not be optimal to generate the best BRET^2 signal. The amount of each fusion protein construct to use in co-transfection experiments depends on the affinity of the two protein interacting domains and the level at which each construct is expressed. A transfection matrix experiment should be performed with various ratios of each construct to determine the combination that will generate the BRET^2 signal with the greatest difference in signal to background values (*see* **Note 9**). **Table 16.1** is an example of a transfection matrix.

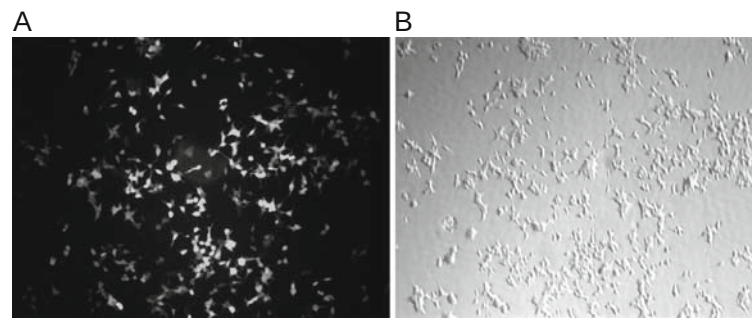

Fig. 16.2. Transfection efficiency of the GFP^2-C-ERα at 24 hours post-transfection showing green fluorescence (**A**) and phase contrast (**B**) in HEK-293 cells.

Table 16.1
Example of the BRET^2 transfection matrix used to optimize the ratio of Rluc to GFP^2 cDNA used for cotransfections. (Adapted from Koterba KL, Rowan BG. Nucl Recept Signal 2006; 4:e021)

	Rluc-Protein B			
	0 μg	**1 μg**	**3 μg**	**10 μg**
0 μg	Condition 1	Condition 2	Condition 7	Condition 12
3 μg	–	Condition 3	Condition 8	Condition 13
10 μg	–	Condition 4	Condition 9	Condition 14
20 μg	–	Condition 5	Condition 10	Condition 15
40 μg	–	Condition 6	Condition 11	Condition 15

3.2. BRET^2 Preliminary and Standardization Experiments

Preliminary experiments must be performed prior to the BRET^2 determination to verify the functionality and expression of all combinations of fusion proteins. Fusion protein expression can be assayed using standard immunoblotting techniques such as Western blots using whole cell lysates or immunoprecipitated protein extracts. Addition of donor and acceptor molecules may also affect protein function and therefore experiments must be performed to ensure that the fusion proteins generated are still functional. Confocal microscopy can also be used to verify the correct subcellular localization of the fusion protein.

3.2.1. Detection of the GFP^2 Signal

1. See Section 3.1 for cell culture and transfection.
2. Aliquot 50,000 transfected cells/well in a 96-well black Optiplate (PerkinElmer).
3. Add 175 μl BRET^2 buffer.
4. Read on microplate reader (Fluorescence mode) using the following settings:
   a. Read time: 0.5 s
   b. Temperature: Room temperature
   c. PMT voltage: 1000 volts
   d. Gain: 1
   e. Excitation: 425/20
   f. Emission: 515/30

3.2.2. Detection of the Rluc Signal

1. See Section 3.1 for cell culture and transfection.
2. Aliquot 50,000 transfected cells per well in a 96-well white Optiplate (PerkinElmer).
3. Add 150 µl BRET^2 buffer.
4. Add DeepBlueC at a final concentration of 5 µM.
5. Incubate covered with foil for 18 min.
6. Read on microplate reader (Luminescence mode) using the following settings:
   a. Read time: 1 s
   b. Temperature: Room temperature
   c. PMT voltage: 900 volts
   d. Gain: 1
   e. Emission: 410 nm

3.3. BRET^{2}Assay

1. 24–72 hours post-transfection, trypsinize transfected HEK-293 cells using 0.05% trypsin for 2–5 min at 37°C. The trypsinized cells are resuspended in BRET^2 buffer.
2. Wash cell pellet two times in BRET^2 buffer with centrifugation at 500–1000 × g for 2 min between washes.
3. Count and resuspend cells in BRET^2 buffer to obtain cell concentrations in the range of 1–4 × 10^6 cells/ml (*see* **Note 10**).
4. Aliquot 50 µl of cells in triplicate into a 96-well white Optiplate (PerkinElmer). This constitutes the non-treated experimental group. Aliquot another 50 µl of cells in triplicate for each ligand as needed (*see* **Note 11**).
5. Let cells equilibrate in Optiplate for 20 min.
6. Add ligand, for example 10^{-8}M 17β-estradiol (E2), 10^{-7}M Tamoxifen (Tam) or 20 ng/ml Amphiregulin (rhAR), (diluted in BRET^2 buffer) or buffer alone to each well.
7. Incubate for 30 min at room temperature or other time points.
8. Prepare DeepBlueC (DBC) in excess.
9. Start BRET^2 reaction by adding DBC substrate for a final concentration of 5 µM one well at a time for a total assay volume of 50–100 µl. Donor and acceptor light outputs are measured immediately by a dual channel plate reader in luminescence mode before the addition of the substrate to the next well. A dual channel plate reader equipped with an automatic injector is ideal. BRET^2 determination instrument settings should be the following:
   a. Read time: 1 s per channel
   b. Temperature: Room temperature

c. PMT voltage: 1100 volts

d. Gain: 25–100

e. Filters: donor 410/80; acceptor 515/30

3.4. BRET^2 Assay Data Analysis

The data obtained from the BRET^{2}analysis (see **Tables 16.2, 16.3 and 16.4**) is calculated as the BRET^2 signal. This signal is the ratio (BRET^2 Ratio) of the GFP^2 emission or fluorescence signal (515 nm) divided by the Rluc emission or luminescence signal (410 nm). This ratio uses the average readings between the triplicate wells of non-transfected cells subtracted from the average readings of transfected cells for each wavelength (*see* **Note 12**).

There are two widely accepted calculations for the BRET^2 signal, the BRET^2 Ratio and the Corrected BRET^2 Ratio. Both adhere to the principle of resonance energy transfer and either one could be used depending on the experimental parameters being tested. Calculation #1 (BRET^2 Ratio) measures basal interactions and is most applicable to ligand-dependent versus ligand-independent experiments.

$$\text{BRET}^2\ \text{Ratio} = \frac{\text{transfected GFP}^2\ \text{emission (515 nm)} - \text{non-transfected GFP}^2\ \text{emission (515 nm)}}{\text{transfected GFP}^2\ \text{emission (410 nm)} - \text{non-transfected Rluc emission (410 nm)}}$$

Calculation #2 (Corrected BRET^2 Ratio) utilizes the additional component of the correction factor (Cf) which takes into account possible false-positive resonance transfer signal due to forced interactions of overexpressed fusion proteins. The correction factor measures the BRET^2 ratio obtained from the Rluc fusion protein and the expression of the GFP^2 empty vector.

$$\text{Corrected BRET}^2\ \text{Ratio} = \text{BRET}^2\ \text{Ratio} - \text{Correction Factor (Cf)}$$

where Cf = BRET^2 Ratio of the Rluc vector expressed alone.

An example of results obtained from BRET^2 signal generated using calculation #2 or the Corrected BRET^2 Ratio is illustrated in **Fig. 16.3**. A positive BRET^2 signal can occur at 10–100 Å. A BRET^2 ratio of 0.1 can be significant as long as it is significantly different than the Rluc alone ratio.

To illustrate BRET^2 in a ligand inducible system, recruitment of SRC-1 to ERα was measured. A COOH-terminus *Renilla* luciferase (Rluc) SRC-1 fusion protein was used as the donor moiety, and an N-terminus GFP^2-ERα fusion protein was used as the acceptor moiety for BRET^2 **(Fig. 16.3)**.

Table 16.2
Example of GFP BRET^2 data obtained from the 515 nm channel.

	Untreated			E2			Tam			rhAR		
	1	2	3	1	2	3	1	2	3	1	2	3
Untransfected	30	30	30	15	31	21	13	44	37	48	21	0
Rluc-C-SRC-1 alone	63	103	109	90	84	122	112	72	0	47	0	15
Rluc-C-SRC-1 + GFP^2-C Vector	9	52	27	54	19	75	90	40	69	42	37	124
Rluc-C-SRC-1 + GFP^2-C ERa	96	98	77	147	45	125	165	63	76	64	90	91

Table 16.3
Example of Rluc BRET^2 data obtained from the 410 nm channel.

	Untreated			E2			Tam			rhAR		
	1	2	3	1	2	3	1	2	3	1	2	3
Untransfected	5	5	5	128	81	70	85	23	73	110	43	10
Rluc-C-SRC-1 alone	1506	2040	2737	2431	2890	2222	1886	1786	590	102	87	2273
Rluc-C-SRC-1 + GFP^2-C-Vector	1066	824	946	598	876	921	566	867	769	738	1097	757
Rluc-C-SRC-1 + GFP^2-C-ERa	1259	1050	954	950	904	1330	989	899	883	684	835	1085

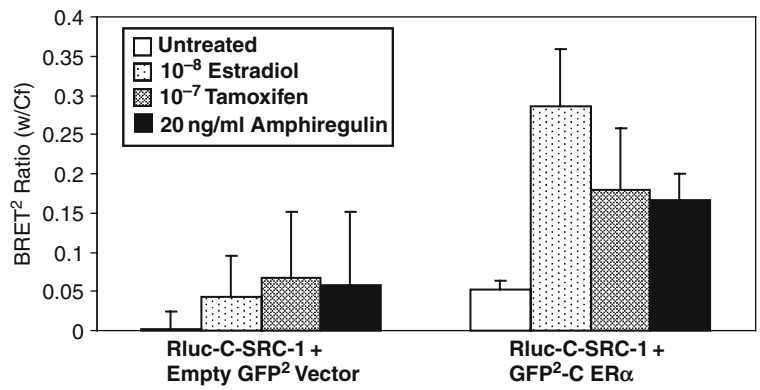

Fig. 16.3. Recruitment of SRC-1 to ERα as assessed by BRET^2. To determine the ligand-dependent and ligand-independent recruitment of SRC-1 to ERα, HEK-293 cells were transfected with 10 μg of Rluc-C-SRC-1 in combination with an empty GFP^2 vector or GFP^2-C-ERα and treated for 30 min with 10^{-8}M estradiol, 10^{-7}Tamoxifen or 20 ng/ml Amphiregulin.

Table 16.4
Example of BRET^2 data analysis showing the calculation of the BRET^2 Ratio for the interaction of SRC-1 and ERα. The numbers used in the calculations were obtained from Tables 2-3.

	Untreated			E2			Tam			rhAR		
	1	2	3	1	2	3	1	2	3	1	2	3
Rluc-C-SRC-1 alone	0.022	0.036	0.029	0.033	0.019	0.047	0.055	0.016	-0.072	0.125	-0.477	0.007
Rluc-C-SRC-1 + GFP^2-C Vector	-0.020	0.027	-0.003	0.083	-0.015	0.063	0.160	-0.005	0.046	-0.010	0.015	0.166
Rluc-C-SRC-1 + GFP^2-C-ERα	0.045	0.065	0.050	0.161	0.017	0.083	0.168	0.022	0.048	0.028	0.087	0.085

4. Notes

1. Aprotinin is a proteases inhibitor used in the sample buffer to preserve phosphorylated residues which may be important in protein−protein interactions. Aprotinin is added to the BRET^2 buffer, prior to use every time.
2. A black Optiplate is used so that the fluorescent signal may be observed.
3. The FLUOStar Optima from BMG Labtech is a dual fluorescence/luminescence microplate reader. Since application of the BRET^2 assay requires fluorescence and luminescence measurements, a plate reader with both capabilities is ideal. Separate instruments can also be used as an alternative. Examples of other dual fluorescence/luminescence microplate readers include POLARstar Optima (BMG Labtech), VICTOR Light (PerkinElmer), and Mithras LB 940 (Berthold Technologies).
4. DeepBlueC is toxic. Suitable protective clothing and gloves must be worn while handling.
5. When generating fusion constructs the stop codon at the end of the protein of interest must be removed so that a single fusion protein is expressed. Labeling of proteins of interest should be validated using expression assays comparing wild type versus labeled proteins.
6. The exact cell number to be plated will vary depending on cell doubling time, size, and transfection system used. Cells with stably transfected fusion proteins may also be used.
7. Use an empty GFP^2 vector when transfecting the Rluc protein alone to keep DNA concentrations constant.
8. A GFP^2 alone transfected group or untransfected group is an acceptable negative control. BRET^2 positive control proteins include a recombinant protein consisting of a GFP^2 molecule directly fused to an Rluc moiety.
9. Titration of GFP^2 and Rluc fusion proteins should be performed to obtain the BRET^{2}ratio. Excessive expression of the Rluc fusion protein will contribute to a decrease in the BRET^2 signal. It is more desirable to express higher levels of the GFP^2 fusion protein relative to the Rluc fusion protein.
10. To further optimize the BRET^2 signal, alter the number of cells assayed. Using the optimized transfection ratio, titrate the number of cells from 50,000 to 200,000 cells/well.
11. Volumes are included throughout this section to obtain a final reaction volume of 70 µl in a 96-well plate. Volumes

may be adjusted according to the size of the wells and optimal volume per well for the individual instrument used to read the $BRET^2$ signal.

12. Substitute a zero value for calculated $BRET^2$ ratios that are less than zero.

Acknowledgments

Financial Support: This project was supported by R01DK068432 and a grant from the Louisiana Cancer Research Consortium to BGR, and by an individual NRSA 1F31CA126489 and a Graduate Alliance for Education in Louisiana (GAELA) Fellowship to TTD.

References

1. Lannigan DA. (2003) Estrogen receptor phosphorylation. Steroids; 68(1):1–9.
2. Nilsson S, Makela S, Treuter E, Tujague M, Thomsen J, Andersson G, Enmark E, Pettersson K, Warner M, Gustafsson. J A (2001). Mechanisms of estrogen action. Physical Rev; **81**:1535–1565.
3. Duan R, Porter W, Safe S. (1998) Estrogen -induced c-fos protooncogene expression in MCF-7 human breast cancer cells – role of estrogen receptor SP1 complex formation. Endocrinology; 139(4):1981–1990.
4. Kelley KM, Rowan BG, Ratnam M. (2003) Modulation of the Folate Receptor alpha Gene by the Estrogen Receptor: Mechanism and Implications in Tumor Targeting. Cancer Res; 63(11):2820–2828.
5. Sun GL, Porter W, Safe S. (1998) Estrogen-induced retinoic acid receptor alpha-1 gene expression – role of estrogen receptor SP1 complex. Mol Endocrinol; 12(6):882–890.
6. Webb P, Lopez GN, Uht RM, Kushner PJ. (1995) Tamoxifen activation of the estrogen receptor/AP-1 pathway: potential origin for the cell-specific estrogen-like effects of antiestrogens. Mol Endocrinol; 9(4):443–456.
7. Stein B, Yang MX. (1995) Repression of the interleukin-6 promoter by estrogen receptor is mediated by NF-kappa B and C/EBP beta. Mol Cell Biol; 15(9):4971–4979.
8. Blobel GA, Sieff CA, Orkin SH. (1995) Ligand-dependent repression of the erythroid transcription factor GATA- 1 by the estrogen receptor. Mol Cell Biol; 15(6):3147–3153.
9. Pfleger KD, Seeber RM, Eidne KA. (2006) Bioluminescence resonance energy transfer (BRET) for the real-time detection of protein–protein interactions. Nat Protoc; 1(1):337–345.

Chapter 17

Detection of Proteins Sumoylated In Vivo and In Vitro

Kevin D. Sarge and Ok-Kyong Park-Sarge

Abstract

Small ubiquitin-related modifier (SUMO) is an ubiquitin-like protein that is covalently attached to a variety of target proteins. Unlike ubiquitination, sumoylation does not target proteins for proteolytic breakdown, but is instead involved in regulating multiple protein functional properties including protein–protein interactions and subcellular targeting, to name a few. Protein sumoylation has been particularly well characterized as a regulator of many nuclear processes as well as nuclear structure, making the characterization of this modification vital for understanding nuclear structure and function. Consequently, there has been intense interest in identifying new proteins that are targets of this modification and determining what role it plays in regulating their functions. This chapter presents methodologies for determining whether a particular protein is a substrate of sumoylation, and for identifying the lysine residue(s) where the modification occurs.

Key words: Sumoylation, SUMO, SUMO-1, testis, ovary, spermatogenesis, ubc9, HSF1, HSF2.

1. Introduction

Small ubiquitin-related modifier (SUMO) was discovered as a modifier of mammalian proteins in 1997 (1, 2). SUMO has since been demonstrated to be a modifier of many important proteins, giving this modification a vital role in modulating a large number of important cellular processes (3–5). SUMO proteins are very similar to ubiquitin structurally, but sumoylation does not promote degradation of proteins and instead regulates key functional properties of target proteins. These properties include subcellular localization, protein partnering, and transactivation functions of transcription factors, among others (3–5). Protein sumoylation plays a particularly vital role in regulating many important processes

O.-K. Park-Sarge, T.E. Curry, Jr. (eds.), *Molecular Endocrinology,* Methods in Molecular Biology 590,
DOI 10.1007/978-1-60327-378-7_17,

occurring in the nucleus, and although sumoylation can be found on proteins that exist in a number of cellular compartments, most of the sumoylation characterized to date occurs on nuclear proteins (3–5). Indeed, proteins of the SUMO conjugation machinery have been found to be localized to nuclear pore complexes, in addition to other locations in the nucleus.

Sumoylation in the testis and ovary has only relatively recently begun to be investigated, but results already suggest that this post-translational modification plays an important role in the regulation and function of both female and male reproductive tissues. For example, sumoylation has been indicated to be important for regulating granulosa cell apoptosis during the differentiation of these cells (6). The existence of a functional connection between SUMO and the progesterone receptor has been suggested as it plays a role in progesterone receptor actions in the ovary (7). Sumoylation has been linked to XY body structure and function, heterochromatin organization, centromere function, and the expression of genes during spermatogenesis (8–10). A number of steroid receptors, including estrogen, progesterone, and androgen receptors have also been shown to be regulated by sumoylation, supporting the likely broad importance of this post-translational modification for proper control of reproductive processes in both females and males (11–13).

SUMO proteins are covalently attached to lysine residues of proteins, which are generally found within the consensus motif ΨKXE where Ψ is a hydrophobic amino acid and X is any residue. Like ubiquitination, the covalent attachment of SUMO to other proteins involves a series of enzymatic steps (**Fig. 17.1**), but the proteins involved are distinct from those in the ubiquitin conjugation pathway. First, the SUMO proteins have to undergo proteolytic processing near their C-terminal end to form the mature proteins, a step which is performed by SUMO proteases (Ulp's). These proteases are dual-functional, as they are also responsible for cleaving SUMO groups from substrate proteins by cleaving the isopeptide bonds by which they are joined (3–5, 14). The mature processed SUMO protein is covalently attached via a thioester bond to the SAE2 (Uba2) subunit of the heterodimeric SUMO E1 activating enzyme in an ATP-dependent reaction (15–18). The SUMO moiety is transferred from the E1 to ubc9, the SUMO E2 enzyme, which then binds to the ΨKXE consensus sequence in target proteins and forms an isopeptide bond between the ε-amino group of the lysine within this sequence and the carboxyl group of the C-terminal glycine of the SUMO polypeptide (19–22). SUMO E3 proteins have been identified that enhance the efficiency of SUMO attachment by interacting with both ubc9 (the E2 enzyme) and the substrate, thereby acting as bridging factors (3–5). Vertebrate cells contain three SUMO paralogs. SUMO-2

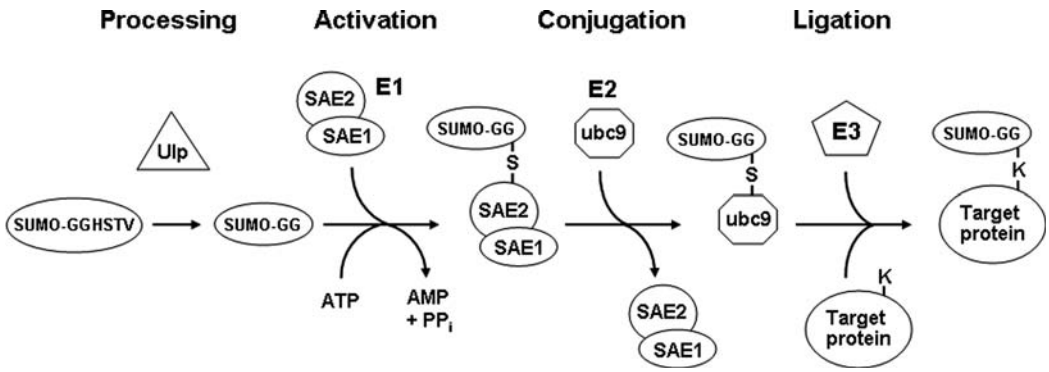

Fig. 17.1. The SUMO conjugation pathway. After they are translated, SUMO proteins must first be processed by a SUMO protease such as Ulp1, which removes four C-terminal residues so that the mature form ends with a glycine. These SUMO proteases are also responsible for removing SUMO groups from proteins. This mature form is then activated in an ATP-dependent manner by forming a thioester bond with a cysteine residue in the SAE2 subunit of the heterodimeric E1 activating enzyme. Following this activation step, the SUMO moiety is transferred to the E2 conjugating enzyme ubc9. In the final step SUMO is transferred in a ligation reaction from ubc9 to substrate proteins, forming an isopeptide bond between the terminal glycine on SUMO and the ε-amino group of a lysine in the target protein. The efficiency of sumoylation of some proteins is enhanced by SUMO ligase E3 proteins, via their ability to bind both ubc9 and the target protein, thereby increasing the kinetics of the SUMO transfer.

and SUMO-3 are very similar to each other in sequence, and have approximately 50% sequence identity with SUMO-1, which is the best characterized of the three vertebrate SUMO proteins.

In this chapter we describe two different experimental approaches for determining whether a specific protein is sumoylated. The first method employs immunoprecipitation of the protein of interest, either endogenous or transfected epitope-tagged protein, followed by Western blot with SUMO antibodies. The second method involves incubating the protein, either as a ^{35}S-labeled in vitro translation product or purified recombinant protein, with a reconstituted in vitro sumoylation enzymatic reaction, followed by SDS-PAGE and autoradiography or Western blot, respectively, to look for the appearance of higher molecular weight bands indicative of sumoylation. By comparing wild-type protein constructs with those containing non-sumoylatable arginine substitutions of candidate target lysine residues, these protocols can also allow identification of those lysine residues where SUMO attachment actually occurs in a given protein. This information then provides the critical reagents for testing the functional consequences of blocking sumoylation of that particular protein. To illustrate the types of data that can be obtained using these methodologies, we present figures showing the results of immunoprecipitation and in vitro sumoylation analyses of a transcription factor, heat shock transcription factor-2 (HSF2).

2. Materials

2.1. Detection of Sumoylated Proteins by Immunoprecipitation Analysis

1. Cells expressing the protein of interest.
2. Phosphate-Buffered Saline (PBS): 137 mM NaCl, 2.7 mM KCl, 4.3 mM Na_2HPO_4, and 1.5 mM KH_2PO_4.
3. Lysis solution: 0.15 M Tris-HCl, pH 6.7, 5% SDS, and 30% glycerol.
4. N-ethylmaleimide.
5. Complete protease inhibitor (Roche; Indianapolis, IN).
6. Protein G-sepharose or protein A-sepharose.
7. Primary antibody capable of immunoprecipitating protein of interest (or against epitope tag if analyzing a transfected tagged protein), species-matched non-specific IgG, and antibodies against SUMO-1, SUMO-2, or SUMO-3 (Invitrogen).
8. 2x SDS sample buffer: 125 mM Tris-HCl, pH 6.7, 4% SDS, 20% glycerol, 0.2 M dithiothreitol, and 0.01% bromophenol blue.
9. 4x SDS sample buffer: 250 mM Tris-HCl, pH 6.7, 8% SDS, 40% glycerol, 0.4 M dithiothreitol, and 0.02% bromophenol blue.
10. Polyacrylamide gel electrophoresis equipment and SDS-PAGE solutions.
11. Reagents for immunoblotting and detection (non-fat dried milk for blocking, and ECL or other detection system).

2.2. Detection of Sumoylated Proteins by In Vitro Sumoylation Analysis

1. Plasmid containing open reading frame of protein of interest oriented to be expressed from a T7 promoter in the vector.
2. pGEX-SUMO-1, pQE30-SUMO-1, pGEX-Ubc9, and pGEX-SAE2/SAE1 bicistronic expression construct, or purified SUMO, ubc9, SAE1/SAE2 available commercially (e.g., LAE Biotech International).
3. Ampicillin and LB media.
4. IPTG (isopropyl-β-D-thio-galactopyranoside).
5. PMSF (phenylmethylsulfonyl fluoride).
6. Glutathione-agarose and Ni-NTA-agarose.
7. In vitro translation kit (e.g Promega TNT T7 Quick for PCR DNA kit).
8. 10x sumoylation buffer: 500 mM Tris-HCl (pH 7.6), 500 mM KCl, 50 mM $MgCl_2$, 10 mM DTT, and 10 mM ATP.
9. Creatine phosphokinase.

10. Creatine phosphate.
11. Inorganic pyrophosphatase.
12. Purified SAE1/SAE2 heterodimer (E1) (AEI international).
13. Purified ubc9 (E2).
14. Purified 6xHis-SUMO-1.
15. French press (Thrermo Scientific).
15. Polyacrylamide gel electrophoresis equipment and SDS-PAGE solutions.
16. Whatman paper, X-ray film, and cassettes for detection of ^{35}S-labeled proteins in sumoylation reaction.
17. Quickchange Site Directed Mutagenesis Kit (Stratagene).

3. Methods

3.1. Detection of Sumoylated Proteins by Immunoprecipitation Analysis

In this protocol, proteins to be tested for sumoylation are immunoprecipitated using lysis buffers designed to block the action of desumoylating enzymes (*see* **Note 1**) and then subjected to Western blot analysis using anti-SUMO antibodies to look for the appearance of a band with a size consistent with a sumoylated form of the protein. Although the theoretical molecular weight of the SUMO proteins is approximately 11 kDa, the size increase for each SUMO added on SDS-PAGE is typically in the range of 15–17 kDa. In the case of a protein with multiple sumoylation sites, or where SUMO chains form on a lysine target site (see **Note 2**), multiples of this size increase are expected, sometimes yielding very large shifts in mobility. Multiple bands representing different sumoylation states of the protein are also possible. This approach can be used to analyze endogenous proteins, or transfected proteins containing an epitope tag (FLAG, myc, etc.) (*see* **Note 3**). The transfection approach can also be used to determine the lysine residue(s) to which the SUMO group is attached, by comparing the sumoylation of wildtype constructs to ones in which candidate lysines have been changed to non-sumoylatable arginines. Two different lysis conditions are described, one using SDS to inhibit desumoylase enzymes and the other containing N-ethylmaleimide, a chemical inhibitor of these enzymes.

1. Tissue culture cells are grown in media appropriate for that cell line or primary cell type, and typically at least 1×10^6 cells are needed for each immunoprecipitation.
2. For harvesting place the plate of cells on ice, remove media by aspiration and add 1 ml of ice-cold PBS to the plate. Scrape cells off plates with a cell scraper, transfer to a 1.5 ml microcentrifuge tube.

3. Collect cells by centrifugation at 13,000*g* for 30 s at room temperature, and remove supernatant by aspiration.
4. Lyse cells in 150 µl of lysis solution, which is then diluted 1:10 in PBS/0.5% NP40 plus complete protease inhibitor (Roche). If the lysate is highly viscous, perform sonication until viscosity is reduced. Centrifuge the lysates at 16,000*g*, 10 min, 4°C to remove cellular debris. Alternatively, the cells can be lysed in any of the standard immunoprecipitation lysis buffers (e.g., RIPA, etc.) known to extract the protein of interest, provided the lysis solution is supplemented with 20 mM N-ethylmaleimide (desumoylase inhibitor, freshly dissolved).
5. While the cell lysate is being centrifuged, prepare 30 µl of 50% protein G-Sepharose (or protein A-sepharose if that is preferential for the particular antibody) as per manufacturer's instructions. After protein G-Sepharose has been prepared add the above cell lysate to the protein G-Sepharose and rotate at 4°C for 30 min to preclear the lysates to reduce non-specific binding.
6. Pellet the protein G-Sepharose by centrifugation (16,000*g*, 20 s, 4°C) and transfer the supernatant to a new tube. At this point take 30 µl of the supernatant, place in a separate tube with 10 µl 4x SDS sample buffer and label "input."
7. Divide the remainder of the supernatant into two equal amounts in separate 1.5 ml centrifuge tubes. To one of the tubes add a sufficient amount of primary antibody and to the other tube add a species-matched non-specific IgG. Place samples on rotator at 4°C for 1 h after which add 20 µl of protein G-Sepharose that has been washed with PBS, and rotate at 4°C for 3 hours.
8. Collect beads by centrifugation (16,000*g*, 10 s, 4°C) and discard supernatant.
9. Wash the beads 4 times with PBS/0.5% NP40 plus complete protease inhibitor, or other lysis buffer if another was chosen, collecting the beads by centrifugation after each wash (16,000*g*, 10 s, 4°C). Add 30 µl 2x SDS sample buffer to beads after removing supernatant from final wash.
10. Boil the samples for 5 min and separate on SDS-PAGE gel. Separate immunoprecipitated proteins by SDS-polyacrylamide gel electrophoresis.
11. Transfer proteins to nitrocellulose or nylon membrane and subject to Western blotting using antibodies against SUMO-1, SUMO-2, or SUMO-3 (commercially available). This methodology can also be used to examine the sumoylation state of an epitope-tagged version of the protein of interest being expressed

in transfected cells (*see* **Note 3**). The results of immunoprecipitation analysis to examine sumoylation of the HSF2 protein in HeLa cell extracts is shown in **Fig. 17.2**.

Fig. 17.2. Detection of sumoylation by immunoprecipitation/SUMO-1 Western blot. HSF2 protein was immunoprecipitated from extracts of HeLa cells followed by Western blot using anti-SUMO-1 antibodies. The positions of molecular weight standards are indicated on the left side of the panel. This figure is from our published work (24), used with permission.

3.2. In Vitro Sumoylation Assay

In this protocol the protein of interest is in vitro translated (typically with ^{35}S-methionine incorporation) and then incubated in a reaction containing the SUMO E1 and E2 enzymes and SUMO-1, followed by SDS-PAGE and autoradiography to determine whether a lower mobility band appears that would be consistent with a sumoylated form of the target protein. Because of the high concentrations of SUMO E1 and E2 enzymes used in this in vitro sumoylation reaction, the need for SUMO E3 proteins is diminished and thus sumoylation can be detected without their addition. Performing the in vitro sumoylation reaction using mutants of the protein in which candidate sumoylation site lysine residues are changed to non-sumoylatable arginines can be used to determine the site(s) at which SUMO attachment is occurring. The expression and purification of the recombinant proteins required for the in vitro sumoylation assay is described in subheadings 3.2.1, and the protocol for performing assay itself is described in subheading 3.2.3.

3.3. Expression of Recombinant SUMO, ubc9 (SUMO E2), and SAE1/SAE2 (SUMO E1) Heterodimer

The SUMO proteins are expressed and purified as fusion proteins with GST or 6xHis at the N-terminal end of the SUMO proteins, and these affinity tags do not need to be removed prior to using these SUMO proteins for the sumoylation reaction. The size difference of GST-SUMO vs. 6xHis-SUMO can also provide a useful control for the sumoylation reaction as it yields a predictable size difference between the sizes of the sumoylation products

(e.g. *see* **Fig. 17.3**). The SUMO E1 is a heterodimer of SAE1/SAE2, and is active when expressed in *E. coli* from a bicistronic construct of GST-SAE2 and untagged SAE1; the two proteins complex can be purified using glutathione-agarose affinity chromatography (23). The SUMO E2 can be expressed which appears to be more active, at least in our hands when the GST tag is removed by thrombin cleavage. The following is the general protocol for expressing and purifying these recombinant proteins needed for the in vitro sumoylation assay. Once purified these recombinant proteins can be stored at −80°C for extended periods of time.

1. Transform expression construct into DH10B *E. coli* cells using standard molecular biology methods.
2. Plate cells on LB plates containing ampicillin and incubate overnight at 37°C.
3. Select single colonies and grow overnight at 37°C in LB media containing ampicillin.
4. Inoculate individual liters of LB containing ampicillin with aliquots (5 mL) of overnight culture and grow cells to an $O.D._{600\ nm}$= 0.6–0.8.
5. Induce the cells with IPTG (1 mM) for 3 hours.
6. After 3 h induction harvest cells by centrifugation (4,000*g*, 5 min, 4°C) and resuspend pellet in PBS (4°C) then repellet cells. At this point the cell pellet can be extracted or stored at −80°C.
7. To extract protein from the cells they are resuspended in PBS (4°C) with PMSF (phenylmethylsulfonyl fluoride) to a final concentration of 1 mM.
8. Pass cells through a French press at 10,000 to 14,000 psi, and repeat to ensure complete lysis.
9. Centrifuge the cell lysate (30,000*g*, 1 h, 4°C) and retain the supernatant.
10. Purify proteins using standard nondenaturing affinity chromatography techniques suitable for their fusion tags (glutathione agarose affinity chromatography for GST-fusion proteins and Ni-NTA-agarose affinity chromatography for 6xHis-fusion proteins).
11. Check purified proteins by Coomassie blue staining of a SDS-PAGE gel (GST-SUMO-1 = 38 kDa, GST-Ubc9 = 44 kDa, and 6xHis-SUMO-1 = 14 kDa).
12. For the in vitro sumoylation assay the GST-Ubc9 needs to be thrombin cleaved to remove the GST-tag. This can be done following manufacturer's protocols. Check thrombin cleavage of GST-Ubc9 by Coomassie staining of a SDS-PAGE gel (Ubc9 = 18 kDa).

3.4. In Vitro Sumoylation of Rabbit Reticulocyte System Translated Proteins

The in vitro sumoylation assay uses ^{35}S-methionine radiolabeled protein as the substrate. We generate radiolabeled protein using the TNT T7 Quick for PCR DNA kit following the manufacturers instructions. Described below is the SUMO modification procedure to be utilized with radiolabeled translated proteins.

1. Translate target protein fresh before each sumoylation assay following the manufacturer's instructions. Place freshly translated protein on ice until step 3.
2. For each sumoylation reaction prepare a mixture containing the following (on ice): 1 µl 10x sumoylation buffer, 0.4 units creatine phosphokinase, 10 mM creatine phosphate, 0.6 units inorganic pyrophosphatase, 100 ng purified SAE1/SAE2 heterodimer (E1), 400 ng purified ubc9 (E2), 1 µg purified 6xHis-SUMO-1, and H_2O to 10 µl. As a negative control, make another mix identical to the one above except that it lacks SUMO protein. If desired a third mix can be made in which GST-SUMO-1 is added instead of 6xHis-SUMO.
3. Set up the reactions (no SUMO control, +6xHis-SUMO, and +GST-SUMO) by adding 2 µl in vitro translated protein to the 10 µl reaction mixes, and then incubate at 37°C for 1 h.
4. Terminate the reaction by adding 12 µl 2x SDS sample buffer. Store at −20°C until gel electrophoresis.
5. Boil the samples for 5 min and separate on SDS-PAGE gel. After electrophoresis the gel is fixed for 10 min in SDS-PAGE fixing solution (50% methanol/10% acetic acid), then dried on Whatman paper, and finally placed on x-ray film. ^{35}S emissions are low energy and so it is advisable not to leave plastic wrap between the dried gel and the X-ray film if possible, as this can increase the required exposure times.
6. One important experiment to do to give confidence in the in vitro sumoylation assay is to do a reconstitution test where each of the components required for sumoylation (E1, ubc9, SUMO-1) are individually left out of the reaction and compared to a reaction where all components are present (**Fig. 17.3A).** As shown in this figure, such an experiment can also reveal the relative efficiency of sumoylation of your target protein by different SUMO proteins (e.g., SUMO-1 vs. SUMO-2). Another experiment which increases confidence that your protein is indeed being sumoylated vs. being targeted by some other modification is to compare the effect of using of 6xHis-SUMO vs. GST-SUMO as the donor SUMO, because this gives a predictable size shift between the sumoylated reactions (**Fig. 17.3B).**
7. To identify the sumoylation site in the protein of interest site directed mutagenesis is done to change candidate lysine (changed to arginine) in the sumoylation consensus sequence

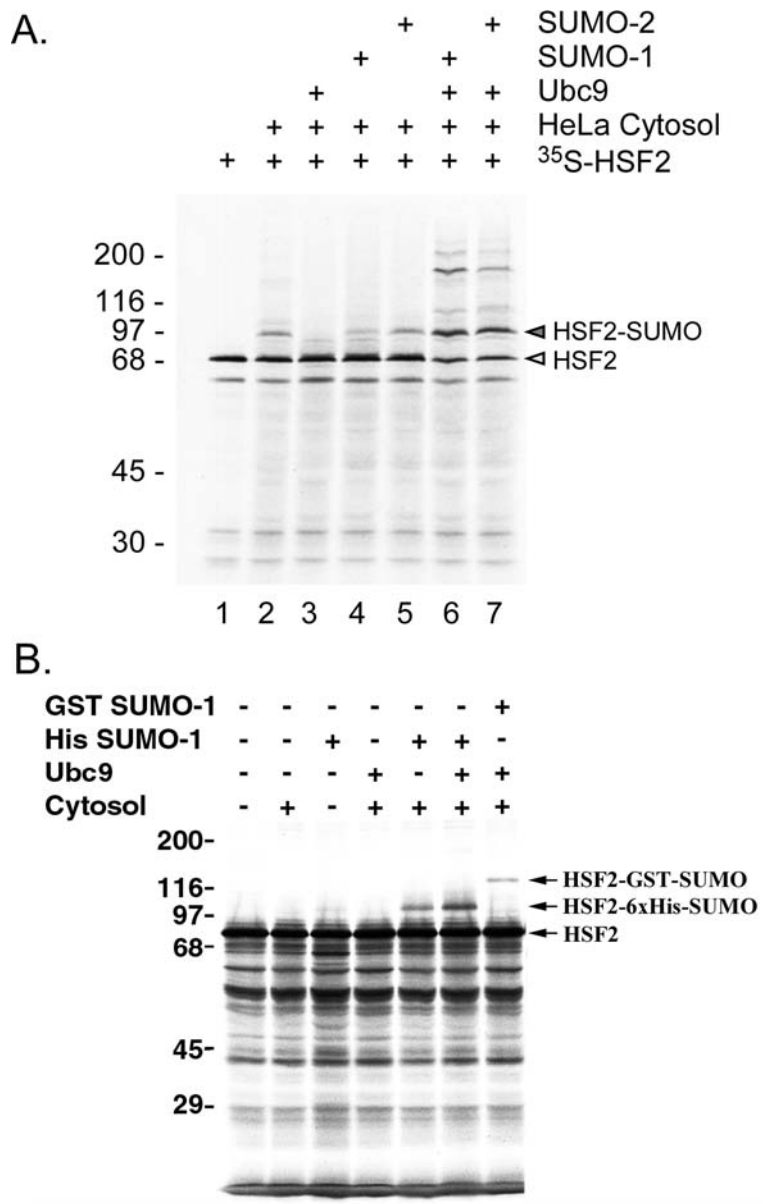

Fig. 17.3. Analysis of SUMO-1 modification by reconstituted in vitro sumoylation reaction. (**A**) In vitro translated ^{35}S-labeled HSF2 protein was incubated with HeLa cytosol (as a source of E1), Ubc9, SUMO-1, SUMO-2 or with various combinations of each of these, and then subjected to SDS-PAGE followed by autoradiography. The positions of unmodified and SUMO-modified HSF2 are indicated to the right of the panel. (**B**) In vitro translated ^{35}S-labeled HSF2 protein was subjected to the in vitro SUMO-1 modification assay using either 6xHis-SUMO-1 or GST-SUMO-1 as the SUMO-1 substrate for the reaction. This figure is from our published work (24), used with permission.

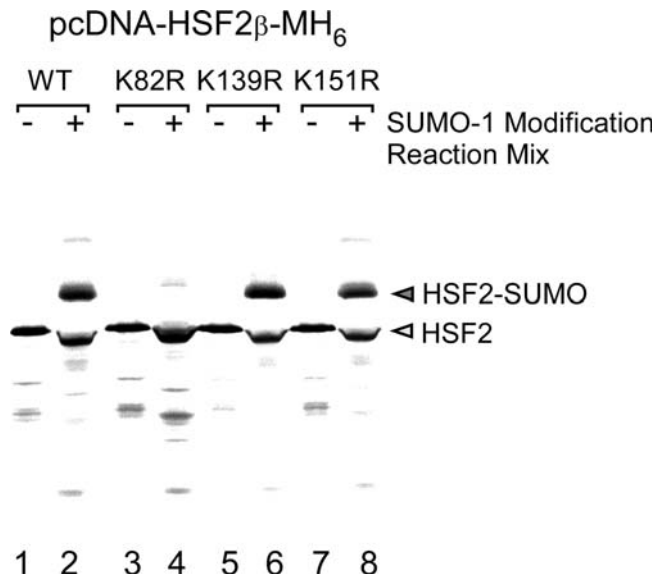

Fig. 17.4 In vitro translated ^{35}S-labeled wild-type HSF2 protein and the HSF2 SUMO-1 consensus site mutants K82R, K139R, and K151R were used as substrates for in vitro SUMO-1 modification reactions. The positions of unmodified and SUMO-modified HSF2 proteins are indicated to the right of the panel. This figure is from our published work (24), used with permission.

(ΨKXE) to non-sumoylatable arginine residues utilizing protocols such as the Quickchange Site Directed Mutagenesis Kit. The extent of sumoylation of the wild type vs. lysine-to-arginine mutant can then be compared using either the transfection/immunoprecipitation approach or the in vitro sumoylation assay. Results of such an experiment using the in vitro sumoylation assay are shown in **Fig. 17.4**.

4. Notes

1. SUMO-modified proteins are highly susceptible to SUMO proteases. The SDS in the lysis buffer described in this protocol inactivates the SUMO proteases allowing for easier detection of sumoylated proteins. However, a common complication with the SDS-lysis method is that the cell lysates tend to be very viscous and sticky due to genomic DNA in the lysate. This problem is remedied by brief sonication which shears the DNA and makes the samples easier to manipulate. SUMO proteases can also be inhibited by the addition isopeptidase inhibitor N-ethylmaleimide (20 mM) to standard lysis buffers such as

NP-40 lysis buffer (50 mM Tris-HCl, pH 8.0, 150 mM NaCl, 1% NP-40) if another lysis buffer besides the SDS-lysis is more desirable.

2. The size of putative sumoylated forms of a protein on SDS-PAGE will depend on how many different SUMO attachment sites the protein has. In addition, SUMO-2 and SUMO-3 have been reported to form polymeric chains reminiscent of ubiquitin, which could result in large increases in size for a sumoylated protein on SDS-PAGE compared to the non-sumoylated form (23). Thus, it is possible to observe bands that are multiples of the approximate 15–17 kDa size of each SUMO unit, as well as multiple bands representing different sumoylation states.
3. Investigating sumoylation may also be done using cells transfected with fusion-tagged plasmid constructs of the protein thought to be sumoylated with immunoprecipitation utilizing fusion tag antibodies which are available from commercial sources (e.g., GFP, FLAG, Myc, and 6xHis tags). In these types of experiments it is advisable to co-transfect the cells with a SUMO expression construct (often this is epitope-tagged) to ensure that sufficient SUMO protein is present in the transfected cells to allow for efficient sumoylation of the transfected target protein being tested.

Acknowledgments

We are very grateful to Mike Matunis (Johns Hopkins), Ron Hay (University of Dundee), and Chris Lima (Sloan Kettering Institute) for providing constructs and reagents.

References

1. Mahajan, R., Delphin, C., Guan, T., Gerace, L., and Melchior, F. (1997) A small ubiquitin-related polypeptide involved in targeting RanGAP1 to nuclear pore complex protein RanBP2. *Cell* **88**, 97–107.
2. Matunis, M. J., Wu, J., and Blobel, G. (1998) SUMO-1 modification and its role in targeting the Ran GTPase-activating protein, RanGAP, to the nuclear pore complex. *J. Cell Biol.* **140**, 499–509.
3. Geiss-Friedlander, R., and Melchior, F. (2007) Concepts in sumoylation: a decade on. *Nat. Rev. Mol. Cell Biol.* **8**, 947–956.
4. Kerscher, O., Felberbaum, R., and Hochstrasser, M. (2006) Modification of proteins by ubiquitin and ubiquitin-like proteins. *Ann. Rev. Cell Dev. Biol.* **22**, 159–180.
5. Hay, R. T. (2005) SUMO: a history of modification. *Mol. Cell* **18**, 1–12.
6. Shao, R., Rung, E., Weijdegard, B., and Billig, H. (2006) Induction of apoptosis increases SUMO-1 protein expression and conjugation in mouse periovulatory granulosa cells in vitro. *Mol. Reprod. Dev.* **73**, 50–60.
7. Shao, R., Zhang, F. P., Rung, E., Palvimo, J. J., Huhtaniemi, I., and Billig, H. (2004)

Inhibition of small ubiquitin-related modifier-1 expression by luteinizing hormone receptor stimulation is linked to induction of progesterone receptor during ovulation in mouse granulosa cells. *Endocrinology* **145**, 384–392.

8. Rogers, R. S., Inselman, A., Handel, M. A., and Matunis, M. J. (2004) SUMO modified proteins localize to the XY body of pachytene spermatocytes. *Chromosoma* **113**, 233–243.
9. Vigodner, M., and Morris, P. L. (2005) Testicular expression of small ubiquitin-related modifier-1 (SUMO-1) supports multiple roles in spermatogenesis: silencing of sex chromosomes in spermatocytes, spermatid microtubule nucleation, and nuclear reshaping. *Dev. Biol.* **282**, 480–492.
10. Vigodner, M., Ishikawa, T., Schlegel, P. N., and Morris, P. L. (2006) SUMO-1, human male germ cell development, and the androgen receptor in the testis of men with normal and abnormal spermatogenesis. *Am. J. Physiol. Endocrinol. Metab.* **290**, E1022–1033.
11. Wu, F., and Mo, Y. Y. (2007) Ubiquitin-like protein modifications in prostate and breast cancer. *Front. Biosci.* **12**, 700–711.
12. Duma, D., Jewell, C. M., and Cidlowski, J. A. (2006) Multiple glucocorticoid receptor isoforms and mechanisms of post-translational modification. *J. Steroid. Biochem. Mol. Biol.* **102**, 11–21.
13. Faus, H., and Haendler, B. (2006) Post-translational modifications of steroid receptors. *Biomed. Pharmacother.* **60**, 520–528.
14. Mukhopadhyay, D., and Dasso, M. (2007) Modification in reverse: the SUMO proteases. *Trends Biochem. Sci.* **32**, 286–295.
15. Johnson, E. S., Schwienhorst, I., Dohmen, R. J., and Blobel, G. (1997) The ubiquitin-like protein Smt3p is activated for conjugation to other proteins by an Aos1p/Uba2p heterodimer. *EMBO J.* **16**, 5509–5519.
16. Desterro, J. M., Rodriguez, M. S., Kemp, G. D., and Hay, R. T. (1999) Identification of the enzyme required for activation of the small ubiquitin-like protein SUMO-1. *J. Biol. Chem.* **274**, 10618–10624.
17. Gong, L., Li, B., Millas, S., and Yeh, E. T. (1999) Molecular cloning and characterization of human AOS1 and UBA2, components of the sentrin-activating enzyme complex. *FEBS Lett.* **448**, 185–189.
18. Okuma, T., Honda, R., Ichikawa, G., Tsumagari, N., and Yasuda, H. (1999) In vitro SUMO-1 modification requires two enzymatic steps, E1 and E2. *Biochem. Biophys. Res. Commun.* **254**, 693–698.
19. Desterro, J. M., Thomson, J., and Hay, R. T. (1997) Ubch9 conjugates SUMO but not ubiquitin. *FEBS Lett.* **417**, 297–300.
20. Johnson, E. S., and Blobel, G. (1997) Ubc9p is the conjugating enzyme for the ubiquitin-like protein Smt3p. *J. Biol. Chem.* **272**, 26799–26802.
21. Rodriguez, M. S., Dargemont, C., and Hay, R. T. (2001) SUMO-1 conjugation in vivo requires both a consensus modification motif and nuclear targeting. *J. Biol. Chem.* **276**, 12654–12659.
22. Sampson, D. A., Wang, M., and Matunis, M. J. (2001) The small ubiquitin-like modifier-1 (SUMO-1) consensus sequence mediates Ubc9 binding and is essential for SUMO-1 modification. *J. Biol. Chem.* **276**, 21664–21669.
23. Tatham, M. H., Jaffray, E., Vaughan, O. A., Desterro, J. M., Botting, C. H., Naismith, J. H., and Hay, R. T. (2001) Polymeric chains of SUMO-2 and SUMO-3 are conjugated to protein substrates by SAE1/SAE2 and Ubc9. *J. Biol. Chem.* **276**, 35368–35374.
24. Goodson, M. L., Hong, Y., Rogers, R., Matunis, M. J., Park-Sarge, O. K., and Sarge, K. D. (2001) Sumo-1 modification regulates the DNA binding activity of heat shock transcription factor 2, a promyelocytic leukemia nuclear body associated transcription factor. *J. Biol. Chem.* **276**, 18513–18518.

Chapter 18

Identification of Alternative Transcripts Using Rapid Amplification of cDNA Ends (RACE)

Oladapo Yeku, Elizabeth Scotto-Lavino, and Michael A. Frohman

Abstract

Many organisms, including humans, have many more proteins than are actually coded for by their genes. This discrepancy is partially explained by the existence of alternative transcripts produced by the same gene. Multiple isoforms of the same gene sometimes perform completely different functions, and as such, knowing the sequence of one of the transcripts is not enough. Rapid Amplification of cDNA Ends (RACE) provides an inexpensive and powerful tool to quickly identify alternative transcripts of a gene when the partial or complete sequence of only one transcript is known. In the following sections, we outline details for rapid amplification of 5' and 3' cDNA ends using the "New Race" technique.

Key words: RACE, new RACE, alternative transcripts.

1. Introduction

Great progress has been made in the sequencing and identification of genes in humans and many other organisms. The advent of microarrays and powerful bioinformatic analysis has not only led to the discovery of new genes but has also provided tools for analysis of existing genes (1–3). Full or partial sequences of newly discovered genes can be aligned against entire organism genomes in search of homology or any other clue that can yield insight into the identity or function of the gene. There are instances, however, where bioinformatic data is unavailable or incomplete. In these instances, Rapid Amplification of cDNA Ends (RACE) can be used to identify alternatively initiated, spliced, or terminated products if the full-length sequence or even part of a gene is known (4–6). RACE can be used to amplify

O.-K. Park-Sarge, T.E. Curry, Jr. (eds.), *Molecular Endocrinology,* Methods in Molecular Biology 590,
DOI 10.1007/978-1-60327-378-7_18,

both the 5' and the 3' ends of genes yielding valuable information such as the location of transcription initiation sites, cis-acting elements, and the localization and stability of the transcript. By using 3' and 5' RACE, alternative transcripts of a known gene can be identified in as little as 3 days.

Since the initial description of RACE (7), many labs and commercial companies have adapted and modified the protocol to increase specificity and user friendliness (8–18) (*see* **Note 1**). Amplification of the 5' end can generally be divided into two classifications: classic RACE and "new RACE." The same principles underlie all RACE protocols and they differ only in terms of specificity, ease of use, and cost. While the principles for classic

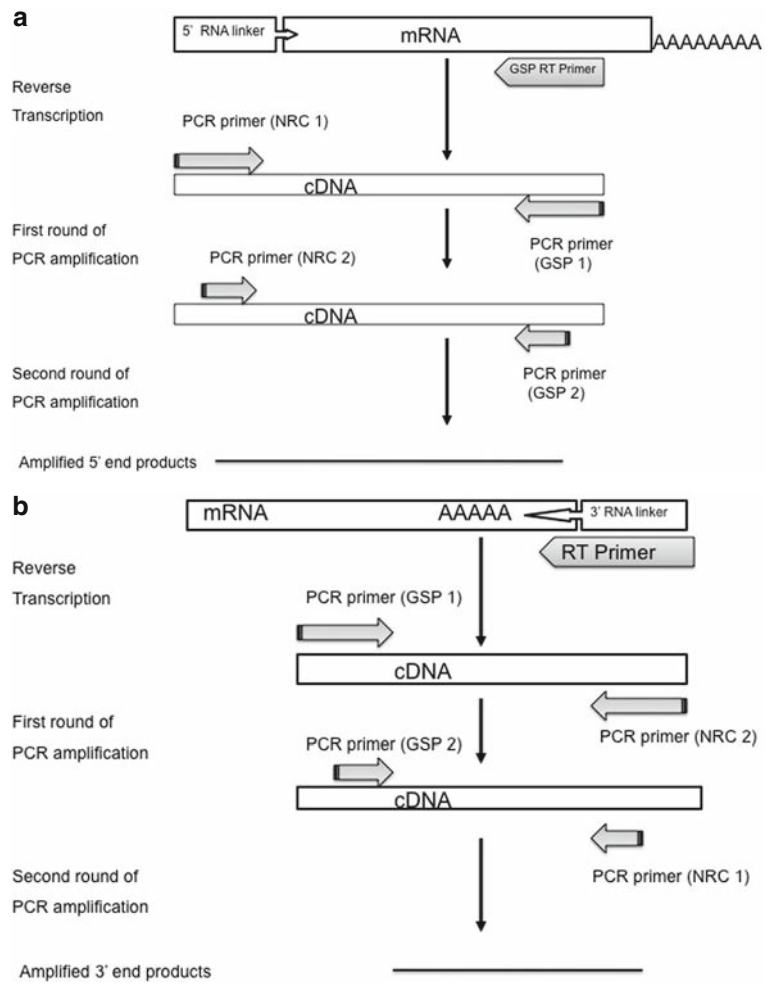

Fig. 18.1. Figure showing the general schematic for Rapid Amplification of cDNA Ends (RACE) starting with an mRNA pool. (a) amplification of the 5' end. See text for full details. (b) amplification of the 3' end. Note that the NRC 1, NRC 2 and NRC 3 primers are the reverse compliments of sequences described in text. RT: Reverse Transcriptase

RACE will be touched on, it has been thoroughly described elsewhere for both 5' (19) and 3' (20) end amplification. This protocol will address the identification of alternative transcripts using the "new RACE" protocol (21).

RACE primarily utilizes RT-PCR (Reverse Transcriptase—Polymerase Chain Reaction) and PCR to amplify the ends of transcripts starting with mRNA and cDNA respectively **(Fig. 18.1)**. In order to perform RACE, the partial or a complete sequence of the mRNA of interest has to be known. This is required to generate the Gene Specific Primers (GSPs) that will be used for the amplifications. A second set of primers that extend from the unknown end of the message back to the known region of the 3' end is provided by the poly (A) tail (or an appended homopolymer), while an appended homopolymer tail is used for the 5' end. Herein lies the first and perhaps most important difference between "classic" and "new" RACE (22, 23). In classic RACE (19), the homopolymer is appended after the mRNA is reverse transcribed, whereas in "new" RACE, the homopolymer is appended before the reverse transcriptase reaction **(Fig.18.2)**. This simple difference eliminates the amplification of non-full length products, which greatly improves the ability to identify transcription start sites. After the mRNA is reverse transcribed to

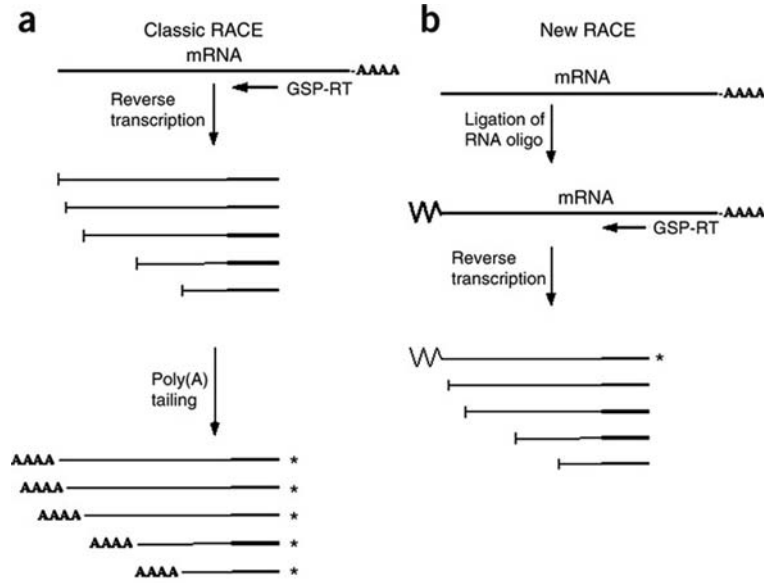

Fig. 18.2. Comparison between "classic RACE" and "New RACE". (a) In "classic RACE", the homopolymer (Poly A tail) is added after the reverse transcription process. This anchor provides specificity for the amplifications downstream of the GSP- reverse transcription step. (b) In "new RACE", the homopolymer is appended before the reverse transcription takes place. This provides ensures full length products from the onset. Figure reproduced from citation 21 (http://www.nature.com/nprot/journal/v1/n6/images/nprot.2006.480-F3.jpg).

cDNA, the 5' and 3' ends are amplified using two nested PCR reactions using gene-specific primers and primers derived from the sequence of the RNA oligonucleotide (appended homopolymer).

The starting mRNA mixture is dephosphorylated with shrimp alkaline phosphatase (SAP). This dephosphorylates degraded and uncapped (non full-length) mRNA's, leaving the full length mRNA's with methylated 'G' caps intact (24). The methylated 'G' cap is then removed with tobacco acid pyrophosphatase (TAP). Treatment with TAP exposes the phosphorylated 5' end of the mRNA and prepares it for ligation to the linker or

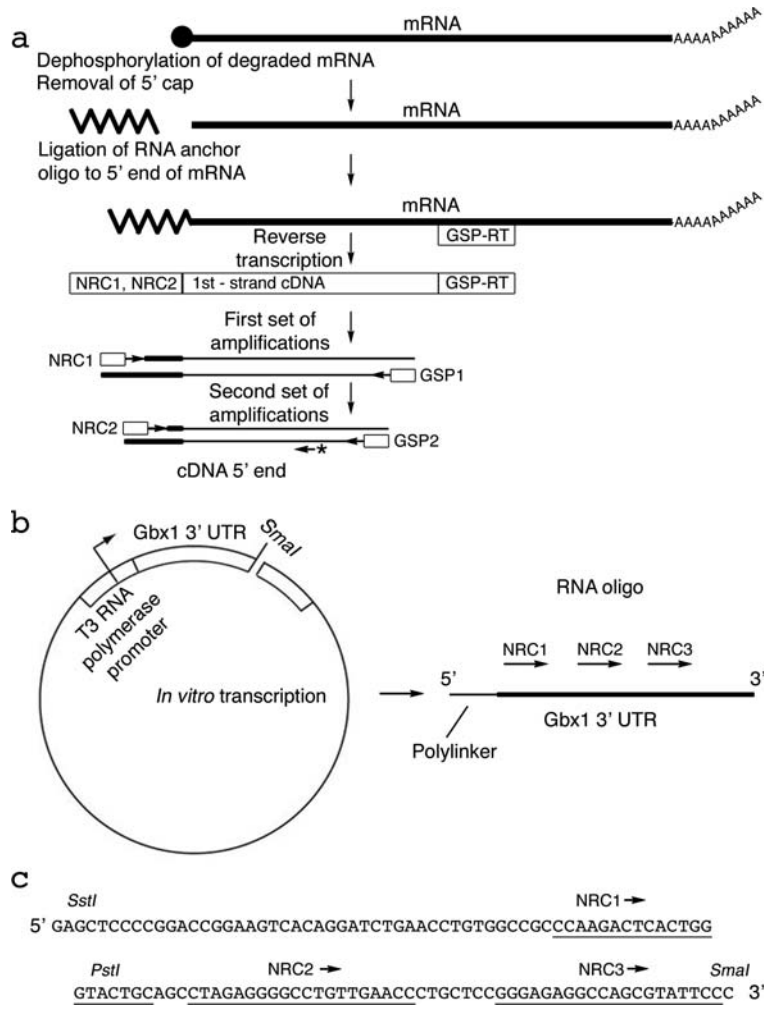

Fig. 18.3. New RACE overview. (a) Outline of steps involved in the amplification of cDNA 5' ends. See text for detailed explanation. (b) Plasmid map and primers used for the example in the text. (c) In vitro transcription of the T3 plasmid in (b) produces a 132-nt product. The sequences for NRC1, NRC2 and NRC3 used for the generation of corresponding primers are underlined. Figure reproduced from citation 21 (http://www.nature.com/nprot/journal/v1/n6/fig_tab/nprot.2006.479_F1.html).

homopolymer. A short synthetic RNA, prepared by in vitro transcription of a linearized plasmid (25), is ligated to the uncapped 5' and 3' end using T4 RNA ligase **(Fig.18.3)**. Degraded or other non-full length mRNA will not be ligated with the synthetic oligonucleotide, since they are dephosphorylated. The mRNA-RNA oligonucleotide hybrids are then reverse-transcribed using a GSP. Full-length cDNA generated from the previous step then contains specific sequences at the 5' and 3' ends that can be used to amplify the full-length cDNA ends. Two nested PCR reactions are used to amplify the full-length cDNA product with high specificity **(Fig.18.3)**.

2. Materials

2.1. DNA/ RNA Purification and Electrophoresis

1. Agarose gel (1%) in TAE buffer.
2. Ethidium bromide.
3. Sodium acetate (3 M, pH 5.2).
4. Phenol/chloroform: 1:1 (vol/vol).
5. Chloroform.
6. Ethanol.
7. Microcon spin filters (Millipore, Billerica, MA).

2.2. Dephosphorylation of Degraded RNA

1. RNA sample (TAP-treated and untreated). All reagents must be RNase free.
2. 10x Phosphatase buffer: 0.1 M Tris-HCl (pH 7.5 at 37°C), 0.1 M $MgCl_2$ and 1 mg/ml BSA.
3. DTT (0.1 M).
4. RNasin (40 U/μl).
5. Shrimp Alkaline Phosphatase SAP (1 U/ml; Fermentas, Glen Burnie, MD).

2.3. Decapping of Intact RNA

1. 10 × Tobacco Acid Pyrophosphatase (TAP) buffer: 0.5 M sodium acetate (pH 6.0), 10 mM EDTA, 1% β-mercaptoethanol, and 0.1% Triton X-100.
2. TAP (5 U/μl; Epicentre, Madison, WI).
3. TE buffer: 10 mM Tris-HCl, pH 7.5, and 1 mM EDTA, pH 8.0.
4. RNA spin column (Qiagen, Valencia, CA).
5. DTT (0.1 M).
6. RNasin (40 U/μl).

2.4. Preparation of RNA Oligonucleotide

1. TE buffer: 10 mM Tris-HCl, pH 7.5, and 1 mM EDTA, pH 8.0.
2. Plasmid template DNA for transcribing RNA oligonucleotide (*see* **Note 2**).
3. Restriction enzymes and buffers.
4. Proteinase K.
5. H_2O treated with diethylpyrocarbonate (DEPC).
6. 5x Transcription buffer.
7. rUTP solution (10 mM).
8. rATP solution (10 mM).
9. rCTP solution (10 mM).
10. rGTP solution (10 mM).
11. DNA-dependent RNA polymerase (20 U/μl).
12. Pancreatic DNase I (RNase-free).
13. 11. DTT (0.1 M).
14. RNasin (40 U/μl).

2.5. RNA Oligonucleotide–Cellular RNA Ligation

1. RNA sample (TAP-treated and untreated).
2. Ligation buffer (10x): 500 mM Tris-HCl, 100 mM $MgCl_2$, 100 mM DTT, 10 mM ATP (pH 7.8 at 25°C) (*see* **Note 3**).
3. RNA oligonucleotide (*see* **Note 4**).
4. ATP (2 mM).
5. T4 RNA ligase (New England BioLabs, Ipswich, MA).

2.6. Reverse Transcription

1. SuperScript II reverse transcriptase (Invitrogen, Carlsbad, CA) and 5x reverse-transcription buffer is supplied with the transcriptase.
2. dNTP solution (containing all four dNTPs, each at 10 mM).
3. Gene-specific antisense primer for 5' end RACE or reverse compliment of NRC3 (New Race Compliment primer) for 3' end RACE (20 ng/μl).
4. RNase H.
5. DTT (0.1 M).
6. RNasin (40 U/μl).
7. TE buffer: 10 mM Tris-HCl, 1 mM EDTA, pH 8.0.

2.7. PCR Amplification

1. 10x Hercules Hot-Start polymerase buffer (Stratagene, La Jolla, CA). Do not add additional nucleotides if they are already contained in the buffer.
2. Hercules Hot-Start polymerase (Stratagene, La Jolla CA). Hot-start protocol is strongly recommended (*see* **Note 5**).

3. User-defined gene-specific oligonucleotide primers GSP1, GSP2, NRC1, and NRC2 to clone the 5' end and the reverse compliment of GSP1, GSP2, NRC1, NRC2, and NRC3 to clone the 3' end (*see* **Note 6** for primer design considerations and **Fig.18.3** for details of primers NRC1 and NRC2).

3. Methods

If large amounts of RNA are used, it is strongly recommended that the quality control steps be performed. Small samples of the RNA can be run on an agarose gel to check for degradation. Aliquots can then be stored at −80°C for future experiments. The quantities presented in this protocol are the ideal amounts of RNA to be used. Reactions can be scaled down in the event that RNA quantities are limited.

3.1. Dephosphorylation of degraded RNA

1. Combine reagents listed in **Table 18.1** in a sterile microfuge tube. Follow the manufacturer's guidelines regarding the use of SAP.
2. The reaction should be incubated for 1 h at 37°C. Dephosphorylation of uncapped mRNA prevents degraded fragments from participating in the subsequent ligation step.
3. Incubate the reaction for 15 min at 65°C to inactivate SAP, then spin briefly in a microcentrifuge. At this point, the products can be stored at −80°C.
4. To visually confirm that the RNA remained intact during the dephosphorylation step, 2 μg (2 μl) of RNA should be analyzed by electrophoresis through a 1% agarose gel (TAE buffer)

Table 18.1
Reaction components for dephosphorylation of degraded RNA

Component	Amount	Final
RNA	50 μg	50 μg
10X phosphatase buffer	5 μl	1x
DTT (0.1 M)	0.5 μl	1 mM
RNasin (40 U ml^{-1})	1.25 μl	50 U
SAP (1 U ml^{-1})	3.5 μl	3.5 U
H_2O	to 50 μl	–

adjacent to a lane containing 2 μg of the original RNA preparation. Upon ethidium bromide staining, degraded RNA will be present as a low molecular weight smear on the gel rather than a discrete band of high molecular weight. If evidence of RNA degradation is observed, then fresh reagents should be prepared and the step repeated.

3.2. Decapping of Intact RNA

1. Combine and mix the reagents listed in **Table 18.2** in a sterile microfuge tube. Note that the quantity of TAP proposed is sufficient for the reaction.
2. Incubate the reaction for 1 h at 37°C, then add 200 μl TE buffer to stop the reaction.
3. Spin columns provided in any RNA extraction kit or from varied companies can be used for separation of the RNA from the reaction components. Elute the RNA from the spin column in 40 μL H_2O. It is permissible to store the products at this point at −80°C.
4. 2 μg of RNA should be analyzed by electrophoresis (through a 1% agarose gel in TAE buffer) adjacent to a lane containing 2 μg of the original RNA preparation; stain the gel with ethidium bromide and visually confirm that the RNA remained intact during the decapping step. A low-molecular weight smear on the gel indicates the presence of RNA fragments whereas a discrete band of high molecular weight corresponds to the desired product.

Table 18.2
Reaction components for decapping of intact RNA

Component	Amount	Final
RNA (obtained in 3.1.4)	48 μg	48 μg
TAP buffer (10 x)	5 μl	1x
DTT (0.1 M)	0.5 μl	1 mM
RNasin (40 U $mL^{?1}$)	1.25 μl	50 U
TAP (5 U ml^{-1})	1 μl	5 U
H_2O	to 50 μl	–

3.3. Preparation of RNA Oligonucleotide

1. Using digestion by appropriate restriction enzymes and buffers, linearize 25 mg of the plasmid to be transcribed. Ensure that the plasmid is reasonably RNase free.

2. Eliminate any residual RNase activity in the reaction by treating the digestion for 30 min at 37°C with 50 μg/ ml with proteinase K. Extract twice with phenol-chloroform and once with chloroform, and collect the DNA by standard ethanol precipitation.
3. Redissolve the template DNA in 25 μl TE buffer, pH 8.0. This yields a final concentration of approximately 1 μg/ μl.
4. Mix the transcription reagents in the order listed in **Table 18.3** in a sterile microfuge tube at room temperature (25°C).
5. Incubate for 1 h at 37°C to allow transcription to occur.
6. Remove the DNA template by adding 0.5 μl DNase (RNase-free) for every 20 μl of reaction volume and incubate for 10 min at 37°C.
7. Analyze 5 μl of the test or preparative reaction by electrophoresis through a 1% agarose gel (TAE buffer). Expect to see a diffuse band of about the right size for the expected product (or a bit smaller) in addition to some smearing up and down the gel.
8. Purify the oligonucleotide by extracting the reaction mixture with phenol-chloroform and then chloroform (keeping the aqueous phase each time). Perform buffer exchange and clean-up of the RNA oligonucleotide by diluting it to 1 ml with H_2O and then concentrating it using a Microcon spin

Table 18.3
Reaction components for preparation of RNA oligonucleotide

Component	Amount (test scale)	Final	Amount (preparative scale)	Final
DEPC-treated H_2O	4 μL	–	80 μL	–
Transcription buffer (5x)	2 μL	1x	40 μL	1x
DTT (0.1 M)	1 μL	10 mM	20 μL	10 mM
rUTP (10 mM)	0.5 μL	0.5 mM	10 μL	0.5 mM
rATP (10 mM)	0.5 μL	0.5 mM	10 μL	0.5 mM
rCTP (10 mM)	0.5 μL	0.5 mM	10 μL	0.5 mM
rGTP (10 mM)	0.5 μL	0.5 mM	10 μL	0.5 mM
Linearized DNA from section 3.3.3 (1 μg μL^{-1})	0.5 μL	0.5 μg	10μL	10.0 μg
RNasin (40 U μL^{-1})	0.25 μL	10 U	5 μL	200 U
RNA polymerase (20 U μL^{-1})	0.25 μL	5 U	5 μL	100 U
Total	10 μL	–	200 μL	–

filter (pre-rinse the spin filter with H_2O before addition of sample). Rinse twice more with 1 ml of H_2O as above. Note that Microcon 10 spin filters have a cutoff size of 20 nucleotides and Microcon 30 spin filters have a cutoff size of 60 nucleotides. Be sure to use Microcon 10 filters for oligonucleotides smaller than 100 nucleotides, and Microcon 30 spin filters for anything larger.

9. To check for the concentration and integrity of the sample, analyze a second aliquot of the oligonucleotide by electrophoresis through a 1% agarose gel in TAE buffer. The oligonucleotide distribution pattern should look like that in step 7 above. A much smaller band likely indicates that degradation has occurred and the procedure should be repeated with fresh material. At this juncture, the product can be stored at −80°C indefinitely.

3.4. RNA Oligonucleotide–Cellular RNA Ligation

1. Set up two sterile microfuge tubes, one with TAP-treated cellular RNA, and another with untreated cellular RNA, and add the remaining components for the ligation reaction (*see* **Table 18.4**). The tube with the untreated cellular RNA serves as a negative control.
2. Incubate for 16 h at 17°C. Overnight is permissible.
3. Purify and concentrate the ligation product by spin filtration with a Microcon 100 spin filter (rinsing product three times with RNase-free H_2O; pre-rinse filter with H_2O). The recovered volume after the Microcon filtration should not exceed 20 µl. Products can be stored at −80°C.

Table 18.4
Reaction components for RNA oligonucleotide–cellular RNA ligation

Component	Amount	Final
Ligation buffer (10x)	3 µL	1x
RNasin (40 U/ml)	0.75 µL	30 U
RNA oligonucleotide[1]	4 µg	4 µg
TAP-treated or untreated RNA	10 µg	10 µg
ATP (2 mM)	1.5 µL	0.1 mM
T4 RNA ligase (20 U ml^{-1})	1.5 µL	30 U
H_2O	to 30 µL	–

[1]RNA oligonucleotides are at a molar excess of 3–6 over target cellular RNA.

4. Analyze 1/3 of the product by electrophoresis through a 1% agarose gel (TAE buffer) to verify the integrity of the ligation. It should look like the previous samples, as discussed in **Section 3.3.7**.

3.5. Reverse Transcription

1. For each experimental and control sample from 3.4.3, assemble the transcription components listed in **Table 18.5** on ice in a sterile microfuge tube.
2. In a separate tube, add 20 ng of a gene-specific antisense primer (e.g., GSP-RT to generate the 5' end and the reverse compliment of NRC3 to generate the 3' end) to the remaining RNA (about 6.7 μg) from 3.4, step 3 in 13 μl H_2O. Incubate for 3 min at 80°C, cool rapidly on ice, and centrifuge for 5 s. To run an optional control reaction, set up an identical tube in parallel to which no reverse transcriptase is added in step 3.
3. Add the RNA-primer mix to the reverse-transcription components, subsequently add 1 ml (200 U) of SuperScript II reverse transcriptase, and incubate for 1 h at 42°C and for 10 min at 50°C.
4. Inactivate the reverse transcriptase by incubating at 70°C for 15 min then centrifuge briefly.
5. Destroy the RNA template by adding 0.75 μl (1.5 U) of RNase H to the reaction mixture and incubating it for 20 min at 37°C.
6. Dilute the reaction mixture to 100 μL with TE buffer and store at 4°C. Note that the 5'-end oligonucleotide–cDNA pool can be stored indefinitely at 4°C. Avoid storing at −20°C, which could snap some of the cDNA strands with repeated freeze-thawings.

Table 18.5
Reaction components for reverse transcription

Component	Amount	Final
Reverse-transcription buffer (5x)	4 μL	1x
dNTP mixture (containing all four dNTPs, each at 10 mM)	1 μL	471 μM
DTT (0.1 M)	2 μL	9.41 mM
RNasin (40 U ml^{-1})	0.25 μL	10 U
Total	7.25 μL	–

3.6. First-Round Amplification

1. In a sterile 0.2 ml microfuge tube, mix the reagents listed in **Table 18.6** for each experimental and control sample from 3.5.6.
2. Add a 1 µl aliquot of the 5'-end oligonucleotide–cDNA pool and 25 pmol each of primers GSP1 and NRC1 (or the reverse compliment of GSP1 and NRC1 if you are cloning the 3' end). A 'no-template' control should also be prepared.
3. Heat in a DNA thermal cycler for 5 min at 98°C to denature the first-strand (and to activate the polymerase). Cool for 2 min to the appropriate annealing temperature (56–68°C), followed by Extend cDNA extension for 40 min at 72°C.
4. Carry out 35 cycles of amplification with a 'step' program as listed in **Table 18.7**. Products can be stored at 4°C.

Table 18.6
Reaction components for first-round PCR amplification

Component	Amount	Final
Hercules Hot-Start polymerase buffer (10x)	5 µl	1x
dNTP solution (10 mM)	1.0 µl	200 mM
Hercules Hot-Start polymerase	2.5 U	2.5 U
H_2O	to 50 µl	–

Table 18.7
Conditions for first-round PCR amplification

Cycle number	Denaturation	Annealing	Polymerization-extension
1–30	10 s at 94°C	10 s at 52–60°C	3 min at 72°C
31–35	10 s at 94°C	10 s at 52–60°C	15 min at 72°C ; then cool to room temperature

3.7. Second-Round Amplification

1. Dilute a portion of the amplification products from the first round amplification 1:20 in TE buffer. Two rounds of amplification ensure the specificity of the yield by quenching the background amplification. The first round generates a lot of background because only one gene-specific primer is utilized. By using a second gene-specific primer, the specificity of the yield is significantly increased.

2. In a sterile 0.2 ml microfuge tube, the reagents listed in **Table 18.8** should be mixed (on ice).
3. Add a 1-ml aliquot of the diluted first-round amplification products (obtained in step 1 above) and 25 pmol each of primers GSP2 and NRC2 (or their reverse compliments for amplifying the 3' end). Set up a 'no-template' control as well.
4. Mix and heat in a DNA thermal cycler for 5 min at 98°C to denature the first-strand products and to activate the polymerase.
5. Carry out 30 cycles of amplification with a 'step' program as described in **Table 18.9**. The product can be stored at 4°C.
6. Separate 20% of the products of first- and second-round amplification by electrophoresis through a 1% agarose gel. Specific partial cDNAs can be checked by Southern blot analysis. Information gained from this analysis can be used to optimize the RACE procedure.

Table 18.8
Reaction components for second-round PCR amplification

Component	Amount	Final
Hercules Hot-Start polymerase buffer (10x)	5 µl	1x
dNTP solution (10 mM)	1.0 µl	200 µM
Hercules Hot-Start polymerase	2.5 U	2.5 U
H_2O	to 50 µl	–

Table 18.9
Conditions for second-round PCR amplification

Cycle number	Denaturation	Annealing	Polymerization-extension
1–29	10 s at 94°C	10 s at 52–68°C	3 min at 72°C
30	10 s at 94°C	10 s at 52–68°C	15 min at 72°C; then cool to room temperature

3.8. Anticipated Results

Depending on the stringency of the amplification cycles, the yield of the desired product could range from less than 1% to 100% of the amplified product. After the second set of amplifications, the expected yield of specific products should be about 100%. If there are alternative transcripts in the starting

pool of mRNA, then several different specific products should be seen after the second round of amplifications. These products are identified as distinct bands when visualized on an ethidium bromide gel. Upon sequencing, the presence of TATA or CCAAT, or other promoter elements, and initiator sites around your gene should identify these products as genuine alternative transcripts.

4. Notes

1. RACE kits are available from Invitrogen (Carlsbad, CA), Clontech (Mountain View, CA), and Ambion (Austin, TX). These ready-made systems are user-friendly and powerful. However they are not suited for every purpose. The investigator might have to optimize the kits using principles outlined in this protocol, e.g., using your own GSP and/or varying the annealing temperature. The entire procedure can be completed in 3 days but will take up to 5 days if the procedure is stopped at the storage points.
2. Adenosine residues are the best 'acceptors' for the ligation of the 3' end of the RNA oligonucleotide to the 5' end of its target, meaning that the restriction enzyme for linearization should be chosen accordingly (e.g., *Nde* I, *Sal* I, or *Xho* I, which terminate in an A at the end of the transcription product). A test transcription should be performed to ensure that all reactions are working properly, and then the reaction can be further "scaled up." The oligonucleotide can be stored indefinitely at −80°C for future experiments. It is also important to synthesize sufficient oligonucleotide to allow for losses due to purification and 'spot-checks' of the oligonucleotide during use. Alternatively, the DNA or RNA oligonucleotide can be ordered from a commercial source.
3. 10x T4 RNA ligase buffers supplied by some manufacturers contain too much ATP (25). If the composition contains more than 1 mM ATP, it is strongly recommended that you make your own. You can do this by regenerating the components used in the supplied buffer and adjusting the ATP concentration to 1 mM (final 1x concentration should be 0.1 mM). Alternatively, the 10x buffer described in ref. (25) can be used.
4. For the synthesis of the RNA oligonucleotide, it is important to select a plasmid that can be linearized at a site about 100 bp downstream from a T7 or T3 RNA polymerase site. A plasmid containing an insert cloned into the first polylinker site should be used because primers made from palindromic polylinker

DNA do not amplify well during PCR. In the scenario presented here, pBS-SK-GBX-1-3'UTR contains the 3' untranslated region of the mouse Gbx1 gene7 cloned into the SstI restriction site of the plasmid pBS-SK (Stratagene, La Jolla CA). This plasmid can be linearized with the restriction enzyme SmaI and transcribed with T3 RNA polymerase to produce a 132-nucleotide RNA oligonucleotide. Any other readily amplifiable sequence can be substituted, but avoid ones derived from abundant endogenous genes (such as actin) to prevent spurious non-specific amplification.

5. The presence of nonspecific amplification products could be the result of inappropriate annealing temperature. Using 'Touch down PCR' is an effective approach to optimize the annealing temperature. Alternatively, the same optimization can be attained by gradually increasing the annealing temperature in 2°C intervals at each relevant step of the protocol.
6. All the primers used for amplification are derived from the RNA oligonucleotide. It is recommended that primer design is software assisted in order to ensure similar melting temperatures. For instance, Primer3 from the Massachusetts Institute of Technology (http://frodo.wi.mit.edu/cgi-bin/primer3/primer3_www.cgi) can be used to generate suitable candidates.

Acknowledgments

This work was supported by NIH awards GM071520 and DK64166 to MAF and an NIH T32 Medical Scientist Training Grant and NIH F31-DK082280 awards to OY.

References

1. Ferreira, E. N., Galante, P. A., Carraro, D. M., and de Souza, S. J. (2007) Alternative splicing: a bioinformatics perspective. *Mol Biosyst* **3**, 473–477.
2. Kashyap, L., Tabish, M., Ganesh, S., and Dubey, D. (2007) Identification and comparative analysis of novel alternatively spliced transcripts of RhoGEF domain encoding gene in *C. elegans* and *C. briggsae*. *Bioinformation* **2**, 43–49.
3. Seim, I., Collet, C., Herington, A. C., and Chopin, L. K. (2007) Revised genomic structure of the human ghrelin gene and identification of novel exons, alternative splice variants and natural antisense transcripts. *BMC Genomics* **8**, 298.
4. Allen, R. D., 3rd, Dickerson, S., and Speck, S. H. (2006) Identification of spliced gammaherpesvirus 68 LANA and v-cyclin transcripts and analysis of their expression in vivo during latent infection. *J Virol* **80**, 2055–2062.
5. Frohman, M. A. (1994) On beyond classic RACE (rapid amplification of cDNA ends). *PCR Methods Appl* **4**, S40–58.
6. Jarosinski, K. W., and Schat, K. A. (2007) Multiple alternative splicing to exons II and

III of viral interleukin-8 (vIL-8) in the Marek's disease virus genome: the importance of vIL-8 exon I. *Virus Genes* **34**, 9–22.

7. Frohman, M. A., Dush, M. K., and Martin, G. R. (1988) Rapid production of full-length cDNAs from rare transcripts: amplification using a single gene-specific oligonucleotide primer. *Proc Natl Acad Sci USA* **85**, 8998–9002.
8. Bertling, W. M., Beier, F., and Reichenberger, E. (1993) Determination of 5' ends of specific mRNAs by DNA ligase-dependent amplification. *PCR Methods Appl* **3**, 95–99.
9. Borson, N. D., Salo, W. L., and Drewes, L. R. (1992) A lock-docking oligo(dT) primer for 5' and 3' RACE PCR. *PCR Methods Appl* **2**, 144–148.
10. Edwards, J. B., Delort, J., and Mallet, J. (1991) Oligodeoxyribonucleotide ligation to single-stranded cDNAs: a new tool for cloning 5' ends of mRNAs and for constructing cDNA libraries by in vitro amplification. *Nucleic Acids Res* **19**, 5227–5232.
11. Fritz, J. D., Greaser, M. L., and Wolff, J. A. (1991) A novel 3' extension technique using random primers in RNA-PCR. *Nucleic Acids Res* **19**, 3747.
12. Frohman, M. A. (1989) *In PCR Protocols and Applications: A Laboratory Manual.*
13. Frohman, M. A. (1993) Rapid amplification of cDNA for generation of full-length cDNA ends: thermal RACE. *Methods Enzymol* **218**, 340–356.
14. Frohman, M. A. M., G. R. (1989) Rapid amplification of cDNA ends using nested primers. *Tech* **1**, 165–173.
15. Jain, R., Gomer, R. H., and Murtagh, J. J., Jr. (1992) Increasing specificity from the PCR-RACE technique. *Biotechniques* **12**, 58–59.
16. Monstein, H. J., Thorup, J. U., Folkesson, R., Johnsen, A. H., and Rehfeld, J. F. (1993) cDNA deduced procionin. Structure and expression in protochordates resemble that of procholecystokinin in mammals. *FEBS Lett* **331**, 60–64.
17. Rashtchian, A., Buchman, G. W., Schuster, D. M., and Berninger, M. S. (1992) Uracil DNA glycosylase-mediated cloning of polymerase chain reaction-amplified DNA: application to genomic and cDNA cloning. *Anal Biochem* **206**, 91–97.
18. Templeton, N. S., Urcelay, E., and Safer, B. (1993) Reducing artifact and increasing the yield of specific DNA target fragments during PCR-RACE or anchor PCR. *Biotechniques* **15**, 48–50, 52.
19. Scotto-Lavino, E., Du, G., and Frohman, M. A. (2006) 5' end cDNA amplification using classic RACE. *Nat Protoc* **1**, 2555–2562.
20. Scotto-Lavino, E., Du, G., and Frohman, M. A. (2006) 3' end cDNA amplification using classic RACE. *Nat Protoc* **1**, 2742–2745.
21. Scotto-Lavino, E., Du, G., and Frohman, M. A. (2006) Amplification of 5' end cDNA with 'new RACE'. *Nat Protoc* **1**, 3056–3061.
22. Fromont-Racine, M., Bertrand, E., Pictet, R., and Grange, T. (1993) A highly sensitive method for mapping the 5' termini of mRNAs. *Nucleic Acids Res* **21**, 1683–1684.
23. Liu, X., and Gorovsky, M. A. (1993) Mapping the 5' and 3' ends of Tetrahymena thermophila mRNAs using RNA ligase mediated amplification of cDNA ends (RLM-RACE). *Nucleic Acids Res* **21**, 4954–4960.
24. Volloch, V., Schweitzer, B., Zhang, X., and Rits, S. (1991) Identification of negative-strand complements to cytochrome oxidase subunit III RNA in *Trypanosoma brucei*. *Proc Natl Acad Sci USA* **88**, 10671–10675.
25. Tessier, D. C., Brousseau, R., and Vernet, T. (1986) Ligation of single-stranded oligodeoxyribonucleotides by T4 RNA ligase. *Anal Biochem* **158**, 171–178.

Chapter 19

Use of Laser Capture Microdissection in Studying Hormone-Dependent Diseases: Endometriosis

Sachiko Matsuzaki, Michel Canis, and Gérard Mage

Abstract

Endometriosis, a common gynecological disorder responsible for infertility and pelvic pain, is defined as the presence of endometrial glands and stroma within extra-uterine sites. Gene expression studies performed on endometriotic tissue homogenates have yielded results reflecting mRNA abundance in a mixture of cell types (including epithelial cells, stromal cells, fibrotic tissue, and muscle tissue). Therefore, a method for quantifying gene expression separately in individual cell populations is essential for identifying genetic markers. Laser capture microdissection is a technique for obtaining pure populations of cells from heterogeneous tissues. This chapter provides methods to obtain high-quality RNA suitable for a variety of different down stream applications from frozen endometrial and endometriotic tissues for laser capture microdissection, using the Arcturus PixCell II system.

Key words: Endometriosis, endometrium, laser capture microdissection, RNA integrity, tissues heterogeneity.

1. Introduction

Gene expression studies performed on endometriotic tissue homogenates have yielded results reflecting mRNA abundance in a mixture of cell types (including epithelial cells, stromal cells, fibrotic tissue, and muscle tissue). Therefore, a method for quantifying gene expression separately in individual cell populations is essential for molecular analysis of endometriosis (1, 2). A relatively new technique for obtaining pure populations of cells from heterogeneous tissues is laser capture microdissection (LCM) (3). This chapter provides methods to obtain high-quality RNA suitable for a variety of different downstream applications from frozen endometrial and endometriotic tissues for laser capture microdissection, using the Arcturus PixCell II system.

O.-K. Park-Sarge, T.E. Curry, Jr. (eds.), *Molecular Endocrinology,* Methods in Molecular Biology 590,
DOI 10.1007/978-1-60327-378-7_19,

2. Materials

2.1. Collection of Samples for Laser Capture Microdissection

1. Human endometrial tissues—Endometrial tissue biopsies are performed, using an endometrial suction catheter (Pipelle, Laboratoire CCD, Paris, France) throughout the menstrual cycle.
2. Human endometriotic tissues.
3. RNAlater® solution (Applied Biosystems/Ambion, Austin, TX, USA).

2.2. Embedding and Cutting

1. Tisseu Tek® O.C.T. ™ Compound (Sakura Finetek, Villeneuve d'Ascq, France).
2. Coated glass slides, e.g., Superfrost® plus (Menzel GmbH, Braunschweig, Germany).

2.3. Staining

1. RNase-free water.
2. Alcohol series: 100, 95, 75% ethanol: add RNase free water to prepare.
3. Xylene.
4. Mayer's Hematoxylin.

2.4. Laser Transfer

1. Arcturus PixCell II (Molecular Devices).
2. Arcturus CapSure™ Macro LCM caps (Molecular Devices).
3. Arcuturus Capsure™ HS LCM caps (Molecular Devices).
4. Extraction Buffer (XB) from the Arcturus PicoPure RNA isolation kit (Molecular Devices).
5. 500 µl Thin-walled PCR Reaction tubes (Applied Biosystems, *see* **Note 1**.

2.5. RNA Extraction

1. CapSure™HS LCM Caps (Molecular Devices).
2. ExtracSure Extraction Device (Molecular Devices).
3. CapSure HS Alignment Tray (Molecular Devices).
4. Incubation Block.
5. CapSure™Macro LCM Caps (Molecular Devices).

2.6. RNA Isolation

1. Arcturus PicoPure RNA isolation kit (Molecular Devices).
2. RNase free DNase (RNase-Free DNase Set, QIAGEN, Courtaboeuf, France).

2.7. Examination of RNA Yield and Integrity

1. Agilent 2100 Bioanalyzer (Agilent Technologies).
2. Chip priming station (Agilent Technologies).
3. IKA Vortex (Agilent Technologies).

4. RNase decontaminating solution (e.g., RNase Away®, Invitrogen).
5. RNase-free water.
6. RNA 6000 Pico LabChip® Kit (Agilent Technologies): Keep all reagents and reagent mixes refrigerated at 4°C when not in use. Allow all reagents to warm up to room temperature for 30 minutes before use.

3. Method

3.1. Collection of Samples for Laser Capture Microdissection

1. Collect immediately fresh samples of endometriosis or endometrium in 5–10 volumes RNA*later*® *Solution* (*see* **Notes 2 and 3**). Before immersion in RNA*later* Solution, cut large endometriotic tissue samples to $\leq$0.5 cm in any single dimension.
2. Store at 4°C overnight (to allow the solution to thoroughly penetrate the tissue), then move to −20°C or −80°C for long-term storage (*see* **Note 4**).

3.2. Embedding and Cutting

The quality of sections is critical for laser capture microdissection, because uniform contact between the thermoplastic and the tissue is necessary for successful transfer.

1. Pre-cool Cryostat temperature (−25°C or less: *see* **Note 5**).
2. Remove and discard old microtome blade.
3. Clean the knife holder and antiroll plate in the cryostat with 100% ethanol to avoid sample cross-contamination.
4. Treat the brushes for manipulation with RNase AWAY and cool them.
5. Place a new disposable microtome blade in the cryostat.
6. Retrieve tissue from RNA *later* Solution with sterile forceps, quickly blot away excess RNA *later* Solution with an absorbent lab wipe or paper towel.
7. To facilitate cutting, the tissue should be relatively small (1 cm^3). If the tissue section is too large it needs to be trimmed to the appropriate size with a scalpel.
8. Place the tissue in O.C.T.
9. Allow the block to equilibrate to the cryostat temperature (−25°C or less) for at least 15 minutes (*see* **Note 6**).
10. Cut 10 μm (or thinner) sections onto coated glass slides (*see* **Notes 7 and 8**).
11. In between sectioning, store slides in a cold slide box placed on dry ice.

12. Store all sections at −80°C to preserve RNA until needed (*see* **Note 9**).
13. Discard slides with folds or wrinkled sections (*see* **Note 10**).

3.3. Staining

The extent of RNA degradation is in proportion to the time the tissue is in an aqueous phase. During the staining procedure, RNase is reactivated when the tissue is exposed to aqueous conditions. Staining improves tissue visualization, but it is not necessary to stain slides for LCM. In general, visual identification of epithelial and stromal cells is not difficult even in unstained tissue sections. If very high integrity of RNA is necessary for your experiment (e.g., Microarray analysis, see **Note 11**), eliminating exposure to water (steps 2–5) could improve RNA integrity (**Fig. 19.1**).

1. Treat the slides in 75% ethanol on ice for 10 seconds.
2. Dip the slides in RNase free water on ice.
3. Incubate the slides in Mayer's Hematoxylin (1:10 dilution) on ice for 10 seconds (*see* **Notes 12–14**).
4. Dip the slides in RNase free water on ice. Repeat this step.
5. Treat the slides in 75% ethanol, 95% ethanol, and 95% ethanol on ice for 10 seconds each.
6. Incubate the slides in100% ethanol for 30 seconds (*see* **Note 15**).
7. Incubate the slides in 100% ethanol for 60 seconds (*see* **Note 15**).
8. Dip the slides in Xylene.
9. Incubate the slides in Xylene (to ensure dehydration of the section) for 3 minutes (*see* **Notes 16 and 17**).
10. Subject the slides to air-dry for approximately 5 minutes.
11. The tissue is now ready for LCM (*see* **Note 18**).

3.4. Laser Transfer

The tissue section must be dry and not coverslipped for effective LCM transfer. The staining appears darker and more granular due to light scattered from the irregular air−tissue interface. The tissue where the polymer melts and bonds after laser activation appears lighter and resembles a coverslipped slide due to the replacement of the air in the tissue with the polymer. This phenomenon is called index-matching or "polymer wetting." An example of this process is shown in **Fig. 19.1**.

1. Perform LCM immediately after preparing LCM slides. Once removed from xylene, microdissection should be completed within 1–2 hours.
2. Inspect the tissue before placing down the cap. If any tissue seems to be mounded or folded, it is best not to place the cap over that area (*see* **Note 19**).
3. Apply cap (*see* **Note 20**).

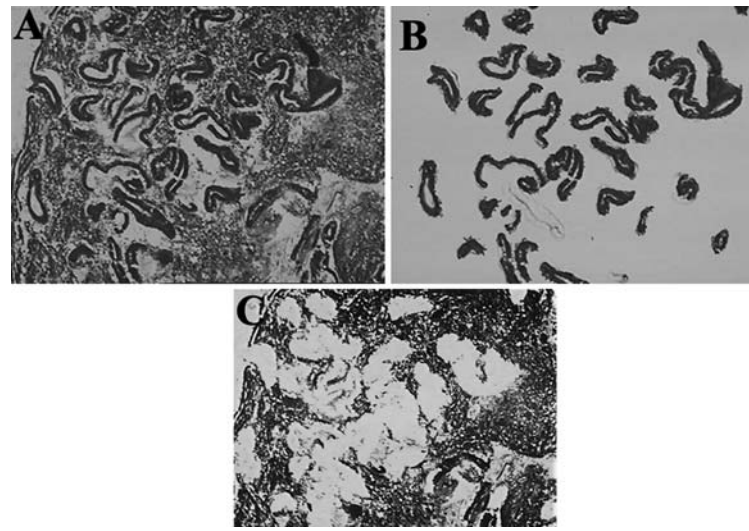

Fig. 19.1. Laser Capture Microdissection (LCM) from hematoxylin-stained sections of endometrium (10 μm). (**A**) Before LCM (**B**) Epithelial cells in endometrium were captured and transferred to film. (**C**) After LCM of epithelial cells.

4. Focus laser spot on section plane (*see* **Note 21**).
5. Set spot size or capture diameter (*see* **Note 22**).
6. Set power and duration of laser pulse. Increasing the Power will achieve better polymer melting and contact with the slide, while increasing the duration will yield spots with larger diameter.
7. Fire laser at desired cells, use joystick to move the stage.
8. Lift the cap so that cells adhered to the film are removed from the tissue section (*see* **Note 17**).
9. Pipette PicoPure Extraction Buffer (XB) (Picopure RNA extraction kit) onto cells acquired by LCM immediately after cell capture. Extraction Buffer (XB) stabilizes RNA by denaturing nucleases.

3.5. RNA Extraction

3.5.1. CapSure™HS LCM Caps

1. Assemble the CapSure HS Cap with the ExtracSure Extraction Device.
2. Place the CapSure–ExtracSure assembly in a CapSure HS Alignment Tray and pipette 20 μl/Extraction Buffer (XB) into the buffer well (*see* **Note 23**).
3. Place a new 0.5 mL microcentrifuge tube (Applied BioSystems) onto the CapSure–ExtracSure assembly. Cover with Incubation Block preheated to 42°C.
4. Incubate assembly for 30 minutes at 42°C.
5. Centrifuge assembly at 800 *g* for 2 minutes to collect.

6. Proceed with RNA isolation protocol or freeze cell extract at −80°C.

3.5.2. CapSure™ Macro LCM Caps

1. Pipette 50 µl Extraction Buffer (XB) into a 0.5 mL microcentrifuge tube (Applied BioSystems).
2. Insert CapSure Macro LCM Cap onto the microcentrifuge tube.
3. Invert the CapSure Cap−microcentrifuge tube assembly.
4. Tap the microcentrifuge tube to ensure all Extraction. Buffer (XB) is covering the CapSure Macro LCM Cap.
5. Incubate assembly for 30 minutes at 42°C.
6. Centrifuge assembly at 800 *g* for 2 minutes to collect.
7. Proceed with RNA isolation protocol or freeze cell extract at −80°C

3.6. RNA Isolation

1. RNA is isolated using the Picopure RNA extraction protocol per the manufacturer's recommendations.
2. To eliminate potential genomic DNA contamination, RNA samples should be treated with DNase at RT for 15 minutes.
3. Total RNA is resuspended in 11 µl RNase-free water and kept at −80°C until needed.

3.7. Examination of RNA Yield and Integrity

RNA Yield and integrity are analyzed using an Agilent Bioanalyser 2100. The Agilent 2100 bioanalyzer, a bio-analytical device based on a combination of microfluidics, microcapillary electrophoresis, and fluorescence detection, provides a platform to record the size distribution of molecules, RNA, DNA, and Protein, in a digital format. The RNA 6000 Pico kit allows determination of integrity of very low amounts of RNA as well as an estimation of the amount of the isolated RNA, which has a linear range of 200–5000 pg/µl.

3.7.1. Preparation of the Agilent 2100 Bioanalyzer

To avoid decomposition of RNA sample, the following decontamination procedure should be performed daily before and after any runs the RNA 6000 Pico kit. In addition, every 6 months, clean the Electrode with RNase decontaminating solution (e.g., RNase Away).

1. If using new electrode cleaners, label one RNase AWAY and the other Water.
2. Take electrode cleaner labeled water and fill one of the wells with 350 µl of RNase free water. Tap to ensure complete coverage of all wells.
3. Place electrode cleaner in Bioanalyser.
4. Close lid and leave for 1 minute.

5. Open lid and remove electrode cleaner.
6. Leave Bioanalyser lid open for a further 30 seconds to allow the water on the electrodes to evaporate.
7. Close the Bioanalyser lid.

3.7.2. Preparation of RNA 6000 Pico Gel Matrix

1. Place 550 µl of RNA 6000 Pico gel matrix on top of spin filter.
2. Spin at 1500 *g* for 10 minutes.
3. Discard the filter and keep the gel matrix for up to 4 weeks.

3.7.3. Preparation of the Gel Dye Mix

1. Vortex Pico dye concentrate (Marked Blue).
2. Add 1 µl of Pico Dye concentrate to a 65 µl aliquot of filtered gel matrix.
3. Cap the tube and vortex thoroughly.
4. Centrifuge the gel dye mix at 13,000 *g* for 10 minutes.
5. Use prepared mix within 1 day.

3.7.4. Sample Preparation

1. To minimize secondary structure formation, denature samples at 70°C for 2 minutes and then, place on ice.

3.7.5. Preparing and Running the Bioanalyzer Chip

1. Place chip on the Chip Priming Station.
2. Pipette 9 µl of the Gel Dye Mix into the bottom of the well-marked G (Bold G) (*see* **Note 24**).
3. Close the Chip Priming Station and press the plunger until held by the chip.
4. Wait exactly 30 seconds and then release the chip.
5. Wait the further 5 seconds and slowly pull up the plunger to the 1 mL position.
6. Pipette 9 µl of the Gel Dye Mix into the bottom of each of the wells-marked G.
7. Pipette 5 µl of the RNA 6000 Pico Marker (Marked Green) into the well marked ladder and into each of the 11 samples wells.
8. Pipette 1 µl of each sample into each of the 11 samples wells (*see* **Note 25**).
9. If there is no samples to be loaded, pipette 1 µl of RNase-free water into the sample well.
10. Pipette 1 µl of the ladder into the well marked ladder.
11. Place the chip into the adapter of the IKA vortex at 2400 rpm for 1 minute.

3.7.6. Running the RNA 6000 Pico Chip

1. Load the chip into an Agilent Bioanalyzer 2100 within 5 minutes.

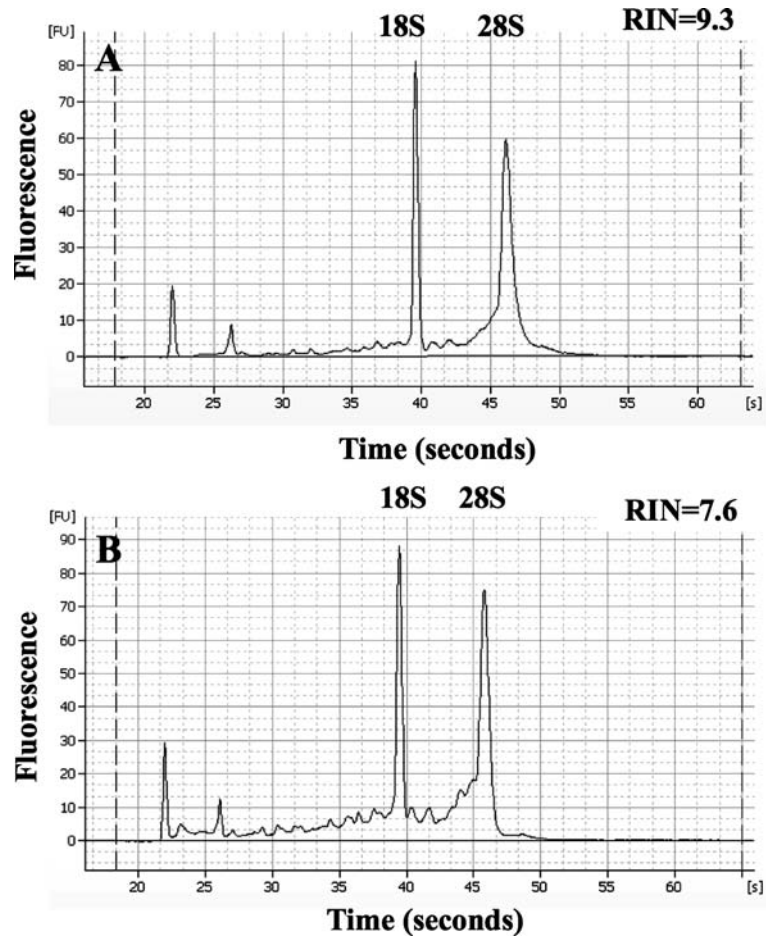

Fig. 19.2. Quality control of total RNA samples using the RNA 6000 pico LabChip kit. RNA damage could occur during the staining steps preparatory to laser capture microdissection (*see* **Notes 11**,**12**, and **14**). FU: frequency units, 18s: 18S band, 28S: 28S band, RIN: RNA integrity number (*see* **Note 11**). (**A**) Frozen total endometrial tissue section before staining, (**B**) microdissected epithelial cells from hematoxylin-stained endometrial tissue.

2. Run Agilent Bioanalyzer 2100.
3. Check RNA Yield and integrity of samples (**Fig. 19.2**).

Now your total RNA sample from LCM might be suitable for downstream applications such asreal-time RT-PCR and Microarray analysis. RNA quality is a critical determinant for the success of many downstream. Fleige and Pfaffl recommended a RNA integrity Number (RIN) (*see* **Note 11**) higher than five as good, but partly degradedtotal RNA quality and higher than eight as perfect total RNA for downstream application (4). A RIN value higher than five and a PCR product length up to 200 bp might be a minimal requirement for a successful and reliable real-time RT-PCR (5).

4. Notes

1. Use of these microcentrifuge tubes is recommended to prevent buffer leakage during extraction.
2. RNA *later*® is an aqueous, non-toxic tissue storage reagent that rapidly permeates tissues to stabilize and protect cellular RNA. It eliminates the need to immediately process or freeze samples; the specimen can simply be submerged in RNA *later* Solution. Samples can be stored at 4°C for 1 month, at 25°C for 1 week. After keeping samples at 4°C overnight to allow the solution to thoroughly penetrate the tissue, samples can be stored at −20°C indefinitely.
3. Does RNA*later* preserve the histology of tissues? Some researchers reported RNA*later* significantly alters histology; thus, they recommended preservation of tissues in RNA*later* might not be suitable for laser capture microdissection. However, we detected no significant alterations of tissue integrity after preservation of endometrial or endometriotic tissues in RNA*later*.
4. Do not freeze samples in RNA*later* Solution immediately; store at 4°C overnight to allow the solution to thoroughly penetrate the tissue.
5. It is necessary to cool Cryostat at a lower temperature than usual for cutting tissues kept in RNA*later*.
6. A longer time than usual is necessary for tissues kept in RNA*later*.
7. If necessary the sections may be cut thinner or thicker. For optimal transfer of frozen tissue sections it is best to keep sections <10 μm thick. Thicker sections are more difficult to visualize. In our laboratory, 8-μm thick frozen sections are prepared for endometriotic tissues and 10-μm thick frozen sections for endometrium.
8. Optimal placement of tissue is within the middle third of the slide. Avoid to place the tissue section near the edges or the end of the slide.
9. Check the RNA integrity in tissue on slides before staining and LCM, using an Agilent 2100 Bioanalyzer. RNA quality is a critical determinant for the success of many downstream applications and it can be defined as the sum of RNA integrity (traditionally 18S: 28S ratio) and RNA purity (260/280 ratio). The most common method used to assess the integrity of total RNA is to run an aliquot of the RNA sample on a denaturing agarose gel stained with ethidium bromide (EtBr). Generally, at least 200 ng of RNA must be loaded onto a denaturing agarose gel in order to be visualized with EtBr.

However, RNA preparations, from laser capture microdissected samples, result in very low yields. In these cases, it may be impossible to spare 200 ng of RNA to assess integrity before proceeding with downstream applications. It might be also impossible to measure a 260/280 ratio by conventional method. Alternative nucleic acid stains, such as SYBR Gold and SYBR Green II RNA gel stain (Molecular Probes Europe BV, Leiden, The Netherlands), offer a significant increase in sensitivity compared to the traditional EtBr stain in agarose gels. Using a 300 nm transilluminator (6 × 15 W bulbs) and a special filter, as little as 1 ng of RNA can be detected with SYBR Gold and 2 ng with SYBR Green II RNA gel stain, allowing less sample to be used for pre-experimental integrity assessment. RNA quantities could be measured with the Ribo-Green RNA Quantitation Kit (Molecular Probes Europe BV, Leiden, The Netherlands). The RiboGreen RNA quantitation assay can detect as little as 1 ng/mL RNA.

10. If there are folds in the tissue the cap may not make direct contact with the entire surface at that area which hinders tissue collection.
11. A new tool for RNA quality assessment using an Agilent 2100 Bioanalyzer is the RNA integrity Number (RIN) developed by Agilent Technologies (6). The softwareand algorithm allows the classification of total RNA on a numbering system from 1 to 10, with 1 being the most degraded profile and 10 being the most intact. A RIN higher than eight might be perfect total RNA for downstream application (5, 7). However, The RIN cut-off is tissue dependent, therefore the reader is advised to do a preliminary experiment to decide the cut-off for their sample.
12. We use a light hemotoxylin stain alone to limit exposure to inhibitory factors and contaminants that might affect the integrity of the cellular RNA.
13. Eosin staining of the cytoplasm is not necessary for visualization of cells during microdissection.
14. According to a credible but nonpeer-reviewed study by Agilent Technologies (8), methyl green was best for RNA isolation when compared to the other stains (Hematoxylin/Eosin, Nuclear Fast Red, Methylene Blue). However, we detected no significant difference in terms of RNA yield and integrity between the Methyl Green stain and Hematoxylin stain.
15. 100% ethanol should be changed after processing up to a maximum of 4 slides. 100% ethanol becomes hydrated after repeated use.
16. Stained slides can be held in Xylene until initiation of laser capture microdissection.

17. Dehydration is vital for two reasons:

    First, moisture impedes film wetting and capture:Poor transfers may result if the slide is not fully dehyrated (i.e., the 100% ethanol becomes hydrated after repeated use). The final xylene rinse facilitates the efficiency of transfer with LCM. If a tissue section does not transfer well, a longer xylene rinse may help. It does not alter RNA integrity. Second,. RNA degradation is most rapid in a hydrated sample through RNAse activity and auto-degradation.

18. Store in a dessicator for no more than 1 hour. Using frozen tissue, one has to be aware of endogeneous RNases that may still be active after short fixation steps.

19. If there are folds in the tissue, the cap may not make direct contact with the enitre surface at that area.

20. CapSure^{TM}Macro is ideal for large area capture. CapSure HS LCM caps enable the highly sensitive extraction and detection of biological molecules from small numbers of cells. "HS" stands for High Specificity. We use LCM Macro caps for endometrium and LCM HS caps for endometriosis.

21. It is only necessary to focus the laser, with the small (7.5 μm) spot size setting and the $\times 10$ objective.

22. In our laboratory, we use a 7.5-μm and 15-μm beam diameter for epithelial cells and for stromal cells, respectively.

23. In the Picopure RNA extraction protocol, it is described to pipette 10 μl of Extraction Buffer. However, to ensure all ExtractionBuffer (XB) is covering the Cap, we recommend to apply 20 μl of Extraction Buffer.

24. It is critical to avoid bubbles in the chip wells. When dispensing liquids into wells ensure that the tip is flush with the bottom of the well, do not expel air bubbles into the well, or expel past the first stop point. Placing the tip at the edge of the well may lead to bubbles and poor quality results.

25. Always run a positive control (a sample that is known to give good results with this method) with new samples.

Acknowledgments

This work was supported in part by Karl Storz Endoscopy & GmbH (Tuttlingen, Germany) and le Conseil Régional d'Auvergne (Recherche et Innovation Technologique) (Clermont-Ferrand, France).

References

1. Matsuzaki S, Canis M, Vaurs-Barriere C, Pouly JL, Boespflug-Tanguy O, Penault-Llorca F, Dechelotte P, Dastugue B, Okamura K, Mage G. (2004) DNA microarray analysis of gene expression profiles in deep endometriosis using laser capture microdissection. Mol Hum Reprod. 10:719–28.
2. Matsuzaki S, Canis M, Vaurs-Barriere C, Boespflug-Tanguy O, Dastugue B, Mage G. (2005) DNA microarray analysis of gene expression in eutopic endometrium from patients with deep endometriosis using laser capture microdissection. Fertil Steril, 84 Suppl 2:1180–90.
3. Emmert-Buck, M.R., Bonner, R.F., Smith, P.D., Chuaqui, R.F., Zhuang, Z., Goldstein, S.R., Weiss, R.A. and Liotta, L.A. (1996) Laser capture microdissection. Science, 274, 998–1001.
4. Fleige S, Pfaffl MW. (2006) RNA integrity and the effect on the real-time qRT-PCR performance. Mol Aspects Med. 2006; 27:126–39.
5. Fleige S, Walf V, Huch S, Prgomet C, Sehm J, Pfaffl MW (2006). Comparison of relative mRNA quantification models and the impact of RNA integrity in quantitative real-time RT-PCR. Biotechnol Lett. 28:1601–13.
6. Schroeder A, Mueller O, Stocker S, Salowsky R, Leiber M, Gassmann M, Lightfoot S, Menzel W, Granzow M, Ragg T (2006). The RIN: an RNA integrity number for assigning integrity values to RNA measurements. BMC Mol Biol. 7:3.
7. Strand C, Enell J, Hedenfalk I, Fernö M (2007). RNA quality in frozen breast cancer samples and the influence on gene expression analysis–a comparison of three evaluation methods using microcapillary electrophoresis traces. BMC Mol Biol. 8:38.
8. Gassmann, M. (2003) Quality Assurance of RNA derived from laser microdissected tissue samples obtained by the PALM(R) MicroBeam System using the RNA 6000 Pico LabChip(R) kit. 1-8. Agilent Technologies.

Chapter 20

Reporter Mice for the Study of Intracellular Receptor Activity

Adriana Maggi and Gianpaolo Rando

Abstract

During the past decade the remarkable progress in molecular genetics and the possibility to engineer cells to express genes reporting on the activity of specific promoters has produced major changes in biological research. The description and validation of reporter mice for non-invasive assessment of biological and biochemical processes in living subjects and the results obtained with the models reporting on the activity of estrogen and peroxisome proliferator receptors clearly showed that such technologies have the potential to enhance our understanding of disease and drug activity. Although reporter-gene technology is in its infancy, reporter animals already represent a valuable tool for biomedical investigation. The present chapter aims at critically illustrating the methodology to be applied when dealing with reporter systems and in vivo imaging.

Key words: Reporter mice, molecular imaging, intracellular receptors, estrogen receptor, bioluminescence, CCD camera imaging.

1. Introduction

Intracellular receptors (IR) belong to a large family of molecules of growing interest because of their relevance for the control of reproductive and major metabolic functions in mammals (1). Most IR are present in a wide variety of cells and tissues and some of them may be considered as ubiquitously expressed. IR are transcription factors regulated by lipophylic hormones. Upon binding to their cognate ligands IR undergo a series of structural modifications facilitating the attraction of co-regulators thus inducing/blocking the formation of the transcription initiation complex (2, 3). Co-regulators are indispensable elements for IR activity; because of that, IR action may be finely tuned depending on the specific tridimensional

O.-K. Park-Sarge, T.E. Curry, Jr. (eds.), *Molecular Endocrinology,* Methods in Molecular Biology 590,
DOI 10.1007/978-1-60327-378-7_20,

conformation induced by the given ligand and by the accessibility of co-activators and co-repressors. The availability of co-activators and co-repressors is cell-specific and variable in time (4, 5). This "tripartite" mechanism of action provides IR with a significant variety of effects on transcription depending on the cell and promoter taken in consideration. The peculiar mechanism of action and the wide distribution of IR has represented an obstacle for the identification of their precise physiological functions and for the generation of drugs with a well-focused therapeutic activity.

However, the nature of transcription factors has facilitated the generation of novel experimental model systems, like reporter mice. Applying molecular imaging with reporter mice enables one to investigate IR *spatio-temporal* activity in living organisms. Such an approach facilitates the understanding of their pathophysiological activity and the identification of drugs devoid of major side-effects (6, 7). These animals have already shown their potential for physiological and pharmaco-toxicological studies (8–10). The present protocol aims at indicating the modalities for the application of reporter mice engineered to express a bioluminescent protein in biological studies as exemplified by showing data obtained in our lab with the ERE-Luc reporter mouse model.

2. Materials

2.1. Reporter Mice

With the term reporter mice we refer to animals genetically engineered to express a reporter gene under the control of IR responsive promoters. Appropriate care must be taken to ensure that the reporter is not susceptible to local restraint (such as silencers or enhancers) and that, in all cells, is freely accessible to the activated IR and to the transcriptional apparatus. From a theoretical point of view, several protocols may be applied to the generation of reporter animals; however, to our knowledge, only a few of the models currently available ensure an expression of the reporter which is ubiquitous and appropriately reflects the state of activity of the receptor (*see* **Notes 1, 2**).

The strategy followed by our laboratory in the production of transgenic reporter mice consists in the exploitation of insulator sequences. For the generation of the transgenic reporter mouse, the transgene to be injected in the male pronucleus is flanked by insulator sequences (such as matrix attachment regions –MAR- and beta-globin hypersensitive site 4 –HS4-): this has enabled the production of animals where the expression of the reporter is ubiquitous and regulated by the hormone-receptor complex (11–13).

The promoter driving the reporter transcription is generally constituted by a sequence from the TK promoter ensuring a basal level of transcription and by a multimerized hormone responsive element (HRE): the exact location of the multimerized HRE and the number of its units is selected experimentally with the creation of a series of stably transfected cell lines where the expression of the reporter in the absence/presence of hormonal stimulation is evaluated (9, 11).

The reporter is selected among genes encoding for proteins with a short turn-over rate (to enable the dynamic view of the state of promoter activity) and easily detectable by non-invasive imaging technologies. So far, we have generated mainly reporter animals for bioluminescence employing as a reporter the fire-fly luciferase: this choice was driven by the short half life of the enzyme and by the relatively easy and cost efficient application of bioluminescence imaging (BLI) to small animals (14).

2.2. Imaging

1. Anesthetic solution composed of a water solution containing 78% v/v ketamine and 15% v/v xylazine.
2. Luciferine: 250 mg of Beetle luciferine potassium salt (Promega) are dissolved in 9.42 ml of bidistilled water then vortexed. The solution is kept in aliquots at −20°C. Fresh aliquots are used for each imaging session.
3. CCD camera or Bioluminescence Imaging work station: several apparatus are available—Lumina (Caliper, Hopkinton Mass, USA), NightOwl (Berthold Technologies, Bad Wildbad, Germany), Photon Imager (Biospace, Paris, France), and Carestream (Kodak, Rochester, NY,USA)
4. Imaging software: Each workstation is marketed with a dedicated imaging software to operate the machine and calculate photon emission.
5. Luminescence standards: Tritium-based light-emission sources (Glowell, Lux Biotechnology, Edinburgh, UK).

2.3. Luciferase Enzymatic Assay

1. Phosphate lysis buffer: 100 mM KPO4 lysis buffer, pH 7.8, 1 mM, dithiothreitol, 4 mM EGTA, 4 mM EDTA, and 0.7 mM phenylmethylsulfonylfluoride (PMSF).
2. Luciferase assay reagent solution: 10 mM luciferin, 1 M dithiothreitol, 200 mM ATP dissolved in 100 mM phosphate buffer, pH 7.0.
3. Luminometer: Single tube or microplate luminomiters available from a variety of suppliers such as Glomax from Promega (Madison Wi, USA) and Centro from Berthold.

3. Methods

In mice carrying as a reporter luciferase, the activity of the promoter may be evaluated: (a) directly in living animals by measuring photon emission resulting from luciferase enzymatic activity; (b) ex vivo in tissues dissected from the animal; (c) by measuring luciferase enzymatic activity in tissue extracts.

The possibility to measure photon emission by means of CCD cameras has the advantage that the effect of a given compound or physiological changes can be measured by observing a single animal over time. The disadvantage of this approach is that the equipment available at present time provides bi-dimensional analysis of photon emission and does not allow the investigator to acquire an unequivocal estimate of the exact origin of photon emission. Furthermore, it is well known that the different layers of tissue shield the photons, therefore impairing the measurements of luciferase activity from the inner most organs. Thus, the in vivo analysis must be complemented either by ex vivo imaging of the tissues immediately after isolation from the reporter animal or by the quantitative measurement of the enzymatic activity of luciferase accumulated in the tissues of interest.

3.1. Reporter Mice

A detailed description of the generation of a reporter mouse was previously described by Ciana et al. (11). The different steps can be summarized as follows:

1. Design a series of promoter sequences and clone them in a pMAR plasmid (11).
2. Amplify and sequence the plasmids generated.
3. Stably transfect each single reporter plasmid into at least two cell lines of different origin and determine experimentally the plasmid providing the best response to the given stimulus.
4. Inject the DNA of the selected plasmid into a fertilized mouse oocytes and reimplant them in a foster mother.
5. Screen the litter to identify the transgenic mice and proceed with the generation of separate lines of mice, each to be tested for the responsiveness to the selected stimulus/drug.

3.2. Imaging

3.2.1. In Vivo Imaging

In vivo imaging requires the use of specific CCD slow-scan cameras equipped with appropriate image processors and software for image reconstruction and localization of photon emission. For the bioluminescence detection:

1. Mice are anesthetized by s.c. injection of a 50 μl anesthetic solution or with isofluorane.
2. The substrate luciferine is administered to anesthetized mice (50 mg/kg i.p.) about 20 min before bioluminescence quantification.

3. For the imaging session, mice are placed in the light-tight chamber and a gray-scale photo is first taken with dimmed light, photon emission is then measured by integrating data over a period of time defined in the initial dose-and time-response study. With our models, we generally use a 5 min observation time.
4. To measure photon emission from the different body regions the gray-scale and pseudocolor images are merged using the software provided by the imaging workstation. Alternatively, open sources software are available (http://rsb.info.nih.gov/ij/) and can be effectively adopted.
5. Photon emission is calculated as counts per unit of time and area [cts/(cm^2s)] in specific regions of the mouse body using an electronic grid to identify reproducibly the different body areas: typically we measure photon emission in head, limbs, thymus, chest, abdomen, genital area, and tail **(Fig. 20.1)**. Alternatively, appropriate algorithms for image analysis can be employed under Imagej or Matlab environment.

Preliminary experiments are needed aimed to ensure that the substrate luciferin reaches all tissues at saturating concentrations, these studies are carried out first injecting the mice with a high dose of luciferin (e.g., 150 mg/kg) and measuring photon emission at for 5 min sessions at 5, 10, 15, 20, 25, 30, 35, 40 min after substrate injection. Photon emission is calculated in head, limbs, thymus, chest, abdomen, limb, and tail. This experiment will enable the investigator to evaluate the time necessary for the substrate to reach all parts of the body (typically between 5 and 40 min). The time selected will be used for a second experiment aimed at establishing the dosage of luciferin necessary and sufficient to saturate the enzyme in all body regions. This second experiment will be done by injecting the animals with increasing concentrations of luciferin (typically, 8–80 mg/kg, i.p.) and exposing them to the CCD camera for a 5 min session at the time selected in the previous experiment **(Fig. 20.2)**. The concentration of luciferin giving maximal response in all organs is then selected for future experiments.

3.2.2. Ex Vivo Imaging

Ex vivo bioluminescence imaging assay is simply carried out by exposing the dissected organs to the CCD camera. To this aim, animals need to be injected with luciferin as before. Generally, once the imaging session ends, the tissue is rapidly frozen for the preparation of tissue extracts where luciferase enzymatic activity can be measured.

Ex vivo imaging is of particular interest for the study of luciferase activity in the central nervous system. In this case, due to the limited diffusion of luciferin through the blood brain barrier, the substrate is administered by intracerebroventricular (ICV) injection

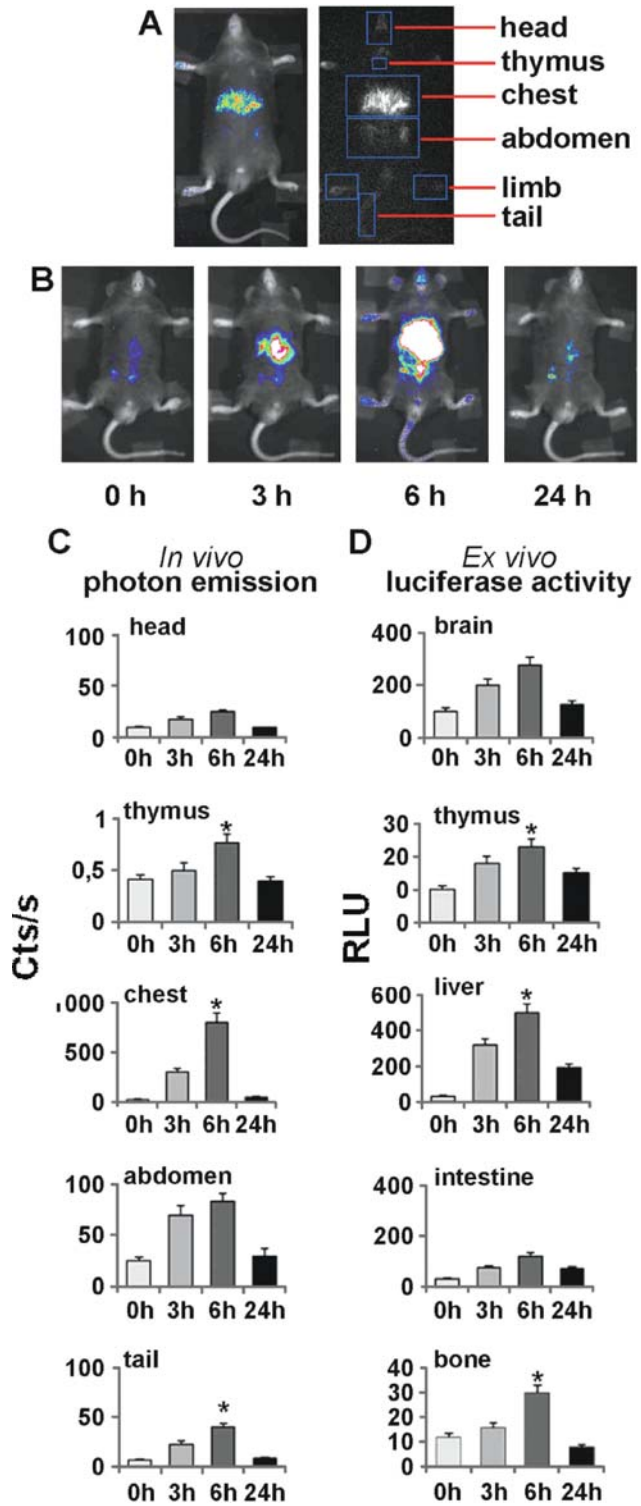

Fig. 20.1. Application of the effect of bioluminescence for the study of the time-dependent activation of the estrogen receptor in adult male ERE-Luc mouse. Groups of 5 ERE-Luc male mice were injected i.p. with either vehicle of

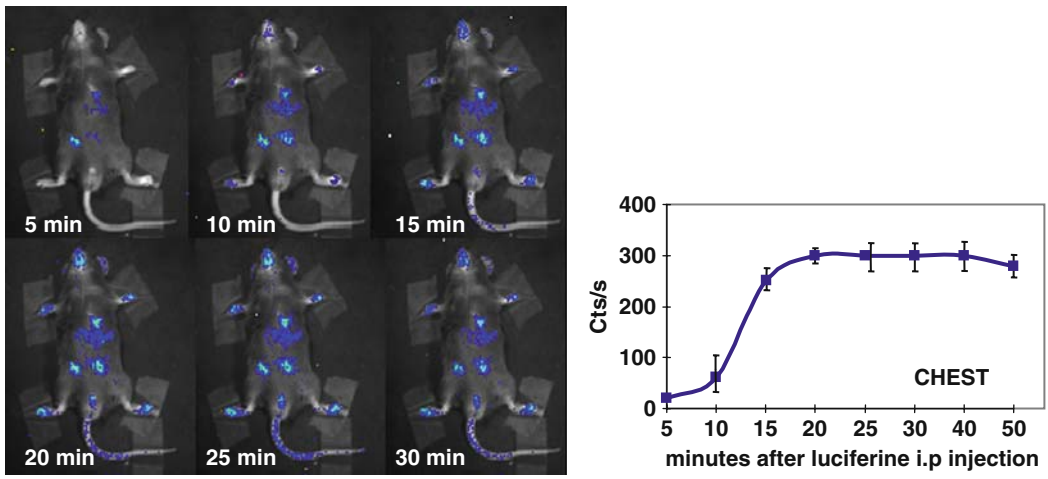

Fig. 20.2. Time course of photon emission in chest of ERE-luc male mouse after luciferine injection. Male ERE-Luc mice were injected i.p. with 150 mg/kg aqueous solution of luciferin and photon emission was measured at 5–30 min intervals. By the 30th min luciferin has reached all body areas.

in anesthetized animals. The injection is done according to specific stereotaxic coordinates (Bregma, –0.25 mm; lateral, 1 mm; depth, 2.25 mm) and by the use of an Hamilton syringe rotated on the coronal plate of about 3° from the orthogonal position, as previously described (15). Mice are euthanized 20 min after the ICV injection of luciferin (75 μg/3 μl saline). Brains are rapidly dissected and sectioned by means of a "brain matrix" (Brain Matrix, Adult Mouse, coronal and sagittal, 1 mm spacing; Ted Pella, Redding, CA) and sections are immediately visualized by the CCD camera. Gray-scale images of the sections are first taken with dimmed light. Photon emission is measured in a 15-min exposure time. Pseudo-color images associated to photon emission are generated by the appropriate image processor and transferred via video cable to a PCI frame grabber. For co-localization of the bioluminescent photon emission, gray-scale and pseudo-color images are merged. Luminescence of the brain slices is expressed as the integration of photon emission per time unit (cts/s); to be able to compare the extent of photon emission in brain nuclei characterized by a

Fig. 20.1. (continued) 17β-estradiol. BLI was carried out with a Night Owl imaging unit (Berthold Technologies) consisting of a Peltier-cooled charge-coupled device slow camera equipped with a 25-mm, f/0.95 lens. Images were generated by the Night Owl LB981 image processor and transferred via video cable to a peripheral component interconnected with a grabber using WinLight software (Berthold Technologies). For the imaging session, the animals were anestethized with a ketamine-xilazine solution as previously described (9). In parallel, ERE-Luc mice treated in the same way were euthanized at 3, 6, and 24 h after treatment, and the tissues were extracted for the detection of luciferase enzymatic activity. Panel **A**: black and white photo merged to the pseudocolor image generated by the CCD camera and example of the electronic grid generated for the quantification of photon emission. Panel **B**: representative example of the imaging data collected. Panel **C**: comparative study of the quantitative analysis of luciferase production as done by in vivo imaging and by ex vivo enzymatic assay.

different area, data are expressed as cts/s/Pixel. Photon emission in selected brain areas is quantified by means of a grid generated with the aid of a brain atlas **(Fig. 20.3)**.

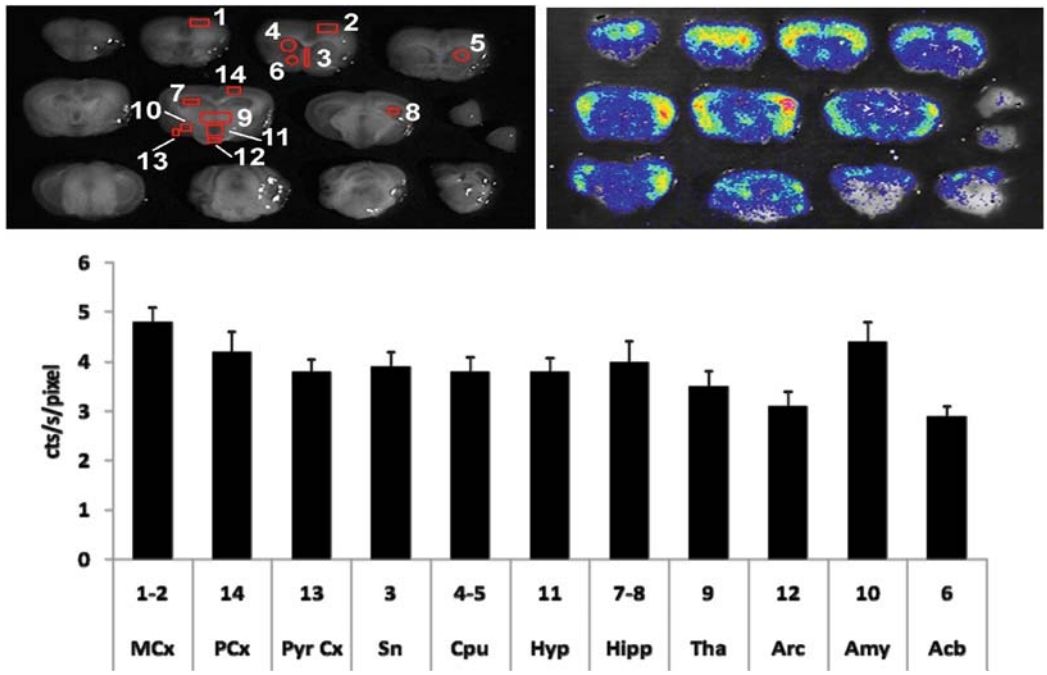

Fig. 20.3. Ex vivo quantitative analysis of bioluminescence in the brain of ERE-Luc mice. *Upper left panel*. Black and white photo of brain slices with an indication of the areas used for the quantitative analysis of photon emission by CCD camera. *Right panel*: merge of the pseudocolor image. Animals were injected icv with luciferin and brains dissected and analyzed 20 min after treatment. Data are expressed as the integration of the average photon emission unit (cts/s) and represent the mean ± SEM (n = 6–10 mice per group). As indicated in the bottom panel, in the brain of untreated male brain luciferase accumulates differentially in the various brain regions (MCx: motor cortex; PCx parietal cortex; PyrCx: pyrophorm cortex; Sn: substantia nigra; Cpu: caudate putamen; Hyp: hypothalamus; Hipp: hippocampus; Tha: thalamus; Arc: arcuate nucleus; Amy: amygdale; Acb: accumbens).

3.3. Luciferase Enzymatic Assay

1. Freshly dissected tissues are immediately frozen and stored at –80°C for the biochemical assay.
2. Tissues (20–100 mg) or cells (~100,000) are homogenized by TissueLyser using 300 µl of the phosphate lysis buffer and stainless steel beads in 1.2 ml polyethylene microtubes containing the tissue fragments or the cells.
3. Protein concentrations in the supernatants are measured using the Bradford assay using solutions and protocols commercially available.
4. The homogenates are frozen on dry ice and thawed in water, then are centrifuged (4900g for 30 min at 4°C).
5. Supernatant are collected and diluted to a protein concentration of 1 mg/ml.

6. 20 µl of the supernatant is transferred to a white opaque 96-well plate for luminescence quantification by luminometer (Glomax, Promega). Typically, luminescence is measured in an integration time of 10 s, after automatically injecting 100 µl of luciferase assay reagent. Light measurements are recorded by the luminometer software.
7. Luminescence data, normalized over protein content of each sample, are finally expressed as relative light units (RLU) per µg of protein.

4. Notes

1. To validate the faithfulness of the reporter of interest, it is advisable to evaluate its activity in parallel with the activity of endogenous genes. However, differences in the spatio-temporal accumulation of the reporter and the products of the endogenous genes is expected due to the fact that all endogenous genes are under the control of complex promoters which may influence the overall transcription rate of the reporter differentially; in addition, the turnover rate of the endogenous gene may differ from the reporter: therefore a time-course experiment must be carried out.
2. A further step necessary to validate the activity of the reporter consists in immunocytochemical studies aimed at demonstrating that the molecules active on the reporter co-localize with the product of the reporter gene.

Acknowledgment

The work done in the laboratory is supported by grants from the European Community (STREP EWA LSHM-CT-2005-518245; NoE EMIL LSHC-CT-2004-503569; NoE DIMI LSHB-CT-2005-512146; IP CRESCENDO LSHM-CT-2005-018652) and by NIH (RO1AG027713).

References

1. http://www.nursa.org/index.cfm
2. Yang, X., Lamia, K.A. and Evans R.M. (2007) Nuclear receptors, metabolism, and the circadian clock. *Cold Spring Harb. Sym. Quant. Biol.* **72**:387–94.
3. Lonard, D.M. and O'Malley B.W. (2007) Nuclear receptor coregulators: judges, juries, and executioners of cellular regulation. *Mol. Cell.* **27**:691–700.
4. Nettles, K.W. and Greene G.L. (2005) Ligand control of coregulator recruitment to nuclear receptors. *Ann. Rev. Physiol.* **67**:309–33.

5. Katzenellenbogen J.A., O'Malley, B.W. and Katzenellenbogen, B.S. (1996) Tripartite steroid hormone receptor pharmacology: interaction with multiple effector sites as a basis for the cell- and promoter-specific action of these hormones. *Mol. Endocrinol.* **10**:119–31.
6. Maggi, A. and Ciana, P. (2005) Reporter mice and drug discovery and development. *Nat. Rev. Drug. Discov.* **4**:249–55.
7. Mussi, P., Liao, L., Park, S.E., Ciana, P., Maggi, A., Katzenellenbogen, B.S., Xu, J. and O'Malley B.W. (2006) Haploinsufficiency of the corepressor of estrogen receptor activity (REA) enhances estrogen receptor function in the mammary gland. *Proc. Natl. Acad. Sci. USA.* **103**, 16716–21.
8. Ciana, P., Raviscioni, M., Mussi, P., Vegeto, E., Que, I., Parker, M.G., Lowik, C. Maggi, A. (2003) In vivo imaging of transcriptionally active estrogen receptors. *Nat. Med.* **9**:82–6.
9. Ciana, P., Biserni, A., Tatangelo, L., Tiveron, C., Sciarroni, A.F., Ottobrini, L., Maggi, A. (2007) A novel peroxisome proliferator-activated receptor responsive element-luciferase reporter mouse reveals gender specificity of peroxisome proliferator-activated receptor activity in liver. *Mol. Endocrinol.* **21**, 388–400.
10. Di Lorenzo, D., Villa, R., Biasiotto, G., Belloli, S., Ruggeri, G., Albertini, A., Apostoli, P., Raviscioni, M., Ciana, P. and Maggi, A. (2002) Isomer-specific activity of dichlorodyphenyltrichloroethane with estrogen receptor in adult and suckling estrogen reporter mice. *Endocrinology* **143**:4544–51.
11. Ciana, P., Di Luccio, G., Belcredito, S., Pollio, G., Vegeto, E., Tatangelo, L., Tiveron, C. and Maggi, A. (2001) Engineering of a mouse for the in vivo profiling of estrogen receptor activity. *Mol. Endocrinol.* **15**: 1104–13.
12. Stief, A., Winter, D.M., Strätling W.H. and Sippel,A.E. (1989) A nuclear DNA attachment element mediates elevated and position-independent gene activity. *Nature* **341**:343–5
13. Chung, J.H., Whiteley, M. and Felsenfeld, G. (1993) A 5' element of the chicken beta-globin domain serves as an insulator in human erythroid cells and protects against position effect in Drosophila. *Cell* **13**:505–14
14. Stell, A., Belcredito, S., Ramachandran, B., Biserni, A., Rando, G., Ciana, P. and Maggi A. (2007) Multimodality imaging: novel pharmacological applications of reporter systems. *Q J Nucl. Med. Mol. Imag.* **51**:127–38.
15. Vegeto, E., Belcredito, S., Etteri, S., Ghisletti, S., Brusadelli, A., Meda, C., Krust, A., Dupont, S., Ciana, P., Chambon, P. and Maggi, A. (2003) Estrogen receptor-alpha mediates the brain antiinflammatory activity of estradiol. *Proc Natl Acad Sci USA.* **100**:9614–9.

Chapter 21

Real-Time Non-invasive Imaging of ES Cell-Derived Insulin Producing Cells

Sudhanshu P. Raikwar and Nicholas Zavazava

Abstract

ES cells are a potential source for insulin producing cells (IPCs). However, two major handicaps are establishing reliable differentiation protocols and the lack of imaging techniques that allow monitoring of these cells post-transplantation. Here, we describe a new approach for monitoring the in vitro differentiation and real-time, non-invasive imaging of ES cell-derived IPCs in vivo. ES cells were molecularly engineered so that the rat insulin promoter (RIP) driven luciferase (Luc) expression was specifically turned on and up regulated following their differentiation into IPCs. The rationale underlying this approach is that the transcriptional activation of RIP leads to Luc expression in IPCs providing an extremely sensitive reporter for monitoring the earliest differentiation events in real-time both in vitro and in vivo.

Key words: Embryonic stem (ES) cells, bioluminescence imaging, diabetes, luciferase, insulin producing cells, pancreatic islets, MRI, Quantum dots, rat insulin promoter (RIP), transplantation.

1. Introduction

Type 1 diabetes is a complex, genetic autoimmune disease characterized by hyperglycemia, due to the immunological destruction of insulin-producing pancreatic β cells. Diabetes leads to microvascular pathological lesions in the retina, renal glomerulus, and humoral defects of peripheral nerves and arteries (1). Currently, whole organ pancreatic transplantation is the preferred treatment that leads to sustained euglycemia and insulin independence in a vast majority of the patients with an overall 1-year graft survival rate as high as 78% (2). Despite significant progress, pancreatic transplantation is associated with perioperative mortality and significant morbidity which leads to early re-laparotomy in almost 20% of the patients (3, 4).

O.-K. Park-Sarge, T.E. Curry, Jr. (eds.), *Molecular Endocrinology,* Methods in Molecular Biology 590,
DOI 10.1007/978-1-60327-378-7_21,

However, following transplantation, islet perfusion is severely compromised until neovascularization is established (5). Without more definitive imaging techniques, the damage to the transplant often remains obscured. The major caveat to a wider application of this potentially curative therapy remains an inadequate supply of islets. Moreover, since the deceased-donor derived islets are histo-incompatible to the recipient, it necessitates a lifelong immunosuppressive therapy with potentially undesirable side effects. These major caveats show the need for the development of new therapeutic strategies for the treatment of type 1 diabetes. In this regard, ES cells and induced pluripotent stem (iPS) cells have emerged at the forefront and offer one of the most promising approaches for the generation of the much needed IPCs (6–17).

In order to improve the differentiation potential as well as the transplantation steps of ES cells into IPCs, we have focused on understanding the molecular mechanisms underlying ES cell differentiation into IPCs as well as to develop molecular imaging modalities. In addition, we have improved on non-invasive imaging of ES cell derived IPCs. We have further exploited the transcriptional activity of a pancreatic beta cell specific promoter for real-time non-invasive in vivo bioluminescence imaging (BLI). This strategy will facilitate a minimally invasive intravital imaging modality for in vivo monitoring of the fate, functional characterization of graft survival, neo-vasculature development, and tracking of transplanted insulin-producing cells in recipient mice. In addition, we have applied nanoparticles to imaging of IPCs. These nanoparticles composed of cadmium, selenium, and zinc can be suitably modified for any required function such as conjugation with biomolecules including antibodies to specifically target certain tissues. The anticipated data from these studies will eventually lead to a novel paradigm in the field of molecular regenerative medicine for a possible cure and management of type 1 diabetes.

2. Materials

2.1. Generation of Primary Mouse Embryonic Fibroblasts

1. E13.5-14.5 pregnant female mouse.
2. 1xPBS: 137 mM NaCl, 2.7 mM KCl, 4.3 mM Na_2HPO_4, 1.47 mM KH_2PO_4, pH 7.4.
3. 0.25% Trypsin-EDTA.
4. DNaseI (10 mg/ml).
5. 70 μm cell strainer (BD Falcon).
6. Dulbecco's Modified Eagle's Medium (DMEM).
7. Fetal Bovine Serum (FBS)

8. Penicillin-streptomycin.
9. Gamma irradiator: (^{137}Cs)-using a Cesium-source.
10. Mitomycin C (Sigma)

2.2. Generation of ES Cell Lines Expressing Luciferase

1. The ES cell lines Elm-3, R1, and DBA (Specialty Media/Millipore) are maintained in an undifferentiated state in DMEM (Invitrogen).
2. Leukemia inhibitory factor (LIF, ESGRO, ESG1107, Chemicon International Inc./Millipore).
3. EmbryoMax ES cell qualified FBS (Millipore) is heat inactivated at 56°C for 30 minutes and used at 15% v/v.
4. 100x Non-essential amino acids (Invitrogen).
5. 100x Sodium pyruvate (Invitrogen).
6. 100x Penicillin and streptomycin (Invitrogen).
7. 2-Mercaptoethanol (Sigma).
8. Nucleoside mix (dissolve 80 mg adenosine, 85 mg guanosine, 73 mg cytidine and 73 mg uridine in 100 ml double distilled water, filter through 0.22 μm filter, and store at 4°C).
9. Autoclaved 0.1% (w/v) gelatin solution in double distilled water.
10. Vector pGL4-RIP-Luc2/Puro.
11. Lipofectamine 2000 (Invitrogen)
12. Puromycin (Invivogen)
13. Forward and reverse RIP primers for PCR (Integrated DNA Technologies).
14. pCR2.1 TOPO vector (Invitrogen).
15. ES cell Nucleofector kit (VTPH-1001, Amaxa Biosystems/Lonza) containing sterile cuvettes, Nucleofector solution, Nucleofector supplement, plastic fine tip pipettes and pmaxGFP control plasmid for optimizing nucleofection.
16. Nucleofector II device: (Amaxa Biosystems/Lonza).

2.3. In Vitro Differentiation of ES Cells into IPCs

1. α-Monothioglycerol (Sigma).
2. Low glucose DMEM (Invitrogen).
3. DMEM/F12 (1:1) medium supplemented with 25 ng/ml bFGF (R & D System Inc.).
4. ITSFn medium (DMEM/F12 supplemented with 5 μg/ml insulin, 50 μg/ml transferring, 30 nM selenium chloride and 5 μg/ml fibronectin).
5. N2 and B27 supplements (Invitrogen).
6. Nicotinamide (Sigma).

2.4. Analysis of IPC Function In Vivo

1. 129/SvJ mice (The Jackson Laboratory).
2. Streptozotocin (50 mg/kg body weight) freshly dissolved in citrate buffer (pH 4.5). Citrate buffer is prepared by dissolving 1.47 g of Sodium citrate in 50 ml double distilled water and the pH is adjusted to 4.5. The solution is sterile filtered using 0.22 μm filter (*see* **Note 1**).
3. Collagenase P from *Clostridium histolyticum* (Roche). Prepare collagenase P solution by dissolving 1.5 mg/ml in Hank's balanced salt solution containing 10 mM Hepes.
4. RPMI.
5. Ficoll-Eurocollin's solution (density 1.108, 1.096, 1.069, and 1.037).
6. Dual luciferase reporter assay system (Promega).
7. 5x lysis buffer (Promega) is a component of the Dual luciferase reporter assay system.

2.5. Functional Assay

1. D-Luciferin (Xenogen Corporation/ Caliper Life Sciences or Gold Biotechnology) (*see* **Note 2**).
2. 1.5% isofluorane in air.
3. IVIS 200 (Xenogen Corporation/ Caliper Life Sciences).
4. IgorPro software package (WaveMetrics Corporation/Caliper Life Sciences).
5. IVIS 2.50 Living Image software package (Xenogen).
6. MRI (Varian Inc.).

2.6. Use of the Nanoparticles for the Real-Time Non-invasive Imaging

1. Qtracker 655 cell labeling kit with QDots (Invitrogen).
2. 129/ SvJ mice (The Jackson Laboratory).
3. βTC-6 cells (ATCC).

3. Methods

3.1. Generation of Primary Mouse Embryonic Fibroblasts

1. Select an E13.5-14.5 pregnant female mouse and sacrifice it by carbon-dioxide (CO_2) asphyxiation.
2. Swab it with 70% ethanol, lay it on its back and make a fine incision to expose the abdominal cavity carefully.
3. Locate the uterine horns and carefully dissect them out into a sterile 10 cm^2 tissue culture petri dish containing 1x PBS. PBS Wash the uterine horns carefully and transfer them into a second sterile petri dish containing 1x PBS.

4. Dissect out the uterine horns and gently remove the embryos from the embryonic sacs and transfer all of the embryos into another sterile Petri dish containing 1x PBS.
5. Dissect the embryo and perform evisceration under a dissecting microscope to remove various internal organs.
6. Transfer the remainder of the embryo into a sterile petri dish and finely mince it using sharp surgical blade and add sufficient 0.25% Trypsin-EDTA to completely cover the minced tissue.
7. Incubate the contents at 37°C for 15 minutes. Repeat this process with fresh trypsin solution 2 more times. If the solution becomes viscous, add 100 µl of DNaseI (10 mg/ml) per 10 ml of the suspension and pass through a 70 µm cell strainer into a 50 ml conical tube to remove the undigested tissue chunks. Add DMEM containing 10% FBS to inactivate the residual trypsin activity.
8. Centrifuge at 290*g* for 10 minutes at 4°C. Discard the supernatant and resuspend the tissue pellet in 50 ml of DMEM supplemented with 10% FBS, 1x Penicillin-Streptomycin. Take 10 µl of cells and add 90 µl of trypan blue. Load 10 µl of the cell suspension on the improved Neubauer hemocytometer to determine cell viability and cell numbers. Count the number of viable cells in each of the four corner squares which in turn contain 16 small squares each. Each large square of the hemocytometer with the coverslip includes a total volume of 0.1 mm^3 or 10^{-4} cm^3. Since 1 cm^3 is equivalent to 1.0 ml, the final cell concentration is determined as follows:

$$\text{Cells/ml} = \text{average cell count per square} \times \text{dilution factor} \times 10^4$$

9. On an average, normally 5×10^7–10^8 primary mouse embryonic fibroblasts are obtained from 10 embryos. Aliquot 5×10^6 cells of tissue suspension each into 10 separate 15 cm tissue culture dishes containing 15 ml DMEM supplemented with 10% FBS, 1x Penicillin–Streptomycin and incubate these tissue culture plates at 37°C with 5% CO_2.
10. Change the media after 2 days and incubate these tissue culture plates at 37°C with 5% CO_2 for 2 more days until the culture becomes confluent.
11. Remove the media, wash the monolayer with PBS, and add 10 ml of Trypin-EDTA to the confluent cell monolayer for 3–5 minutes. Collected cells are centrifuged at 200*g* for 10 minutes. Wash the cell pellet with 1x PBS. The cells can either be expanded further or frozen down in liquid nitrogen as small aliquots using a mixture of 10% DMSO + 90% FBS.

12. Before freezing the primary mouse embryonic fibroblasts (PMEFs) they must be irradiated using a Gamma irradiator at 3500 Rads for approximately 15 minutes. This step is essential so that PMEFs are just viable and able to provide growth factors to the plated ES cells without undergoing replication and competing with the ES cells for the nutrients. Replicating PMEFs will rapidly deplete the nutrients from the medium and turn it acidic.
13. Alternatively, the PMEFs can be treated with 15 ml DMEM+10%FBS containing 150 µl of 1 mg/ml mitomycin C solution for 2 hours at 37°C with 5% CO_2. These mitomycin C treated cells can either be frozen down or used to seed gelatin coated tissue culture plates for ES cell culture. Gelatin-coated tissue culture plates are prepared by treating the tissue culture surface with a sterile 0.1% gelatin solution for 15 minutes at room temperature. The gelatin solution is removed and the plates are air dried in the tissue culture hood for 15 minutes prior to using them. The gelatin-coated tissue culture plates and flasks can be stored safely at room temperature for an extended period.
14. One confluent 15 cm dish of mitomycin C treated PMEFs can seed approximately 5×10 cm^2 tissue culture dishes for cultivating ES cells. Generally, PMEFs are incubated in DMEM + 10%FBS at 37°C with 5% CO_2 overnight prior to plating the ES cells (*see* **Note 3**).

3.2. Generation of ES Cell Lines Expressing Luciferase

1. The ES cell lines Elm-3, R1, and DBA are maintained in an undifferentiated state in DMEM containing 1000 IU/ml leukemia inhibitory factor (LIF) and 15% EmbryoMax ES cell qualified FBS on PMEF feeder layer (*see* step 3.1.14).

3.2.1. Culture of ES Cell Lines

2. An ES cell line Elm-3-RIP-Luc is generated by transfecting undifferentiated Elm-3 cells with expression vector pGL4-RIP-Luc2/Puro which contains the rat insulin promoter (RIP) driven Luciferase (Luc) gene and SV40 promoter driven puromycin resistance gene (*see* **Section 3.2.2**).
3. Transient transfection is carried out using Lipofectamine 2000 followed by selection using growth medium supplemented with puromycin at a concentration of 2 µg/ml.
4. Puromycin resistant ES cell clones are obtained in 7–10 days, amplified and subjected to differentiation. These ES cells are subjected to in vitro differentiation into IPCs and are analyzed by luciferase (Luc) assay (*see* **Section 3.3**).

3.2.2. Generation of pGL4-RIP-Luc2/Puro

1. This is achieved by cloning RIP (−671 bp to +86 bp) upstream of the luciferase gene in pGL4.20[Luc2/Puro] vector (Promega). In this vector the SV40 promoter drives

the expression of the puromycin resistance gene for the stable selection of clones. The RIP is amplified by PCR using the rat genomic DNA and the following PCR primers:

RIP-F (forward primer): 5'-TCTAGACTTGAATTCTGC TTTCCTTCTACC-3'

RIP-R (reverse primer): 5'-ACCGGTGGAGAGTACA-TACCTGCTTGCT-3'.

2. The PCR is performed by denaturation at 95°C for 5 minutes followed by 30 cycles, each comprising of denaturation at 94°C, primer annealing at 60°C, and extension at 72°C for 1 minute. A final extension step at 72°C for 8 minutes is included.
3. The PCR amplified RIP is cloned into pCR2.1 TOPO vector sequenced and subcloned into pGL4.20 Luc2/Puro vector (**Fig. 21.1A**).
4. The transcriptional activity of RIP is examined by measuring the luc activity following transient transfection of pGL4-RIP-Luc2/Puro in undifferentiated ES cells and the mouse βTC-6 insulinoma cells. In the undifferentiated ES cells the luc activity is at the baseline level since the RIP is transcriptionally inactive. The βTC-6 insulinoma cells display significantly higher relative luciferase activity (~100,000 fold) due to transcriptional activation of RIP. Since the ES cell-derived IPCs represent approximately ≥3–5% of the total differentiated cell population, the relative luc activity is much lower as compared to the βTC-6 insulinoma cells (**Fig. 21.1A**) (*see* **Notes 8–10**).

3.2.3. Nucleofection of ES Cells

1. Undifferentiated ES cells are cultivated without feeder cells on a gelatin-coated T75 flask 48 hours prior to nucleofection. Feed the ES cell cultures 4–12 hours prior to nucleofection (*see* **Notes 4 and 5**).
2. On the day of nucleofection, exponentially growing ES cells are trypsinized, washed in PBS and centrifuged at 100x g for 10 minutes, and resuspended in 10 ml 1x PBS containing 5% FBS in a 15 ml conical centrifuge tube (*see* **Note 6**).
3. Take 10 µl of cells and 90 µl trypan blue dye and use 10 µl cell suspension to determine cell viability and number.
4. Each nucleofection requires 2–5 $\times$ 10^6 cells. Depending upon the number of nucleofections to be performed, the desired number of ES cells are transferred into 15 ml conical centrifuge tubes, resuspended in 10 ml 1x PBS and centrifuged at 80–100*g* for 5–10 minutes at 4°C.

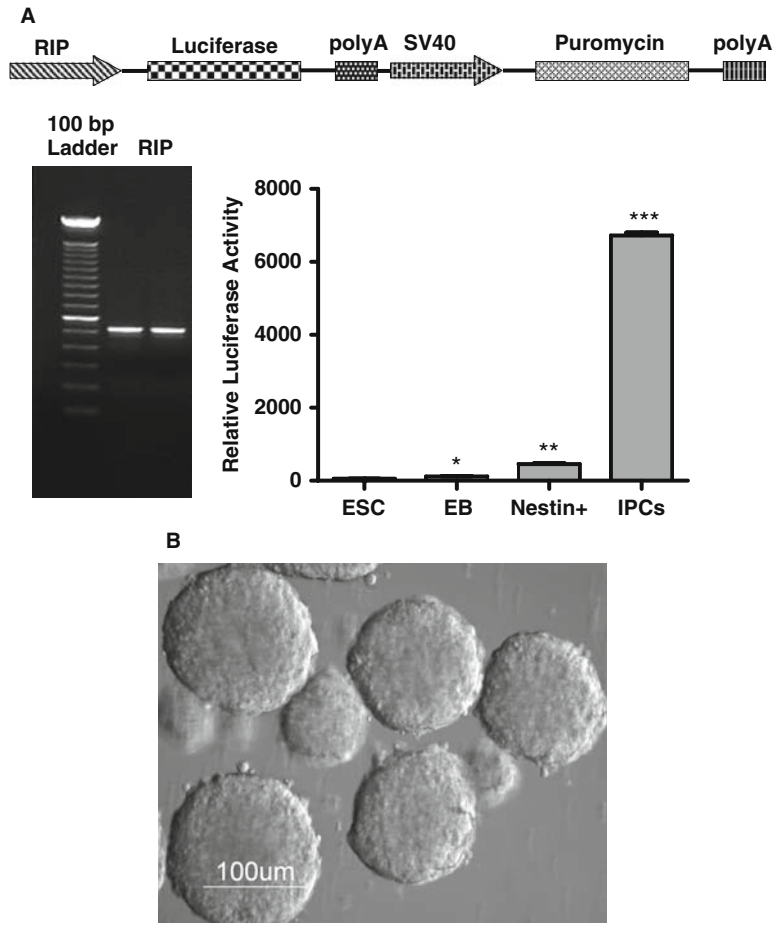

Fig. 21.1. Generation of pGL4-RIP-Luc2/Puro vector and monitoring in vitro differentiation of ES cells into IPCs by luciferase assay. **(A)** The figure depicts the design of the pGL4-RIP-Luc2/Puro vector. In this expression vector, RIP drives the expression of luciferase (Luc) gene while SV40 promoter drives the expression of the puromycin resistance gene for the generation of stable cell lines. The rat insulin promoter (RIP) sequence was amplified from rat genomic DNA by PCR, separated on 1% agarose gel by electrophoresis, cloned into pCR2.1-TOPO vector and sequenced. The RIP was isolated as an EcoRI fragment, Klenow treated, and cloned into pGL42.0-Luc2/Puro vector to generate pGL4-RIP-Luc2/Puro. A stable ES cell line expressing RIP-Luc was generated by puromycin selection. Stable ES cell harboring RIP driven luc was subjected to a multi-step differentiation protocol to generate IPCs and luc activity was monitored at different stages. A significant increase in the luc activity was observed following the differentiation of the ESC into IPCs suggesting that this novel approach can be used to sequentially monitor the events underlying the differentiation of ESC into IPCs. **(B)** The ES cells were grown on ultra low attachment cell culture plates to generate embryoid bodies which are capable of differentiating into specialized cells of all the three germinal layers.

5. Aliquot 2–10 μg Endo-toxin free plasmid DNA in 10 μl of supplemented Nucleofector solution in a 1.5 ml sterile Eppendorf tube. The plasmid to be used for nucleofection is routinely isolated using EndoFree plasmid Maxi Kit (Qiagen).
6. Pre-warm the supplemented mouse ES cell nucleofector solution to room temperature. The PBS is removed carefully and the cell pellet is resuspended in 90 μl of the mouse ES cell Nucleofector solution.
7. Prepare the required number of the 10 cm^2 plates by adding appropriate amount of pre-warm medium and incubate them at 37°C.
8. Gently mix the cell suspension together with the plasmid DNA from step 6 by pipetting three times and taking care to avoid air bubbles. Transfer the cell suspension into the cuvette and close it with the cap.
9. Nucleofection is performed by using one of the program settings. The supplier recommends optimizing the nucleofection for ES cells using either or all of the four programs: A-013, A-023, A-024, or A-030. Place the cuvette into the Nucleofector II device and run the program.
10. Upon successful nucleofection, remove the cuvette from the holder, add 500 μl of pre-warmed culture medium, and gently take out the cell suspension in a 1.5 ml Eppendorf tube and incubate it at 37°C for 15 minutes.
11. Transfer the nucleofected cells into 10 cm^2 plates containing 10 ml of pre-warm ES cell media and incubate at 37°C. Transgene expression of the fluorescent proteins can be monitored by fluorescence microscopy approximately 6 hours post nucleofection. For example, the expression vector pAcGFP N1 (Clontech) encodes a green fluorescent protein from *Aequorea coerulescens* which can be monitored using the fluorescence microscopy following excitation at 475 nm and emission at 505 nm. Any gene of interest can be fused in frame at the N terminus of AcGFP by PCR and the expression of the resulting fusion protein can be monitored by fluorescence microscopy (*see* **Notes 7 and 14**).

3.3. In Vitro Differentiation of ES Cells into IPCs

1. The mouse ES cells are maintained in an undifferentiated state by cultivating them on primary mouse embryonic fibroblast feeder (PMEF) cells in the presence of LIF as in 3.2. Prior to differentiation, the ES cells are passaged twice in the absence of PMEF. The undifferentiated ES cells are subjected to differentiation using a multi-step protocol (*see* **Notes 4 and 5**).

2. The ES cells are trypsinized using 0.05% Trypsin EDTA solution for 2 minutes at 37°C, washed with PBS, and centrifuged at 100*g* for 10 minutes at 4°C. 1×10^7 cells are plated on to ultra-low attachment culture dishes in 10 ml DMEM containing 10% FBS and 9 µl of freshly prepared (1:10 dilution in PBS) of α-Monothioglycerol to promote embryoid body (EB) formation. EB formation represents a three-dimensional spherical cluster of cells capable of differentiating into functional cell types and lineages representing all the three germinal layers (**Fig. 21.1B**).
3. The EBs are cultivated in serum-free DMEM supplemented with ITSFn to enrich for nestin positive cells for 6 days **(***see* **Note 11)**.
4. This step ensures that a vast majority of cells except the nestin positive fail to survive thereby ultimately leading to selective enrichment of nestin positive cells..
5. The nestin positive cells are grown in DMEM/F12 (1:1) medium supplemented with 25 ng/ml bFGF N2 and B27 supplements and cultured for 6–8 days.
6. The endocrine precursors obtained at the end of this stage are further propagated for 6 days in low glucose DMEM supplemented with N2, B27, and 10 mM Nicotinamide to enrich IPCs.

3.4. Analysis of IPC Function In Vivo

1. All animal experiments are performed according to IACUC guidelines.
2. Six- to eight-week-old 129/ SvJ mice are used for the isolation of pancreatic islets.

3.4.1. Transplantation of IPCs in Streptozotocin-Treated Mice

3. Diabetes is induced in 129/ SvJ mice fasted for 4 hours by intra-peritoneal (i.p.) injection of streptozotocin (50 mg/kg body weight) freshly dissolved in citrate buffer (pH 4.5) **(***see* **Notes 1 and 12)**.
4. Three to five days later, diabetes is confirmed by weight loss, polyuria and blood glucose levels >250 mg/dl.
5. With mice under anesthesia (100 mg/kg body weight ketamine and 10 mg/kg body weight xylazine administered by intraperitoneal injection) the kidney is exposed through a small lateral incision and IPCs are gently placed under the kidney capsule. The abdominal incision is closed with absorbable surgical sutures while the skin incision is closed using non-absorbable nylon surgical sutures.

3.4.2. Isolation of Pancreatic Islets

1. Mice are anesthetized using pentobarbital. Abdominal cavity is exposed by a midline incision and the sphincter Odii is clamped at its junction into the duodenum.
2. An ice cold 3 ml, 0.2% collagenase P solution is injected using a 30 gauze needle to perfuse the pancreas through the common bile duct.

3. The pancreas is harvested and treated with additional 2 ml collagenase P solution (1.5 mg/ml in HBSS) at 37°C for 8 minutes with continuous shaking.
4. Following the digestion, the solution is agitated vigorously to break the large clumps of the pancreatic tissue.
5. The islets are subjected to centrifugation at 100*g* for 2 minutes, the centrifuge is switched off and the tubes are removed carefully and the supernatant is aspirated off leaving 5 ml behind.
6. The cell pellet is resuspended by tapping vigorously and adding 45 ml RPMI. The suspension is centrifuged again at 100*g* for 2 minutes and processed as described earlier. The resuspended pellet is transferred to a 15 ml tube and centrifuged as above, and the supernatant is discarded completely.
7. The pellet is resuspended in 7 ml of Ficoll-Eurocollin's solution (density 1.108) and layered with 2 ml of Ficoll-Eurocollin's solution with densities in the order 1.096, 1.069, and 1.037.
8. The step gradient is centrifuged at 200*g* for 20 minutes at 4°C with the break at the off position. The islets are picked by gentle aspiration from the second layer and washed three times to remove the traces of Ficoll solution.
9. The purified islets are maintained in RPMI containing 10% FBS and 1x non-essential amino acids.

3.4.3. Luciferase Assay

1. For quantifying the luc activity during the differentiation of ES cells into IPCs, a dual luciferase reporter assay system (Promega) is used as per the recommendations of the manufacturer.
2. Briefly, equal number of cells from various stages of differentiation are lysed using 1x passive lysis buffer (Promega) on a rocking platform at room temperature (RT) for 15 minutes, centrifuged and the resulting supernatant is used to perform luciferase assay using FLUOstar OPTIMA microplate reader (BMG Labtech).

3.5. Functional Analysis

3.5.1. Real Time In Vivo Bioluminescene Imaging

1. Mice injected with an adenoviral vector expressing CMV promoter driven luciferase or transplanted with ES cell-derived insulin producing cells under the renal capsule are subjected to real-time in vivo bioluminescence imaging.
2. Mice are anesthetized using a 1.5% mixture of isofluorane and oxygen in the anesthesia induction chamber, injected i.p. with 150 mg/kg D-Luciferin) and placed into the camera chamber equipped with a controlled flow of 1.5% isofluorane and oxygen administered through a nose cone (*see* **Note 2**).

3. Mice are subjected to non-invasive bioluminescence imaging using IVIS 200 system within 5 minutes post D-Luciferin injection. To get the best results, place the mice in a dorsal, ventral, or lateral position such that it gives the best signal.
4. Following the acquisition of the photographic image, luminescent images are acquired with a 1 minute exposure. Continue to take images every minute up to 30 minutes in order to generate the kinetic curve for your model. The images are obtained with 25 cm^2 field of view (depends upon the number of animals), binning factor of 8, an f-stop setting at 1, and the filter at open position.
4. The resultant gray-scale photographic and pseudocolor luminescent images are automatically superimposed by the Living Image 2.50.1 software to render the optical signals with location of the IPCs transplanted in mice. The optical images are displayed and analyzed with the IgorPro software package and IVIS 2.50 Living Image software package. The signals are quantified as photons/sec/cm^2/steradian. An example is shown in **Fig. 21.2A**. Systemic delivery of Ad-CMV-Luc results in a robust expression of luc in the liver and the spleen, because following systemic tail vein injection most of the adenoviral vectors are selectively taken up by the liver due to high-level expression of adenovirus specific CAR receptors (18, 19). Similarly, the RIP-driven luc expression in the βTC-6 cells and ES cell-derived IPCs could be detected at the transplantation site (**Fig. 21.2B, C**). Interestingly, IPCs are identified as a distinct signal in the transplanted kidney (**Fig. 21.2C**).

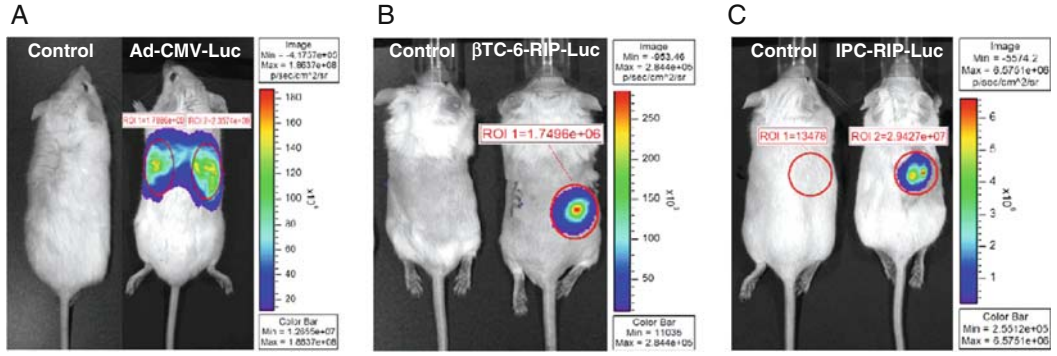

Fig. 21.2. Real-time non-invasive Bioluminescence Imaging (BLI) of IPCs in vivo. (**A**) The mice are injected with 4 × 10^9 Pfu of Ad-CMV-Luc by systemic tail vein injection. BLI is performed 2 days post-adenoviral injection on anesthetized mice following d-Luciferin injection using the IVIS 200 system. The mice injected with Ad-CMV-Luc exhibit strong bioluminescence signal in the liver and spleen ranging from 1.7 to 2.35 photons/s/cm^2/steradian. **(B)** 1 × 10^6 βTC-6 cells stably expressing luc under the transcriptional control of RIP are transplanted under the renal capsule of the 129/SvJ mice and subjected to BLI 5 days post-transplantation. The mice transplanted with βTC-6 cells exhibit strong bioluminescence signal from the kidney corresponding to 1.74 × 10^6 photons/s/cm^2/steradians. **(C)** 2.94 × 10^7 ES cell-derived IPCs are transplanted under the kidney capsule in the 129 SvJ mice and subjected to BLI 5 days post-transplantation. The mice transplanted with ES cell-derived IPCs exhibit a strong signal corresponding to 2.94 × 10^7photons/s/cm^2/steradians.

3.5.2. Magnetic Resonance Imaging

1. Mice are anesthetized using ketamine/xylazine mixture (100 mg/kg body weight ketamine and 10 mg/kg body weight xylazine administered by intraperitoneal injection).
2. The MRI equipment consists of a horizontal bore Varian Unity/INOVA 4.7 T unit with a gradient system having 10 cm bore and capable of gradient amplitudes of 270 mT/m. Mice are placed prone on the imaging carrier and moved into the standard radio frequency coil such that the kidneys are approximately located at the center of the coil.
3. The carrier and the radio frequency coil are then placed in the magnet bore. After a series of coil tuning steps, a set of three 2 mm thick scout images in each of the three principal imaging planes (axial, sagittal, and coronal) for a total of nine images are acquired for localization.
4. The scout images are used to prescribe a set of 20–30 contiguous axial slices of 0.6 mm thickness covering both kidneys completely. First, a fast spin echo pulse sequence acquires images over the volume with in-plane resolution of 0.12×0.24 mm^2using parameters TR/TE = 5000/50 ms, an echo train length of 8, and two signal averages to improve image quality (scan time = 3 minutes).
5. Next, a pair of gradient echo acquisitions are taken over an identical set of slices ($0.12 \times 0.24 \times 0.6$ mm^3 resolution) with two different echo times to generate two susceptibility (T2*) weightings. Acquisition parameters are TR/TE = 1000/6 ms and 1000/12 ms and two signal averages (scan time = 4 minutes each).
6. From the axial images, a set of 15–20 contiguous coronal slices are prescribed to cover both kidneys. The same three data sets (fast spin echo and two gradient echo sequences) are acquired in the coronal orientation with the parameters as for the axial images.

3.6. Use of the Nanoparticles by Real-Time Non-invasive Imaging

3.6.1. Quantum Dot (Qdot) Labeling of the IPCs

1. 2×10^4 βTC-6 cells are labeled with a 10 nM solution of Qdot (ferromagnetic materials) for 45 minutes at 37°C
2. Qdot-labeled cells are washed gently three times with 1x PBS to remove any unbound Qdots.
3. The cells are examined under fluorescence microscope to determine the labeling efficiency. This procedure generally results in almost 100% labeling of the cells with the Q dots (**Fig. 21.3A**).

3.6.2. Functional Assay In Vivo

1. 1×10^6 Qdot-labeled βTC-6 cells are transplanted by microsurgery under the renal capsule in anesthetized mice (**Fig. 21.3B**).

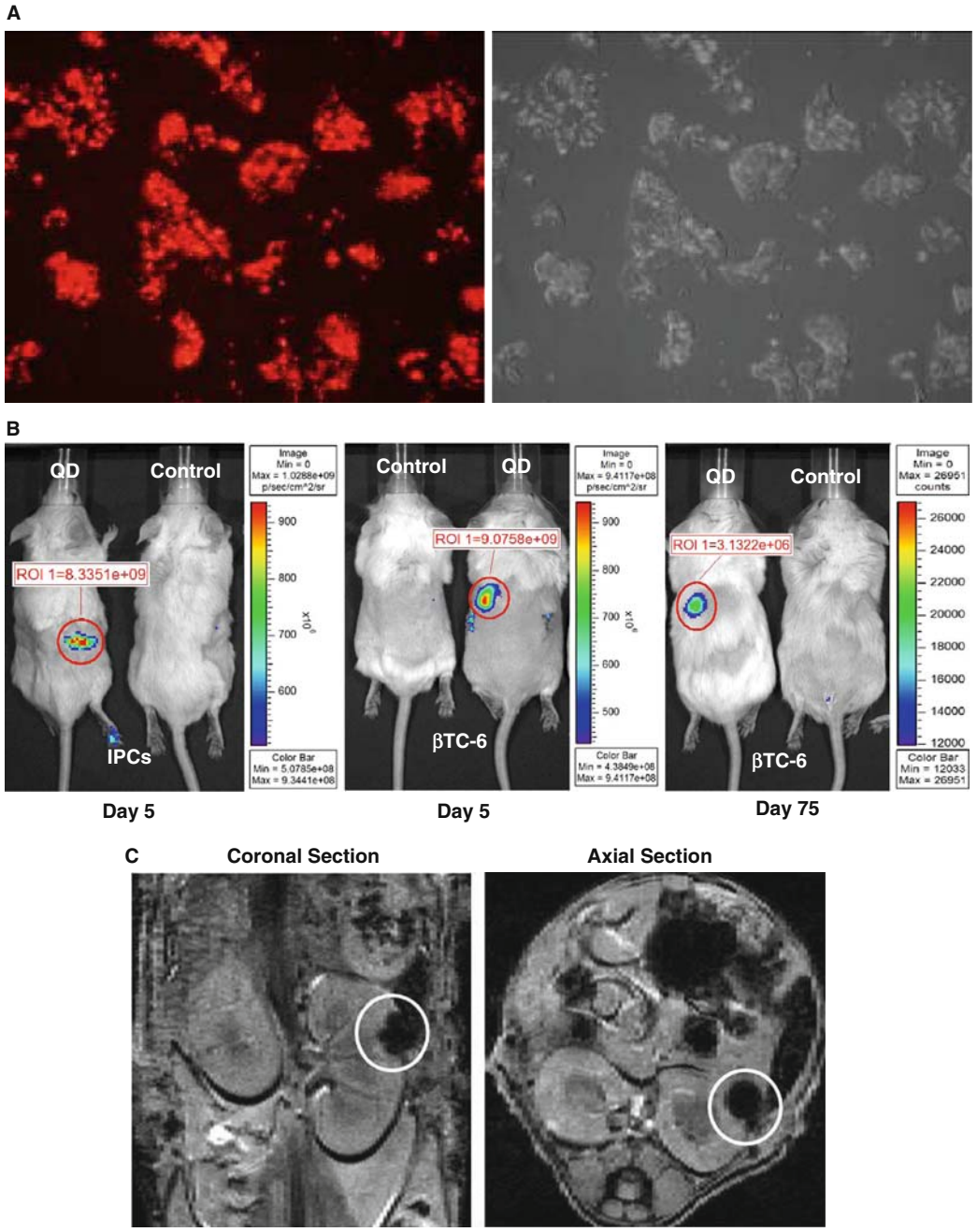

Fig. 21.3. Imaging of IPCs and βTC-6 cells in vivo using Qdots. **(A)** βTC-6 cells were labeled with Qdots. Phase contrast image of Qdot-labeled cells (panel i) and fluorescent image (panel ii) reveal specific labeling of βTC-6 cells. **(B)** 1×10^6 Qdot labeled ES cell- derived IPCs or βTC-6 cells were transplanted either subcutaneously or under the kidney capsule of the recipient mouse and imaged on day 5 and 75 using the IVIS 200 system. The signal intensity of the Qdot-labeled cells did not significantly change over time demonstrating the stability of Qdots. **(C)** The fate of Qdot-labeled βTC-6 cells was examined by MRI following an intra-peritoneal injection of Gadodiamide. The panel (i) shows contiguous 0.8 mm coronal slices whereas the panel (ii) shows 1.0 mm axial slices from an in vivo multi-slice gradient echo acquisition detecting susceptibility-induced signal loss resulting from the introduction of the Qdot-labeled βTC-6 cells. The MRI data indicate that Qdot-labeled βTC-6 cells were specifically localized under the renal capsule thereby indicating the sensitivity of MRI to follow the in vivo fate of IPCs, non-invasively post-transplantation.

2. The mice are subjected to real-time non-invasive in vivo BLI at day 5 and 75 post-transplantation. Our results indicate that these Qdot-labeled cells could be successfully visualized by BLI as early as 5 days post-transplantation and subsequently without any significant reduction in the signal intensity beyond 75 days post-transplantation (**Fig. 21.3B**).
3. Since the Qdots are made up of heavy metals, the same animals that had been examined by BLI could be subjected to MRI. An example is shown in **Fig. 21.3C**. The Qdot-labeled βTC-6 cells are easily identifiable as light sparing surfaces.
4. These results indicate the sensitivity of the BLI as well as MRI which can be successfully used in real-time to non-invasively monitor the in vivo fate as well as the function of the transplanted cells repetitively. The Qdot-labeled βTC-6 cells emitted a strong intensity fluorescent signal without any background. The mice transplanted with Qdot-labeled cells could be subjected to non-invasive BLI as required over 75 days without loss of signal (**Fig. 21.3B**). These data suggest that in addition to the real-time non-invasive BLI of RIP-mediated luc expression in the ES cell-derived IPCs, Qdots provide a unique and novel approach to non-invasively follow the fate of the transplanted IPCs over time (*see* **Note 13**).

4. Notes

1. Streptozotocin: 2-Deoxy-2-(3-methyl-3-nitrosoureido)-d-glucopyranose is a pale yellow solid, diabetogenic compound that acts as a nitric oxide donor in pancreatic islets and causes DNA alkylation and DNA strand breaks in the pancreatic islets cells. For best results we use streptozotocin (Calbiochem, Catalog No. 572201). Always store streptozotocin at −20°C. For diabetes induction prepare 7.5 mg/ml solution of streptozotocin in sodium citrate buffer (pH 4.5) in an aluminum foil covered 1.5 ml Eppendorf tube, immediately before injection.
2. Reconstitute the entire 1.0 g of D-Luciferin, firefly, potassium salt, 1.0 g vial (Xenogen Catalog No. XR1001) in 66.6 ml of Ca^{++} and Mg^{++} free DPBS (Gibco Catalog No. 14190-144) and filter the solution using 0.22 μm filter. Alternatively, prepare a fresh stock solution of D-Luciferin at either 15 mg/ml or 30 mg/kg body weight in DPBS and filter sterilize using a 0.2 μm filter.
3. Mitomycin C is highly toxic with potential carcinogenic (classified 2B by IARC) and mutagenic effects. Therefore extreme caution must be exercised while handling Mitomycin C.

4. ES cells generally should not be split at ratios lower than 1:4 or higher than 1:10. Plating too sparsely ($<0.5 \times 10^5$cells/cm^2) or plating too densely ($>4 \times 10^5$cells/cm^2) will invariably cause them to differentiate.
5. Failure to change the ES cell media every alternate day, allowing cells to get too confluent, allowing the colonies to get too large and failure to add the appropriate amount of LIF will invariably cause them to differentiate.
6. It is very critical to centrifuge the ES cells at 80–100 *g* in order to achieve the highest nucleofection efficiency.
7. Unlike transfection, nucleofection directly delivers the DNA into the nucleus of the cells with a high efficiency. Therefore transgene expression in most cases can be detected as early as 4–6 hours post-nucleofection.
8. *Gaussia princeps* luciferase (Gluc), naturally secreted form of luciferase is over 2000-fold more sensitive than the luciferases from Photinus and Renilla reniform and can be substituted for the firefly luciferase if one needs to determine the amount of secreted luciferase.
9. Gluc is 20,000-fold more sensitive than secreted alkaline phosphatase (SEAP) when expressed in mammalian cells.
10. Gluc assay can be performed in blood or serum samples in a few seconds, whereas SEAP activity cannot be measured in blood as hemoglobin inhibits it.
11. Nestin is a 206,994 dalton (1864 amino acids) type VI intermediate filament-associated protein expressed in the dividing cells during the early stages of development in the neural crest cells, central nervous system stem cells as well as non-neural cell types in the embryo including the cells within the pancreatic islets of Langerhans and the limb bud.
12. Different strains of mice require different doses of streptozotocin to induce diabetes. While C57/Bl6 mice require a dose of 250 mg/kg body weight of streptozotocin/day for 5 consecutive days, 129 SvJ mice require only 50 mg/kg body weight of streptozotocin for 5 days to render them diabetic.
13. A potential pitfall of the real-time, non-invasive BLI imaging modality is that it cannot be applied clinically even though it is extremely sensitive.
14. Alternatively, the fraction of cells expressing either single fluorescent reporters like AcGFP, DsRed, mCherry etc. or simultaneously coexpressing two or more fluorescent reporters can be monitored as well as sorted for either single or double fluorescent reporters using FACS.

Acknowledgments

This study was made possible by Grant Number NIH/NHLBI #R01 HLO73015, a VA Merit Review Award, Grant No. 0455585Z of the American Heart Association and a grant by the ROTRF to N.Z. and by a NIH Pilot Grant to S.R. from the University of Iowa, Center for Gene Therapy of Cystic Fibrosis and Other Genetic Diseases, Grant Number NIH/NIDDK #P30DK054759. The authors gratefully acknowledge Dr. Daniel R. Thedens, Division of Diagnostic Radiology, for his immense help with the MRI studies.

References

1. Eisenbarth, G.S. 1986. Type I diabetes mellitus. A chronic autoimmune disease. *N. Engl. J. Med.* **314**:1360–1368.
2. Sollinger, H.W., Odorico, J.S., Knechtle, S.J., D'Alessandro, A.M., Kalayoglu, M., and Pirsch, J.D. 1998. Experience with 500 simultaneous pancreas-kidney transplants. *Ann. Surg.* **228**:284–296.
3. Humar, A., Kandaswamy, R., Granger, D., Gruessner, R.W., Gruessner, A.C., and Sutherland, D.E. 2000. Decreased surgical risks of pancreas transplantation in the modern era. *Ann. Surg.* **231**:269–275.
4. Manske, C.L. 1999. Risks and benefits of kidney and pancreas transplantation for diabetic patients. *Diabetes Care* **22 Suppl 2**:B114–B120.
5. Ricordi, C., and Strom, T.B. 2004. Clinical islet transplantation: advances and immunological challenges. *Nat. Rev. Immunol.* **4**: 259–268.
6. Brambrink, T., Foreman, R., Welstead, G.G., Lengner, C.J., Wernig, M., Suh, H., and Jaenisch, R. 2008. Sequential expression of pluripotency markers during direct reprogramming of mouse somatic cells. *Cell Stem Cell* **2**:151–159.
7. Chan, K.M., Raikwar, S.P., and Zavazava, N. 2007. Strategies for differentiating embryonic stem cells (ESC) into insulin-producing cells and development of non-invasive imaging techniques using bioluminescence. *Immunol. Res.* **39**:261–270.
8. Hanna, J., Wernig, M., Markoulaki, S., Sun, C.W., Meissner, A., Cassady, J.P., Beard, C., Brambrink, T., Wu, L.C., Townes, T.M. et al. 2007. Treatment of sickle cell anemia mouse model with iPS cells generated from autologous skin. *Science* **318**:1920–1923.
9. Nakagawa, M., Koyanagi, M., Tanabe, K., Takahashi, K., Ichisaka, T., Aoi, T., Okita, K., Mochiduki, Y., Takizawa, N., and Yamanaka, S. 2008. Generation of induced pluripotent stem cells without Myc from mouse and human fibroblasts. *Nat. Biotechnol.* **26**: 101–106.
10. Okita, K., Ichisaka, T., and Yamanaka, S. 2007. Generation of germline-competent induced pluripotent stem cells. *Nature* **448**:313–317.
11. Park, I.H., Zhao, R., West, J.A., Yabuuchi, A., Huo, H., Ince, T.A., Lerou, P.H., Lensch, M.W., and Daley, G.Q. 2008. Reprogramming of human somatic cells to pluripotency with defined factors. *Nature* **451**: 141–146.
12. Raikwar, S.P., Mueller, T., and Zavazava, N. 2006. Strategies for developing therapeutic application of human embryonic stem cells. *Physiology (Bethesda)* **21**:19–28.
13. Takahashi, K., and Yamanaka, S. 2006. Induction of pluripotent stem cells from mouse embryonic and adult fibroblast cultures by defined factors. *Cell* **126**:663–676.
14. Wernig, M., Meissner, A., Foreman, R., Brambrink, T., Ku, M., Hochedlinger, K., Bernstein, B.E., and Jaenisch, R. 2007. In vitro reprogramming of fibroblasts into a pluripotent ES-cell-like state. *Nature* **448**: 318–324.
15. Wernig, M., Lengner, C.J., Hanna, J., Lodato, M.A., Steine, E., Foreman, R., Staerk, J., Markoulaki, S., and Jaenisch, R. 2008. A drug-inducible transgenic system for direct reprogramming of multiple somatic cell types. *Nat. Biotechnol.* **26**: 916–924.
16. Yu, J., Vodyanik, M.A., Smuga-Otto, K., ntosiewicz-Bourget, J., Frane, J.L., Tian,

S., Nie, J., Jonsdottir, G.A., Ruotti, V., Stewart, R. et al. 2007. Induced pluripotent stem cell lines derived from human somatic cells. *Science* **318**:1917–1920.

17. Raikwar, S.P., and Zavazava, N. 2008. Insulin producing cells derived from embryonic stem cells: Are we there yet? *J. Cell Physiol.* **218**:256–263.
18. Bergelson, J.M., Cunningham, J.A., Droguett, G., Kurt-Jones, E.A., Krithivas, A., Hong, J.S., Horwitz, M.S., Crowell, R.L., and Finberg, R.W. 1997. Isolation of a common receptor for Coxsackie B viruses and adenoviruses 2 and 5. *Science* **275**: 1320–1323.
19. Tomko, R.P., Xu, R., and Philipson, L. 1997. HCAR and MCAR: the human and mouse cellular receptors for subgroup C adenoviruses and group B coxsackieviruses. *Proc. Natl. Acad. Sci. USA* **94**:3352–3356.

Chapter 22

Transgenic Mouse Technology: Principles and Methods

T. Rajendra Kumar, Melissa Larson, Huizhen Wang, Jeff McDermott, and Illya Bronshteyn

Abstract

Introduction of foreign DNA into the mouse germ line is considered a major technical advancement in the fields of developmental biology and genetics. This technology now referred to as transgenic mouse technology has revolutionized virtually all fields of biology and provided new genetic approaches to model many human diseases in a whole animal context. Several hundreds of transgenic lines with expression of foreign genes specifically targeted to desired organelles/cells/tissues have been characterized. Further, the ability to spatio-temporally inactivate or activate gene expression in vivo using the "Cre-lox" technology has recently emerged as a powerful approach to understand various developmental processes including those relevant to molecular endocrinology. In this chapter, we will discuss the principles of transgenic mouse technology, and describe detailed methodology standardized at our institute.

Key words: Transgene, mouse embryo, pseudopregnancy, microinjection, gene manipulation, reporter genes, integration of foreign DNA.

1. Introduction

Gene manipulation has been the constant pursuit of geneticists since the end of the 19th century. Although initially started as a means to improve and select for the good qualities of species, the potential of gene manipulation was not realized until random mutagenesis screens were devised in bacteriophages and fruit flies in order to score the resultant phenotypes (1). Several advances in gene cloning, chromosomal mapping, and DNA sequencing and a wealth of breeding data on various species have heralded a new era of introducing foreign DNA into chromosomes of the host species (2). This technology often known as the transgenic animal technology has become the most popular method of introducing foreign DNA into a host genome. Mice are routinely used for this purpose, because they are relatively inexpensive, easy to

O.-K. Park-Sarge, T.E. Curry, Jr. (eds.), *Molecular Endocrinology,* Methods in Molecular Biology 590,
DOI 10.1007/978-1-60327-378-7_22,

maintain and breed and a large amount of data are available with regard to chromosomal mapping and linkage analysis of many mouse genes (2). Moreover, micromanipulation of one-cell mouse embryos is considered technically relatively easy when compared to that in other species. Our group has generated several lines of transgenic mice that phenocopy many human reproductive diseases. In the following sections, we will discuss general principles of transgenic mouse technology and provide detailed methods in later sections.

1.1. Principles

Foreign DNA can be introduced into the mouse genome mainly by three ways. The first method involves DNA delivery by retroviral infection of mouse embryos at different developing stages. Because of many technical problems, this method is not in practice for routine production of transgenic mice (2).

The second method that has been widely used since its discovery almost 25 years ago involves the direct microinjection of foreign DNA into the pronuclei of fertilized one-cell mouse embryos. Because the transgene randomly integrates as one or more copies into the mouse genome prior to embryo cleavage, all cells including those of extraembryonic origin will eventually carry the transgene (3, 4). The microinjected embryos are transferred into oviducts of pseudopregnant foster mothers that subsequently produce the transgene carrying founders at varying frequencies. The founders are typically identified by either a Southern blot or genomic PCR assay, often using the proteinase-K-digested tail DNA. These founders will eventually be used to establish independent lines that will vary with regard to the transgene integration site as well as in its copy number. This technology became very popular by the pioneering efforts of Ralph Brinster and Richard Palmiter. Although this technology has revolutionized virtually every discipline of biology, it has a significant association with the field of molecular endocrinology. This stems from the fact that one of the very first strains of transgenic mice created were gigantic as a result of over expression of growth hormone, a key pituitary hormone (5).

The third method exploits the targeted manipulation of mouse embryonic stem (ES) cells at desired loci by introducing loss or gain of function mutations as small as a single base pair change to megabase range chromosomal alterations (6–9). ES cells are derived from the inner cell mass of embryonic 3.5-day-old mouse blastocysts. These cells are pluripotent and can contribute to all cell lineages of the embryo proper when injected into recipient blastocysts (6–9). Typically, the donor and recipient blastocysts are obtained from different coat color mice that enable the easy identification of the resulting offspring, called chimeras that display a characteristic patchy distribution of coat colors. The germline transmission of the mutant allele is achieved by breeding the chimeric male mice with

normal control female mice. The resulting heterozygous mice are intercrossed to obtain the homozygous mutant mice usually at 25% frequency, if the mutation is not detrimental to embryo survival and development (6–9). In addition to the above standard gene targeting approach, gene inactivation can also be achieved both spatially and temporally and in a cell-specific conditionally restricted manner (10–12). The reader is referred to excellent reviews and various other sources for a detailed description of the principles and methods of gene-targeting strategies in mice (13, 14). In the following sections, we will describe the standard methodology used at our Transgenic and Gene-targeting Institutional Facility (http://www.kumc.edu/TGIF/transgenic2) at the Kansas University Medical Center.

2. Materials

2.1. Purification of DNA Construct

1. Montage DNA Gel Extraction Kit (Millipore, Billerica, MA) or any other suitable DNA gel extraction kit.
2. 1x Modified TAE Buffer: 40 mM Tris-Acetate, pH 8.0, 0.1 mM Na_2EDTA. Add 1 part 50x modified TAE buffer (Montage DNA Gel Extraction Kit) to 49 parts nuclease-free water.
3. 3 M Sodium Acetate, pH 5.5 (Sigma-Aldrich, St. Louis, MO).
4. 70% and 100% molecular biology grade ethanol (Sigma-Aldrich).
5. EmbryoMax Injection Buffer (Millipore).

2.2. Superovulation and Setting Up Mating of Donor Females

1. Mice of choice (*see* **Note 1**).
2. Pregnant Mare's Serum Gonadotrophin (PMSG) (Sigma-Aldrich G-4877) reconstituted to 50 IU/ml in sterile physiological saline (0.9%) or Dulbecco's Phosphate Buffered Saline (D-PBS). Aliquot into 1.5 ml microcentrifuge tubes and store at −80°. PMSG may also be administered in the form of P.G. 600 (Intervet, Millsboro, DE), a product sold in vials of 400 IU PMSG and 200 IU hCG combined. Reconstitute one vial in 8 ml PBS to achieve 50 IU/ml PMSG.
3. Human Chorionic Gonadotrophin (hCG) (Sigma-Aldrich C-1063) reconstituted to 50 IU/ml. Aliquots may then be frozen at −80° until use.
4. Donor female mice in groups of 5 or 10 between 3 and 4 weeks of age. (See Notes regarding choice of donor strain.)

2.3. Production of Pseudopregnant Recipient Females

1. Vasectomized male mice of unimportant genetic status (20 to 30), e.g. outbred CD-1 (Charles River, MA) or Swiss Webster (Harlan, IN). Mice may be requested with vasectomy surgery completed prior to shipment. Alternatively, perform vasectomy on 6-week-old males.
2. Working solution of 2.5% Avertin anesthetic, prepared from 100% Avertin solution. Prepare stock 100% Avertin by suspending 5 g 2,2,2-Tribromoethanol in 5 ml tert-Amyl alcohol in an amber Boston round glass bottle with an open-closure top (septum screw cap). Allow the suspension to remain overnight at room temperature or heat gently with agitation. Prepare working solution in small batches by diluting 0.25 ml of 100% Avertin solution with 9.75 ml sterile D-PBS (or 0.9% sterile saline). Dissolve overnight or heat gently until the Avertin crystals dissipate, then filter through a 0.22 μm syringe filter using a 10 cc syringe. Store at 4°C in an amber glass bottle and protect from light. As an alternative, a combination of Ketamine (100 mg/kg body weight) and Xylazine (10 mg/kg body weight) may be administered as an injectable anesthetic. Prepare a cocktail of these two drugs by diluting with PBS: 2 ml Ketamine (50 mg/ml), 0.5 ml Xylazine (20 mg/ml), and 7.5 ml PBS. Store at 4°C.
3. Surgical instruments, including #5 Swiss jeweler forceps; 3 ½ " iris scissors; McPherson-Vannas micro iris scissors; clip applicator and clips; and 5-0 absorbable suture with a tapered needle.
4. Recipient female mice (available pool of approximately 50) of unimportant genetic status between the ages of 2–5 months, e.g. outbred CD-1 or Swiss Webster.

2.4. Collection of Embryos

1. M2 mouse embryo culture medium buffered with HEPES (MR-015-D, Millipore). This medium is used for handling embryos outside the incubator. Thaw overnight at 4°C prior to use. Medium has a shelf-life of 2 weeks from thaw date when stored at 4°C.
2. Hyaluronidase for the dispersion of cumulus cells from the surface of the harvested embryos. Prepare by suspending 30 mg of Type IV Hyaluronidase (Sigma-Aldrich H-4272) in 3 ml sterile D-PBS. Aliquot 100 μl into microcentrifuge tubes and store at −20°C until use.
3. Bicarbonate buffered mouse embryo culture medium, KSOM (MR-106-D Millipore). This medium is used to culture embryos in an atmosphere with 5% CO_2. Thaw overnight at 4°C prior to use. Medium has a shelf life of 2 weeks from thaw date when stored at 4°C.

4. Light mineral oil (M-8410, embryo tested, Sigma-Aldrich).
5. Surgical instruments, including four pair of #5 Swiss jeweler forceps, 3 ½:" iris scissors; and micro iris scissors.
6. Petri dishes, 35 mm.
7. Transfer pipettes are purchased in packs of 20 (#14314 Vitrolife, Englewood, CO). They can also be prepared from 1.5 mm OD × 1.17 mm ID glass transfer capillary (GC150T-10, Harvard Apparatus Part #30-0062, Hollis-ton, MA) using mouth pipetting device (15" aspirator tube assembly, Drummond Scientific 2-000-000, Broomall, PA) (*see* **Notes 2**).
8. CO_2 incubator maintained at 5% CO_2, 20% air or a tri-gas incubator maintained at 5% CO_2, 5% O_2.

2.5. Preparation of DNA Construct for Microinjection

1. Microinjection buffer (modified TE buffer): 10 mM Tris-HCl, pH 7.5, 0.1 mM EDTA (or MR-095-10F, Millipore).

2.6. Pronuclear Microinjection of Embryos

1. Inverted microscope equipped with either Hoffman Modulation Contrast (HMC) or Differential Interference Contrast (DIC) optics (Nikon Ti-U). The microscope should also be equipped with a stage warmer set at 37°C (Brook Industries, OH) (**Figs. 22.1**, **22.2**, **22.3**, and **22.4**).
2. Plastic dishes for microinjection with HMC or glass depression slides for DIC.
3. Micrometer (Eppendorf Cell Tram Air and/or Oil) for controlling the suction of the holding pipette, and a microinjector or micrometer to allow injection of DNA (Eppendorf Femtojet), as well as manipulators to control the motion of both the holding pipette and injection needle.
4. Glass capillary tools: holding pipettes (VacuTip Eppendorf #930001015 or Vitrolife #14318) or prepare from glass capillary (GC100-15, Harvard Apparatus Part #30-0017) (*see* **Notes 3**); injection needle (InJek needle, MicroJek, Kansas City, MO) or prepare from 1.0 mm OD × 0.78 mm ID glass capillary with an internal filament (GC100TF-10, Harvard Apparatus Part #30-0038) (*see* **Notes 4**).
5. Incubator maintained at 37°C and 5% CO_2.
6. Stereomicroscope (Nikon SMZ-1000, Japan).
7. 60 mm Petri dish for microinjection with HMC optics.
8. M2 mouse embryo handling medium (Millipore).
9. Light mineral oil (Sigma-Aldrich).

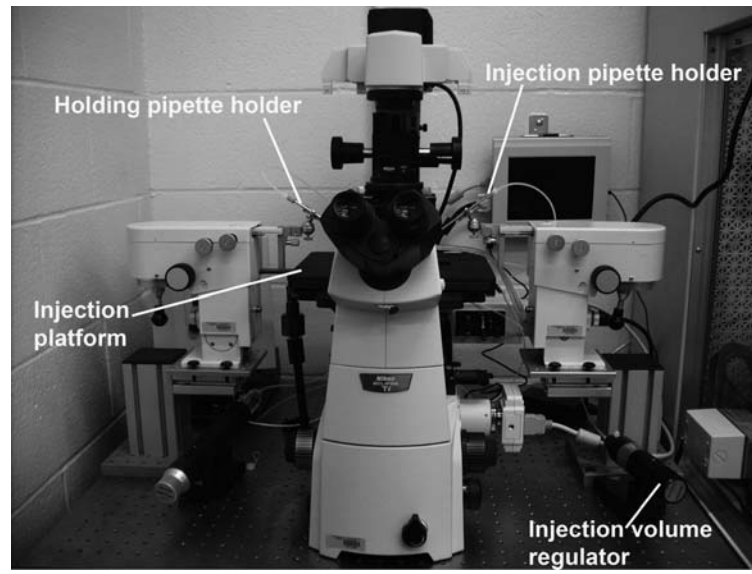

Fig. 22.1. Photograph of a micromanipulator.

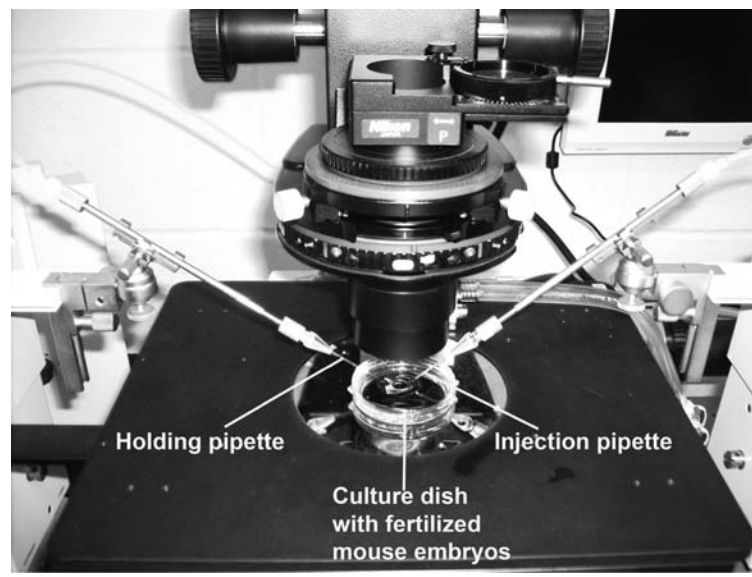

Fig. 22.2. Injection platform of a micromanipulator.

2.7. Embryo Transfer into Recipient Females

1. Stereomicroscope (Nikon SMZ-1000).
2. Working solution of 2.5% Avertin.
3. Animal weighing scale.
4. Mouth pipetting device and glass transfer pipette.
5. 35 mm petri dish.

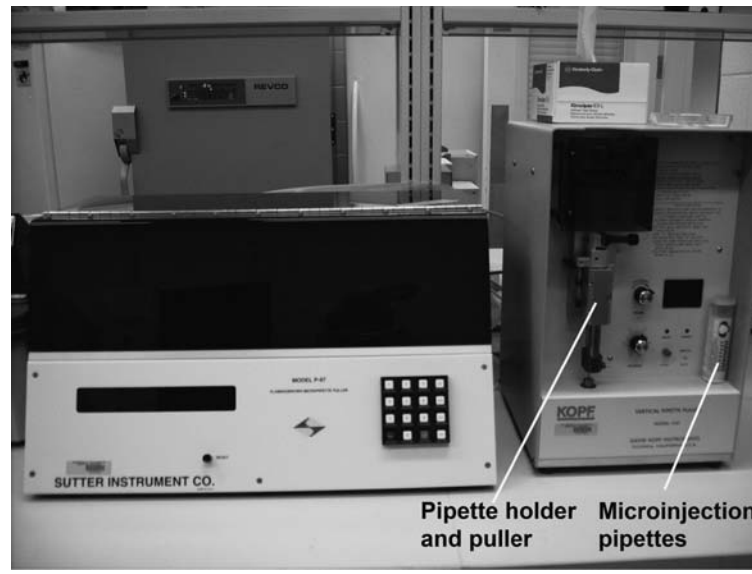

Fig. 22.3. Injection needle pullers.

6. M2 mouse embryo medium (Millipore).
7. Animal clippers with a #50 blade.
8. Alcohol swabs and povidone iodine prep pads.

2.8. Genotyping of Pups for Transgene Positives

1. Dissecting scissors and forceps.
2. Lysis buffer: 50 mM Tris pH 7.6, 100 mM EDTA, 1.0% SDS. Prepare buffer fresh from reagent stock solutions just prior to use.
3. 20.0 mg/ml Proteinase K.
4. Saturated NaCl greater than 6 M (should have precipitate on bottom of bottle).
5. 70% and 100% molecular biology grade ethanol.
6. TE buffer: 10 mM Tris-Cl, pH 7.5, 1.0 mM EDTA.
7. Taq polymerase and components: Taq DNA Polymerase (5 U/μL), 10X PCR Buffer (contains 15 mM $MgCl_2$), dNTP Mixture (2.5 mM each dNTP) (Taq HS DNA Polymerase, Hot Start Version, Takara Bio USA, Madison, WI).
8. DNA primer stocks (Integrated DNA Technologies, Coralville, IA) (*see* **Notes 5**). Reconstitute samples with ddH_2O to a stock concentration of 100 μM and store at −80°C. Dilute to a working concentration of 10 μM prior to use and store working solution at −20°C.

Fig. 22.4. Pipette polisher.

3. Methods

3.1. Purification of Transgene DNA Fragment

1. Purify the undigested plasmid containing the transgene construct either by CsCl gradient or by a membrane column method (e.g., Qiagen Plasmid Maxi/Midi Kit or Promega Wizard Plasmid Purification Kit). The design of typical transgene constructs is illustrated in **Fig. 22.5**.
2. Restriction digest the vector with appropriate restriction enzymes to completely release and separate the transgene from vector/prokaryotic sequence. The construct must therefore be designed with unique restriction enzyme(s) at

each terminus of the transgene (at both junctions with the prokaryotic backbone), permitting isolation by restriction enzyme digest.

3. Electrophorese the products of the restriction digest through a <1.25% agarose gel in 1x Modified TAE buffer.
4. Using a transilluminator, excise the DNA band with a razor and place into the Montage DNA Gel Extraction Device. The size of the gel piece should be less than 100 mg.
5. Close lid and spin assembled device for 10 min at 5000*g*. When finished, discard the Sample Filter Cup and Gel Nebulizer.
6. Determine the volume of your sample. Add 1/10 volume of 3 M sodium acetate pH 5.5 and 2.5 volumes 100% ethanol. Mix and centrifuge at 15,000*g* for 15 min. Wash with 70% ethanol, air dry, and resuspend in EmbryoMax Injection Buffer. Concentration should be greater than 2.0 ng/μl.

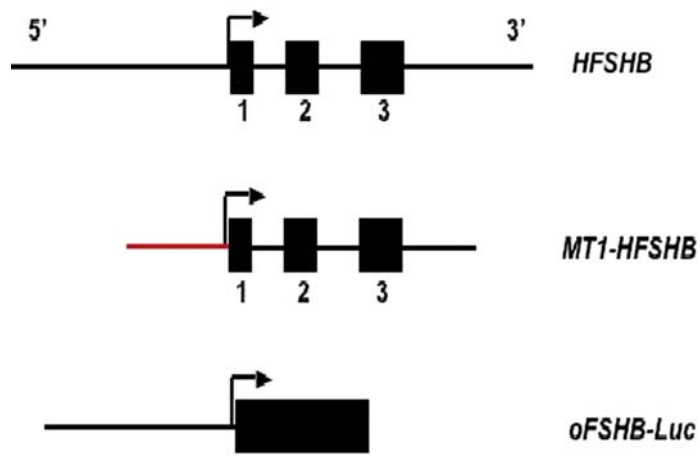

Fig. 22.5. Design of transgenes. Some representative examples of transgenes that we and other groups have used are shown. The top construct contains 10 kb of *HFSHB* sequences (~4 kb of 5' promoter sequences, 2 kb of 3' downstream sequences and all three exons shown as black boxes with numbers below) and was designed to test the gonadotrope-specific and hormonal regulation in pituitaries of transgenic mice (15). Middle panel contains a 1.8 kb mouse metallothionein-1 (MT1) promoter that drives the expression of *HFSHB*sequences. This transgene was designed to achieve *FSHB* expression to multiple ectopic tissues (37, 69). The bottom panel shows a 4.7 kb sheep *FSHB* promoter-luciferase transgene (*oFSHB-Luc*) that was designed to test the regulation of sheep FSHB promoter by GnRH, activins, and various other transcription factors (70, 71).

3.2. Superovulation

1. Day 0 is day of embryo microinjection. Begin superovulation on day 3. Thaw desired aliquots of PMSG gently by holding in your hand until all ice has melted. Invert the tube to mix and load a 1 cc insulin syringe. Restrain female mouse and expose abdomen for an intraperitoneal (i.p.) injection.

Administer PMSG at 5 IU per female; therefore dose each female 100 µl or 0.1 cc. Time of administration should be early afternoon, e.g. 2:00 pm. After injection, return females to their regular housing.

2. Administer hCG 46–48 h after PMSG injection (day 1) by i.p. injection at 5 IU per mouse. After injection, pair females with a singly housed, intact stud males and allow to mate overnight.
3. The next morning, remove females from the males and check for copulation plugs.
4. Also on day 1, prepare embryo culture dishes by placing four 20 µl drops of KSOM on the bottom of two 35 mm petri dishes. Overlay with light mineral oil and equilibrate overnight at 37°C in a humidified incubator at 5% CO_2 (and 5% O_2 if tri-gas incubator is available).

3.3. Production of Pseudopregnant Recipient Females

1. Assuming outbred stud males are purchased already vasectomized from a commercial source, breeding of recipient females needs to begin at least the day before embryo microinjection is scheduled (d -1).
2. If in-house vasectomies are performed, the following procedure can be used.
   a) Anesthetize a 6-week-old CD-1 male by i.p. injection of 2.5% Avertin at 0.015 ml per gram of body weight. Check that the male is unconscious by toe pinch reflex.
   b) Lay the male on his back and clip the hair of the lower abdomen with a #50 blade. Prep the incision site with alcohol, povidone iodine, and alcohol again.
   c) Sterilize instruments by immersing the tips in a bead sterilizer at 250°C. Using forceps, grasp the skin just antral of the penis and make a transverse incision.
   d) Using clean forceps, grasp the body wall and cut transversely just antral of the fat pads that lie beneath the skin. A testicular complex can be exteriorized by grasping the fat pad that lies adjacent to the bladder.
   e) As the testis appears, a long curved tube can be seen. Grasp the vas deferens with a pair of forceps and hold away from the body cavity. Over a burner, flame the tips of a pair of forceps and when red, grasp the tube on both sides of the forceps, effectively removing a loop of the vas deferens while cauterizing the ends.
   f) Return the testis to the body cavity and repeat on the other side.
   g) Stitch body wall with 5-0 absorbable suture with a tapered needle. Close skin with two wound clips. Allow the male to recover in a cage on a warmed surface until ambulatory.

h) Remove wound clips at 1 week. Check that vasectomy is complete by test-mating males 2 weeks after surgery by pairing naturally cycling adult outbred female mice with vasectomized males at 1–2 females per male.

i) Euthanize the female the next morning and look for sperm in the reproductive tract, or allow it to mate and wait 10 days to determine if pregnant. If no sperm or pregnancies, males can be used to generate pseudopregnant recipients.

3. Pair naturally cycling adult outbred female mice with vasectomized males at 1–2 females per male. Add the females to the male's cage, rather than adding the male to the females' cage. Establish at least 15 mating pairs.
4. The next morning, remove females from the males and check for copulation plugs. The morning of plugging is considered day 0.5, these females are suitable for oviduct transfer.

3.4. Collection of Embryos

1. Prepare 35 mm dishes of medium by transferring in a sterile manner 3 ml of M2 into three dishes. To one dish, thaw and add the aliquot of hyaluronidase that was previously prepared.
2. Sterilize surgical instruments by immersing the tips in a bead sterilizer for 15 s. Allow to cool down while keeping the tips clean.
3. Euthanize plugged female mice by cervical dislocation or CO_2 inhalation. Prepare females by laying on their back on an absorbent surface and wetting the abdomen with 70% ethanol (to reduce the distribution of cut hair).
4. Grasp the skin of the lower abdomen of each mouse and make a single transverse cut with the iris scissors. The skin may then be pulled back by grasping the incision site and the tail and pulling in opposite directions.
5. Now grasp the body wall. Again make a transverse cut across the lower abdomen, and use the scissors to increase the cuts to either side of the body. Fold body wall back on top of the thorax.
6. Using clean forceps, displace the intestines to the outside of the body cavity and locate the kidneys along each side of the spine. The ovaries will lie rostral to each kidney, with the oviducts and uterine horns attached. Pick up an ovary with one hand and stretching gently, use the micro iris scissors to cut the connective membrane between the ovary and the oviduct. Now grasp the space between the oviduct and uterine horn and cut this connection in a similar manner. Place the excised oviduct into a dish of M2. Repeat this procedure for both oviducts of all donor mice.
7. Transfer the excised oviducts to the dish of M2 and hyaluronidase. Under a stereo microscope, use clean forceps to immobilize

one oviduct on the bottom of the dish. Locate the ampulla (the swollen section of the oviduct, which will appear extended and clear) and tear open with the tip of the other forceps. The cumulus mass containing the embryos will "pour" out of the oviduct, usually with no further manipulation required. Remove the empty oviduct from the dish and repeat the process for all of the remaining oviducts.

8. After all oviducts have been removed from the dish, attach a transfer pipette to a mouth aspirator assembly. Pick up embryos that have fallen out of the cumulus mass as the cells disperse in the hyaluronidase.
9. Wash embryos in the third dish of M2, wash in KSOM, transfer to a culture drop of KSOM and place in incubator until microinjection.

3.5. Preparation of Transgene DNA for Microinjection

1. Just prior to microinjection, prepare 50 μl of a working dilution of the transgene DNA at 1 ng/μl in microinjection buffer.
2. Spin small constructs at high speed for 10 min in order to pellet any particulate debris in the suspension. Carefully remove the top half of the suspension and transfer to a clean microcentrifuge tube. Maintain at 4°C for use that day.

3.6. Microinjection

1. Prepare a microinjection dish by placing a 75–100 μl drop of M2 in the center of a 60 mm petri dish. Overlay the drop with light mineral oil. Place the injection dish on the inverted scope and turn on stage warmer to 37°C.
2. Assemble holding pipette and place on manipulator.
3. Pull a microinjection needle and carefully place the blunt end into the DNA solution. Allow the tip to load by capillary action. Load needle into holder and turn on Femtojet. The microinjector will require some time to establish pressure within the system, but a needle must be loaded prior to turning on the Femtojet. Similarly, any time that a needle requires changing, the Femtojet must be paused.
4. Lower both the holding pipette and the injection needle into the microinjection drop, first manually and then adjust with the vertical control of the manipulators. Both instruments should be positioned horizontally across the field of view.
5. Remove embryos from the incubator and transfer a small quantity (20 if learning, 50 or more when proficient) to a dish of M2. (Return the KSOM dish with remaining embryos to the incubator.) Pick embryos up in a small volume of M2 and on low magnification on the inverted microscope, deposit in the microinjection drop just south of the glass capillary tools.

6. While on low magnification, dial back on the holding pipette to establish suction and attempt to pick up an embryo **(Fig. 22.6)**. Adjust vertical position of the pipette as necessary, to be as close as possible to the level of the embryo without the pipette dragging on the bottom of the dish.
7. Switch to high magnification. Position the embryo so that the pronuclei are not obscured by the polar bodies. Also minimize the real estate of the embryo that must be traversed prior to reaching a pronucleus with the injection needle. For obvious reasons, it is prudent to aim for the larger of the two pronuclei.
8. Once the embryo is positioned, bring the pronuclear membrane into focus by adjusting the fine focus on the microscope. Next, bring the injection needle close to the edge of the embryo. Focus the very tip of the needle by raising and/or lowering the manipulator, without adjusting the focus on the microscope. In this way, the needle will be on the same plane of focus as the pronucleus.
9. Advance the needle into the embryo and puncture the pronuclear membrane **(Fig. 22.7)**. Inject the DNA solution until the pronucleus visibly swells, then withdraw the needle swiftly but gently (*see* **Notes 7–9**). Injection needles may need to be changed with some frequency during injection, as they may become clogged or sticky.
10. Move the injected embryo to the top of the microinjection dish and repeat with the next embryo. When all embryos in the dish have been injected, pick up the embryos, wash through KSOM, transfer back into a culture drop of KSOM and return to the incubator for keeping until embryo transfer surgery. Remove the next group of embryos for microinjection and repeat the process until all are injected.

3.7. Transfer of Embryos to Recipient Females

1. Embryo transfer surgery requires area for animal preparation, embryo handling, surgery, and recovery. Begin by weighing the recipient female (identified earlier by copulation plug). Avertin (2.5%) is administered i.p. at 0.015 ml per gram of body weight (BW). Alternatively, Ketamine/Xylazine is administered i.p. at 0.01 ml/g BW. Allow the anesthetic several minutes to take effect.
2. Remove injected embryos from the incubator and transfer to a dish of M2. Sort embryos into groups of 25 after removing all embryos that lysed following microinjection.

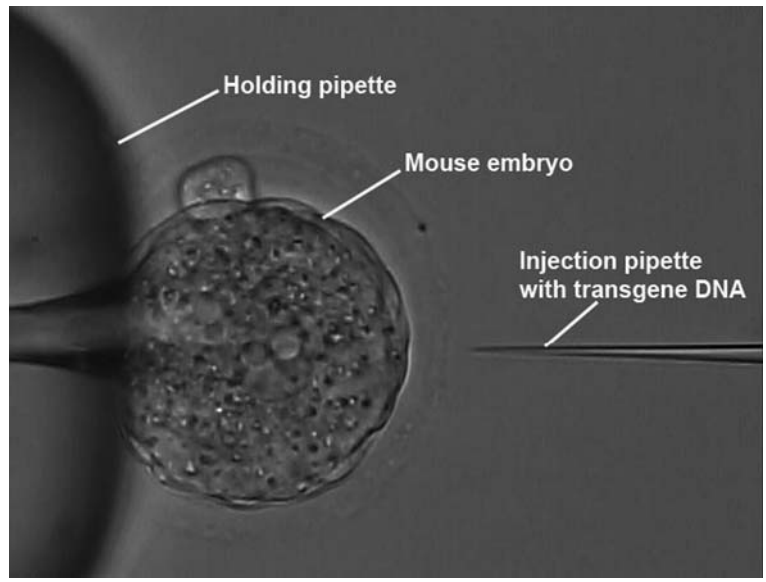

Fig. 22.6. A mouse embryo held with a holding pipette is ready for microinjection of DNA.

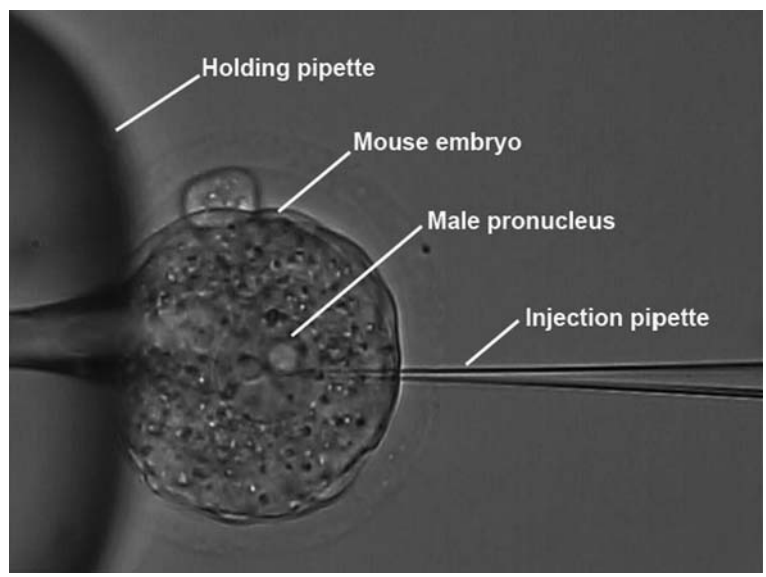

Fig. 22.7. A mouse embryo photographed just after microinjection of transgene DNA into the male pronucleus.

3. Remove the hair from the back of the mouse by clipping with a #50 blade. Wipe the clipped area with an alcohol prep pad to remove hair and scrub with a povidone prep pad. Follow with another alcohol wipe and move the mouse to the surgery area.

4. Sterilize all instruments by immersing the tips in a bead sterilizer at 250°C. With forceps, pick up the skin lying immediately over (dorsal) the area of the kidney on one side of the mouse and make a small incision with iris scissors.
5. With clean forceps, pick up the body wall beneath the incision and make a small opening. The ovary will lie rostral to the kidney and can be identified by the large fat pad attached to it. Grasp the fat pad, exteriorize the reproductive tract, and lay over the back of the mouse by clamping the fat pad with a bulldog Serrafin clamp.
6. Load embryos into the transfer pipette in as small a volume as possible. Load M2 medium, an air bubble, medium, another air bubble, and the embryos in single file. Aspirate an additional air bubble and a small amount of medium after the embryos at the tip of the transfer pipette. The loaded aspiration assembly can then be suspended over the microscope eyepiece while the oviduct is exposed.
7. Move the mouse to the stage of the microscope and focus on the oviduct. The infundibulum will lie dorsal and slightly below the rest of the oviduct (at the junction with the ovary). Identify the infundibulum and using clean forceps tear the bursa immediately above the opening of the oviduct, taking care to avoid blood vessels.
8. Pick up the aspiration assembly and position the transfer pipette at the opening of the infundibulum. Insert the pipette and grasp the outside of the oviduct over the pipette with forceps in the opposite hand. Expel the contents of the pipette until two air bubbles appear in the ampulla (those before and after the embryos in the transfer pipette).
9. Remove the clamp and return the tract to the body cavity. It is not necessary to suture the body wall. Close the skin with a wound clip. Place the recipient female in a new cage and allow to recover on a warmed surface until ambulatory. Repeat for any additional embryos and recipients. If there are insufficient recipients on day 0, embryo transfers may be performed at the two-cell stage the following day into 0.5 day recipients.

3.8. Genotyping and Identification of Founders

1. Pups will be born between day 19 and 21. Wean pups at 3 weeks of age and collect tail biopsies. Scruff pups, identify by ear punch or other means, and cut off a small piece of the tail (0.5 cm). Place the tail biopsy in a microcentrifuge tube and mark with the identification number of the mouse. Place on ice while other samples are collected. Rinse dissecting scissors and forceps with 70% ethanol between each sample. Store all tail biopsies at −20°C until ready to process.

2. If the DNA extracted from the tail is just for PCR analysis, modern DNA isolation kits will work (Sigma's REDExtract-N-Amp Tissue PCR Kit, Sigma, St. Louis, MO) and have been proven to be cheap, quick, and reliable. If further analysis of the DNA is needed (e.g., Southern blotting), most kits are not suitable as they will shear the genomic DNA to a size less than 10 kb. The following is a traditional proteinase K digestion that will yield genomic DNA to a size greater than 40 kb.
3. Lyse tail in 500 µl Lysis Buffer (50 mM Tris pH7.6, 100 mM EDTA, 1.0% SDS). Add 20 µl 20 mg/ml Proteinase K and incubate at 55°C overnight.
4. Add 250 µl saturated 6 M NaCl.
5. Shake tube approximately 500 times. Do not vortex to prevent shearing of genomic DNA.
6. Chill on ice for 10 min. Centrifuge at 4,400*g* for 10 min.
7. Aspirate 650 µl of supernatant and transfer to new microcentrifuge tube. Add 2 volumes of 100% ethanol, invert 10–20 times. Spool DNA with a glass rod (capillary tube with one end sealed) and rinse with 70% ethanol. Resuspend in 50 µl TE buffer.
8. Determine the quality of the DNA prep by spectrophotometer (good quality = 260/280 reading between 1.6 and 2.0). If quality of the prep is poor (spectrophotomer 260/280 reading > 2.0 or < 1.6), a phenol–chloroform extraction can be performed to decrease the DNA contaminants. The DNA must be precipitated again after phenol–chloroform extraction. Store resuspended DNA at −20°C.
9. Thaw all PCR reagents, templates, and controls on ice. Taq polymerase should be kept at −20°C.
10. Mix following in PCR tube for each reaction. A Master Mix of buffer, dNTP's, primers, Taq, and water can be prepared and aliquoted into PCR tubes, to which the sample DNA is then added for each tail sample.

Templates (25-200 ng/µl)	**x µl**
10x Buffer (with $MgCl_2$)	5.0 µl
2.5 mM dNTP	4.0 µl
10 µM Primer-Forward	2.0 µl
10 µM Primer-Reverse	2.0 µl
Taq(1.25 U/µl)	0.25 µl

Add sterile ddH2O to a final volume of 50 µl (*see* **Note 10**).

12. Place into thermocycler and program the PCR reaction as follows:

Step	Temperature (°C)	Time
1	94	2 min
2	94	15 s
3	*	15 s
4	72	**
5	Goto step 2	30 times
6	72	5 min
7	10	–

*Annealing temperature may vary from primer set to primer set, optimizing may be necessary. $^{o}C = [4(G + C) + 2(A + T)] - 5$, for only primers < 20 bp.
** For extension times use 1 min per 1 kb expected fragment size.

13. Run PCR products on an agarose gel and visualize on a transilluminator **(Fig. 22.8)**.

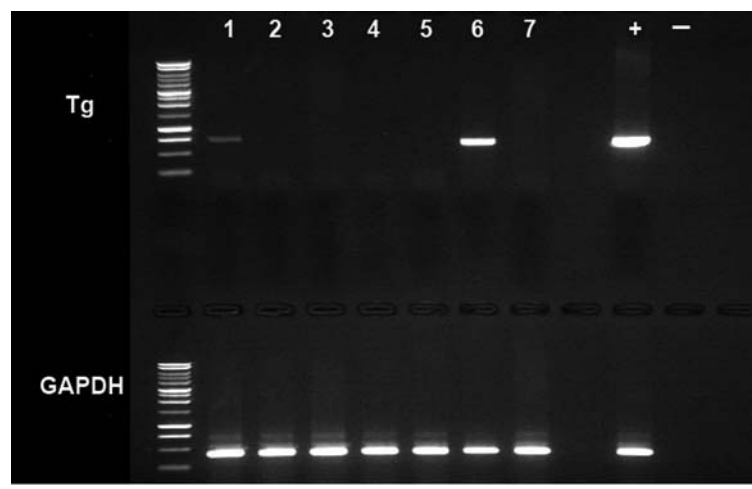

Fig. 22.8. Example of a typical genomic PCR gel depicting amplified products from a transgene (Brca1) and an internal control (GAPDH) gene. The left most lane in *top* and *bottom panels* contains 100 bp DNA size markers. Tg: transgene fragment amplified in founder mice. GAPDH: Primers for glyceraldehydes-3-phosphate dehydrogenase encoding gene (GAPDH) used as an internal control for checking the presence of DNA in each lane. +: Amplified products from positive control plasmids containing Tg (*top panel*) or GAPDH (*lower panel*) DNA sequences.

3.9. Applications of Transgenic Technology

Transgenic technology offers limitless opportunities to determine in vivo gene functions in numerous ways. In general, the transgenes are expressed in a tissue/cell-specific manner using either homologous (i.e., mouse) or heterologous (e.g., rat, cow, sheep, human, pig, etc.,) gene regulatory sequences (3, 4). Mouse genes or cDNAs appropriately marked with random oligos or engineered with heterologous downstream polyadenylation DNA sequences are also used (3, 4). The effects of overexpression of transgenes on organ development and/or physiology are then monitored. In some instances, ectopic expression of the transgene is also achieved by purposefully directing its expression to tissues/cells different from those in which the corresponding mouse gene is normally expressed (3, 4).

In several instances, data obtained with cell transfection studies on mapping the regulatory regions of genes that confer tissue/cell specific expression most often are not very well correlated or difficult to interpret, compared to the corresponding in vivo scenario. In such cases, transgenic approach is often used to identify, map, and define the minimal regulatory elements of a given promoter that dictate tissue/cell specific expression and hormonal regulation. This is usually achieved by first engineering a series of deletion constructs from a larger piece of the gene that is known to confer tissue/cell specific expression. Subsequently, the truncated transgenes are microinjected to produce transgenic mice and their expression in the selected cell type is monitored at the RNA and/or protein level as an endpoint (15). Similar strategies have also been used in which a known transcription factor-binding site is mutated on a given promoter driving the expression of a transgene and its functional consequence tested in vivo (16–20). In case the promoter elements of a given gene are already identified and characterized, these can be used to direct the expression of useful reporters that can be quantitatively assayed. The commonly used reporters for quantifying the promoter activity include lacZ from *E. coli*, chloramphenicol acetyl transferase and the firefly luciferase (2).

Developmental expression of many genes that have important endocorine function can be tracked using lineage marking and cell fate mapping. Depending on specificity and expressivity of the gene regulatory sequences and the earliest time at which these are activated as early as during embryogenesis, expression of either lacZ, alkaline phosphatase, or various fluorescent reporters (e.g., GFP, CFP, YFP, or dsRed) can be targeted to specific cell types (2). Tissues/cells are harvested in such cases, and the activity of lacZ (formation of a blue product), alkaline phosphatase (formation of blue or red product) or the visualization of distinct colors under ultraviolet illumination is monitored starting from embryonic stages (2). Thus, tracking such "reporter-tagged" cells through distinct developmental stages will provide a novel way to study the linage specification and

differentiation of desired cell types. Furthermore, cell–cell interactions during organogenesis can sometimes be visualized on a short-term basis in a Petri dish by live cell imaging using confocal microscopy. Because cells expressing fluorescent reporters can be sorted by fluorescence activated cell sorting, these transgenic mice will also provide novel resources to purify desired cell types from a tissue consisting of heterogeneous populations of various other cells (21–23). These can be further used for gene/protein expression profiling under normal physiological or pathological conditions.

Transgenic approaches that identify cell/specific regulatory elements have also been useful for selectively ablating cells at desired times and study the consequences of the loss of hormones secreted from these cells (2). This has been achieved by expressing either diphtheria toxin (17), or herpes simplex virus thymidine kinase (24), or viral-specific ion channels (25). In the latter two cases, either an appropriate substrate (gancyclovir) or an ionophore (calcium or sodium channel activator or blocker) is used to produce either a cell-toxic product or changes in ion flux that affect hormone secretion, respectively. These approaches have been used, e.g., to study the consequences of ablation of gonadotropes on gonadal development and reproduction (24). More recently, ablation of Sertoli cells has been achieved to study the consequences on germ cell development and function that consequently impact male reproduction (26).

Transgenic strategies permit immortalization of rare cell types that are often difficult to obtain in large numbers and good purity for routine cell transfection analyses (27–32). This is usually achieved by targeted expression of viral oncogenes to immortalize desired cell types in vivo (33). Moreover, novel cell lines are derived from these tumors and established as useful in vitro tools for various studies. Since many cell types within the endocrine organs are post-mitotic, this approach has been particularly very useful for immortalizing these endocrine cell types and establishing novel cell lines (27–32). Many of these cell lines have been used to investigate specific signal transduction pathways, and transcriptional regulation (27–32). In some cases, these tumor-prone mouse models also phenocopy known human cancers and thus have tremendous potential to understand the pathobiology of the human disease (29). Furthermore, these models can also be a useful resource for identifying novel cancer biomarkers.

In many cases, the expression of a given transgene is dependent on the promoter that drives its expression, and in some cases the site of its integration and copy number will also dictate the expression of the transgene. In addition, some promoters also exhibit high basal activity in many tissues (34, 35). This feature has been exploited to ectopically express various hormones in multiple tissues at high basal

levels and the consequences analyzed (36–38). Some of these promoters are also inducible, e.g., metallothionein-1 promoter is induced by heavy metals such as zinc and cadmium (34, 35).

A strategy to temporally induce transgene expression has also been developed. In this approach, the desired protein encoding cDNA or gene is engineered downstream of a conditionally activated "gene switch" (39, 40). This "gene switch" consists of DNA sequences that often encode a bacterial repressor protein and an operator region that is linked to the gene/cDNA of interest. The repressor binds to the adjacent operator DNA sequence that is fused in tandem with the gene/cDNA of interest and keeps it inactive. This entire "gene switch" cassette along with the gene/cDNA of interest is engineered under the regulation of a tissue/cell specific promoter. When a drug that binds the repressor and prevents it from binding to the operator region is administered to transgenic mice, it allows the transcription of the desired gene/cDNA at specific times. Based on this principle, transgenic mice have been developed using tet ^{on}(41), ecdysone (39, 42), RU486 (43), tamoxifen (44) gene switches as inducible gene expression models.

Many transgenic lines of mice have also been successfully used in gene targeting experiments to genetically rescue knockout mutant mice, spatio-temporally inactivate genes by using the Cre-lox approach, cell fate mapping, and gene/protein expression profiling.

3.10. Resources

In the above sections we have described a summary of various principles of transgenic mouse technology. We encourage the reader to browse through excellent mouse genome resources available as public databases (**Table 22.1**). The Jackson Labs in Barr Harbor, ME, and the mouse genome informatics are great resources for all the mouse genome–based information. This is tightly linked to the National Center for Biotechnology Information (NCBI) that provides various mouse genomics tools. Similarly, ENSEMBL website maintained by The Sanger Institute in Cambridge, UK, has numerous resources related to genomes of mouse, human, and other species. A number of Institution-based web sites also provide transgenics (66) and other mouse genome resources (**Table 22.2**). There are several ready-to-use practical manuals and reference books that describe various aspects of transgenic and knockout mouse technologies (2, 14, 45). Finally, species other than mouse have also been successfully used for transgenesis including chicken (46, 47), cow (48–50), fish (salmon and zebra fish) (51–54), frog (55, 56), goat (57–59), sheep (50, 60), pig (61, 62), rabbit (63–65), rat, and monkey (67, 68). However, several methodological refinements are ongoing in several laboratories to routinely achieve transgenesis in species other than rodents.

Table 22.1
List of web links to some useful mouse genome resources

International Gene Trap Consortium	http://www.genetrap.org
Baygenomics	http://baygenomics.ucsf.edu
The Jackson Laboratory (General site)	http://jax.org
Federation of International Mouse Resources	www.fimre.org
European Mouse Mutant Archive	http://www.emma.rm.cnr.it
Ensembl Mouse	http://www.ensembl.org/Mus_musculus/index.html
Mouse Genome Informatics	http://www.informatics.jax.org
Trans-NIH Mouse Initiative	http://nih.gov/science/models/mouse/resources/index.html
Lexicon Genetics	http://www.lexicon-genetics.com/index.php
Baylor College of Medicine (ENU project)	http://www.mouse-genome.bcm.tmc.edu
Cornell University (ENU project)	http://www.vertebrategenomics.cornell.edu
The Jackson Laboratory (Infertility website)	http://jaxmice.jax.org/library/notes/496c.html
The Sloan-Kettering Mouse Project	http://mouse.ski.mskcc.org

Table 22.2
Useful Institutional websites for transgenic core facilities

Institute	Website
1. Johns Hopkins University Transgenic Core Laboratory	www.hopkinsmedicine.org/core/home.htm
2. University Pennsylvania Transgenic & Chimeric Mouse Facility	www.med.upenn.edu/genetics/core-facs/tcmf
3. Stanford University Transgenic Mouse Research Facility	med.stanford.edu/transgenic
4. University of Michigan Transgenic Animal Model Core	www.med.umich.edu/tamc
5. University Pittsburgh Transgenic & Chimeric Mouse Facility	www.genetics.pitt.edu/services/labpage.html?whichlab=tcmf
6. Duke University Transgenic Mouse Facility	www.cancer.duke.edu/tmf/about

(continued)

Table 22.2 (continued)

Institute	Website
7. Yale University Animal Genomics Services	www.ags.med.yale.edu
8. Washington University Mouse Genetics Core	www.mgc.wustl.edu
9. Baylor College of Medicine Genetically Engineered Mouse Core	www.bcm.edu/gemcore/home.htm
10. University of Texas M.D. Anderson Cancer Center	www.mdanderson.org/departments/gemf/

4. Notes

1. The embryo donor strain is dependent upon the desired background strain for the transgenic line, tempered by the strain with which an injector is willing to work. Inbred C57BL/6 embryos are increasingly requested, as this strain has become the gold standard for experimental research. However, C57BL/6 mice and their embryos present a number of difficulties which decrease the efficiency of producing transgenic mice: a great number of ovulated ova are uninjectable; the cytoplasm of the embryo is granular and the pronuclei are small, which make them difficult to inject; a high proportion of the embryos lyse following microinjection; and few embryos develop to term and live-born pups. For these reasons, many transgenic facilities choose to inject C57BL/6 hybrid embryos, e.g. C57BL/6 x SJL = B6/SJL, providing hybrid vigor on a partial C57BL/6 background. If C57BL/6 mice are not desired, FVB/N embryos are the easiest to microinject, due to their clear cytoplasm, large pronuclei, and high survivability following microinjection. Inbred C57BL/6 mice should be superovulated between 3 and 4 weeks of age. Expect as many as 40–50 ova per mouse, of which only 20 may be injectable. Hybrid C57BL/6 mice may be superovulated between 4 and 5 weeks of age. The number of ova per mouse should average about 30, most of which should be injectable. Inbred FVB/N mice respond well to superovulation between 5 and 6 weeks of age. These mice yield fewer ova, about 20 per mouse, but nearly all should be injectable.
2. Transfer pipettes are prepared by pulling a capillary tube by hand. Hold a GC150T-10 capillary at both ends, heat the center of the tube over a low flame (either ethanol burner or Bunsen burner) until pliable, and pull hands apart in a swift and

steady motion. The thin neck of the capillary can then be scored with a diamond pen and separated into two pipettes. The tip of the transfer pipette can be polished by holding close to the flame or the heating filament on a microforge, to prevent gouging the bottom of a plastic dish and potentially damaging embryos, especially for users new to manual pipetting. The internal diameter should be approximately 150 μm; a smaller diameter provides greater control but requires a steadier hand to pick up embryos.

3. Holding pipettes are prepared in a manner similar to transfer pipettes. Heat a GC100-15 capillary over a flame and pull apart. Score and separate the two pieces, and place one pipette on the microforge. Polish the tip of the pipette by lowering close to the heating filament, without touching, and heat until the opening of the pipette is almost closed. This will prevent damage to the embryos when immobilizing in the injection dish, and the small opening will prevent the embryos from being drawn into the pipette when suction is applied.
4. Injection needles are pulled on a mechanical pipette puller (Kopf or Sutter P-97). Load the injection capillary GC100TF-10, taking care not to touch one end of the tube. After pulling, remove the clean half and backload DNA by immersing the back end in the DNA solution. The tip of the needle will fill with DNA by capillary action through the internal filament.
5. When designing primers, a unique product must be generated to distinguish the introduced transgene from the host genome. Once the sequence is decided upon, primer selection can be based on traditional rules of thumb (avoid runs over 3 nucleotides; primer length of 18-26 bp; GC content between 40% and 60%; 3' end should be G or C; avoid palindromes and hairpin sequences; avoid complementation between primer pairs; and select melting temperature between 55 and 70°C) or use online primer design programs (**Primer3: WWW primer tool**, University of Massachusetts Medical School, MA).
6. Primer sets should be tested and optimized prior to genotyping. Optimal annealing temperature and $MgCl_2$ concentration should be determined using genomic DNA (negative control) and genomic DNA spiked with linearized transgene at one copy number per genome (positive control).
7. If DNA fails to cause the pronucleus to swell, check that the microinjector (Femtojet) is in inject mode. Test the needle by attempting to inject an embryo. If the pronucleus does not swell, the tip of the injection needle may

need to be broken. If so, focus on the holding pipette and adjust the manipulator height until the tip of the needle is also in focus. Insert the very tip of the needle into the opening of the holding pipette and gently brush the needle against the side of the holding pipette. This should break the tip, creating an opening through which DNA can pass. If it appears that the needle is broken open sufficiently and still no DNA comes out, it may be that material is covering the opening of the needle. In this case, discard the needle and prepare and load a new needle.

8. Another common problem occurs when embryos lyse after microinjection. A proficient microinjectionist may lyse only 1–5% of injected embryos, but the standard rate of lysis post-injection is between 10 and 20%. New injectionist will likely see a much higher rate of lysis (50% or greater). Embryos will lyse if the opening of the injection needle is too great and causes irreparable damage to the membranes. If this is the case, discard the needle and try again with a fresh needle. Similarly, lysis will be high if the rate of DNA flow is too great. This may happen if the pressure is too high on the Femtojet or if the opening of the injection needle is too large. Flow can be ascertained after penetrating the plasma membrane: if movement of the cytoplasm is evident, the flow is too high. Another common source of lysis occurs when withdrawal of the injection needle pulls out the nucleoli of the pronucleus. The tip of the needle is likely sticky, either from embryo debris or large pieces of DNA. It is possible that attempts to remove the material by brushing against the holding pipette may work, but it is advisable to change the needle. The embryos will likely lyse in time, even if they appear intact immediately following injection.
9. Very large DNA constructs, such as bacterial and yeast artificial chromosomes (BACs and YACs), require special handling to ensure that the construct remains intact before and during microinjection. But it should also lead to a greater number of transgenic mice incorporating the entire construct versus fragments of the BAC or YAC. Inject the freshly prepared BAC/YAC at a concentration of 0.5–1.0 ng/μl, using wide bore tip. It will be necessary to break the tip to create a larger opening (than for small DNA constructs). Avoid vigorous pipetting as this will likely lead to a DNA shearing and higher incidence of lysis.
10. The concentration of $MgCl_2$can be optimized by using 10x PCR buffer without $MgCl_2$and increasing the final concentration from 0.5 to 2.5 mM by increments of 0.5 mM $MgCl_2$until a strong band can be visualized when the PCR products are run on an agarose gel.

Acknowledgments

T.R.K. acknowledges funding support from NIH (NCRR Center for Biomedical Research Excellence Program Grant RR024214, HD04394, HD056082 and K-INBRE P20 RR016475) and The Hall Family Foundation, Kansas City, MO. H.W. is the recipient of a postdoctoral fellowship from the Biomedical Research Training Program at the Kansas University Medical Center.

References

1. Griffiths, A.J.F., Wessler, S.R., Lewontin, R.C., Carroll, S.B. (2008) *Introduction to genetic analysis*. W.H. Freeman & Co., New York.
2. Nagy, A., Gertsenstein, M., Vintersten, K., Behringer, R. (2003) *Manipulating the mouse embryo: A laboratory manual*; 3rd Edition, Cold Spring Harbor Laboratory, New York.
3. Palmiter, R.D., Brinster, R.L. (1986) Germline transformation of mice.*Ann Rev Genet.* **20,** 465–499.
4. Brinster, R.L., Palmiter, R.D. (1984) Introduction of genes into the germ line of animals. *Harvey Lectures.* **80,** 1–38.
5. Palmiter, R.D., Brinster, R.L., Hammer, R.E., Trumbauer, M.E., Rosenfeld, M.G., Birnberg, N.C., Evans, R.M. (1982) Dramatic growth of mice that develop from eggs microinjected with metallothionein-growth hormone fusion genes. *Nature.* **300,** 611–615.
6. Bradley, A, van der Weyden, L. (2006) Mouse: Chromosome Engineering for Modeling Human Disease. *Ann Rev Genomics Human Genetics.* **7,** 247–276.
7. Capecchi, M.R. (2005) Gene targeting in mice: functional analysis of the mammalian genome for the twenty-first century. *Nat Rev Genet.* **6,** 507–512.
8. Evans, M. (2005) Embryonic stem cells: a perspective. *Novartis Found Symp.* **265,** 98–103; discussion 103–106.
9. Koller, B.H., Smithies, O. (1992) Altering genes in animals by gene targeting. *Ann Rev Immunol.* **10,** 705–730.
10. Le, Y., Sauer, B. (2001) Conditional gene knockout using Cre recombinase. *Mol Biotechnol.* **17,** 269–275.
11. Sauer, B., Henderson, N. (1989) Cre-stimulated recombination at loxP-containing DNA sequences placed into the mammalian genome. *Nucleic Acids Res.* **17**, 147–161.
12. Porret, A., Merillat, A.M., Guichard, S., Beermann, F., Hummler, E. (2006) Tissue-specific transgenic and knockout mice. *Methods Mol Biol.* **337,** 185–205.
13. Austin, C.P., Battey, J.F., Bradley, A., Bucan, M., Capecchi, M., Collins, F.S., et al. (2004) The knockout mouse project. *Nat Genet* **36**, 921–924.
14. Joyner, A.L. (2001) *Gene Targeting: A practical approach*. 2nd edition. Oxford University Press, New York.
15. Kumar, T.R., Schuff, K.G., Nusser, K.D., Low, M.J. (2006) Gonadotroph-specific expression of the human follicle stimulating hormone beta gene in transgenic mice. *Mol Cell Endocrinol.* **247,** 103–115.
16. Hamernik, D.L., Keri, R.A., Clay, C.M., Clay, J.N., Sherman, G.B., Sawyer, H.R., et al. (1992) Gonadotrope- and thyrotrope-specific expression of the human and bovine glycoprotein hormone alpha-subunit genes is regulated by distinct cis-acting elements. *Mol Endocrinol.* **6,** 1745–1755.
17. Kendall, S.K., Saunders, T.L., Jin, L, Lloyd, R.V., Glode, LM, Nett TM, et al. (1991) Targeted ablation of pituitary gonadotropes in transgenic mice. *Mol Endocrinol.* **5,** 2025–2036.
18. Keri, R.A., Bachmann, D.J., Behrooz, A., Herr, B.D., Ameduri, R.K., Quirk, C.C., et al. (2000) An NF-Y binding site is important for basal, but not gonadotropin-releasing hormone-stimulated, expression of the luteinizing hormone beta subunit gene. *J Biol Chem.* **275,** 13082–13088.
19. Keri, R.A., Nilson, J.H. (1996) A steroidogenic factor-1 binding site is required for activity of the luteinizing hormone beta subunit promoter in gonadotropes of transgenic mice. *J Biol Chem.* **271,** 10782–10785.
20. Quirk, C.C., Lozada, K.L., Keri, R.A., Nilson, J.H. (2001) A single Pitx1 binding

site is essential for activity of the LHbeta promoter in transgenic mice. *Mol Endocrinol.* **15,** 734–746.

21. Balthasar, N., Mery, P.F., Magoulas, C.B., Mathers, K.E., Martin, A., Mollard, P., et al. (2003) Growth hormone-releasing hormone (GHRH) neurons in GHRH-enhanced green fluorescent protein transgenic mice: a ventral hypothalamic network. *Endocrinology.* **144,** 2728–2740.
22. Bonnefont, X., Lacampagne, A., Sanchez-Hormigo, A., Fino, E., Creff, A., Mathieu, M.N., et al. (2005) Revealing the large-scale network organization of growth hormone-secreting cells. *Proc Natl Acad Sci USA.* **102,** 16880–16885.
23. Magoulas, C., McGuinness, L., Balthasar, N., Carmignac, D.F., Sesay, A.K, Mathers, K.E., et al. (2000) A secreted fluorescent reporter targeted to pituitary growth hormone cells in transgenic mice. *Endocrinology.* **141,** 4681–4689.
24. Markkula, M., Kananen, K., Klemi, P., Huhtaniemi, I. (1996) Pituitary and ovarian expression of the endogenous follicle-stimulating hormone (FSH) subunit genes and an FSH beta-subunit promoter-driven herpes simplex virus thymidine kinase gene in transgenic mice; specific partial ablation of FSH-producing cells by anti-herpes treatment. *J Endocrinol.* **150,** 265–273.
25. Le Tissier, P. R., Carmignac, D.F., Lilley, S., Sesay, A. K., Phelps, C.J., Houston P, et al. (2005) Hypothalamic growth hormone-releasing hormone (GHRH) deficiency: targeted ablation of GHRH neurons in mice using a viral ion channel transgene. *Mol Endocrinol* **19,** 1251–1262.
26. Ahtiainen, M., Toppari, J., Poutanen, M., Huhtaniemi, I. (2004) Indirect Sertoli cell-mediated ablation of germ cells in mice expressing the inhibin-alpha promoter/herpes simplex virus thymidine kinase transgene. *Biol Reprod.* **71,** 1545–1550.
27. Alarid, E.T., Holley, S., Hayakawa, M., Mellon, P.L. (1998) Discrete stages of anterior pituitary differentiation recapitulated in immortalized cell lines. *Mol Cell Endocrinol.* **140,** 25–30.
28. Alarid, E.T., Windle, J.J., Whyte, D.B., Mellon, P.L. (1996) Immortalization of pituitary cells at discrete stages of development by directed oncogenesis in transgenic mice. *Development.* **122,** 3319–3329.
29. Kumar, T. R., Graham, K. E., Asa S. L., Low, M. J. (1998) Simian virus 40 T antigen-induced gonadotroph adenomas: a model of human null cell adenomas. *Endocrinology* **139,** 3342–3351.
30. Pernasetti, F., Spady, T. J., Hall, S. B., Rosenberg, S. B., Givens, M. L., Anderson S., et al. (2003) Pituitary tumorigenesis targeted by the ovine follicle-stimulating hormone beta-subunit gene regulatory region in transgenic mice. *Mol Cell Endocrinol.* **203,** 169–183.
31. Thomas, P., Mellon, P.L., Turgeon, J., Waring, D.W. (1996) The Lbeta-T2 clonal gonadotrope: a model for single cell studies of endocrine cell secretion. *Endocrinology.* **137,** 2979–2989.
32. Windle, J. J., Weiner, R. I., Mellon, P. L. (1990) Cell lines of the pituitary gonadotrope lineage derived by targeted oncogenesis in transgenic mice. *Mol Endocrinol.* **4,** 597–603.
33. Hanahan, D. (1985) Heritable formation of pancreatic beta-cell tumours in transgenic mice expressing recombinant insulin/simian virus 40 oncogenes. *Nature.* **315,** 115–122.
34. Palmiter, R.D. (1987) Molecular biology of metallothionein gene expression. *Experientia Suppl.* **52,** 63–80.
35. Palmiter, R. D., Norstedt, G., Gelinas, R.E., Hammer, R.E., Brinster, R. L. (1983) Metallothionein-human GH fusion genes stimulate growth of mice. *Science.* **222,** 809–814.
36. Guo, Q., Kumar, T. R., Woodruff, T. K., Hadsell, L. A., DeMayo, F. J., Matzuk, M. M. (1998) Overexpression of mouse follistatin causes reproductive defects in transgenic mice. *Mol Endocrinol.* **12,** 96–106.
37. Kumar, T. R., Palapattu, G., Wang, P., Woodruff, T. K., Boime, I., Byrne M. C., et al. (1999) Transgenic models to study gonadotropin function: the role of follicle-stimulating hormone in gonadal growth and tumorigenesis. *Mol Endocrinol.* **13,** 851–865.
38. Matzuk, M. M., DeMayo, F. J., Hadsell, L. A., Kumar, T. R. (2003) Overexpression of human chorionic gonadotropin causes multiple reproductive defects in transgenic mice. *Biol Reprod.* **69,** 338–346.
39. Ryding, A. D., Sharp, M. G., Mullins, J. J. (2001) Conditional transgenic technologies. *J Endocrinol.* **171,** 1–14.
40. Schnutgen, F., Doerflinger, N., Calleja, C., Wendling, O., Chambon, P., Ghyselinck, N.B. (2003) A directional strategy for monitoring Cre-mediated recombination at the cellular level in the mouse. *Nat Biotechnol.* **21,** 562–565.
41. Zhu, Z., Zheng, T., Lee, C. G., Homer, R. J., Elias, J. A. (2002) Tetracycline-controlled transcriptional regulation systems:

advances and application in transgenic animal modeling. *Semin Cell Dev Biol.* **13,** 121–128.

42. Karzenowski, D., Potter, D.W., Padidam, M. (2005) Inducible control of transgene expression with ecdysone receptor: gene switches with high sensitivity, robust expression, and reduced size. *Biotechniques.* **39,** 191–192, 194, 196.
43. Pierson, T.M., Wang, Y., DeMayo, F. J., Matzuk, M. M., Tsai, S. Y., O'Malley, B. W. (2000) Regulable expression of inhibin A in wild-type and inhibin alpha null mice. *Mol Endocrinol.* **14,** 1075–1085.
44. Albanese, C., Hulit, J., Sakamaki, T., Pestell, R. G. (2002) Recent advances in inducible expression in transgenic mice. *Semin Cell Dev Biol.* **13,** 129–141.
45. Marten, H., Hofker, J. V. D., Deursen, J.V. (2003) *Transgenic Mouse*: *Methods and Portocols* (*Methods in Molecular Biology.* **V. 209**, Humana Press, Totowa, N.J.
46. Han, J. Y. (2008) Germ cells and transgenesis in chickens. *Comp Immunol Microbiol Infect Dis.*[Epub ahead of print].
47. Houdebine, L. M. (2008) Production of pharmaceutical proteins by transgenic animals. *Comp Immunol Microbiol Infect Dis.* [Epub ahead of print].
48. Laible, G., Wells, D. N. (2006) Transgenic cattle applications: the transition from promise to proof. *Biotechnol Genet Eng Rev.* **22,** 125–150.
49. Melo, E. O., Canavessi, A. M., Franco, M. M., Rumpf, R. (2007) Animal transgenesis: state of the art and applications. *J Appl Genet.* **48,** 47–61.
50. Robl, J. M., Wang, Z., Kasinathan, P., Kuroiwa, Y. (2007) Transgenic animal production and animal biotechnology. *Theriogenology.* **467,** 127–133.
51. Halpern, M. E., Rhee, J., Goll, M.G., Akitake, C.M., Parsons, M., Leach, S.D. (2008) Gal4/UAS transgenic tools and their application to zebrafish. *Zebrafish.* **5**, 97–110.
52. Higashijima, S. (2008) Transgenic zebrafish expressing fluorescent proteins in central nervous system neurons. *Dev Growth Differ.* **50,** 407–413.
53. Houdebine, L. M., Chourrout, D. (1991) Transgenesis in fish. *Experientia.* **47,** 891–897.
54. Male, R., Lorens, J. B., Nerland, A. H., Slinde, E. (1993) Biotechnology in aquaculture, with special reference to transgenic salmon. *Biotechnol Genet Eng Rev.* **11,** 31–56.
55. Chesneau, A., Sachs, L. M., Chai, N., Chen, Y., Du Pasquier, L., Loeber, J., et al. (2008) Transgenesis procedures in Xenopus. *Biol Cell.* **100,** 503–521.
56. Ishibashi, S., Kroll, K. L., Amaya, E. (2008) A method for generating transgenic frog embryos. *Methods Mol Biol.* **461,** 447–466.
57. Niemann, H., Kues, W., Carnwath, J. W. (2005) Transgenic farm animals: present and future. *Rev Sci Tech.* **24,** 285–298.
58. Niemann, H, Kues, W. A. (2003) Application of transgenesis in livestock for agriculture and biomedicine. *Anim Reprod Sci.* **79,** 291–317.
59. Van Cott, K.E, Velander, W. H. (1998) Transgenic animals as drug factories: a new source of recombinant protein therapeutics. *Expert Opin Investig Drugs.* **7,** 1683–1690.
60. Campbell, K. H., Fisher, P., Chen, W. C., Choi, I., Kelly, R. D., Lee, J. H., et al. (2007) Somatic cell nuclear transfer: Past, present and future perspectives. *Theriogenology.* **68** *Suppl.* **1,** S214–S231.
61. Dobrinski, I. (2006) Germ cell transplantation in pigs–advances and applications. *Soc Reprod Fertil Suppl.* **62,** 331–339.
62. Prather, R. S., Sutovsky, P., Green, J. A. (2004) Nuclear remodeling and reprogramming in transgenic pig production. *Exp Biol Med (Maywood).* **229,** 1120–1126.
63. Chrenek, P., Makarevich, A. V., Pivko, J., Massanyi, P., Lukac, N. (2009) Characteristics of rabbit transgenic mammary gland expressing recombinant human factor VIII. *Anat Histol Embryol.* **38,** 85–88.
64. Kondo M, Sakai T, Komeima K, Kurimoto Y, Ueno S, Nishizawa Y, et al. (2008) Generation of a transgenic rabbit model of retinal degeneration. *Invest Ophthalmol Vis Sci.*[Epub ahead of print].
65. Li, S., Guo, Y., Shi, J., Yin, C., Xing, F., Xu, L., et al. (2008) Transgene expression of enhanced green fluorescent protein in cloned rabbits generated from in vitro-transfected adult fibroblasts. *Transgenic Res.*[Epub ahead of print].
66. Murphy, D. (2008) Production of transgenic rodents by the microinjection of cloned DNA into fertilized one-celled eggs. *Methods Mol Biol.* **461,** 71–109.
67. Chan, A. W., Chong, K.Y., Martinovich, C., Simerly, C., Schatten, G. (2001) Transgenic monkeys produced by retroviral gene transfer into mature oocytes. *Science.* **291,** 309–312.
68. Chan, A. W., Luetjens, C. M., Dominko, T., Ramalho-Santos, J., Simerly, C. R., Hewitson L, et al. (2000) TransgenICSI reviewed:

foreign DNA transmission by intracytoplasmic sperm injection in rhesus monkey. *Mol Reprod Dev*. **56,** 325–328.

69. Kumar, T. R., Low, M. J., Matzuk, M. M. (1998) Genetic rescue of follicle-stimulating hormone beta-deficient mice. *Endocrinology*. **139,** 3289–3295.
70. Huang, H. J., Sebastian, J., Strahl, B. D., Wu, J. C, Miller, W. L. (2001) Transcriptional regulation of the ovine follicle-stimulating hormone-beta gene by activin and gonadotropin-releasing hormone (GnRH): involvement of two proximal activator protein-1 sites for GnRH stimulation. *Endocrinology*. **142,** 2267–2274.
71. Huang, H. J., Sebastian, J., Strahl, B. D., Wu, J. C., Miller, W. L. (2001) The promoter for the ovine follicle-stimulating hormone-beta gene (FSHbeta) confers FSHbeta-like expression on luciferase in transgenic mice: regulatory studies in vivo and in vitro. *Endocrinology*. **142,** 2260–2266.

Chapter 23

Breast Tumor-Initiating Cells Isolated from Patient Core Biopsies for Study of Hormone Action

Carolyn G. Marsden, Mary Jo Wright, Radhika Pochampally, and Brian G. Rowan

Abstract

In recent years, evidence has emerged supporting the hypothesis that cancer is a stem cell disease. The cancer stem cell field was led by the discovery of leukemia stem cells (Tan, B.T., Park, C.Y., Ailles, L.E., and Weissman, I.L. (2006) The cancer stem cell hypothesis: a work in progress. *Laboratory Investigation*. **86**, 1203–1207), and within the past few years cancer stem cells have been isolated from a number of solid tumor including those of breast and brain cancer among others (Al-Hajj M., Wicha M.S., Benito-Hernandez A., Morrison, S.J., and Clarke, M.F. (2003) Prospective identification of tumorigenic breast cancer cells. *Proc. Natl. Acad. Sci. USA* **100**, 3983–3988; Singh, S.K., Clarke, I.D., Terasaki, M., Bonn, V.E., Hawkins, C., Squire, J., and Dirks, P.B. (2003) Identification of a Cancer Stem Cell in Human Brain Tumors. *Cancer Research.* **63**, 5821–5828). Cancer stem cells exhibit far different properties than established cells lines such as relative quiescence, multidrug resistance, and multipotency (Clarke, M.F., Dick, J.E., Dirks, P.B., Eaves, C.J., Jamieson, C.H.M., Jones, D.L., Visvader, J., Weissman, I.L., and Wahl, G.M. (2006) Cancer Stem Cells-Perspectives on Current Status and Future Directions: AACR Workshop on Cancer Stem Cells. *Cancer Research.* **66**, 9339–9344). In addition, our laboratory has demonstrated that breast cancer stem cells exhibit a strong metastatic phenotype when passaged in mice. Since stem cells exhibit these somewhat unique properties, it will be important for endocrinologists to evaluate hormonal action in these precursor cells for a more thorough understanding of cancer biology and development of more effective treatment modalities. A relatively easy and low cost method was developed to isolate breast cancer stem cells from primary needle biopsies taken from patients diagnosed with primary invasive ductal carcinoma during the routine care of patients with consent and IRB approval. Fresh needle biopsies (2–3 biopsies at 2 cm in length) were enzymatically dissociated in a collagenase (300 U/ml)/hyaluronidase (100 U/ml) solution followed by sequential filtration. Single cell suspensions were cultured on ultra low attachment plastic flasks in defined medium and formed non-adherent tumorspheres. The tumorspheres exhibited surface marker expression of $CD44^{+}/CD24^{low/-}/ESA^{+}$, previously defined as a "breast cancer stem cell" phenotype by Al Hajj et al. (Al-Hajj M., Wicha M.S., Benito-Hernandez A., Morrison, S.J., and Clarke, M.F. (2003) Prospective identification of tumorigenic breast cancer cells. *Proc. Natl. Acad. Sci. USA* **100**, 3983–3988).

Key words: Breast cancer, tumor-initiating cells, primary cell culture, tumorspheres, invasive ductal carcinoma, cancer stem cells.

O.-K. Park-Sarge, T.E. Curry, Jr. (eds.), *Molecular Endocrinology,* Methods in Molecular Biology 590,
DOI 10.1007/978-1-60327-378-7_23,

1. Introduction

An understanding of the mechanisms for hormone action and endocrine therapy response in breast cancer in limited due to the complexity of this disease, the numerous disease subtypes, and de novo and acquired resistance to endocrine therapies. Part of the complexity in breast cancer is likely due to the presence of limiting numbers of cancer stem cells. By definition, cancer stem cells are tumor cells that (a) have the ability to self-renew and (b) can recapitulate the entire cellular heterogeneity of tumor from which the cells were derived when transplanted into an immunodeficient mouse model (1). In this regard, the cancer stem cell would be the progenitor of all the differentiated tumor cells that constitute the bulk of a breast tumor. Whereas the more differentiated breast tumor cells are sensitive to chemotherapy and endocrine therapy for breast cancer, the cancer stem cells are insensitive to these therapeutics by virtue of a relatively quiescent phenotype, expression of membrane pumps, and uncertain nuclear receptor status.

Tumor initiating cells (T-ICs), a term used to describe a putative stem cell population, are a population of cells that contain a sub-population of cancer stem cells (1). T-ICs have the capacity to initiate and maintain tumor growth; however the term refers to a more heterogeneous population of cells containing a population of cancer stem cells (1). Isolation of T-ICs will provide an important laboratory tool to understand endocrine regulation of these multipotent cells. This chapter describes methods for isolation, culturing, and characterization of breast T-ICs.

Breast T-ICs can be isolated using a variety of methods. Fluorescence activated cell sorting (FACS) utilizes the expression of identified cell surface markers to isolate T-ICs (2,3). The advantage of using FACS to isolate breast T-ICs is that the initial cell population will be less heterogeneous. However, propagation in vitro as tumorspheres will most likely yield a heterogeneous population of cells ranging from cancer stem cells to more differentiated progenitor cells. The low number of cells recovered from FACS is a caveat of the technique, depending on the size of the tissue and hence the total number of cells initially isolated from the primary tissue. For the isolation of breast T-ICS, an alternative to isolating T-ICs from primary tissue is FACS sorting of established breast cancer cell lines (4). This method offers accessibility and convenience due to the unlimited resource of cell lines. However, similar to the parental cell line, T-ICs sorted from cancer cell lines present translational limitations and complications from long-term culture.

The method presented in this chapter for isolating breast T-ICs is more accessible for researchers without consummate stem cell experience and cheaper than alternative methods described above.

The following method is a variation of a valid isolation method developed by Ponti et al. (5) and uses specific culture conditions to isolate non-adherent cells that form tumorspheres in vitro. One disadvantage to the following method is that a heterogeneous population of cells is isolated as compared to FACS sorting to isolate population based on specific cell surface markers. However this method provides a robust and reliable approach to isolate T-ICs for studies in which the degree of "stemness" of isolated cells is not as critical as the tumor formation efficiency and the serial transplantability. Isolated primary T-ICs provide a tumor model that more closely recapitulates the primary tumor when injected into the mammary fat pad of immunodeficient mice. For that reason, tumor models derived from T-ICs are more relevant for investigation of basic tumor biology, metastasis, and response to hormones and therapeutics.

2. Materials

2.1. Isolation of Breast T-ICs from Biopsy Core Samples

1. 1x Hanks' balanced salt solution (HBSS) with phenol red.
2. 1x Phosphate buffered solution (PBS), pH 7.0.
3. Dulbecco's Phosphate Buffered Saline (DPBS), sterile-filtered, cell culture tested (Sigma-Aldrich).
4. 7.5% bovine serum albumin (BSA) in DPBS.
5. Disposable scalpels.
6. Dulbecco's Modified Eagles Medium/Ham's F-12 (DMEM: F-12): 1:1 mix, with L-glutamine and 15 mM HEPES (#11330-032, Invitrogen).
7. 10x Collagenase (3000 U/ml)/Hyaluronidase (1000 U/ml) in Dulbecco's Modified Eagle's Medium with glucose (1000 mg D-Glucose/L) (Stem Cell Technologies).
8. Sterile Petri dishes.
9. BD Falcon Filter Cell Strainer, 100 μm and 40 μm pore size.
10. B-27 supplement (50X) (GIBCO-Invitrogen).
11. Human recombinant epidermal growth factor (EGF) is dissolved at 20 μg/ml in 10 mM acetic acid/0.1% BSA and stored in 500 μl aliquots at –20°C. The working concentration is 20 ng/ml and therefore used at a 1:1000 dilution.
12. Insulin, human recombinant (SAFC Biosciences) diluted in autoclaved ddH_2O at 400 μg/ml, using hydrochloric acid to adjust the pH to dissolve (about pH 2.7). Aliquots of 400 μg/ml stored at −20°C and used at a working concentration of 4 μg/ml.

13. Human recombinant basic fibroblast growth factor (bFGF) is dissolved at 25 μg/ml in DMEM:F-12 and stored in aliquots at –20°C. The working concentration is 10 ng/ml.
14. DMEM:F-12 complete medium. To prepare 500 ml of DMEM:F-12 complete medium, add 5 ml of 400 μg/ml of human recombinant insulin, 500 μl of 20 μg/ml human EGF, 200 μl of 25 μg/ml of bFGF, 26.7 ml of 7.5% BSA in DPBS, and 10 ml of 50X B-27 supplement to 447.6 ml of DMEM:F12. Sterile filter the final solution (*see* **Note 1**).
15. Ultra low attachment culture 75 cm^2 flasks/100 mm dishes/6-well plates/24-well plates/96-well plates (Corning), depending on the number of cells and types of experiments to be performed.

2.2. Culture Conditions and Maintenance In Vitro

1. DMEM:F-12 as in 2.1.
2. B-27 supplement (50X).
3. hEGF (20 ng/ml).
4. Insulin (4 μg/ml).
5. Human bFGF (10 ng/ml).
6. 7.5% BSA in DPBS.
7. Ultra low attachment culture 75 cm^2 flasks/100 mm dishes/6-well plates/24-well plates/96-well plates (Corning), depending on the number of cells and types of experiments to be performed.
8. 1x Trypsin with EDTA (0.05%) (Invitrogen).
9. 1x Trypsin inhibitor from *glycine max* (soybean) stored in 1 –2 ml aliquots at −20°C (Sigma-Aldrich).

2.3. Immunocytochemistry on Isolated Tumorspheres

1. 1x PBS with 2% fetal bovine serum (FBS), pH 7.4.
2. 1x PBS with 1% BSA, pH 7.4.
3. Cytocentrifuge (Cytofuge 2, Statspin).
4. Filter concentrators (FF01/FF01-B) and stainless steel clips (FFCL, Statspin).
5. Cardboard filters (supplied with concentrator and used to concentrate the cells at one spot on the slide).
6. Superfrost plus microscope slides, pre-cleaned.
7. Acetone.

2.4. Immunocytochemistry on Tumorsphere Cytospins

1. 1x PBS, pH 7.4.
2. Normal goat serum.
3. Nonidet-P40 (NP40), reagent grade.

4. Humidified chamber; an unused pipette tip box with wet paper towels and a small amount of ddH_2O in the bottom.
5. IgG1-FITC/IgG2a-PE antibody mixture (Beckman Coulter). This mixture of two nonspecific antibodies that are isotype matched for the CD44-PE antibody and CD24-FITC antibodies is used as a negative control for nonspecific staining. If using different primary antibodies then choose the appropriate isotyped matched IgG control antibody to assess nonspecific staining.
6. CD44-PE antibody and CD24-FITC antibody (BD Biosciences).
7. ESA-FITC antibody (Biomeda).
8. Hoechst 33342 dye (1 mM) to be diluted in 1x PBS, pH 7.4 to a working concentration of 10 μM.
9. Prolong Gold Antifade reagent.
10. Coverglass slips 24 × 30 mm.

3. Methods

Isolating primary breast T-ICs from patient core biopsies can be challenging. With an approved IRB protocol and patient consent, tumor biopsies may be obtained either at the time of initial patient diagnosis or following tumor resection. During initial patient diagnosis, ultrasound guided needle biopsies are efficient for obtaining core biopsies from the tumor and not the surrounding normal tissue. However all resultant cultures must be evaluated by a pathologist for cellular and nuclear morphology to determine whether cells are from cancer or normal tissue origin. There is always variability in the number of T-ICs isolated from different biopsies. Regardless of the variability, a limited number of T-ICs will be isolated from a small amount of tissue such as a core biopsy. Alternately, biopsies obtained by the surgeon following tumor resection (True-cut biopsies) may also be used as a source for T-ICs and would provide a larger amount of starting material. Once again, resection samples would have to be evaluated by a pathologist to ensure separation of cancerous tissue from normal tissue prior to isolating T-ICs. A further concern for resection samples would occur if the patient received any neoadjuvant therapy prior to resection that could introduce variability in the T-ICs. It has been demonstrated that neoadjuvant chemotherapy may actually enrich for the number of T-ICs obtained from resection

biopsies (6). Nonetheless, cultures established from resection samples should be carefully evaluated with the expectation that not all tissue samples will yield T-ICs.

Due to the possible infectious nature of the patient tissue samples, safety precautions are needed during dissociation of the tissue and during all subsequent culturing and handling of the samples. The user should consult with the appropriate safety officials for proper protection against infectious agents. Since there is no penicillin/streptomycin added to the complete medium, precise and careful cell culture techniques need to be employed. In addition, if there are established cell lines present in the same cell culture laboratory, primary cells should be used in a separate hood and designated incubator that will not contain established cell lines to minimize cross contamination.

3.1. Isolation of Breast T-ICs from Biopsy Core Samples

1. Upon receipt of core biopsies, immediately place the biopsy pieces into a 15 ml conical tube containing 1x HBSS (4°C) and place on ice for immediate transport to the laboratory.
2. Once back in the laboratory, transfer the core biopsy pieces and 1x HBSS into a sterile Petri dish in a sterile tissue culture hood.
3. Thaw 3–5 ml (depending on the amount of tissue) of 10x collagenase/hyaluronidase in a 37°C water bath. Pre-warm DMEM:F-12 in a 37°C water bath for diluting the 10x collagenase/hyaluronidase.
4. Remove the 1x HBSS from the dish and discard into a 50 ml conical tube containing bleach (*see* **Note 2**).
5. Wash the core biopsies twice with 1x PBS, pH 7.4. Removing and disposing of the 1x PBS should be done in the same manner as the 1x HBSS in 3.1.4.
6. Place the core biopsies into a new sterile Petri dish (or a sterile tissue culture plate) and add 8–10 ml of 1x PBS, pH 7.4. Using two sterile disposable scalpels mince the tumor pieces into ~2 mm pieces in 1x PBS, pH 7.4. Do not use excessive mechanical dissociation of the tissue or increased cell death will occur.
7. Transfer the minced tissue pieces in PBS to a 50 ml conical tube. Allow the tumor pieces to settle to the bottom (about 5–10 minutes).
8. While waiting, dilute the pre-thawed 10x collagenase/hyaluronidase to 1x in pre-warmed DMEM:F-12 and mix thoroughly.
9. From step 3.1.7, remove the 1x PBS supernatant without disturbing the settled minced tumor pieces and dispose the PBS in bleach as in step 3.1.4.
10. Add 30–50 ml of 1x collagenase/hyaluronidase to the minced tumor pieces and gently agitate, either by pipetting up and down or by brief and slow pulse on a vortexer (*see* **Note 3**).

11. Incubate the 50 ml conical tube containing the tumor pieces in a 37°C water bath for 3–4 hours, agitating every 15–25 minutes by pipetting up and down in the tissue culture hood. If an overnight incubation for the enzymatic digestion is preferred, additional growth factors etc. must be added to the DMEM:F-12/collagenase/hyaluronidase mixture to prevent excessive cell death. Usually, 3–4 hour enzymatic dissociation at 37°C is sufficient for enzymatic dissociation.
12. Prepare DMEM:F-12 complete medium during the enzymatic dissociation step (*see* 2.1.13).
13. Upon completion of the enzymatic dissociation, sequentially filter the cell suspension through a 100 μm pore filter, and then a 40 μm pore filter and collect the flow through into a fresh 50 ml conical tube. This step is used to remove undigested tissue and clumps of cells that will not pass through the filters and should be discarded. The flow through will contain single cells that will be used in the next step.
14. Centrifuge the resultant single cell suspension at 350g for 10 minutes. Resuspend the cell pellet in complete medium with gentle pipetting. Remove 10 μl of the resuspended cell solution for cell counting by trypan blue exclusion.
15. Plate 1000 cells/ml in an ultra low attachment plate/flask (6), depending on the total number of isolated cells in the single cell suspension. Culture cells at 37°C with 5% CO_2. Tumorspheres should be visualized by light microscopy within 3–6 days of culture. A general flow chart of the procedure and an image of a tumorsphere are shown in **Fig. 23.1**. Maintain tumorspheres under non-adherent culture conditions in the DMEM:F-12 complete media.

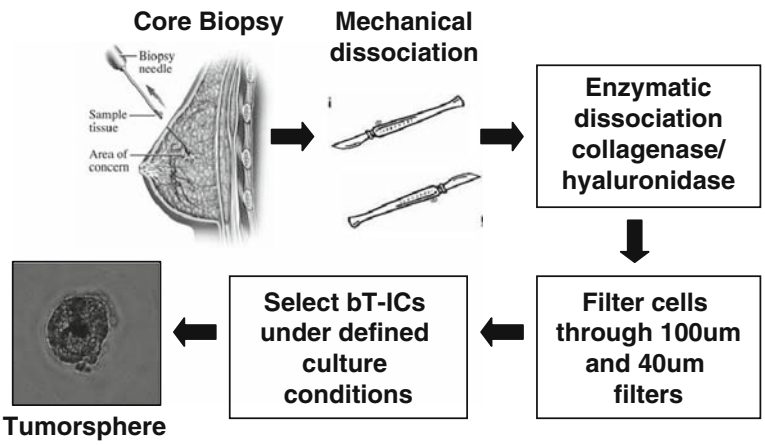

Fig. 23.1. A flow chart illustrating the general isolation procedure for bT-ICs including an image of a "tumorsphere" in vitro.bT-ICs; breast tumor initiating cells.

3.2. Culture Conditions and Maintenance In Vitro

1. When approximately 50% of the tumorspheres reach 60 μm in diameter, collect all tumorspheres in a 50 ml conical tube and centrifuge at 300*g* for 10 minutes (tumorspheres that are larger than 60 μm in diameter develop a darkened center).
2. While cells are in the centrifuge, thaw a sufficient number of aliquots of trypsin inhibitor in a 37°C water bath.
3. Carefully aspirate the supernatant (*see* **Note 4**) and gently resuspend the cells in 1 ml of 0.05% trypsin-EDTA keeping bubble formation to a minimum.
4. Incubate the 50 ml conical tube containing the cells in a 37°C water bath for 10 minutes with gentle agitation after 5 minutes.
5. After the 10 minute incubation, add an equal volume of trypsin inhibitor to the cells (e.g., if cells were incubated in 1 ml of trypsin, add 1 ml of trypsin inhibitor). Pipette the cells up and down about 40 times using a Rainin P1000 pipettor with sterile plugged pipette tips, minimizing bubble formation.
6. Centrifuge the cells at 350*g* for 10 minutes (*see* **Note 5**).
7. Gently resuspend the cell pellet in complete media with a Rainin P1000 pipettor and sterile plugged pipette tips (keeping bubble formation to a minimum). Remove 10 μl of the resuspended cell solution for cell counting by trypan blue exclusion.
8. Plate the cells at 1000 cells/ml on ultra low attachment plates/flasks in DMEM:F-12 complete medium.
9. Every 3 days, collect cells by centrifugation at 350*g* for 10 minutes and replate cells with fresh complete media containing EGF and bFGF.

3.3. Tumorsphere Cytospins

1. Harvest >100 tumorspheres in a conical tube and centrifuge at 300*g* for 10 minutes.
2. Wash (pipette up and down 3–4 times) the tumorspheres in cold 1x PBS, pH7.4 supplemented with 2% FBS twice, centrifuging at 300*g* for 10 minutes after each wash.
3. After the second wash, resuspend the tumorspheres in 100 μl of 1x PBS, pH7.4 supplemented with 1% BSA (using cotton plugged sterile pipette tips) and keep tumorspheres on ice.
4. Label the Superfrost Plus microscope slides appropriately. Be aware of the slide orientation when placing slides into the cytocentrifuge to avoid loading cells into the incorrect wells of the filter concentrators. Once assembled, it is very difficult to see the labels on the slides.
5. Assemble the filter concentrators and cardboard filters as per the manufacture instructions. Cardboard filters are used to concentrate the cells at one spot on the glass slide. Be sure that

the hole in the cardboard filter is in the proper position and the filter and the slide are flush to ensure the cells can reach the slide.

6. Place the assembled filter concentrators into the appropriate positions in the cytocentrifuge.
7. Add 100 µl of 1x PBS, pH7.4 supplemented with 1% BSA to the wells of the filter concentrators (*see* **Note 6**). Centrifuge at 500*g* for 2 minutes.
8. Quickly add 100 µl of each tumorsphere sample to the appropriate wells of the filter concentrators. Centrifuge at 500*g* for 10 minutes.
9. Remove the filter concentrator apparatus from the cytocentrifuge. Remove the metal clips being careful not to scrape the filter across the slide with the attached cells (the circle of liquid on the slide indicates the location of the cells on the slide).
10. Carefully open the filter concentrator separating the cardboard filter from the slide without any lateral motion that would disturb the attached cells on the slide.
11. Dry the slides overnight at room temperature (in a secure location to avoid any disturbance).
12. Add acetone to the slides for 5 minutes at 4°C to fix the cells.
13. Wash the slides three times with 1x PBS, pH 7.4 for 5 minutes each wash at room temperature.
14. Dry slides at room temperature but avoid excessive drying (*see* **Note 7**). Store slides at –20°C if staining won't be performed immediately.

3.4. Immunocytochemistry on Tumorsphere Cytospins

1. Blocking step: using the slides from step 3.3.14, add ~200 µl of blocking buffer (10% normal goat serum and 0.2% NP-40 in 1x PBS, pH 7.4) to slides. Incubate slides for 30 minutes in a humidified chamber at room temperature.
2. During the 30 minute blocking step, prepare primary antibody dilutions in blocking buffer (*see* step 3.4.1). For antibody incubations, at least 200 µl of diluted antibody will be needed per slide. Antibody dilutions should be determined empirically. As an example, CD44-PE, CD24-FITC, and ESA-FITC antibodies were diluted 1:100 in blocking buffer. All experiments should make use of appropriate controls (incubation of slides with isotype matched nonspecific antibody or peptide competition of primary antibody). As an example, a mixture of IgG1-FITC and IgG2a-PE (Beckman Coulter) served as isotype matched control antibodies for CD44-PE, CD24-FITC, and ESA-FITC. Control antibodies should be prepared at the same dilution in blocking buffer

(or the same mass/volume) as the primary antibodies. Some primary antibodies may be incubated concomitantly (e.g., CD44-PE and CD24-FITC antibodies may be incubated together). Keep all antibodies on ice and protected from light (*see* **Note 8**).

3. Wash the slides twice with cold 1x PBS, pH 7.4, blotting the slides on paper towels to remove the excess 1x PBS, pH 7.4 after each wash. Be sure to only touch the edge of the slide to the paper towel to avoid disturbing the attached tumorspheres.
4. Turn off as many lights in the workspace as possible before working with fluorophore-conjugated antibodies. Prepare your workspace such that exposure to light during the addition of the diluted antibodies is minimized.
5. Add ~200 µl of each antibody dilution to the appropriately labeled slides.
6. Cover the humidified chamber with aluminum foil without tipping the chamber, since this may cause loss of liquid from the desired location on the slide.
7. Incubate the slides in the humidified chamber for 90 minutes at room temperature.
8. Dilute 1 mM of Hoechst dye (*see* **Note 9**) 1:100 in 1x PBS, pH 7.4 to make a 10 µM working solution. Make enough working solution to add 500 µl to each slide. Keep working solution on ice and protect from light.
9. Remove the Prolong Gold Antifade reagent from –20°C to equilibrate to room temperature before use.
10. Wash slides twice with 1x PBS, pH 7.4 for 5 minutes each. Blot the edge of the slides on a paper towel to remove excess 1x PBS, pH 7.4 after each wash.
11. Add ~500 µl of 10 µM Hoechst 33342 dye to each slide. Incubate at room temperature for 15–20 minutes, in the humidified chamber with aluminum foil.
12. Wash slides once with 1XPBS, pH 7.4.
13. Blot the side of the slides gently on a paper towel to remove excess 1x PBS, pH 7.4.
14. Using a Pasteur pipette, make a thin line of the Prolong gold antifade reagent along one edge of the slide, adjacent to the attached tumorspheres. Pick up a coverslip using a forceps and touch the edge of the coverslip to the thin line of the Prolong gold antifade reagent. Gently drop the coverslip onto the slide. Once the Prolong gold reagent has dispersed under the coverslip, check for bubbles. If there are excess bubbles, use the forceps to gently push the bubbles to the edge of the coverslip for removal.

15. Allow the preparation to cure overnight, protected from light, before imaging. Images of the staining, including controls, are shown in **Fig. 23.2**.

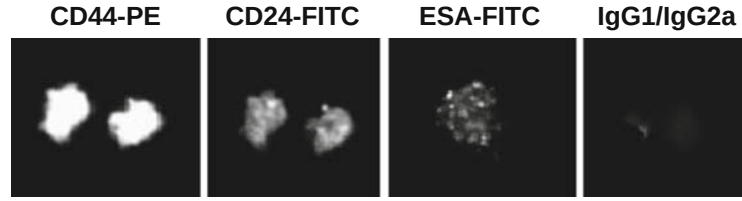

Fig. 23.2. Immunocytochemistry of stained cytospins of tumorspheres derived from breast cancer biopsy demonstrating a $CD44^{+}/CD24^{low/-}/ESA^{+}$ phenotype.

4. Notes

1. Replace the growth factors, EGF and bFGF, every 3–4 days. Store complete media for up to 1 month at 4°C, protected from light.
2. Before beginning, setup several 50 ml conical tubes containing bleach. All reagents and supplies that come into contact with the tissue pieces should be placed into the bleach before disposal.
3. For two core biopsies, typically 30 ml of 1x collagenase/hyaluronidase is sufficient for complete enzymatic digestion. For each addition core biopsy, in general, increase the amount of 1x collagenase/hyaluronidase by 10 ml.
4. Depending on the number and size (from 40 to 100 μm) of the tumorspheres in culture, a pellet may or may not be visible following centrifugation. Prior to centrifugation, mark the region of the tube where the pellet should form. If there is no pellet visible, aspirate the majority of the supernatant and then hold the tube at a 15–45° angle to the working surface of the tissue culture hood while pressing the aspirating pipette to the side of the tube to aspirate the supernatant at the bottom of the tube where the cells are pelleted (although not visible). Do not hold the tube at a sharp angle to aspirate for any length of time as the cells may detach from the bottom of the tube. In addition, do not repeatedly agitate the supernatant at the bottom of the tube while aspirating at an angle since this will detach cells from the bottom of the tube and the number of cells recovered will be significantly reduced.
5. Some protocols filter the dissociated cells through a 50–40 μm pore filter at this step to ensure a single cell suspension. We do not include this step because of cell loss during filtration. For the purpose of tumorsphere formation assays, flow

cytometry and any other assays that require a single cell suspension with the exclusion of doublets, triplets, etc. should include this filtration step. However, for the sole purpose of passaging and expanding the tumorspheres in culture, filtration is not necessary at this step.

6. If a significant number of tumorspheres were obtained and cell loss is not a concern, wetting the filter with 1x PBS, pH7.4 supplemented with 1% BSA is not necessary. Wetting the filter with 1x PBS, pH7.4 supplemented with 1% BSA before adding the tumorspheres will increase the number of cells that are deposited on the slide following centrifugation.
7. Allow slides to dry just enough to prevent crystal formation from residual PBS during storage at –20°C. Avoid excessive drying of the slide as this could decrease the efficiency and quality of subsequent staining.
8. The fluorophores conjugated to the various antibodies are photosensitive. For optimal visualization of the fluorescent signal, the antibodies should be protected from light throughout the procedure.
9. Hoechst 33342 is the preferred Hoechst dye used for this protocol. However other Hoechst dyes that are not cell permeable will also function well with this protocol since the cells were permeabilized during the fixation step with acetone and subsequent incubation with blocking buffer that contains the membrane solubilizing detergent NP-40.

Acknowledgments

This project was supported, in part, by grants from the Louisiana Cancer Research Consortium (BGR) and by a Louisiana Board of Regents Predoctoral Fellowship (CGM).

References

1. Clarke, M.F., Dick, J.E., Dirks, P.B., Eaves, C.J., Jamieson, C.H.M., Jones, D.L., Visvader, J., Weissman, I.L., and Wahl, G.M. (2006) Cancer Stem Cells-Perspectives on Current Status and Future Directions: AACR Workshop on Cancer Stem Cells. *Cancer Research.* **66**, 9339–9344.
2. Al-Hajj M., Wicha M.S., Benito-Hernandez A., Morrison, S.J., and Clarke, M.F. (2003) Prospective identification of tumorigenic breast cancer cells. *Proc. Natl. Acad. Sci. USA* **100**, 3983–3988.
3. Yu, F., Yao, H., Zhu, P., Zhang, X., Pan, Q., Gong, C., Huang, Y., Hu, X., Su, F., Lieberman, J., and Song, E. (2007) *let-7* Regulates Self Renewal and Tumorigenicity of Breast Cancer Cells. *Cell.* **131**, 1109–1123.
4. Fillmore, C.M., and Kuperwasser, C. (2008) Human breast cancer cell lines contain stem-like cells that self-renew, give rise to

phenotypically diverse progeny and survive chemotherapy. *Breast Cancer Research.* **10**, R25.

5. Ponti, D., Costa, A., Zaffaroni, N., Pratesi, G., Petrangolini, G., Coradini, D., Pilotti, S., Pierotti, M.A., and Daidone, M.G. (2005) Isolation and *In vitro* Propagation of Tumorigenic Breast Cancer Cells with Stem/Progenitor Cell Properties. *Cancer Research.* **65**, 5506–5511.
6. Dontu, G., Abdallah, W.M., Foley, J.M., Jackson, K.W., Clarke, M.F., Kawamura, M.J., and Wicha, M.S. (2003) In vitro propagation and transcriptional profiling of human mammary stem/progenitor cells. *Genes & Development.* **17**, 1253–1270.

Chapter 24

Markers of Oxidative Stress and Sperm Chromatin Integrity

Ashok Agarwal, Alex C. Varghese, and Rakesh K. Sharma

Abstract

Oxidative stress (OS) is an imbalance between the amount of reactive oxygen species (ROS) produced and the ability of the antioxidants to scavenge these. OS has been established as a major etiological cause of male infertility. High levels of ROS are harmful and cause damage to sperm nuclear DNA. Evaluation of OS-related damage to spermatozoa is therefore highly relevant in assisted reproductive techniques (ART) such as intracytoplasmic sperm injection (ICSI). ICSI is an effective therapy for severe male factor infertility that bypasses the majority of reproductive tract deficiencies. Despite the controversial findings in the existing literature, there is now enough evidence to show that sperm DNA damage is detrimental to reproductive outcomes. In addition to impairment of fertility, such damage might increase the transmission of genetic diseases to the offspring. Standardization of protocols to assess ROS, antioxidant status, and DNA damage is very important for implementation of these tests in clinical practice. Estimation of seminal ROS levels and extent of sperm DNA damage, especially in an infertile male, may help develop new therapeutic strategies and improve the success of ART.

Key words: Spermatozoa, reactive oxygen species, DNA damage, caspases, apoptosis.

1. Introduction

It is evident from the research in the last decade that oxidative stress (OS), sperm DNA damage and apoptosis are associated with various clinical and laboratory manifestations that may be present in infertile males. Sperm DNA contributes one-half of the genomic material to offspring, and the integrity of sperm DNA is of crucial importance for balanced transmission of genetic information to future generations. DNA-fragmented sperm has been interpreted as a fraction of cells that have failed to complete maturation and, in particular, to complete the packaging of chromatin during spermiogenesis (1).

O.-K. Park-Sarge, T.E. Curry, Jr. (eds.), *Molecular Endocrinology,* Methods in Molecular Biology 590,
DOI 10.1007/978-1-60327-378-7_24,

When a spermatozoon is subjected to oxidative stress, both the plasma membrane and the DNA integrity are under attack. The concomitant loss of genomic integrity and functional competence seen at the highest levels of oxidative stress represent a biological safeguard designed to ensure that spermatozoa possessing highly fragmented DNA are unlikely to participate in the process of conception. However, the chances of such cells fertilizing the oocyte clearly would be enhanced if the collateral damage to the sperm plasma membrane was circumvented through the use of intracytoplasmic sperm injection (ICSI) (2). The incidence of DNA-fragmented sperm in human ejaculate is documented, in particular in men with poor semen quality (3–6). Although the sperm cells are endowed with antioxidant enzymes such as glutathione peroxidase and superoxide dismutase, the restricted volume of cytoplasm limits the protection available from these antioxidant enzymes. However, the fluids that bathe the sperm cells are rich in enzymatic and non-enzymatic antioxidants which afford protection from oxidative attack and peroxidative damage to the vulnerable sperm biomembrane, which is vital for the fertilizing capacity of these cells. Studies clearly indicate that excessive reactive oxygen species (ROS) generation and diminished antioxidant capacity of seminal plasma are present in infertile males (7, 8).

The cascade of effects inducted by oxidative stress on sperm cells warrants a multilevel analysis of the endpoints of oxidative injury. This will help not only in understanding various unknown causes of male infertility but also will open up new, novel diagnostic tools for male factor evaluation. Since current male factor evaluation solely depends on the "gold standard test" i.e. semen analysis, which by itself provides only limited information, novel and robust diagnostic test are needed. This chapter outlines the various tests available for the analysis of human spermatozoa and seminal plasma under oxidative stress, one of the major causes of idiopathic male infertility.

2. Materials

2.1. Measurement of Global ROS

1. Clean wide mouth specimen container.
2. Sperm counting chamber (Microcell, Conception Technologies, San Diego, CA or Cell VU, Fertility Technology Research, Marietta, GA)
3. Luminol (5-amino-2,3 dehydro-1.4 phthalazinedione).
4. H_2O_2.
5. Lucigenin (Sigma-Aldrich, St. Louis, MO).

6. Phase contrast microscope.
7. Computer-assisted semen analyzer.
8. Dimethyl sulfoxide (DMSO; Sigma-Aldrich).
9. 1x Dulbecco's Phosphate-Buffered Saline Solution (PBS).
10. Luminometer (Berthold Technologies, Oakwood, TN).

2.2. Measurement of Intracellular ROS by Flow Cytometry

1. 100 μM Dichlorofluorescin diacetate (DCFH-DA, Sigma-Aldrich) in DMSO: make this working solution fresh from the stock DCFH-DA (1 mM in DMSO). DCFH-DA is sensitive to light but can be stored in the dark at −20°C up to 1 week (*see* **Note 1**).
2. 100 μM Hydroethidine (HE, Sigma-Aldrich) in DMSO: make this working solution fresh from the stock HE (5 mM in DMSO). This should also be stored in dark.
3. Propidium iodide (Sigma-Aldrich): the working solution is 50 μg/mL.
4. Yo-pro stain (Sigma-Aldrich): the working solution is 10 μg/mL.
5. Flow cytometer.

2.3. Measurement of Lipid Peroxidation

1. 1x Dulbecco's Phosphate-Buffered Saline Solution.
2. BWW medium: Biggers, Whitten, and Whittingham (95 mM NaCl/44 μM sodium lactate/25 mM $NaHCO_3$/20 mM Hepes/5.6 mM d-glucose/4.6 mM KCl/1.7 mM $CaCl_2$/1.2 mM KH_2PO_4/1.2 mM $MgSO_4$/0.27 mM sodium pyruvate/0.3% wt/vol BSA, 5 units per ml penicillin/5 μg/ml streptomycin, pH 7.4).
3. 4 mM Ferrous sulfate, 7 H_2O.
4. 20 mM Sodium ascorbate.
5. Thibarbituric acid (TBA) assay mixture: 200 μL sodium dodecylsulfate, 2 mL hydrochloric acid, 300 μL phosphotungstic acid, 100 μL butylated hydroxytoluene, 1 mL thiobarbituric acid.
6. Butanol.
7. H_2SO_4.

2.4. Measurement of Total Antioxidant Capacity (TAC) in Seminal Plasma

1. Antioxidant assay kit (Cayman Chemical, Ann Arbor, Michigan): 10x antioxidant assay buffer, chromogen, metmyoglobin, trolox, hydrogen peroxide solutions are prepared according to the manufacturer's instructions provided. Once the assay kit is thawed, it should be used within 24 hours.
2. ELx800™ Absorbance Microplate Reader (BioTek Instruments Inc., Winooski, VT).

3. Deionized water or HPLC-grade water.

2.5. Measurement of DNA Damage in Spermatozoa

1. Sperm counting chamber.
2. 3% Paraformaldehyde (w/v in 1x PBS, pH7.4).
3. Positive (6552LZ) and negative (6553LZ) controls supplied by the manufacturers.
4. APO-DIRECT^{TM} kit (BD Biosciences, San Jose, CA): supplied with components for TUNELwash buffer, TUNEL staining solution, TUNEL rinse buffer, and TUNEL PI/RNase staining buffer.
5. Fluorescence light microscope.
6. 'Sperm counting chamber (MicroCell, Conception Technologies, San Diego, CA or Cell VU, Fertility Technology Research, Marietta, GA)'.
7. AO equilibrium buffer: 0.037 M citric acid, 0.126 M Na_2HPO_4, 1.1 mM EDTA disodium, 0.15 M NaCl, pH 6.0.
8. TNE buffer: 0.01 M Tris-HCl, pH 7.4, 0.15 M NaCl, 1 mM EDTA.
9. Low-pH Detergent solution: 0.1% Triton X-100, 0.15 M NaCl, and 0.08 N HCl, pH 1.2.
10. Phosphate citrate buffer: 0.2 M Na_2HPO_4, 1 mM EDTA, 0.15 M NaCl, 0.1 M citric acid, pH 6.0.
11. Acridine Orange (AO) staining solution: 6 μg/mL Acridine Orange in phosphate citrate buffer.
12. PC/flow cytometer system (Cicero System, Cytomation, Fort Collins, CO)
13. Software for calculating the SCSA parameters: LISTVIEW (Phoenix Flow Inc., San Diego, CA), WINLIST (Verity Software House Inc., Topsham, MN), and FCS EXPRESS (DeNovo Software, Ontario, CA) (*see* **Note 2**).
14. Low-melt agarose.
15. Halosperm kit (Halotech DNA SL, Madrid, Spain).
16. Agarose precoated slide.
17. Acid denaturation solution (0.08 N HCl).
18. Neutralizing and lysing solution: 0.4 M Tris, 0.8 M DTT, 1% SDS, and 50 mM EDTA, pH 7.5.
19. Tris-Borate-EDTA(TBE) buffer: 0.09 M Tris-borate, 0.002 M EDTA, pH 7.5.
20. DAPI (4',6-diamidino-2-phenylindole) (2 μg/mL) (Sigma-Aldrich).
21. Carnoy's solution (3 parts methanol: 1 part glacial acetic acid).

22. Fluorescent beads for alignment.
23. Mini-capsule filter (0.45 μm).
24. Acridine orange (AO), chromatographically purified (Sigma-Aldrich).
25. Staurosporine (Sigma-Aldrich).
26. FLICA Apotosis Detection kit (FAM-VAD-FMK): supplied with 10x FLICA wash buffer concentrate, and FLICA reagent (Chemicon, Temecula, CA).
27. Hoechst stain (200 μg/mL).
28. Annexin V-FITC apoptosis detection kit (BD Biosciences).
29. Annexin V binding buffer (BD Biosciences, San Jose, CA): 0.1 M HEPES/ NaOH (pH 7.4) 1.4 M NaCl, 25 mM $CaCl_2$. This is supplied with the kit (*see* **Note 3**).
30. Purified recombinant annexin V (BD Biosciences) (*see* **Note 4**).
31. Microbeads (Militenyi Biotec, Auburn, CA).
32. MACS columns (Militenyi Biotec).
33. MACS separators (Militenyi Biotec).
34. Annexin V MicroBead kit (MiniMACS; Militenyi Biotec).

3. Methods

Highly reactive chemical molecules that have one or more unpaired electrons are called free radicals. They have the ability to oxidatively modify all the biomolecules that they encounter, causing them to react almost instantly with any substance in their vicinity (9). Free oxygen radicals such as superoxide anion ($O_2^{-\bullet}$), hydrogen peroxide (H_2O_2) hypochlorite (OHCl) and hydroxyl radical ($OH^{-\bullet}$) are called reactive oxygen species (ROS). These are mainly produced by white blood cells (WBC), especially the granulocytes, and by abnormal sperm (mainly spermatozoa with cytoplasmic droplet). Low levels of ROS are essential for physiological functions such as acrosome reaction, hyperactivation, motility, capacitation, and zona pellucida binding (10). Sperm quality is impaired because of the presence of excessive amounts of ROS. ROS levels can be measured by the chemiluminescence method using luminol/ lucigenin as the probe. Luminol can measure H_2O_2, $O_2^{-\bullet}$, and $OH^{-\bullet}$ levels, although it cannot distinguish these oxidants from one another (7). The lucigenin probe is more specific for measurement of extracellular superoxide anions (11).

The cutoff values for abnormal ROS levels using luminol depend on the type of sample used to measure ROS, i.e. sperm prepared by density gradient or after simple washing and resuspending of the sample in sperm wash media or in the native (unprocessed or neat) seminal ejaculate (12).

ROS values $>1 \times 10^6$ cpm/ 20×10^6 sperm have been reported for washed samples and are considered to be ROS-positive. For neat samples, values $>0.2 \times 10^6$ cpm/20×10^6 sperm have been reported (13). Similarly ROS cutoff has been established in clinical patients with and without leukocytospermia (14). Here we report the measurement of ROS in native seminal ejaculate after liquefaction without any further processing. This is important because estimation of ROS level in neat semen provides the true picture of oxidative stress to sperm cells emanating not only from morphologically abnormal spermatozoa but also from other cells and the amount of various antioxidants in the seminal plasma. Oxidative stress can also be induced during sperm preparation procedures. Once the semen sample is prepared, the protocol is essentially identical except for the reference values of the ROS measured in different sperm preparations.

3.1. Measurement of Global ROS

Global ROS, i.e. both extracellular and intracellular ROS, can be measured by the chemiluminescence method using a luminol probe. Luminol is extremely sensitive and reacts with a variety of ROS at neutral pH. Free radicals have a very short half-life and are produced continuously. The free-radical combines with luminol to produce a light signal that is converted to an electrical signal (photon) by a luminometer. The number of free radicals produced is measured as counted photons per minute (cpm) (12–14).

3.1.1. Semen Analysis

1. Semen sample is collected into a clean, wide-mouthed glass or plastic container. A minimum of 48–72 h of sexual abstinence should be observed. Record the name of the subject, period of abstinence, date, time the sample is produced, and semen age.
2. Allow the specimen to liquefy for 30 minutes in an incubator.
3. Record the initial physical characteristics such as volume, color, pH, and presence of round cells and leukocytospermia by peroxidase staining (Peroxidase staining is also called the Endtz test).
4. Load 5 μL of the sample on a sperm counting chamber.
5. Perform semen analysis for sperm concentration, motility, and round cells.

3.1.2. Measurement of ROS by Luminol

The steps involved in measurement of ROS by chemiluminiscence are shown in **Fig. 24.1**

1. Prepare working luminol solution (5 mM luminol in DMSO).
2. Label seven tubes as follows: (1) for a blank, (2–3) for an internal negative control, (4–5) for patient 1, (6–7) for patient 2.
3. For preparation of the internal positive control, add 50 μL of H_2O_2 (30%) to 400 μL of sperm suspension (*see* **Notes 5–6**).
4. Add reagents as follows:

Tube	Labeled polystyrene tube	PBS-1x	Neat* specimen	Probe 5 mM luminol
1	Blank	400 μL	–	
2	Control 1	400 μL	–	10 μL
3	Control 1	400 μL	–	10 μL
4	Patient 1	–	400 μL	10 μL
5	Patient 1	–	400 μL	10 μL
6	Patient 2	–	400 μL	10 μL
7	Patient 2	–	400 μL	10 μL

*Neat is liquefied, unprocessed ejaculated sperm.

5. Gently vortex to uniformly mix the aliquots in the tubes.
6. Measure the chemiluminiscence as counted photons per minute (cpm) according to the manufacturer's protocol.
7. Calculate the ROS by the equation of patient's ROS in cpm (counted photons per minute) = Average of patient sample readings (cpm) − average of control sample readings (cpm) (*see* **Note 7**). The results are expressed in cpm/20 × 10^6 sperm. The acceptable control reading is <0.02 × 10^6 cpm and the normal range of patient's reading is <0.2 × 10^6cpm/20 × 10^6 sperm.

3.1.3. Measurement of ROS by Lucigenin

Luminol reacts with a variety of reactive oxygen species, especially in samples with leukocytospermia where H_2O_2 appears to be the predominant form of ROS. Lucigenin yields a chemiluminescence that is more specific for extracellular $O_2^{-\bullet}$(15–17).

1. Add 400 μL of seminal ejaculate in a sample tube and mix with 4 μL of a 25 mM lucigenin stock solution dissolved in DMSO.
2. Prepare negative assay controls by adding 4 μL of lucigenin to 400 μL of 1x PBS.
3. All the remaining steps are identical to those described above for luminol (steps 1–7 of the Section 3.1.2).

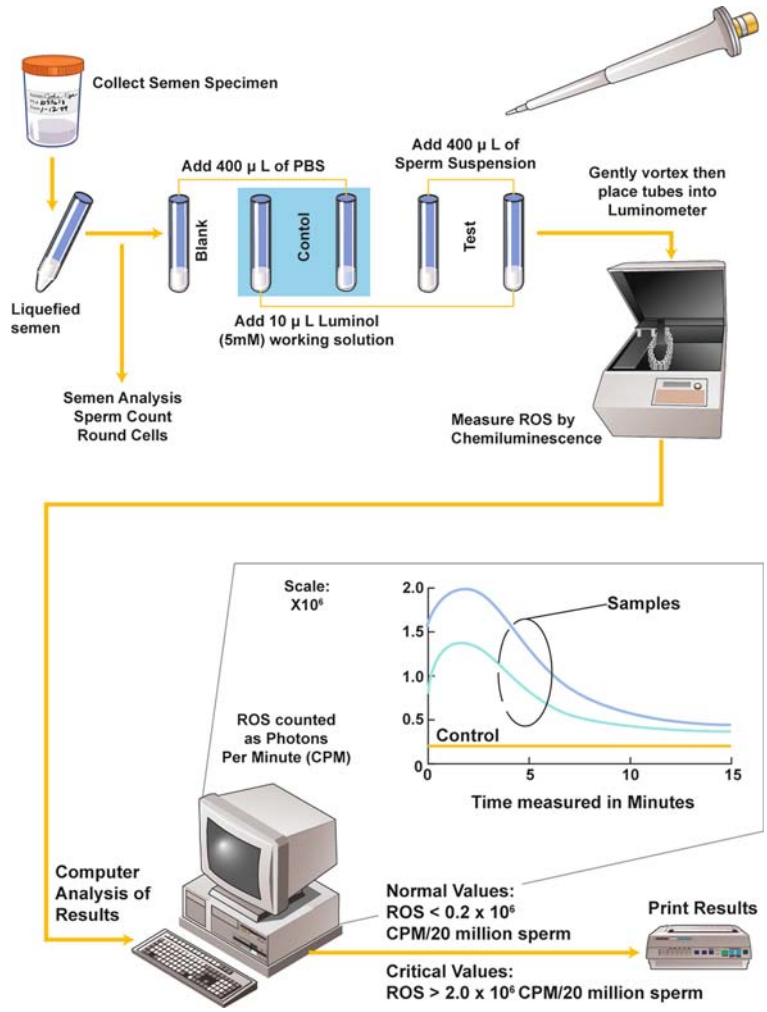

Fig. 24.1. Measurement of reactive oxygen species using the chemiluminescence assay.

3.2. Measurement of Intracellular ROS by Flow Cytometry

Intracellular generation of ROS can originate from a number of potential sources, including NADPH oxidase and complex III within the mitochondrial electron transport chain. Dichlorofluorescin (DCFH) can detect intracellular H_2O_2 and dihydroethidium (DHE) can detect intracellular $O_2^{-\bullet}$ (18, 19).

1. Add 100 µL of the working solution of DCFH-DA to 300 µL of sperm sample.
2. Add 5 µL of the working solution of HE to 395 µL of sperm sample.
3. Incubate positive sample (H_2O_2-induced OS) and negative (no OS induction) and test samples in duplicate at 25°C for 40 minutes for DCFH-DA and 20 minutes for HE before analyzing by flow cytometry.

4. Analyze each aliquot using a flow cytometer equipped with 488 nm argon laser as a light source (Becton Dickinson FACScan, San Jose, CA). Green fluorescence (DCFH) is evaluated between 500 and 530 nm, while red fluorescence (HE) is evaluated between 590 and 700 nm (excitation: 488 nm; emission: 525–625 nm in the FL2 channel). Data is expressed as the percentage of fluorescent spermatozoa. Apoptotic spermatozoa are excluded by using counterstain dye for nucleic acid. Propidium iodide (PI) is a counterstain dye for DCFH (stains red) and Yo-Pro-1 is a counterstain dye for the HE (stains green). PI-stained cells indicate necrosis. Yo-Pro-positive and PI-negative stained cells indicate early apoptosis, whereas Yo-pro-stained and PI-positive staining indicate late apoptosis (19).

3.3. Measurement of Lipid Peroxidation

Oxidative stress can have major detrimental effects on sperm and their lipid membranes, which are rich in polyunsaturated fatty acids. Thus, by increasing the level of membrane lipid peroxidation, they diminish the membrane fluidity and its functions. It is proposed that the impeded propagation of peroxidation initiated by Fenton or Haber-Weiss reactions would lead to the accumulation of lipid peroxides in the spermatozoa. These peroxides decompose during the $Fe^{(2+)}$-promoted thibarbituric acid (TBA) assay, stimulating a lipoperoxidative chain reaction and resulting in malondialdehyde formation (20).

1. Follow steps for semen analysis and sperm preparation in ROS estimation (3.1).
2. Resuspend the pellet after centrifugation in 10 mL of BWW medium.
3. Add 10 μL ferrous sulfate and 20 μL sodium ascorbate to 1 mL sperm suspension and incubate at 37°C for 2 hours.
4. Add 200 μL of incubated sperm suspension to 360 μL of TBA assay mixture (*see* **Note 8**).
5. After cooling to room temperature, extract the malonaldehyde–thiobarbituric acid adduct by the addition of 500 μL of butanol.
6. Fluorescence of thiobarbituric acid reactive substances (TBARS) in the butanol layer is measured at excitation and emission wavelengths of 532 and 553 nm, respectively.
7. A standard curve is generated using malondialdehyde bisdimethyl acetal after hydrolysis in 2% H_2SO_4 for 30 minutes. The amount of TBARS is expressed as malondialdehyde (MDA) equivalents and the concentration is given in μmol/L.
8. Lipid peroxide products can also be quantified directly using the lipid peroxidation (LPO) assay kit (Cayman Chemical Company, Ann Arbor, MI).

3.4. Measurement of Total Antioxidant Capacity (TAC) in Seminal Plasma

ROS are produced as a consequence of normal aerobic metabolism. Unstable free radical species attack cellular components causing damage to lipids, proteins, and DNA resulting in an onset of a variety of diseases. Living organisms are endowed with a complex antioxidant system to counteract the effects of ROS and reduce damage to biological structures. The antioxidant system of living organisms includes enzymes such as superoxide dismutase, catalase and glutathione peroxidase; macromolecules such as albumin, ceruloplasmin, and ferritin; and an array of small molecules, including ascorbic acid, α-tocopherol β-carotene, reduced glutathione, uric acid, and bilirubin. The sum of endogenous and food-derived antioxidants represents the total antioxidant activity of the extracellular fluid.

The seminal plasma is well-endowed with an array of antioxidants that act as free radical scavengers to protect spermatozoa against oxidative stress. The overall antioxidant capacity may give more relevant biological information compared to that obtained by the measurement of individual components, as it considers the cumulative effect of all antioxidants present in plasma and body fluids. The combined index from ROS generation and TAC score is reported to be a better marker of oxidative stress (21). TAC levels have been shown to be significantly lower in the leucocytospermic, varicocele, male factor infertility, or idiopathic infertility groups compared with control groups, suggesting that seminal TAC itself is a good marker in male infertility evaluation (22–29).

The assay relies on the ability of antioxidants in the sample to inhibit the oxidation of ABTS (2,2′-azino-di-[3-ethylbenzthiazoline sulfonate]) to ABTS·+ by metmyoglobin. Under the reaction conditions used, the antioxidants in the seminal plasma cause suppression of the absorbance at 750 nm to a degree that is proportional to their concentration. The capacity of the antioxidants present in the sample to prevent ABTS oxidation is compared with that of standard Trolox—a water-soluble tocopherol analogue. Results are reported as micromoles of Trolox equivalent. This assay measures the combined antioxidant activities of all its constituents including vitamins, proteins, lipids, glutathione, uric acid, etc. (28, 29).

1. Follow steps 1–5 of the **Section 3.1.1.**
2. After complete liquefaction, centrifuge the sample at 300*g* for 10 minutes. Aliquot clear seminal plasma into clearly labeled cryovials/microcentrifuge tubes and store at −70°C until the time of assay. Samples can be batched for this assay.
3. All reagents should be equilibrated at room temperature before beginning the assay. Bring the frozen seminal plasma to room temperature and centrifuge in a microfuge at high speed for 5 min.
4. Transfer clear seminal plasma to a new tube and dilute the sample 1:10 using assay buffer (supplied with the kit) in a microfuge tube.

5. Use the plate template to note the sample being added to each well is duplicate (standard and test samples) as described below (*see* **Note 9**).
6. Prepare the standards in seven clean tubes and mark them A–G. Add the amount of reconstituted Trolox and 1x assay buffer to each tube as shown below.

Tube	Reconstituted Trolox (μL)	Assay buffer(μL)	Final Conc(mM Trolox)
A	0	1000	0
B	30	970	0.044
C	60	940	0.088
D	90	910	0.135
E	120	880	0.18
F	150	850	0.225
G	220	780	0.330

7. Add 10 μL of Trolox standard (tubes A–G) or sample in duplicate + 10 μL of metmyoglobin + 150 μL of chromogen per well (*see* **Note 10**).
8. Initiate the reaction by adding 40 μL hydrogen peroxide working solution using multichannel pipette. This step should be completed as quickly as possible (within 1 minute). H_2O_2 can be pipetted from a flat container using a multichannel pipette.
9. Cover the plate with the plate cover and incubate on a shaker for 5 min at room temperature. Since the procedure involves enzymatic reaction, proper maintenance of room temperature is vital to obtain consistent results.
10. Remove the cover and read the absorbance at 750 nm using a plate reader.
11. Calculate the antioxidant concentration of the samples using the equation obtained from the linear regression of the standard curve by substituting the average absorbance values for each sample into the equation.

$$\text{Antioxidant}(\mu M) = (A_{750}\,\text{for unknown} - \text{Y intercept})/\text{slope} \times \text{dilution} \times 1000$$

In addition the information can also be derived from the worksheet provided by the manufacturer and plugging each value in the spreadsheet available at www.caymanchem.com. The result >1000 μM Trolox should be considered normal.

3.5. Measurement of DNA Damage in Spermatozoa

DNA damage in spermatozoa from infertile men has been associated with infertility in numerous studies, and a decrease in pregnancy rates has been observed with ejaculates containing a large number of DNA-damaged sperm (30–33). Direct assessment of DNA damage can be obtained by means of the terminal deoxynucleotidyl transferase-mediated deoxyuridine triphosphate-nick end labeling (TUNEL), comet, in situ nick translation, or sperm chromatin structure assay (SCSA) techniques.

3.5.1. Terminal Deoxynucleotidyl Transferase dUTP Nick-End Labeling (TUNEL) Assay

DNA fragmentation is a process which results from the activation of endonucleases during apoptosis. These nucleases degrade the higher order sperm chromatin structure into fragments ~30 kb and subsequently into smaller DNA pieces about ~50 kb in length. This method is used to detect fragmented DNA and utilizes a reaction catalyzed by exogenous terminal deoxynucleotidyl transferase (tdt) and is termed as "end labeling" or terminal deoxynucleotidyltransferase dUTP nick-end labeling (TUNEL) assay (34, 35).

1. Follow steps 1–5 of the Section 3.1.1.
2. Following liquefaction, evaluate semen specimens for volume, sperm concentration, total cell count, motility, and morphology.
3. Aliquot and load a 5 μL aliquot of the sample on a sperm counting chamber for manual evaluation of concentration and motility. Check the concentration of sperm in the sample. Adjust it to 2–3 $\times$ 10^6/mL.
4. Suspend the cells in 3% paraformaldehyde at a concentration of 1–2 $\times$ 10^6sperm/ mL.
5. Place the cell suspension on ice for 30–60 minutes.
6. Store cells in 1 mL of ice-cold 70% ethanol at −20°C until use. Samples can be batched and stored at −20°C till analysis.
7. Resuspend the positive (6552LZ) and negative (6553LZ) control cells provided in the kit by swirling the vials.
8. Remove 1 mL aliquots of the control cell suspensions (approximately 1 $\times$ 10^6 cells/mL) and place in 12 $\times$ 75 mm centrifuge tubes. Centrifuge the control cell suspensions for 5 min at 300*g* and remove the 70% ethanol by aspiration, being careful to not disturb the cell pellet.
9. Resuspend each tube of control cells with 1.0 mL of TUNELwash buffer (supplied by the manufacturer). Centrifuge as before and remove the supernatant by aspiration.
10. Repeat the TUNEL wash buffer treatment.
11. Resuspend each tube of the control cell pellets in 50 μL of the TUNEL staining solution (prepared as described below) (*see* **Note 11**).

Staining Solution	1 assay	6 assays	12 assays
Reaction buffer	10.00 µL	60.00 µL	120.00 µL
TdT enzyme	0.75 µL	4.50 µL	9.00 µL
FITC-dUTP	8.00 µL	48.00 µL	96.00 µL
Distilled H_2O	32.25 µL	193.05 µL	387.00 µL
Total volume	51.00 µL	306.00 µL	612.00 µL

12. Incubate the sperm in the staining solution for 60 min at 37°C. The reaction also can be carried out at room temperature overnight for the control cells. For test samples, the 60 min incubation time at 37°C may need to be adjusted to longer periods of time.
13. At the end of the incubation time, add 1.0 mL of TUNEL rinse buffer to each tube and centrifuge each tube at 300*g* for 5 min. Remove the supernatant by aspiration.
14. Repeat the cell rinsing with 1.0 mL of rinse buffer, centrifuge, and remove the supernatant by aspiration.
15. Resuspend the cell pellet in 0.5 ml of the TUNEL PI/RNase staining buffer (*see* **Note 12**).
16. Incubate the cells in the dark for 30 min at room temperature.
17. Analyze the cells in TUNEL PI/RNase solution by flow cytometry (*see* **Note 13**).
18. Percentage of cells showing DNA fragmentation is calculated. Less than 15% DNA damage is considered normal.

3.5.2. Sperm Chromatin Structure Assay

Sperm chromatin integrity is vital to the accurate transmission of paternal genetic information, and normal sperm chromatin structure is important for sperm fertilizing ability. Routine semen examination, which includes sperm concentration, motility, and morphology, does not identify defects in sperm chromatin structure (36). The SCSA utilizes the metachromatic properties of acridine orange to distinguish between low pH or heat-denatured (red fluorescence = single-stranded) and native (green fluorescence = double-stranded) DNA in sperm chromatin. The SCSA is a robust and clinically accepted assay for evaluating sperm DNA factor infertility. Spermatozoa with defective DNA can fertilize an oocyte, produce high quality early stage embryos, and then, in relationship to the extent of DNA damage, fail in producing a successful term pregnancy (37–39).

The growing concern about transmission of genetic diseases through ICSI has intensified the focus on the genomic integrity of the male gamete. ICSI bypasses processes of natural selection

during sperm–oocyte interaction, which is still present in conventional IVF. The SCSA is a rapid, reliable, and practical test; previous data show that it has a clinical value in human as well as in animal fertility assessment. A potential patient attending an ART fertility clinic can have an aliquot of his semen analyzed by SCSA prior to any proposed IVF/ICSI procedure to assist him in making a final decision on whether to proceed with the ART procedure. The SCSA could also aid in the decision of a young male patient just diagnosed with cancer on whether his semen should be frozen and stored for future use (31, 40–44).

The protocol listed below describes the methodology for DNA damage assessment by SCSA. The original protocol that describes each step in detail is available in the landmark paper by Evenson and Jost (45). The assay essentially consists of three main parts: cell preparation and staining, FCM, and data analysis. Liquefied semen samples are examined for count and motility and immediately frozen (−70 to −110°C).

1. Place a tube of AO equilibrium buffer on the instrument to flow through the sample lines while preparing the sample.
2. Thaw fresh or frozen semen/sperm in a 37°C water bath and dilute to 1–2 $\times$ 10^6 sperm/mL with TNE buffer.
3. Mix 200 μL aliquots of diluted samples with 400 μL of a low-pH detergent solution for 30 seconds.
4. Stain the cells by adding 1.2 mL of AO staining solution in a phosphate citrate buffer.
5. Immediately at the moment of staining, analyze the cells using a FACS XL, red ($F \geq_{630}$) and green ($F_{515-530}$) fluorescence flow cytometer (Becton Dickinson) equipped with an air-cooled argon laser. Under these conditions, AO intercalated into double-stranded DNA emits green fluorescence, and AO associated with single-stranded DNA emits red fluorescence.
6. Collect measurements on 5000 cells per sample and store in list mode on the interfaced computer. Analyze the flow cytometry data using the WimnDi 2.9 Software (free version).
7. The extent of DNA denaturation is quantified by the calculated parameter alpha-t [αt = red/(red + green) fluorescence] (46). This ratio is calculated on each of the 5000 cells measured in the sample and this forms an αt distribution (histogram) with its own population statistics, including mean channel ($X\alpha t$) and standard deviation ($SD\alpha t$). $SD\alpha t$ describes the extent of chromatin structure abnormality within a population, and $X\alpha t$ indicates shifts and trends in the whole population of cells. The percent of **C**ells **O**utside the **M**ain **P**opulation of this distribution ($COMP\alpha t$; i.e., the percent of cells with

denatured DNA) is also derived from the αt histogram. The actual αt values are calculated from the αt frequency histogram. Normal, native chromatin remains structurally sound and produces a narrow αt distribution with relatively low αt values. DNA in sperm with abnormal chromatin structure exhibits increased red fluorescence usually yielding a broader distribution with an increased Xαt and SDαt and more cells with denatured DNA (%COMPαt) (36, 37). COMPαt is now called %DNA Fragmentation Index (%DFI), a ratio expressed as a percentage of sperm DNA, which is fragmented ssDNA (red fluorescence) divided by total sperm fluorescence, with both unfragmented dsDNA (green fluorescence) and fragmented ssDNA (red fluorescence) (*see* **Note 14**).

8. Mean green fluorescence reflects DNA content and/or degree of sperm chromatin condensation, of which the latter inhibits DNA stainability. Percentage of high DNA-stainable (%HDS) sperm, formerly called %HGRN (the percentage of high green) identifies the cells with immature nuclei due to lack of nuclear condensation. Fertility potential is categorized as follows (31): Excellent $\leq$15 %DFI; Good: 15–24 %DFI; Fair: 30 %DFI; Poor: >30% DFI.

3.5.3. Sperm Chromatin Decondensation Test

Sperm chromatin dispersion (SCD) assay has been reported recently as a unique test for its ability to diagnose different degrees of DNA fragmentation—with severe damage being characterized as degraded DNA. The SCD test is developed and marketed as the Halosperm kit (Halotech DNA SL, Madrid, Spain).

1. Dilute each semen sample to a concentration of 10 million/mL and mix with 1% low-melting point agarose gel (47, 48).
2. Pipette 15 μL of the mixture onto an agarose precoated slide and cover with a coverslip.
3. Place the slide on a cold plate (4°C) for 5 minutes to produce a microgel with the sperm trapped in the agarose.
4. After removing the coverslip, immediately immerse the slide horizontally in a tray of freshly prepared acid denaturation solution for 7 minutes at room temperature. This generates restricted single-stranded DNA (ssDNA) motifs from DNA breaks.
5. Terminate the denaturation reaction and remove proteins by transferring the slides to a tray with neutralizing and lysing solution for 10 minutes at room temperature.
6. Wash the slides thoroughly in TBE buffer for 2 minutes.
7. Dehydrate the slides in sequential 70%, 90%, and 100% ethanol baths (2 minutes each) and air dry.

8. Stain the cells with DAPI (4',6-diamidino-2-phenylindole) (2 μg/mL) for fluorescence microscopy. Score a minimum of 500 spermatozoa per sample under the 100x objective of the fluorescence microscope. An example is shown in **Fig. 24.2.** Scoring 1–5 is based on the different halo sizes using the minor diameter of the core from their own nucleoid as a reference to which the halo width is compared (49).

Score 1: Sperm cells with large halos: Halo width is similar to or higher than the minor diameter of the core.

Score 2: Sperm cells with medium-size halos: Halo size is between those with high and with very small halos.

Score 3: Sperm cells with very small halos: Halo width is similar to or smaller than one-third of the minor diameter of the core.

Score 4: Sperm cells without a halo.

Score 5: Sperm cells without a halo-degraded: Similar to No. 4 but weakly or irregularly stained sperm cells with very small halos, without halos, and without halo-degraded contain fragmented DNA.

Nucleoids that do not correspond to sperm cells are scored separately.

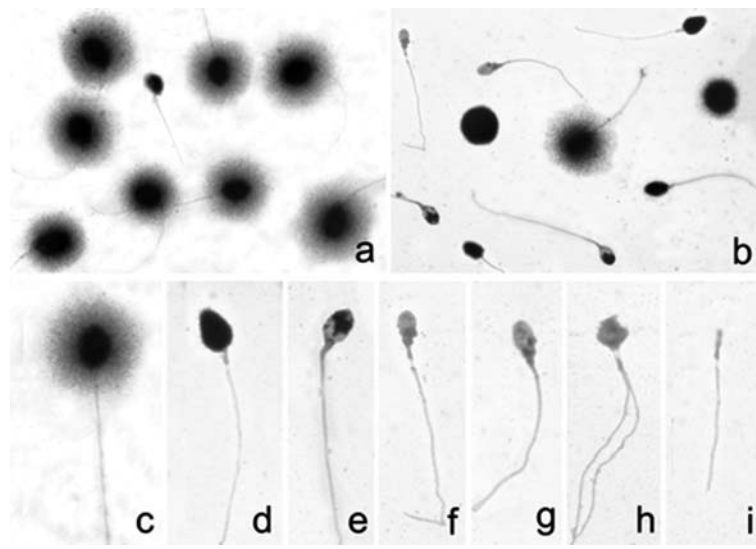

Fig. 24.2. Sperm DNA fragmentation determined with the sperm chromatin dispersion (SCD) test using the Halosperm kit. **(a)** Sample from a fertile subject, only showing a sperm nucleus with fragmented DNA in the microscopic field, evidenced by the absence of halo. **(b)** Sample from an individual with varicocele, showing 7 sperm cells with fragmented DNA. Four of them correspond to the degraded type, with irregular or lower staining. Moreover, 2 non-sperm cells, with big nucleus and without tail, are evident. Detailed images are presented in **(c–i)**. **(c)** Sperm cell without DNA fragmentation, with big halo. **(d)** Sperm cell with fragmented DNA, without halo. **(e–i)** Selected sperm cells with DNA fragmentation and degraded. (Enciso et al. (2006) *J Androl.* **27**, 106–111).

3.5.4. Acridine Orange Staining

Acridine orange staining is used to detect human sperm DNA damage using fluorescent microscopy. Acridine orange staining has been suggested as a screening test to predict DNA damage in human sperm and to predict fertilization rates (30, 50). AO fluoresces green when it intercalates as a monomer into native DNA (double-stranded and normal) and red when it binds to denatured DNA (single-stranded) as an aggregate. The AO fluorescence of the sperm nucleus is determined by the thiol disulfide status of DNA-associated protamines. The sperm nucleus exhibits red AO fluorescence when treated with acid while its protamines are poor in disulfides. Acridine orange binds to denatured (single-stranded) DNA as aggregates and emits red fluorescence. DNA that is associated with disulfide-rich protamines is apparently resistant to denaturation procedures; hence AO binds to native (double-stranded) DNA as a monomer and emits green fluorescence.

1. Prepare AO staining solution (*see* **Note 15**).
2. Allow the semen to liquefy for 20–30 minutes.
3. Prepare a smear from each sample on a clean, glass slide and allow to air dry for 20 minutes.
4. Fix the slides in Carnoy's solution for at least 2 hours, preferably overnight.
5. Wash the slides in distilled water and stained with AO solution for 5 minutes.
6. Gently rinse the slides in a stream of deionized water.
7. Place a coverslip before the slide dry. Place a paper towel over the mounted slide and firmly squeeze the excess water using a rubber roller.
8. Seal the coverslip with nail polish.
9. Read the slides on the same day on a fluorescent microscope using a 490-nm excitation filter and a 530-nm barrier filter. Observation time per field should be no longer than 40 seconds.
10. Calculate the percentage of spermatozoa with normal DNA by counting at least 300 spermatozoa at $\times 400$ magnifications (see **Notes 16–18**). Spermatozoa with normal, intact, double-stranded DNA stain green and those with denatured DNA show red or orange fluorescence.

3.5.5. Detection and Evaluation of Active Caspases

Caspases are involved in a series of reactions that are triggered in response to pro-apoptotic signals and result in the cleavage of protein substrates, causing the disassembly of the cell (51). In apoptosis, caspases are responsible for proteolytic cleavages that lead to cell disassembly (effector caspases) and are involved in upstream regulatory events (initiator caspases). Caspases can be

detected via immunoprecipitation, immunoblotting techniques using caspase specific antibodies, or by employing fluorochrome substrates that become fluorescent upon cleavage by the caspase.

Active caspases-8, -9, -1, and -3 can be detected in living spermatozoa using carboxyfluorescein-labeled caspase (52). The fluorogenic substrate becomes fluorescent upon cleavage by the caspases and has been shown to be reliable for detection of early caspase activation (53–56). Cells that contain the bound, labeled reagent can be analyzed by 96-well plate-based fluorometry, fluorescence microscopy, or flow cytometry.

1. Prepare sperm at a concentration of 1×10^6 cells/mL.
2. Induce apoptosis (by staurosporine, 10 μM for 3 h) and concurrently incubate a negative control cell population (non-induced) at the same concentration (10^6 cells/ mL).
3. Induced and non-induced samples should be assayed for each labeling condition. For example, if using both the FLICA reagent and the Hoechst stain, make 8 populations for (a) unlabeled, induced vs. non-induced, (b) FLICA-labeled, induced vs. non-induced, (c) FLICA- and Hoechst-labeled, induced vs. non-induced, and (d) Hoechst-labeled, induced vs. non-induced.
4. Transfer 290–300 μL of each cell suspension ($\sim 10^6$ cells) to sterile tubes.
5. Add 10 μL of freshly prepared 30x FLICA reagent and mix cells by slightly flicking the tubes.
6. Incubate tubes for 1 hour at 37°C under 5% CO_2, protecting tubes from light. Swirl tubes once or twice during this time to gently resuspend settled cells.
7. Add 2 mL of 1x FLICA wash buffer to each tube and gently mix.
8. Centrifuge the cells at $<400g$ for 5 minutes at room temperature.
9. Carefully remove and discard supernatant, and gently vortex cell pellet to disrupt any cell-to-cell clumping.
10. Repeat wash using 1 ml of 1x FLICA wash buffer.
11. Resuspend the cell pellet in 400 μL of 1x FLICA wash buffer.
12. Add 2 μL of propidium iodide (250 μg/mL) to one cell suspension. Set aside a second suspension without propidium iodide.
13. Add 40 μL fixative (3% paraformaldehyde) to the cell suspension without propidium iodide. Keep fixed cells at 2–8°C protected from light for analyses. The cell suspension with propidium iodide is analyzed without being fixed.
14. Levels of activated caspase-8, -9, -1, and -3 can be evaluated using flow cytometric analyses (fluorescence activated cell sorting, FACS, Becton Dickinson). A minimum of 10,000

spermatozoa are examined for each assay at a flow rate of <100 cells/s. The sperm population is gated using 90-degree and forward-angle light scatter to exclude debris and aggregates. An argon laser at 15 mW is used and green fluorescence (480–530 nm) measured in the FHL1 channel. The percentage of positive cells and the mean fluorescence are calculated on a 1023 channel scale using the flow cytometer software CellQuest™ (version 3.3, BD Biosciences, San Jose, CA).

3.5.6. Annexin Labeling

Apoptosis is a normal physiological process that occurs during embryonic development and also helps in the maintenance of tissue homeostasis. The apoptotic program is characterized by certain morphological features, including loss of plasma membrane asymmetry and attachment, condensation of the cytoplasm and nucleus, and internucleosomal cleavage of DNA. Loss of plasma membrane is one of the earliest features. In apoptotic cells, the membrane phospholipid phosphatidylserine (PS) is translocated from the inner to the outer leaflet of the plasma membrane, thereby exposing PS to the external cellular environment. Annexin V is a 35–36 kDa Ca^{2+} dependent phospholipid-binding protein that has a high affinity for PS and binds to cells with exposed PS. Annexin V may be conjugated to fluorochromes such as FITC. This format retains its high affinity for PS and thus serves as a sensitive probe for flow cytometric analysis of cells that are undergoing apoptosis (57–59).

Since externalization of PS occurs in the earlier stages of apoptosis, annexin V-FITC staining can identify apoptosis at an earlier stage than assays based on nuclear changes such as DNA fragmentation. Annexin V-FITC staining precedes the loss of membrane integrity that accompanies the latest stages of cell death resulting from either apoptotic or necrotic processes. Therefore, staining with annexin V-FITC typically is used in conjunction with a vital dye such as propidium iodide to identify early apoptotic cells.

Cells that are viable are annexin V-FITC-negative and PI-negative; cells that are in early apoptosis are annexin V-FITC-positive and PI-negative; and cells that are in late apoptosis or dead are both annexin V-FITC- and PI-positive. This assay does not distinguish per se cells that already have undergone apoptotic death and those that have died as a result of a necrotic pathway because in either case the dead cells stain with both annexin-FITC and PI. However, when apoptosis is measured over time, cells can be identified as annexin V-FITC- and PI-negative (viable, or no measurable apoptosis), annexin V-FITC-positive and PI-negative (early apoptosis, membrane integrity is present) or annexin V-FITC-and PI-positive (end-stage apoptosis and death). The movement of cells through these three stages suggests apoptosis. In contrast, a single observation indicating that cells are both annexin V-FITC-and PI-positive, in itself, reveals less information about the process by which the cells underwent their demise (35).

Annexin V-FITC is used to determine quantitatively the percentage of cells within a population that are actively undergoing apoptosis. It is based on the property of cells to lose membrane asymmetry in the early phases of apoptosis. In apoptotic cells, the membrane phospholipid phosphatidylserine (PS) is translocated from the inner leaflet of the plasma membrane to the outer leaflet, thereby exposing PS to the external environment.

Annexin V is a Ca_2^+-dependent phospholipid-binding protein that has a high affinity for PS, and is useful for identifying apoptotic cells with exposed PS. PI is a standard flow cytometric viability probe and is used to distinguish viable from non-viable cells (35).

1. Wash cells twice with cold PBS and then resuspend cells in 1x Annexin V binding buffer at a concentration of 1×10^6 cells/mL.
2. Transfer 100 µL of the solution (1×10^5 cells) to a 5 mL culture tube.
3. Add 5 µL of annexin V-FITC and 5 µL of propidium iodide (250 µg/mL).
4. Gently vortex the cells and incubate for 15 min at RT (25°C) in the dark.
5. Add 400 µL of 1x annexin V binding buffer to each tube.
6. Analyze by flow cytometry within 1 hour.
7. An EPICS Elite ESP flow cytometer (Beckman Coulter), equipped with an argon-ion laser (488 nm) is used to analyze sperm labeled with annexin V and propidium iodide. Green fluorescence (FITC) is detected with PMT2 (behind 550 DL and 525 BP filters) and red fluorescence (PI) with PMT4 (behind 600 DL and 575 BP filters). The sperm population can be identified by a combination of side-scatter (PMT1) and forward-scatter (FS) information. Acquisition gates on the FS x PMT1, two-dimensional histogram are used to eliminate small particles and cell debris from subsequent analyses. Ten thousand spermatozoa are analyzed per sample.

3.5.7. Magnetic Activated Cell Sorting Preparation

Numerous reports link the presence of apoptosis markers in human sperm with the failure of in vivo and in vitro fertilization (5, 60–63). Therefore, the current suboptimal ART success rates may be attributed, at least in part, to the inclusion of apoptotic sperm as a result of absent in vivo sperm selection barriers. This hypothesis has generated a motivation to develop new protocols for sperm selection based on the presence of apoptosis or apoptosis-like markers and manifestations. Such an approach represents the inevitable evolution of sperm preparation techniques that expand to include molecular characteristics in addition to the physical properties. Some sperm selected for ART are likely to display features of apoptosis despite their normal appearance, which may be partially responsible for the low fertilization and implantation rates seen with ART.

One of the features of apoptosis is the externalization of phosphatidylserine (PS) residues, which normally are present on the inner leaflet of the sperm plasma membrane. Colloidal super-paramagnetic microbeads (~50 nm in diameter) conjugated with annexinV bound to PS are used to separate dead and apoptotic spermatozoa by magnetic-activated cell sorting (MACS) (64–66). Cells with externalized PS will bind to these microbeads, while non-apoptotic cells with intact membranes do not bind and could be used during ART. We have conducted a series of experiments to investigate whether MACS technology could be used to improve ART outcomes (54, 66–68).

Our results clearly indicate that integrating MACS into sperm preparation techniques will improve semen quality and cryosurvival rates by eliminating apoptotic sperm (68). Non-apoptotic spermatozoa prepared by MACS display higher quality in terms of routine sperm parameters and apoptosis markers. This higher sperm quality is represented by an increased oocyte penetration potential and cryosurvival rates. Thus, the selection of non-apoptotic spermatozoa by MACS should be considered to enhance ART success rates.

During apoptosis, phosphatidyl serine residues are translocated from the inner membrane of the spermatozoa to the outside. Annexin V has a strong affinity for phosphatidyl serine but cannot pass the intact sperm membrane. Colloidal superparamagnetic beads (~ 50 nm in diameter) are conjugated to highly specific antibodies to annexin V and used to separate dead and apoptotic spermatozoa by MACS. Annexin V binding to spermatozoa indicates compromised sperm membrane integrity.

1. Mix 100 μL of the sperm suspension isolated from the pellet (10 million total spermatozoa) with 100 μL of MACS Microbeads and incubate at room temperature for 15 min.
2. Load mixture on top of the separation column placed in the magnetic field (0.5 Tesla (T) between the poles of the magnet and 1.5 T within the iron globes of the column).
3. Rinse the column with buffer. The entire unlabeled (annexin V-negative non-apoptotic) sperm fraction passes through the column. The entire annexin-positive (apoptotic) fraction is retained in the column.
4. Remove column from the magnetic field.
5. Elute annexin V-positive fraction using the annexin V-binding buffer and calculate sperm recovery.

$$\text{Sperm recovery} = (\#\ \text{of spermatozoa after separation} / \#\ \text{of spermatozoa before separation}) \times 100$$

4. Notes

1. Cover the tubes in aluminum foil due to the light sensitivity of DCF-DA and HE. Store it in the −20° C in dark (valid for 1 week).
2. To avoid instrument drift, reference samples are used to set the red and green photomultiplier tube voltages. In addition a reference sample of semen is run in every assay.
3. This solution should be sterile-filtered.
4. Store the annexin V protein at −80°C and avoid repeated freeze/thaw cycles to prevent protein degradation.
5. This procedure takes place in a semi-dark room.
6. To avoid contamination, use fresh pipette tips each time for adding luminol to tubes 2–7.
7. If the sperm concentration is different from 20×10^6 sperm/mL, calculate a factor that adjusts the concentration to 20×10^6 sperm/mL. Use this factor to multiply the final ROS result to adjust the difference in the sperm concentration. For example,

$$\text{Sperm Count} = 8.5 \times 10^6 \text{ sperm/mL}, \; 20 \times 10^6 \text{ sperm/mL} = 2.35(\text{factor}) \times \text{final ROS result } 8.5 \times 10^6 \text{ sperm/mL}$$

8. This mixture must be prepared fresh every time. Place in a boiling (100°C) water bath for 30 minutes.
9. Any errors during pipetting can be highlighted on the template for any discrepancy in the final results.
10. A multichannel pipette should be used to pipette chromogen taken in a flat disposable container.
11. The appropriate volume of staining solution to prepare for a variable number of assays is based upon multiples of the component volumes needed for one assay. Mix only enough staining solution to complete the number of assays prepared per session. The staining solution is active for approximately 24 h at 4°C.
12. If the cell density is low, decrease the amount of PI/ RNase staining buffer to 0.3 mL.
13. Cells must be analyzed within 3 hours of staining. Cells may begin to deteriorate if left overnight before analysis.
14. It is **NOT**appropriate to use software or hardware configurations that define αt as red (>630 nm)/total (515 longpass) fluorescence; this adds the unknown component of (530–630 nm) wavelength data into the equation.

15. Store the stock solution in the dark at 4°C and prepare fresh AO stain. It is important to fix sperm smears on the same day of analysis and stain on the very next day. Storage of either fixed or non-fixed smears for later staining could affect results.
16. Using clean, grease-free, high quality microscopic slides for making the sperm smears is important. Ideally, stained smears should be evaluated immediately in a dark room. Storage of slides can cause fading of fluorescence. If a delay in evaluating smears is unavoidable, slides may be stored at dark in 4°C but for not longer than 24 hours.
17. Since high-back ground staining is a major hurdle in the AO test, use of freshly prepared AO solution and removal of seminal plasma by slow speed centrifugation is useful.

References

1. Muratori, M., Piomboni, P., Baldi, E., Filimberti, E., Pecchioli, P., Moretti, E., Gambera, L., et al. (2000) Functional and ultrastructural features of DNA-fragmented human sperm. *J Androl.* ***21,*** 903–912.
2. Aitken, R.J., Gordon, E., Harkiss, D., Twigg, J.P., Milne, P.J. Irvine, D.S. (1998) Relative impact of oxidative stress on the functional competence and genomic integrity of human spermatozoa. *Biol Reprod.* ***59,*** 1037–1046.
3. Sun, J.G., Jurisicova A, Casper, R.F. (1997) Detection of deoxyribonucleic acid fragmentation in human sperm: correlation with fertilization in vitro. *Biol Reprod.* ***56,*** 602–607.
4. Lopes, S., Sun, J.G., Jurisicova, A., Meriano, J., Casper, R.F. (1998) Sperm deoxyribonucleic acid fragmentation is increased in poor-quality semen samples and correlates with failed fertilization in intracytoplasmic sperm injection. *Fertil Steril.* ***69,*** 528–532.
5. Host, E., Lindenberg, S., Kahn, J.A., Christensen, F. (1999) DNA strand breaks in human sperm cells: a comparison between men with normal and oligozoospermic sperm samples. *Acta Obstet Gynecol Scand.* ***78,*** 336–339.
6. Irvine, D.S., Twigg, J.P., Gordon, E.L., Fulton, N., Milne, P.A., Aitken, R.J. (2000) DNA integrity in human spermatozoa: relationships with semen quality. *J Androl.* ***21,***33–44.
7. Sharma, R.K., Agarwal A. (1996) Role of reactive oxygen species in male infertility. *Urology* ***48,*** 835–850.
8. Hammadeh, M.E., Radwan, M., Al-Hasani, S., Micu, R., Rosenbaum, P., Lorenz, M., Schmidt W. (2006) Comparison of reactive oxygen species concentration in seminal plasma and semen parameters in partners of pregnant and non-pregnant patients after IVF/ICSI. *Reprod Biomed Online* ***13,*** 696–706.
9. Warren, J.S., Johnson, K.J., Ward, P.A. (1987) Oxygen radicals in cell injury and cell death. *Pathol Immunopathol Res.* ***6,*** 301–315.
10. Griveau, J.F., Renard, P., Le Lannou, D. (1995) Superoxide anion production by human spermatozoa as a part of the ionophore-induced acrosome reaction process. *Int J Androl.* ***18,***67–74.
11. Aitken, R.J., Buckingham, D. (1992) Enhanced detection of reactive oxygen species produced by human spermatozoa with 7-dimethyl amino-naphthalin-1, 2-dicarbonic acid hydrazide. *Int J Androl.* ***15,*** 211–219.
12. Agarwal, A, Allamaneni, S.S.R., and Said, T.M. (2004) Chemiluminescence technique for measuring reactive oxygen species. *Reprod Biomed Online* ***9,*** 466–468.
13. Allamaneni, S.S.R., Agarwal, A., Nallella, K., Sharma, R.K., Thomas, A.J., Jr, Sikka, S.C. (2005) Characterization of oxidative stress status by evaluation of reactive oxygen species levels in whole semen and isolated spermatozoa. *Fertil Steril.* 83:800–803.
14. Athayde, K.S., Cocuzza, M., Agarwal, A., Krajcir, N., Lucon, A.M., Srougi, M., Hallak, J. (2007) Development of normal reference values for seminal reactive oxygen species and their correlation with leukocytes and semen parameters in a fertile population. *J Androl.* ***28,*** 613–620.
15. Aitken, R.J., Buckingham, D.W., West, K.M. (1992) Reactive oxygen species and

human spermatozoa: analysis of the cellular mechanisms involved in luminol- and lucigenin-dependent chemiluminescence. *J Cell Physiol.* ***151,*** 466–477.

16. Aitken, R.J., Ryan, A.L., Curry, B.J., and Baker, M.A. (2003) Multiple forms of redox activity in populations of human spermatozoa. *Mol Hum Reprod.* ***9,*** 645–661.
17. Said, T., Agarwal, A., Sharma, R.K., Mascha, E., Sikka, S.C., Thomas, A.J.Jr. (2004) Human sperm superoxide anion generation and correlation with semen quality in patients with male infertility. *Fertil Steril.* ***82,*** 871–877.
18. Guthrie, H.D., Welch, G.R. (2006) Determination of intracellular reactive oxygen species and high mitochondrial membrane potential in Percoll-treated viable boar sperm using fluorescence-activated flow cytometry. *J Anim Sci.* ***84,*** 2089–2100.
19. Mahfouz, R., Sharma, R., Lackner, J., Aziz, N, Agarwal, A. (2008) Evaluation of chemiluminescence and flowcytometry as tools in assessing production of hydrogen peroxide and superoxide anion in human spermatozoa. *Fertil Steril.* Aug 16. [Epub ahead of print], PMID: 18710706.
20. Aitken, R.J., Harkiss, D., Buckingham, D. (1993) Relationship between iron-catalysed lipid peroxidation potential and human sperm function. *J Reprod Fertil.* ***98,*** 257–265.
21. Sharma, R.K., Pasqualotto, F.F., Nelson, D.R., Thomas, A.J., Jr., and Agarwal, A. (1999) The reactive oxygen species – total antioxidant capacity score is a new measure of oxidative stress to predict male infertility. *Hum Reprod.* **14,** 2801–2807.
22. Pasqualotto, F.F., Sundaram, A., Sharma, R.K., Borges, E. Jr, Pasqualotto, E.B., Agarwal, A. (2008) Semen quality and oxidative stress scores in fertile and infertile patients with varicocele. *Fertil Steril.* **89,** 602–607.
23. Hendin, B.N., Kolettis, P.N., Sharma, R.K., Thomas, A.J., Jr., and Agarwal, A. (1999) Varicocele is associated with elevated spermatozoal reactive oxygen species production and diminished seminal plasma antioxidant capacity. *J Urol.* ***161,*** 1831–1834.
24. Pasqualotto, F.F., Sharma, R.K., Nelson, D.R., Thomas, A.J., Jr., and Agarwal, A. (2000) Relationship between oxidative stress, semen characteristics, and clinical diagnosis in men undergoing fertility investigation. *Fertil Steril.* ***73,*** 459–464.
25. Saleh, R.A., Agarwal A., Kandirali, E., Sharma, R.K., Thomas, A.J. Jr., Nada, E.A., Evenson, D.P., and Alvarez, J.G. (2002) Leukocytospermia is associated with increased reactive oxygen species production by human spermatozoa. *Fertil Steril.* ***78,*** 1215–1224.
26. Saleh, R.A., Agarwal, A., Nada, E.A., El-Tonsy, M.H., Sharma, R.K., Meyer, A., et al. (2003) Negative effects of increased sperm DNA damage in relation to seminal oxidative stress in men with idiopathic and male factor infertility. *Fertil Steril.* ***79,*** 1597–1605.
27. Pasqualotto, F.F., Sharma, R.K., Pasqualotto, E.B., Agarwal, A. (2008) Poor semen quality and ROS-TAC scores in patients with idiopathic infertility. *Urol Int.* **3,** 263–270.
28. Mahfouz, R., Sharma, R., Sharma, D., Sabanegh, E., Agarwal, A. (2009) Diagnostic value of the total antioxidant capacity (TAC) in human seminal plasma. *Fertil Steril.* **91,** 805–811.
29. Said, T.M., Kattal, N., Sharma, R.K., Sikka, S.C., Thomas, A.J., Jr, Mascha, E., Agarwal, A. (2003) Enhanced chemiluminescence assay vs colorimetric assay for measurement of the total antioxidant capacity of human seminal plasma. *J Androl.* ***24,*** 676–680.
30. Hoshi, K., Katayose, H., Yanagida, K., Kimura, Y., Sato, A. (1996) The relationship between acridine orange fluorescence of sperm nuclei and the fertilizing ability of human sperm. *Fertil Steril.* ***66,*** 634–639.
31. Evenson, D.P., Jost, L.K., Marshall, D., Zinaman, M.J., Clegg, E., Purvis, K., de Angelis, P. et al. (1999) Utility of the sperm chromatin structure assay as a diagnostic and prognostic tool in the human fertility clinic. *Hum Reprod.* ***14,*** 1039–1049.
32. Gopalkrishnan, K., Hurkadli, K., Padwal, V., Balaiah, D. (1999) Use of acridine orange to evaluate chromatin integrity of human spermatozoa in different groups of infertile men. *Andrologia* ***31,*** 277–282.
33. Larson, K.L., DeJonge, C.J., Barnes, A.M., Jost, L.K., Evenson, D.P. (2000) Sperm chromatin structure assay parameters as predictors of failed pregnancy following assisted reproductive techniques. *Hum Reprod.* ***15,*** 1717–1722.
34. Sergerie, M., Laforest, G., Bujan, L., Bissonnette, F., and Bleau, G. (2005) Sperm DNA fragmentation: threshold value in male fertility. *Hum Reprod.* ***20,*** 3446–3451.
35. Mahfouz, R.Z., Sharma, R.K., Poenicke, K., Jha, R., Paasch, U., Grunewald, S., Agarwal, A. (2009) Evaluation of poly (ADP-ribose)

polymerase cleavage (cPARP) in ejaculated human sperm fractions after induction of apoptosis. *Fertil Steril.* **91,** 2210–20.

36. Evenson, D.P., Darzynkiewicz, Z., Melamed, M.R. (1980) Relation of mammalian sperm chromatin heterogeneity to fertility. *Science* ***240,*** 1131–1133.
37. Boe-Hansen, G.B., Fedder, J., Ersboll, A.K., and Christensen, P. (2006) The sperm chromatin structure assay as a diagnostic tool in the human fertility clinic.*Hum Reprod.* ***21,*** 1576–1582.
38. Wyrobek, J., Eskenazi, B., Young, S., Arnheim, N., Tiemann-Boege, I., Jabs, E.W., Glaser, R.L., Pearson, F.S., and Evenson, D. (2006) Advancing age has differential effects on DNA damage, chromatin integrity, gene mutations, and aneuploidies in sperm. *PNAS* ***103,*** 9601–9606.
39. Ahmadi, A., Ng, S.C. (1999) Developmental capacity of damaged spermatozoa. *Hum Reprod.* ***14,*** 2279–2285.
40. Spanò M, Bonde JP, Hjøllund HI, Kolstad HA, Cordelli E, Leter G. (2000) Sperm chromatin damage impairs human fertility. The Danish First Pregnancy Planner Study Team. *Fertil Steril. 73,* 43–50.
41. Agarwal, A., and Said, T.M. (2003) Role of sperm chromatin abnormalities and DNA damage in male infertility. *Hum Reprod Update* ***9,*** 331–345.
42. Larson-Cook, K.L., Brannian, J.D., Hansen, K.A., Kasperson, K.M., Aarnold, E.T. and Evenson, D.P. (2003) Relationship between the outcomes of assisted reproductive techniques and sperm DNA fragmentation as measured by the sperm chromatin structure assay. *Fertil Steril.* ***80,*** 895–902.
43. Bungum, M., Humaidan, P., Spano, M., Jepson, K., Bungum, L., and Giwercman, A. (2004) The predictive value of sperm chromatin structure assay (SCSA) parameters for the outcome of intrauterine insemination, IVF and ICSI. *Hum Reprod.* ***19,*** *1401–1408.*
44. Erenpreiss, J., Bungum, M., Spano, M., Elzanaty, S., Orbidans, J., and Giwercman, A. (2006) Intra-individual variation in sperm chromatin structure assay parameters in men from infertile couples: clinical implications. *Hum Reprod.* ***21,*** 2061–2064.
45. Evenson, E. and Jost, L. (2000) Sperm chromatin structure assay is useful for fertility assessment. *Methods Cell Sci* ***22,*** 169–189.
46. Darzynkiewicz, Z., Traganos, F., Sharpless, T., Melamed, M.R. (1975) Thermal denaturation of DNA in situ as studied by acridine orange staining and automated cytofluorometry. *Exp Cell Res.* ***90,*** 411–428.
47. Fernandez, J.L., Muriel, L., Rivero, M.T., Goyanes, V., Vazquez, R., Alvarez, J.G. (2003) The sperm chromatin dispersion test: a simple method for the determination of sperm DNA fragmentation. *J Androl.* ***24,*** 59–66.
48. Enciso, M., Lopez-Fernandez, C., Fernandez, J.L., Garcia, P., Gosalbez, A., Gosalvez, J. (2006) A new method to analyze boar sperm DNA fragmentation under bright-field or fluorescence microscopy. *Theriogenology* ***65,*** 308–316.
49. Fernandez, J.L., Muriel, L., Goyanes, V., Segrelles, E., Gosalvez, J., Enciso, M., LaFromboise, M. et al. (2005) Simple determination of human sperm DNA fragmentation with an improved sperm chromatin dispersion test. *Fertil Steril.* ***84,*** 833–842.
50. Tejada, R.I., Mitchell, J.C., Norman, A., Marik, J.J., Friedman, S. (1984) A test for the practical evaluation of male fertility by acridine orange (AO) fluorescence. *Fertil Steril.* ***42,*** 87–91.
51. Said, T.M., Paasch, U., Glander, H-J., and Agarwal, A. (204) Role of caspases in male infertility.*Hum Reprod Update* ***10,*** *39–51.*
52. Ekert, P.G., Silke, J., Vaux, D.L. (1999) Caspase inhibitors. *Cell Death Differ.* ***6,*** 1081–1086.
53. Bedner, E., Smolewski, P., Amstad, P., Darzynkiewicz, Z. (2000) Activation of caspases measured in situ by binding of fluorochrome-labeled inhibitors of caspases (FLICA): correlation with DNA fragmentation. *Exp. Cell Res.* ***259,*** 308–313.
54. Paasch, U., Grunewald, S., Agarwal, A., Glander, H.J. (2004a) Activation pattern of caspases in human spermatozoa. *Fertil Steril.* ***81,*** 802–809.
55. Paasch, U, Sharma, R.K., Gupta, A.K., Grunewald, S., Mascha, E.J., Thomas, A.J., Jr., Glander, H-J., and Agarwal, A. (2004b) Cryopreservation and thawing is associated with varying extent of activation of apoptotic machinery in subsets of ejaculated human spermatozoa. *Biol Reprod.* ***71,*** 1828–1837.
56. Grunewald, S., Paasch, U., Said, T.M., Sharma, R.K., Glander, H.J., Agarwal, A. (2005) Caspase activation in human spermatozoa in response to physiological and pathological stimuli. *Fertil Steril.* ***83,*** 1106–1112.
57. Glander, H-J., and Schaller, J. (1999) Binding of annexin V to plasma membranes of

human spermatozoa: a rapid assay for detection of membrane changes after cryostorage. *Mol Hum Reprod.* ***5,*** 109–115.

58. Barroso, G., Morshedi, M., and Oehninger, S. (2000) Analysis of DNA fragmentation, plasma membrane translocation of phosphatidylserine and oxidative stress in human spermatozoa. *Hum Reprod.* ***15,*** 1338–1344.
59. Said, T., Agarwal, A., Grunewald, S., Rasch, M., Baumann, T., Kriegel, C., Li, L., Glander, H-J., Thomas, A.J., Jr., and Paasch, U. (2006) Selection of nonapoptotic spermatozoa as a new tool for enhancing assisted reproduction outcomes: An in vitro model.- *Biol Reprod.* ***74,*** 530–537.
60. Barroso, G., Taylor, S., Morshedi, M., Manzur, F., Gaviño, F. and Oehninger, S. (2006) Mitochondrial membrane potential integrity and plasma membrane translocation of phosphatidylserine as early apoptotic markers: a comparison of two different sperm subpopulations. *Fertil Steril.* ***85,*** 149–154.
61. Tesarik, J., Greco, E., Mendoza, C. (2001) Assisted reproduction with in-vitro-cultured testicular spermatozoa in cases of severe germ cell apoptosis: a pilot study. *Hum Reprod.* ***16,*** 2640–2645.
62. Henkel, R., Hajimohammad, M., Stalf, T., Hoogendijk, C., Mehnert, C., Menkveld, R., Gips, H., Schill, WB., Kruger, T.F. (2004) Influence of deoxyribonucleic acid damage on fertilization and pregnancy. *Fertil Steril.* ***81,***965–972.
63. Seli, E., Gardner, D.K., Schoolcraft, W.B., Moffatt, O., Sakkas, D. (2004) Extent of nuclear DNA damage in ejaculated spermatozoa impacts on blastocyst development after in vitro fertilization. *Fertil Steril.* ***82,*** 378–383.
64. Said, T.M., Grunewald, S., Paasch, U., Glander, H.J., Baumann, T., Kriegel, C., Li, L., Agarwal, A. (2005) Advantage of combining magnetic cell separation with sperm preparation techniques. *Reprod Biomed Online* ***10,*** 740–746.
65. Aziz N, Said T, Paasch U, Agarwal A. (2007) The relationship between human sperm apoptosis, morphology and the sperm deformity index. *Hum Reprod.* ***22,*** 1413–1419.
66. Said, T., Agarwal, A., Zborowski, M., Grunewald, S., Glander, H-J., and Paasch U. (2008) Utility of magnetic cell separation as a molecular sperm preparation technique.*J Androl.* ***29,*** 134–142.
67. Said, T., Agarwal, A., Grunewald, S., Rasch, M., Baumann, T., Kriegel, Li, L., Glander, H-J., Thomas, A.J., Jr., and Paasch, U. (2006) Selection of nonapoptotic spermatozoa as a new tool for enhancing assisted reproduction outcomes: An in vitro model. *Biol Reprod.* ***74,*** 530–537.
68. Said, T.M., Grunewald, S., Paasch, U., Rasch, M., Agarwal, A., Glander, H-J. (2005) Effects of magnetic-activated cell sorting on sperm motility and cryosurvival rates. *Fertil Steril.* ***83,*** 1442–1446.

Chapter 25

Planning and Executing a Genome Wide Association Study (GWAS)

Michèle M. Sale, Josyf C. Mychaleckyj, and Wei-Min Chen

Abstract

In recent years, genome-wide association approaches have proven a powerful and successful strategy to identify genetic contributors to complex traits, including a number of endocrine disorders. Their success has meant that genome wide association studies (GWAS) are fast becoming the default study design for discovery of new genetic variants that influence a clinical trait or phenotype. This chapter focuses on a number of key elements that require consideration for the successful conduct of a GWAS. Although many of the considerations are common to any genetic study, the greater cost, extreme multiple testing, and greater openness to data sharing require specific awareness and planning by investigators. In the section on designing a GWAS, we reflect on ethical considerations, study design, selection of phenotype/s, power considerations, sample tracking and storage issues, and genotyping product selection. During execution, important considerations include DNA quantity and preparation, genotyping methods, quality control checks of genotype data, *in silico* genotyping (imputation), tests of association, and replication of association signals. Although the field of human genetics is rapidly evolving, recent experiences can help guide an investigator in making practical and methodological choices that will eventually determine the overall quality of GWAS results. Given the investment to recruit patient populations or cohorts that are powered for a GWAS, and the still substantial costs associated with genotyping, it is helpful to be aware of these aspects to maximize the likelihood of success, especially where there is an opportunity for implementing them prospectively.

Key words: Linkage disequilibrium, haplotype, association, population, genetic, genome, genome wide, single nucleotide polymorphism.

1. Introduction

The sequencing of the human genome (1, 2), and SNP discovery and genotyping efforts (3) led to the discovery that the human genome is arranged in blocks of high linkage disequilibrium (LD), separated by hotspots of recombination (4). Resources from the

O.-K. Park-Sarge, T.E. Curry, Jr. (eds.), *Molecular Endocrinology,* Methods in Molecular Biology 590,
DOI 10.1007/978-1-60327-378-7_25,

International HapMap Project (5–7) and affordable, accurate, high-throughput genotyping technologies have permitted analysis of the entire human genome using association methods, exploiting the fact that common variation in the human genome can be surveyed by genotyping only a fraction of the estimated 10–15 million single nucleotide polymorphisms (SNPs) that exist in the human population (8–10). This approach, using either tagging SNPs or protein coding non-synonymous SNPs, has revolutionized human genetics over the past 5 years. Recent analyses have identified loci for several endocrine measures and disorders, including type 2 diabetes (11, 12), type 1 diabetes and other autoimmune diseases (13), thyroid disease or thyroid measures

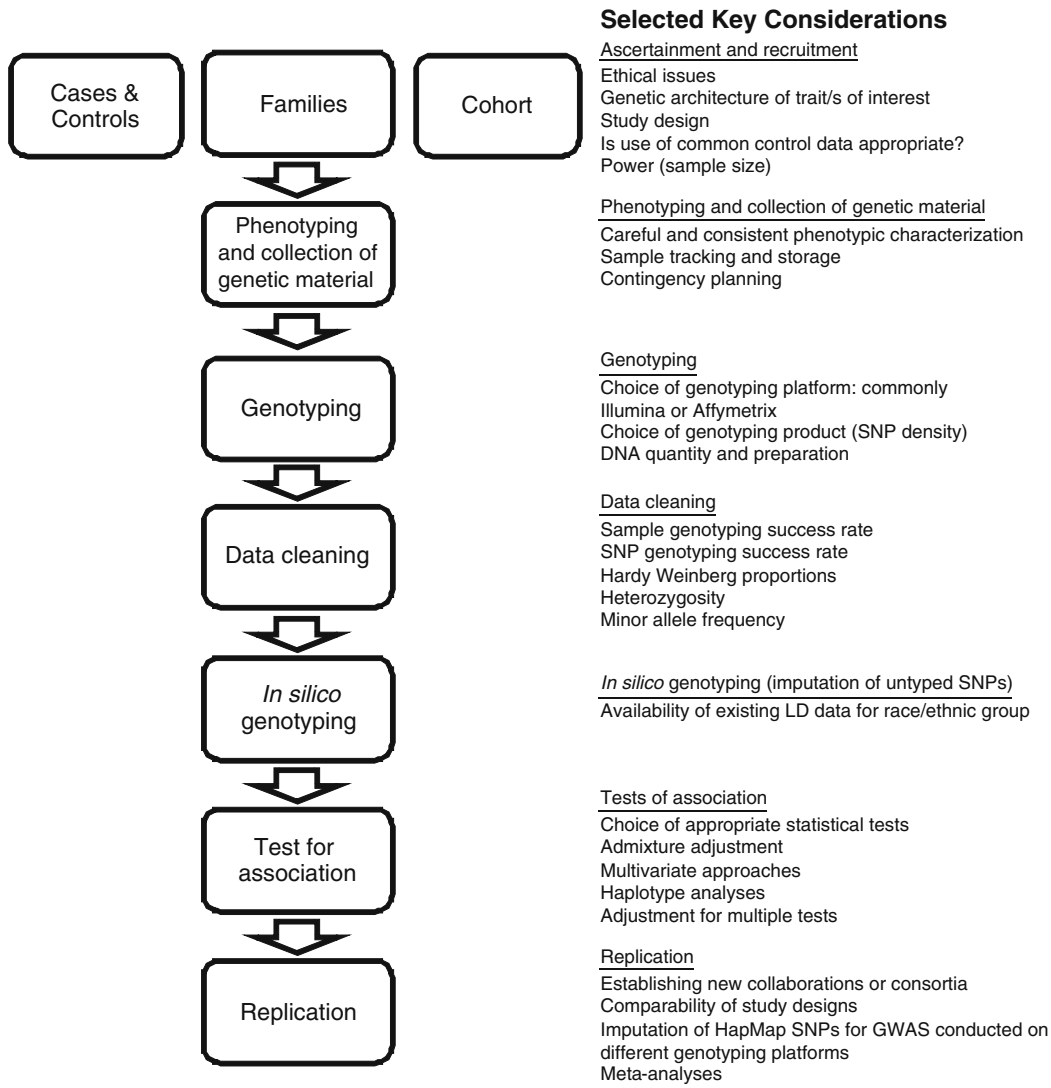

Fig. 25.1. Schematic of GWAS process.

(14, 15), bone mineral density and osteoporosis (16, 17), obesity (18–20), and adult height (21–24). In many cases, the newly identified associated genes and regions have provided insights on novel pathways and potential therapeutic targets (25).

This chapter focuses on a number of key elements to consider in the planning and successful conduct of a genome wide association study (GWAS), summarized in **Fig. 25.1**. Although this is an evolving and dynamic field of active research with many diverse opinions on approaches, some general recommendations can be made. Where possible, we point to in-depth reviews by other authors that provide more detailed explanation of these issues.

2. Planning a Genome Wide Association Study (GWAS)

2.1. Ethical Considerations

The scope of existing consent documents is an important consideration before embarking on a GWAS. Many studies were designed and initiated prior to the availability of GWAS technology and did not have to confront the issues of individual identifiability and mandated sharing of data under national biobank policies. An example of such a policy is the current National Institutes of Health policy for awards that include a GWAS component (available at http://grants.nih.gov/grants/gwas/) and the deposition of de-identified data in the National Institutes of Health's Database of Genotype and Phenotype (dbGaP) (26). Recent policy changes reflect new concerns over potential identification of individual participants from summary data (27). Retrospective extension of existing clinical trial or observational studies to test genetic hypotheses raises major and profound issues of the applicability of an existing informed consent to the genetic study being considered. Consents may contain language that restricts data sharing to investigators of the trial or study only, or may preclude the use of the research data for studying diseases other the main study outcome. It is important to review consent wording in terms of participant intent and data sharing potential. For new studies, the possibility that de-identified data may be able to be matched against a second sample given by the same participant should be explicitly stated and explained during consent, since aggregated genetic data of this magnitude will undoubtedly constitute a unique genetic profile. Investigators are strongly urged to consult with local experts in ethics and genetics on their local research review board.

2.2. Study Design Issues

Although family designs can be used for GWAS projects, and the resulting data can be analyzed under family-based tests of association (e.g., 28–29), many of the early successes with GWAS have

come from retrospective case-control study designs. Case-control designs offer advantages in relative efficiency of recruitment of independent sampling units, ease of analysis, and power for tests of common genetic variants that contribute only modest-to-low relative risk.

For a case-control design, matching of samples is critical to avoid biases that will inflate the overall type 1 error rate and lead to the identification of thousands of apparently significant SNPs. Matching can be performed at the individual level in a 1:1 or 1:*M* design (where *M* is an integer), or could be based on equalizing the frequency of known study subpopulations. For potential confounders for which matching may not be feasible, post-hoc adjustments can be performed during statistical analysis. It is critical that cases and controls are matched for ethnicity as closely as possible to avoid confounding and spurious associations. In this regard, GWA studies draw from the same design principles employed for any observational or clinical trial.

Several studies have demonstrated the utility of genotyping a common set of population controls for analyses of multiple traits. In particular, The Wellcome Trust Case-Control Consortium (WTCCC) (30) genotyped 500,000 SNPs in a common set of 3,000 controls drawn from the 1958 British birth cohort and the UK Blood Services collection, and have used these for a number of disease-based GWAS. Tests of association using a Cochran-Armitage additive trend statistic showed a high degree of concordance of the separately ascertained, but ethnically matched, UK controls. Similarly, use of previously genotyped population controls ascertained from an independent study can result in a considerable cost saving or increase in power (31), but the population must be substantially free of the disease or phenotype under investigation, and must be ethnically well-matched.

Many of the issues relating to study design, phenotype measures, and power are reviewed in (25, 32, 33). Considerations for designing a study, including the genetic architecture of complex traits, population stratification, and phenotype data are considered in detail by (34), while the role of family study designs in GWAS is reviewed in (35).

2.3. Selection of Phenotype/s

Often under-appreciated aspects of GWAS are the choice of phenotype definition and method of measurement of the primary phenotype and potential confounders. Large, well-designed prospective cohort studies are often advantageous since protocols are consistent across sites. However, even smaller single-site investigations need to consider the spectrum of phenotypic data that may be useful for GWAS analyses in order to provide insight into molecular mechanisms. Given the need for large-scale, often international, collaborative efforts to establish

replication or identify alleles of modest effect, it is helpful to develop standardized phenotypic protocols to facilitate comparable cross-study analyses and meta-analyses of data.

2.4. Power Considerations

The power to detect association is a function of the effect size, sample size (number of cases and controls, or families), and the tested association disease model. These factors are themselves influenced by the prevalence of the disease, disease allele frequency and the genotypic relative risk (GRR). For a typical study design that plans to genotype 1,000 cases and 1,000 controls for 300,000 markers, a disease-predisposing variant with GRR = 1.415 under a multiplicative model, with prevalence 0.1 and risk allele frequency 0.5 can be detected with 80% power. To reduce the high cost of genotyping, a two-stage design has been proposed where a proportion of samples are genotyped on every marker in stage 1, and a proportion of these markers are later followed up by genotyping them on the remaining samples in stage 2. For the above example, nearly the same power (77%) can be achieved with only 34% as many genotypes by using 30% of samples in stage 1 and 5% markers in stage 2. The software package CaTS (36) provides a convenient way for users to plan the sample size and power for their studies.

2.5. Sample Tracking and Storage

A known potential source of error for any GWAS is sample handling within the laboratory. A number of sample tracking and evaluation steps can be put in place to reduce the potential for sample mishandling or mislabeling. The National Cancer Institute's Office of Biorepositories and Biospecimen Research (http://biospecimens.cancer.gov/) is a useful resource for best practices and policies for biospecimen storage and tracking, and has also developed a suite of informatics tools available through the cancer Biomedical Informatics Grid (caBIG). At entry into the lab, a digital photographic record showing original sample sources (e.g., tubes) and label details is often useful. Allocation of a unique barcoded ID at the point of sample receipt enables tracking within the laboratory. Sample ID, receipt date, sample type, and storage location, together with any other available information, should be electronically logged into a secure database and, following DNA isolation, the quality and quantity of the genetic material should be assessed using standard methods (*see* **Section 3.1**). To enable back-referencing as the sample moves through sample processing stages (e.g., source sample, DNA isolation, aliquoting, dilution, plating, and genotyping), a number of alternate and complementary strategies can be implemented, depending on sample volume and financial resources. The simplest is to store a back-up sample of the original source material, such as an aliquot of frozen whole blood (or saliva, frozen tissue, etc.) or, for liquid samples, by spotting onto an FTA card (Whatman, Kent, UK) or equivalent product. These samples can be accessed later for DNA isolation

and genotyping, or direct PCR, if a sample handling mix-up is suspected. Another option is to conduct a simple PCR-based sex check immediately following DNA isolation, since this approach can often pick up mislabeling during recruitment, or wider sample handling problems during DNA isolation. Finally, generating a "mini-fingerprint" of highly polymorphic genetic variants (SNPs or microsatellites) on all incoming samples can serve as a more specific sample reference, but typically requires additional financial and personnel resources for sample processing and genotyping. The forensic community typically uses 13 short tandem repeat (STR) CODIS (Combined DNA Index System) markers that have been developed for utilization in forensic casework, although approximately 30 well-chosen SNPs would provide a similar information content.

For long-term storage, stock DNA samples can be placed in a −80°C ultra-low temperature freezers and should be stored in physically separate, duplicate locations on backup generator outlets (or in freezers with CO_2 backup). However, DNA samples that are accessed frequently can be stored at 4°C in the short-term to avoid multiple freeze-thaw cycles that can compromise DNA fragment length.

2.6. Genotyping Product Selection

The molecular methods described in this chapter utilize the Illumina Infinium assay (Illumina Inc., San Diego, CA) since we have most experience with this platform, however other genotyping platforms are available. The most commonly used alternative is the Affymetrix platform (Affymetrix Inc., Santa Clara, CA). Selection of the appropriate fixed content Illumina BeadChip is generally based on coverage in the population of interest and cost considerations. For example, the HumanCNV370-Quad BeadChip provides mean genomic coverage at $r^2 > 0.8$ for 0.87 of the genome, and, when combined with imputation methods, is generally adequate for populations of European ancestry where financial resources are limited (37). The higher SNP density of the Human1M-Duo BeadChip provides similar coverage (0.86 with $r^2 > 0.8$) in the HapMap Yoruba (YRI) population from Nigeria (http://www.illumina.com/pages.ilmn?ID=261).

3. Executing a GWAS

3.1. DNA Quantity and Preparation

Two key predictors of genotyping success are DNA quality and quantity. The 260/280 nm ratio, although a good measure of nucleic acid contamination of protein, is a poor measure of DNA contamination by protein (38). Visualization of DNA samples on gel to assess potential template degradation, and records of the sample storage and extraction methods, are likely to yield a more

accurate representation of overall quality. Although picogreen quantitation methods are recommended by Illumina Inc., we have had good success in GWAS assays using DNA samples quantitated using non-fluorescent methods, such as the NanoDrop-8000 spectrophotometer (NanoDrop Technologies; Wilmington, DE), provided input quantities exceed the specified minimum DNA quantity requirement. Illumina's fixed content GWAS products require a minimum input DNA of 400 ng for "Duo" products that process two samples per BeadChip, or 200 ng for "Quads" (four DNAs per BeadChip).

For a case-control study, case and control DNA samples should be intercalated in the wells of the genotyping daughter plates that will be used to prepare BeadChip assays. Case and control samples that have been separately ascertained, or collected and isolated, naturally lead to segregation of the case and control DNA samples into separate stock plates. While it is easiest to mirror this configuration of samples in daughter plates, plate-level biases in the genotyping assay or laboratory handling can lead to extreme plate-level effects that create spurious associations. If the samples are mixed on plates in approximately equal numbers, latent biases in the genotyping of an individual plate are less likely to generate spurious association results. From our experience, it is possible for a single plate to lead to spurious associations of more than 5 orders of magnitude in the measured *p*-values of association. Plate-level quality control checks of the samples in one plate compared to its sample complement should reveal plate(s) that appear to be outliers by SNP allele frequency or missing data.

3.2. Genotyping

Illumina's Infinium assay (39) is capable of multiplexing approximately 6,000 to 1 million SNPs/CNVs, either using fixed content products for GWAS, or customizable focused-content products (termed iSelect). At present, fixed content products for GWAS in humans range from approximately 370,000 to over 1 million markers per sample. Content is derived from HapMap data (6, 7), with a higher density of tagSNPs within 10 kb of a gene or in evolutionarily conserved regions.

In brief, Illumina's Infinium assay (39) consists of four modular components: (a) a single-tube whole-genome amplification step, (b) an array-based hybridization capture step, (c) an 'on array' enzymatic single base extension (SBE) step, and (d) an amplified-signal detection step. SBE uses a single 50 bp probe designed to hybridize adjacent to the SNP query site. After hybridization of target DNA to the BeadChip (a microelectromechanical systems (MEMS)-patterned substrate on silica slides), the SNP locus-specific primers, attached to 3-micron silica beads, are extended in the presence of hapten-labeled dideoxynucleotides. Biotin-labeled ddCTP and ddGTP, and 2,4-dinitrophenol (DNP)-labeled ddATP and ddUTP are efficiently incorporated

by polymerases and allow detection with a dual-color, orthogonal, multi-layer immune-histochemical sandwich assay. Biotin and DNP are simultaneously detected by staining with a combination of Alexa555-labeled streptavidin (SA) and Alexa647-labeled rabbit primary antibody against DNP, counterstaining with biotinylated anti-SA and DNP-labeled goat anti-rabbit secondary antibody. The signal is amplified by re-staining with Alexa555-SA/Alexa647-rabbit anti-DNP.

Physically separated pre- and post-PCR preparation areas are recommended to minimize possible cross-contamination of SBE primers from one assay to the next. It is advisable to use aerosol pipette tips, with separate boxes for pre- and post-PCR areas, and usual personal protective equipment such as latex gloves. Automation using robotics and incorporation of Laboratory Information Management Systems (LIMS), such as the Illumina's Infinium LIMS, can further reduce the possibility of error and contamination during processing of the Infinium assay.

Visualization of the resulting signal and decoding of SNP position is performed using a BeadArray Reader (Illumina Inc., San Diego, CA) and Illumina's proprietary data collection software. Data are initially analyzed using BeadStudio software (Illumina Inc., San Diego, CA), which automates clustering of genotypes and allele calling, as well as providing quality metrics to assist user inspection and removal of suspect data (*see* **Section 3.4**). This approach can be scaled to unlimited levels of multiplexing without compromising data quality, although in practical terms, the number of SNPs that can be assayed is limited by the number of probes on the array. Illumina has recently introduced a range of high-density (HD) BeadChips and has made minor adjustments to the protocol for this suite of products (40).

3.3. Quality Control Checks of Genotyping Data

Rigorous quality control is a crucial component of any GWAS since subtle biases in raw data can lead to hundreds or thousands of false positive results, confounding efforts to validate lead SNPs at the replication stage. Quality control steps to reject SNPs or samples are necessarily a trade-off between stringency to prevent type 1 error against loss of data, reducing power. The thresholds used in the individual steps reflect common values that are currently in use, but can be modified to be more or less tolerant of type 1 error. This decision will depend on study design, availability, and size of replication study samples, and willingness to include downstream manual steps to review cluster patterns of many SNP loci that appear to show significant association.

The first step involves use of vendor software to identify SNPs or samples that have obviously failed the assay or have generated significantly poorer quality data. Data checks from Infinium assays are initially conducted using Illumina's BeadStudio module. Given differences in allele frequencies, it is often advantageous to cluster

SNPs on the basis of individual race/ethnicity groups. Low-quality samples from the dataset can be identified and removed based on low signal intensities (less than 1000), low p10GC score (a quality metric, measuring distance from center of the cluster), and poor call rates (<95%). After removal of problem samples, all SNPs can be re-clustered and the call rates recalculated. SNPs with <95% call rate are classified as poor quality and removed. A large proportion of missing data indicates a non-robust SNP assay and is the best correlate of genotyping error or miscalling. We recommend the following pipeline of quality control checks:

1. Minor allele frequency (MAF): Retain only SNPs with MAF > 1%. Very low MAF SNPs are more susceptible to small biases in genotype calling algorithm.
2. Hardy Weinberg Equilibrium (HWE): Exclude SNPs with exact HWE test (41) jointly $p < 10^{-5}$. Deviations can indicate systematic genotype miscalling.
3. Cryptic duplicates: Test for outlier samples by examining the mean identity by state (IBS) between sample pairs by calculating the kappa coefficient. Pairs with extreme sharing suggest cryptic biological relationships or sample duplication.
4. Mean heterozygosity: Plots of heterozygosity distribution can reveal relative pairs (low) and contaminated samples (high).
5. X-linked heterozygosity: Plots of log odds ratio (sample is male/sample is female) can detect mis-specified study sex versus genetically inferred sex, indicating sample or data mix-up.

A potential problem for a GWAS is the presence of undetected population structure that may confound tests of association, leading to an increased rate of false positives or to false negative true associations (42). The effects of population structure increase with sample size, and for the size of study needed to detect typical genetic effects in common diseases, even the modest levels of population structure within population groups should not be ignored (43). A range of statistical issues for GWAS, including population substructure, are reviewed in (44). One approach is to use EIGENSTRAT (45, 46), which will detect outliers that are more than 6 standard deviations in any of 10 principal component (PC) dimensions by default, supplemented with a multivariate outlier detection algorithm. The optimal reduced principal components can be used as stratification adjustments in the generalized linear models for cross-sectional and longitudinal analysis (*see* **Section 3.5**). This approach has been shown to dramatically reduce the effects of population admixture, although we suggest carefully reviewing the principal components after computation and rationally choosing those to include as statistical model adjustments, to prevent over-adjustment.

Further genotype quality control measures are performed following initial analysis of association; this may involve visual

inspection of genotype cluster plots for the entire cohort for all SNPs deemed significant and all SNPs that show a distribution outside of HWE (at $P < 0.001$; this will include several thousand SNPs). This analysis is performed to ensure that there are no errors in automated calling and that any SNPs with potential errors can be discarded. Only if cluster plots reveal an obvious and correctible error is the SNP re-clustered and retained.

Quantile-quantile (QQ) plots are a particularly effective way to visually review the entire distribution of association or quality control statistics for all SNPs. These plots show the empirical distribution of statistics derived from the GWAS analysis plotted against the expected value for each ranked SNP under the global null hypothesis of no association or no significant test result for any SNP. A systematic difference in the empirical versus expected values across a fraction of the distribution may represent latent inflation of type 1 error through biases in the study populations, or may reflect true associations. Under a common variant complex model we expect to see true associated deviation from the expected null values for many SNPs in the more highly significant tail of the distribution.

As an illustrative example, genome-wide association scans were carried out using publicly available HapMap data (29, 47) to study the genetic basis of natural variation in gene expression. The data consist of gene-expression measurements (*CHI3L2* in this example) for 156 individuals in twenty 3-generation CEPH pedigrees, each with 12–17 individuals. Genotypes for 864,360 SNPs were generated for a subset of 90 individuals in these families in phase I of the International HapMap Project. Genotypes for 6,728 SNPs for the complete families, including 168 individuals, were also genotyped previously by the SNP Consortium. The GWA scan (*see* **Fig. 25.2**) maps gene *CHI3L2* to chromosome 1 with *p*-value $<10^{-9}$(29), and the *cis*-association has been confirmed by a functional assay analysis (47). The Q–Q plot for the GWA test statistics shows that overall the *p*-values are distributed uniformly between 0 and 1, and the log Q–log Q plot focuses attention on the tail of the distribution.

3.4. In Silico Genotyping

To improve genomic coverage of the selected marker panel, imputation methods have been implemented in software packages MACH (48) and IMPUTE (49) amongst others. Imputation improves the coverage of SNP panels as well as the power of a GWAS. Imputed SNPs are anticipated to lead to increased signal strength (lower *p*-values) near a signal from a true typed SNP, and also allow cross-genotyping platform analysis. The imputation method in MACH uses Markov models to identify stretches of shared chromosome between individuals, and then infer intervening genotypes by contrasting study samples with densely typed HapMap samples. Currently 2.5 million HapMap SNPs can be imputed for each individual, regardless of different genotyping

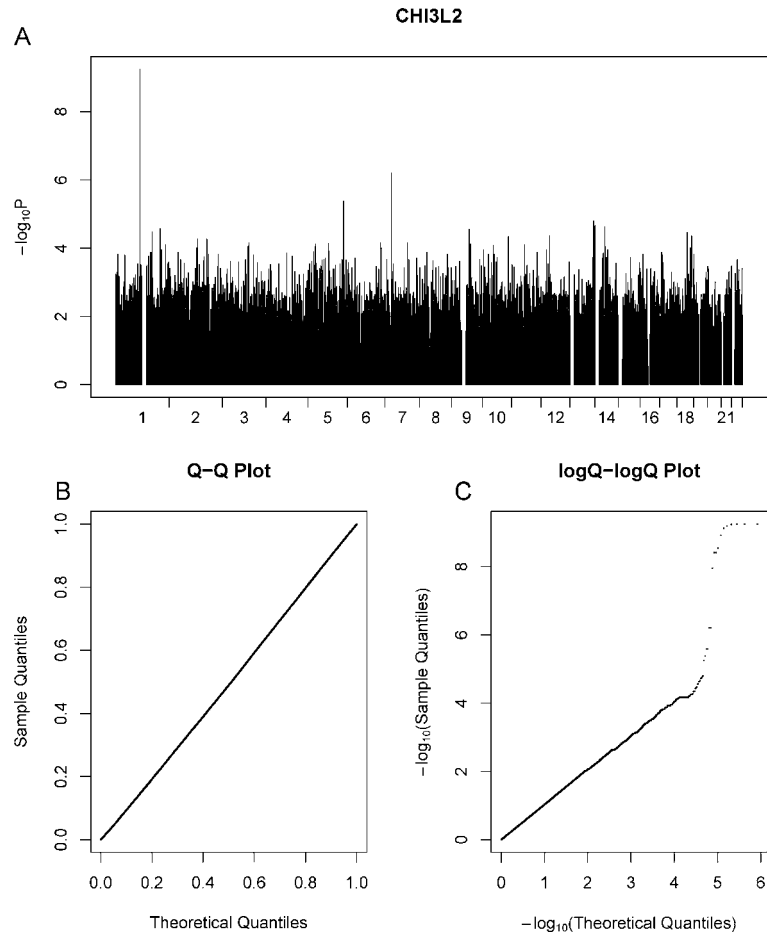

Fig. 25.2. Genome scan for *CHI3L2*expression levels. The gene maps to chromosome 1, and the association has also been confirmed by a functional analysis. (**A**) Genome scan using 90 individuals genotyped by the HapMap Consortium and 66 individuals with imputed genotypes. (**B**) Q–Q plot. (**C**) log Q–log Q plot.

platforms used. The imputation is accurate: in a few studies examined (50), focusing on top 95% top quality (measured by a correlation estimate between predicted and true genotypes) imputations, the error rate per SNP is about 1.1%. African samples were the most difficult to impute, with overall error rates ranging between 5.13% for the Yoruba and 11.86% for a sample from the San tribe when the HapMap YRI panel was used as a reference. In contrast, using the HapMap Centre d'Etude du Polymorphisme Human (CEPH) sample for European populations, and Chinese and Japanese HapMap samples for East Asian populations, resulted in overall error rates of <3.34 and 2.89% respectively (50). However, the accuracy can be further improved by tuning the quality metric threshold. It is prudent to confirm associated imputed genotyped by subsequent direct genotyping. For example, in a GWAS of

fasting glucose, the imputed SNP with the strongest association in gene G6PC2 was later genotyped and the discrepancy rate per allele between the imputed and typed genotypes was 1.4% (51).

3.5. Tests of Association

Although a variety of approaches can be used to analyze a GWAS, in this section we suggest some widely used applications, as well as a method uniquely capable of handling multivariate data. For single SNP analyses in case-control datasets, PLINK (http://pngu.mgh.harvard.edu/purcell/plink/) (52) has been developed specifically for the analysis of GWAS data. For example, point tests of association can be estimated for each SNP using standard allelic and inheritance model association tests, or the Cochran-Armitage test for trend. For both discrete and quantitative traits, univariate and multivariable analyses can be performed to examine the contribution at each SNP to the specific trait of interest, depending on the hypothesis. The baseline linear regression framework allows for adjustment for environmental and other factors known or suspected to be confounding variables (e.g., age, sex, EIGENSTRAT principal components), as well as gene-by-gene and gene-by-environment interactions. Under a model of stratification, Cochran-Mantel-Haenzsel tests the conditional independence of the case-control disease status.

A multivariate trait GWA algorithm has been implemented the software package Ghost (Chen WM, personal communication, http://people.virginia.edu/~wc9c/ghost/). This implementation can help systematically identify genetic variants that are responsible for multiple traits.

For longitudinal data, the generalized estimating equation (GEE) method, using a sandwich estimator of the variance under an exchangeable correlation and allowing adjustment for covariates as well as gene-by-gene and gene-by-environment interactions, can take into account correlations of repeated measures, and association results will be less sensitive to the trait distribution (and thus more robust). Note this GEE based GWAS does not add computational complexity, and permutation testing can be easily followed to adjust for multiple testing.

Although it is possible under disease models of SNP-SNP interaction that haplotype tests could have greater power to detect association than single SNP tests, genome wide haplotype testing increases the total number of GWAS hypothesis tests conducted, and leads to reduced power resulting from the necessary increased stringency threshold for increased multiple testing. The usual approach is to perform single SNP tests first, utilizing the high accuracy of imputation methods to effectively increase marker density, and follow-up with targeted haplotype analyses where an associated SNP is contained within a haplotype block (4). Few, if any, current studies have power to detect and fully replicate genetic predisposition arising from gene–gene or SNP–SNP interactions.

To assess whether SNPs or haplotypes are associated with clinical outcomes, the Kaplan–Meier method of survival analysis can be used to estimate the survival functions for subjects with different genotypes in the follow up period, and a logrank test performed to compare the survival distributions. Cox's proportional hazards model can also be used by treating the genotype as a risk factor.

A number of analytical approaches for analyses of GWAS data are reviewed in (53).

3.6. Replication

Since the discovery stage of most GWAS designs is underpowered to detect the modest effects observed for the majority of complex diseases, such studies are anticipated to generate a substantial number of false positive results (type 1 errors) (54). Additionally, the initial effect estimates are likely to be inflated due to the phenomenon known as the "winner's curse" (55, 56). Replication in an independent population therefore remains a critical step in a GWAS to confirm initial results (57). Several different strategies have been employed, including the two-stage design mentioned previously (*see* **Section 2.4**). However, due to the large sample sizes required, large-scale meta-analyses across several independent studies have been a mainstay of GWAS reports. These studies frequently combine heterogeneous study designs, ascertainment and recruitment criteria, genotyping platforms, and QC metrics. A set of useful guidelines for imputation and meta-analyses have been developed by (58), and many of the relative merits, caveats, statistical approaches, and diagnostic tests for meta-analyses are reviewed in (59). It should be noted that lack of replication may reflect any one of a number of possible scenarios, including appropriate refutation of a false lead, false non-replication, or true genetic heterogeneity across studies (60).

4. Summary and Future Directions

Recent successes using GWAS approaches have generated considerable enthusiasm about the utility of this approach to identify variants that contribute to human variation and disease susceptibility. In a relatively short space of time, considerable advances have already been made in genotyping efficiency and cost, imputation approaches, and analytical methods. In future, further understanding of the roles of epistasis (gene–gene interactions), gene–environment interactions, copy number variants, and epigenetic phenomena are anticipated to provide additional insights into our understanding of complex human disorders.

Acknowledgments

We wish to thank Andrew Singleton, Ph.D., National Institute on Aging, Kathleen H. Day, University of Virginia and Fang-Chi Hsu, Ph.D., Wake Forest University School of Medicine, for helpful discussion and comments.

References

1. Lander ES, Linton LM, Birren B, Nusbaum C, Zody MC, Baldwin J, Devon K, Dewar K, Doyle M, FitzHugh W et al.: Initial sequencing and analysis of the human genome. *Nature* 2001, 409(6822):860–921.
2. Venter JC, Adams MD, Myers EW, Li PW, Mural RJ, Sutton GG, Smith HO, Yandell M, Evans CA, Holt RA et al.: The sequence of the human genome. *Science* 2001, 291(5507):1304–1351.
3. Sachidanandam R, Weissman D, Schmidt SC, Kakol JM, Stein LD, Marth G, Sherry S, Mullikin JC, Mortimore BJ, Willey DL et al.: A map of human genome sequence variation containing 1.42 million single nucleotide polymorphisms. *Nature* 2001, 409(6822):928–933.
4. Gabriel SB, Schaffner SF, Nguyen H, Moore JM, Roy J, Blumenstiel B, Higgins J, DeFelice M, Lochner A, Faggart M et al.: The structure of haplotype blocks in the human genome. *Science* 2002, 296(5576):2225–2229.
5. Olivier M: A haplotype map of the human genome. *Physiol Genomics* 2003, 13(1):3–9.
6. The International HapMap Consortium: A haplotype map of the human genome. *Nature* 2005, 437(7063):1299–1320.
7. Frazer KA, Ballinger DG, Cox DR, Hinds DA, Stuve LL, Gibbs RA, Belmont JW, Boudreau A, Hardenbol P, Leal SM et al.: A second generation human haplotype map of over 3.1 million SNPs. *Nature* 2007, 449(7164):851–861.
8. de Bakker PI, Yelensky R, Pe'er I, Gabriel SB, Daly MJ, Altshuler D: Efficiency and power in genetic association studies. *Nat Genet* 2005, 37(11):1217–1223.
9. Gu CC, Yu K, Ketkar S, Templeton AR, Rao DC: On transferability of genome-wide tagSNPs. *Genet Epidemiol* 2008, 32(2): 89–97.
10. Gu CC, Yu K, Rao DC: Characterization of LD structures and the utility of HapMap in genetic association studies. *Adv Genet* 2008, 60:407–435.
11. Frayling TM: A new era in finding Type 2 diabetes genes-the unusual suspects. *Diabet Med* 2007, 24(7):696–701.
12. Lindgren CM, McCarthy MI: Mechanisms of disease: genetic insights into the etiology of type 2 diabetes and obesity. *Nat Clin Pract Endocrinol Metab* 2008, 4(3): 156–163.
13. Duffy DL: Genetic determinants of diabetes are similarly associated with other immune-mediated diseases. *Curr Opin Allergy Clin Immunol* 2007, 7(6):468–474.
14. Hwang SJ, Yang Q, Meigs JB, Pearce EN, Fox CS: A genome-wide association for kidney function and endocrine-related traits in the NHLBI's Framingham Heart Study. *BMC Med Genet* 2007, 8 Suppl 1:S10.
15. Todd JA, Walker NM, Cooper JD, Smyth DJ, Downes K, Plagnol V, Bailey R, Nejentsev S, Field SF, Payne F et al.: Robust associations of four new chromosome regions from genome-wide analyses of type 1 diabetes. *Nat Genet* 2007, 39(7):857–864.
16. Richards JB, Rivadeneira F, Inouye M, Pastinen TM, Soranzo N, Wilson SG, Andrew T, Falchi M, Gwilliam R, Ahmadi KR et al.: Bone mineral density, osteoporosis, and osteoporotic fractures: a genome-wide association study. *Lancet* 2008, 371(9623): 1505–1512.
17. Kiel DP, Demissie S, Dupuis J, Lunetta KL, Murabito JM, Karasik D: Genome-wide association with bone mass and geometry in the Framingham Heart Study. *BMC Med Genet* 2007, 8 Suppl 1:S14.
18. Fox CS, Heard-Costa N, Cupples LA, Dupuis J, Vasan RS, Atwood LD: Genome-wide association to body mass index and waist circumference: the Framingham Heart Study 100 K project. *BMC Med Genet* 2007, 8 Suppl 1:S18.
19. Frayling TM, Timpson NJ, Weedon MN, Zeggini E, Freathy RM, Lindgren CM, Perry JR, Elliott KS, Lango H, Rayner NW et al.: A common variant in the FTO gene is

associated with body mass index and predisposes to childhood and adult obesity. *Science* 2007, 316(5826):889–894.

20. Scuteri A, Sanna S, Chen WM, Uda M, Albai G, Strait J, Najjar S, Nagaraja R, Orru M, Usala G et al.: Genome-wide association scan shows genetic variants in the FTO gene are associated with obesity-related traits. *PLoS Genet* 2007, 3(7):e115.
21. Weedon MN, Lettre G, Freathy RM, Lindgren CM, Voight BF, Perry JR, Elliott KS, Hackett R, Guiducci C, Shields B et al.: A common variant of HMGA2 is associated with adult and childhood height in the general population. *Nat Genet* 2007, 39(10): 1245–1250.
22. Lettre G, Jackson AU, Gieger C, Schumacher FR, Berndt SI, Sanna S, Eyheramendy S, Voight BF, Butler JL, Guiducci C et al.: Identification of ten loci associated with height highlights new biological pathways in human growth. *Nat Genet* 2008, 40(5): 584–591.
23. Sanna S, Jackson AU, Nagaraja R, Willer CJ, Chen WM, Bonnycastle LL, Shen H, Timpson N, Lettre G, Usala G et al.: Common variants in the GDF5-UQCC region are associated with variation in human height. *Nat Genet* 2008, 40(2):198–203.
24. Weedon MN, Lango H, Lindgren CM, Wallace C, Evans DM, Mangino M, Freathy RM, Perry JR, Stevens S, Hall AS et al.: Genome-wide association analysis identifies 20 loci that influence adult height. *Nat Genet* 2008, 40(5):575–583.
25. McCarthy MI, Abecasis GR, Cardon LR, Goldstein DB, Little J, Ioannidis JP, Hirschhorn JN: Genome-wide association studies for complex traits: consensus, uncertainty and challenges. *Nat Rev Genet* 2008, 9(5):356–369.
26. Mailman MD, Feolo M, Jin Y, Kimura M, Tryka K, Bagoutdinov R, Hao L, Kiang A, Paschall J, Phan L et al.: The NCBI dbGaP database of genotypes and phenotypes. *Nat Genet* 2007, 39(10):1181–1186.
27. Homer N, Szelinger S, Redman M, Duggan D, Tembe W, Muehling J, Pearson JV, Stephan DA, Nelson SF, Craig DW: Resolving individuals contributing trace amounts of DNA to highly complex mixtures using high-density SNP genotyping microarrays. *PLoS Genet* 2008, 4(8):e1000167.
28. Martin ER, Monks SA, Warren LL, Kaplan NL: A test for linkage and association in general pedigrees: the pedigree disequilibrium test. *Am J Hum Genet* 2000, 67(1): 146–154.
29. Chen WM, Abecasis GR: Family-based association tests for genomewide association scans. *Am J Hum Genet* 2007, 81(5): 913–926.
30. Wellcome Trust Case Control Consortium: Genome-wide association study of 14,000 cases of seven common diseases and 3,000 shared controls. *Nature* 2007, 447(7145): 661–678.
31. Cooper JD, Smyth DJ, Smiles AM, Plagnol V, Walker NM, Allen JE, Downes K, Barrett JC, Healy BC, Mychaleckyj JC et al.: Meta-analysis of genome-wide association study data identifies additional type 1 diabetes risk loci. *Nat Genet* 2008.
32. Zondervan KT, Cardon LR: Designing candidate gene and genome-wide case-control association studies. *Nat Protoc* 2007, 2(10):2492–2501.
33. Amos CI: Successful design and conduct of genome-wide association studies. *Hum Mol Genet* 2007, 16 Spec No. 2:R220–225.
34. Kraft P, Cox DG: Study designs for genome-wide association studies. *Adv Genet* 2008, 60:465–504.
35. Cupples LA: Family study designs in the age of genome-wide association studies: experience from the Framingham Heart Study. *Curr Opin Lipidol* 2008, 19(2):144–150.
36. Skol AD, Scott LJ, Abecasis GR, Boehnke M: Joint analysis is more efficient than replication-based analysis for two-stage genome-wide association studies. *Nat Genet* 2006, 38(2):209–213.
37. Anderson CA, Pettersson FH, Barrett JC, Zhuang JJ, Ragoussis J, Cardon LR, Morris AP: Evaluating the effects of imputation on the power, coverage, and cost efficiency of genome-wide SNP platforms. *Am J Hum Genet* 2008, 83(1):112–119.
38. Glasel JA: Validity of nucleic acid purities monitored by 260 nm/280 nm absorbance ratios. *Biotechniques* 1995, 18(1):62–63.
39. Steemers FJ, Chang W, Lee G, Barker DL, Shen R, Gunderson KL: Whole-genome genotyping with the single-base extension assay. *Nat Methods* 2006, 3(1):31–33.
40. Illumina Inc.: Infinium HD Assay Super, Manual – Experienced User Card. In.: Part # 11294825.
41. Wigginton JE, Cutler DJ, Abecasis GR: A note on exact tests of Hardy-Weinberg equilibrium. *Am J Hum Genet* 2005, 76(5):887–893.
42. Pritchard JK, Donnelly P: Case-control studies of association in structured or admixed populations. *Theor Popul Biol* 2001, 60(3): 227–237.

43. Marchini J, Cardon LR, Phillips MS, Donnelly P: The effects of human population structure on large genetic association studies. *Nat Genet* 2004, 36(5):512–517.
44. Teo YY: Common statistical issues in genome-wide association studies: a review on power, data quality control, genotype calling and population structure. *Curr Opin Lipidol* 2008, 19(2):133–143.
45. Price AL, Patterson NJ, Plenge RM, Weinblatt ME, Shadick NA, Reich D: Principal components analysis corrects for stratification in genome-wide association studies. *Nat Genet* 2006, 38(8):904–909.
46. Li Q, Yu K: Improved correction for population stratification in genome-wide association studies by identifying hidden population structures. *Genet Epidemiol* 2008, 32(3):215–226.
47. Cheung VG, Spielman RS, Ewens KG, Weber TM, Morley M, Burdick JT: Mapping determinants of human gene expression by regional and genome-wide association. *Nature* 2005, 437(7063): 1365–1369.
48. Li Y, Abecasis GR: Mach 1.0: Rapid haplotype reconstruction and missing genotype inference. *American Journal of Human Genetics* 2006, S79:2290.
49. Marchini J, Howie B, Myers S, McVean G, Donnelly P: A new multipoint method for genome-wide association studies by imputation of genotypes. *Nat Genet* 2007, 39(7):906–913.
50. Huang L, Li Y, Singleton AB, Hardy JA, AbeCasis G, Rosenberg NA, Scheet P: Genotype-imputation accuracy across worldwide human populations. *American Journal of Human Genetics* 2009, 84(2):230–250.
51. Chen WM, Erdos MR, Jackson AU, Saxena R, Sanna S, Silver KD, Timpson NJ, Hansen T, Orru M, Grazia Piras M et al.: Variations in the G6PC2/ABCB11 genomic region are associated with fasting glucose levels. *J Clin Invest* 2008, 118(7):2620–2628.
52. Purcell S, Neale B, Todd-Brown K, Thomas L, Ferreira MA, Bender D, Maller J, Sklar P, de Bakker PI, Daly MJ et al.: PLINK: a tool set for whole-genome association and population-based linkage analyses. *Am J Hum Genet* 2007, 81(3):559–575.
53. Langefeld CD, Fingerlin TE: Association methods in human genetics. *Methods Mol Biol* 2007, 404:431–460.
54. Senn S: Transposed conditionals, shrinkage, and direct and indirect unbiasedness. *Epidemiology* 2008, 19(5):652–654; discussion 657–658.
55. Ioannidis JP: Why most discovered true associations are inflated. *Epidemiology* 2008, 19(5):640–648.
56. Kraft P: Curses—winner's and otherwise—in genetic epidemiology. *Epidemiology* 2008, 19(5):649–651; discussion 657-648.
57. Willett WC: The search for truth must go beyond statistics. *Epidemiology* 2008, 19(5): 655–656.
58. de Bakker PI, Ferreira MA, Jia X, Neale BM, Raychaudhuri S, Voight BF: Practical aspects of imputation-driven meta-analysis of genome-wide association studies. *Hum Mol Genet* 2008, 17(R2):R122-128.
59. Kavvoura FK, Ioannidis JP: Methods for meta-analysis in genetic association studies: a review of their potential and pitfalls. *Hum Genet* 2008, 123(1):1–14.
60. Ioannidis JP: Non-replication and inconsistency in the genome-wide association setting. *Hum Heredity* 2007, 64(4): 203–213.

Subject Index

A

Ok-Kyong Park-Sarge, Thomas E. Curry (eds.), *Molecular Endocrinology,* Methods in Molecular Biology 590,
DOI 10.1007/978-1-60327-378-7, © Humana Press, a part of Springer Science+Business Media, LLC 2009

B

C

D

E

F

G

H

I

J

K

L

M

N

O

P

Q

R

S

T

U

V

W

Y